

## Stereospecific Polymerization of 2-Substituted- 1,3-butadienes. I. Crystalline Polymers of 2-*tert*- Butyl-1,3-butadiene

W. MARCONI, A. MAZZEI, S. CUCINELLA, and M. CESARI, *SNAM*  
*Laboratori Riuniti Studi e Ricerche, S. Donato, Milan, Italy*

### Synopsis

Some results obtained in the stereospecific polymerization of 2-*tert*-butyl-1,3-butadiene are reported. The catalysts employed were prepared from  $TiCl_4$  and aluminum alkyls or soluble aluminum hydride derivatives. Polymers thus obtained were crystalline with a melting point of 106°C. and soluble in common solvents. X-ray investigation shows the polymer to have a helical chain structure built on 11 monomeric units with *cis* configuration, distributed on three turns. The identity period along the chain axis is 15.3 Å. A comparison of the infrared spectra of the crystalline and amorphous polymers is given. Attempts to obtain a crystalline 1,4-*trans* polymer failed; this is in accord with the lower stability of such a configuration due to steric repulsion of the bulky group.

### INTRODUCTION

The greatest part of the research on polymerization of 2-alkyl-substituted butadiene relates to stereospecific polymers of isoprene having a predominantly *cis*-1,4-structure, due to the enormous commercial interest in such polymers as substitutes for natural rubber. However, some papers on the polymerization of 2-alkyl-butadienes with alkyl group other than  $-CH_3$  are reported in the literature. For instance, 2-ethyl-1,3-butadiene and 2-isopropyl-1,3-butadiene<sup>1,2</sup> can be polymerized by using metallic lithium or its organic derivatives as catalysts; rubbery materials are obtained whose gum vulcanizates possess high strength and elastic properties comparable to those of natural rubber.

The glass transition temperatures change in the order isoprene, 2-ethyl-1,3-butadiene, 2-isopropyl-1,3-butadiene, from  $-72^\circ C.$  to  $-76^\circ C.$  and  $-52^\circ C.$ , respectively.

Furthermore high molecular weight polymers having a predominantly 1,4 structure are claimed from 2-ethyl-1,3-butadiene, 2-propyl-1,3-butadiene, 2-phenyl-1,3-butadiene, and 2-neopentyl-1,3-butadiene with complex catalysts prepared from aluminum alkyls and transition metal salts, as reported in a recent patent.<sup>3</sup>

No previous description has been given of the polymerization of 2-*tert*-butyl-1,3-butadiene by means of stereospecific catalysts.

Overberger,<sup>4</sup> in a paper dealing with the synthesis and properties of polymers obtained from 2-alkyl-butadienes, describes the emulsion polymerization of 2-*tert*-butyl-1,3-butadiene by use of the conventional GR-S recipe and some physical properties of the polymers. The poly-2-*tert*-butyl-1,3-butadiene thus obtained is a powder at room temperature which softens above 30°C. and has some elastic properties. The second-order transition point of this polymer is +20°C., i.e., higher than that of poly-2-isopropyl butadiene (-47°C.), poly-2-*n*-heptylbutadiene (-83°C.), and poly-2-*n*-decylbutadiene (-53°C.).

It is assumed that the increase in the second-order transition temperature is due to side-chain branching.

We wish now to report our results on the stereospecific polymerization of 2-*tert*-butyl-1,3-butadiene using catalytic systems prepared from TiCl<sub>4</sub> and aluminum alkyls or aluminum hydride derivatives.

Characteristics and some properties of the new crystalline polymers are also reported; a detailed study of their crystalline structure will appear later.

## EXPERIMENTAL

### Materials

Pure 2-*tert*-butyl-1,3-butadiene monomer was prepared in our laboratories by catalytic ethynylation of pinacolone followed by selective hydrogenation and dehydration over alumina. The monomer was distilled on Na-K alloy at reduced pressure just before use and maintained at -78°C. under an inert atmosphere.

TiCl<sub>4</sub> was the commercial product and was used without further purification. Triethyl aluminum produced by Ethyl Co. (about 97% pure) was used. Aluminum hydride derivatives were prepared according to methods described in the literature.<sup>5,6</sup>

Reagent-grade benzene (or *n*-heptane) was purified and refluxed over sodium, then distilled in a nitrogen atmosphere before use as solvent.

### Polymerizations

The polymerizations were carried out in screw-cap bottles by a technique already described.<sup>7</sup> The order of addition of materials to the bottle was solvent, TiCl<sub>4</sub>, monomer, and aluminum compound. The bottles were kept in a thermostatic rotating bath for the desired time, and the polymer then precipitated with methanol in the presence of an antioxidant.

### Physicochemical Measurements

X-ray diffraction patterns were obtained with a Philips diffractometer equipped with proportional counter.

The infrared spectra were measured with a Perkin-Elmer Model 21 spectrophotometer on carbon disulfide solutions of the polymer or films obtained by slow evaporation of the solvent.

Intrinsic viscosity determinations were carried out in toluene solution at 30°C. in a Ubbelohde suspended-level viscometer.

## RESULTS AND DISCUSSION

### Polymerizations

**Triethylaluminum and Titanium Tetrachloride System.** The results obtained with this system are summarized in Table I.

TABLE I  
Polymerization of 2-*tert*-Butyl-1,3-butadiene by the Al(C<sub>2</sub>H<sub>5</sub>)<sub>3</sub>-TiCl<sub>4</sub> System<sup>a</sup>

No.	Solvent	Al/Ti molar ratio	Time, hr.	Yield, %	Relative crystallinity, %	[ $\eta$ ] (30°C.), dl./g.
1	<i>n</i> -Heptane	0.6	17	6	Low	—
2	"	0.8	17	23	66	1.21
3 <sup>b</sup>	"	1	17	47	46	1.70
4	"	1.2	17	13	40	—
5	"	1.4	17	6	Low	—
6	Benzene	0.8	62	70	55	1.49
7	"	1	62	56	44	1.34

<sup>a</sup> Polymerization conditions: monomer, 7.4 g.; TiCl<sub>4</sub>, 0.6 × 10<sup>-3</sup> moles; solvent, 30 ml.; polymerization temperature, +15°C.

<sup>b</sup> Melting point 103°C.

It is known that in polymerizing diolefins with such a catalyst<sup>8-10</sup> the polymer structure is strongly dependent on the Al/Ti mole ratio. However, polymers of 2-*tert*-butylbutadiene obtained in the range of Al/Ti ratios from 0.5 to 1.5 show identical infrared spectra and crystalline structure.

Instead, the yield of solid polymer is strongly dependent on Al/Ti ratios: for Al/Ti ratios lower than 0.5 and higher than 1.5 no solid products are formed. The highest conversion values are obtained at Al/Ti ratios near 1.

The nature of the solvent does not affect the structure of the products obtained by polymerization, as ascertained from comparison tests carried out in aromatic or aliphatic solvents.

**Systems with Aluminum Hydride Derivatives and Titanium Tetrachloride.** Recently in a number of studies on the polymerization of diolefins it was found that complex catalysts obtained from TiCl<sub>4</sub> and soluble aluminum hydride derivatives show a high catalytic activity and give rise to stereoregular polymers.<sup>11</sup>

Some results obtained in the polymerization of 2-*tert*-butyl-1,3-butadiene with catalytic systems prepared from TiCl<sub>4</sub> and AlHCl<sub>2</sub>·O(C<sub>2</sub>H<sub>5</sub>)<sub>2</sub>, AlHCl<sub>2</sub>·N(CH<sub>3</sub>)<sub>3</sub>, AlH<sub>2</sub>N(CH<sub>3</sub>)<sub>2</sub> and AlH<sub>3</sub>·N(CH<sub>3</sub>)<sub>3</sub> are reported in Table II.

Crystalline high molecular weight polymers are obtained with good yields also by the use of such cocatalysts; the structure of these polymers is almost identical to that of the polymers obtained with the use of aluminum alkyls as cocatalysts.

TABLE II  
 Polymerization of 2-*tert*-Butyl-1,3-butadiene by TiCl<sub>4</sub>-Al Hydrides System<sup>a</sup>

No.	Cocatalyst		Al/Ti molar ratio	Time, hr.	Yield, %	[ $\eta$ ] (30°C.), dl./g.	Melting point, °C.	Rela- tive crys- tal-
	Type	Moles $\times 10^3$						linity, %
1	AlHCl <sub>2</sub> ·O(C <sub>2</sub> H <sub>5</sub> ) <sub>2</sub>	0.97	1.6	1 30	48	2.37	104	50
2	AlHCl <sub>2</sub> ·N(CH <sub>3</sub> ) <sub>3</sub>	0.9	1.5	66	74.5	1.79	106	60
3	AlH <sub>2</sub> N(CH <sub>3</sub> ) <sub>2</sub>	0.36	0.6	1 30	65	2.95	103	50
4	AlH <sub>3</sub> ·N(CH <sub>3</sub> ) <sub>3</sub>	0.24	0.4	65	41	1.56	103	50

<sup>a</sup> Polymerization conditions: benzene, 30 ml.; monomer, 10 ml.; TiCl<sub>4</sub> 0.6  $\times 10^{-3}$  moles; polymerization temperature, +15°C.

The poly-2-*tert*-butyl-1,3-butadiene obtained with these aluminum hydride derivatives as catalysts shows a melting point of 103–106°C. and a glass transition temperature of +25°C., a value near the one found<sup>4</sup> for traditional emulsion polymers.

The polymer is completely soluble at room temperature in diethyl ether, carbon disulfide, benzene, *n*-heptane, chloroform, and carbon tetrachloride.

Boiling acetone extracts an oily fraction (10–25%) consisting of low molecular weight polymers. Infrared examination shows that the content of 3,4 structure in this fraction is higher than that of the bulk unextracted polymer. Also, the residue after extraction shows a higher crystallinity.

### Crystallinity and Crystalline Structure

The polymers obtained by the methods previously described show a fairly high degree of crystallinity when examined by x-ray diffraction techniques.

In Figure 1 are shown the diffraction patterns of two crystalline samples (A and B) and of one amorphous sample, obtained by radical polymerization.

The degree of crystallinity, calculated by using the ratio of x-ray energy diffused from crystalline and amorphous portion of the polymers, is 60–70% for sample A and 20–30% for sample B, although no particular attempt has been made to improve the accuracy of the method.

The change in crystallinity as function of temperature in a highly crystalline sample was investigated by using a high temperature attachment with the diffractometer; in this case, the intensity of the reflection corresponding to the spacing  $d = 11.60$  Å. was used as a measure of the relative crystalline content. The resulting melting point is 106°C. (Fig. 2). The sharp decrease of crystallinity even at low temperature is surprising for such a highly crystalline polymer.

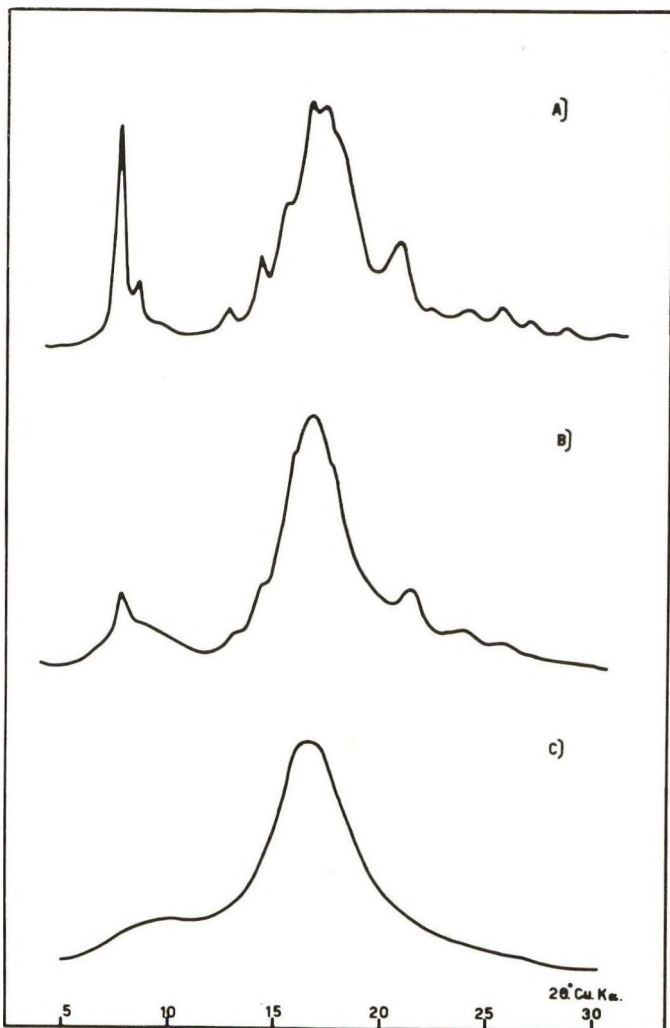


Fig. 1. Smooth trace of x-ray diffractometer patterns of poly-2-*tert*-butyl-1,3-butadiene: (A) highly crystalline; (B) moderately crystalline; (C) amorphous.

The Bragg spacings corresponding to the peaks of the amorphous halos are 10.5 and 5.2 Å.

The reflections due to crystalline portion of the polymer, observed in powder pattern, are reported in Table III. Only the reflections corresponding to the equatorial reflections of the fiber spectrum (Fig. 3) are indexed on the basis of a rectangular cell, having axes  $a' = 13.95$  Å. and  $b' = 20.78$  Å.

Oriented fibers may be drawn from polymer melts or solutions. As has been reported in a previous communication,<sup>12</sup> interpretation of the fiber spectrum leads to a chain structure of helical type, with identity period  $c = 15.3$  Å. The helix is built on 11 monomers units distributed on three

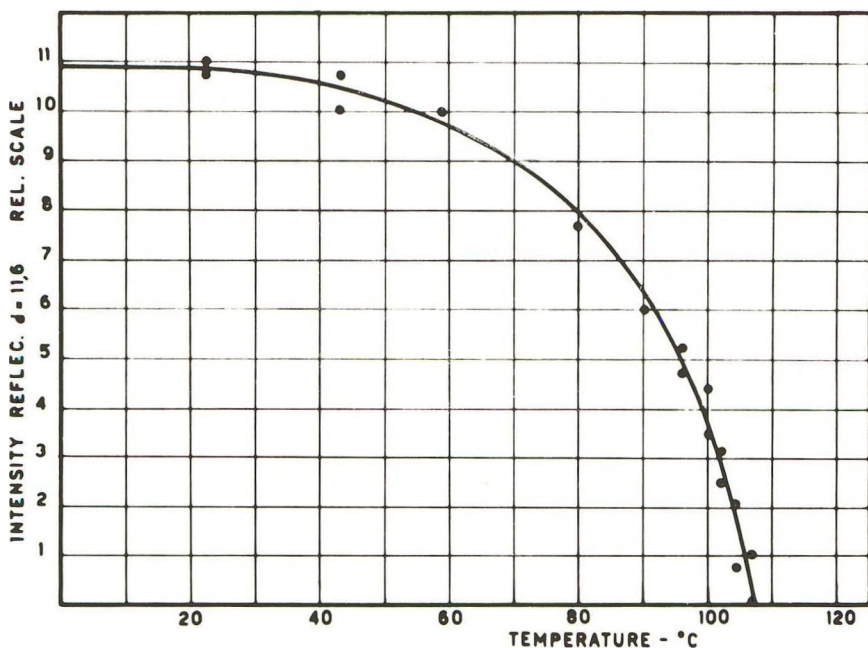


Fig. 2. Melting point curve of poly-2-*tert*-butyl-1,3-butadiene by roentgenographic method.

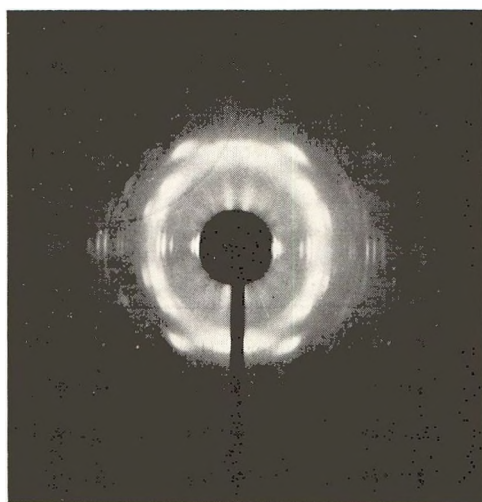


Fig. 3. X-ray diffraction photograph of a fiber of poly-2-*tert*-butyl-1,3-butadiene.

turns. A model of such a helix, which gives a satisfactory explanation of the distribution of the intensity in the eight layer observed in the fiber spectrum, requires a *cis* configuration of monomeric units. On the other hand, no helical chain structure with *trans* conformation would be possible without imposing drastic and unacceptable deformations in bond and internal rotational angles.

TABLE III  
Reflections in Powder X-Ray Pattern

$I_{obs.}$	$d_{obs.}, \text{ \AA}$	$hko$
<i>vs</i>	11.60	110
<i>m</i>	10.46	020
<i>m</i>	6.98	200
<i>ms</i>	6.20	130
<i>s</i>	5.75	<sup>b</sup>
<i>s</i>	5.30	<sup>b</sup>
<i>s</i>	5.10	<sup>b</sup>
<i>s</i>	4.23	240
<i>vw</i>	3.98	150
<i>w</i>	3.80	330
<i>w</i>	3.48	400
<i>w</i>	3.30	420

<sup>a</sup> Intensity: *vs* = very strong; *s* = strong; *ms* = moderately strong; *w* = weak; *vw* = very weak.

<sup>b</sup> Not Indexed.

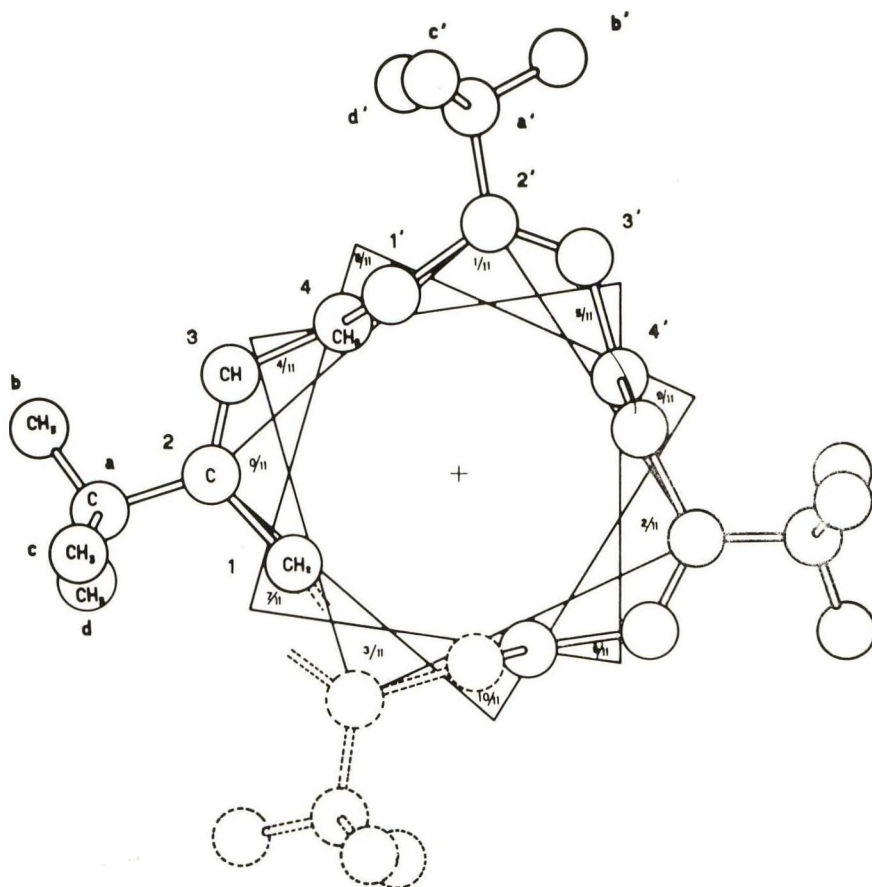


Fig. 4. Projection on the plane perpendicular to chain axis of the helix.

A sketch of the proposed model is given in Figure 4, where the helix is projected on the plane perpendicular to its axis; only three units are entirely represented and hydrogen atoms are omitted. It is worthy of note that the helical structure of this polymer is exceptional when compared to the known zigzag type structure of diolefin polymers having a 1,4 enchainment. A detailed account on chain structure will be reported later.

### Infrared Examination

The spectrum of a crystalline stereoregular polymer whose structure, as determined by x-ray, agrees with a *cis* configuration, is reported in Figure 5 together with the spectrum of an amorphous polymer prepared by radical initiators.

The main differences in the two spectra lie in the 11–12  $\mu$  range where both the polymers show, even with different intensity, the same bands at 11.20–11.70 and 11.85  $\mu$ . Moreover only the stereoregular polymer shows an absorption band at 11.45  $\mu$ . The difference in intensity of the CH deformation band at 11.20  $\mu$  in the two spectra shows that the amount of 3,4 addition product is larger in the amorphous polymer than in the stereospecific one. This is also confirmed by the position of the bands in the C=C stretching region in both the samples.

With reference to the spectrum of polyisoprene,<sup>13</sup> the absence of an absorption band at 11.45  $\mu$  in the amorphous polymer and the differences in

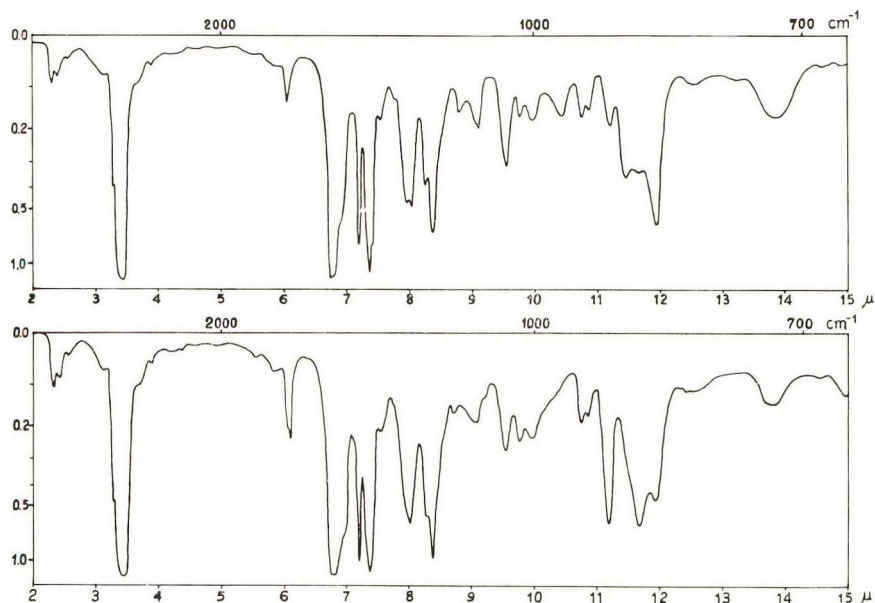


Fig. 5. Infrared spectra of poly-2-*tert*-butyl-1,3-butadiene: (top) crystalline polymer obtained by stereospecific catalysts; (bottom) amorphous polymer obtained by radical mechanism.



the absorption at 9.55 and 7.57  $\mu$  in the two samples could be explained on the basis of the differences in degree of crystallinity as found by x-ray.

The 11.90  $\mu$  band, present in both samples with different intensity, could be related to the *cis*-1,4-poly-*tert*-butylbutadiene concatenation. In fact the intensity of this band is stronger in the stereoregular polymer than in the polymers with high 3,4 configuration.

In order to confirm the 11.90  $\mu$  assignment we have tried to synthesize *trans*-1,4-polymers. Unfortunately, the use of the  $VCl_3$ -aluminum alkyl catalyst system<sup>14</sup> or the attempt to isomerize the polymer with techniques used with *cis* polybutadiene and natural rubber<sup>15,16</sup> have not given good results.

The authors wish to thank Dr. R. Onesta for the monomer preparation and Prof. G. Daniele for the infrared measurements.

### References

1. Livshits, I. A., and L. M. Korobova, *Vysokomol. Soedin.*, **3**, 891 (1961).
2. Livshits, I. A., and L. M. Korobova, *Dokl. Akad. Nauk. SSSR*, **121**, 474 (1958).
3. Goodrich-Gulf Chemical Co., U.S. Pat. 2,977,349, (Mar. 28, 1961).
4. Overberger, C. G., L. H. Arond, R. H. Wiley, and R. R. Gerrett, *J. Polymer Sci.*, **7**, 431 (1951).
5. Wiberg, E., K. Moedritzer, and R. Uson, *Rev. Acad. Cienc. Exact. Fis. Quim. Nat., Zaragoza*, **9**, No. 1, 91 (1954).
6. Ruff, J. K., and M. F. Hawthorne, *J. Am. Chem. Soc.*, **82**, 2141 (1960).
7. Marconi, W., A. Mazzei, S. Cucinella, and M. De Maldé, *Chim. Ind. (Milan)*, **44**, 121 (1962).
8. Natta, G., L. Porri, A. Mazzei, and D. Morero, *Chim. Ind. (Milan)*, **41**, 398 (1959).
9. Saltman, W. M., W. E. Gibbs, and J. Lal, *J. Am. Chem. Soc.*, **80**, 5615 (1958).
10. Yen, T. F., *J. Polymer Sci.*, **35**, 533 (1959); *ibid.*, **38**, 133 (1959).
11. Marconi, W., A. Mazzei, S. Cucinella, and M. De Maldé, *Makromol. Chem.*, **71**, 118 (1964); *ibid.*, **71**, 134 (1964); see also: A. Mazzei, S. Cucinella, W. Marconi, and M. De Maldé, *Chim. Ind. (Milan)*, **45**, 528 (1963).
12. Cesari, M., *J. Polymer Sci.*, in press.
13. Binder, J. L., *J. Polymer Sci.*, **A1**, 37 (1963).
14. Natta, G., L. Porri, P. Corradini, and D. Morero, *Chim. Ind. (Milan)*, **40**, 362 (1958).
15. Golub, M. A., *J. Polymer Sci.*, **25**, 373 (1957); *ibid.*, **36**, 523 (1959); *J. Am. Chem. Soc.*, **80**, 1794 (1958); *ibid.*, **81**, 54 (1959).
16. Bishop, W. A., *J. Polymer Sci.*, **55**, 827 (1961).

### Résumé

On donne quelques résultats obtenus dans la polymérisation stéréospécifique du 2-*tert*-butyle-1,3-butadiène. Les catalyseurs employés sont préparés à partir de  $TiCl_4$  et d'alkylaluminium ou de dérivés solubles d'hydrures d'aluminium. Les polymères ainsi obtenus sont cristallins avec un point de fusion de 106°C et sont solubles dans les solvants courants. L'étude aux rayons-X montre que le polymère possède une structure en chaînes hélicoïdales construite de 11 unités monomériques de configuration *cis* distribuées sur trois boucles. La périodicité le long de l'axe de la chaîne est de 15.3 Å. On donne une comparaison des spectres infra-rouges des polymères cristallins et amorphes. Les essais en vue d'obtenir un polymère cristallin *trans* 1,4 ont échoué; ceci est en accord avec le plus faible stabilité d'une telle configuration due à la répulsion stérique du groupe volumineux.

### Zusammenfassung

Es werden einige Ergebnisse der stereospezifischen Polymerisation von 2-*tert.*-Butyl-1,3-butadien mitgeteilt. Die verwendeten Katalysatoren wurden aus  $TiCl_3$  und Aluminiumalkylen oder löslichen Aluminiumhydridderivaten hergestellt. Die auf diese Weise erhaltenen Polymere sind kristallin mit einem Schmelzpunkt bei  $106^\circ C$  und sind in üblichen Lösungsmitteln löslich. Röntgenuntersuchung zeigt, dass das Polymere eine aus 11 Monomereinheiten mit *cis*-Konfiguration, verteilt auf drei Windungen, aufgebaute Helixkettenstruktur aufweist. Die Identitätsperiode entlang der Kettenachse ergibt sich zu 15,3 Å. Ein Vergleich der Infrarotspektren der kristallinen und amorphen Polymeren wurde durchgeführt. Versuche, ein kristallines 1,4-*trans*-Polymere zu erhalten, schlugen fehl; dies stimmt mit der geringeren auf der sterischen Abstossung der Hauptgruppe beruhenden Stabilität der Konfiguration überein.

Received October 15, 1963

## Polymerization in Liquid Sulfur Dioxide. Part XXI. Effect of Liquid Sulfur Dioxide Concentration on Cationic Copolymerization of Styrene with Methyl Acrylate in Liquid Sulfur Dioxide

MINORU MATSUDA, KOICHI OHSHIMA, and NIICHIRO TOKURA,  
*The Chemical Research Institute of Non-aqueous Solutions, Tohoku University,  
Sendai, Japan*

### Synopsis

The effect of liquid sulfur dioxide concentration on cationic copolymerization of styrene ( $M_1$ ) with methyl acrylate ( $M_2$ ) was carried out with the use of boron trifluoride-ether complex as a catalyst. The reaction was carried out at 0°C. The monomer reactivity ratios  $r_1$  and  $r_2$  increased with increase in liquid sulfur dioxide concentration, and  $r_1$  was changed from  $r_1 = 0.30$  at  $[\text{liq. SO}_2]_0 = 6.58$  mole/l., to  $r_1 = 1.50$  at  $[\text{liq. SO}_2]_0 = 13.16$  mole/l., but  $r_2$  was not changed. These facts indicated that reactivity of carbonium ion of styrene in the propagation step was increased with increasing liquid sulfur dioxide concentration. The relation between the overall rate of copolymerization and liquid sulfur dioxide concentration is the same as in the case of the cationic homopolymerization of styrene, and polymolecular contribution of liquid sulfur dioxide on the overall copolymerization is shown from these observations.

### INTRODUCTION

Liquid sulfur dioxide is an aprotic solvent, and is supposed to have no affinity with a proton. Therefore, there are some peculiarities in cationic polymerization in this solvent: (1) the overall rate of polymerization is considerably higher than those in such organic solvents as benzene, nitrobenzene, and carbon tetrachloride, and this cannot be explained by dielectric constant;<sup>1,2</sup> (2) in the equation for the overall rate of polymerization  $R_p$  as shown by eq. (1)<sup>3</sup>

$$R_p = \text{const} \times [M]_0 [C]_0^{1-3} [\text{liq. SO}_2]_0^4 \quad (1)$$

liquid sulfur dioxide, the solvent, makes polymolecular contribution to the rate equation; (3) polymers having higher molecular weight are easily obtained in this solvent.

Among these peculiarities, the polymolecular contribution of liquid sulfur dioxide used as a solvent is a unique characteristic which has not been hitherto reported on other solvents. If this characteristic can be explained quantitatively, it will present information concerning the nature of liquid

sulfur dioxide as a solvent. A copolymerization system was chosen for the purpose to study in which step of the polymerization reactions liquid sulfur dioxide may be participating. The reason why methyl acrylate was chosen as a comonomer for styrene is that methyl acrylate is poor in cationic polymerizability and, therefore, the effect of liquid sulfur dioxide concentration can be neglected in the propagation step of polymerization between methyl acrylate molecules; thus the analysis of data obtained from the copolymerization experiments is simplified.

Solvent effects in cationic copolymerization on the monomer reactivity ratios have been reported by Overberger<sup>4,5</sup> and Okamura, Higashimura, et al.<sup>6</sup> A comparison of results obtained by these investigators in various solvents having different dielectric constants confirms a certain relation between the monomer reactivity ratios and dielectric constants.

The authors set up the condition in this experiment in such a way that the effects of dielectric constant in the copolymerizing system were negligible; this facilitated determination of the exact effect of concentration of liquid sulfur dioxide.

## EXPERIMENTAL

Styrene monomer (St), liquid sulfur dioxide (liq.  $\text{SO}_2$ ), boron trifluoride-ether complex,  $\text{BF}_3 \cdot \text{O}(\text{C}_2\text{H}_5)_2$ , carbon tetrachloride, and nitrobenzene were used after purification by the same method as previously reported.<sup>7</sup> Methyl acrylate and dioxane were purified by the usual method.

Polymerizations were carried out by the same method as previously reported.<sup>3</sup> When the initial concentration of liquid sulfur dioxide was changed, an amount of solvent corresponding to the volume of  $\text{SO}_2$  omitted had to be added. A mixture of carbon tetrachloride and nitrobenzene having a dielectric constant (15.12) is almost equal to that of liquid sulfur dioxide at its polymerizing temperature ( $0^\circ\text{C}.$ ) was thus made, and this mixture was added to compensate for the amount of liquid sulfur dioxide.

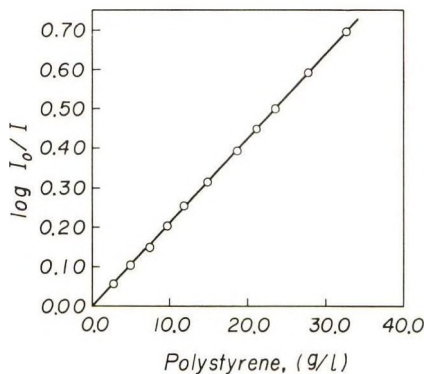


Fig. 1. Relationship between concentration of styrene units in the copolymer and infrared absorbancy used for quantitative measurement.

Thus, the change in dielectric constant with change in liquid sulfur dioxide concentration was minimized.

The overall rate of polymerization was obtained gravimetrically, and the polymerization was carried out by the same procedure as previously reported.<sup>3</sup>

The intrinsic viscosity was measured with a Ubbelohde-type viscometer in dioxane solution at 30°C.

Composition of the copolymer were obtained from the results of infrared spectroscopy. The molar fraction of styrene in the copolymer was calculated by measuring the absorption of monosubstituted benzene in dioxane at 700  $\text{cm}^{-1}$ . The relationship between concentration of styrene units in the copolymer and infrared absorbancy used for quantitative measurement (the relationship between  $\log I_0/I$  and the concentration of polystyrene) is shown in Figure 1. The concentration employed for measurement of infrared absorption spectra of the copolymer was in most cases about 25 g. copolymer/l. dioxane.

## RESULTS

### Initial Concentration of Liquid Sulfur Dioxide and Monomer Reactivity Ratios ( $r_1$ and $r_2$ )

The initial concentration of the catalyst,  $[\text{BF}_3 \cdot \text{O}(\text{C}_2\text{H}_5)_2]_0$ , was kept constant at  $5.88 \times 10^{-3}$  mole/l., and the dielectric constant of the reaction medium involving liquid sulfur dioxide  $[\text{liq. SO}_2]_0$  was kept constant by using a mixture of nitrobenzene and carbon tetrachloride as the added solvent. The initial concentration  $[\text{liq. SO}_2]_0$  was varied between 6.58 and 13.16 mole/l.; the temperature employed for the polymerization was 0°C. The conversions were kept below 5% in all cases. The results of copolymerization of styrene and methyl acrylate at  $[\text{liq. SO}_2]_0 = 6.58$  mole/l. are shown in Table I. Composition curves for the copolymers are shown in Figures 2 and 3 for initial liquid  $\text{SO}_2$  concentrations of 6.58 and 13.16 mole/l., respectively. The monomer reactivity ratios,  $r_1$  and  $r_2$ , for the

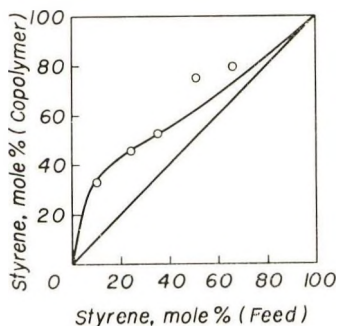


Fig. 2. Copolymer composition curve obtained from cationic copolymerization of styrene with methyl acrylate in liquid sulfur dioxide.  $[\text{liq. SO}_2]_0 = 13.16$  mole/l.; polymerization temperature 0°C.

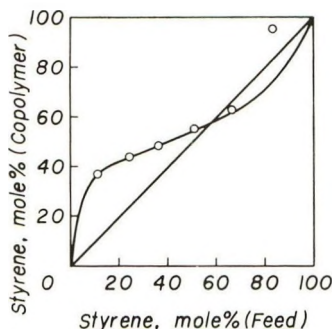


Fig. 3. Copolymer composition curve obtained from cationic copolymerization of styrene with methyl acrylate in liquid sulfur dioxide.  $[\text{liq. SO}_2]_0 = 6.58$  mole/l.; polymerization temperature  $0^\circ\text{C}$ .

cationic copolymerization of styrene ( $M_1$ ) and methyl acrylate ( $M_2$ ) were determined from these curves by the curve-fitting method. The results are shown in Table II, together with the product of  $r_1$  and  $r_2$ .

TABLE I  
Results of Styrene-Methyl Acrylate Copolymerization in  
Liquid Sulfur Dioxide (6.58 mole/l.)  $0^\circ\text{C}$ .

Feed		Conver- sion (wt.-%)	Concn. of polymer used, g./2.0 ml.	log $I_0/I$	St in copoly- mer, g./l.	Copolymer	
St, mole- %	MA, mole- %					St, mole- %	MA mole- %
11.6	88.4	1.18	0.0564	0.2219	0.0236	37.3	62.7
23.9	76.1	1.69	0.0658	0.3340	0.0314	43.1	56.9
37.1	62.9	0.76	0.0576	0.3251	0.0305	48.2	51.8
51.2	48.8	2.38	0.0602	0.3804	0.0357	54.7	45.3
66.3	33.7	1.56	0.0434	0.3098	0.0291	62.8	37.2
82.4	17.6	3.24	0.0539	0.5531	0.0519	95.6	4.4

TABLE II  
Relationship between Initial Concentration of Liquid  $\text{SO}_2$  and the Monomer  
Reactivity Ratios,  $r_1$  and  $r_2$ , for the Cationic Copolymerization of Styrene ( $M_1$ ) and  
Methyl Acrylate ( $M_2$ )

$[\text{liq. SO}_2]_0$ , mole/l.	$r_1$	$r_2$	$r_1r_2$
6.58	$0.30 \pm 0.02$	$0.12 \pm 0.02$	0.036
7.90	$0.45 \pm 0.05$	$0.13 \pm 0.03$	0.059
9.22	$0.60 \pm 0.08$	$0.14 \pm 0.04$	0.084
10.53	$0.70 \pm 0.07$	$0.11 \pm 0.02$	0.077
11.85	$1.00 \pm 0.06$	$0.13 \pm 0.03$	0.13
13.16	$1.50 \pm 0.05$	$0.15 \pm 0.05$	0.23

### Relationship between Initial Liquid Sulfur Dioxide Concentration and Overall Rate of Copolymerization

The molar ratio of styrene monomer and methyl acrylate (37.1:62.9) and the initial  $[\text{BF}_3 \cdot \text{O}(\text{C}_2\text{H}_5)_2]_0$  concentration ( $3.90 \times 10^{-2}$  mole/l.) were kept constant, and cationic copolymerization was carried out by changing  $[\text{liq. SO}_2]_0$  from 5.27 to 13.16 mole/l. In order to keep constant the whole volume (17.0 ml.) and the dielectric constant of the system, the previously noted mixture was used. The copolymerization was carried out at  $0^\circ\text{C}$ . The time-conversion curves are shown in Figure 4, and a logarithmic plot of

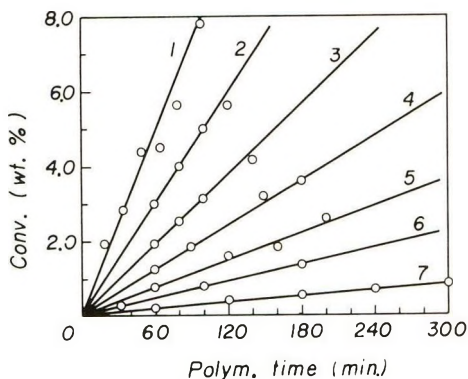


Fig. 4 Time-conversion curves obtained from cationic copolymerization of styrene with methyl acrylate in liquid sulfur dioxide at various initial concentrations of liquid  $\text{SO}_2$ : (1) 13.16 mole/l.; (2) 11.85 mole/l.; (3) 10.53 mole/l.; (4) 9.22 mole/l.; (5) 7.90 mole/l.; (6) 6.58 mole/l.; (7) 5.27 mole/l.  $[\text{Styrene}]_0 = 37.1$  mole-%;  $[\text{methyl acrylate}]_0 = 62.9$  mole-%;  $[\text{BF}_3 \cdot \text{O}(\text{C}_2\text{H}_5)_2]_0 = 3.90 \times 10^{-2}$  mole/l.; polymerization temperature  $0^\circ\text{C}$ .

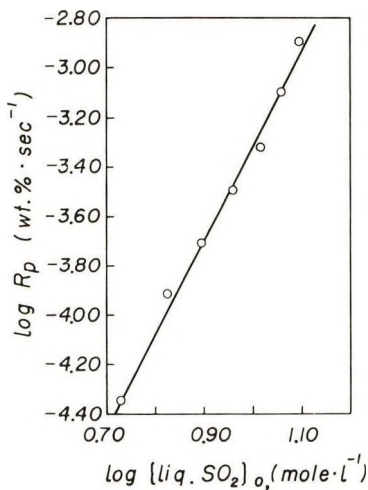


Fig. 5. Logarithmic plot of the overall rate of copolymerization vs. liquid sulfur dioxide concentration (obtained from Fig. 4).

$R_p$  versus  $[\text{liq. SO}_2]_0$  is shown in Figure 5. From the slope in Figure 5, eq. (2) was obtained.

$$R_p = \text{const} \times [\text{liq. SO}_2]_0^4 \quad (2)$$

### Initial Concentration of Liquid Sulfur Dioxide and Intrinsic Viscosity of the Copolymers

The relation between  $[\text{liq. SO}_2]_0$  in the copolymerization system and intrinsic viscosity  $[\eta]$  of the copolymers obtained at  $[\text{St}]_0 = 37.1$  mole-% and  $[\text{MA}]_0 = 62.9$  mole-% is shown in Figure 6.

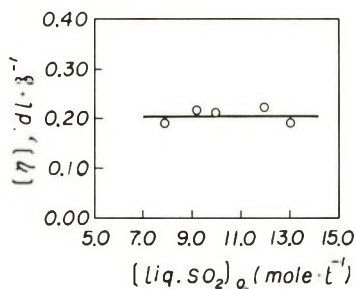


Fig. 6. Relationship between initial concentration of liquid sulfur dioxide and intrinsic viscosity of the copolymers.

### Composition of the Feed and Intrinsic Viscosity

The relation between  $[\eta]$  of the copolymers obtained at constant initial catalyst concentration  $[\text{BF}_3\cdot\text{O}(\text{C}_2\text{H}_5)_2]_0 = 3.90 \times 10^{-2}$  mole/l. and constant liquid sulfur dioxide concentration  $[\text{liq. SO}_2]_0 = 13.16$  mole/l. and varying composition of the feed styrene is shown in Figure 7.

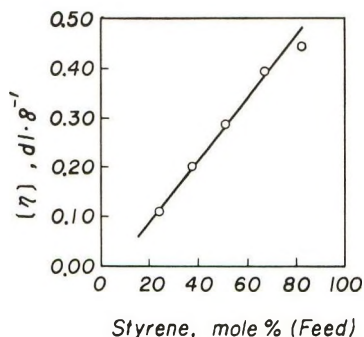


Fig. 7. Relationship between initial concentration of styrene and intrinsic viscosity of the copolymers.

### Cationic Polymerization of Methyl Acrylate

Polymers were not obtained in appreciable amounts when the reaction was carried out at 60°C. for 60 hr. with  $[\text{MA}]_0 = 4.59$  mole/l.,  $[\text{liq. SO}_2]_0 = 13.18$  mole/l., and  $[\text{BF}_3\cdot\text{O}(\text{C}_2\text{H}_5)_2]_0 = 3.90 \times 10^{-2}$  mole/l.



## DISCUSSION

As has been shown by Overberger and Kamath,<sup>5</sup> the monomer reactivity ratios are not related to the macroscopic parameter, the dielectric constant, in cationic copolymerization. However, the present authors kept constant the dielectric constant of the copolymerizing systems in order to determine precisely the effects of liquid sulfur dioxide concentration. When concentration of one solvent in the mixed solvent system is changed, it is hard to keep exactly constant the dielectric constant of the whole system; also, the effect of the solvent added to keep constant the dielectric constant cannot be neglected. The solvent system used in this experiment was a ternary system consisting of liquid sulfur dioxide, carbon tetrachloride, and nitrobenzene. In this mixed solvent system, carbon tetrachloride acts as a diluent;<sup>7</sup> on the other hand, the effect of nitrobenzene is ambiguous when mixed with liquid sulfur dioxide. However, monomer reactivity ratios ( $r_1$  and  $r_2$ ) were the same when cationic copolymerization of styrene with *p*-bromostyrene was carried out in the mixed solvent systems, liquid sulfur dioxide–nitrobenzene, and liquid sulfur dioxide–benzene, provided that liquid sulfur dioxide concentration was equal in the both mixed solvent systems.<sup>8</sup> As nitrobenzene is deemed to be an acid, it may have no affinity for liquid sulfur dioxide or carbonium ions at the growing chain end but benzene has.<sup>7</sup> These facts show that liquid sulfur dioxide acts selectively in the copolymerization reaction. The effect of nitrobenzene in the copolymerization system is small compared with that of liquid sulfur dioxide, so that the effect is negligible.

Variation of the monomer reactivity ratios with the change in liquid sulfur dioxide concentrations is considered first. To consider the value of  $r_1$  and  $r_2$  for the cationic copolymerization of styrene ( $M_1$ ) with methyl acrylate ( $M_2$ ) is really to consider the effect of liquid sulfur dioxide on the propagation reaction. The copolymerization of styrene with methyl acrylate was selected for study in this investigation just because  $k_{22}$  is considerably smaller than  $k_{11}$ .<sup>9</sup> As has been described above, this was verified by the fact that no polymer was obtained when methyl acrylate was polymerized at 0°C. for 60 hr. in liquid sulfur dioxide with boron trifluoride–ether complex as the catalyst at the same monomer concentration as in the copolymerization experiment.  $r_2$  values (Table II) were not affected by liquid sulfur dioxide concentration, and the values are small. This means that the reactivities of both carbonium ion of the acrylate and acrylate monomer are small, and that the reactivity of styrene monomer is not influenced by liquid sulfur dioxide concentration. On the other hand,  $r_1$  values increased with increase in liquid sulfur dioxide concentration. This means that  $k_{11}$  is affected more than  $k_{12}$  by liquid sulfur dioxide concentration. This is clarified from the fact that the reactivity of methyl acrylate monomer is not affected by liquid sulfur dioxide concentration.

Then, the step affected among four steps in the propagation of the copolymerization is  $k_{11}$ . However, it has not been satisfactorily shown that  $k_{11}$  is

greater than  $k_{21}$ , and therefore the effect of liquid sulfur dioxide on this latter propagation step may also be important.

The effect of liquid sulfur dioxide on the termination reaction is known from the intrinsic viscosity  $[\eta]$  of the copolymers.  $[\eta]$  was independent of liquid sulfur dioxide concentration, and this due to the fact that carbonium ions cannot participate in the chain transfer reaction with liquid sulfur dioxide, and that the chain transfer to both carbon tetrachloride and nitrobenzene is very small. The molecular weight of the copolymer may therefore be determined by unimolecular termination and chain transfer to both monomers. Accordingly,  $[\eta]$  is independent of liquid sulfur dioxide concentration.

The effect of liquid sulfur dioxide concentration on the overall rate of copolymerization  $R_p$  is, as seen from Figure 5, proportional to the fourth power of the initial concentration of liquid sulfur dioxide. This result is in good accord with results of cationic homopolymerization of styrene.<sup>3</sup> From the fact that polymerizabilities of methyl acrylate and its carbonium ion are poor, and that the overall rate of copolymerization is proportional to the fourth power of liquid sulfur dioxide concentration, liquid sulfur dioxide is considered to affect only polymerization of styrene ( $k_{11}$ ) of the four steps in the propagation of copolymerization. No assumptions are made for the results when the comonomer pair is change, and the result may not be extended to all cationic copolymerizations. The polymolecular contribution of liquid sulfur dioxide to any elementary reaction, i.e., to initiation, propagation, or termination, may also be a matter of conjecture. However, considering the relation between the monomer reactivity ratios and liquid sulfur dioxide concentration, and the relation between the intrinsic viscosity and liquid sulfur dioxide concentration it is most probable that liquid sulfur dioxide contributes mostly in the initiation step.

## References

1. Asami, R., and N. Tokura, *J. Polymer Sci.*, **42**, 545, 553 (1960).
2. Tokura, N., R. Asami, M. Matsuda, and H. Negishi, *Kogyo Kagaku Zasshi*, **64**, 717 (1961).
3. Tokura, N., M. Matsuda, and H. Negishi, *Kogyo Kagaku Zasshi*, **64**, 1502 (1961).
4. Overberger, C. G., and V. G. Kamath, *J. Am. Chem. Soc.*, **81**, 2910 (1959).
5. Overberger, C. G., and V. G. Kamath, *J. Am. Chem. Soc.*, **85**, 446 (1963).
6. Higashimura, T., *Kagaku (Kyoto)*, **16**, Special Issue No. 7, 33 (1961).
7. Tokura, N., M. Matsuda, and Y. Watanabe, *J. Polymer Sci.*, **62**, 135 (1962).
8. Tokura, N., M. Matsuda, and M. Iino, *Bull. Chem. Soc. Japan*, **36**, 278 (1963).
9. Landler, Y., *J. Polymer Sci.*, **8**, 63 (1952).

## Résumé

L'effet de la concentration en anhydride sulfureux liquide sur la copolymérisation cationique du styrène ( $M_1$ ) avec l'acrylate de méthyle, ( $M_2$ ) a été examiné en employant le complexe trifluorure de bore—éther comme catalyseur. La réaction a été effectuée à 0°C  $r_1$ , le rapport des réactivités des monomères ( $r_1$  et  $r_2$ ) augmente avec une augmentation de la concentration en anhydride sulfureux liquide et  $r_1$  passe de  $r_1 = 0.30$  pour  $(\text{liq SO}_2)_0 = 6.58$  mole/l, à  $r_1 = 1.50$  pour  $(\text{liq SO}_2)_0 = 13.16$  mole/l, mais  $r_2$  ne change pas.

A partir de ces faits on a pu montrer que la réactivité de l'ion carbonium du styrène dans l'étape de propagation augmente avec une augmentation de la concentration en anhydride sulfureux liquide. La relation entre la vitesse globale de la copolymérisation et la concentration en anhydride sulfureux liquide est la même que dans le cas de l'homopolymérisation cationique du styrène, et ces observations ont montré une contribution polymoléculaire de l'anhydride sulfureux liquide à la copolymérisation totale.

### Zusammenfassung

Die Wirkung der Konzentration von flüssigem Schwefeldioxyd auf die kationische Copolymerisation von Styrol ( $M_1$ ) mit Methacrylat ( $M_2$ ) wurde unter Verwendung eines Bortrifluoridätherkomplexes als Katalysator untersucht. Die Reaktion wurde bei  $0^\circ\text{C}$  durchgeführt.  $r_1$ , wobei  $r_1$  und  $r_2$  die Monomerreaktivitätsverhältnisse sind, nahm mit einem Zuwachs der Konzentration von flüssigem Schwefeldioxyd zu,  $r_1$  änderte sich von  $r_1 = 0,30$  bei  $[\text{fl. SO}_2]_0 = 6,58 \text{ Mol/l}$ , auf  $r_1 = 1,50$  bei  $[\text{fl. SO}_2]_0 = 13,16 \text{ Mol/l}$ , wobei sich  $r_2$  nicht änderte. Aus diesen Tatsachen ergibt sich, dass die Reaktivität des Carboniumions des Styrols beim Wachstumsschritt mit wachsender Konzentration an flüssigem Schwefeldioxyd zunimmt. Die Beziehung zwischen der Bruttogeschwindigkeit und der Konzentration an flüssigem Schwefeldioxyd ist dieselbe wie im Falle der kationischen Homopolymerisation von Styrol; der polymolekulare Beitrag von flüssigem Schwefeldioxyd zur Bruttocopolymerisation wird durch diese Beobachtungen gezeigt.

Received September 9, 1963

Revised October 21, 1963

## **Polymerization in Liquid Sulfur Dioxide. Part XXII. Comparison of Retarding Effects of Bases on the Radical Polymerization of Acrylonitrile in Liquid Sulfur Dioxide**

MINORU MATSUDA and NIICHIRO TOKURA, *The Chemical Research  
Institute of Non-Aqueous Solutions, Tohoku University, Sendai, Japan*

### **Synopsis**

The radical polymerization of acrylonitrile was carried out in liquid sulfur dioxide and in benzene, with addition of aniline, dimethylaniline, dimethyl-*o*-toluidine, and diethylaniline to these systems. The temperatures of polymerization were 40, 50, and 60°C. It was found that the chain transfer reaction occurs more easily in liquid sulfur dioxide than in benzene; this was attributed to the differences in the polarity of the terminal radical of the growing chain in both solvents. The difference of activation energies due to the difference of bases is not so large. The frequency factors are rather important in both solvents for chain transfer reactions. The isokinetic relation is also discussed.

### **INTRODUCTION**

It was reported previously<sup>1</sup> that both the overall rate of polymerization and the degree of polymerization of acrylonitrile polymers are decreased in the case of the radical polymerization in liquid sulfur dioxide by the addition of aniline and its derivatives. These bases acted as retarders for the polymerization. The present report is concerned with the results of further study of this retardation. The chain transfer constant was determined in liquid sulfur dioxide and benzene, and the difference of the activation energies of the chain transfer reaction and the propagation reaction was calculated. The characteristics of the radical polymerization of acrylonitrile in liquid sulfur dioxide was presumed from the difference of the activation energies and the ratio of the frequency factors. Acrylonitrile was used as the monomer because it was expected to be affected by the bases in the propagation process as a result of the polar nature of the monomer.

Imoto, Otsu, Ota, Takatsugi, and Matsuda<sup>2</sup> have studied the mechanism of such a chain transfer reaction in benzene. The characteristic nature of liquid sulfur dioxide as the solvent can be studied by close comparison of the results in benzene with those in liquid sulfur dioxide.

### Experimental

Liquid sulfur dioxide (liq.  $\text{SO}_2$ ), acrylonitrile (AN),  $\alpha, \alpha'$ -azobisisobutyronitrile (AIBN), dimethylformamide (DMF), aniline (An), dimethylaniline (DMA), dimethyl-*o*-toluidine (DMoT), and diethylaniline (DEA) were purified by the usual methods. The polymerization and the preparation of the mixed solutions of liquid sulfur dioxide and aniline derivatives were carried out by the same methods as previously reported.<sup>1,3</sup>

The intrinsic viscosity of the polymers was measured in dimethylformamide at 25°C. and the degree of polymerization of the polymers was calculated by using eq. (1).

$$[\eta] = 1.75 \times 10^{-3} M_n^{0.66} \quad (1)$$

### RESULTS

#### Liquid Sulfur Dioxide-Acrylonitrile-Aniline Derivative System

The concentrations of liquid sulfur dioxide, acrylonitrile and azobisisobutyronitrile ( $[\text{liq. SO}_2]_0$ ,  $[\text{AN}]_0$ , and  $[\text{AIBN}]_0$ ) were kept constant at 10.11, 7.54, and  $3.05 \times 10^{-2}$  mole/l., respectively, all through the experi-

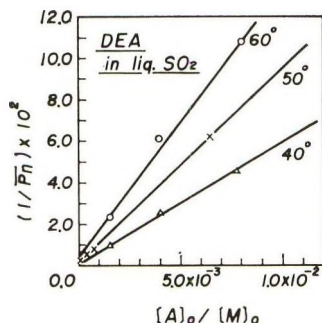


Fig. 1. Relation between  $[\text{A}]_0/[\text{M}]_0$  and the reciprocal degree of polymerization  $1/P_n$  obtained with the addition of diethylaniline to a system consisting of acrylonitrile and liquid  $\text{SO}_2$ .

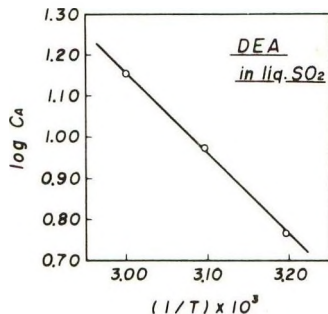


Fig. 2. Arrhenius plot of the chain transfer constant ( $C_A = k_{tr,A}/k_p$ ) obtained for the polymerization of acrylonitrile in liquid sulfur dioxide with addition of diethylaniline.

ment. The temperature of the polymerization was 40, 50, or 60°C. Figure 1 shows the relation between the ratio  $[A]_0/[M]_0$  and the reciprocal of the degree of polymerization,  $1/\bar{P}_n$ , obtained with the addition of DEA, where  $[A]_0$  and  $[M]_0$  are the initial concentrations of DEA and acrylonitrile, respectively. Figure 2 shows the Arrhenius plot of the chain transfer constant ( $C_A = k_{tr}/k_p$ ) obtained at various temperatures. The difference of the activation energies was also determined for the cases of An and DMA by a similar method and the ratio of the frequency factors was calculated from these. The results are summarized in Table I together with the  $pK_a$  values of aniline derivatives.

TABLE I  
Results Obtained for the Liquid Sulfur Dioxide-Acrylonitrile-Aniline Derivatives Systems

Added species	Polymerization temp., °C.	$C_A$	$\Delta E_{tr} \dagger - \Delta E_p \dagger$ , kcal./mole	$\log (A_{tr}/A_p)$	$pK_a$
An	60	1.22	6.86	3.98	4.62
	50	0.96			
	40				
DMA	60	2.18	8.18	5.27	5.06
	50	1.54			
	40	1.19			
DEA	60	14.32	9.29	6.82	6.56
	50	9.38			
	40	5.81			
DMoT	50	3.02			5.86

### Benzene-Acrylonitrile-Aniline Derivatives System

The initial concentrations  $[C_6H_6]_0$ ,  $[AN]_0$ , and  $[AIBN]_0$  were kept constant at 5.58, 7.54, and  $3.05 \times 10^{-2}$  mole/l., respectively. The results with DEA are shown in Figures 3 and 4. The results obtained in benzene are summarized in Table II.

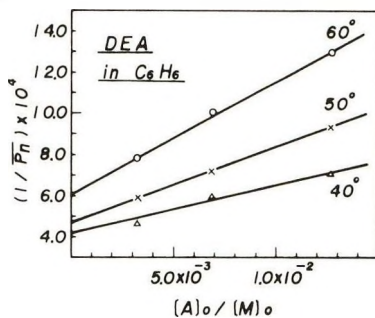


Fig. 3. Relation between  $[A]_0/[M]_0$  and  $1/\bar{P}_n$  obtained with the addition of diethylaniline to a system consisting of acrylonitrile and benzene.

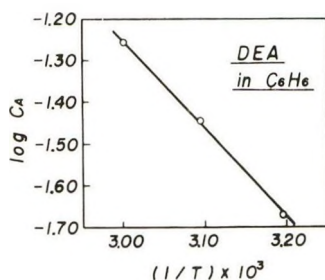


Fig. 4. Arrhenius plot of the chain transfer constant  $C_A$  obtained for the polymerization of acrylonitrile in benzene with addition of diethylaniline.

TABLE II  
Results Obtained for the Benzene-Acrylonitrile-Aniline  
Derivatives Systems

Added species	Polymerization temp., °C.	$C_A$	$\Delta E_{tr} \dagger - \Delta E_p \dagger$ kcal./mole	$\log (A_{tr}/A_p)$	$pK_a$
An	60				
	50	$4.40 \times 10^{-3}$	6.34	1.50	4.62
	40	$3.20 \times 10^{-3}$			
DMA	60	$9.64 \times 10^{-2}$			
	50	$7.08 \times 10^{-2}$			
	40	$6.05 \times 10^{-2}$			
DMoT	60	$4.63 \times 10^{-2}$	6.82	2.71	5.86
	50	$3.34 \times 10^{-2}$			
	40	$2.72 \times 10^{-2}$			
DEA	60	$5.47 \times 10^{-2}$	9.82	4.75	6.56
	50	$3.59 \times 10^{-2}$			
	40	$2.15 \times 10^{-2}$			

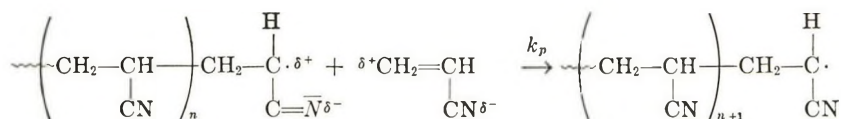
## DISCUSSION

The polymerization proceeds as a heterogeneous system both in benzene and in liquid sulfur dioxide. Consequently, a comparison of the chain transfer constants, which are dependent on the kind of bases, cannot be made if the heterogeneity of the system changes by the addition of a base such as An, DMA, DMoT, or DEA. The overall rate equation of the polymerization in liquid sulfur dioxide was determined with and without the addition of DMA.<sup>2</sup> In the preceding paper,<sup>1</sup> it was confirmed from the comparison of the overall rate equations that the heterogeneity of the system is not changed from the kinetic point of view by the addition of the bases. It was also mentioned in the preceding report that the retardation effect comes from the transfer of the terminal radical of the growing chain end of polyacrylonitrile to the added base. Thus, the base which accepted the radical stabilizes itself by resonance and loses the ability to reinitiate the polymerization.

It is found by the comparison of the chain transfer constants obtained for the polymerization in liquid sulfur dioxide and in benzene that the value in liquid sulfur dioxide is much larger than that in benzene. The aniline derivatives are solvated by liquid sulfur dioxide molecules.<sup>5</sup> This solvation is supported by the facts that the mixed solvent is colored and that, when cooled, it yields a white precipitate below about  $-50^{\circ}\text{C}$ ., indicating the formation of an additional compound. The temperature of formation of this addition compound is dependent upon the kind and the concentration of the bases.



It is reasonable to consider that the base is more stable in liquid sulfur dioxide. Nevertheless the chain transfer constant is larger in liquid sulfur dioxide than in benzene. This may be attributed to the fact that liquid sulfur dioxide is a dipolar solvent and the ionization ability of liquid sulfur dioxide is larger than benzene, since the radical polymerization of acrylonitrile is largely affected by polar factors during the propagation step. This is due to the  $+E$  effect of the nitrile group:



Consequently,  $k_p$  is small for the radical polymerization in those solvents which make this polarity larger. This view is supported by the fact that the overall rate of polymerization is larger in benzene than in liquid sulfur dioxide. The chain transfer constant, which is the ratio of the rate constant, is larger in liquid sulfur dioxide. The order of magnitude of the transfer constants is  $\text{DEA} > \text{DMoT} > \text{DMA} > \text{An}$  in liquid sulfur dioxide. This order is the same as that of the  $\text{p}K_a$  of these bases. It was also mentioned in the preceding report that the value of the  $\text{p}K_a$  is in linear relation with the Alfrey-Price  $e_{tr}$ , calculated from the results at  $50^{\circ}\text{C}$ .<sup>1</sup> On the other hand the order is  $\text{DMA} > \text{DEA} > \text{DMoT} > \text{An}$  in benzene. This order does not agree with that of  $\text{p}K_a$  and the order in liquid sulfur dioxide. The magnitude of the chain transfer constant of DMA in benzene is different from the expected value. The disagreement of the relation with  $\text{p}K_a$  is also seen in the Menshutkin reaction in benzene, nitrobenzene, and liquid sulfur dioxide,<sup>6</sup> so it is likely that the behavior is often seen in a particular solvent; however, the reason for this has not yet been discovered.

No large difference is found in the activation energies in the two solvents. Bases are solvated in liquid sulfur dioxide as mentioned above, so it is expected that the activation energies become larger by the amount required to release the solvation in order to react with the terminal radical of the growing chain, but the polarity of the radical is larger in liquid sulfur dioxide so these factors cancel each other and the value is almost equal to that in benzene. When a comparison is made for various bases, the order



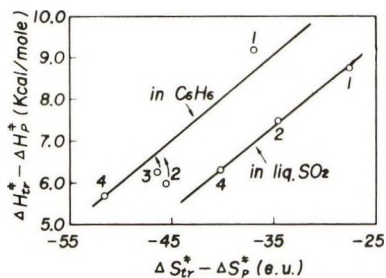


Fig. 5. Relation between the entropy and the enthalpy for the polymerization of acrylonitrile in liquid sulfur dioxide and in benzene.

is  $\text{DEA} > \text{DMoT} > \text{DMA} > \text{An}$  in both solvents. This order is just opposite to that expected from the values of the chain transfer constant.

But the difference of the activation energies of DEA and An ( $[\Delta E_{tr}^\ddagger - \Delta E_p^\ddagger]_{\text{DEA}} - (\Delta E_{tr}^\ddagger - \Delta E_p^\ddagger)_{\text{An}}$ ) is 2.43 kcal./mole in liquid sulfur dioxide and 3.48 kcal./mole in benzene. It is clearly noticed that the difference of the frequency factors of the reaction affects primarily the chain transfer reactions in both solvents rather than the activation energy; namely, the frequency factor ( $A$  factor) of DEA is the largest and is about  $2 \times 10^4$  times that of An in benzene. It is also shown from the comparison of DMA and DEA in benzene that the chain transfer constant of DMA is larger than that of DEA, but the  $A$  factor of DEA is much larger than that of DMA. The order of the magnitude of the  $A$  factor is the same as the order of the magnitude of  $pK_a$ .

Figure 5 shows the relation between the entropy and the activation enthalpy. From the linear relation, eq. (2) holds:

$$\Delta H_{*}^\ddagger = \Delta H_{0,*}^\ddagger + \beta \Delta S_{*}^\ddagger \quad (2)$$

where  $\beta$  is the gradient of the curve shown in Figure 5. (The subscript asterisk (\*) indicates the difference of the chain transfer and propagation reaction.) In the present research, the value of  $\beta$  in benzene is approximately the same as that in liquid sulfur dioxide. Also, it was reported previously that the chain transfer constant of DMA in benzene is much larger than that expected from the values of other bases. The behavior deviated from linearity in the isokinetic relation, and it was confirmed that the behavior is almost anomalous.

## References

1. Matsuda, M., S. Abe, and N. Tokura, *J. Polymer Sci.*, **A2**, 3877 (1964).
2. Imoto, M., T. Otsu, T. Ota, H. Takatsugi, and M. Matsuda, *J. Polymer Sci.*, **22**, 137 (1956).
3. Tokura, N., M. Matsuda, and F. Yazaki, *Makromol. Chem.*, **42**, 108 (1960).
4. Houtz, R. C., *Textile Res. J.*, **20**, 786 (1950).
5. Kashtanov, L. I., and N. V. Kazanskaya, *Zh. Fiz. Khim.*, **28**, 1547 (1954).
6. Tokura, N., and Y. Kondo, *Bull. Chem. Soc. Japan*, **37**, 133 (1964).

### Résumé

On a polymérisé l'acrylonitrile dans l'anhydride sulfureux liquide et dans le benzène en présence de radicaux, en ajoutant de l'aniline, de la diméthylaniline, de la diméthyl-*o*-toluidine, et de la diéthylaniline. La température de polymérisation était 40, 50 et 60°C. On a trouvé que la réaction de transfert de chaîne est plus facile dans le dioxyde de soufre liquide que dans le benzène et on a expliqué ce fait par les différences de polarité du radical terminal de la chaîne en croissance dans les deux solvants. La différence d'énergie d'activation à cause des différentes bases n'était pas très importante. Les facteurs de fréquence pour les réactions de transfert de chaîne sont assez importants pour les deux solvants. On a discuté la relation isocinétique.

### Zusammenfassung

Die radikalische Polymerisation von Acrylnitril wurde in flüssigem Schwefeldioxyd und Benzol unter Zusatz von Anilin, Dimethylanilin, Dimethyl-*o*-toluidin und Diäthylanilin zu diesen Systemen durchgeführt. Die Polymerisationstemperatur betrug 40, 50 und 60°C. Es zeigte sich, dass die Kettenübertragungsreaktion in flüssigem Schwefeldioxyd leichter auftritt als in Benzol. Dies wurde durch die Unterschiede der Polarität des endständigen Radikals der wachsenden Kette in beiden Lösungsmitteln erklärt. Mit den verschiedenen Basen treten keine grossen Unterschiede in der Aktivierungsenergie auf. In beiden Lösungsmitteln sind die Frequenzfaktoren für die Kettenübertragungsreaktionen wichtig. Auch die isokinetische Beziehung wurde diskutiert.

Received September 17, 1963

Revised January 3, 1964

## Isomorphism in Copolyamides Containing the *p*-Phenylene Linkage

T. C. TRANTER, *Research Department, British Nylon Spinners Ltd.,  
Pontypool, Monmouthshire, England*

### Synopsis




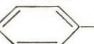
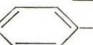
Since the observations of Edgar and Hill on polyhexamethylene adipamide/polyhexamethylene terephthalamide copolymers, a linear melting point/composition relationship has become widely accepted as a criterion for isomorphous replacement. In a series of binary copolymers based on homopolymers prepared from hexamethylene diamine and *p*-phenylene dipropionic (3P3), 3-(*p*-carboxymethyl) phenyl butyric (2P4), 2-(*p*-carbomethoxy) phenyl propionic (3P02), hydroquinone diacetic (2OPO2), terephthalic (T), adipic (6), or sebacic (10) acids, only the 6.3P3/6.3P02 system showed a linear softening point/composition curve, although the differences in repeating unit length were certainly no greater and often much less than with adipic and terephthalic acids. X-ray examination, however, revealed that all the systems behaved in the same basic manner, the second component dissolving in the lattice of the first until a certain critical concentration was reached when the lattice changed fairly abruptly to that of the second component in which the first component was now dissolved. The changeover point generally, but not always, coincided with the position of a minimum in the softening point/composition curve. Infrared and density measurements did not show any reduction in crystallinity at this point. These copolyamides, thus, afford no exception to the assumption that close similarity in length of repeating units is a necessary, but perhaps not the only, prerequisite for the occurrence of segmental change. The form of the softening point/composition curve is, therefore, not a reliable criterion for isomorphous replacement and it seems likely that this conclusion applies equally to the melting point/composition curve.

### INTRODUCTION

The general effects of copolymerization of mixtures of different monomers are well known.<sup>1</sup> Introduction of the second component usually brings about a reduction in melting point and second-order transition point and an increase in solubility, i.e., changes normally associated with a reduction in crystallinity. These almost certainly result from inability to fit a repeating unit of different size into the lattice of the first component without producing considerable disturbances. In these circumstances the melting point versus composition curve usually shows a minimum. Such minima have been shown to exist in copolymers of nylon 66 and poly(hexamethylene tetrahydrofuran-2,5-dipropionamide)<sup>2</sup> and for 6.6/6,<sup>3,4</sup> 6.6/6.9<sup>5</sup>, and 6.6/6.10<sup>6</sup> copolymers. However, several exceptions to this general rule have been reported. Edgar and Hill<sup>7</sup> showed that the softening point versus

composition curve for the system polyhexamethylene adipamide/polyhexamethylene terephthalamide possessed no such minimum. This behavior was attributed to the close similarity in overall length of the adipyl and terephthalyl groups so that they could replace one another in the crystalline lattice without appreciable distortion; this conclusion was supported by density measurements, which showed a linear increase with increasing proportion of the terephthalamide unit. The term isomorphous replacement was used to describe this phenomenon. It has since become standard practice in studies of isomorphism in polymers to use the existence of a linear melting point versus composition relationship as the criterion for isomorphous replacement (although Levine and Temin<sup>8</sup> apparently also accept a sigmoidal relationship). Cremer and Beaman<sup>9</sup> studied copolyamides prepared from heptamethylene diamine (7), bis(3-aminopropyl) ether (303), adipic acid, (6) and terephthalic acid (T). They found that the system 303.6/7.6 showed isomorphous behavior, while the copolyamides 303.T/7.T, 303.6/7.T, and 7.6/303.T showed a decreasing tendency to isomorphism and 303.6/303.T showed a definite minimum in the softening point vs. composition curve. Hayashi and Hachihama<sup>2</sup> prepared copolyamides from hexamethylene diamine (6) azelaic acid, (9) and tetrahydrofuran dipropionic acid (TDA). It was concluded that the system 6.9/6.TDA showed isomorphous behavior and thus confirmed the earlier conclusion of Cremer and Beaman that an aliphatic ether oxygen was a good substitute for a methylene group. The present work describes an extension of such observations to systems containing aryl-oxy links. In particular it was hoped to establish the significance of the length of the monomer unit in relation to the phenomenon of isomorphous replacement since, in the absence of precise structural studies, some doubt existed regarding the exact role which it played. For this purpose the binary copolyhexamethylene amides of the acids given in Table I were used.

TABLE I

Acid	Formula	Abbreviation
<i>p</i> -Phenylenedipropionic	$\text{HOOC}(\text{CH}_2)_2$  $\text{CH}_2\text{COOH}$	3P3
3-( <i>p</i> -Carboxymethyl)-phenylbutyric	$\text{HOOCCH}_2$  $(\text{CH}_2)_3\text{COOH}$	2P4
2-( <i>p</i> -Carboxymethoxy)-phenylpropionic	$\text{HOOC}(\text{CH}_2)_2$  $\text{OCH}_2\text{COOH}$	3PO2
Hydroquinone diacetic	$\text{HOOCCH}_2\text{O}$  $\text{OCH}_2\text{COOH}$	2OPO2
Terephthalic	$\text{HOOC}$  $\text{COOH}$	T
Adipic	$\text{HOOC}(\text{CH}_2)_4\text{COOH}$	6
Sebacic	$\text{HOOC}(\text{CH}_2)_8\text{COOH}$	10

To obtain direct information regarding any changes in the crystalline lattice, x-ray diffraction patterns of the various copolymers were obtained

and the principal lattice spacings calculated. To date, very little use has been made of this technique in the study of isomorphism in copolymers.

## EXPERIMENTAL

### Preparation of Copolyamides

Hexamethylene salts of the acids were made by established procedures.<sup>10</sup> Polymers containing more than 30% of 6.T were not obtained because the melting point then becomes too high for preparation by conventional methods. For the remaining ten salt pairs, at least seven mixtures were made up covering the complete composition range. The copolyamides were ob-

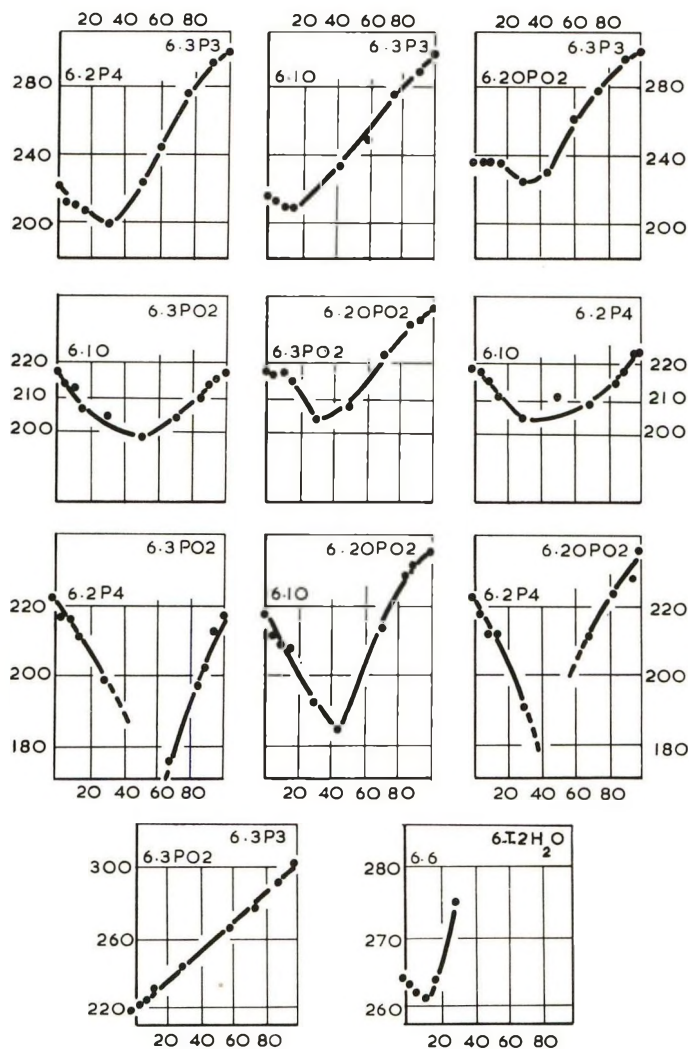


Fig. 1. Softening point vs. composition curves.

tained by a one-stage heating process, the time and temperature of heating depending to some extent on the particular mixture. Their intrinsic viscosity in *m*-cresol was 0.3–0.5.

### Measurement of Softening Points

The softening points were determined with a penetrometer. The copolymers were, in general, highly crystalline and gave sharp collapse points. With a total load of 300 g. results were reproducible to within 2°C.

### Softening Point versus Composition Curves

The softening point curves which are shown in Figure 1 are of three main types.

(a) The introduction of a second component immediately depresses the softening point of the lower melting first component. The curves all showed a minimum. This result was obtained with the systems 6.2P4/6.3P3, 6.10/6.3PO<sub>2</sub>, 6.10/6.3P3, 6.10/6.2OPO<sub>2</sub>, 6.2P4/6.2OPO<sub>2</sub>, 6.2P4/6.3PO<sub>2</sub>. In two cases the minima were ill defined and softening occurred over a wide temperature range.

(b) Addition of the second component does not produce a depression of the softening point until about 15% has been added. The curve then passes through a minimum. The results for the 6.2OPO<sub>2</sub>/6.3P3 and 6.3PO<sub>2</sub>/6.2OPO<sub>2</sub> systems are of this type.

(c) In one case only, the softening point versus composition plot is a straight line. Addition of 6.3P3 to 6.3PO<sub>2</sub> produces an immediate increase in softening point, the increase being proportional to the quantity of additive.

### X-Ray Examination of Copolyamides

From the bulk polymer samples pieces about 1 mm. thick were cut and then photographed with Ni-filtered CuK $\alpha$  radiation, a flat film fiber camera and a film-specimen distance of 3.5 cm. being used. The diameters of the Debye-Scherrer circles were measured with a centimeter scale and the lattice spacings calculated. This procedure was deemed adequate, since the objective was to establish the nature of any changes in the crystalline lattice rather than to characterize the spacings with high precision. Generally the lattice changes abruptly at a composition corresponding with the minimum in the softening point curve. Even when, as in 6.3PO<sub>2</sub>/6.3P3, the softening point versus composition curve is linear, changes still occur in the nature of the crystalline lattice with composition. On the other hand when, as in the 6.3PO<sub>2</sub>/6.2P4 copolymers, no changes in the lattice spacings with composition are observed, the softening point curve nevertheless shows a pronounced minimum. These features are illustrated by the photographs reproduced in Figure 2 which relate to systems with different softening point versus composition curves and by the selected lattice spacing versus composition diagrams in Figure 3.

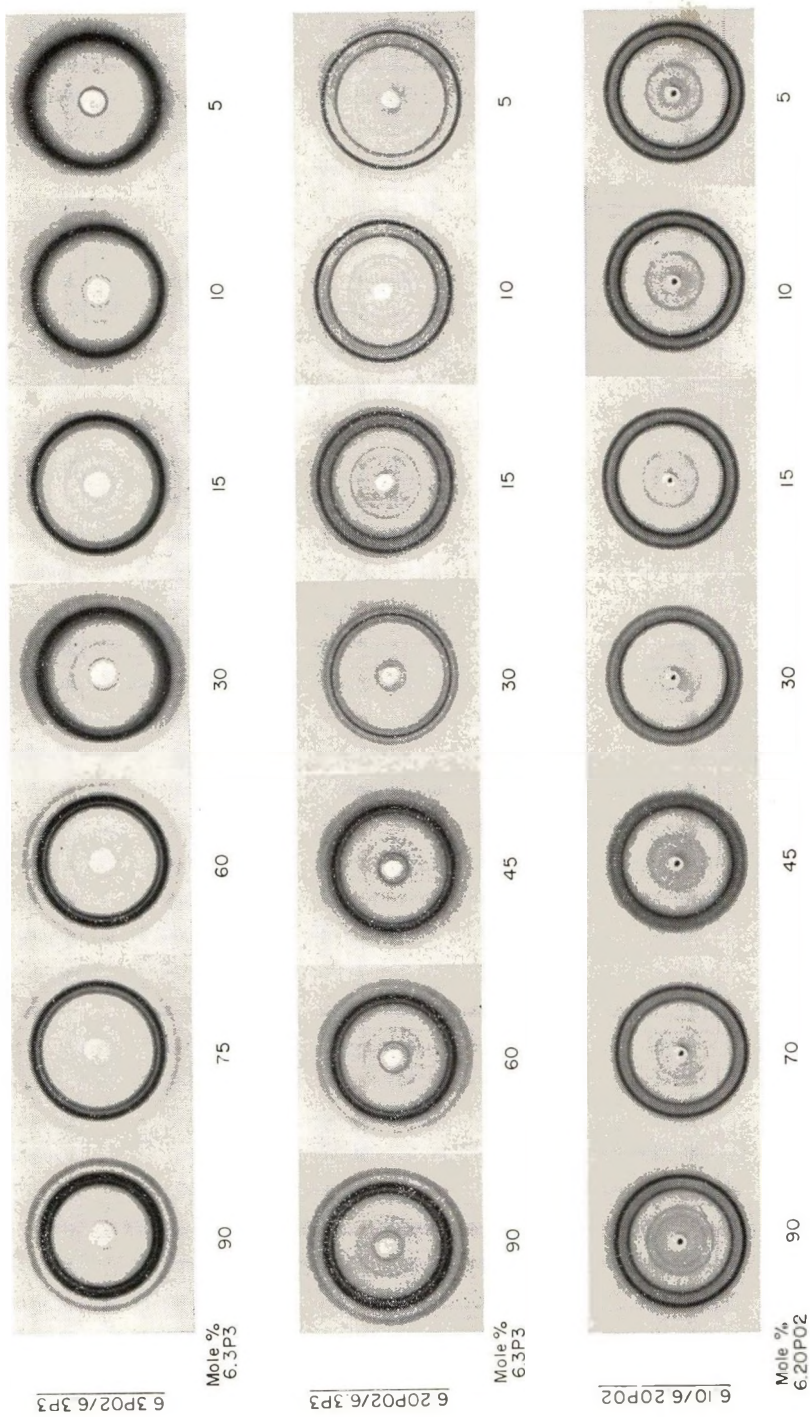


Figure 2.

The available 6.6/6.T copolymers were also examined because even in this first reported case of isomorphism, its existence was not confirmed with

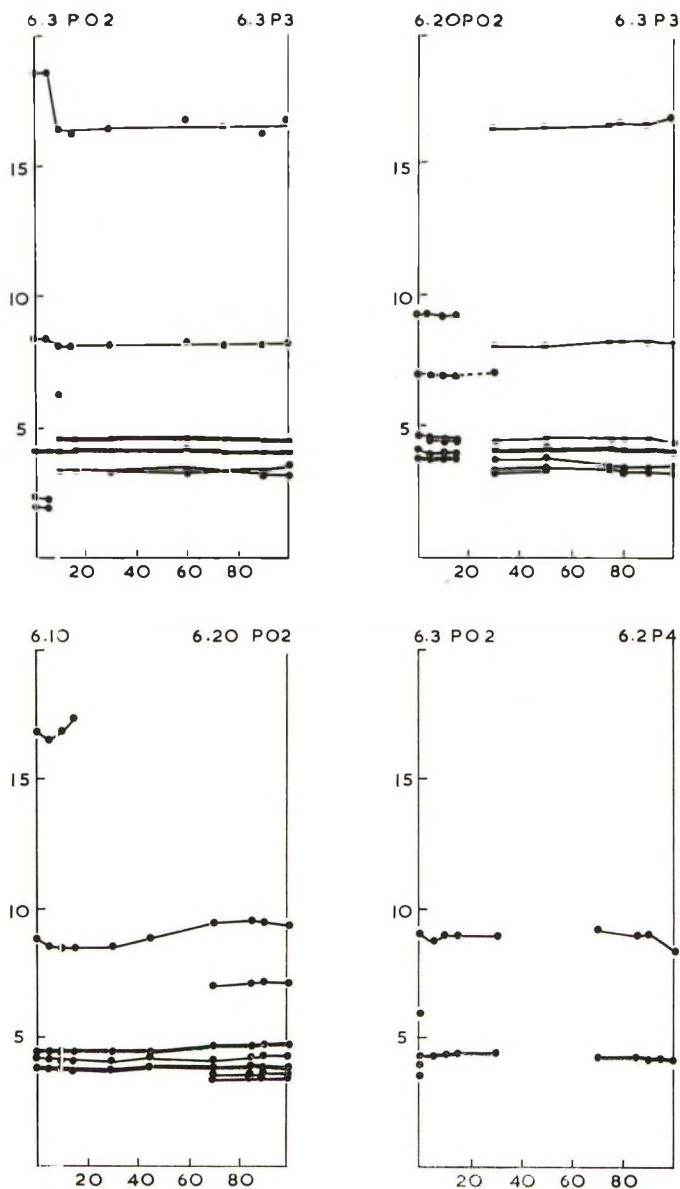


Fig. 3. Changes in lattice spacing (A.) with composition.

x-rays. Up to 30% of 6.T there is no change in the lattice which is clearly that of 6.6 polymer, although there is a progressive decrease in the diameter of the outer Debye-Scherrer circle as the concentration increases.



### Density and Infrared Measurements

The densities of 6.2OPO2 and two 6.10/6.2OPO2 copolymers were determined by using a density gradient column. Mixtures of nitrobenzene and chlorobenzene were used for the copolymers and nitrobenzene and bromobenzene for the homopolymer. In each case some 20 samples were employed, and the mean density values are plotted in Figure 4. It is clear that the density of the 45:55 copolymer is not lower than that to be expected from a simple mixture law. There is thus no evidence of any decrease in crystallinity at the composition corresponding with the minimum in the softening point curve.

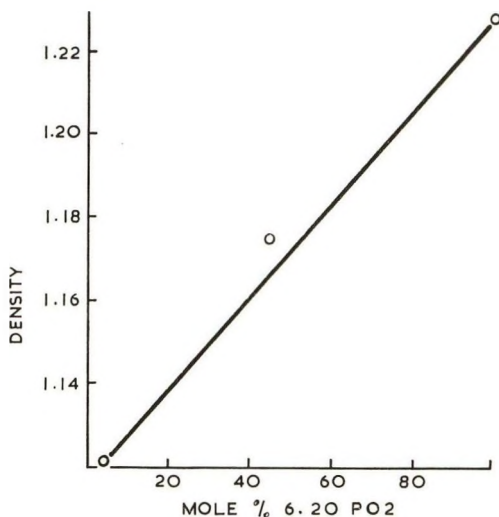


Fig. 4. Density: 6.10-6.20 PO2 copolymers. The density units are g./cm.<sup>3</sup>.

The infrared spectra were recorded with a Unicam SP.700 spectrometer. After mounting the film in a cell and removing adsorbed water by evacuation, a very weak shoulder was detected at 3428 cm.<sup>-1</sup> in the 55:45 6.10/6.2OPO2 copolymer. A similar shoulder was present in the 6.2OPO2 homopolymer. This band indicates the presence of less than 1% of unassociated NH groups. The intensity of the band in the homopolymer 6.2OPO2 was more than twice that in its copolymer with 6.10. Again, there is no sign of any decrease in hydrogen bonding in the region of the softening point curve minimum which might be associated with a lower degree of crystallinity.

## DISCUSSION

### Similarity in Identity Period and Isomorphous Replacement

The results of Edgar and Hill<sup>7</sup> suggested that close similarity in the identity period was the most important requisite for the occurrence of isomor-

phous replacement or the interchange of different repeating units within the crystal lattice without reduction in crystallinity. The polymers investigated here should show an even closer resemblance in overall length of the repeating unit than adipic and terephthalic acids. Thus: (a) 3P3 and 2P4 acids should be almost identical in molecular length, the only difference being the position of the benzene ring; (b) the difference in molecular length between sebacic and 3P3 and 2P4 acids, respectively, is the same as that for terephthalic and adipic acids, the difference being that each acid has an extra four  $-\text{CH}_2-$  groups; (c) the relationship between 3P3 and 3PO2 acids is the same as that between 3PO2 and 2OPO2 acids.

The different copolymers should, therefore, permit a more comprehensive test of the general validity or otherwise of this hypothesis. Considering this close similarity in overall length it was very surprising to find that only one copolymer system, viz., 6.3PO2/6.3P3, gave a linear softening point versus composition curve. Either other factors besides similarity in the length of the component units are important in determining isomorphism or the form of the softening point curve is not a reliable criterion of isomorphous replacement. The x-ray examination was undertaken in order to decide between these two alternatives.

### Changes in the Crystalline Lattice

Although the softening points suggest that only one binary copolymer system exhibits isomorphous replacement, an examination of the x-ray results shows that this conclusion is not reliable. The changes in lattice spacings (Fig. 3) reveal no grounds for differentiating any of these copolymers from the remainder. Basically they all behave similarly. In general, the second component dissolves in the lattice of the first until a certain critical concentration is reached, when a fairly abrupt change in lattice type occurs and the first component is now dissolved in the lattice of the second. This behavior is, therefore, completely analogous to the well-known phenomenon in the metal field of substitutional solid solution formation over limited ranges. Generally the change in lattice type occurs at a composition corresponding approximately with the minimum in the softening point curve. This is normally around 50/50 mole-% composition but considerable deviations from this occur. Thus in the 6.10/6.3P3 system it takes place between 15 and 40 mole-% of 6.3P3. Intermediate compositions were not examined, but the exact changeover point would be expected to lie near the lower value in agreement with the position of the minimum in the softening point curve. It is probable that the exact position of the transition depends on the quality of the fit of the second component in the lattice of the first. It is doubtful, however, whether any quantitative treatment of this problem is possible as yet.

Occasionally there were minor signs of instability in the changeover region; a line from the first lattice might persist for a short while, as, for example, in Figure 3*b*, where the 7.1 Å spacing is still present in the polymer containing 30 mole-% 6.3P3. There were, however, no obvious features

such as increased broadness of the lines or a reduction in their number to suggest any significant decrease in crystallinity.

### **Polyhexamethylene Adipamide/Polyhexamethylene Terephthalamide Copolymers**

It is surprising how the use of a linear melting point versus composition relationship as a criterion for isomorphous replacement has developed when the early results of Edgar and Hill<sup>7</sup> do not in fact afford such a relationship. Subsequent work also confirms the nonlinearity. Yu and Evans<sup>11</sup> describe the curve as sigmoidal, and in the present work, which relates to softening points, there is a slight minimum. This amounts, however, to only 2°C., which is of the order of the error of measurement. Levine and Temin,<sup>8</sup> referring to the paper of Edgar and Hill, state: "in this case only a small depression of the melting points of the copolymers, hexamethylene diammonium terephthalate (6T. salt) and hexamethylene diammonium adipate (nylon 6.6 salt) occurred." The only really characteristic feature is, therefore, the absence of a pronounced minimum.

The x-ray observations confirm the interchange of adipyl and terephthalyl groups within the crystal lattice, but there is clear evidence of some degree of misfit. The spacing of the (010) planes increases steadily from 3.73 Å. to 3.88 Å. when 30% of 6.T is present. This change indicates decreasing lattice perfection. In the absence of results for the remaining copolymer compositions there is no reason for inferring that the behavior of this system is basically different from that of any of the other copolymer systems which form the basis of the present work.

### **Isomorphism, Isomorphous Replacement, and Solid Solutions**

The transfer of the term isomorphous to copolymer systems is unfortunate, since its usual significance has to be modified somewhat for this purpose. Normally two materials are said to be isomorphous if they have identical structures and the cell edges do not differ by more than a few tenths of an Angström unit.

In polymers, where the structures are usually of relatively low symmetry, the prospects of finding two polymers with identical unit cells are remote and genuine isomorphous replacement can be little more than an academic curiosity. Of the examples studied here, the 6.3PO2/6.2P4 system offers the closest approach, since no lattice change was observed over the entire composition range examined (5–95 mole-% 6.3PO2). However, this cannot be regarded as a genuine example of isomorphous replacement, since the copolymers were less crystalline than the homopolymers.

The phenomenon of greater interest is the satisfactory inclusion of the segments of one polymer within the crystalline regions of another. If the resemblance in shape and size is sufficient, then interchange within the crystal lattice should be possible without a reduction in crystallinity. This phenomenon is more adequately described as solid solution or mixed crystal formation and is already well known in metallurgy. With the ex-

ception of the 6.3PO2/6.2P4 system, all the examined copolymer systems showed this behavior.

It might be suggested that the lattice changes observed are not conclusive evidence for segmental interchange, since the component whose diffraction pattern is not observed may actually be present in the amorphous regions. This seems very unlikely in the present instance, since one lattice may remain stable over a very wide composition range and experience has shown that the crystalline fraction is very sensitive to small degrees of misfit and rapidly tends to an amorphous state if proper accommodation in the lattice is not possible. Density measurements likewise showed no decrease in packing density in the region of the changeover, such as would be expected if there were any significant increase in amorphous content. Infrared measurements also showed no decrease in hydrogen bonding—in fact the free—NH in the 55:45 copolymer was only about half what it was in the 6.2OPO2 homopolymer. Thus the two different acid residues in the copolymer allow more complete association of the amide groups possibly due to the greater flexibility of the  $-(CH_2)_8-$  segment of the sebacic acid. In accord with this hypothesis the band was not detectable in nylon 610. The composition intervals were often large in the changeover regions so that it is not possible to rule out entirely the possibility in some cases of a decrease in crystallinity within a narrow composition interval about the transition point. There is no doubt, however, that at the compositions actually examined, genuine segmental interchange is occurring in the crystalline regions. None of these copolymers, therefore, affords any exception to the rule that close similarity in the repeating distance is a prime requirement for the occurrence of isomorphous replacement.

In general, the compositions at which the changeovers occurred corresponded well with the position of the minima in the softening point versus composition curves. The 6.2PO2/6.2P4 copolymers are again notable exceptions since, in spite of the absence of any lattice changes, the softening point versus composition curve nevertheless shows a minimum. Clearly, a wide range of degrees of misfit is possible, and it is these which determine the solubility relationships and hence the position of the changeover point on the composition scale. It follows, therefore, from the nature of the phenomenon that no sharp line of demarcation between isomorphous and nonisomorphous polymers is to be expected but rather a continuous gradation depending on the degree of similarity of the repeating units. As the differences increase, the polymers will become increasingly amorphous in the middle composition range. The problem of so-called isomorphous replacement is then one of determining the factors which control this type of lattice interchange.

### The Repeating Distance and Isomorphous Replacement

In the first reported example of polymer isomorphism,<sup>7</sup> the segmental interchange was attributed to close similarity in the overall length of the adipic and terephthalic acids. The authors concluded that the distances

between the carboxyl groups differed by only 0.31 Å. This figure is based on an inaccurate value for the distance between the terminal carbon atoms in a chain of six methylene groups. The corrected difference is 0.50 Å., and it is debatable whether this really constitutes very close agreement. In fact, Yu and Evans<sup>11</sup> are forced to incline the benzene axis at an angle of 35°16' to the molecular direction in order to achieve a reasonable fit. Under these conditions it is not possible to say that there is no distortion of the lattice and the gradual reduction in crystallinity shown by the decreasing separation of the two strong reflections with increasing 6.T content is in agreement with this.

However, the assumption that close similarity in the length of the repeating units is a necessary prerequisite for segmental interchange seems a very reasonable one. The 6.6/6.T results would suggest that a tolerance of at least 10% is permissible. It is, therefore, necessary to enquire why, in the polyamides containing the *p*-phenylene link examined here, where the differences in the overall length of the repeating units are certainly not more than in 6.6/6.T, and mostly much less, that on the basis of the softening point curves only one binary copolymer should be adjudged isomorphous. The x-ray results, however, show that, if isomorphism is considered in the modified form suggested above, then all the binary copolymers examined exhibit segmental interchange and may be described as isomorphous. There is thus a direct relationship between isomorphous replacement and the overall length of the component dicarboxylic acids. This does not imply that this is necessarily the sole criterion. It is quite likely that the conclusion of Frunze and Korshak<sup>12</sup> that similarity in repeating length is not always sufficient to ensure isomorphism is correct, but this cannot be accepted as established experimentally since it is again based on the form of the melting point versus composition curve.

#### Relationship between Crystalline Structure and Softening Point Curve

At first sight it is surprising that there is so little connection between the changes in the crystalline lattice and the form of the softening point curve. Further, although the transition usually takes place at a composition corresponding closely with the position of the minimum in the softening point curve, exceptions again occur. In the 6.3PO<sub>2</sub>/6.3P<sub>3</sub> system, which shows no minimum, there is a lattice transition at about 10 mole-% of 6.3P<sub>3</sub>, while on the other hand the 6.4PO<sub>2</sub>/6.2P<sub>4</sub> copolymers show no abrupt lattice change, but there is a pronounced minimum in the softening point versus composition curve. It might be suggested that the softening point as measured with a penetrometer is more a function of the amorphous regions, so that a close parallel between the lattice changes as studied by x-rays and the softening point versus composition curve is not to be expected. On the other hand, the very close agreement between softening points and optical melting points obtained for the 6.3PO<sub>2</sub>/6.2P<sub>4</sub> copolymers (Fig. 5) suggests a very close connection between the softening points as measured and the crystalline regions. It could be that these polymers

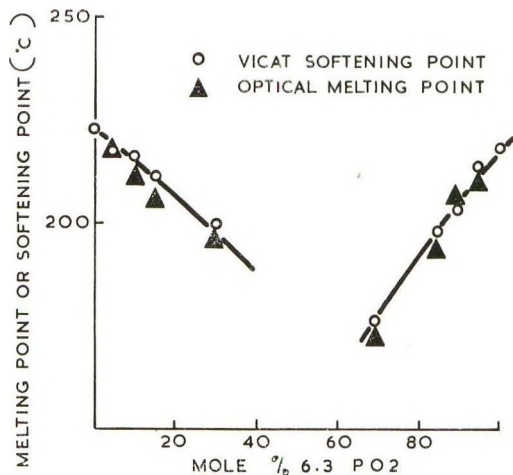


Fig. 5. Softening and optical melting points. 6.3PO<sub>2</sub>-6.2P<sub>4</sub> copolymers.

contain very little amorphous material and the penetrometer is, in fact, measuring the melting of the crystalline regions. It follows, therefore, that the x-ray line positions serve to determine the lattice structure, but that segmental interchange within such a lattice does not usually occur without some modifications of its cohesive properties.

#### Softening Point Curve as a Criterion for Isomorphous Replacement

The present results leave no doubt that the form of the softening point curve is quite useless for determining the occurrence or absence of segmental interchange. The series of copolymers based on polymers containing the *p*-phenylene link show a wide variety of softening point curves, ranging from linear to curves with deep minima, yet there is no fundamental distinction in their behavior; they all show the same type of solid-solution phenomenon.

The question then arises as to whether the melting point curves follow a similar pattern to the softening point curves. The optical melting points of the 6.3PO<sub>2</sub>/6.2P<sub>4</sub> copolymers suggest that they do.

It seems reasonable, therefore, to expect that the conclusion arrived at for the softening point curves is equally valid for the melting point versus composition curves. This has important implications, since considerable confusion has thereby developed in the literature relating to isomorphous replacement. Many cases of isomorphism may in this way have been wrongly classed as nonisomorphous. Yu and Evans<sup>11</sup> found that four methylene groups and a *p*-phenylene unit were not always isomorphically replaceable but it depended on whether there was an even or odd number of methylene groups between the benzene ring and the functional group. Since the length of the repeating unit is the same in both cases, a reexamination of these systems is necessary. Yu and Evans<sup>11</sup> have also interpreted more subtle features of the melting point versus composition curves in

structural terms. They distinguish cases of partially isomorphous copolyamides where A can enter the crystalline lattice of B to some extent, but B cannot enter the lattice of A. This conclusion was arrived at because in some systems showing a typical eutectic type curve the addition of aliphatic comonomer to the aryl homopolymer did not immediately produce a depression of the melting point. This initial curvilinear portion of the curve was taken to imply limited or partial isomorphism. On the basis of our work with copolymers we conclude that all examples of polymer isomorphism are partial in character, and the situation postulated by Yu and Evans is merely a limiting state of this general condition. While the phenomenon suggested is theoretically possible, it seems somewhat unlikely that if the repeating unit of B resembles that of A sufficiently to be capable of entering the A lattice that A would not also be able to enter the lattice B to some extent. In the circumstances, this conclusion is not acceptable on the basis of the form of the melting point versus composition curve alone.

It is remarkable that the form of the melting point versus composition curve has been used almost exclusively in the study of isomorphism, while x-ray techniques, which allow the changes in the crystalline lattice to be easily and directly followed, have hardly been used at all. The confusion thereby introduced necessitates a critical reappraisal of the problem of isomorphous replacement in polymers. Some of the rather artificial models put forward to explain apparent anomalies might well then be dispensed with.

The author expresses his thanks to Dr. F. P. Chappel for the determination of the optical melting points, to Mr. B. D. Herrington for the density determinations, to Dr. B. C. Stace for the infrared measurements, to Mr. P. R. Thomas and Dr. G. J. Tyler for supplying the copolymers and softening point data, and to Mr. R. C. Collins for preparing the x-ray diffraction patterns.

### References

1. Baker, W. O., and C. S. Fuller, *J. Am. Chem. Soc.*, **64**, 2399 (1942).
2. Hayashi, I., and G. Hachihama, *Kogyo Kagaku Zasshi*, **59**, 104 (1956).
3. Hosina, K., and K. Aikawa, *Nippon Kagaku Zasshi*, **63**, 1182 (1942).
4. Mokudai, W., M. Ishihara, T. Kamiyama, and R. Oda, *Bull. Inst. Phys. Chem. Res.*, **21**, 350 (1942).
5. Oda, R., W. Mokudai, M. Ishihara, and T. Morisita, *Bull. Inst. Phys. Chem. Res.*, **19**, 1448 (1940).
6. Catlin, W. E., E. P. Czerwin, and R. H. Wiley, *J. Polymer Sci.*, **2**, 412 (1947).
7. Edgar, O. B., and R. Hill, *J. Polymer Sci.*, **8**, 1 (1952).
8. Levine, M., and S. C. Temin, *J. Polymer Sci.*, **49**, 241 (1961).
9. Cramer, F. B., and R. G. Beaman, *J. Polymer Sci.*, **21**, 237 (1956).
10. Thomas, P. R., and G. J. Tyler, Brit. Pat. 797,617 (1958); Brit. Pat. 804,225 (1958).
11. Yu, A. J., and R. D. Evans, *J. Am. Chem. Soc.*, **81**, 5361 (1959).
12. Frunze, T. M., and V. V. Korshak, *Vysokomol. Soedin.*, **1**, 287 (1959).

### Résumé

Depuis les observations d'Edgar et Hill concernant les copolymères polyhexaméthylène adipamide/polyhexaméthylène téréphtalamide, on admet, en général, que l'existence d'une relation linéaire entre le point de fusion et la composition constitue un critère

d'échange isomorphe. Dans une série de copolymères linéaires, dont les homopolymères ont été préparés au moyen d'hexaméthylène diamine d'une part et d'acide *p*-phénylène dipropionique (3P3), d'acide 3-(*p*-carboxyméthyl) phénylbutyrique (2P4), d'acide 2-(*p*-carboxyméthoxy) phénylpropionique (3PO2), d'acide hydroquinone diacétique (2OPO2), d'acide téréphthalique (T), d'acide adipique (6) ou d'acide sébacique (10) d'autre part, seul le système 6-3P3/6-3PO2 présente une relation linéaire entre la composition et le point de ramollissement, et cela bien que les différences entre les longueurs des unités périodiques n'y soient pas plus grandes et même plutôt moindres que dans le cas des acides adipiques et téréphthaliques. L'examen aux rayons-X montre toutefois que tous les systèmes se comportent fondamentalement de la même façon, à savoir la dissolution du second constituant dans le réseau du premier jusqu'à l'atteinte d'une concentration critique où le réseau se transforme brusquement en un autre réseau; celui du second constituant au sein duquel le premier constituant se retrouve à présent dissous. Le point de transition coïncide généralement mais pas toujours avec la position du minimum dans la courbe: point de ramollissement en fonction de la composition. Les mesures de densité et les spectres infra-rouges n'indiquent aucune réduction de la cristallinité en ce point. Ces copolyamides ne constituent donc pas une exception à l'hypothèse suivant laquelle une similitude de longueur des unités de répétition soit une condition préalable nécessaire, mais peut-être pas unique, à la réaction d'échange des segments. La forme de la courbe du point de ramollissement en fonction de la composition n'est pas, de ce fait, un critère de l'existence d'un échange isomorphe et il semble probable que cette conclusion s'applique également à la courbe du point de fusion en fonction de la composition.

### Zusammenfassung

Seit den Beobachtungen von Edgar und Hill an Polyhexamethylenadipamid-Polyhexamethylenterephthalamid-Kopolymeren wurde eine lineare Beziehung zwischen Schmelzpunkt und Zusammensetzung als Kriterium für eine isomorphe Vertretbarkeit allgemein angenommen. In einer Reihe von binären Kopolymeren auf Grundlage von Homopolymeren aus Hexamethyldiamin und *p*-Phenylendipropion- (3P3), 3-(*p*-Carboxymethyl)-Phenylbutter- (2P4), 2-(*p*-Carboxymethoxy)-Phenylpropion- (3PO2), Hydrochinondiessig- (2OPO2), Terephthal- (T), Adipin- (6) oder Sebacin- (10) -Säure zeigte nur das 6.3P3-6.3PO2-System eine lineare Erweichungspunkt-Zusammensetzungskurve, obwohl die Unterschiede in der Länge des Grundbausteins sicher nicht grösser und oft sogar viel geringer als bei Adipin- und Terephthalsäure waren. Röntgenuntersuchung zeigte jedoch, dass alle Systeme sich grundsätzlich gleich verhielten, da sich nämlich die zweite Komponente im Gitter der ersten bis zu einer kritischen Konzentration löste, bei der das Gitter sich ziemlich plötzlich in dasjenige der zweiten Komponente umwandelte, in welcher nun die erste gelöst war. Der Umwandlungspunkt fiel im allgemeinen, aber nicht immer, mit der Lage des Minimums in der Erweichungspunkt-Zusammensetzungskurve zusammen. Infrarot- und Dichtemessungen liessen an diesem Punkt keine Herabsetzung der Kristallinität erkennen. Diese Kopolyamide bilden daher keine Ausnahme zu der Annahme, dass eine starke Ähnlichkeit der Länge der Grundeinheit eine notwendige, aber vielleicht nicht die einzige, Voraussetzung für das Auftreten von Segmentumwandlungen ist. Die Form der Erweichungspunkt-Zusammensetzungskurve bildet daher kein verlässliches Kriterium für isomorphe Vertretbarkeit, und es scheint wahrscheinlich, dass dieser Schluss auch auf die Schmelzpunkt-Zusammensetzungskurve in gleicher Weise anwendbar ist.

Received August 5, 1963



## A Critical Evaluation of Mathematical Molecular Weight Distribution Models Proposed for Real Polymer Distributions. I. Effects of a Low Molecular Weight Cut-Off Value

A. M. KOTLIAR,\* *Esso Research and Engineering Company, Linden, New Jersey*

### Synopsis

It is of considerable practical importance to be able to describe the distribution of molecular sizes of a polymeric material by a convenient mathematical expression. Since the various molecular averages of any distribution are obtained from a summation process, the general models require an analytical expression of the differential distribution and a corresponding definite integral generally having the integration limits of zero and infinity. In general, real polymer distributions do not fit these integration limits and an error, which can be very large, is therefore introduced. If the error in the various molecular weight averages due to changes in integration limits is of the order of or less than the error generally encountered in the experimental evaluation of the average, the distribution function can be considered to be applicable from a practical point of view. In addition, the selected model should fulfill the requirements of fitting known experimental facts such as: the polymerization kinetics, the effects of random degradation and crosslinking, fractionation data, and the effects of polymerization and processing on the differential distribution maxima. It should also conform to the rheological behavior based on current theoretical ideas. The integration limit criteria are applied to logarithmic normal type distributions, e.g., Wesslau, and generalized exponential type distributions, e.g., Schulz-Zimm and Tung. The results show that logarithmic normal type distributions cannot be considered as useful models, while the generalized exponential type distributions can be valid and useful representations.

### Introduction

Two general type distribution functions have been used to characterize the relative amounts of different molecular sizes found in a polymeric material. They are the generalized logarithmic normal [eq. (1)] and the generalized exponential [eq. (2)] distributions<sup>1</sup>

$$W(P) = \frac{P^n N}{\beta \pi^{1/2}} \exp \left\{ - \frac{1}{\beta^2} \ln^2 P/P_0 \right\} \quad (1)$$

\* Present address: Central Research Laboratory, Allied Chemical Corporation, Morristown, New Jersey.

where

$$\begin{aligned}\bar{P}_n &= P_0 \exp \{ (2n + 1)\beta^2/4 \} \\ \bar{P}_w &= P_0 \exp \{ (2n + 3)\beta^2/4 \} \\ \bar{P}_z &= P_0 \exp \{ (2n + 5)\beta^2/4 \} \\ \bar{P}_i &= P_0 \exp \{ (2n + i + 2)\beta^2/4 \}\end{aligned}$$

and

$$W(P) = \frac{(a + 1)y^{a + 1/m}}{\Gamma\left(\frac{a + 1}{m} + 1\right)} P^a e^{-yP^n} \quad (2)$$

where

$$\begin{aligned}\bar{P}_n &= \Gamma\left(\frac{a + 1}{m}\right) / y^{1/m} \Gamma\left(\frac{a}{m}\right) \\ \bar{P}_w &= \Gamma\left(\frac{a + 2}{m}\right) / y^{1/m} \Gamma\left(\frac{a + 1}{m}\right) \\ \bar{P}_z &= \Gamma\left(\frac{a + 3}{m}\right) / y^{1/m} \Gamma\left(\frac{a + 2}{m}\right) \\ \bar{P}_i &= \Gamma\left(\frac{a + i}{m}\right) / y^{1/m} \Gamma\left(\frac{a + i - 1}{m}\right)\end{aligned}$$

$P$  is the molecular size and is equal to the degree of polymerization;  $N$  is a normalization constant, and  $n$ ,  $\beta$ ,  $P_0$ ,  $m$ ,  $a$ ,  $y$  are distribution parameters. The molecular weight of species of size  $P$  is then  $m_0P$ , where  $m_0$  is the molecular weight of the repeating unit. The  $i$ th molecular weight average is then

$$\bar{M}_i = m_0 \bar{P}_i \quad (3)$$

The Lansing-Kramer<sup>2</sup> and Wesslau<sup>3</sup> distributions are obtained by setting  $n$  in eq. (1) as  $n = 0$  and  $n = -1$ , respectively. The Schulz-Zimm,<sup>4</sup> Poisson, and Tung<sup>5</sup> type distributions are obtained by setting  $m$  in eq. (2) as  $m = 1$  with  $a > 0$ ,  $m = 1$  with  $a \gg 1$ , and  $m = a + 1$  with  $a > 0$ , respectively.

It is extremely important to note the necessary requirement of the equalities of the ratios  $\bar{P}_w/\bar{P}_n = \bar{P}_z/\bar{P}_w = \bar{P}_z + 1/\bar{P}_z$  for logarithmic normal type distributions, while  $\bar{P}_w/\bar{P}_n > \bar{P}_z/\bar{P}_w > \bar{P}_z + 1/\bar{P}_z$  for the generalized exponential type distribution. We shall generally assume in all that follows that a distribution model which fulfills the requirements of yielding the correct values for the ratio of  $\bar{P}_w/\bar{P}_n$ ,  $\bar{P}_z/\bar{P}_w$ ,  $\bar{P}_z + 1/\bar{P}_z$  will be sufficient to characterize the distribution, although it does not necessarily describe the fine details of the differential distribution.

In general we may know at best the number-average and weight-average molecular weight of the particular polymeric material. When the ratio of

$\bar{P}_w/\bar{P}_n$  is less than 2, it may easily be shown that the differences between various distribution functions become relatively insignificant and less than the errors generally associated with the measurements of the respective molecular weight averages. We may, therefore, as a matter of mathematical convenience, represent the relative amounts of different molecular sizes in fractionated polymers by the Schulz-Zimm type distributions. When the ratio of  $\bar{P}_w/\bar{P}_n$  becomes greater than 2, we have a difficult situation, in that a large number of distinctly different distribution types can fit this ratio. Since direct measurements of higher molecular weight averages are currently not possible, we must resort to supplementary information in order to reject as many distribution types as possible as being physically or mathematically unreal.

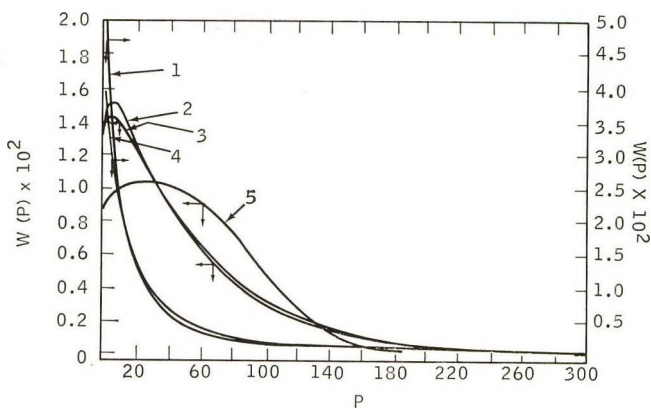


Fig. 1. Differential weight distribution for (1) Wesslau, (2) Schulz-Zimm, (3) Tung, and generalized exponential (4) with  $m = 0.2$  and (5) with  $m = 3$ .  $\bar{P}_w/\bar{P}_n = 11$ ,  $\bar{P}_w = 55$ .

Although we are not usually concerned with the exact differential distribution of the polymer, it is useful to examine the shape of the distribution, particularly around the peak of the distribution. Figures 1 and 2 show some typical types having  $\bar{P}_w/\bar{P}_n$  values of 11 and 21. Since a particular polymer is generally made by a polymerization process over a period of time during which the molecular weight averages vary to some extent, and since finished commercial polymer lots are subsequently obtained by combining smaller quantities having somewhat different molecular weight averages, it is physically unrealistic to expect rather narrow peaked distributions. This indicates that logarithmic type distributions and generalized exponential distributions with small values for  $m$  are not realistic. Although it may be argued that blending of two or more disperse distributions of the same type having different  $\bar{P}_w$  values will tend to broaden the peak, the effect of low and high molecular cut-off values described in parts I and II<sup>6</sup> of this series make such combinations of broad distributions mathematically impossible.

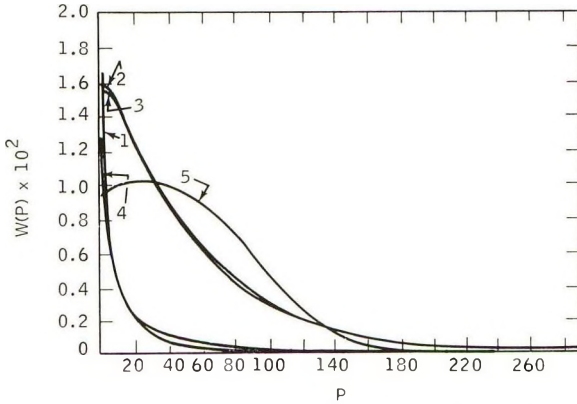


Fig. 2. Differential weight distribution for (1) Wesslau, (2) Schulz-Zimm, (3) Tung, and generalized exponential (4) with  $m = 0.2$  and (5) with  $m = 3$ .  $\bar{P}_w/\bar{P}_n = 21$ ,  $\bar{P}_w = 55$ .

The analysis of removal of low and high molecular species is extremely useful, since the distribution models proposed [eqs. (1) and (2)] and are normalized so that

$$\bar{P}_n = \sum_1^{\infty} W(P) / \sum_1^{\infty} \frac{W(P)}{P} \cong \int_0^{\infty} W(P) dP / \int_0^{\infty} W(P)/P dP \quad (4)$$

$$\bar{P}_w = \sum_1^{\infty} P W(P) / \sum_1^{\infty} W(P) \cong \int_0^{\infty} P W(P) dP / \int_0^{\infty} W(P) dP$$

$$P_i = \sum_1^{\infty} P^i W(P) / \sum_1^{\infty} P^{i-1} W(P) \cong \int_0^{\infty} P^i W(P) dP / \int_0^{\infty} P^{i-1} W(P) dP$$

and

$$\sum_1^{\infty} W(P) \cong \int_0^{\infty} W(P) dP = 1$$

The replacement of the summation process by an integral sign and the changing of the limits from 1 to 0 generally introduces negligible errors in the evaluation. If  $\bar{P}_n$  is large, e.g.,  $10^3$  or greater, this error is generally less than 3% in  $\bar{P}_n$  and negligible for the higher molecular weight averages.

In general, all polymeric materials which have no gel component have a high molecular weight cut-off generally less than  $10^7$  if they have been subjected to extrusion or filtration during their production or characterization history. In addition, the polymers are generally subject to an extraction process during which unreacted monomer and low molecular species are removed. Again, the exact value to use as an effective cut-off value is somewhat arbitrary. When the rejection process takes place under phase equilibrium conditions the weight fraction of the eluted phase is given by<sup>7</sup>

$$W(P)_{\text{eluted}} = \frac{W(P)}{1 + Re^{\sigma P}} \quad (5)$$

where  $R$  is the ratio the volume of the concentrated phase to the volume of the dilute phase and  $\sigma$  is a parameter describing the partitioning of every component species between the two phases. An extremely important consequence of the theory is that every component species is more soluble in the concentrated (precipitated) phase, since the basis for separation is the exponential  $\sigma P$  term, inefficient though it be, with most of the smaller species being retained in the more dilute phase merely as a consequence of its large volume. Therefore, all species present in the initial distribution will also be present in the rejected polymer. For calculation purposes, it is quite reasonable to consider the rejected polymer as having an effective low molecular weight cut-off of  $q\bar{P}_n$ , where  $q$  has a limiting value of about 0.025 for high number-average molecular weights of the order of  $10^5$  and increases with decreasing molecular weight.

### Theory

The number-average molecular weight of a distribution is defined by

$$\bar{P}_n' = \frac{\sum_i W(P_i)}{\sum_i W(P_i)/P_i} \quad (6)$$

where the symbol  $\sum_i$  indicates a summation of all species present. In this section, we shall not be concerned with the upper limit, since the high molecular weight material, i.e.,  $P > 10^5$ , generally contributes insignificantly to the number average. Since  $\bar{P}_n$ , and higher molecular weight averages are insensitive to low ends (other than by a dilution effect), we shall omit discussion of these averages in this section.

In order to compare eq. (6) with eq. (4) of the generalized distribution functions, we can write eq. (6) as

$$\bar{P}_n' = \frac{\sum_{k=1}^{\infty} W(P_k) - \sum_{k=1}^{q\bar{P}_n} W(P_k)}{\sum_{k=1}^{\infty} \frac{W(P_k)}{P_k} - \sum_{k=1}^{q\bar{P}_n} \frac{W(P_k)}{P_k}} \quad (6a)$$

without loss of generality. For values of  $q \leq 0.1$ , the factor

$$\sum_{k=1}^{q\bar{P}_n} W(P_k)$$

is generally very small. Hence

$$\bar{P}_n' / \bar{P}_n \cong = \frac{1}{1 - \bar{P}_n \sum_{k=1}^{q\bar{P}_n} W(P_k)/P_k} \quad (7)$$

where  $\bar{P}_n$  is given by eq. (4) for the generalized distribution functions.

The experimental determination of  $\bar{P}_n'$ , which is a colligative property, is generally accomplished by using an osmometer having a semipermeable membrane. Unfortunately, all known usable membranes which have

reasonable permeation rates for solvent molecules, are also permeable to low molecular weight polymeric species. A generally accepted value for an effective cut-off molecular weight is about 15,000. Therefore, the measured  $\bar{P}_{n,osm}$  will be given by

$$\bar{P}_{n,osm} = \sum_i W(P_i) \left/ \sum_i \frac{W(P_i)}{P_i} \right. - \sum_1^{i\bar{P}_n} W(P_i)/P_i \quad (8)$$

Equation (8) may be written for the generalized distribution as

$$\frac{\bar{P}_{n,osm}}{\bar{P}_n} = \frac{1}{1 - \bar{P}_n \sum_1^{i\bar{P}_n} W(P_i)/P_i}$$

The true error of the osmotic pressure measurement for a polymer having a low molecular cut-off value is given by  $\bar{P}_{n,osm}/\bar{P}_n'$ . When this ratio is greater than one, which is generally the case for broad distributions, the  $\bar{P}_{n,osm}$  limiting value for a particular distribution having the normalization limits of 1 to  $\infty$  may be evaluated by successive approximations assuming cut-off values for the distribution and the membrane. In the limit,  $(\bar{P}_{n,osm}/\bar{P}_n)$  corrected will equal  $\bar{P}_n'/\bar{P}_n$ . The ratio  $\bar{P}_n'/\bar{P}_n$  may be considered as a measure of the applicability of the distribution model to the real polymer distribution. We shall assume that  $\bar{P}_n'/\bar{P}_n \leq 1.1$  constitutes a good fit, since the error in the absolute determination of  $\bar{P}_n'$  is certainly of this order or perhaps greater for dispersed polymers.

### Results and Discussion

The effects of a low molecular weight cut-off value, as reflected by the ratio of  $\bar{P}_n'/\bar{P}_n$ , are shown in Tables I-XXI and Figures 3-16. In order to

TABLE I  
Wesslau Distribution,  $\bar{P}_w/\bar{P}_n = 1.5$

Cut-off parameter $q$ or $i$	$\bar{P}_n'/\bar{P}_n$	$\bar{P}_{n,osm}/\bar{P}_n$	Cumulative number fraction	Cumulative weight fraction
0.025	1.00	1.00	0.000	0.000
0.050	1.00	1.00	0.000	0.000
0.100	1.00	1.00	0.000 <sub>5</sub>	0.000
0.200	1.01	1.01	0.001	0.002
0.300	1.05	1.06	0.058	0.014
0.400	1.11	1.15	0.132	0.040
0.500	1.18	1.28	0.221	0.080
0.600	1.27	1.46	0.315	0.132
0.700	1.38	1.68	0.405	0.190
0.800	1.46	1.95	0.488	0.252
0.900	1.56	2.28	0.561	0.315
1.000	1.67	2.67	0.625	0.375
1.500	2.21	5.90	0.830	0.625
2.000	2.77	12.55	0.920	0.780

TABLE II  
 Wesslau Distribution,  $\bar{P}_w/\bar{P}_n = 2$ 

Cut-off parameter $q$ or $j$	$\bar{P}_n'/\bar{P}_n$	$\bar{P}_{n,osm}/\bar{P}_n$	Cumulative number fraction	Cumulative weight fraction
0.025	1.00	1.00	0.000	0.000
0.050	1.00	1.00	0.000	0.000
0.100	1.01	1.01	0.010	0.000 <sub>7</sub>
0.200	1.06	1.07	0.065	0.010
0.300	1.14	1.18	0.152	0.031
0.400	1.24	1.33	0.247	0.065
0.500	1.35	1.51	0.339	0.106
0.600	1.47	1.73	0.422	0.152
0.700	1.59	1.98	0.496	0.199
0.800	1.71	2.27	0.559	0.247
0.900	1.83	2.59	0.614	0.294
1.000	1.95	2.96	0.626	0.339
1.500	2.58	5.46	0.817	0.528
2.000	3.20	9.45	0.894	0.662

 TABLE III  
 Wesslau Distribution,  $\bar{P}_w/\bar{P}_n = 3$ 

Cut-off parameter $q$ or $j$	$\bar{P}_n'/\bar{P}_n$	$\bar{P}_{n,osm}/\bar{P}_n$	Cumulative number fraction	Cumulative weight fraction
0.025	1.00	1.00	0.002	0.000
0.050	1.01	1.01	0.010	0.000 <sub>4</sub>
0.100	1.05	1.05	0.048	0.003
0.200	1.16	1.19	0.157	0.020
0.300	1.30	1.36	0.267	0.047
0.400	1.44	1.57	0.364	0.081
0.500	1.59	1.80	0.446	0.118
0.600	1.74	2.07	0.515	0.156
0.700	1.89	2.34	0.573	0.194
0.800	2.04	2.65	0.662	0.231
0.900	2.18	2.98	0.664	0.266
1.000	2.38	3.33	0.700	0.300
1.500	3.06	5.52	0.819	0.446
2.000	3.78	8.48	0.882	0.555

evaluate the width parameter,  $a$  or  $\beta$ , which describes the differential weight distribution of the models described above in the interval  $P$  (low cut-off)  $\leq P \leq P$  (high cut-off), two different molecular weight averages are needed. The most experimentally accessible averages are  $\bar{P}_n'$  and  $\bar{P}_w''$ , where  $\bar{P}_w''$  is the weight-average molecular size for a distribution having a high molecular weight cut-off value as described in part II of this series.<sup>6</sup> Since  $\bar{P}_w''$  is less than  $\bar{P}_w$  (particularly for a Wesslau type distribution) and  $\bar{P}_n'$  is greater than  $\bar{P}_n$ , the measured ratio of  $\bar{P}_w''/\bar{P}_n'$  can be considerably less than the true value derived from the width parameter which describes

TABLE IV  
 Wesslau Distribution,  $\bar{P}_w/\bar{P}_n = 6$ 

Cut-off parameter $q$ or $j$	$\bar{P}_n'/\bar{P}_n$	$\bar{P}_{n, \text{osm}}/\bar{P}_n$	Cumulative number fraction	Cumulative weight fraction
0.025	1.02	1.02	0.019	0.000 <sub>3</sub>
0.050	1.06	1.06	0.059	0.002
0.100	1.16	1.17	0.148	0.009
0.200	1.38	1.42	0.298	0.031
0.300	1.59	1.69	0.410	0.059
0.400	1.80	1.98	0.494	0.088
0.500	2.01	2.28	0.561	0.118
0.600	2.21	2.59	0.613	0.147
0.700	2.40	2.91	0.657	0.175
0.800	2.60	3.25	0.693	0.202
0.900	2.79	3.61	0.723	0.227
1.000	2.97	3.98	0.749	0.252
1.500	3.89	6.05	0.835	0.357
2.000	4.76	8.50	0.882	0.440

 TABLE V  
 Wesslau Distribution,  $\bar{P}_w/\bar{P}_n = 11$ 

Cut-off parameter $q$ or $j$	$\bar{P}_n'/\bar{P}_n$	$\bar{P}_{n, \text{osm}}/\bar{P}_n$	Cumulative number fraction	Cumulative weight fraction
0.025	1.06	1.06	0.055	0.001
0.050	1.14	1.14	0.124	0.003
0.100	1.30	1.31	0.239	0.012
0.200	1.60	1.66	0.396	0.035
0.300	1.88	2.00	0.499	0.061
0.400	2.14	2.34	0.573	0.086
0.500	2.39	2.69	0.628	0.111
0.600	2.64	3.05	0.672	0.135
0.700	2.87	3.41	0.707	0.158
0.800	3.11	3.79	0.736	0.179
0.900	3.34	4.17	0.760	0.200
1.000	3.56	4.56	0.781	0.220
1.500	4.64	6.67	0.850	0.304
2.000	5.67	9.03	0.889	0.372

the differential weight distribution. Hence we must more or less arbitrarily select a somewhat larger value for  $\bar{P}_w/\bar{P}_n$  in order to get a better estimate of the effects of a low molecular cut-off on  $\bar{P}_n$  for the various distribution models under consideration. Since the most confirmed data on disperse distributions<sup>8</sup> indicate  $\bar{P}_w''/\bar{P}_n'$  values of about 14, it is best to compare the various distribution models at a value for the ratio  $\bar{P}_w/\bar{P}_n$  of about 20, noting that  $(\bar{P}_n'/\bar{P}_n)q$  is rather insensitive to small changes in  $\bar{P}_w/\bar{P}_n$  in this region. It is also quite reasonable to assume a cut-off parameter,  $q$ , of about 0.1 for  $\bar{M}_n'$  values of the order of 10,000–30,000, since



TABLE VI  
 Wesslau Distribution,  $\bar{P}_w/\bar{P}_n = 21$ 

Cut-off parameter $q$ or $j$	$\bar{P}_n'/\bar{P}_n$	$\bar{P}_{n, \text{osm}}/\bar{P}_n$	Cumulative number fraction	Cumulative weight fraction
0.025	1.12	1.12	0.109	0.002
0.050	1.24	1.25	0.201	0.005
0.100	1.47	1.49	0.328	0.014
0.200	1.85	1.92	0.481	0.036
0.300	2.20	2.34	0.573	0.059
0.400	2.52	2.75	0.636	0.081
0.500	2.83	3.15	0.683	0.102
0.600	3.12	3.56	0.719	0.122
0.700	3.41	3.97	0.748	0.141
0.800	3.69	4.38	0.772	0.159
0.900	3.95	4.80	0.792	0.176
1.000	4.22	5.10	0.808	0.192
1.500	5.49	7.42	0.865	0.261
2.000	6.68	9.78	0.898	0.317

 TABLE VII  
 Generalized Exponential Distribution,  $m = 1$  (Schulz-Zimm),  $\bar{P}_w/\bar{P}_n = 1.5$ 

Cut-off parameter $q$ or $j$	$\bar{P}_n'/\bar{P}_n$	$\bar{P}_{n, \text{osm}}/\bar{P}_n$	Cumulative number fraction	Cumulative weight fraction
0.025	1.00	1.00	0.001	0.000
0.050	1.00	1.00	0.005	0.000
0.100	1.02	1.02	0.018	0.001
0.200	1.06	1.07	0.062	0.008
0.300	1.11	1.14	0.122	0.023
0.400	1.18	1.24	0.192	0.048
0.500	1.25	1.36	0.265	0.081
0.600	1.33	1.51	0.338	0.121
0.700	1.41	1.69	0.409	0.167
0.800	1.49	1.91	0.475	0.217
0.900	1.58	2.16	0.538	0.270
1.000	1.67	2.47	0.594	0.324
1.500	2.13	5.03	0.801	0.577
2.000	2.60	10.93	0.909	0.762

species having a molecular weight below about 1000 are likely to be removed. It is important to bear in mind that the parameter  $q$  refers to  $\bar{M}_n$  which can be considerably less than  $\bar{M}_n'$ . This effective cut-off parameter is a function of the rejection process, weight fraction removed, distribution model, and any subsequent operation which can regenerate low molecular species, e.g., polymer degradation and condensation polymer interchange reactions. Comparison of the various distribution models, using the above values of  $\bar{P}_w/\bar{P}_n$  and  $q$ , show that 10, 20, and 40% of the total number of molecules are excluded for the generalized exponential

TABLE VIII  
Generalized Exponential Distribution,  $m = 1$  (Schulz-Zimm),  $\bar{P}_w/\bar{P}_n = 2$

Cut-off parameter $q$ or $j$	$\bar{P}_n'/\bar{P}_n$	$\bar{P}_{n, osm}/\bar{P}_n$	Cumulative number fraction	Cumulative weight fraction
0.025	1.03	1.03	0.025	0.0003
0.050	1.05	1.05	0.049	0.001
0.100	1.10	1.11	0.095	0.005
0.200	1.20	1.22	0.181	0.018
0.300	1.30	1.35	0.259	0.037
0.400	1.40	1.49	0.330	0.062
0.500	1.50	1.65	0.393	0.090
0.600	1.60	1.82	0.451	0.122
0.700	1.70	2.01	0.503	0.156
0.800	1.80	2.22	0.550	0.191
0.900	1.90	2.46	0.593	0.228
1.000	2.00	2.72	0.632	0.264
1.500	2.50	4.47	0.777	0.442
2.000	2.99	7.36	0.864	0.594

TABLE IX  
Generalized Exponential Distribution,  $m = 1$  (Schulz-Zimm),  $\bar{P}_w/\bar{P}_n = 3$

Cut-off parameter $q$ or $j$	$\bar{P}_n'/\bar{P}_n$	$\bar{P}_{n, osm}/\bar{P}_n$	Cumulative number fraction	Cumulative weight fraction
0.025	1.12	1.12	0.108	0.001
0.050	1.19	1.19	0.159	0.003
0.100	1.29	1.30	0.230	0.008
0.200	1.45	1.48	0.327	0.023
0.300	1.59	1.66	0.398	0.040
0.400	1.72	1.83	0.455	0.060
0.500	1.85	2.01	0.502	0.081
0.600	1.96	2.19	0.543	0.104
0.700	2.07	2.38	0.579	0.127
0.800	2.18	2.57	0.611	0.151
0.900	2.29	2.77	0.639	0.175
1.000	2.39	2.98	0.664	0.199
1.500	2.85	4.18	0.761	0.318
2.000	3.26	5.69	0.824	0.428

$m = 3$ ,  $m = 1$  (Schulz-Zimm), and Wesslau type distributions, respectively. Since the experimental errors involved in measuring  $\bar{M}_n$  values of disperse distributions in the molecular weight range  $10^4$ – $10^5$  is certainly as great as 10%, the generalized exponential distribution, having an  $m$  value of 3, appears to introduce a minimum amount of error when applied to disperse distributions.

It is important to note that  $(\bar{P}_n'/\bar{P}_n)_q$  as a function of  $\bar{P}_w/\bar{P}_n$  exhibits a maximum for the generalized exponential distribution when the  $m$  parameter is equal to or greater than one. Hence for lower values of  $\bar{P}_w/\bar{P}_n$ ,

TABLE X  
Generalized Exponential Distribution,  $m = 1$  (Schulz-Zimm),  $\bar{P}_w/\bar{P}_n = 6$

Cut-off parameter $q$ or $j$	$\bar{P}_n'/\bar{P}_n$	$\bar{P}_{n, osm}/\bar{P}_n$	Cumulative number fraction	Cumulative weight fraction
0.025	1.25	1.25	0.203	0.002
0.050	1.34	1.35	0.258	0.004
0.100	1.46	1.47	0.321	0.008
0.200	1.62	1.65	0.393	0.019
0.300	1.71	1.78	0.439	0.030
0.400	1.82	1.90	0.473	0.042
0.500	1.89	2.00	0.500	0.054
0.600	1.96	2.10	0.523	0.067
0.700	2.01	2.19	0.543	0.080
0.800	2.06	2.27	0.560	0.092
0.900	2.10	2.35	0.575	0.105
1.000	2.14	2.43	0.589	0.118
1.500	2.27	2.78	0.641	0.182
2.000	2.33	3.09	0.676	0.245

TABLE XI  
Generalized Exponential Distribution,  $m = 1$  (Schulz-Zimm),  $\bar{P}_w/\bar{P}_n = 11$

Cut-off parameter $q$ or $j$	$\bar{P}_n'/\bar{P}_n$	$\bar{P}_{n, osm}/\bar{P}_n$	Cumulative number fraction	Cumulative weight fraction
0.025	1.22	1.23	0.184	0.001
0.050	1.29	1.29	0.225	0.003
0.100	1.36	1.37	0.268	0.006
0.200	1.44	1.46	0.315	0.013
0.300	1.49	1.52	0.344	0.020
0.400	1.53	1.57	0.365	0.027
0.500	1.56	1.62	0.381	0.035
0.600	1.58	1.65	0.395	0.042
0.700	1.60	1.68	0.406	0.050
0.800	1.62	1.71	0.416	0.057
0.900	1.63	1.74	0.425	0.065
1.000	1.64	1.76	0.433	0.072
1.500	1.66	1.86	0.464	0.110
2.000	1.66	1.94	0.485	0.147

i.e., values in the range of about 3-6, the error introduced by relating a mathematical distribution model to a real polymer distribution with part of the low ends removed can be greater for the generalized exponential type distribution than for Wesslau type distributions at a given  $q$  value. However, in actual practice, a given weight fraction is removed which reflects different  $q$  values for different distribution models considered. Inspection of Figures 1, 2, 17, and 18, indicate that upon extraction of a given weight fraction, the effective  $q$  value of a Wesslau distribution is always considerably larger than that for exponential distributions when  $m$  is equal to or

TABLE XII  
Generalized Exponential Distribution,  $m = 1$  (Schulz-Zimm),  $\bar{P}_w/\bar{P}_n = 21$

Cut-off parameter $q$ or $j$	$\bar{P}_n'/\bar{P}_n$	$\bar{P}_{n, osm}/\bar{P}_n$	Cumulative number fraction	Cumulative weight fraction
0.025	1.15	1.15	0.128	0.001
0.050	1.18	1.18	0.153	0.002
0.100	1.22	1.22	0.180	0.004
0.200	1.25	1.26	0.208	0.008
0.300	1.29	1.29	0.224	0.012
0.400	1.30	1.31	0.236	0.016
0.500	1.31	1.32	0.245	0.020
0.600	1.31	1.34	0.253	0.024
0.700	1.32	1.36	0.259	0.028
0.800	1.32	1.36	0.265	0.033
0.900	1.32	1.37	0.270	0.037
1.000	1.32	1.38	0.274	0.041
1.500	1.32	1.41	0.291	0.062
2.000	1.32	1.44	0.303	0.083

TABLE XIII  
Generalized Exponential Distribution,  $m = 3$ ,  $\bar{P}_w/\bar{P}_n = 6$

Cut-off parameter $q$ or $j$	$\bar{P}_n'/\bar{P}_n$	$\bar{P}_{n, osm}/\bar{P}_n$	Cumulative number fraction	Cumulative weight fraction
0.025	1.22	1.22	0.180	0.001
0.050	1.29	1.29	0.220	0.003
0.100	1.35	1.36	0.265	0.006
0.200	1.44	1.45	0.313	0.013
0.300	1.49	1.52	0.343	0.020
0.400	1.53	1.57	0.365	0.028
0.500	1.56	1.62	0.382	0.036
0.600	1.58	1.66	0.397	0.044
0.700	1.60	1.69	0.409	0.052
0.800	1.62	1.73	0.421	0.060
0.900	1.63	1.76	0.430	0.069
1.000	1.64	1.78	0.439	0.077
1.500	1.67	1.91	0.475	0.121
2.000	1.67	2.01	0.501	0.167

greater than 1. For example, a rejection process, described by eq. (5), removing 6.6 and 7.0% of the low ends of a Wesslau and Schulz-Zimm distribution, having  $\bar{P}_w/\bar{P}_n$  ratios of 6, results in  $\bar{P}_n'/\bar{P}_n$  ratios of 1.5 and 1.3, respectively, when the ratio of the volume of the concentrated phase to the volume of the dilute phase is 0.001. Hence logarithmic normal type distributions are generally poor models for disperse polymer distributions having a fraction of the low ends removed. In addition, it will be shown in part II of this series<sup>6</sup> that a high molecular weight cut-off value mathe-

TABLE XIV  
Generalized Exponential Distribution,  $m = 3$ ,  $\bar{P}_w/\bar{P}_n = 11$

Cut-off parameter $q$ or $j$	$\bar{P}_n'/\bar{P}_n$	$\bar{P}_{n, osm}/\bar{P}_n$	Cumulative number fraction	Cumulative weight fraction
0.025	1.15	1.15	0.132	0.001
0.050	1.19	1.19	0.159	0.002
0.100	1.23	1.23	0.187	0.004
0.200	1.27	1.28	0.216	0.008
0.300	1.29	1.31	0.234	0.013
0.400	1.30	1.33	0.247	0.017
0.500	1.32	1.35	0.257	0.022
0.600	1.32	1.36	0.265	0.026
0.700	1.33	1.37	0.272	0.031
0.800	1.34	1.39	0.278	0.036
0.900	1.34	1.40	0.284	0.040
1.000	1.34	1.41	0.289	0.045
1.500	1.34	1.44	0.308	0.069
2.000	1.34	1.47	0.322	0.094

TABLE XV  
Generalized Exponential Distribution,  $m = 3$ ,  $\bar{P}_w/\bar{P}_n = 21$

Cut-off parameter $q$ or $j$	$\bar{P}_n'/n$	$\bar{P}_{n, osm}/\bar{P}_n$	Cumulative number fraction	Cumulative weight fraction
0.025	1.09	1.09	0.083	0.000 <sub>6</sub>
0.050	1.11	1.11	0.099	0.001
0.100	1.13	1.13	0.115	0.002
0.200	1.15	1.15	0.132	0.005
0.300	1.16	1.16	0.141	0.007
0.400	1.16	1.17	0.149	0.010
0.500	1.17	1.18	0.154	0.012
0.600	1.17	1.19	0.158	0.015
0.700	1.17	1.20	0.162	0.017
0.800	1.18	1.20	0.166	0.020
0.900	1.18	1.20	0.169	0.022
1.000	1.18	1.21	0.171	0.025
1.500	1.18	1.22	0.182	0.038
2.000	1.18	1.23	0.189	0.050

matically prohibits disperse high molecular weight polymers from being described by logarithmic type distributions.

When the number-average molecular weight is evaluated from osmotic pressure measurements, there is a procedural error due to the smaller molecular species diffusing or reflecting a permeability through the membrane.<sup>9</sup> The cut-off limit for most useful membranes is generally in the range of 10,000–20,000, depending on the membrane type and the conditioning it has received. Tables I–XXI and Figures 8–12 show the pro-

TABLE XVI  
Generalized Exponential Distribution,  $m = 1 + z$  (Tung),  $\bar{P}_w/\bar{P}_n = 6$

Cut-off parameter $q$ or $j$	$\bar{P}_n'/\bar{P}_n$	$\bar{P}_{n, \text{osm}}/\bar{P}_n$	Cumulative number fraction	Cumulative weight fraction
0.025	1.25	1.25	0.200	0.002
0.050	1.33	1.34	0.251	0.003
0.100	1.44	1.45	0.310	0.008
0.200	1.57	1.60	0.375	0.017
0.300	1.67	1.72	0.417	0.028
0.400	1.74	1.81	0.448	0.038
0.500	1.80	1.90	0.473	0.050
0.600	1.86	1.98	0.494	0.061
0.700	1.90	2.05	0.512	0.073
0.800	1.94	2.12	0.528	0.085
0.900	1.97	2.18	0.542	0.096
1.000	2.00	2.24	0.554	0.108
1.500	2.10	2.52	0.603	0.168
2.000	2.13	2.76	0.637	0.228

TABLE XVII  
Generalized Exponential Distribution,  $m = 1 + a$  (Tung),  $\bar{P}_w/\bar{P}_n = 11$

Cut-off parameter $q$ or $j$	$\bar{P}_n'/\bar{P}_n$	$\bar{P}_{n, \text{osm}}/\bar{P}_n$	Cumulative number fraction	Cumulative weight fraction
0.025	1.21	1.21	0.177	0.001
0.050	1.27	1.27	0.215	0.003
0.100	1.34	1.34	0.257	0.006
0.200	1.41	1.43	0.300	0.012
0.300	1.46	1.49	0.327	0.019
0.400	1.52	1.53	0.347	0.026
0.500	1.52	1.57	0.362	0.033
0.600	1.54	1.60	0.375	0.040
0.700	1.55	1.63	0.386	0.047
0.800	1.57	1.65	0.395	0.054
0.900	1.58	1.68	0.404	0.061
1.000	1.58	1.70	0.411	0.068
1.500	1.60	1.79	0.440	0.104
2.000	1.60	1.85	0.461	0.139

cedural errors that can occur as a function of the type of distribution when the lower limit of the distribution is zero. For a polymer having a low molecular weight cut-off value, the error is decreased by the factor  $\bar{P}_n'/\bar{P}_n$  depending on the appropriate  $q$  and  $j$  parameters.

The results of Billmeyer and co-workers<sup>8</sup> (Table XXII) clearly demonstrate the procedural errors that can occur in osmotic pressure determinations. However, the results should be treated with some reservation, since he reports a change from  $1.27 \times 10^4$  to  $3.64 \times 10^4$  in the  $\bar{M}_n$  of sample 84 upon removal of 0.33 wt.-% of material, the value of  $3.64 \times 10^4$  being

TABLE XVIII  
Generalized Exponential Distribution,  $m = 1 + a$  (Tung),  $\bar{P}_w/\bar{P}_n = 21$

Cut-off parameter $q$ or $j$	$\bar{P}_n'/\bar{P}_n$	$\bar{P}_{n, \text{osm}}/\bar{P}_n$	Cumulative number fraction	Cumulative weight fraction
0.025	1.14	1.14	0.124	0.001
0.050	1.17	1.17	0.149	0.002
0.100	1.21	1.21	0.174	0.003
0.200	1.24	1.25	0.201	0.007
0.300	1.26	1.28	0.217	0.011
0.400	1.28	1.30	0.228	0.015
0.500	1.29	1.31	0.237	0.019
0.600	1.29	1.32	0.244	0.023
0.700	1.30	1.33	0.250	0.027
0.800	1.30	1.34	0.256	0.031
0.900	1.30	1.35	0.261	0.036
1.000	1.31	1.36	0.265	0.040
1.500	1.31	1.39	0.281	0.060
2.000	1.31	1.41	0.293	0.080

TABLE XIX  
Generalized Exponential Distribution,  $m = 0.2$ ,  $\bar{P}_w/\bar{P}_n = 6$

Cut-off parameter $q$ or $j$	$\bar{P}_n'/\bar{P}_n$	$\bar{P}_{n, \text{osm}}/\bar{P}_n$	Cumulative number fraction	Cumulative weight fraction
0.025	1.08	1.08	0.071	0.001
0.050	1.15	1.16	0.135	0.003
0.100	1.29	1.31	0.236	0.011
0.200	1.55	1.60	0.375	0.031
0.300	1.78	1.89	0.470	0.055
0.400	2.00	2.17	0.540	0.080
0.500	2.21	2.47	0.595	0.105
0.600	2.41	2.77	0.639	0.129
0.700	2.61	3.08	0.675	0.153
0.800	2.80	3.40	0.706	0.175
0.900	2.99	3.73	0.732	0.198
1.000	3.17	4.06	0.754	0.219
1.500	4.06	5.92	0.831	0.314
2.000	4.90	8.06	0.876	0.392

in good agreement with the  $\bar{M}_n$  value of  $3.17 \times 10^4$  determined osmotically. For this to be true, the removed fraction would have to have an  $\bar{M}_n$  of about 60. Since the membranes employed generally have a molecular weight cut-off between 10,000 and 20,000, it is very difficult to believe that the measurements on the extracted material are valid. On the basis of the above distribution models, assuming that the 0.33% extracted material represents a sharp cut-off, the  $\bar{M}_n'$  (extracted) should have a value in the range 15,000–17,000 as an upper limit. Hence a more realistic interpretation is that the true  $\bar{M}_n'$  is in the range of 10,000–20,000, and that the error

TABLE XX  
Generalized Exponential Distribution,  $m = 0.2$ ,  $\bar{P}_w/\bar{P}_n = 11$

Cut-off parameter $q$ or $j$	$\bar{P}_n'/\bar{P}_n$	$\bar{P}_{n, osm}/\bar{P}_n$	Cumulative number fraction	Cumulative weight fraction
0.025	1.19	1.19	0.159	0.002
0.050	1.32	1.32	0.244	0.005
0.100	1.53	1.55	0.354	0.013
0.200	1.87	1.94	0.483	0.032
0.300	2.17	2.29	0.564	0.051
0.400	2.45	2.63	0.620	0.071
0.500	2.70	2.97	0.663	0.090
0.600	2.94	3.30	0.670	0.109
0.700	3.17	3.63	0.725	0.126
0.800	3.39	3.96	0.748	0.144
0.900	3.61	4.30	0.767	0.160
1.000	3.82	4.63	0.784	0.176
1.500	4.79	6.37	0.843	0.248
2.000	5.67	8.20	0.878	0.308

TABLE XXI  
Generalized Exponential Distribution,  $m = 0.2$ ,  $\bar{P}_w/\bar{P}_n = 21$

Cut-off parameter $q$ or $j$	$\bar{P}_n'/\bar{P}_n$	$\bar{P}_{n, osm}/\bar{P}_n$	Cumulative number fraction	Cumulative weight fraction
0.025	1.33	1.34	0.252	0.002
0.050	1.51	1.52	0.343	0.006
0.100	1.79	1.81	0.448	0.013
0.200	2.11	2.16	0.537	0.025
0.300	2.53	2.65	0.623	0.045
0.400	2.82	3.00	0.667	0.060
0.500	3.09	3.33	0.700	0.075
0.600	3.33	3.65	0.726	0.089
0.700	3.55	3.95	0.747	0.102
0.800	3.76	4.24	0.764	0.115
0.900	3.95	4.53	0.779	0.127
1.000	4.14	4.81	0.792	0.139
1.500	4.93	6.11	0.836	0.193
2.000	5.56	7.32	0.863	0.239

TABLE XXII  
Molecular Weight of Polyethylene Determined by Osmometry and Cryoscopy

Sample	$\bar{M}_n$ , Osmometry	$\bar{M}_n$ , Cryoscopy
75	30,300	10,700
76	26,600	13,300
77	31,400	19,100
84	31,700	12,700
85		11,500



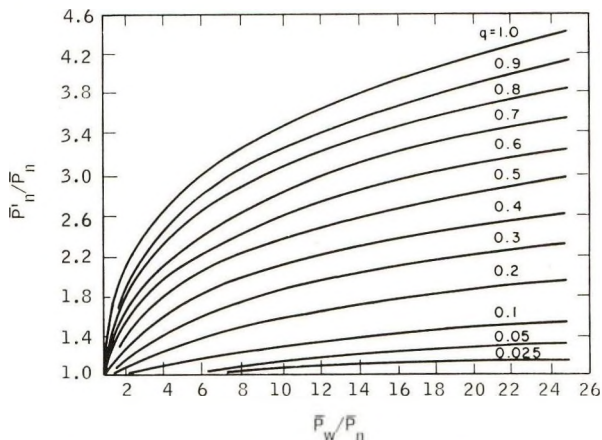


Fig. 3. Effect of a low molecular weight cut-off on the number average of the distribution. Wesslau type.

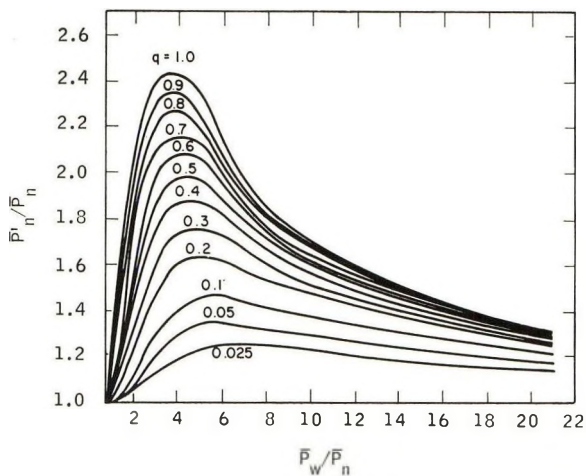


Fig. 4. Effect of a low molecular weight cut-off on the number average of the distribution. Schulz-Zimm type.

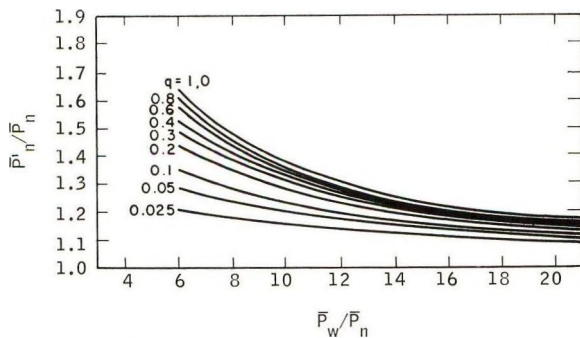


Fig. 5. Effect of a low molecular weight cut-off on the number average of the distribution. Generalized exponential type,  $m = 3$ .

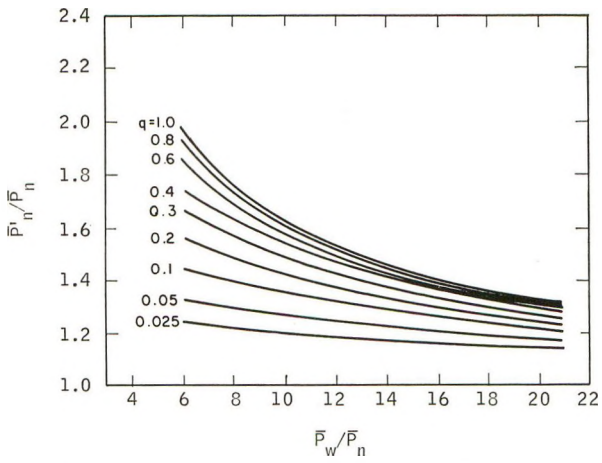


Fig. 6. Effect of a low molecular weight cut-off on the number average of the distribution. Tung type.

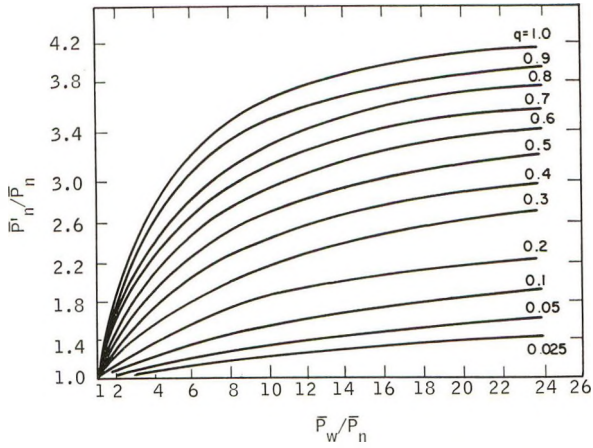


Fig. 7. Effect of a low molecular weight cut-off on the number average of the distribution. Generalized exponential type,  $m = 0.2$ .

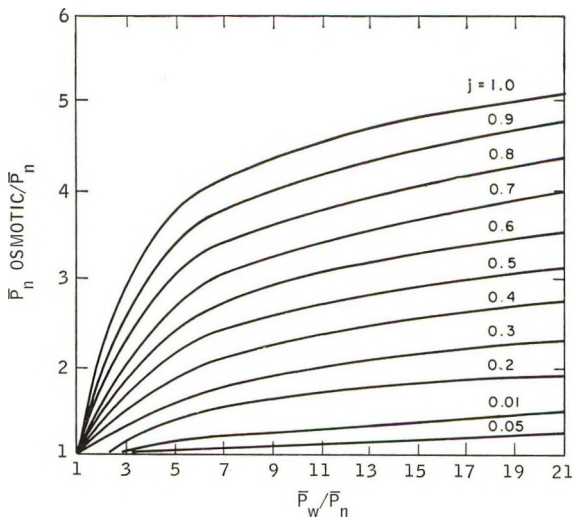


Fig. 8. Effect of the membrane cut-off value on the number average determined osmotically. Wesslau distribution.

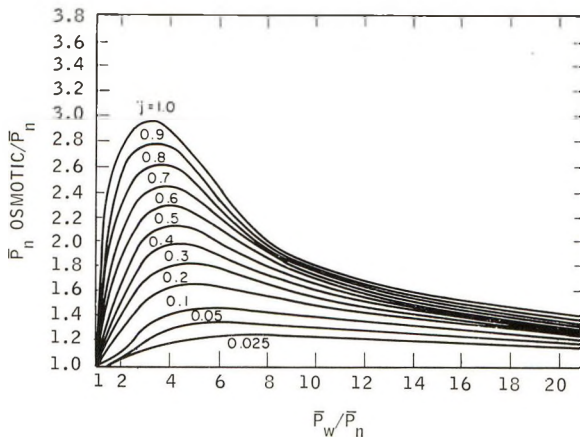


Fig. 9. Effect of the membrane cut-off value on the number average determined osmotically. Schulz-Zimm distribution.

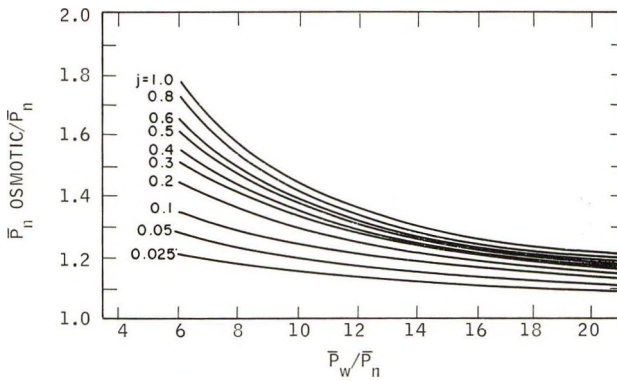


Fig. 10. Effect of the membrane cut-off value on the number average determined osmotically. Generalized exponential distribution,  $m = 3$ .

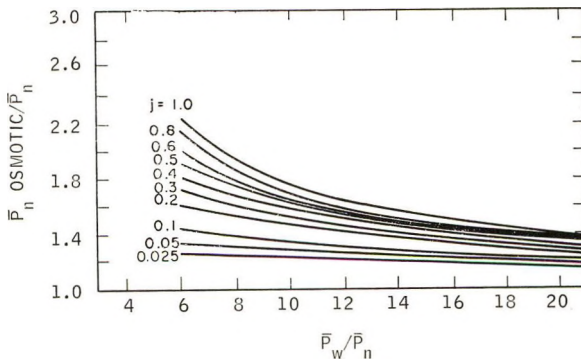


Fig. 11. Effect of the membrane cut-off value on the number average determined osmotically. Tung distribution.

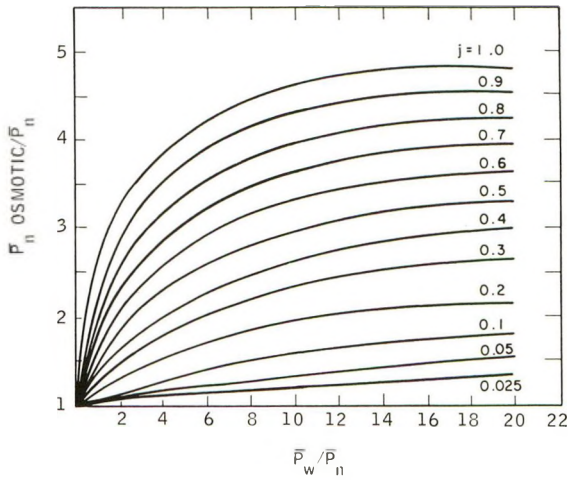


Fig. 12. Effect of the membrane cut-off value on the number average determined osmotically. Generalized exponential distribution,  $m = 0.2$ .

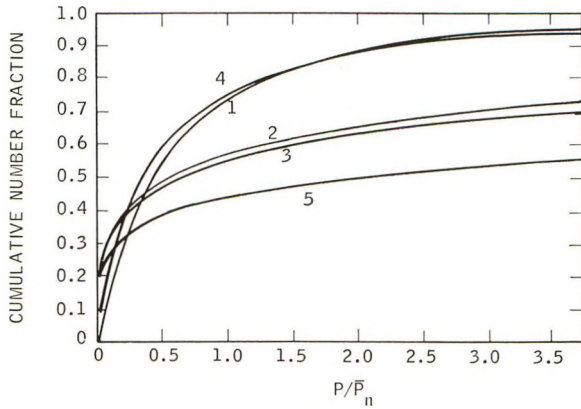


Fig. 13. Cumulative number fraction for (1) Wesslau, (2) Schulz-Zimm, (3) Tung, and generalized exponential distributions (4) with  $m = 0.2$  and (5) with  $m = 3$ .  $P_w/P_n = 6$ .

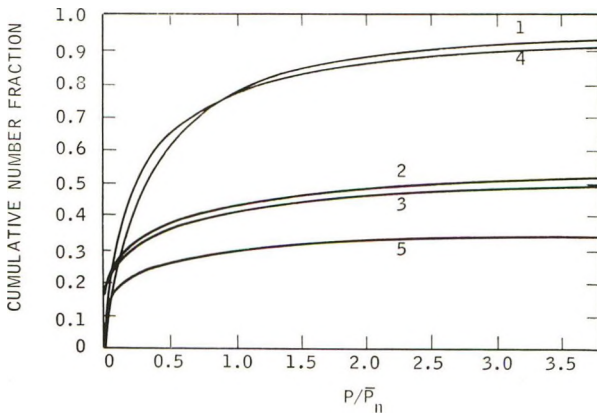


Fig. 14. Cumulative number fraction for (1) Wesslau, (2) Schulz-Zimm, (3) Tung, and generalized exponential distributions (4) with  $m = 0.2$  and (5) with  $m = 3$ .  $P_w/P_n = 11$ .

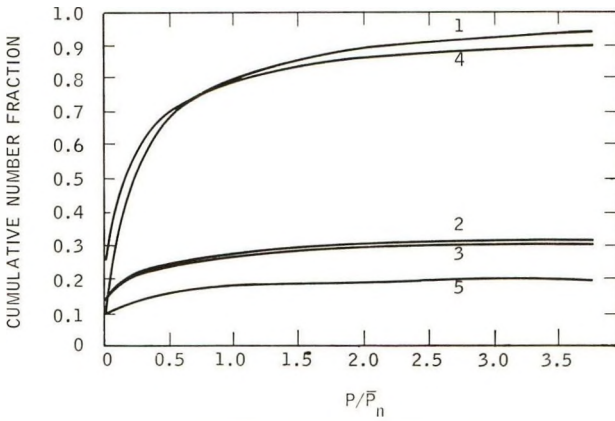


Fig. 15. Cumulative number fraction for (1) Wesslau, (2) Schulz-Zimm, (3) Tung, and generalized exponential distributions (4) with  $m = 0.2$  and (5) with  $m = 3$ .  $P_w/P_n = 21$ .

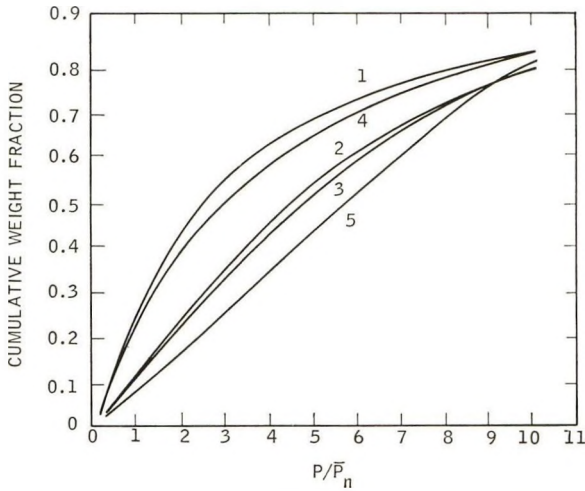


Fig. 16. Cumulative weight fraction for (1) Wesslau, (2) Schulz-Zimm, (3) Tung, and generalized exponential with (4)  $m = 0.2$  and (5)  $m = 3$ .  $P_w/P_n = 6$ .

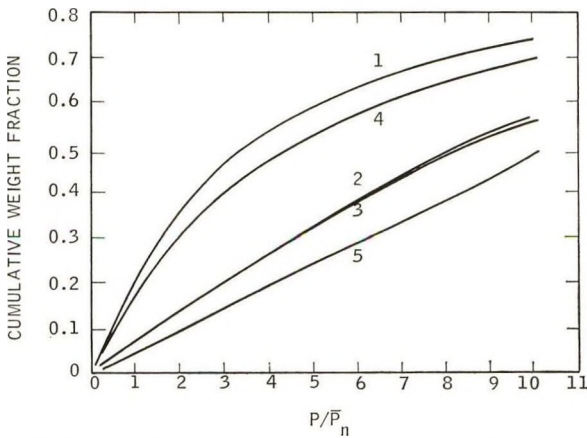


Fig. 17. Cumulative weight fraction for (1) Wesslau, (2) Schulz-Zimm, (3) Tung, and generalized exponential distributions (4) with  $m = 0.2$  and (5) with  $m = 3$ .  $P_w/P_n = 11$ .

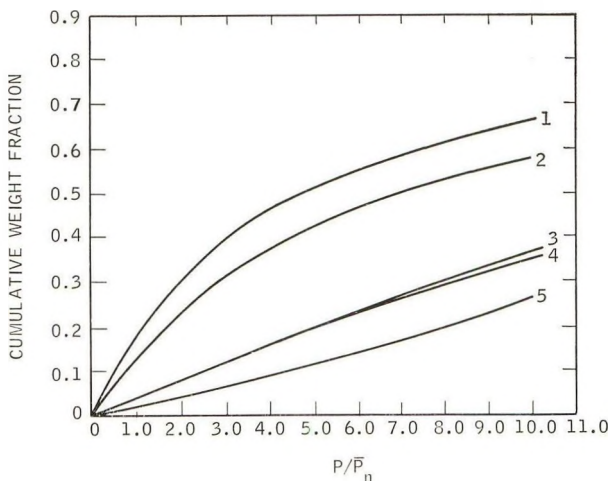


Fig. 18. Cumulative weight fraction for (1) Wesslau, (2) Schulz-Zimm, (3) Tung, and generalized exponential distributions (4) with  $m = 0.2$  and (5) with  $m = 3$ .  $P_w/P_n = 21$ .

in using cryoscopy, boiling point elevation, or vapor phase osmometry in this range of molecular weights can be rather large. In addition, the calculations show that for valid evaluation of  $\bar{M}_n'$  from osmotic pressure measurements on rather disperse molecular weight distributions, the number-average molecular weight should in general be at least five times the effective cut-off molecular weight, i.e., about  $10^5$ .

### Conclusions

It is shown that logarithmic normal type distributions cannot be considered as useful models for disperse polymer distributions having a fraction of the low ends removed. The generalized exponential distribution model, however, can be a useful and valid representation.

The author wishes to express his gratitude to Dr. D. Poller and Mr. R. Kruse for helpful discussions and to Mr. H. Oakley and Miss D. Mahon for performing the computer calculations.

### References

1. Muus, L. T., and W. H. Stockmayer, quoted by F. W. Billmeyer, Jr., in *Textbook of Polymer Chemistry*, Interscience, New York-London, 1962.
2. Lansing, W. D., and E. O. Kraemer, *J. Am. Chem. Soc.*, **57**, 1368 (1935).
3. Wesslau, H., *Makromol. Chem.*, **20**, 111 (1956).
4. Schulz, G. V., *Z. Phys. Chem.*, **B43**, 25 (1939); B. H. Zimm, *J. Chem. Phys.*, **16**, 1093 (1948).
5. Tung, E. H., *J. Polymer Sci.*, **20**, 495 (1956).
6. Kotliar, A. M., *J. Polymer Sci.*, **A2**, 4321 (1964).
7. Flory, P. J., *J. Chem. Phys.*, **12**, 425 (1944).
8. Kokle, V., F. W. Billmeyer Jr., L. T. Muus, and E. J. Newitt, *J. Polymer Sci.*, **62**, 251 (1962).
9. Staverman, A. J., *Rec. Trav. Chim.*, **70**, 345 (1951); **71**, 673 (1952).

### Résumé

Il est d'une importance considérable de pouvoir décrire la distribution des poids moléculaires d'un polymère par une expression mathématique. Puisque les différentes moyennes moléculaires d'une distribution sont obtenues à partir d'une sommation, le modèle général demande une expression analytique de la distribution différentielle et une intégrale définie correspondante à des limites zéro et l'infini. En général, de vraies distributions de polymères n'entrant pas dans ces limites d'intégration et une erreur, qui peut être très grande, est alors introduite. Si l'erreur dans les différentes moyennes de poids moléculaires, due aux changements des limites d'intégration, est de l'ordre de grandeur ou plus petite que l'erreur faite en général dans l'évaluation expérimentale de la moyenne, on peut considérer la fonction de distribution comme applicable du point de vue pratique. De plus, le modèle envisagé devra remplir les conditions requises par les données expérimentales telles que: les cinétiques de polymérisation, les effets de dégradation et de ramification, les données de fractionnement, les effets de polymérisation et le maximum de distribution différentielle. Il faut également un accord avec le comportement rhéologique, basé sur les théories courantes. Les critères de limites d'intégration ont été appliqués aux distributions de type normal logarithmique, par exemple, Wesslau, et aux distributions de type général exponentiel, par ex. Schulz-Bimm et Tung. Les résultats montrent que les distributions de type normal et logarithmique ne peuvent pas être considérés comme des modèles utiles, tandis que les distributions de type exponentiel généralisé peuvent être des représentations valables et utiles.

### Zusammenfassung

Es ist von beträchtlicher praktischer Bedeutung, die Molekulargrößenverteilung eines Polymermaterials durch einen handlichen mathematischen Ausdruck beschreiben zu können. Da die verschiedenen Molekularmittel einer Verteilung aus einer Summierung erhalten werden, verlangen die üblichen Modelle einen analytischen Ausdruck für die differentielle Verteilung und ein damit korrespondierendes bestimmtes Integral, im allgemeinen mit den Grenzen Null und Unendlich. Im allgemeinen erfüllen reale Polymerverteilungen diese Grenzen nicht, wodurch ein möglicherweise sehr grosser Fehler auftritt. Wenn der Fehler in den verschiedenen Molekulargewichtsmitteln infolge Änderung der Integrationsgrenzen in der Grössenordnung oder kleiner als der allgemein bei experimenteller Ermittlung des Mittels auftretende Fehler ist, so kann die Verteilungsfunktion als praktisch anwendbar betrachtet werden. Ausserdem sollte das ausgewählte Modell dem Erfordernis genügen, bekannten experimentellen Verhältnissen wie: Polymerisationskinetik, Einfluss des statistischen Abbaus und Vernetzung, Fraktionierungsdaten und dem Einfluss der Polymerisation und der Verarbeitung auf die differentielle Verteilungsmaxima angepasst werden zu können. Es sollte sich auch dem rheologischen Verhalten aufgrund von gängigen Vorstellungen anpassen. Die Kriterien für die Integrationsgrenzen werden auf die logarithmische Normalverteilung, z.B. Wesslau, und auch verallgemeinerte Exponentialverteilungstypen, z.B. Schulz-Zimm und Tung angewandt. Die Ergebnisse zeigen, dass die logarithmische Normalverteilung nicht als brauchbares Modell angewandt werden kann, während die verallgemeinerten Exponentialverteilungen nützlich und gültig sind.

Received October 8, 1963

Revised December 12, 1963

## A Critical Evaluation of Mathematical Molecular Weight Distribution Models Proposed for Real Polymer Distributions. II. Effects of a High Molecular Weight Cut-Off Value

A. M. KOTLIAR,\* *Esso Research and Engineering Company,  
Linden, New Jersey*

### Synopsis

It is shown that logarithmic normal type distributions, e.g., Wesslau, cannot describe real polymer distributions having low and high molecular weight cut-off values. However, certain cases of the generalized exponential type distribution do appear to be useful and valid models.

### Introduction

Part I of this series<sup>1</sup> has shown that a low molecular weight cut-off value seriously affects the normalization of logarithmic normal distributions of the Wesslau type. However, with certain cases of the generalized exponential type distributions, the normalization remains relatively unaffected, i.e. only about 10% of the total number of molecules are lost. Since physically real polymer distributions have high molecular weight cut-off values, it is important to know to what extent the change of the upper integration limit of infinity to some multiple of the weight-average molecular weight affects the assumed distribution model.

### Theory

All physically real polymer distributions having no gel component have a high molecular cut-off value which generally only affects the higher molecular weight averages, since the number fraction of molecules of size  $P = n\bar{P}_w$  is very small and, therefore, the contribution to the number average is small, i.e.,

$$\sum_{nP_w}^{\infty} \frac{W(P)}{P} \ll \sum_{qP_n}^{nP_w} \frac{W(P)}{P} \quad \begin{matrix} n > 1 \\ q < 1 \end{matrix} \quad (1)$$

Similarly, when  $n$  has a value  $n > 5$  and when  $q < 1$ ,

\* Present address: Central Research Laboratory, Allied Chemical Corporation, Morristown, New Jersey.



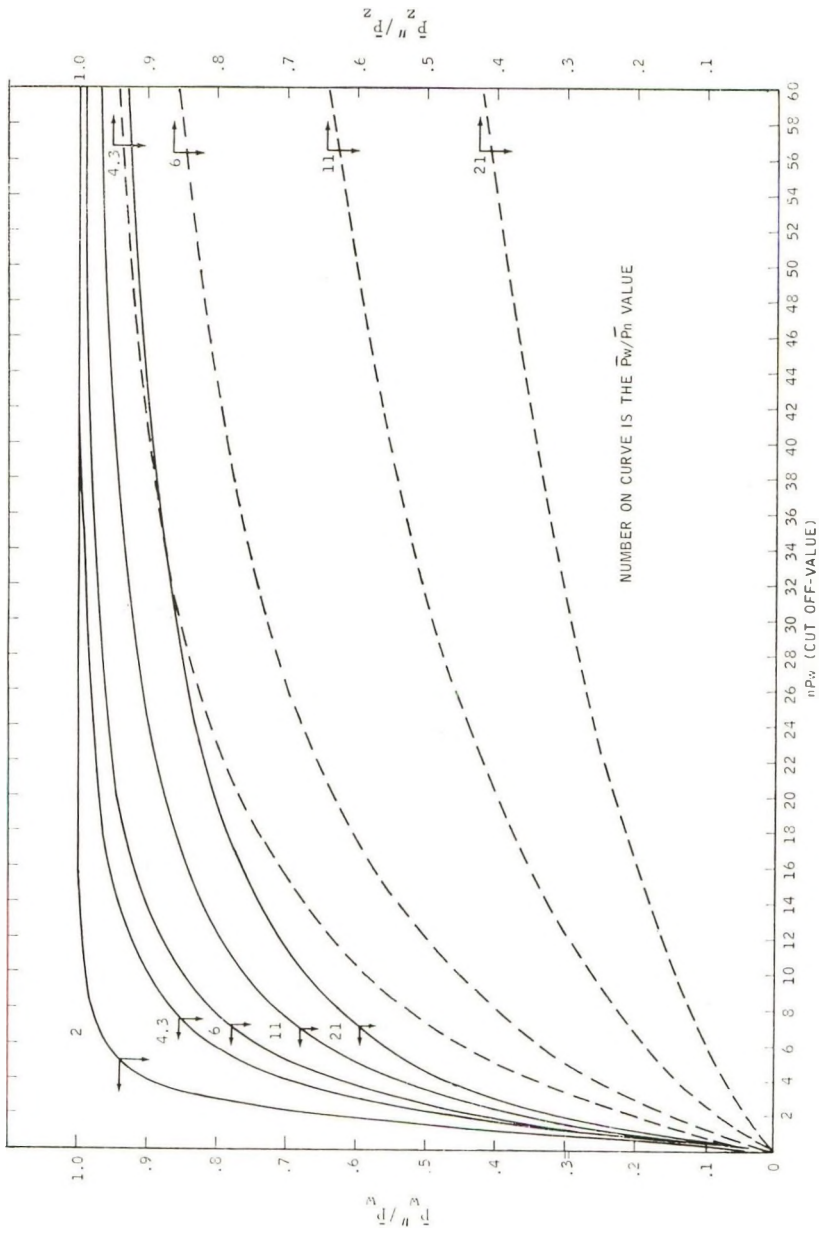


Fig. 1. Effect of high molecular cut-off value on the  $\bar{P}_w^1$  and  $\bar{P}_z^1$  for a Wesslau distribution.

$$\sum_{q=1}^{n\bar{P}_w} W(P) \cong 1 \quad (2)$$

with an error generally less than 2%.

The effective value for  $n\bar{P}_w$  unfortunately is difficult to evaluate. We can safely assume that it is less than  $2 \times 10^5$  and consider the resulting changes in  $\bar{P}_w''$ ,  $\bar{P}_z''$ , and  $\bar{P}_{z+1}''$  as a function of  $n\bar{P}_w$ ,  $\bar{P}_w/\bar{P}_n$ , and the distribution models given by eqs. (1) and (2) in part I. The double primes will be used to indicate the value of the respective molecular size average with a cut-off value. These averages will be defined by

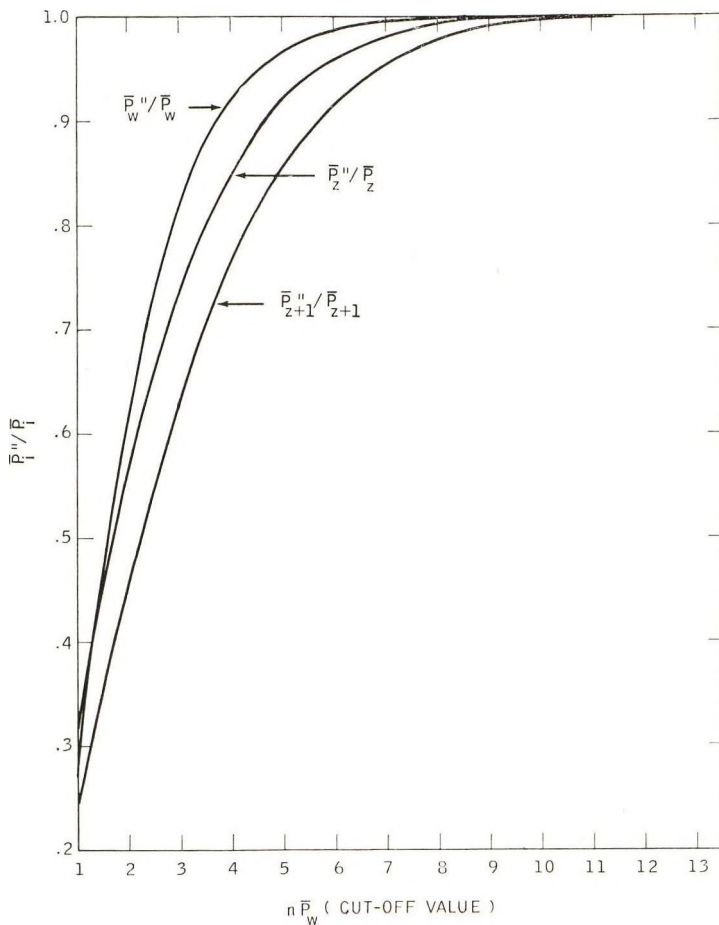


Fig. 2. Effect of high molecular weight cut-off value on the  $\bar{P}_w$ ,  $\bar{P}_z$ , and  $\bar{P}_{z+1}$  for a Schulz-Zimm distribution with  $\bar{P}_w/\bar{P}_n = 21$ .

TABLE I  
Effect of a High Molecular Weight Cut-Off on the Weight-, Z-, and Z + 1-Average  
Molecular Weights; Schulz-Zimm Distribution

Case	$n\bar{P}_w$	$\Sigma W(P)$	$\bar{P}_w''/\bar{P}_w$	$\bar{P}_z''/\bar{P}_z$	$P_{z+1}''/\bar{P}_{z+1}$
Case 1:					
$\bar{P}_w/\bar{P}_n = 2$	1	0.599	0.328	0.445	0.372
	2	0.910	0.765	0.746	0.657
	3	0.983	0.939	0.906	0.844
	4	0.997	0.986	0.971	0.941
	5	0.999	0.997	0.993	0.981
	6	1.000	1.000	0.998	0.995
	7	1.000	1.000	1.000	0.999
	8	1.000	1.000	1.000	1.000
Case 2:					
$\bar{P}_w/\bar{P}_n = 3$	1	0.612	0.304	0.386	0.313
	2	0.889	0.696	0.665	0.567
	3	0.970	0.892	0.840	0.754
	4	0.992	0.966	0.932	0.876
	5	0.997	0.990	0.974	0.943
	6	0.999	0.997	0.991	0.977
	7	0.999	0.999	0.997	0.991
	8	0.999 (1.000 <sup>a</sup> )	1.000	0.999	0.997
	9	0.999 (1.000 <sup>a</sup> )	1.000	1.000	0.999
	10	0.999 (1.000 <sup>a</sup> )	1.000	1.000	1.000
Case 3:					
$\bar{P}_w/\bar{P}_n = 4.33$	1	0.618	0.292	0.358	0.286
	2	0.878	0.661	0.624	0.523
	3	0.962	0.863	0.801	0.706
	4	0.987	0.950	0.905	0.834
	5	0.994	0.982	0.958	0.914
	6	0.997	0.994	0.983	0.959
	7	0.997	0.998	0.993	0.982
	8	0.997	0.999	0.998	0.992
	9	0.998	1.000	0.999	0.997
	10	0.998 (1.000 <sup>a</sup> )	1.000	1.000	0.999
	11	0.998 (1.000 <sup>a</sup> )	1.000	1.000	1.000
Case 4:					
$\bar{P}_w/\bar{P}_n = 6$	1	0.621	0.284	0.342	0.271
	2	0.872	0.642	0.600	0.498
	3	0.956	0.846	0.778	0.678
	4	0.984	0.939	0.887	0.808
	5	0.992	0.977	0.947	0.894
	6	0.995	0.992	0.976	0.945
	8	0.996	0.997	0.990	0.974
	9	0.996 (1.000 <sup>a</sup> )	0.999	0.996	0.988
	10	0.996 (1.000 <sup>a</sup> )	1.000	0.998	0.995
	11	0.996 (1.000 <sup>a</sup> )	1.000	0.999	0.998
	12	0.996 (1.000 <sup>a</sup> )	1.000	1.000	0.999
	13	0.996 (1.000 <sup>a</sup> )	1.000	1.000	1.000

(continued)

TABLE I (continued)

Case	$n\bar{P}_w$	$\Sigma W(P)$	$\bar{P}_w''/\bar{P}_u$	$\bar{P}_z''/\bar{P}_z$	$\bar{P}_z''_{+1}/\bar{P}_z_{+1}$
Case 5:					
$\bar{P}_w/\bar{P}_n = 11$	1	0.624	0.276	0.325	0.255
	2	0.865	0.620	0.574	0.472
	3	0.950	0.826	0.751	0.647
	4	0.979	0.926	0.865	0.778
	5	0.989	0.970	0.932	0.870
	6	0.992	0.988	0.967	0.928
	7	0.994	0.995	0.985	0.962
	8	0.994	0.998	0.994	0.981
	9	0.994	0.999	0.997	0.991
	10	0.994 (1.000 <sup>a</sup> )	1.000	0.999	0.996
	11	0.994 (1.000 <sup>a</sup> )	1.000	1.000	0.998
	12	0.994 (1.000 <sup>a</sup> )	1.000	1.000	0.999
	13	0.994 (1.000 <sup>a</sup> )	1.000	1.000	1.000
Case 6:					
$\bar{P}_w/\bar{P}_n = 21$	1	0.625	0.272	0.316	0.247
	2	0.861	0.609	0.561	0.458
	3	0.946	0.814	0.737	0.630
	4	0.976	0.918	0.853	0.762
	5	0.987	0.965	0.923	0.856
	6	0.991	0.986	0.962	0.917
	7	0.992	0.994	0.982	0.955
	8	0.992	0.998	0.992	0.977
	9	0.993	0.999	0.996	0.988
	10	0.993	1.000	0.998	0.994
	11	0.993 (1.000 <sup>a</sup> )	1.000	0.999	0.997
	12	0.993 (1.000 <sup>a</sup> )	1.000	1.000	0.999
	13	0.993 (1.000 <sup>a</sup> )	1.000	1.000	1.000

<sup>a</sup> Error due to change in limits of 1 to 0 with  $\bar{P}_w$  normalized at 55.

TABLE II

Effect of a High Molecular Weight Cut-Off on the Weight-, Z-, and Z + 1-Average Molecular Weights; Generalized Exponential Distribution,  $m = 3.0$

Case	$n\bar{P}_w$	$\Sigma W(P)$	$\bar{P}_w''/\bar{P}_w$	$\bar{P}_z''/\bar{P}_z$	$\bar{P}_z''_{+1}/\bar{P}_z_{+1}$
Case 1:					
$\bar{P}_w/\bar{P}_n = 6$	1	0.544	0.284	0.478	0.448
	2	0.921	0.823	0.854	0.821
	3	0.995	0.993	0.991	0.986
	4	0.997 (1.000 <sup>a</sup> )	1.000	1.000	1.000
Case 2:					
$\bar{P}_w/\bar{P}_n = 11$	1	0.546	0.279	0.467	0.436
	2	0.914	0.806	0.840	0.805
	3	0.993	0.990	0.988	0.981
	4	0.996 (1.000 <sup>a</sup> )	1.000	1.000	1.000
Case 3:					
$\bar{P}_w/\bar{P}_n = 21$	1	0.547	0.276	0.461	0.430
	2	0.910	0.797	0.832	0.797
	3	0.992	0.989	0.986	0.978
	4	0.996 (1.000 <sup>a</sup> )	1.000	1.000	1.000

<sup>a</sup> Error due to change in limits of 1 to 0 with  $\bar{P}_w$  normalized at 55.

TABLE III  
 Effect of a High Molecular Weight Cut-Off on the Weight-,  $Z$ -, and  $Z + 1$ -Average  
 Molecular Weights; Wesslau Distribution

Case	$n\bar{P}_w$	$\Sigma W(P)$	$\bar{P}_w''/\bar{P}_w$	$\bar{P}_z''/\bar{P}_z$	$\frac{P_z''_{+1}/}{\bar{P}_z_{+1}}$
Case 1:					
$\bar{P}_w/\bar{P}_n = 2$	1	0.665	0.343	0.315	0.044
	2	0.895	0.663	0.513	0.078
	3	0.959	0.818	0.648	0.106
	4	0.981	0.895	0.740	0.128
	5	0.991	0.936	0.806	0.147
	6	0.995	0.959	0.852	0.162
	7	0.997	0.973	0.886	0.174
	8	0.998	0.981	0.911	0.185
	9	0.999	0.987	0.930	0.194
	10	0.999	0.991	0.944	0.201
	15	1.000	0.998	0.980	0.225
	20	1.000	0.999	0.991	0.236
	30	1.000	1.000	0.998	0.245
	60	1.000	1.000	1.000	0.250
Case 2:					
$\bar{P}_w/\bar{P}_n = 4.33$	1	0.730	0.275	0.128	0.002
	2	0.881	0.488	0.220	0.004
	3	0.935	0.620	0.294	0.005
	4	0.960	0.706	0.357	0.006
	5	0.974	0.766	0.410	0.008
	6	0.982	0.810	0.456	0.009
	7	0.987	0.842	0.496	0.010
	8	0.990	0.867	0.532	0.011
	9	0.992	0.887	0.564	0.012
	10	0.994	0.903	0.592	0.013
	15	0.998	0.949	0.699	0.017
	20	0.999	0.969	0.769	0.021
	30	1.000	0.986	0.852	0.026
	60	1.000	0.997	0.944	0.036
Case 3:					
$\bar{P}_w/\bar{P}_n = 6$	1	0.749	0.254	0.089	0.000 <sub>6</sub>
	2	0.882	0.441	0.155	0.001
	3	0.931	0.561	0.210	0.001
	4	0.955	0.644	0.258	0.002
	5	0.968	0.704	0.300	0.002
	6	0.977	0.749	0.337	0.002
	7	0.982	0.784	0.370	0.003
	8	0.986	0.812	0.400	0.003
	9	0.988	0.835	0.428	0.003
	10	0.990	0.854	0.454	0.004
	15	0.995	0.912	0.555	0.005
	20	0.997	0.942	0.628	0.006
	30	0.998	0.969	0.725	0.008
	60	0.999 (1.000 <sup>a</sup> )	0.992	0.861	0.013

(continued)

TABLE III (continued)

Case	$n\bar{P}_w$	$\Sigma W(P)$	$\bar{P}_w''/\bar{P}_w$	$\bar{P}_z''/\bar{P}_z$	$\bar{P}_{z+1}''/\bar{P}_{z+1}$
Case 4:					
$\bar{P}_w/\bar{P}_n = 11$	1	0.772	0.221	0.046	0.000
	2	0.879	0.373	0.082	0.000
	3	0.921	0.475	0.113	0.000
	4	0.942	0.549	0.140	0.000
	5	0.955	0.605	0.165	0.000
	6	0.963	0.649	0.188	0.000
	7	0.968	0.686	0.209	0.000
	8	0.972	0.715	0.229	0.000
	9	0.975	0.741	0.247	0.000
	10	0.978	0.762	0.265	0.000
	15	0.984	0.835	0.339	0.000
	20	0.986	0.877	0.398	0.000
	30	0.988	0.923	0.488	0.001
	60	0.989 (1.000 <sup>a</sup> )	0.969	0.646	0.001 <sub>5</sub>
Case 5:					
$\bar{P}_w/\bar{P}_n = 21$	1	0.776	0.193	0.023	0.000
	2	0.864	0.318	0.042	0.000
	3	0.899	0.405	0.058	0.000
	4	0.918	0.469	0.073	0.000
	5	0.929	0.520	0.087	0.000
	6	0.937	0.562	0.100	0.000
	7	0.942	0.596	0.112	0.000
	8	0.946	0.625	0.123	0.000
	9	0.949	0.651	0.134	0.000
	10	0.951	0.673	0.145	0.000
	15	0.958	0.752	0.191	0.000
	20	0.961	0.801	0.230	0.000
	30	0.963	0.859	0.294	0.000
	60	0.965	0.930	0.423	0.000 <sub>1</sub>

<sup>a</sup> Error due to change in limits with  $\bar{P}_w$  normalized at 55.

$$P_i'' = \frac{\sum_{q=1}^{n\bar{P}_w} P^q W(P)}{\sum_{q=1}^{q\bar{P}_n} P^{i-1} W(P)} \cong \frac{\sum_{1}^{n\bar{P}_w} P^i W(P)}{\sum_{1}^{n\bar{P}_w} P^{i-1} W(P)} \quad (3)$$

The values for  $\bar{P}_w''/\bar{P}_w$ ,  $\bar{P}_z''/\bar{P}_z$ , and  $\bar{P}_{z+1}''/\bar{P}_{z+1}$  as a function of  $n\bar{P}_w$  are shown in Figures 1-3 and Tables I-V. As can be seen, the Wesslau distribution cannot be considered a useful model for polymers having a  $\bar{P}_w/\bar{P}_n > 2$  unless the molecular weight is very low. It is also important to note the large contribution to the  $\bar{P}_w$ ,  $\bar{P}_z$ , and  $\bar{P}_{z+1}$  averages made by the high molecular weight ends, which amount to less than 2 wt.-% of the distribution. However, we can conclude that the generalized exponential distribution models having  $m$  values of about 1 or greater appear to be good

TABLE IV  
Effect of a High Molecular Weight Cut-Off on the Weight-,  $Z_1$ , and  $Z + 1$ -Average  
Molecular Weights; Tung Distribution

Case	$n\bar{P}_w$	$\Sigma W(P)$	$\bar{P}_w''/\bar{P}_w$	$\bar{P}_z''/\bar{P}_z$	$\bar{P}_{z+1}''/\bar{P}_{z+1}$
Case 1:					
$\bar{P}_w/\bar{P}_n = 6$	1	0.609	0.287	0.367	0.301
	2	0.877	0.668	0.645	0.554
	3	0.963	0.877	0.827	0.745
	4	0.988	0.960	0.927	0.872
	5	0.994	0.989	0.973	0.944
	6	0.996	0.997	0.991	0.978
	7	0.996 (1.000 <sup>a</sup> )	0.999	0.997	0.992
	8	0.996 (1.000 <sup>a</sup> )	1.000	0.999	0.998
	9	0.996 (1.000 <sup>a</sup> )	1.000	1.000	0.999
	10	0.996 (1.000 <sup>a</sup> )	1.000	1.000	1.000
Case 2:					
$\bar{P}_w/\bar{P}_n = 11$	1	0.617	0.278	0.340	0.273
	2	0.868	0.636	0.601	0.504
	3	0.954	0.845	0.782	0.687
	4	0.982	0.940	0.892	0.819
	5	0.991	0.979	0.951	0.904
	6	0.993	0.993	0.980	0.954
	7	0.994	0.998	0.992	0.979
	8	0.994	0.999	0.997	0.991
	9	0.994	1.000	0.999	0.996
	10	0.994 (1.000 <sup>a</sup> )	1.000	1.000	0.999
	11	0.994 (1.000 <sup>a</sup> )	1.000	1.000	1.000
Case 3:					
$\bar{P}_w/\bar{P}_n = 21$	1	0.621	0.273	0.324	0.257
	2	0.863	0.617	0.575	0.476
	3	0.948	0.825	0.754	0.653
	4	0.988	0.926	0.869	0.785
	5	0.991	0.971	0.935	0.876
	6	0.992	0.989	0.970	0.933
	7	0.993	0.996	0.987	0.966
	8	0.993 (1.000 <sup>a</sup> )	0.999	0.994	0.984
	9	0.993 (1.000 <sup>a</sup> )	0.999	0.998	0.993
	10	0.993 (1.000 <sup>a</sup> )	1.000	0.999	0.997
	11	0.993 (1.000 <sup>a</sup> )	1.000	1.000	0.999
	12	0.993 (1.000 <sup>a</sup> )	1.000	1.000	1.000

<sup>a</sup> Error due to change in limits of 1 to 0 with  $\bar{P}_w$  normalized at 55.

models for polymers having high molecular weight cut-off point at reasonable values of  $n\bar{P}_w$  for  $\bar{P}_w$  as high as 10.<sup>4</sup>

### Conclusions

On the basis of random degradation effects<sup>2</sup> and a knowledge of the effects of low and high molecular weight cut-off values, Wesslau type distributions are shown to be rather poor models for representing real polymer distributions. Prior justifications for this model was primarily based on the

TABLE V

Effect of a High Molecular Weight Cut-Off on the Weight-,  $Z$ -, and  $Z + 1$ -Average Molecular Weights; Generalized Exponential Distribution,  $m = 0.2$ 

Case	$n\bar{P}_w$	$\Sigma W(P)$	$\bar{P}_w''/\bar{P}_w$	$\bar{P}_z''/\bar{P}_z$	$\bar{P}_{z+}''/\bar{P}_{z+}$
Case 1:					
$\bar{P}_w/\bar{P}_n = 6$	1	0.715	0.260	0.150	0.064
	2	0.870	0.479	0.262	0.120
	3	0.928	0.620	0.353	0.170
	4	0.955	0.715	0.430	0.216
	5	0.970	0.780	0.495	0.259
	6	0.979	0.827	0.550	0.299
	7	0.984	0.862	0.598	0.336
	8	0.988	0.889	0.640	0.371
	9	0.990	0.909	0.676	0.403
	10	0.992	0.924	0.708	0.433
	15	0.995	0.967	0.819	0.560
	20	0.996	0.983	0.883	0.654
	30	0.998	0.995	0.945	0.779
	60	0.998 (1.000 <sup>a</sup> )	1.000	0.991	0.931
Case 2:					
$\bar{P}_w/\bar{P}_n = 11$	1	0.729	0.235	0.108	0.040
	2	0.862	0.424	0.192	0.076
	3	0.914	0.552	0.264	0.109
	4	0.940	0.643	0.325	0.139
	5	0.955	0.709	0.379	0.169
	6	0.965	0.760	0.427	0.196
	7	0.971	0.798	0.470	0.222
	8	0.975	0.829	0.508	0.247
	9	0.978	0.854	0.543	0.271
	10	0.980	0.874	0.575	0.294
	15	0.985	0.934	0.695	0.395
	20	0.986	0.962	0.774	0.477
	30	0.987	0.984	0.867	0.603
	60	0.988 (1.000 <sup>a</sup> )	0.998	0.963	0.810
Case 3:					
$\bar{P}_w/\bar{P}_n = 21$	1	0.731	0.215	0.082	0.027
	2	0.849	0.382	0.147	0.051
	3	0.897	0.499	0.203	0.074
	4	0.922	0.585	0.253	0.095
	5	0.936	0.650	0.298	0.116
	6	0.946	0.701	0.338	0.135
	7	0.952	0.742	0.375	0.154
	8	0.956	0.775	0.409	0.172
	9	0.960	0.802	0.440	0.190
	10	0.962	0.825	0.469	0.207
	15	0.968	0.897	0.584	0.284
	20	0.970	0.934	0.668	0.350
	30	0.972	0.968	0.777	0.460
	60	0.972 (1.000 <sup>a</sup> )	0.993	0.915	0.672

<sup>a</sup> Error due to change in limits of 1 to 0 with  $\bar{P}_w$  normalized at 55.



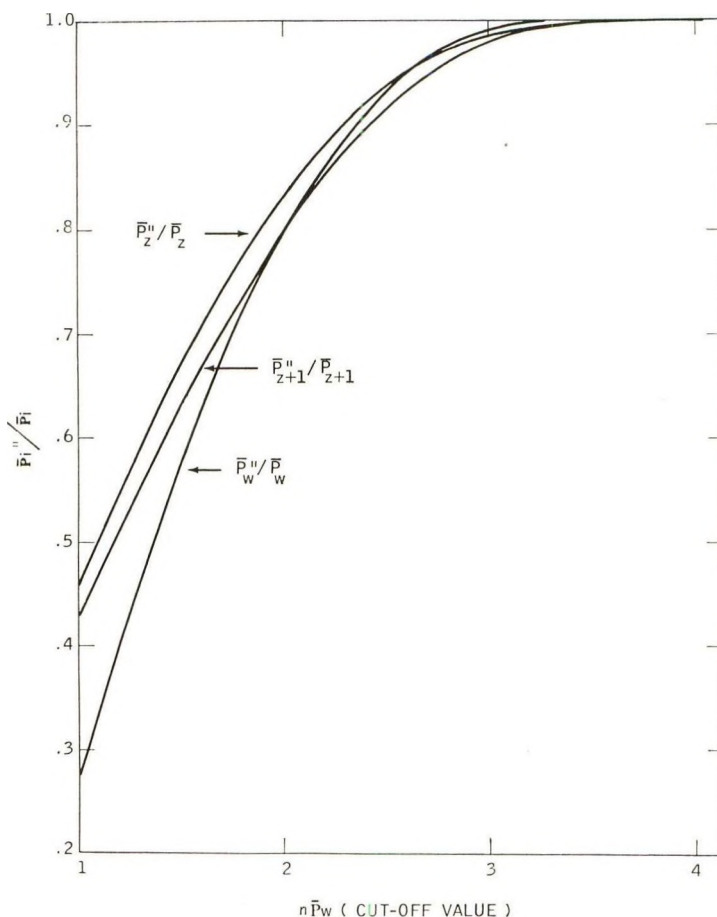


Fig. 3. Effect of high molecular weight cut-off value on the  $\bar{P}_w$ ,  $\bar{P}_z$ , and  $\bar{P}_{z+1}$  for a generalized exponential distribution with  $m = 3.0$  and  $\bar{P}_w/\bar{P}_n = 21$ .

apparent linearity of the cumulative weight versus molecular weight of fractionated cuts when plotted on logarithmic probability paper. However, the method assumes the Schulz-Dinglinger<sup>3</sup> approximation is valid and generally omits consideration of the low and high ends. Aside from the poorness of the Schulz-Dinglinger approximation for disperse polymers,<sup>4</sup> i.e.,  $P_w/P_n > 2$ , the importance of the low and high molecular weight fractions of about 2% are generally overlooked. However, these two low and high fractions, respectively, generally contain about 40% of the number of molecules and contribute to about 30%, 80%, and 100% of the total  $\bar{M}_w$ ,  $\bar{M}_z$ , and  $\bar{M}_{z+1}$  values, respectively. Hence, a good correlation of the fractionation data omitting these factors can hardly be used as justification for the model.

The generalized exponential type distributions, where  $m$  is of the order of or greater than 1, do show good correlations with the effects of random degradation with small errors due to low and high molecular weight cut-off values, and rather broad maximum for the differential weight distributions.

The author wishes to express his gratitude to Dr. D. Poller and Mr. R. Kruse for helpful discussions and to Mr. H. Oakley and Miss D. Mahon for the computer calculations.

### References

1. Kotliar, A. M., *J. Polymer Sci.*, **A2**, 4297 (1964).
2. Kotliar, A. M., *J. Polymer Sci.*, **A2**, 1057 (1964).
3. Schulz, G. V., and A. Dinglinger, *Z. Physik. Chem.*, **B43**, 47 (1939).
4. Kotliar, A. M., *J. Polymer Sci.*, **A2**, 1373 (1964).

### Résumé

Les distributions du type logarithmique normal, par exemple de Wesslau, ne peuvent pas décrire la distribution réelle d'un polymère dépourvu des bas et hauts poids moléculaires. Cependant dans certain cas, une distribution du type exponentiel généralisé donne des modèles intéressants et valables.

### Zusammenfassung

Es wird gezeigt, dass die logarithmischen Normalverteilungen, z.B. Wesslau, tatsächliche Polymerverteilungen bei Abschneiden der niedrigen und hohen Molekulargewichte nicht beschreiben können. Jedoch scheinen gewisse Fälle der verallgemeinerten Exponentialverteilungen nützliche und gültige Modelle zu sein.

Received October 8, 1963

Revised December 12, 1963

## On the Relation between Different Morphological Forms in High Polymers\*

H. D. KEITH, *Bell Telephone Laboratories, Incorporated,  
Murray Hill, New Jersey*

### Synopsis

It is suggested that all of the morphological forms commonly observed in high polymers are closely related. These forms are considered to represent different stages in a development from single crystal into spherulite under the influence of species rejected by growing crystals. Single crystals undergo this transformation in habit when of a size roughly equal to  $\delta = D/G$ , where  $D$  is the diffusion coefficient in the crystallizing medium and  $G$  is the rate of crystal growth. New experimental results show that when  $\delta$  is unusually large, single crystals may be grown from polymer melts, and when  $\delta$  is reduced by the use of high molecular weight polymer and/or viscous solvents, spherulites may be grown from polymer solutions. It is shown that single crystals of polyethylene crystallized from solution in paraffinic solvents exhibit a different habit from those crystallized under equivalent conditions from xylene. This affords a simple explanation for the radial  $b$  orientation found in spherulites of polyethylene.

### Introduction

Synthetic high polymers are known to exhibit several different types of crystalline morphology. When crystallized from very dilute solution in solvents such as xylene, for example, they commonly yield lamellar (chain-folded) single crystals,<sup>1</sup> and from more concentrated (>0.5% approximately) solution in these same solvents they generally yield multilayer aggregates<sup>2</sup> of such crystals. In the case of polyethylene, these aggregates are often found to consist of lamellae which diverge from a central spine or axis; they are then known as axialites.<sup>2</sup> When crystallized from the melt, on the other hand, high polymers almost always form spherulites.<sup>3,4</sup> However, thin films of melt may also give rise, under certain conditions, to multilayer aggregates of lamellar crystals. On account of their polyhedral outlines, these aggregates have been termed hedrites.<sup>5</sup> The present paper is not concerned so much with elaboration of these various morphological forms, each of which has been described in detail elsewhere, as with clarifying the relation between them. An attempt is made to account for the different morphologies realized under different experimental conditions and,

\* Paper presented at American Physical Society Meeting, St. Louis, Missouri, in March 1963.

in particular, to examine means by which polymer spherulites evolve from single crystal nuclei.

The point of view to be developed has its origin in recent work by Padden and the author<sup>6,7</sup> which has emphasized the importance of fractionation and impurity segregation in the crystallization of polymers from the melt. It has been shown that a typical high polymer is to be regarded as a multi-component system, some components of which, principally molecules of low molecular weight and stereoirregular molecules, are rejected preferentially by growing crystals. These crystallization-rejected components (which have previously been referred to under the generic term "impurities") tend to accumulate in the neighborhood of any advancing face of a growing crystal. Continuing growth of such a face then requires that readily crystallizable species diffuse to growth sites through impurity-rich layers, and that the impurities themselves diffuse out of the way of the oncoming solid front. In examining the influence of these diffusion processes on crystal habits it is helpful to consider the characteristic length  $\delta = D/G$ , where  $D$  is the diffusion coefficient for impurity in the unsolidified crystallizing medium and  $G$  is the rate of advance of a growing crystal face. This length has physical significance both as a measure of the distance through which rejected impurities can diffuse out of the way of oncoming growth fronts in the case of small crystals, and also as a measure of the widths of the impurity-rich layers that surround growing crystals of larger size. In fact, rejected impurities should be able to diffuse away readily from the surfaces of a crystal that is still small in comparison with  $\delta$ , whereas they cannot do so in the case of a crystal that is already larger than  $\delta$ . In polymer melts, for which values of  $\delta$  are generally small ( $<1 \mu$ ), growing crystals would normally come under the influence of these impurities while still too small to be resolved under the optical microscope. They would then suffer an instability of surface profile such as would cause growth fronts to become cellular and would lead ultimately to the development of crystals possessing a fibrous habit. According to Keith and Padden,<sup>6</sup> it is this instability which is largely responsible for the growth of spherulites in polymer melts and, in the view of these authors, spherulites consist for the most part of radiating arrays of fibers formed in this way. As these fibers grow outward, rejected impurities are swept aside and accumulate in highly impure interfibrillar regions. In this case,  $\delta$  now serves as a rough measure of the widths of the fibers, that is, as a gauge of the "coarseness" of the fibrous texture. Previous experiments have already shown that many of the morphological properties of polymer spherulites, and variations in coarseness of texture in particular, can be understood on this basis.<sup>7</sup>

As a simple extension of the foregoing, the following broad generalization may now be suggested. It is proposed that differences between the various morphological forms noted earlier arise principally for the reason that, in some cases, we are observing crystals that are still small in comparison with  $\delta$  so that their habits are as yet insensitive to rejected impurities.

whereas, in other cases, we are dealing with crystals that are already larger than  $\delta$  so that they have become spherulitic under the influence of rejected impurities.

As pointed out above, spherulitic crystallization from the melt is certainly consistent with such a view. We now note that the growth of single crystals from dilute solution also appears to accord with our suggestion. For polyethylene crystallizing in xylene, for example, we would have  $D \geq 10^{-6}$  cm.<sup>2</sup>/sec.\* and  $G \leq 10$   $\mu$ /sec.<sup>8</sup> so that an extreme lower limit for the magnitude of  $\delta$  is 10  $\mu$ . Generally speaking,  $\delta$  is about 100  $\mu$  or more, appreciably larger than most observed single crystals. Consequently, the habits of these crystals are unlikely to be much affected by impurities, and should reflect as close an approach to equilibrium forms as is allowed, first, by nucleation processes (which favor chain folding and cause the crystals to be lamellar in character) and, secondly, by increasing instability with respect to dendritic development at faster rates of growth. For the most part, observed single crystals are indeed polyhedral lamellae bounded by low index planes.

Further experimental evidence is needed, however, before it can be decided whether or not the generalization we have proposed also applies to the growth of hedrites. For it to do so would imply that hedrites are formed only under conditions of unusually large  $\delta$  so that single crystals might then grow from the melt to appreciable (observable) size. The first series of experiments to be described in this paper confirms that this is the case. By allowing us to observe single crystals directly as they grow from sizes smaller to sizes larger than  $\delta$ , these experiments also demonstrate a number of early stages in the transformation of single crystals into spherulites.

A further series of experiments is also described in which an attempt is made to bring about spherulitic crystallization in solutions of polyethylene. Although successful in a limited sense only, these offer a simple explanation for the hitherto puzzling observation that, whereas polyethylene dendrites grown from dilute solution in xylene display  $a$  as the fastest growing axis, melt-grown spherulites exhibit radial orientation of the  $b$  axis. They also show how screw dislocations are introduced into growing polyethylene crystals, and indicate a means by which axialites may be formed. Both results are helpful in understanding spherulitic crystallization in this and other polymers.

### Growth of Single Crystals from the Melt

Polystyrene was chosen for this study for the reason that it is one of the few polymers for which there is sufficient data to allow estimates to be made of  $D$ , the coefficient of self-diffusion in the melt. Even then, these estimates have to be based on the assumption that there is little difference

\* This inequality is based upon the knowledge that, for simple liquids at room temperature,  $D \approx 10^{-5}$  cm.<sup>2</sup>/sec.

in  $D$  between isotactic and atactic polymer of the same molecular weight at the same temperature. Rudd<sup>9</sup> has measured the melt viscosities of a number of atactic fractions of polystyrene at 227°C., and values of  $D$  may be calculated from these by using a relation given by Bueche.<sup>10</sup> For a fraction for which  $\bar{M}_w = 51,400$ , for example, the value  $10^{-10}$  cm.<sup>2</sup>/sec. may be derived for  $D$  at 227°C. This provides a basis for estimating  $\delta$  in the following experiments in which we have used extracted isotactic polystyrene of molecular weight 60,000 blended on occasion with the same atactic fraction ( $\bar{M}_w = 51,400$ ) as used by Rudd.  $D$  has been assumed to vary with temperature in accordance with an activation energy of 35 kcal./mole,<sup>7</sup> and with molecular weight according to  $D \propto \bar{M}^{-3.14}$ , which is based upon Rudd's empirical relation  $\eta \propto \bar{M}^{3.14}$ . For temperatures within 50°C. of the melting point (230°C.) and molecular weights not too far removed from 50,000, this procedure, though primitive, probably yields values of  $D$  accurate to within an order of magnitude. Corresponding values of  $G$  were measured directly from the radial growth rates of spherulites (see Keith and Padden<sup>7</sup>). Values of  $\delta$  ( $= D/G$ ) estimated in this way for a blend containing 25% of isotactic ( $\bar{M}_w = 60,000$ ) and 75% of atactic ( $\bar{M}_w = 51,400$ ) polymer are 0.2, 0.21, and 1.6  $\mu$  at 165, 182.5, and 200°C., respectively, in good agreement with observed coarseness of texture in spherulites grown at these temperatures.<sup>6</sup> Similar estimates indicate that  $\delta$  increases markedly as the temperature is raised above 200°C., attaining at 210°C. a value of about 5  $\mu$  in the isotactic polymer and slightly higher in blends containing the atactic diluent. Crystallization of these systems at 210°C. should provide a means, therefore, of studying growth from the melt of crystals that are of observable size but still smaller than  $\delta$ .

Samples of polymer in the form of thin (2–20  $\mu$ ) films sandwiched between glass cover slips were crystallized isothermally either in an oven or in silicone oil. In the centers of the specimens, which were protected from oxidative degradation or from plasticization by the silicone oil, the only structures observed at temperatures below 200°C. were spherulites. As 200°C. was approached, these became coarser in texture, and it also became apparent that many of them developed from small, strongly birefringent, sheaflike precursors. Between 200 and 210°C., small hexagonal structures also began to appear which, on reaching a size usually between 5 and 10  $\mu$ , became rounded and increasingly spherulitic in appearance. Unfortunately, it was not possible to extend controlled experiments to temperatures much above 210°C. because of decreasing growth rates and increasing degradation of the polymer (see later). It was clear at these higher temperatures, however, that hexagonal structures were more common and also that they grew to sizes appreciably larger than 10  $\mu$  before becoming rounded in profile.

These hexagonal structures vary considerably in appearance depending upon the thickness of the films in which they are formed. Those grown in thinner films are lamellar crystals which in themselves show no birefringence when viewed at normal incidence, although they usually develop

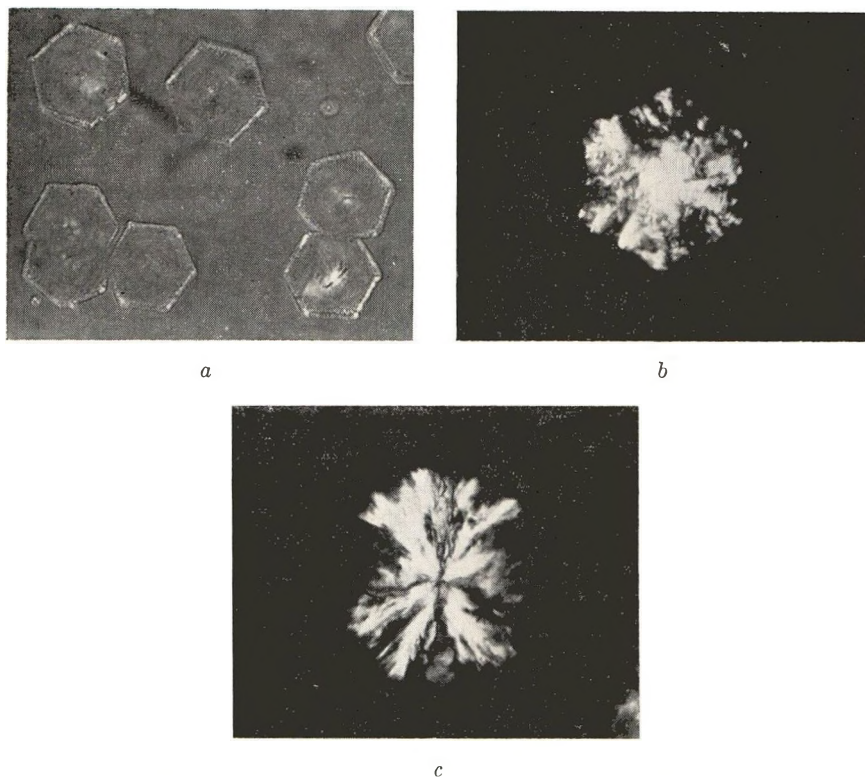


Fig. 1. Hedrites grown in isotactic polystyrene at 210°C. showing: (a) hedrites with birefringent edges (slightly uncrossed polarizers,  $\times 890$ ); (b) birefringent overgrowths on a thicker hedrite (crossed polarizers,  $\times 920$ ); (c) strongly birefringent, seemingly fibrous, overgrowths on a hedrite formed in a fairly thick film (Crossed polarizers,  $\times 1450$ .)

weakly birefringent edges as they grow larger (Fig. 1a). Those grown in thicker films are somewhat less regular in outline and generally exhibit irregular patches of birefringence or, in some instances, strongly birefringent overgrowths (Fig. 1b). Microscopic examination suggests that these various structures are related as follows. The seemingly nonbirefringent hexagonal lamellae appear to be chain-folded single crystals of polystyrene oriented with the *c* axis of the (hexagonal) unit cell normal to the planes of the specimens. These crystals usually develop a number of layers in parallel orientation, probably through the agency of screw dislocations in the manner now familiar in the case of solution-grown crystals of many polymers. In the restricted space allowed in very thin films there are relatively few, and often no more than one or two such layers; generally speaking, in thicker films there are many. Successive layers tend to peel away from one another, however, and this appears to be the origin of weak birefringence at the edges of thinner aggregates. This peeling is more pronounced in thicker aggregates, and in extreme cases the topmost layers

curl up and present the appearance of strongly birefringent, seemingly fibrous, overgrowths (Fig. 1c).

As far as these observations are concerned, there is little difference between isotactic polystyrene ( $\bar{M}_v = 60,000$ ) and blends containing up to 75% of atactic polymer ( $\bar{M}_w = 51,400$ ) as diluent. Corresponding differences in  $\delta$  would also be slight. Substitution of other atactic diluents, however, causes appreciable changes in behavior. In blends containing 50–75% of an atactic polystyrene of molecular weight 4,500, for example, it is found that hexagonal aggregates grow to sizes of the order of 50–100  $\mu$  at 210°C. before their profiles become rounded. Furthermore, small hexagonal crystals can be discerned in these blends at crystallization temperatures as low as 190°C. Substitution of an atactic fraction of molecular weight 247,000 in similar proportions, on the other hand, suppresses the appearance of hexagonal aggregates at all but the highest temperatures (210°C. and above). Apparently, these variations in behavior reflect appreciable changes in  $\delta$  (an increase in the first case and a decrease in the second) such as might be expected from drastic differences in molecular weight distribution between the samples. Since the melt surrounding growing crystals becomes enriched in rejected impurity (atactic polymer), these changes in  $\delta$  may be even larger than would be estimated solely from changes in overall composition of the samples.<sup>6</sup> Other experiments, to be described later, lend further support to the conclusions that may even now be drawn from these observations: (a) that polyhedral single crystals may be grown in polymer melts but only up to sizes of the order of  $\delta$ , and (b) that, as these crystals grow to sizes larger than  $\delta$ , their habits are modified by rejected impurities. It would follow that, for single crystals of observable size to be formed,  $\delta$  must be appreciably larger than 1  $\mu$ .

Rounding of the profiles of individual single crystal layers has been examined in greater detail in very thin films. Figure 2 shows a number of typical crystals at different stages of growth. Initially these are relatively perfect hexagonal lamellae (Fig. 2a) whose appearance and optical properties are consistent with a chain-folded single crystal structure.\* They then develop star-shaped profiles (Fig. 2b), apparently in response to an increasing accumulation of impurities near the midpoints of their sides. (Similar crystals have been reported earlier by Danusso and Sabbioni.<sup>11</sup>)

With further growth, protruding spurs are formed along the sides of the stars and the outlines of the crystals become heavily serrated (Fig. 2c). This serration is thought to illustrate the phenomenon of cellulation commonly observed in crystals growing in impure melts<sup>12</sup> and to support the arguments advanced by Keith and Padden in an earlier paper on spherulitic

\* The extended lengths of polystyrene molecules of molecular weight 60,000 (1300 A.) are so close to the estimated thicknesses of the crystals ( $\sim 1000$  A.) that there may be doubt as to their being folded. The question is not resolved, but the likelihood of folding is confirmed, by the observation that, using silicone oil as a plasticizer to enlarge values of  $\delta$ , similar crystals can be grown in polystyrene of molecular weight 1,250,000.



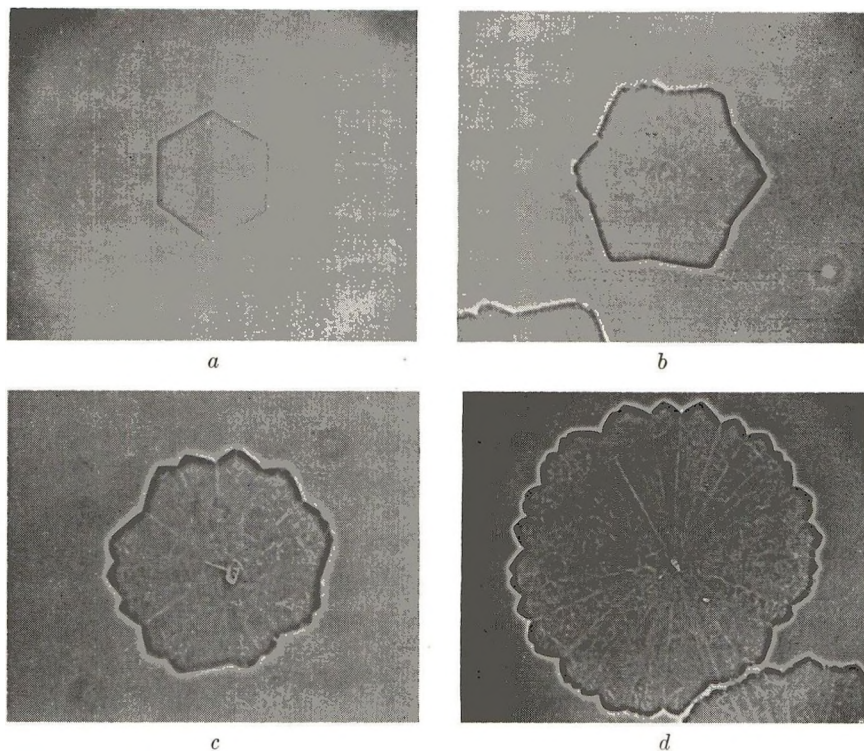


Fig. 2. Various stages of disordering in hedrites grown in a very thin film of isotactic polystyrene at 215°C. All are shown in phase contrast at various magnifications: (a)  $\times 510$ ; (b)  $\times 275$ ; (c), (d)  $\times 185$ .

crystallization.<sup>6</sup> The formation of re-entrant corners between spurs causes the character of the crystals to be greatly changed. Severe disorder is built into the crystals at these corners such that neighboring sectors (clearly delineated by radial markings in Figures 2*b-d*) become misaligned crystallographically one with respect to another. As a result, the addition of more and more spurs soon converts the crystals into radiating polycrystalline structures such as shown in Figure 2*d*.

A major factor contributing to this development of polycrystalline aggregate from single crystal is the following. Figure 3 shows, at high magnification, a common and significant feature of all polystyrene crystals we have grown from the melt in this way. Along radii extending inward from the tips of protruding corners, which in chain-folded crystals would mark boundaries between different fold domains, there are obvious signs of extensive crystalline imperfection. Molecular chains apparently experience difficulty in negotiating these boundaries in the course of being deposited in folded conformations on growth faces. The disorder which causes misalignments between sectors in crystals such as shown in Figure 2*d* seems to arise because molecules encounter a more serious problem with fold domain boundaries at re-entrant corners. Not only is the concentra-

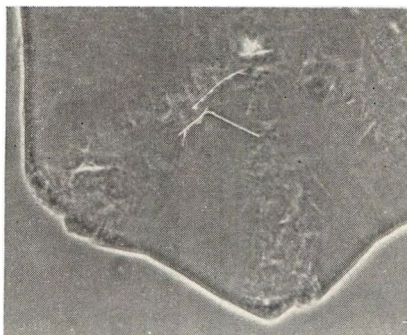


Fig. 3. Large hedrite in isotactic polystyrene showing disorder in the vicinity of fold domain boundaries. Phase contrast,  $\times 920$ .

tion of rejected impurities likely to be considerable at these corners, but crystallizing molecules are also more closely confined and would have less opportunity for adjustment to well-adapted conformations.

The various layers in multilayer crystals develop rounded profiles and radiating polycrystalline character in similar fashion, and it may easily be seen how this process, combined with a divergence of peeling layers, could lead in an unrestricted volume of melt to the growth of spherulitic aggregates. Indeed, many polymer spherulites may well be formed in such a manner, and lamellar fibers of the kind commonly found in these spherulites<sup>4,13</sup> may originate from sectors such as shown in Figure 2*d*.

Hexagonal aggregates were found more commonly in our experiments than the above account might suggest. Their growth appears to be facilitated in large measure by degradation\* or by plasticization of the polymer, for they were frequently found in profusion around the edges of sandwich specimens, and uniformly throughout films crystallized with one side freely exposed to the atmosphere or to silicone oil. In these circumstances, hexagonal structures began to appear in the isotactic polymer at crystallization temperatures around 185°C. and grew to substantial sizes (50–100  $\mu$ ) at temperatures (200°C. and above) where small hexagonal crystals could first be discerned in the protected interiors of films sandwiched between glass surfaces. It has been noted previously<sup>7</sup> that degradation and plasticization also cause a marked coarsening of texture in spherulites grown in polystyrene at lower temperatures. In each instance, the results are as though these changes in the polymer cause values of  $\delta$  to be substantially increased. It is scarcely surprising that plasticization would have such an effect, since coefficients of diffusion are considerably enhanced but growth rates are not so greatly affected<sup>7</sup>. In the case of degradation, however, it is less obvious how appreciable increases in  $\delta$  can arise. Evidently, they result (at least in part) from the formation of products of low molecu-

\* This degradation, which is reduced (but not prevented) by a nitrogen atmosphere, appears to result from two processes, one requiring access to oxygen and the other not. Both processes accelerate rapidly above 200°C.

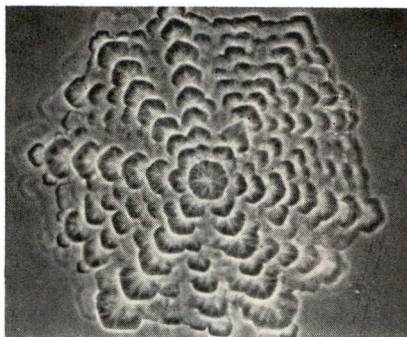


Fig. 4. Polyhedral aggregate of crystals formed at the edge of a film of isotactic polystyrene crystallized at 200°C. Phase contrast,  $\times 600$ .

lar weight, modest amounts of which, acting as impurities accumulating at growth fronts, could exert a disproportionately large influence on  $\delta$ .

Hedrites found in gutta-percha,<sup>14</sup> polyoxymethylene,<sup>5</sup> polyethylene oxide,<sup>5</sup> poly-4-methylpentene-1,<sup>15</sup> and polypropylene,<sup>16</sup> are usually similar to the multilayer crystals we have observed in thicker films of polystyrene. (Single crystals of less regular outline have also been reported in nylons<sup>17</sup> and polytetrafluoroethylene.<sup>18</sup>) However, insufficient detail has been given for it to be decided with certainty whether these hedrites, too, were formed under conditions of unusually large  $\delta$ . Nevertheless, it is significant that slow growth at small supercoolings and the use of thin films under conditions likely to cause appreciable degradation are features common to almost all of them. Both circumstances would tend to give rise to relatively large values of  $\delta$  and we suggest that, in most of the instances reported, the appearance of hedrites reflects increases in  $\delta$  brought about in this way.

Of course, aggregates of crystals may be formed from time to time which remain polyhedral in overall outline principally because of branching that is crystallographic (see, for example, Fig. 4); these might well achieve dimensions considerably larger than  $\delta$ , and the formation of such aggregates, therefore, does not necessarily imply correspondingly large values of  $\delta$ .

### Approaches to Spherulitic Crystallization in Solutions of Polyethylene

In terms of morphological investigations, polyethylene is by far the most commonly and most thoroughly studied crystalline polymer. As a result, previous attempts to explain how growth processes that give rise to single crystals in dilute solution are related to those that cause spherulitic crystallization in the melt have dealt almost exclusively with this material. From an experimental standpoint, however, there are considerable difficulties in the way of elucidating such a relation. Attempts at direct observation of early stages of spherulitic growth in the melt are unrewarding, principally for the reason that molten polyethylene cannot be quenched into a glassy state (as can easily be done with polystyrene). Attempts to

approach spherulitic growth by crystallization from concentrated solution, though more informative, suffer similarly from a serious disadvantage. Polyethylene solutions of the highest concentrations that allow the crystallized polymer to be dispersed for reliable identification of morphological forms do not yield single crystals or spherulites, but instead yield axialites whose crystal habits are intermediate between these two.<sup>2</sup>

This lack of evidence notwithstanding, it has generally been supposed that polymer spherulites, which usually consist of radiating arrays of ribbonlike fibers, represent something in the nature of a dendritic development of lamellar single crystals.<sup>19,21</sup> It has also been suggested that the formation of polycrystalline aggregates by a repeated twinning of such crystals may be a possible stage in this development.<sup>21</sup> However, there is a major difficulty with this line of reasoning. Polyethylene crystals grown from dilute (concentrations less than about 0.1%) solution in xylene, toluene or similar solvents, are usually rhombic in shape, the *a* axis of the unit cell lying parallel to the long, and the *b* axis parallel to the short, diagonals. In dendritic growth at large supersaturations, the acute apices of these crystals develop preferentially, leading to greater elongation of *a*-oriented, rather than of *b*-oriented, branches.<sup>20,22</sup> In sharp contrast, it is the *b* axis that is found to lie parallel to the long axes of radial fibers in melt-grown spherulites.<sup>23</sup> Various suggestions have been made as to how these *b*-oriented fibers might be formed but, in each case, as yet without substantiation.<sup>24-26</sup>

There is a further difficulty with the view that a dendritic development of single crystals might lead in some simple way to the formation of spherulites in concentrated solutions or in the melt. This has been brought to light by recent experiments which have shown that a significant factor in spherulitic crystallization is the behavior of crystallization-rejected impurities.<sup>7</sup> Despite this difficulty, however, it is a view which still appears reasonable in broad outline. As has been pointed out elsewhere,<sup>6</sup> spherulites formed by cellulation and fibrillation in impure melts can indeed be regarded as dendritic aggregates, but in a restricted sense only.\* What is needed, therefore, in addition to an explanation for radial orientation of the *b* axis in polyethylene spherulites, is a clearer understanding of the parts played by impurities and by solvent in these various cases.

The most promising approach to these problems, of course, is the systematic study of crystallization in solutions of increasing concentration. Bassett, Keller, and Mitsuhashi<sup>2</sup> have recently shown that, at all concentrations ranging from about 0.3 to 40% (the limit at which the crystallized polymer can still be dispersed), solutions of polyethylene in xylene do not form spherulites but, as mentioned above, form axialites. These consist

\* Diffusion of latent heat away from growth sites appears to play a minor part in controlling the habits of these aggregates. By far the more important factor is the diffusion of readily crystallizable species to growth sites and the diffusion of rejected impurities away from them. However, the concentration gradients responsible for these diffusion processes are confined to regions very close to growth fronts.

of many superimposed lamellae attached to one another along a central axis or spine but otherwise splaying like the leaves of a partly opened book. The lamellae are roughly hexagonal in shape, and correspond to rhombs so heavily truncated that they are often longer along their  $b$  axes (parallel to the spines of the aggregates) than along their  $a$  axes. The splaying of lamellae is so marked that, as the axialites tumble about in suspension, they usually resemble spherulites (with radial  $a$  orientation) when seen edge-on. But, as we have said, these aggregates are *not* spherulites; apart from considerations of orientation, they fall short of being spherulitic in the fullest sense of the term for the reason that the radiating crystals do not exhibit a fibrous habit. (By a crystal of fibrous habit we mean one considerably larger in one dimension than in either of the other two. The ribbonlike lamellar crystals found in polyethylene spherulites grown from the melt can thus be regarded, in this sense, as being fibers.)

Nevertheless, it is clear that a transition to a spherulitic growth of fibrous crystals must occur in polyethylene solutions if their concentrations can be increased sufficiently. For, in the limit of high concentrations, these solutions would be equivalent to plasticized melts which are known to crystallize spherulitically. Now, in spherulites grown from the melt, a fibrous crystal habit is brought about by a segregation of crystallization-rejected impurities. In an effort to see how best to promote a transition to spherulitic crystallization in solutions of relatively low concentration, let us now give some thought to the likely influence of impurity species (and to the significance of  $\delta$ ) in systems containing relatively large concentrations of solvent.

The impurities which play an important role in the crystallization of a polymer from the melt are all constituents of the original polymer but, in crystallization from solution, the solvent behaves as an additional crystallization-rejected component of the system. The relation between crystallization from the melt and crystallization from solution is now made clearer, perhaps, by adopting the following viewpoint. Crystallization from the melt can be regarded as a crystallization of stereoregular polymer of higher molecular weight from concentrated solution in stereoirregular polymer or in polymer of lower molecular weight; that is, from solution in the "impurity" present in the system. All that is changed in crystallization from dilute solution in xylene, for example, is the concentration of the solution and the nature of the species (xylene and low molecular weight polymer) which now play the dual role of crystallization-rejected impurity and of solvent. In these terms, an impurity-rich layer surrounding a crystal growing in the melt may be considered the analog of a layer of depleted solute concentration enveloping a crystal growing in dilute solution. Instability with respect to cellulation and subsequent fibrillation in the former case<sup>6</sup> may similarly be considered a counterpart of instability with respect to dendritic growth in the latter.

From this undoubtedly oversimplified viewpoint, one can conceive (in principle) of a gradation ranging continuously from dendritic growth in

dilute solution, as one extreme, to spherulitic crystallization in highly concentrated solution or in the melt, as the other.\* Provided that transport in these media is limited to diffusion,  $\delta$  would serve throughout this range as a rough measure of the sizes of crystals whose habits will be modified by impurities. In dilute solutions, however, where there may be convective mixing at elevated temperatures, crystals might well remain unmodified up to sizes appreciably larger than  $\delta$ ; however, in more concentrated solutions exhibiting larger viscosities, the significance of  $\delta$  in this respect will be relatively free from such complications. Now, as the concentration of a solution is raised, or as the molecular weight of the polymer is increased,  $\delta$  will take smaller and smaller values until, at some stage, there must be a transition from the growth of what are primarily dendritic single crystals to the formation of (polycrystalline) spherulites. Earlier experiments<sup>6,7</sup> suggest that this comes about at some small value of  $\delta$  such that fibers are formed which then begin to branch profusely in a noncrystallographic manner. Thus, in order for this transition to take place at relatively low concentrations (to facilitate microscopic examination of crystal habits), some advantage might be gained by reducing  $\delta$  through the use of high molecular weight polymer and also of solvents more viscous than xylene.† Accordingly, in the experiments now to be described, polyethylene was crystallized from solution in polyisobutylene and in long chain paraffins. Though less viscous than polyisobutylene, these paraffins were chosen for the reason that they provide growing crystals with an environment not unlike that which polyethylene crystals encounter in growing from the melt. It was hoped that their use might provide some clue as to the causes of radial orientation of the *b* axis in polyethylene spherulites.

To reduce complications arising from polydispersity, two fractionated polyethylenes (viscosity-average molecular weights 168,000 and 4,500) were used for most of the experiments. In order to conserve the limited quantities of these fractions available and, at the same time, work with moderately concentrated solutions, the following procedure was adopted. Polymer and solvent (polyisobutylene or long-chain paraffin), in the correct proportions for the final solution desired, were dissolved in heated decalin. Drops of decalin solution were then spread on glass cover slips at

\* At this point in the discussion we are concerned only with means whereby crystals of fibrous, as distinct from simple polyhedral, habit are formed in solutions covering a wide range of concentrations. For the moment, we shall ignore the further consideration that, whereas fibers in dendritic aggregates generally branch in accordance with simple crystallographic rules, a truly spherulitic growth regime involves not only the formation of fibrous crystals but also the requirement that these fibers should branch noncrystallographically.<sup>6</sup>

† It is to be borne in mind that there is considerable variation in behavior between different polymers. Polypropylene, for example, differs quite markedly from polyethylene in that it readily forms spherulites when crystallized from solution in xylene at concentrations above 0.5%.<sup>27</sup> Less is known of the morphology of this polymer, however, but there are indications that impurities may cause fibrous growth in polypropylene by means other than cellulation, so that a small value of  $\delta$  may not be a prerequisite for spherulitic growth.<sup>13</sup>

140°C. The decalin evaporated fairly rapidly, leaving thin films of polymer solution which were transferred subsequently to hot plates at controlled temperatures for crystallization. After crystallization, the solvent was removed by washing in xylene at room temperature.

One of the solutions studied in some detail contained 10% of the high molecular weight fraction dissolved in *n*-dotriacontane (*n*-C<sub>32</sub>H<sub>66</sub>; m.p. 68.5°C.). This composition is well suited to a study of correlations between modes of crystallization realized under a wide range of conditions,

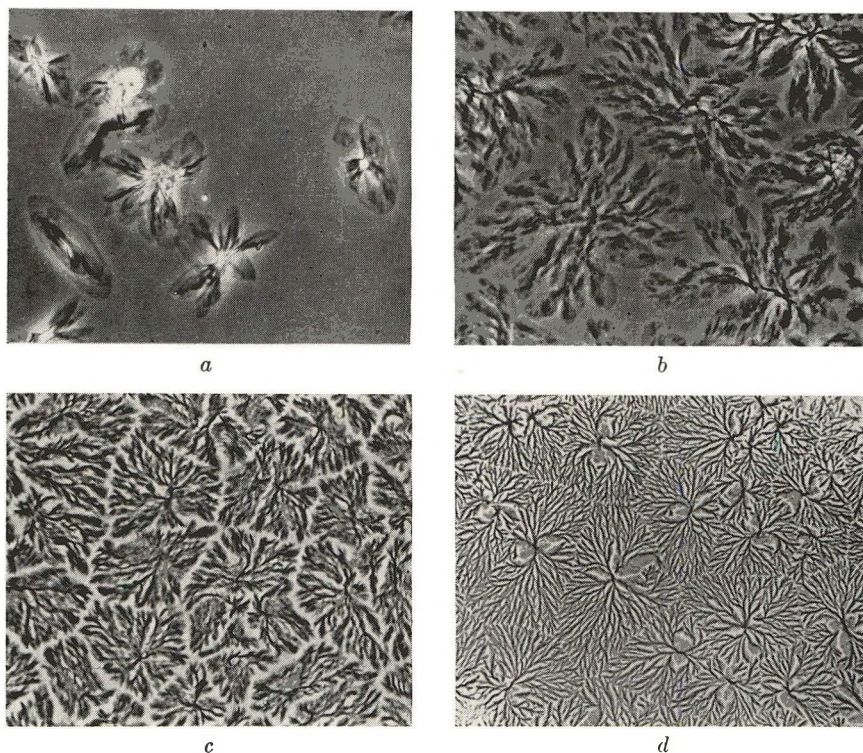


Fig. 5. Aggregates of polyethylene crystals formed from a solution containing 10% of a polymer fraction ( $\bar{M}_v = 168,000$ ) in C<sub>32</sub>H<sub>66</sub> at (a) 110°C.; (b) 100°C.; (c) 90°C.; (d) 75°C. All phase contrast,  $\times 460$ .

for it can be considered either as a solution or as a specially constituted polyethylene possessing an unusual bimodal distribution of molecular weights. Thus, depending upon viewpoint, crystallization at temperatures above 68.5°C. might be regarded either as crystallization from solution in a paraffinic solvent or, alternatively, as crystallization of polyethylene from the melt. Figure 5 illustrates typical results obtained after crystallization at the temperatures indicated in the legend and after removal of solvent. The structures range from multilayer aggregates reminiscent of the axialities described by Bassett et al.<sup>2</sup> (Fig. 5a) to what are clearly two-dimensional spherulites.

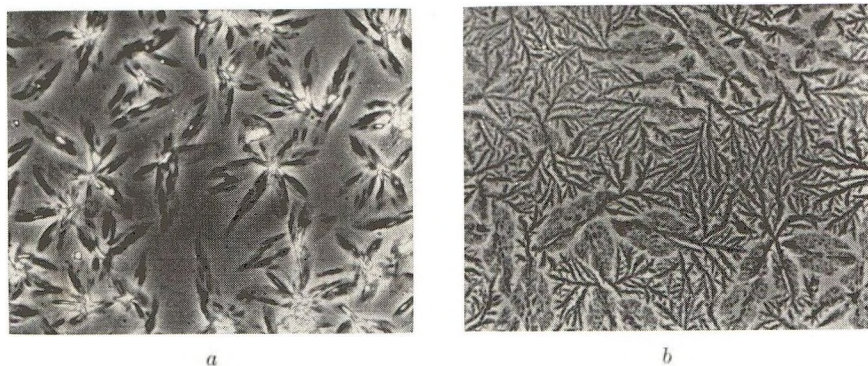


Fig. 6. Aggregates of polyethylene crystals formed from a solution containing 10% of a polymer fraction ( $\bar{M}_v = 4,500$ ) in  $C_{32}H_{66}$  at (a) 90°C. and (b) 75°C. Phase contrast,  $\times 460$ .

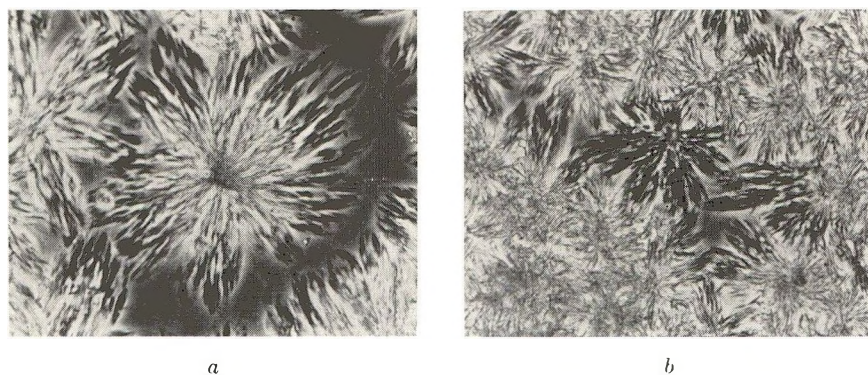


Fig. 7. Aggregates formed at 110°C. by crystallization of (a) 30% and (b) 50% solutions of a polyethylene fraction ( $\bar{M}_v = 4,500$ ) in  $C_{32}H_{66}$ . Phase contrast,  $\times 900$ .

For comparison, Figure 6 shows aggregates grown in a solution containing 10% of the low fraction ( $\bar{M}_v = 4,500$ ) in  $n-C_{32}H_{66}$ , and Figure 7 shows aggregates formed in more concentrated solutions (30 and 50%) of this fraction in the same solvent. Structures formed at 100°C. in solutions containing 10% of the high fraction in polyisobutylene polymers of molecular weight 625 and 1,190 are illustrated in Figure 8. In the latter cases, the crystals are still immersed in viscous solvent.

Structures grown in thin films in this way are not necessarily representative of those formed in bulk solution under otherwise identical conditions. Except for relatively dilute solutions, however, it is difficult to determine exactly what is formed in the latter case. Unmistakably, bulk solutions of polyethylene in  $n-C_{32}H_{66}$  at concentrations up to about 2% yield axialites. More compact aggregates formed at concentrations up to 10% (where dispersal becomes extremely difficult) are indistinct as they swirl around in solution, and even more so after they shrivel up on drying. These aggregates could not be identified reliably; they show no clear evi-



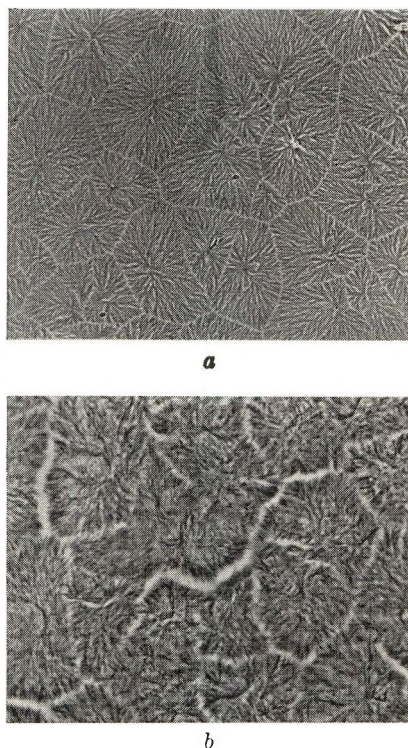


Fig. 8. Aggregates formed by the crystallization at 100°C. of solutions containing 10% of a polyethylene fraction ( $\bar{M}_v = 4,500$ ) in polyisobutylenes of molecular weight (a) 625 and (b) 1,200. Phase contrast,  $\times 415$ .

dence of possessing a fibrous habit, and it seems likely that they too are axialites. Our various observations suggest the following connection between the structures we have found to grow in thin films and structures formed in the corresponding bulk solutions.

There is very little difference between structures of these two types in the case of slow growth at higher temperatures. Indeed, multilayer crystals such as shown in Figure 5*a* appear to be axialites in which the proliferation of layers, which would be abundant in bulk solution, has been limited by film thickness. With faster growth at lower temperatures, however, crystals grown in thin films develop into irregular radiating structures (Figs. 5*b-d*) while bulk solutions, apparently, still yield axialites. This difference seems to be attributable to the fact that, whereas growing aggregates are free to tumble about in bulk solutions, there is poor mixing in solutions spread as thin films. In the former situation, crystal growth would be less susceptible to diffusion control occasioned by depletion of solute. In these terms, the use of thin films may be providing, adventitiously, a convenient means of inducing dendritic growth at relatively low concentrations such that aggregates can still be examined in detail. At concentrations as high as 30% in  $n\text{-C}_{32}\text{H}_{66}$  (Fig. 7), however, spherulites of

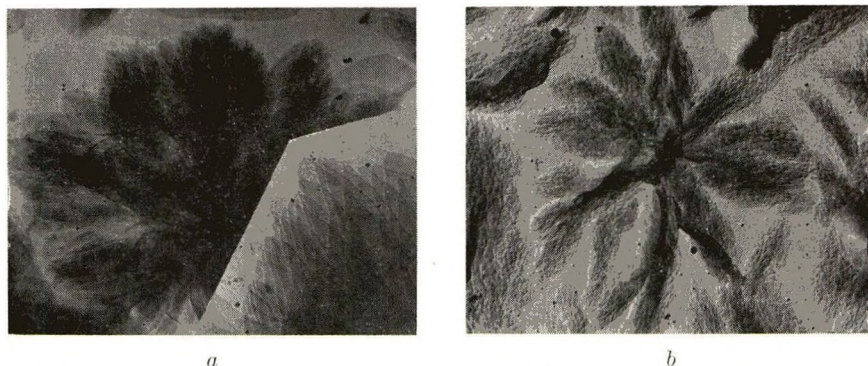


Fig. 9. Electron micrographs of aggregates grown in a 10% solution of a polyethylene fraction ( $\bar{M}_v = 168,000$ ) in  $C_{32}H_{66}$  at (a) 110°C. and (b) 80°C. (Compare with Fig. 5.) The insert in (a) shows at higher magnification ( $\times 7,360$ ) details of the top left-hand corner of the overall aggregate ( $\times 1,380$ ). The magnification in (b) is  $\times 2,300$ .

fairly fine texture are formed even in comparatively thick films, and it seems likely that spherulites would be formed in bulk solutions as well under these conditions.

Throughout our experiments, of which Figures 6–8 show typical and representative results, there is evidence of variations in coarseness of texture which parallel similar variations in spherulites crystallized from polymer melts.<sup>7</sup> From rough estimates of growth rates and of the relative viscosities of the solutions, it is clear that coarseness increases with decreasing viscosity, and with increasing temperature of crystallization, in a manner qualitatively consistent with variation in  $\delta$ . These results not only complement previous findings with polymer spherulites; they also allow more detailed correlation of coarseness (as a subjective evaluation of apparent fibrosity<sup>7</sup>) with the dimensions of individual radial fibers. Spherulites such as illustrated earlier in Figures 5b and 5c are shown in Figures 9a and 9b as they appear under low magnification in the electron microscope. It may easily be seen that the widths of the numerous spear-shaped lamellae which comprise the radial arms of the aggregates increase in concert with overall coarseness of texture.

Electron diffraction patterns obtained from selected areas ( $2.5 \mu$  in diameter) of aggregates such as shown in Figure 5 reveal several interesting results. Most significant is the fact that the spherulites all show radial orientation of the  $b$  axis of the unit cell. The same axis also lies parallel to the long axes of multilayer crystals formed at higher temperatures (Fig. 5a). As reported previously by Agar, Frank, and Keller,<sup>28</sup> the crystallinity of the polymer is rapidly destroyed by electron bombardment. Figure 10 shows a typical series of diffraction patterns taken in rapid succession at very low beam intensity from the same area (Fig. 10d). At first only the (020) reflections appear strongly (Fig. 10a); then these weaken as (200) and (110) reflections gain in intensity (Fig. 10b) and give way finally to a halo indicative of polymer now in an amorphous state (Fig. 10c).

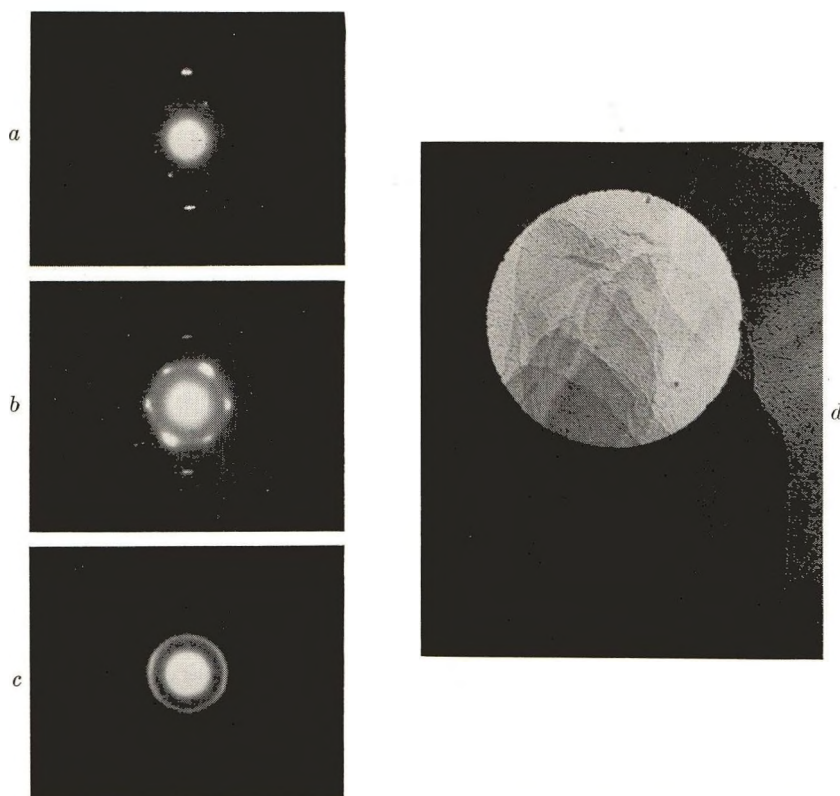


Fig. 10. Time lapse series of diffraction patterns obtained from the tips of elongated crystals found in radiating aggregates as shown in Fig. 5b. The diffracting area is indicated at (d)  $\times 9,200$ .

The positions of the (020) reflections allow the orientation of the aggregate to be determined unambiguously. Moreover, it is clear from the early absence of inner reflections that the molecular chains are at first inclined to the electron beam (normal to the plane of the specimen) and are later brought into alignment with it by a rotation about the (radial)  $b$  axis. This rotation probably indicates that the original crystals were composed of chains with folds staggered as in pyramidal crystals formed in dilute solution.<sup>29-31</sup> However, in view of the profusion of re-entrants formed at growing faces (see Fig. 9a), it is unlikely that these crystals are divided neatly into sectors in a relatively simple way as are solution-grown pyramidal crystals.

Apparently, the key to the radial orientation of the  $b$  axis in these aggregates lies in a severe truncation of habit when polyethylene crystals are grown from solution in long-chain paraffinic solvents. In Figure 5a we have already seen that crystals grown from  $n\text{-C}_{32}\text{H}_{66}$  are truncated to the extent that they are longer in the  $b$  than in the  $a$  direction. Apart from some rounding of form, the habits of these crystals owe little to the fact

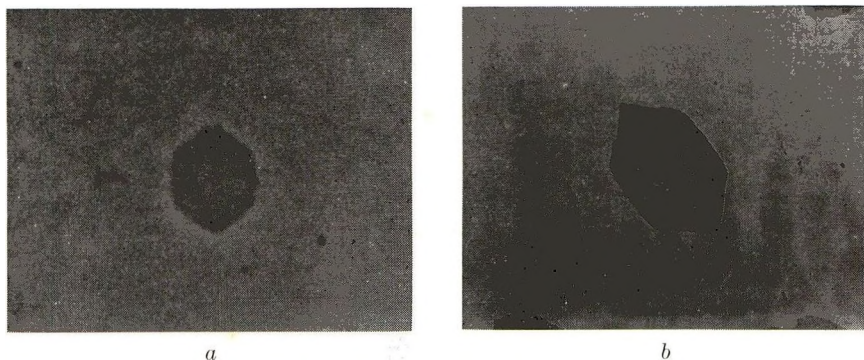


Fig. 11. Crystals formed at 75°C. in a 0.1% solution of a polyethylene fraction ( $\bar{M}_n = 4,500$ ) in  $C_{32}H_{66}$ : (a) in phase contrast,  $\times 1520$  (photographic enlargement  $\times 15$ ); (b) electron micrograph  $\times 2,300$ .

that they were grown in thin films, for it is found that individual layers in axialites grown in bulk solution are similarly truncated. Truncation is less pronounced in crystals grown at lower concentration and lower temperatures, but is still considerable in crystals grown from a 0.1% solution in  $n-C_{32}H_{66}$  at 75°C. (Fig. 11).<sup>\*</sup> A systematic study of the habits of crystals grown from dilute (0.005–1%) solution in various alkanes shows that this truncation increases with the length of the paraffinic chain in the solvent. Crystals grown from  $n$ -hexane are either rhombic or slightly truncated ( $a$  axis still longer than  $b$ ); those grown in  $n$ -decane vary widely in habit but are roughly hexagonal in shape if grown slowly at higher temperatures; crystals grown from  $n$ -octadecane are heavily truncated and, except insofar as their corners are less rounded, are almost indistinguishable from those grown from  $n$ -dotriacontane. Truncation also increases with concentration and with temperature. No reason can be given for these modifications of habit other than to remark that they obviously reflect differences in the relative surface energies of (110) and (100) faces in different solvents. However, it is clear that  $b$  is the fastest growing axis of the heavily truncated crystals and their prominent corners are such as to lead naturally to preferential elongation of the  $b$  axis in dendritic growth.<sup>32</sup> In these terms, it is not surprising that  $b$  is the fiber axis of the radiating units in spherulites grown from molten polyethylene, a medium comprising long-chain paraffinic molecules.

Electron microscopic examination of structures such as shown in Figure 5a suggests that the proliferation of layers in axialites may be brought about by a mechanism by which growth pyramids have previously been observed to form at the edges of single crystal lamellae.<sup>33</sup> Growing crystals are often serrated along their faster growing faces, and Figure 12 shows several examples of how neighboring spikes can be displaced out of the same plane and give rise to what are effectively screw dislocations.

\* Crystals grown under the same conditions from xylene are rhombic in habit and, in dendritic growth, develop mostly along the  $a$  axis.

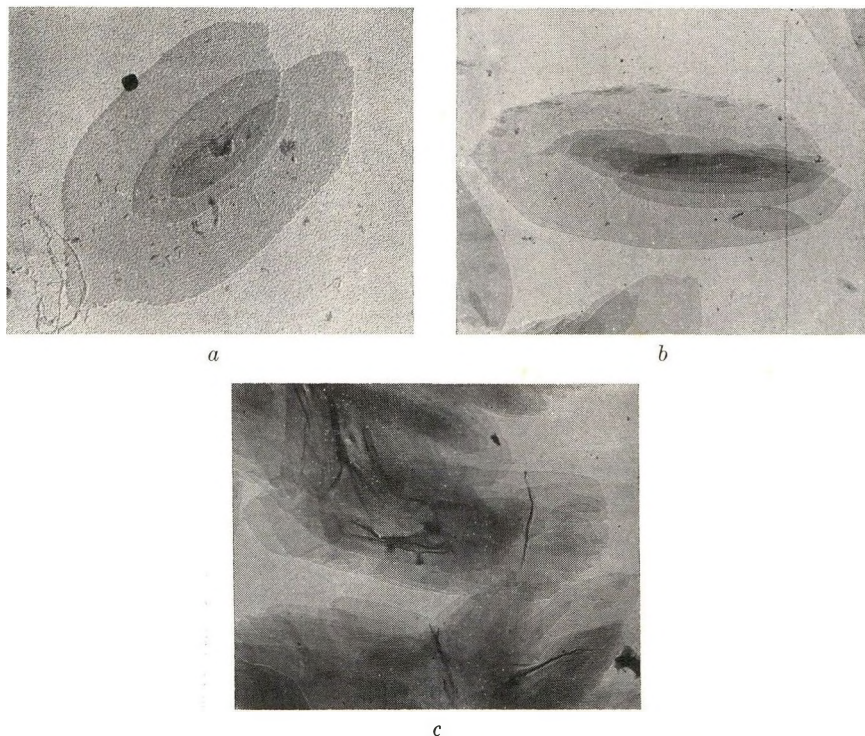


Fig. 12. Showing the generation of screw dislocations at the fast-growing surfaces of polyethylene crystals formed in: (a) 0.5% solution in  $C_{32}H_{66}$  at  $90^{\circ}C$ . ( $\times 13,800$ ); (b) 10% solution in  $C_{32}H_{66}$  at  $110^{\circ}C$ . ( $\times 2,300$ ); (c) 10% solution in  $C_{32}H_{66}$  at  $113^{\circ}C$ . ( $\times 3,680$ ). All are electron micrographs.

(It is not known whether these displacements are caused mechanically or as a result of domain boundaries being formed partly along planes involving relatively large Miller indices.) Rows of these dislocations are frequently formed along the faster growing  $b$  axes of aggregates of the kind shown in Figure 12b. These dislocations probably account not only for the proliferation of layers in axialites, but also for the observation that there is a compact packing of superimposed layers along their  $b$ -oriented spines.

### Discussion of Results

The various crystallization processes dealt with in previous sections are undoubtedly complex, and we have done no more than touch upon some of what are, perhaps, their more salient aspects. Nevertheless, it is clear that the morphological forms considered are related, and might be regarded as representing different stages in a development from single crystal to spherulite.

Regardless of whether they are growing in solution or in the melt, polymer single crystals are lamellar in habit, and usually retain relatively simple polyhedral outlines as long as they remain smaller than  $\delta$  in size.



Fig. 13. Aggregates grown in isotactic polystyrene at 200°C. Note that hedritic aggregates seen obliquely appear as sheaflike objects. Phase contrast,  $\times 515$ .

Concomitant with this growth, there is a pronounced tendency in all but very dilute solutions for a proliferation of layers, caused in the main by screw dislocations whose Burgers vectors lie normal to the planes of the crystals. For reasons that are far from clear, these layers splay and give rise to aggregates which appear sheaflike when viewed edge-on. In crystallization from solution we recognize these aggregates as multilayer crystals or as axialites. Similar aggregates formed in thin films of melt also appear sheaflike if nucleated so as to lie obliquely to the planes of the films. When lying in the planes of the films, however, these aggregates splay less and appear as hedrites (see Fig. 13). Further growth to sizes considerably larger than  $\delta$  usually leads in both instances to spherulites, presumably because individual layers respond to rejected impurities by breaking up into lamellar fibers (see again Figs. 2 and 9).

So far we have largely ignored an important step in achieving a spherulitic, as distinct from any other fibrous, habit. This is the introduction of noncrystallographic branching<sup>6</sup> without which, generally speaking, aggregates with radiating polycrystalline orientation would not be formed. With spherulites in polymers, however, radiating orientation of this kind is realized at the outset as a result of the splaying of layers in sheaflike precursors. But, in order that further growth will lead to spherulites of relatively compact texture, this splaying must be followed by a continuing and fairly profuse noncrystallographic branching of radial fibers. Details of how this comes about are as yet uncertain. The origin of the branches may well be found in the splaying of new layers generated at screw dislocations, and in disorder introduced at fold domain boundaries at re-entrant corners in growth fronts. However, the fact that there is comparatively little branching unless  $\delta$  is small<sup>6,7</sup> suggests that other considerations may also be involved. Clearly, this is an important problem for future study.

Finally, it may be pointed out that some of the questions raised in this study have also been discussed in a recent paper by Bassett, Keller, and Mitsuhashi.<sup>2</sup> The conclusions we have reached are essentially in agreement with the viewpoint adopted by these authors. The principal dif-

ferences arise in connection with the role of impurity segregation in crystallization (and the significance of  $\delta$ ), and the reasons for radial orientation of the  $b$  axis in spherulites of polyethylene.

Thanks are due to Dr. R. D. Heidenreich for invaluable assistance with the difficult technique of studying polymer crystals by electron diffraction; and also to Dr. F. Khoury for permission to quote results prior to publication. The manuscript has profited from critical reviews by Drs. D. C. Bassett, D. W. McCall, F. J. Padden, Jr., and E. Passaglia, all of which are gratefully acknowledged.

### References

1. Keller, A., *Phil. Mag.*, **2**, 1171 (1957).
2. Bassett, D. C., A. Keller, and S. Mitsuhashi, *J. Polymer Sci.*, **A1**, 763 (1963).
3. Bunn, C. W., and T. C. Alcock, *Trans. Faraday Soc.*, **41**, 317 (1945).
4. Keith, H. D., *Physics and Chemistry of the Organic Solid State*, Interscience, New York, 1963, Chap. 8.
5. Geil, P. H., *Growth and Perfection of Crystals*, Wiley, New York, 1958, p. 579.
6. Keith, H. D., and F. J. Padden, Jr., *J. Appl. Phys.*, **34**, 2409 (1963).
7. Keith, H. D., and F. J. Padden, Jr., *J. Appl. Phys.*, **35**, 1270, 1286 (1964).
8. Holland, V. F., and P. H. Lindenmeyer, *J. Polymer Sci.*, **57**, 589 (1962).
9. Rudd, J. F., *J. Polymer Sci.*, **44**, 459 (1960).
10. Bueche, F., *J. Chem. Phys.*, **20**, 1957 (1952).
11. Danusso, F., and F. Sabbioni, *Rend. Inst. Lomb. Sci. Letters*, **A92**, 435 (1958).
12. Chalmers, B., and J. W. Rutter, *Can. J. Phys.*, **31**, 151 (1953).
13. Keith, H. D., and F. J. Padden, Jr., to be published.
14. Schlesinger, W., and H. M. Leeper, *J. Polymer Sci.*, **11**, 203 (1953).
15. Leugering, H. J., *Kolloid-Z.*, **172**, 184 (1960).
16. Geil, P. H., *J. Appl. Phys.*, **33**, 642 (1960).
17. Magill, J. H., and P. H. Harris, *Polymer*, **3**, 252 (1962).
18. Symons, N. K. J., *J. Polymer Sci.*, **A1**, 2843 (1963).
19. Keith, H. D., and F. J. Padden, Jr., *J. Polymer Sci.*, **39**, 123 (1959).
20. Wunderlich, B., and P. Sullivan, *J. Polymer Sci.*, **61**, 195 (1962).
21. Lindenmeyer, P. H., *J. Polymer Sci.*, **C1**, 5 (1963).
22. Geil, P. H., and D. H. Reneker, *J. Polymer Sci.*, **51**, 569 (1961).
23. Keller, A., *J. Polymer Sci.*, **17**, 351 (1955).
24. Frank, F. C., A. Keller, and A. O'Connor, *Phil. Mag.*, **3**, 64 (1958).
25. Bassett, D. C., and A. Keller, *J. Polymer Sci.*, **40**, 565 (1959).
26. Niegisch, W. D., *J. Polymer Sci.*, **40**, 263 (1959).
27. Khoury, F., private communication.
28. Agar, A. W., F. C. Frank, and A. Keller, *Phil. Mag.*, **4**, 32 (1959).
29. Niegisch, W. D., and P. R. Swan, *J. Appl. Phys.*, **31**, 1906 (1960).
30. Reneker, D. H., and P. H. Geil, *J. Appl. Phys.*, **31**, 1916 (1960).
31. Bassett, D. C., and A. Keller, *Phil. Mag.*, **6**, 345 (1961).
32. Keith, H. D., *J. Appl. Phys.*, in press.
33. Bassett, D. C., and A. Keller, *Phil. Mag.*, **7**, 1553 (1962).

### Résumé

Il est suggéré que toutes les formes morphologiques, généralement observées dans les hauts polymères, sont étroitement liées. Ces formes sont considérées comme représentant les différentes étapes dans le développement de cristaux uniques en sphérulites, sous l'influence d'espèces, rejetées par des cristaux en croissance. Les cristaux uniques subissent cette transformation de configuration quand ils ont environ la grandeur donnée par  $\delta = D/G$ ,  $D$  étant le coefficient de diffusion dans le milieu cristallin,  $G$  étant la vitesse de

la croissance des cristaux. De nouveaux résultats expérimentaux montrent que, quand  $\delta$  est exceptionnellement grand, des cristaux peuvent naître dans les polymères fondus, et que quand  $\delta$  est diminué par l'emploi de polymères à haut poids moléculaire et/ou de solvants visqueux, les sphérulites peuvent naître d'une solution de polymère. Il est démontré que des mono-cristaux de polyéthylène cristallisés dans une solution de solvant paraffinique ont une configuration différente de ceux cristallisés dans les mêmes conditions dans le xylène. Ceci nous fournit une explication simple pour l'orientation radiale  $b$  trouvée dans les sphérulites de polyéthylène.

### Zusammenfassung

Eine enge Beziehung zwischen den gewöhnlich bei Hochpolymeren beobachteten morphologischen Formen wird angenommen. Diese Formen scheinen verschiedene Stufen einer Entwicklung vom Einkristall zum Sphärolithen unter dem Einfluss einer von den wachsenden Kristallen abgewiesenen Spezies zu sein. Bei Einkristallen tritt diese Habitusumwandlung dann auf, wenn sie ungefähr die Grösse  $\delta = D/G$  besitzen, wo  $D$  der Diffusionskoeffizient im kristallisierenden Medium und  $G$  die Kristallwachstumsgeschwindigkeit ist. Neue Versuchsergebnisse zeigen, dass bei ungewöhnlich grossem  $\delta$  Einkristalle aus Polymerschmelzen gezogen werden können und dass bei Herabsetzung von  $\delta$  durch Verwendung von Polymerem mit hohem Molekulargewicht oder viskosen Lösungsmitteln aus Polymerlösungen Sphärolithe gezogen werden können. Es wird gezeigt, dass aus paraffinischen Lösungsmitteln kristallisierte Polyäthyleneinkristalle einen von den unter gleichen Bedingungen aus Xylol kristallisierten verschiedenen Habitus zeigen. Dies gibt eine einfache Erklärung für die in Sphärolithen von Polyäthylen gefundene radiale  $b$ -Orientierung.

Received October 28, 1963



## Polyether-Ester Copolymer Prepared from *p*- $\gamma$ -Hydroxypropoxy Benzoate and Bis- $\beta$ -hydroxyethyl Terephthalate

MATAHUMI ISHIBASHI, *Research and Development Laboratories,  
Nippon Rayon Company, Ltd., Uji, Kyoto, Japan*

### Synopsis

Polyether-ester copolymers were prepared from methyl *p*- $\gamma$ -hydroxypropoxy benzoate and bis- $\beta$ -hydroxyethyl terephthalate over the entire composition range by a condensation reaction. It was found by means of x-ray diffraction that the copolymers showed high crystallinity over the entire range of copolymer composition. The melting point curve of the copolymers showed a eutectic type. The x-ray diffraction patterns of the copolymers were different from both those of poly(ethylene terephthalate) and of poly(*p*-1,3-propylene oxybenzoate). These results showed that in each of the copolymers both the repeating units, the ethylene terephthalate unit and the *p*-1,3-propylene oxybenzoate unit, could be incorporated into the chain of a crystallizable polymer without hindering crystallization of the resulting copolymer, i.e., the copolymers were isomorphous over the entire composition range.

### Introduction

The copolymer prepared from *p*- $\beta$ -hydroxyethoxy benzoate and bis- $\beta$ -hydroxyethyl terephthalate, hereafter called EB/ET copolymer, has been the subject of at least two publications.<sup>1,2</sup> Kawaguchi and Nukushina<sup>2</sup> have pointed out that crystallization could not be observed in EB/ET copolymer whose content of *p*-ethylene oxybenzoate was between 50 and 90 mole-% and that x-ray diffraction patterns of EB/ET copolymer showed that up to about 40 mole-% of *p*-ethylene oxybenzoate the original poly(ethylene terephthalate) structure still persisted, but the size of the crystals was greatly reduced. The same behavior was observed when small amounts of ethylene terephthalate were added to *p*-ethylene oxybenzoate; the crystals were still of the same type as the original poly(*p*-ethylene oxybenzoate). We have investigated the possibility of the formation of mixed crystals in copolymers prepared from other *p*-hydroxyalkoxy benzoates and bis- $\beta$ -hydroxyethyl terephthalate and have found a crystallizable copolymer prepared from methyl *p*- $\gamma$ -hydroxypropoxy benzoate and bis- $\beta$ -hydroxyethyl terephthalate, hereafter called PB/ET copolymer, over the entire range of copolymer composition.

### Experimental

The starting materials, methyl *p*- $\gamma$ -hydroxypropoxy benzoate and bis- $\beta$ -hydroxyethyl terephthalate, were prepared at this laboratory. The melting point of methyl-*p*- $\gamma$ -hydroxypropoxy benzoate, which is believed to be a new compound, is 54°C.; that of bis- $\beta$ -hydroxyethyl terephthalate is 107°C. and agreed well with that reported in the literature.

To prepare PB/ET copolymer, the two starting materials were weighed separately to give the correct mole ratio, mixed thoroughly, and transferred quantitatively to the reaction flask for polymerization. In this work, the molar ratio of methyl *p*- $\gamma$ -hydroxypropoxy benzoate was increased by 10% each time.

TABLE I  
Melting Points of *p*-Propylene Oxybenzoate and Ethylene Terephthalate Copolymer (PB/ET Copolymer), and *p*-Ethylene Oxybenzoate and Ethylene Terephthalate Copolymer (EB/ET Copolymer)

PB or EB, mole-%	Melting point, °C.	
	PB/ET copolymer	EB/ET copolymer <sup>a</sup>
0	262	262
10	241	247
20	225	229
30	207	208
40	183	180
50	164	—
60	159	—
70	174	—
80	182	—
90	195	189
100	211	203

<sup>a</sup> Data of Kawaguchi and Nukushina.<sup>2</sup>

The copolymer was obtained by heating the mixture for 6 hr. at 275°C., first under nitrogen atmosphere then under reduced pressure (0.5 mm.), to a high degree of polymerization.

The melt spinning apparatus used in this work was a Shimadzu Model KOKA flow tester<sup>3</sup> in which the polymer was melted in an electrically heated cell and was extruded through a spinneret. The monofilaments, about 1000 den., were drawn 4.5 times their original length at 60°C.

The melting points were determined by observing solid particles of the copolymer between crossed Nicol polarizers on an electrically heated hot-stage microscope. The temperature at which the last trace of birefringent crystallinity completely disappeared was taken as the melting point.

X-ray diffraction patterns were taken on flat plate film at a sample-to-film distance of 50.0 mm. with nickel-filtered copper  $K\alpha$  radiation.

## Results

All PB/ET copolymer was highly crystalline. The melting points of crystalline PB/ET copolymer were determined. The results are listed in Table I together with those of EB/ET copolymer. Plots of melting point versus composition for PB/ET copolymer show a eutectic type; these are presented in Figure 1. The x-ray diffraction patterns of drawn fibers of PB/ET copolymer are shown in Figure 2. The copolymer has new crystal structures which give sharp x-ray diffraction patterns.

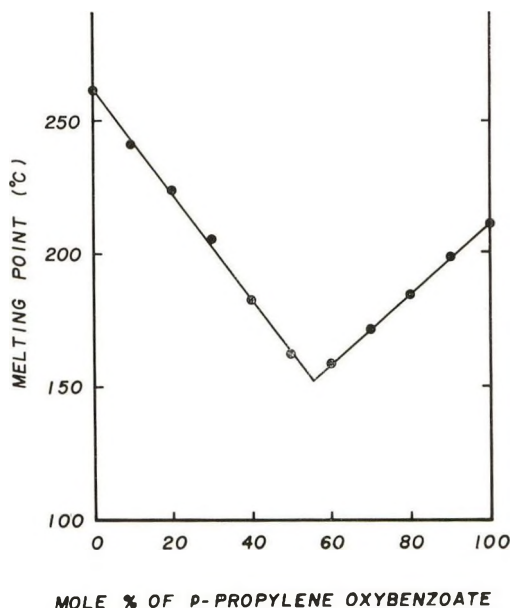


Fig. 1. Melting points of *p*-propylene oxybenzoate-ethylene terephthalate copolymer plotted against content of *p*-propylene oxybenzoate.

## Discussion

The formation of a mixed crystal, an isomorphic phenomenon, has often been observed in low molecular weight compounds in which the molecules are similar in size and chemical nature. However, this phenomenon occurs only rarely in synthetic macromolecular substances. In a copolymeric system, a mixed crystal involves the introduction of repeating units having different structures into a single crystalline lattice. Several instances of the formation of mixed crystals in copolymeric systems have been reported for copolyamides,<sup>4-6</sup> for stereoregular copolymers of styrene and substituted styrene,<sup>7</sup> and for copolycarbonates.<sup>8</sup>

The preparation and structure of copolymers containing the ethylene terephthalate unit and another unit have been investigated by many workers. In almost all of these cases it has been revealed that the formation of mixed crystals containing both units could not be observed, that the

achievable amount of crystallinity is much lower in the copolymer than in the individual homopolymers, and that the melting range of the crystallites in the copolymer is lower than that of the corresponding homopolymer.

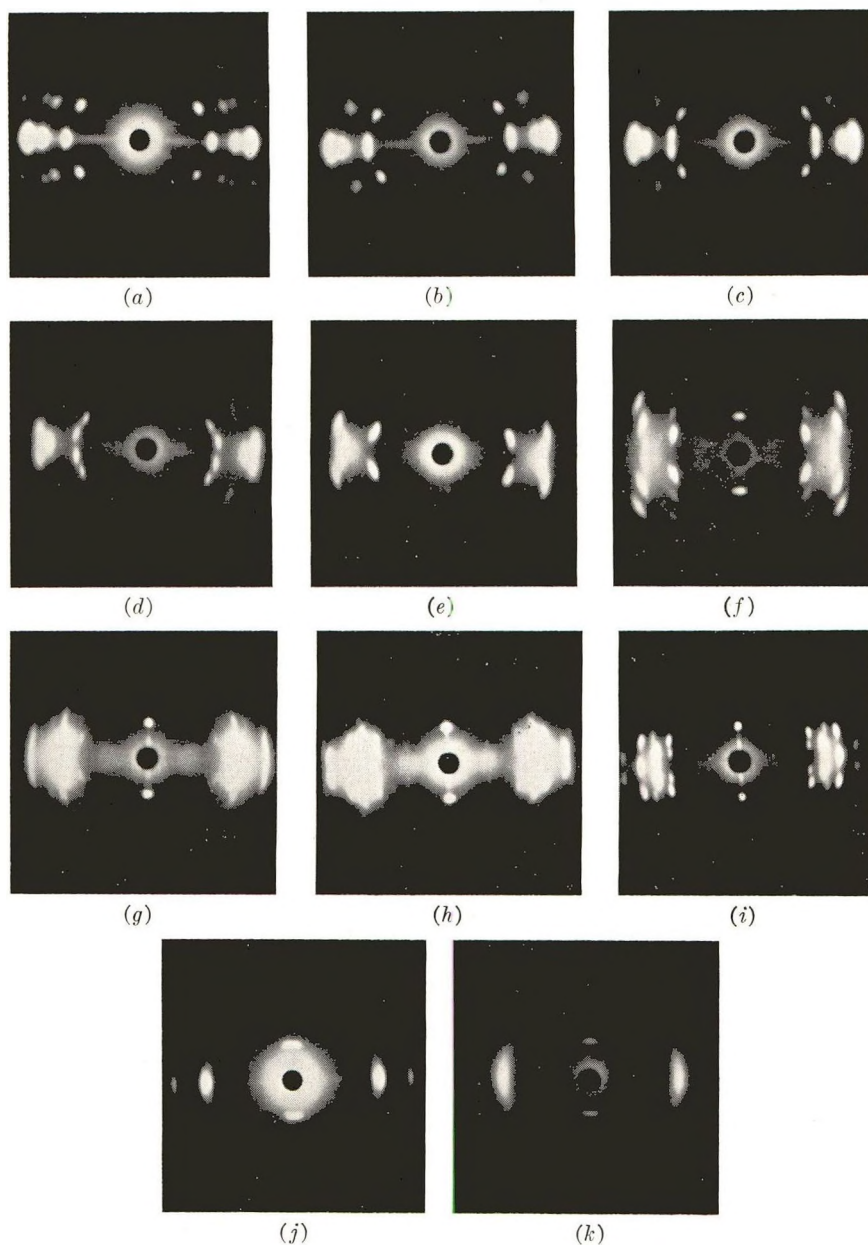


Fig. 2. X-ray diffraction patterns of *p*-propylene oxybenzoate-ethylene terephthalate copolymers with various contents of *p*-propylene oxybenzoate: (a) 0 mole-%; (b) 10 mole-%; (c) 20 mole-%; (d) 30 mole-%; (e) 40 mole-%; (f) 50 mole-%; (g) 60 mole-%; (h) 70 mole-%; (i) 80 mole-%; (j) 90 mole-%; (k) 100 mole-%.

For instance, Edgar and Hill<sup>9</sup> carried out a very careful investigation of the systems ethylene terephthalate–ethylene adipate and ethylene terephthalate–ethylene sebacate. With addition of ethylene adipate or ethylene sebacate to the ethylene terephthalate system, the melting point drops rapidly. X-ray diffraction patterns of the copolymer show that up to about 70 mole-% of ethylene adipate or ethylene sebacate the poly(ethylene terephthalate) structure still persists, though the amount of background scattering increases with the proportion of ethylene adipate or ethylene sebacate.

It is understood from the results of Table I or Figure 1 that PB/ET copolymer is a random one and repeating units of two different structures are therefore introduced statistically along copolymer chains. As shown in Figure 2, the x-ray diffraction patterns of PB/ET copolymer are different from those of poly(ethylene terephthalate) (Fig. 2a) and poly(*p*-1,3-propylene oxybenzoate) (Fig. 2k). There are many differences between Figures 2a, 2b, and 2c in the diffraction spots on layer lines in original negative plates, though they are only barely visible in Figure 2. It is observed from Figure 2 that the amount of background does not increase with increasing content of the second component and that the x-ray diffraction spots do not become broad at any of the intermediate compositions. These results reveal that mixed crystallites containing both units are formed, and that the structure of the mixed crystallites changes with the proportion of the second component. The detailed structure of the mixed crystalline form of the copolymer is being studied, and it will be reported in a subsequent paper.

One of the most probable reasons, for the formation of mixed crystallites in the PB/ET copolymer system is the identity of the repeat period of each component. The value of the repeat period calculated from the molecular configuration of *p*-propylene oxybenzoate unit is 11.07 Å. and that for the ethylene terephthalate unit<sup>10</sup> is 10.9 Å. Therefore different repeating units are incorporated into the chain of the crystallizable polymer without hindering the crystallization of the resulting copolymer.

## References

1. Griehl, W., and H. Lückert, U. S. Pat. 3,056,761 (1962).
2. Kawaguchi, T., and Y. Nukushina, *Kobunshi Kagaku*, **20**, 529 (1963).
3. Arai, T., *A guide to the testing of rheological properties with KOKA flow tester* (in English), Maruzen, Tokyo, Japan, 1958.
4. Cramer, F. B., and R. G. Beaman, *J. Polymer Sci.*, **21**, 237 (1956).
5. Yu, A. J., and R. D. Evans, *J. Am. Chem. Soc.*, **81**, 5361 (1959).
6. Levine, M., and S. C. Temin, *J. Polymer Sci.*, **49**, 241 (1961).
7. Natta, G., P. Corradini, D. Sianesi, and D. Morero, *J. Polymer Sci.*, **51**, 527 (1961).
8. Rubin, I. D., *J. Polymer Sci.*, **A1**, 1645 (1963).
9. Edgar, O., and R. Hill, *J. Polymer Sci.*, **8**, 1 (1952).
10. Daubeny, R. de P., C. W. Bunn, and C. J. Brown, *Proc. Roy. Soc. (London)*, **A226**, 531 (1954).

### Résumé

On a préparé des copolymères de polyéther-ester à partir du *p*- $\gamma$ -hydroxypropoxybenzoate et du téréphtalate de bis- $\beta$ -hydroxyéthyls pour des rapports de compositions variées par une réaction de condensation. On a trouvé par des études de diffraction aux rayons-X que les copolymères montrent une cristallinité élevée pour l'ensemble des rapports de composition du copolymère. La courbe de fusion des copolymères est du type eutectique. Les diagrammes de diffraction aux rayons-X des copolymères ne correspondent ni à ceux du téréphtalate de polyéthylène ni à ceux de l'oxybenzoate de poly-*p*-1,3-propylène. Les résultats montrent que dans chacun des copolymères, les deux unités, le téréphtalate d'éthylène et l'oxybenzoate de *p*-1,3-propylène, peuvent être incorporés dans la chaîne d'un polymère cristallisable sans gêner la cristallisation du copolymère résultant. Ceci veut dire que les copolymères sont isomorphes pour tous les rapports de composition.

### Zusammenfassung

Polyätheresterkopolymere wurden aus Methyl-*p*- $\gamma$ -Hydroxypropoxybenzoat und Bis- $\beta$ -Hydroxyäthylterephthalat über den ganzen Zusammensetzungsbereich durch eine Kondensationsreaktion hergestellt. Mittels Röntgenstreuung wurde gefunden, dass die Kopolymeren über den ganzen Bereich der Kopolymerzusammensetzung hohe Kristallinität zeigen. Die Schmelzpunktkurve der Kopolymeren war von eutektischen Typ. Die Röntgenbeugungsdiagramme der Kopolymeren stimmten weder mit denen von Polyäthylenterephthalat noch mit denen von Poly-*p*-1,3-Propylenoxybenzoat überein. Diese Ergebnisse zeigen, dass in jedes der Kopolymeren beide Grundbausteine, nämlich der Äthylenterephthalat und der *p*-1,3-Propylenoxybenzoatbaustein in die Kette eines kristallisationsfähigen Polymeren ohne Behinderung der Kristallisation des resultierenden Kopolymeren eingebaut werden können; d.h. die Kopolymeren sind im ganzen Zusammensetzungsbereich isomorph.

Received December 6, 1963

## Applicability of Polymer Network Theories to Gels Obtained by Crosslinking a Polymer in Solution\*

B. MUKHERJI and W. PRINS, *Laboratory of Physical Chemistry, Technische Hogeschool, Delft, The Netherlands*

### Synopsis

Current polymer network theories exhibit inconsistencies which show up particularly clearly when one considers the three-dimensional deformation (swelling) of networks which are prepared by crosslinking a polymer in solution. A check on the theories can only be obtained if one knows precisely the number of crosslinks in the network and if a range of deformations (range of swelling ratios) is imposed on the network. To this end a series of seven gels was prepared by crosslinking secondary cellulose acetate (D.S. = 2.42) in dioxane solution (5-10%) with dianisidine diisocyanate. The number of chemical crosslinks was determined by reacting unused isocyanate groups with  $C^{14}$ -labeled methanol. Subsequently, changes in the degree of swelling of the gel, induced by increasing concentrations of cellulose acetate in dioxane and methyl acetate solutions around the gel, were followed by measuring accurately the changes in length of 2-cm. strips under a travelling microscope. At equilibrium swelling the activities of the solvent inside and outside the gel are equal. For the outside solutions the activities were derived from osmometry. The inside activities derive from a mixing term and an elastic deformation term. The mixing term was approximated by using the Flory-Huggins expression with an interaction parameter, as obtained from osmometry on a derivative, which was prepared by reacting cellulose acetate with an excess of diisocyanate, thus avoiding network formation. By means of the various known theoretical expressions for the elastic deformation term, the swelling data allow the calculation of the number of crosslinks in the gels. All theories lead to far fewer crosslinks than are known to be there on the basis of the chemical analysis. This has never been observed to the same extent before, but may be specific for gels obtained by crosslinking in solution. One is forced to conclude that none of the existing theories are applicable. The data can be explained, however, by postulating that the configurations of the chains between crosslinks do not follow a Gaussian distribution, but are instead given by  $\omega(\mathbf{r})d\mathbf{r} = \omega_x(x)\omega_y(y)\omega_z(z) dx dy dz$ , where  $\omega_x(x) = C|x|^n \exp\{-bx^2\}$ . Such a non-Gaussian distribution might arise because of topological restrictions, possibly including those due to the excluded volume. For the free energy of elastic deformation we find, following James and Guth's reasoning but using the new distribution function:

$$\Delta F_{el}/kT = \nu[(n+1)/2][\lambda_x^2 + \lambda_y^2 + \lambda_z^2 - 3] - \nu n \ln \lambda_x \lambda_y \lambda_z$$

where  $\nu$  is the number of chains in the network and  $\lambda_x$ ,  $\lambda_y$ , and  $\lambda_z$  are the deformation ratios with respect to the unstrained state. In the well known Gaussian theories, the term  $n+1$  is absent and in front of the logarithm instead of  $n$  either 0,  $2/f$ , or 1 ( $f$  = functionality of the crosslink) is found, depending on whether the result of James and Guth, Flory and Wall, or Hermans is used, respectively.

\* Based on a thesis submitted by B. Mukherji to the Graduate School, State University College of Forestry, Syracuse, N. Y., in partial fulfillment of the requirements for the Ph.D., 1963.

## INTRODUCTION

Various theoretical derivations of the free energy of elastic deformation of polymer networks exist in the literature. A review of these has recently been given by Staverman.<sup>1</sup> All treatments so far assume (1) that the elastic free energy is not affected by intermolecular forces, (2) that the constraints imposed by the network structure are delivered only at the crosslinks, (3) that the components of the mean end-to-end distance of the chains are changed by the deformation in the same ratio as the corresponding dimensions of the sample, and (4) that the end-to-end distribution for the "free" chains is Gaussian.<sup>2</sup> The final equation obtained by Hermans<sup>3</sup> is:

$$\Delta F_{e1} = kT[(\nu/2)(\lambda_x^2 + \lambda_y^2 + \lambda_z^2 - 3) - \nu \ln \lambda_x \lambda_y \lambda_z] \quad (1)$$

Flory and Wall<sup>4</sup> find

$$\Delta F_{e1} = kT[(\nu/2)(\lambda_x^2 + \lambda_y^2 + \lambda_z^2 - 3) - (2\nu/f) \ln \lambda_x \lambda_y \lambda_z] \quad (2)$$

and James and Guth, in one of their papers,<sup>5</sup> consider

$$\Delta F_{e1} = kTK(\lambda_x^2 + \lambda_y^2 + \lambda_z^2 - 3) \quad (3)$$

to be the most probable expression for the elastic free energy. In these equations  $\lambda_x$ ,  $\lambda_y$ , and  $\lambda_z$  are the elastic deformation ratios,  $\nu$  is the number of chains which take an active part in the deformation,  $f$  is the functionality of the crosslinks, i.e., the number of chains connected in one crosslink;  $K$  in eq. (3) is a constant depending on  $\nu$  but also in an as yet unspecified way on the structure of the network.

For a deformation without a change in volume, the controversial term  $\ln \lambda_x \lambda_y \lambda_z$  drops out. Furthermore, if the deformation ratios are large, the logarithmic term becomes negligible compared to the  $\lambda^2$  terms and thus again drops out. However, for a three-dimensional deformation, such as occurs in the isotropic swelling of a polymer network in a diluent, the disputed logarithmic term may exert a measurable influence if the volume occupied by the network in the unstrained state is not very small compared to the volume of the swollen network, in other words if the  $\lambda$ 's are not too large. This can be realized by employing networks which are prepared by crosslinking a polymer in solution.

A first attempt to follow this trend of thought was made by Rijke and Prins,<sup>6</sup> who crosslinked secondary cellulose acetate solutions in dioxane with oxalyl chloride. Swelling measurements were performed in a series of cellulose acetate solutions. If the equilibrium swelling of a network is described as due to the balance of a free energy of mixing term,  $\Delta F_m^g$ , and the elastic free energy,  $\Delta F_{e1}$ , one can write for the thermodynamic potential of the solvent in the gel (g):

$$\mu_g = \partial \Delta F_m^g / \partial N + \partial \Delta F_{e1} / \partial N$$

where  $N$  is the number of solvent molecules in the swollen gel. For the



thermodynamic potential of the solvent outside the gel (s) we will have only a mixing term:

$$\mu^s = \partial \Delta F_m^s / \partial N$$

Introducing now the Flory-Huggins expressions for  $\Delta F_m^s$  and  $\Delta F_m^g$  and inserting in eqs. (1)–(3) yields

$$\lambda_x = \lambda_y = \lambda_z = (q/q_0)^{1/3}$$

where  $q$  is the degree of swelling and  $q_0$  the degree of swelling at which the chains in the network are unstrained (i.e., where  $\Delta F_{cl} = 0$ ), and defining

$$p = V_{dry}/\nu v$$

$$K' = V_{dry}/2Kv$$

with  $V_{dry}$  denoting the dry volume of the network and  $v$  the molecular volume of the solvent, Rijke and Prins obtain<sup>6</sup> from the equilibrium condition  $\mu^s = \mu^g$  for eqs. (1)–(3):

$$\text{from eq. 1:} \quad D\phi_g^{-1/3} = (1/p)q_0^{-2/3} - (1/p)\phi_g^{2/3} \quad (4)$$

$$\text{from eq. 2:} \quad D\phi_g^{-1/3} = (1/p)q_0^{-2/3} - (2/pf)\phi_g^{2/3} \quad (5)$$

$$\text{from eq. 3:} \quad D\phi_g^{-1/3} = (1/K')q_0^{-2/3} \quad (6)$$

where

$$D = kT[\ln(1 - \phi_s) + (1 - 1/x)\phi_s + \chi_s\phi_s^2 - \ln(1 - \phi_g) - \phi_g - \chi_g\phi_g^2]$$

Here  $\phi_s$  and  $\phi_g$  ( $= q^{-1}$ ) are the volume fractions polymer in the solution and in the gel, respectively;  $\chi_s$  and  $\chi_g$  are the respective Flory-Huggins interaction parameters; and  $x$  is the ratio of the molecular volume of a dissolved polymer chain to the volume of a solvent molecule.

From the swelling data in a series of cellulose acetate solutions, it is thus feasible to calculate  $p$  ( $\sim 1/\nu$ ) and  $q_0$  from eq. (4) or (5) if  $x$ ,  $\chi_s$ , and  $\chi_g$  are known, by plotting  $D\phi_g^{-1/3}$  versus  $\phi_g^{2/3}$ . The quantities  $x$  and  $\chi_s$  were obtained by osmometry on the solutions, and an argument was presented to justify the assumption that  $\chi_g = \chi_s$ .\*

It was concluded that eq. (6) cannot apply. Equations (4) and (5) lead to different values for  $p$  and  $q_0$ . In fact, it is easily seen that the  $p$ -values will differ by a factor  $f/2$  and the  $q_0$  values by a factor  $(f/2)^{-3/2}$ . A firm decision between eqs. (4) and (5) could, however, not be made on the basis of the experimental data because no absolutely reliable independent value for  $p$  could be obtained from a chemical analysis of the number of crosslinks introduced in the networks.

Because of this shortcoming, we decided to prepare a wide range of gels with the emphasis on an accurate determination of the number of chemical

\* Off-hand one would think that from any three swelling measurements in three different solutions, all three parameters  $p$ ,  $q_0$ , and  $\chi_g$  should be solvable. Due to the almost vanishing of the coefficient determinant in each set of three linear equations in the unknowns  $\chi_g$ ,  $1/p$ , and  $(1/p)q_0^{-2/3}$  this is not feasible in practice.

crosslinks introduced. Secondary cellulose acetate was chosen as polymeric starting material, not only to allow a comparison with the data of Rijke and Prins<sup>6</sup> but also because it shows less syneresis during crosslinking than other polymers, which were also tried. Crosslinking was carried out with dianisidine diisocyanate, and the degree of crosslinking was determined by a radioactive tracer technique. The equilibrium swelling of the gels in pure solvents was determined in a standard fashion. Small changes in swelling induced by changes in the medium were measured much more accurately than before<sup>6</sup> under a travelling microscope, equipped with a finely adjustable micrometer table. The possible influence of crosslinks on  $\chi_{\kappa}$  was investigated by osmometry on a soluble cellulose acetate derivative prepared by reacting cellulose acetate with an excess of diisocyanate. Since the data do not unequivocally support any of the existing theories, an attempt is made to explain the data by assuming non-Gaussian chain statistics, which are thought to be a result of topological restrictions and of the excluded volume.

## EXPERIMENTAL

### Preparation and Analysis of Cellulose Acetate Networks

Dianisidine diisocyanate, DADI, (3,3'-dimethoxy-4,4'-biphenylene diisocyanate, Carwin Chemical Co., North Haven, Conn.) was purified by vacuum sublimation. The product was colorless and could be titrated to

TABLE I  
Preparation and Analysis of Cellulose Acetate Networks

Gel	$\phi_c$ Volume fraction cross- linked <sup>a</sup>	Structural units/ crosslink <sup>b</sup>	Radioactive, disintegrations/sec. <sup>c</sup>		Structural units/ side branch <sup>d</sup>	Structural units/ chemical crosslink <sup>e</sup>
			Part I	Part II		
1	0.067	7.85	1060		438	8.2
2	0.062	20.23	208	548	2230	20.6
3	0.059	14.13	903	1959	514	14.8
4	0.107	12.98	846	1414	548	13.4
5	0.054	3.74	2203	5508	210	4.9
6	0.077	15.67	582	1183	797	16.4
7	0.063	21.43	658	1227	705	22.5

<sup>a</sup>  $\phi_c$  is the volume fraction of cellulose acetate in solution in which crosslinkages were introduced.

<sup>b</sup> Structural units/crosslink is the number of cellulose acetate structural units (molecular weight 263) per diisocyanate molecule added for crosslinking.

<sup>c</sup> Radioactive disintegrations/sec. is the number of radioactive disintegrations/sec./gm. of the reacted gel (1 mole NCO  $\equiv$  1 mole radioactive methanol  $\cong$   $32 \times 3.81 \times 10^6$  disintegrations/sec.).

<sup>d</sup> Structural units/side branch is the number of structural units per isocyanate side branch in the network.

<sup>e</sup> Structural units/chemical crosslink is the number of structural units per chemical crosslink introduced.

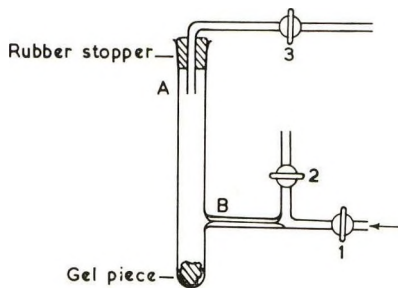


Fig. 1. Assembly for reacting a piece of crosslinked cellulose acetate gel with  $C^{14}$ -labeled methanol in the absence of moisture. For explanation, see text.

more than 99% pure diisocyanate with di-*n*-butylamine and hydrochloric acid. The secondary cellulose acetate was the same as used in the study of Rijke and Prins<sup>6</sup> (D.S. = 2.42,  $\bar{M}_n \approx 50,000$ ). It was dried in vacuum at 75°C. over  $P_2O_5$ . The dioxane used as a solvent during preparation was always freshly purified and dried by the usual methods.

The crosslinking was carried out in sealed Pyrex glass tubes of 2.5 cm. I.D., 15 cm. length, and 2 mm. wall thickness. Appropriate amounts of carefully determined cellulose acetate solution in pure dry dioxane and DADI were introduced in the tubes (see Table I) in a drybox. The mixtures were subsequently purged with dry nitrogen and cooled in liquid air under a nitrogen stream outside the drybox and sealed under vacuum. The sealed tubes were then placed in an oven at 110°C. and kept there for ten days, after which period the temperature was lowered slowly to room temperature to avoid uneven cooling which gives rise to bubbles in the gel.

At cellulose acetate concentrations lower than 5% or with DADI amounts less than 3 molecules per chain, gelation is not complete. If too large amounts of DADI crosslinks are used, considerable syneresis occurs. The range of gels which can be used for our experimental purpose is therefore limited to the series given in Table I.

For the determination of the number of crosslinks formed during gelation, it is necessary to establish that isocyanate reacts exclusively with the hydroxyl groups on the cellulose acetate chain (D.S. = 2.42). Under the conditions used for crosslinking, reaction with acetyl groups is extremely unlikely.<sup>7</sup> Reaction of the urethane derivative formed from the hydroxyl groups and DADI with additional DADI is in principle possible, but was shown to occur only to a negligible extent by reacting DADI with ethanol. It was found by titration with di-*n*-butylamine that the excess DADI is recovered quantitatively.

With this fact established, the amount of isocyanate groups left after completion of the gelation was determined by reacting them with  $C^{14}$ -labeled methanol. A weighed gel piece was taken from one of the crosslinking tubes under dry nitrogen in a drybox, and inserted in a tube as shown in Figure 1. After removing this tube from the drybox while passing  $N_2$  through stopcocks 1 and 3 a constriction was made at A; the stopcock 2 was opened and the seal completed at A under nitrogen pressure.

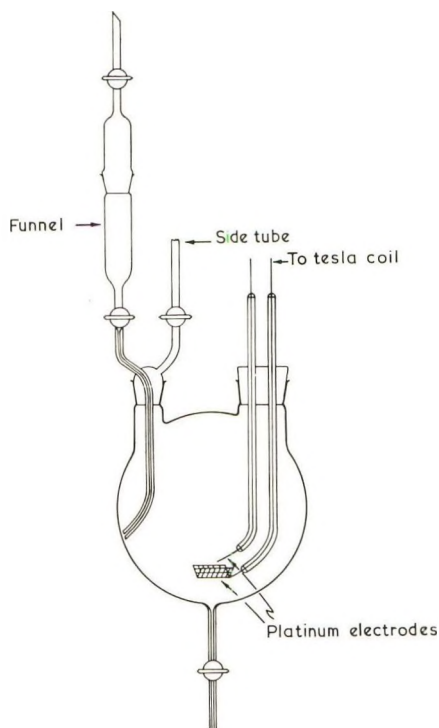


Fig. 2. Modified Schöniger apparatus for the preparation of  $C^{14}$ -labeled  $CO_2$  obtained by burning a dry piece of labeled gel in an oxygen atmosphere.

Through the capillary tube B an excess (0.1–0.2 ml.) of  $C^{14}$ -labeled methanol (activity 0.1 mc./g.) was added, again in the drybox under nitrogen. Stopcocks 1 and 2 were closed, the tube was taken out and sealed at B while passing nitrogen through 1 and 2. In order to ensure complete reaction of the isocyanate groups with the labeled methanol, the tube was heated in an oven at  $100^\circ C.$  for 5 days. The “reacted” gel was divided into two weighed parts (I and II). Part I was extracted in a Soxhlet apparatus with dioxane for 30–40 hr. in order to remove all free radioactive materials (methanol and the product of the reaction of methanol with free DADI). Only the product formed by the reaction of the labeled methanol with one isocyanate group of a DADI molecule which has already reacted at the other end with a hydroxyl group of the cellulose acetate remains in the gel, Part II was dried directly at  $30^\circ C.$ , then allowed to swell in dioxane vapor, and dried again. The process was repeated four times to ensure complete removal of methanol. All the  $C^{14}$  in the active methanol, which has reacted with all isocyanate groups left after the gelation reaction, thus remains in this Part II. It was established separately that the DADI–methanol reaction product is not volatile under the conditions used.

The activities of parts I and II were determined by burning the dried gel pieces to carbon dioxide with oxygen in a modified Schöniger apparatus

carbon dioxide being absorbed in a 1*M* solution in methanol of hyamine [*p*-(diisobutyl-cresoxyethoxyethyl)-dimethylbenzylammonium hydroxide, Packard Instrument Inc., La Grange, Ill]. The apparatus is shown in Figure 2. The oxygen is added through the side tube, the ignition takes place by means of a Tesla coil, and a known volume of Hyamine solution is added through the funnel. After absorption of the carbon dioxide by the Hyamine solution, an aliquot (3 ml.) was taken out through the bottom tube, mixed with a standard volume phosphor solution, and its activity determined in a liquid scintillation counter (Model 6012, Isotope Development Ltd., England). The counting efficiency of the instrument was determined by adding an amount of labeled ethanol of exactly known activity to the above mixture and counting the apparent number of disintegrations per second. It was assumed that the counting efficiency remains the same whether C<sup>14</sup> is present as carbonate or as alcohol. If  $A_a$  is the apparent activity of the gel,  $E_c$  the counting efficiency,  $A_{MeOH}$  the activity of one mole methanol, the number of moles of labeled urethane groups (CH<sub>3</sub>O—CO—NH—) present in the sample is given by  $A_a / (E_c A_{MeOH})$ , which can subsequently be converted to the amount of such groups present in the original gel since all weights are known.

The results in Table I show that the activity left in part I as well as part II is very low, which indicates that almost all DADI introduced has reacted at both ends to form crosslinks (>99%). The results also prove that complications which might arise as a result of side reactions (e.g., ester interchange leading to labeled methyl carbonate and crosslink scission) are unimportant. If side reaction products would occur, this would show up in the difference in activity of parts I and II. Since the measured activities are very small anyway, this proves that these side reactions do not have to be taken into account.

### Swelling Measurements

The equilibrium degrees of swelling,  $q_1$  (swollen volume/dry volume), of all seven gels at 25°C. were determined in pure dioxane and methyl acetate by blotting and weighing large pieces in the swollen and in the dry state, on the basis of the known densities of cellulose acetate and the solvents, and by assuming additivity. The results are given in Table II and in Figures 3 and 4.

For the measurements of the changes in swelling induced by immersing the gels in a series of cellulose acetate solutions of increasing concentration, we first used the swelling balance described by Rijke and Prins.<sup>6</sup> It was observed, however, that in viscous solutions the results were not reproducible due to the adherence of a layer of the solutions to the gels. A much higher accuracy could be reached by measuring one of the dimensions of the gel under a travelling microscope. Pieces of gel were cut in the form of a strip of approximately 2 × 10 × 30 mm. Near the two ends two very small graphite particles or some inorganic insoluble pigment particles were embedded. The strips were then placed in cells with flat windows filled

TABLE II  
Swelling of Gels in Pure Dioxane (DX) and Methyl Acetate (MA) at 26°C.

Gel	Structural units/chemical crosslink	$\phi_c$	$q_c (= 1/\phi_c)$	$p_{\Lambda}^{\text{DX}}$	$q_1^{\text{DX}}$	$p_{\Lambda}^{\text{MA}}$	$q_1^{\text{MA}}$
1	8.2	0.067	14.92	9.2	16.09	9.8	14.94
2	20.6	0.062	16.13	23.3	41.08	24.2	33.92
3	14.8	0.059	16.95	18.1	30.18	19.3	25.50
4	13.4	0.107	9.35	16.9	14.52	18.0	12.98
5	4.9	0.054	18.52	5.5	12.64	5.8	11.32
6	16.4	0.077	12.99	19.3	27.04	20.6	23.14
7	22.5	0.063	15.87	25.8	34.16	27.5	28.27

with the solvent. After noting the distance  $L_1$  between the two markers in the gel as measured under a travelling microscope with an accuracy of 0.03%, the solvent was replaced by a cellulose acetate solution and the resulting change in distance,  $L - L_1$ , between the markers was measured. Since the gels were isotropic, the degrees of swelling then follow from the

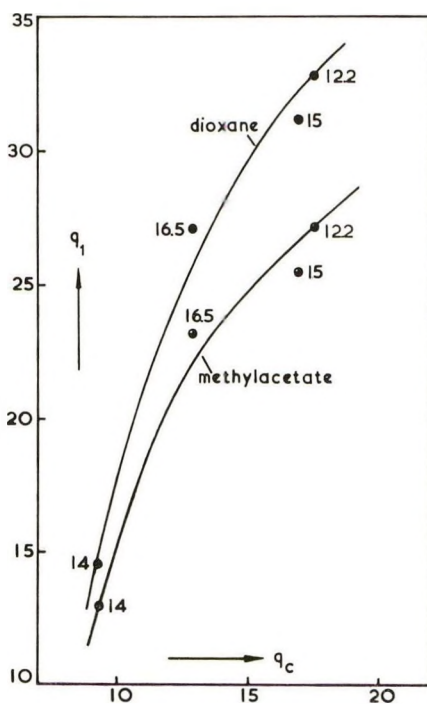


Fig. 3. The degree of swelling,  $q_1$  (swollen volume/dry volume), of the crosslinked cellulose acetate gels in pure dioxane and pure methyl acetate, plotted vs. the degree of dilution,  $q_c$ , prior to crosslinking. The numbers written near the experimental points represent the crosslinking densities, expressed as the number of structural units/chemical crosslink.

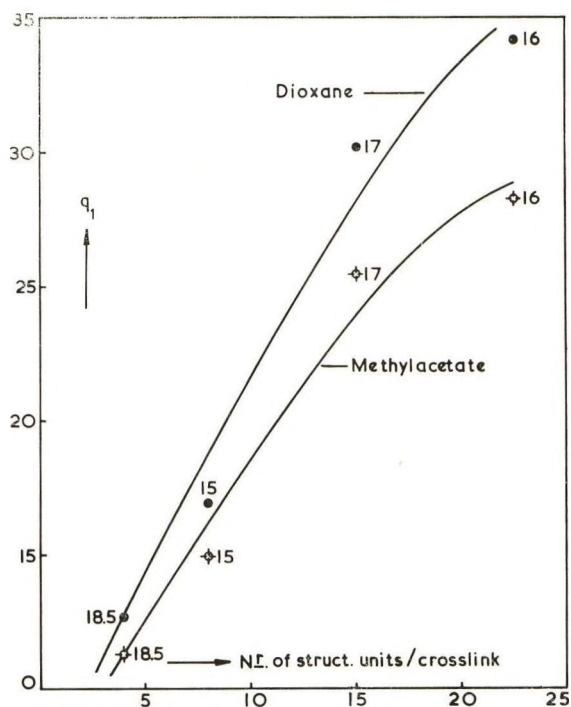


Fig. 4. The degree of swelling,  $q_1$ , of the crosslinked cellulose acetate gels in pure dioxane and methyl acetate plotted vs. the crosslinking density, expressed as the number of structural units/chemical crosslink. The numbers written near the experimental points represent the degree of dilution,  $q_e$ , prior to crosslinking.

TABLE III  
Swelling of Gels in Dioxane Solutions of Cellulose Acetate at 25°C.

$\phi_s \times 10^2$	Gel 1 <sup>a</sup>		Gel 5 <sup>b</sup>	
	$L$ , mm.	$q$	$L$ , mm.	$q$
0.000	33.33	16.09	30.89	12.64
0.066	33.36	16.15	30.89	12.64
0.105	33.32	16.07	30.75	12.47
0.210	33.30	16.05	30.67	12.38
0.307	33.30	16.05	30.62	12.31
0.609	33.29	16.03	30.59	12.28
0.930	33.25	15.97	30.56	12.24
1.140	33.29	15.95	30.56	12.34
1.940	33.01	15.65	30.43	12.09
2.640	32.84	15.41	30.30	11.93
3.160	32.56	15.00	30.11	11.71
4.425	32.18	14.48	29.90	11.45

<sup>a</sup>  $q_e = 14.9$ ;  $p_{\Lambda}^{\text{DN}} = 9.2$ .

<sup>b</sup>  $q_e = 26.4$ ;  $p_{\Lambda}^{\text{DN}} = 5.5$ .

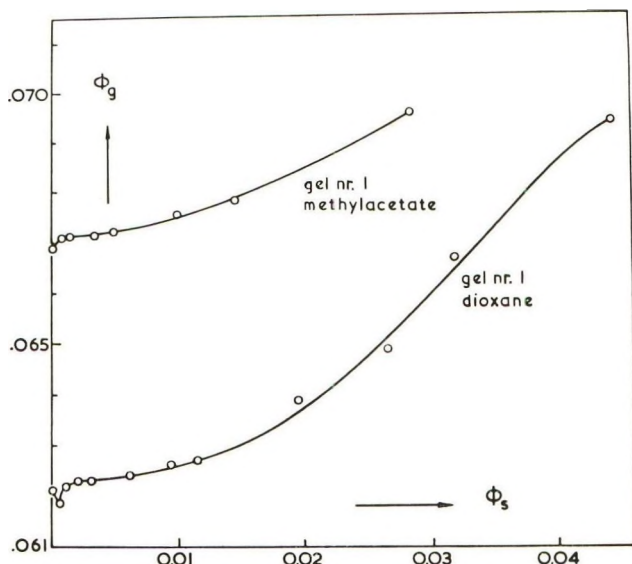


Fig. 5. Deswelling of gel 1 in dioxane and methyl acetate solutions of cellulose acetate at 25°C., plotted as volume fraction crosslinked polymer in the gel,  $\phi_g$ , vs. volume fraction dissolved polymer around the gel,  $\phi_s$ .

relation  $q = q_1(L/L_1)$ .<sup>3</sup> All these experiments were carried out in a constant temperature room regulated at  $25 \pm 0.1^\circ\text{C}$ . The adjustment to a new equilibrium swelling was always found to be complete within 48 hr.

TABLE IV  
Swelling of Gels in Dioxane Solutions of Cellulose Acetate at 25°C.

$\phi_s \times 10^2$	$q$				
	Gel 2 <sup>a</sup>	Gel 3 <sup>b</sup>	Gel 4 <sup>c</sup>	Gel 6 <sup>d</sup>	Gel 7 <sup>e</sup>
0.000	41.08	30.18	14.52	27.04	34.16
0.066	40.65	29.77	14.50	26.95	34.54
0.105	40.21	29.77	14.46	26.79	34.38
0.210	39.89	29.77	14.42	26.74	34.11
0.307	39.40	29.77	14.39	26.58	33.69
0.609	38.04	29.21	14.35	26.28	32.48
0.930	36.86	28.55	14.31	25.81	30.96
1.140	36.52	28.22	14.31	25.65	30.54
1.940	32.05	25.49	14.02	24.17	27.20
2.640	28.63	23.96	13.71	22.61	24.25
3.160	26.57	23.31	13.33	21.43	22.55
4.425	23.65	20.73		19.68	20.36

<sup>a</sup>  $q_c = 16.1$ ;  $p_A^{\text{DX}} = 23.3$ .

<sup>b</sup>  $q_c = 16.9$ ;  $p_A^{\text{DX}} = 18.1$ .

<sup>c</sup>  $q_c = 9.3$ ;  $p_A^{\text{DX}} = 16.9$ .

<sup>d</sup>  $q_c = 13$ ;  $p_A^{\text{DX}} = 19.3$ .

<sup>e</sup>  $q_c = 15.9$ ;  $p_A^{\text{DX}} = 25.8$ .



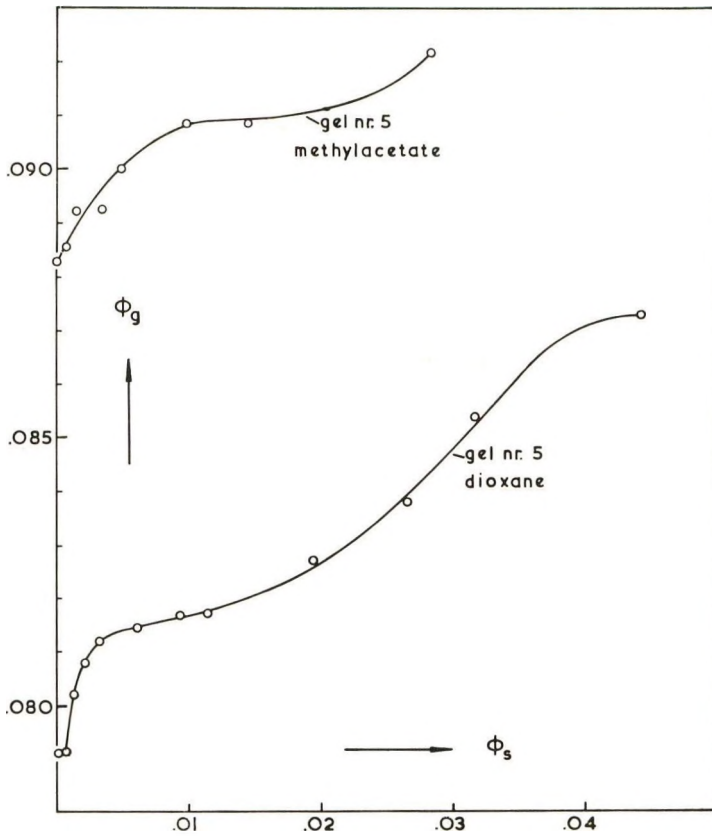


Fig. 6. Deswelling of gel 5 in dioxane and methyl acetate solutions of cellulose acetate, plotted in the same way as in Fig. 5.

TABLE V  
Swelling of Gels in Methyl Acetate Solutions of Cellulose Acetate at 25°C.

$\phi_s \times 10^2$	$q$		
	Gel 1 <sup>a</sup>	Gel 2 <sup>b</sup>	Gel 3 <sup>c</sup>
0.000	14.94	33.92	25.50
0.079	14.90	33.44	25.50
0.143	14.90	33.35	25.37
0.334	14.89	32.98	25.26
0.479	14.87	32.43	24.84
0.986	14.79	30.95	23.89
1.440	14.76	30.20	23.74
1.830	14.37	26.19	21.23

<sup>a</sup>  $q_c = 14.9$ ;  $p_A^{MA} = 9.8$ .

<sup>b</sup>  $q_c = 16.1$ ;  $p_A^{MA} = 24.8$ .

<sup>c</sup>  $q_c = 16.9$ ;  $p_A^{MA} = 19.3$ .

TABLE VI  
Swelling of Gels in Methyl Acetate Solutions of Cellulose Acetate at 25°C.

$\phi_a \times 10^2$	$q$			
	Gel 4 <sup>a</sup>	Gel 5 <sup>b</sup>	Gel 6 <sup>c</sup>	Gel 7 <sup>d</sup>
0.000	12.98	11.32	23.15	28.27
0.079	12.95	11.26	23.00	27.96
0.143	12.95	11.21	22.96	27.86
0.334	12.87	11.21	22.85	27.53
0.479	12.85	11.10	22.75	27.27
0.986	12.73	11.01	22.16	25.95
1.440	12.72	11.01	21.94	25.46
1.830	12.30	10.85	20.29	22.31

<sup>a</sup>  $q_c = 9.3$ ;  $p_A^{MA} = 18.0$ .

<sup>b</sup>  $q_c = 26.4$ ;  $p_A^{MA} = 5.8$ .

<sup>c</sup>  $q_c = 13$ ;  $p_A^{MA} = 20.6$ .

<sup>d</sup>  $q_c = 15.9$ ;  $p_A^{MA} = 27.5$ .

To check whether true equilibrium had been reached several pieces were reimmersed in pure solvent. This always yielded identical distances under the microscope. Illustrative examples of the results are given in Table III and in Figures 5 and 6. The other data are collected in Tables IV-VI. A discussion of the swelling results will be given below.

### Characterization of Cellulose Acetate

Since the cellulose acetate solutions used in the deswelling experiments were made from the same polymer as used by Rijke and Prins,<sup>6</sup> their values for number-average molecular weight and interaction parameter could be used. These values were [see eqs. (4)-(6)] in dioxane:  $x = 420$ ,  $\chi_s = 0.351$ ; and in methyl acetate,  $x = 448$ ,  $\chi_s = 0.434$ .

In order to investigate whether the introduction of crosslinks alters the interaction parameter  $\chi_E$  appreciably, a cellulose acetate derivative was prepared and characterized as follows. A 3-g. portion of cellulose acetate was dissolved in 500 ml. dioxane and added dropwise to a refluxing mixture of an excess of DADI (10 g.) in dioxane. Refluxing was continued for 10 hr. Then 10 ml. methanol was added and the mixture refluxed for another 5 hr. After cooling and filtration to remove microgel, the polymer was precipitated by ethanol, dried and several times redissolved in dioxane and precipitated to remove the reaction product of DADI with methanol.

The nitrogen content of the polymer was found to be 1.14%, which corresponds to one urethane group for four cellulose acetate structural units (M.W. = 263). On the basis of the acetyl content of the original cellulose acetate (D.S. = 2.42), this means that about  $1/3$  to  $2/3$  of all hydroxyls have reacted with DADI. A range of  $1/3$  to  $2/3$  is given because DADI may react at one or at both ends with hydroxyl groups on the polymer backbone.

Further qualitative evidence about the extent of reaction with DADI was obtained from infrared data. Although there is some overlap of hy-

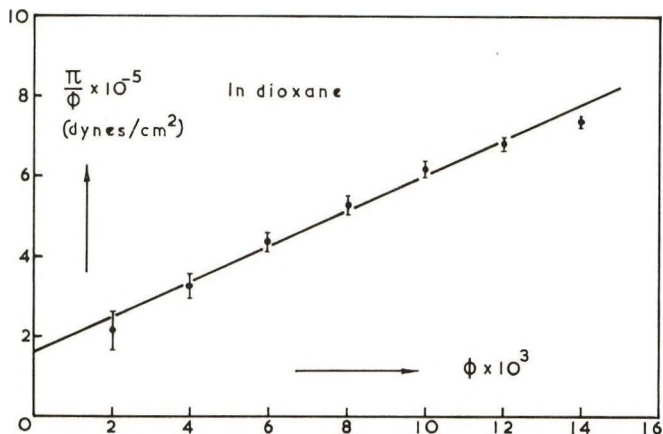


Fig. 7. Reduced osmotic pressure data in dioxane for the soluble polymer obtained by reacting cellulose acetate with an excess of dianisidine diisocyanate.  $\phi$  = volume fraction polymer.

droxyl and amide absorption in the infrared, a comparison of the different spectra against pure dioxane in matched cells, obtained from 2% solutions of the original and the modified cellulose acetate, shows that roughly 50( $\pm 20$ )% of the hydroxyls have disappeared.

Osmotic pressures were measured on a series of dioxane solutions of this derivative in a Zimm-Meyerson osmometer using cellophane membranes (Ultracella filter, Allerfeinst, Membran Filter Gesellschaft, Göttingen, Germany). The solutions were aged for two weeks prior to use because of time effects previously observed by Rijke and Prins.<sup>5</sup> The osmometer was kept in the dark, except during readings, as a precaution against the formation of peroxides and subsequent chain degradation. The reduced osmotic pressures are given in Figure 7. The results indicate in the first place that the molecular weight is considerably higher ( $\bar{M}_n \approx 200,000$ ) than that of the original cellulose acetate ( $M_n \approx 50,000$ ). This must be due to the linking together of several chains by the DADI. This information is, however, not needed for our evaluation. The drawn line in Figure 7 corresponds to  $\chi_s = 0.351$  as reported by Rijke and Prins.<sup>6</sup> It is seen that there is no significant change in  $\chi$  value as a result of the presence of side branches. We are, therefore, justified in using the approximation  $\chi_u = \chi_s$  in our further evaluation of the swelling data with the eqs. (4)–(6).

The osmotic data were taken up to  $\phi = 0.02$ , whereas the volume fractions polymer in and around the gel go up to  $\phi \approx 0.05$ – $0.08$ . In view of this, activity determinations of cellulose acetate solutions were performed at concentrations ranging from  $\phi \approx 0.1$  to  $\phi \approx 0.04$ , by means of a thermoelectric vapor phase osmometer.<sup>15</sup> At still higher concentrations the solutions became too viscous for this instrument. The measurements indicated a constant value of  $\chi = 0.42$ . The discrepancy between the two techniques which can perhaps be traced to a difference in water content of the dioxane,

is not very important at this point. From the measurements we conclude that in any case  $\chi$  remains essentially constant up to  $\phi \approx 0.04$ . The swelling data are evaluated on this basis, with  $\chi = 0.351$ . Inserting the higher value  $\chi = 0.42$  does not alter the essence of our conclusions (see below).

## RESULTS AND DISCUSSION

The degrees of swelling of our gels in pure dioxane,  $q_1^{\text{DX}}$  and in pure methyl acetate,  $q_1^{\text{MA}}$ , can be expected to be governed by the number of crosslinks and by the concentration at which the crosslinks are introduced. The crosslinking densities as determined by the radioactive labeling method are presented in Table II as  $p_A^{\text{DX}}$  and  $p_A^{\text{MA}}$ . These  $p_A$  values, calculated from Table I, represent the ratios of the molecular volume of the average chain between crosslinks and the volume of a solvent molecule. They have been corrected for network imperfections (e.g., wasted crosslinks) in the way indicated by Flory,<sup>8</sup> i.e., by multiplying by the factor  $(1 + 2M_p/\bar{M}_n)$ , where  $M_p$  is the molecular weight between crosslinks and  $\bar{M}_n$  the molecular weight of the original cellulose acetate before crosslinking. In Figure 3,  $q_1$  values for gels with approximately the same crosslinking densities ( $p_A$ ) are plotted against increasing dilution during crosslinking,  $q_c (= \phi_c^{-1})$ . In Figure 4  $q_1$  values for gels prepared at approximately the same dilution ( $q_c$ ) are plotted as a function of decreasing crosslinking density ( $p_A \sim$  number of structural units/crosslink). The trends in both figures are as expected. Of the two parameters,  $q_c$  and  $p_A$ , the former seems to have the larger influence, because gel 2 has a higher swelling than gel 7 in spite of the higher crosslinking density. This must be due to the greater dilution during preparation of gel 2. Also, the swelling in methyl acetate is always lower, because this is the poorer solvent of the two ( $\chi_g = 0.434$  as compared with  $\chi_g = 0.351$  for dioxane).

The results of the deswelling measurements in cellulose acetate solutions are given in Tables III–VII, and some illustrative graphs are shown in Figures 5 and 6. Most of the points (at  $\phi_s$  values between 0.002 and 0.03) follow at least qualitatively the behavior predicted by eqs. (4) and (5)

TABLE VII  
Slopes of the Plots of  $D\phi_s^{-1/3}$  vs.  $\phi_s^{2/3}$  for All Gels and the Values of the Parameter  $n$ , Where  $n$  is Slope Multiplied by  $p_A$

	Gel 1	Gel 2	Gel 3	Gel 4	Gel 5	Gel 6	Gel 7
$\phi_c$	0.067	0.062	0.059	0.107	0.054	0.077	0.063
$p_A^{\text{DX}}$	9.2	23.3	18.1	16.9	5.5	19.3	25.8
Slope in DX	1/22	1/87	1/55	1/24	1/26	1/52	1/184
$n^{\text{DX}}$	1/2.4	1/3.7	1/3.0	1/1.4	1/4.7	1/2.7	1/7.1
$p_A^{\text{MA}}$	9.8	24.8	19.3	18.0	5.8	20.6	27.5
Slope in MA	1/19	1/74	1/72	1/21	1/22	1/50	1/88
$n^{\text{MA}}$	1/1.9	1/3.0	1/3.7	1/1.2	1/3.7	1/2.4	1/3.2

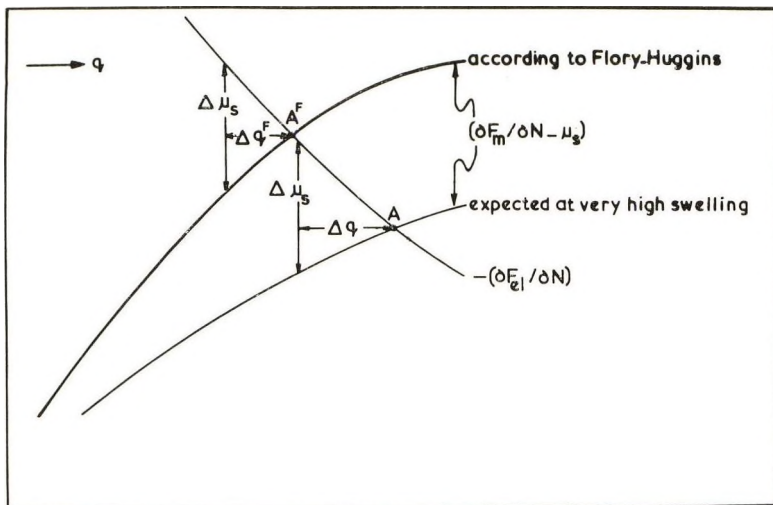


Fig. 8. At very high swelling in pure solvents, deviation from the Flory-Huggins free energy of mixing may occur as a result of insufficient polymer-polymer contacts (see text).

(this will be discussed fully below), but at very low concentrations of cellulose acetate around the gel two interesting deviations occur.

In the first place, when the pure solvent surrounding a gel is replaced by a dilute solution, some of the gels (e.g., gels 1 and 7) exhibit an increase in swelling instead of the expected decrease. The reproducibility of this effect was established by remeasuring in pure solvent. In each case a decrease of swelling was observed. Similar effects were also found by Blokland<sup>9</sup> in our laboratory, who observed that slightly stretched poly(vinyl alcohol) filaments in swelling equilibrium with water exhibit a decrease in retractive force and an increase in diameter if the water is replaced by a sodium carboxymethyl cellulose solution in water of  $\phi_s < 0.001$ . Returning to pure water restores the force and swelling, but this takes a much longer time than in the case of the regular decrease in swelling and increase in force which is observed when  $\phi_s > 0.001$ . A tentative explanation might be that polymer molecules become attached to the surface of the gel. They may actually form a surface layer with higher concentration than exists in the bulk of the solution. They will not be under strain and will try to dilute themselves with solvent. Thus, they may exert a slight pull on the network which leads to slightly increased swelling.

The second "abnormal" effect is that the rate of deswelling  $d\phi_g/d\phi_s$  at very low (but above  $\phi_s = 0.001$ ) concentrations is often higher than predicted from eqs. (4) and (5). Similar observations were also made by Rijke.<sup>10</sup> A possible qualitative explanation is as follows. At equilibrium swelling we have

$$\mu^s = \mu^g = \partial\Delta F_{in}/\partial N + \partial\Delta F_{el}/\partial N$$

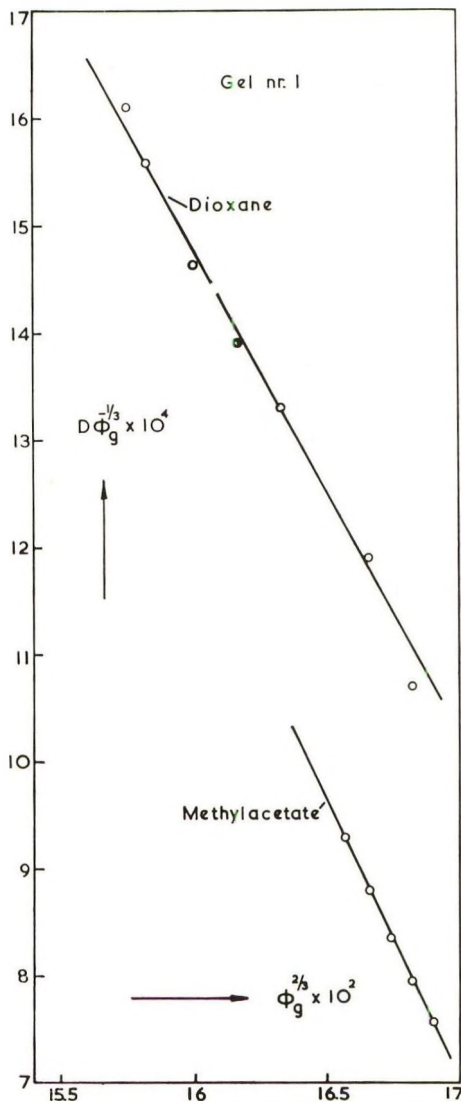


Fig. 9. The deswelling data, plotted as  $D\phi_g^{-1/3}$  vs.  $\phi_g^{2/3}$  for gel 1 in dioxane and methyl acetate solutions, as suggested by the theoretical treatment [eqs. (4), (5), (6), and (8)].

If we plot  $-\partial\Delta F_{el}/\partial N$  and  $(\partial\Delta F_m/\partial N - \mu^s)$  both as functions of the degree of swelling  $q$ , the projection of the intersection of these two graphs on the  $q$  axis will then indicate the equilibrium degree of swelling in a solution of thermodynamic potential  $\mu^s$  (Fig. 8). Now, it is conceivable that at very high degrees of swelling, the free energy of mixing part,  $\partial\Delta F_m/\partial N$ , changes less rapidly with  $q$  than predicted by the Flory-Huggins theory. This might occur, because at these high degrees of swelling the polymer chains may actually become so tautly stretched between crosslinks that no

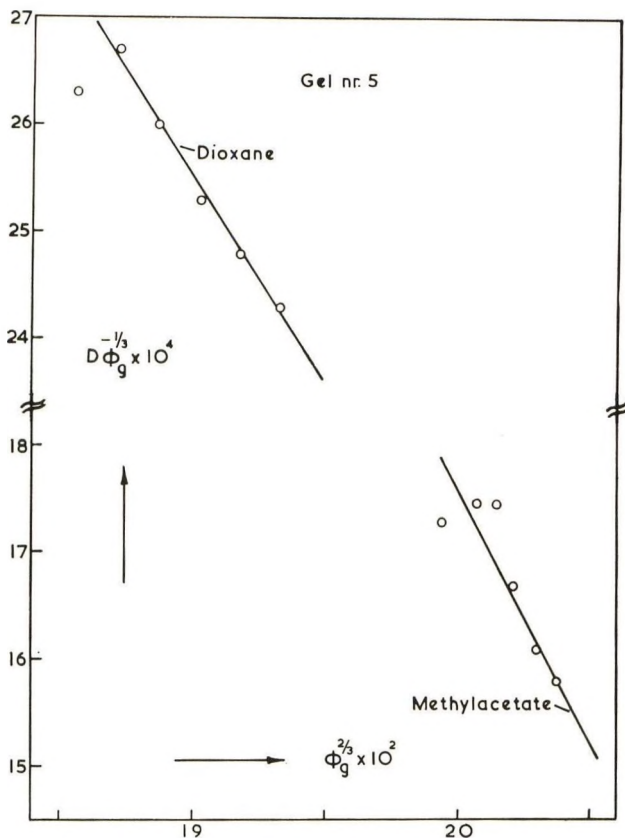


Fig. 10. Plots of  $D\phi_g^{-1/3}$  vs.  $\phi_g^{2/3}$  for gel 5, as in Fig. 9.

real homogeneous polymer-solvent mixing can occur. If now the outside solution is replaced by one of higher concentration with a solvent potential which is lower by an amount  $\Delta\mu^s$ , the amount of deswelling,  $\Delta q$ , will be larger than would be found if the Flory-Huggins expression was applicable (see Fig. 8). One could expect this effect to disappear as soon as sufficient deswelling has occurred to coil the chains sufficiently for mixing according to the Flory-Huggins expression to apply again.

For most of the data, however, the above-mentioned abnormal effects do not interfere, because between  $\phi_s = 0.002$  and  $0.03$  straight lines are obtained if they are plotted according to eqs. (4)–(6), which make use of the Flory-Huggins expression. Examples of the best and the worst straight lines are given for gel 1 and 5 in Figures 9 and 10.

None of the lines has a zero slope, so that on experimental grounds we must reject eq. (6). From the slope of the graphs we obtain the crosslinking densities, expressed as dimensionless average chain length,  $p$ , between crosslinks. In Table VII the slopes are compared with analytically determined values  $p_A$  by writing slope =  $n/p_A$ . According to eq. (4) (Hermans),  $n$  should be 1 and according to eq. (5) (Flory), it should be  $1/2$ .

Experimentally we find  $n$  to vary from 1/1.2 to 1/4.7. We exclude the results for gel 7 in dioxane, because of the large discrepancy between slope in dioxane and in methyl acetate, which is a rather unlikely happenstance not found in the case of the other gels. If we use  $\chi = 0.42$  rather than  $\chi = 0.351$ , the  $n$  values vary from 1/2.1 to 1/6, i.e., the essential features of the results are retained: the  $n$  values vary from gel to gel and neither Flory's nor Hermans' theory describes the data quantitatively.

If short intramolecular loops were formed, a certain number of chemical crosslinks would be wasted as far as the elasticity of the network is concerned. Although this would be a possible explanation for any discrepancy between  $p$  and  $p_A$ , it is not a very likely explanation. In the first place, short loop formation is quite unimportant in our case because of the stiffness and size of the crosslinking agent.<sup>16</sup> Secondly, as Kuhn pointed out,<sup>16</sup> only at much lower polymer concentration would one expect an appreciable amount of intramolecular crosslinking to occur. Our data, however, show a very large discrepancy between  $p$  and  $p_A$ , whereas the polymer concentration is of the order  $\phi_E \approx 0.05$ .

Systematic errors, as e.g., due to the existence of physical entanglements in addition to the chemical crosslinks, would make the  $p_A$  value to be compared with the experimental slope smaller. The parameter  $n$  would then show smaller values than are listed in Table VII. Rather than introduce into  $p_A$  some artificial correction for entanglements, we would prefer to give the parameter  $n$  a specific meaning on the basis of topological restrictions (as, e.g., entanglements) in the network. A theoretical basis for the existence of  $n$  and its dependence on the conditions of network formation are given in the next section.

### Influence of Topological Restrictions

All theories so far have been based on the assumption that the distribution of end-to-end dimensions of free chains is Gaussian, and that in the network there are no interactions between the chains which change this distribution. Thus the chains are supposed to behave like "ghost" chains which can freely pass through each other. Alfrey and Lloyd<sup>11</sup> have, however, shown that even for the simple case where chains of negligible girth exist in a cubical array of network junctions but cannot pass through each other, the end-to-end distribution should be different, albeit that no precise calculation could be performed.

Let us consider a chain between crosslinks in a real network. Due to topological restrictions (the connectivity pattern<sup>11</sup>) and in principle also other restrictions as, e.g., due to the excluded volume, the distribution of end-to-end distances may in general be non-Gaussian. Since calculating this distribution is beyond our power at the moment, we will assume a general distribution function which will exhibit the expected traits<sup>12</sup> and has an adjustable parameter  $n$ , and which for the case  $n = 0$  reduces to the regular Gaussian distribution.



We write for the number of configurations of a chain with length between  $\mathbf{r}$  and  $\mathbf{r} + d\mathbf{r}$

$$\omega(\mathbf{r})d\mathbf{r} = \omega_x(x)\omega_y(y)\omega_z(z)dx dy dz$$

where

$$\omega_x(x)dx = C|x|^n \exp \{-bx^2\}dx$$

Expressions for the  $y$  and  $z$  components are similar. This function, which is shown in Figure 11, exhibits at least the desired characteristic that a chain with  $\mathbf{r} = 0$  cannot exist, which must be so because of volume exclusion.<sup>12</sup> For the rest we do not as yet claim a physical basis for this

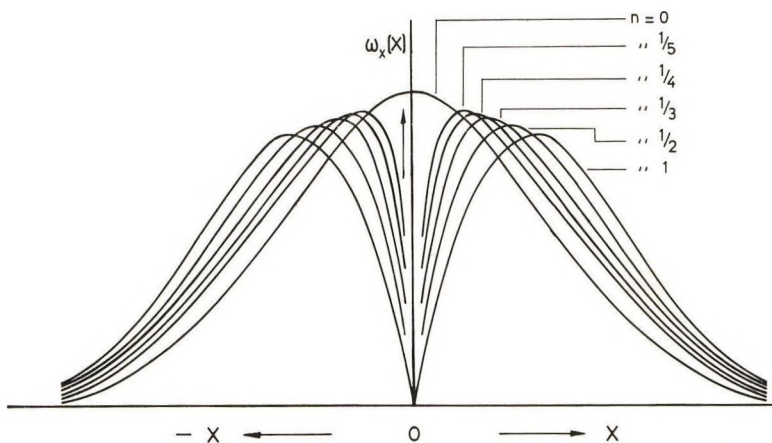


Fig. 11. Non-Gaussian distributions as used in the derivation of eq. (7) in order to take topological restrictions into account; only one-dimensional distributions are shown. With  $\omega_x(x) = C|x|^n \exp \{-bx^2\}$  and similar expressions for the  $y$  and  $z$  components we have:  $\omega(\mathbf{r})d\mathbf{r} = \omega_x(x)\omega_y(y)\omega_z(z)dx dy dz$ .

distribution function with  $n \neq 0$ . The parameter  $b$  is determined by the molecular weight between crosslinks, but  $n$  is assumed to be independent of this.

Following now the reasoning of James and Guth<sup>5</sup> as given in Staverman's review article,<sup>1</sup> we can write the total number of configurations of the network as an integral over all crosslink positions:

$$\Omega = \int \prod_i \omega_i^{\nu_i^K} d\tau_i^K$$

where  $\nu_i^K$  is the number of chains with end-to-end distance  $\mathbf{r}_i$  under the restriction that the crosslinks are in the  $K$  configuration, and  $\omega_i = \omega(\mathbf{r}_i)$ . Approximating the integrand by<sup>1</sup>

$$\prod_i \omega_i^{\nu_i^K} = \left( \prod_i \omega_i^{\nu_i^E} \right) \exp \left\{ -B^2 \sum_K (X_K - X_E)^2 \right\}$$

where  $X_K$  stands for the  $6\nu/f$  coordinates of the crosslinks in the  $K$  con-

figuration and  $X_E$  for the same in the most probable equilibrium (E) configuration, integration yields

$$\Omega = (\prod_i \omega_i^{\nu_i^E}) (\pi^{1/2} B^{-1})^{6\nu/f}$$

According to James<sup>1,5</sup> now, in a first approximation  $B$  will be independent of deformation. The entropy of deformation is thus obtained directly from

$$S = k \ln (\Omega_E' / \Omega_E)$$

where  $\Omega_E$  and  $\Omega_E'$  are given by the expression  $\prod_i \omega_i^{\nu_i^E}$  before and after deformation. Since the numbers  $\nu_i^E$  according to this mode of calculation do not change with deformation, we have only to consider that before deformation

$$\omega_i d\mathbf{r}_i = C(|x_i| |y_i| |z_i|)^n \exp \{-b(x_i^2 + y_i^2 + z_i^2)\} d\mathbf{r}_i$$

represents the number of configurations of a chain with end-to-end distance  $\mathbf{r}_1$  and

$$\omega_i' d\mathbf{r}_i = C(|x_i \lambda_x| |y_i \lambda_y| |z_i \lambda_z|)^n \exp \{-b(x_i^2 \lambda_x^2 + y_i^2 \lambda_y^2 + z_i^2 \lambda_z^2)\} d\mathbf{r}_i$$

the same after deformation. We then obtain for a network of  $\nu (= \sum_i \nu_i^E)$  chains:

$$\Delta S/k = -b[\sum_i x_i^2(\lambda_x^2 - 1) + \sum_i y_i^2(\lambda_y^2 - 1) + \sum_i z_i^2(\lambda_z^2 - 1)] + n\nu \ln \lambda_x \lambda_y \lambda_z$$

Inserting

$$(1/\nu) \sum_i x_i^2 = \langle x^2 \rangle$$

and

$$\langle x^2 \rangle = \langle y^2 \rangle = \langle z^2 \rangle = \langle r^2 \rangle / 3$$

and evaluating

$$\begin{aligned} \langle x^2 \rangle &= \int_{-\infty}^{+\infty} \omega_x x^2 dx / \int_{-\infty}^{+\infty} \omega_x dx = \int_0^{\infty} x^{n+2} \exp \{-bx^2\} dx / \int_0^{\infty} x^n \exp \{-bx^2\} dx \\ &= \int_0^{\infty} y^{(n+1)/2} \exp \{-by\} dy / \int_0^{\infty} y^{(n-1)/2} \exp \{-by\} dy \\ &= \frac{\Gamma[1 + (n+1)/2]}{b^{1+(n+1)/2}} / \frac{\Gamma[1 + (n-1)/2]}{b^{1+(n-1)/2}} = (n+1)/2b \end{aligned}$$

-1 < n < ∞  
0 < b < ∞

we obtain, finally

$$\Delta S/k = -\nu[(n+1)/2](\lambda_x^2 + \lambda_y^2 + \lambda_z^2 - 3) + \nu n \ln \lambda_x \lambda_y \lambda_z \quad (7)$$

The above derivation assumes the network to be composed of  $\nu$  identical chains of average molecular weight  $M_p$  between crosslinks, whereas in reality the network is of course composed of chains which vary in  $M_p$ . By grouping chains with the same  $M_p$  together, applying the above reasoning, and then summing the results,<sup>13</sup> one obtains the same final equation.

For isotropic deformations, as occur in our swelling experiments, we have

$$\lambda_x = \lambda_y = \lambda_z = (q/q_0)^{1/3}$$

and

$$\Delta F_{el}/kT = -\Delta S/k = \nu[3(n+1)/2][(q/q_0)^{2/3} - 1] - \nu n \ln(q/q_0)$$

By applying the condition for equilibrium swelling  $\mu^s = \mu^R$  we obtain an equation similar to eqs. (4)–(6):

$$D\phi_g^{-1/3} = [(n+1)/p]q_0^{-2/3} - (n/p)\phi_g^{2/3} \quad (8)$$

where  $\phi_g$ , as before, is equal to  $q^{-1}$ .

The introduction of a distribution function of the type  $|x|^n \exp\{-bx^2\}$  in this manner thus leads to a slope of the graph  $D\phi_g^{-1/3}$  versus  $\phi_g^{2/3}$ , which is given by  $n/p$  instead of  $1/p$  according to Hermans [eq. (4)] and  $1/2p$  according to Flory [eq. (5)]. The smaller the value of  $n$ , the more Gaussian the distribution of the chains in a network will be. If  $n = 0$ , we obtain the result of James and Guth.

The factor  $(n+1)$  in front of the  $\lambda^2$  terms in eq. (7) (or in front of the  $q_0^{-2/3}$  term in eq. (8)) is another result of our treatment. This factor will show up in nonisotropic deformations, as, e.g., occur in unidirectional stretching. It is possible that the omission of this factor in previous theories is responsible for the discrepancy usually found<sup>14</sup> between  $\nu$  from Young's modulus and  $\nu$  from chemical analysis.

## CONCLUSION

According to eq. (8), a value of  $n$  different from zero indicates non-Gaussian behavior (compare Fig. 11). In our gels we find  $n$  to vary from 1/1.2 to 1/4.7 (or  $1/2$  to  $1/6$  if we use  $\chi = 0.42$ ), as shown in Table VII; that is, in all cases  $n$  is positive as more or less expected on the basis of Schatzki's results. Attention should be drawn to the fact that we find  $n$  to be smaller, the more dilute the polymer solution prior to crosslinking and the lower the crosslinking density. This is to be expected since at high dilution (large  $q_c$ ) and low crosslinking density (large  $p_A$ ), networks with less topological restrictions (e.g., entanglements) will be formed. They will then behave more like a Gaussian network, i.e.,  $n$  approaches zero.

In Table VIII we have listed the  $\phi_0 (= q_0^{-1})$  values which follow from the various equations [eqs. (4), (5), and (8)]. Since dioxane is a better solvent than methyl acetate one might expect the average chain length between crosslinks in the unstrained state to be larger in dioxane than in methyl acetate because of the possible persistence of excluded volume effects in these very highly swollen gels. In the absence of short range

TABLE VIII  
The Parameter  $\phi_0 (= q_0^{-1})$  Calculated According to the Various Theories

	Gel 1	Gel 2	Gel 3	Gel 4	Gel 5	Gel 6	Gel 7
$\phi_e$	0.067	0.062	0.059	0.107	0.054	0.077	0.063
$p_A^{\text{DX}}$	9.2	23.3	18.1	16.9	5.5	19.3	25.3
$p_A^{\text{MA}}$	9.8	24.8	19.3	18.0	5.8	20.6	27.5
$\phi_0$ [Hermans, eq. (1)]							
In DX	0.084	0.037	0.048	0.101	0.130	0.056	0.085
In MA	0.078	0.037	0.049	0.097	0.117	0.055	0.049
$\phi_0$ [Flory and Wall, eq. (2)]							
In DX	0.030	0.013	0.017	0.035	0.046	0.020	0.010
In MA	0.028	0.013	0.017	0.034	0.041	0.019	0.015
$\phi_0$ [our eq. (7)]							
In DX	0.015	0.0037	0.006	0.027	0.011	0.008	0.004
In MA	0.016	0.0044	0.004	0.029	0.013	0.008	0.006

specific solvent effects, one would thus expect  $q_0^{\text{DX}} > q_0^{\text{MA}}$  or  $\phi_0^{\text{DX}} < \phi_0^{\text{MA}}$ . This trait is exhibited only when the calculation is done by means of our eq. (8).

Of course, the occurrence of the descriptive parameter  $n$ , which for our gels seems to vary between 1 and 1/4.7, still has to be based more securely on molecular considerations. This represents, however, a formidable problem as already indicated by the attempt of Alfrey and Lloyd.<sup>11</sup>

Therefore, as a first step, further experiments should be designed to check the consistency of the parameter  $n$  under various types of network deformation. If for example, a unidirectional elongation is applied and the retractive force measured, the factor  $(n + 1)$  in front of the  $\lambda^2$  terms can be measured. Work along this line is in progress in this laboratory.

The authors wish to thank J. H. Parmentier at the Central Laboratory TNO, Delft, The Netherlands, for the use of the liquid scintillation counter facilities and J. van Dam and M. C. A. Donkersloot at our laboratory for performing the thermoelectric vapor pressure osmometry and regular membrane osmometry, respectively. Financial support of the National Science Foundation and the Cellulose Research Institute, Syracuse, N. Y., during the early stages of the work is also gratefully acknowledged.

## References

1. Staverman, A. J., in *Encyclopedia of Physics*, Vol. XIII, S. Flügge, Ed., Springer-Verlag, Berlin, 1962, pp. 432-451.
2. Flory, P. J., in *Unsolved Problems in Polymer Science*, National Academy of Sciences, National Research Council Publication 995, Washington D. C., 1962, p. 142.
3. Hermans, J. J., *Trans. Faraday Soc.*, **43**, 591 (1947); *J. Polymer Sci.*, **59**, 191 (1962).
4. Wall, F. T., and P. J. Flory, *J. Chem. Phys.*, **19**, 1435 (1951); P. J. Flory, *Trans. Faraday Soc.*, **56**, 722 (1960).
5. James, H. M., and E. Guth, *J. Chem. Phys.*, **21**, 1039 (1953); H. M. James, *J. Chem. Phys.*, **15**, 651 (1947).
6. Rijke, A. M., and W. Prins, *J. Polymer Sci.*, **59**, 171 (1962).
7. Saunders, J. H., and K. C. Frisch, *Polyurethanes, Chemistry and Technology*, Part I, Interscience, New York, 1962, p. 275.

8. Flory, P. J., *Principles of Polymer Chemistry*, Cornell Univ. Press, Ithaca, N. Y., 1953, p. 463.
9. Blokland, R. (Laboratory of Physical Chemistry, Technische Hogeschool, Delft, The Netherlands), private communication.
10. Rijke, A. M., Thesis, Leiden, The Netherlands, 1961.
11. Alfrey, T., Jr., and W. G. Lloyd, *J. Polymer Sci.*, **62**, 159 (1962).
12. Schatzki, T. F., *J. Polymer Sci.*, **57**, 337 (1962).
13. Treloar, L. R. G., *The Physics of Rubber Elasticity*, Oxford Univ. Press, 1958, p. 68.
14. Ciferri, A. J., *Polymer Sci.*, **54**, 149 (1961).
15. For a description, see J. Van Dam and W. Prins, in *Methods of Carbohydrate Chemistry*, Vol. V, M. L. Wolfson and R. L. Whistler, Ed., Academic Press, New York, in press; J. Van Dam, *Rec. Trav. Chim.*, **83**, 129 (1964).
16. Kuhn, W., and G. Balmer, *J. Polymer Sci.*, **57**, 311 (1962).

### Résumé

Les théories courantes sur les réseaux de polymères montrent des incohérences particulièrement apparentes, quand nous considérons la déformation tridimensionnelle (gonflement) de réseaux, obtenu par pontage d'un polymère en solution. Un contrôle des théories peut être obtenu uniquement lorsque nous connaissons précisément le nombre de ponts dans le réseau et quant une série de déformations (une série de rapports de gonflement) est imposé au réseau. A cette fin, une série de 7 gels a été préparée par formation de ponts dans l'acétate de cellulose secondaire (D.S. = 2.42) dans une solution de dioxanne (5-10%) avec le diisocyanate de dianisidine. Le nombre de ponts chimiques a été déterminé en faisant réagir les groupements isocyanates restantes avec le méthanol, contenant  $^{14}\text{C}$ . En conséquence, des changements dans le degré de gonflement du gel, induits par accroissement des concentrations de l'acétate de cellulose dans des solutions de dioxanne et d'acétate de méthyle autour du gel, ont été suivis en mesurant avec précision les changements de longueur de bandes de 2 cm à l'aide d'un microscope mobile. Lorsque le gonflement atteint son point d'équilibre, les activités du solvant à l'intérieur et autour du gel sont égales. Pour les solutions environnantes les activités ont été dérivées de mesures osmotiques. Les activités à l'intérieur sont dérivés d'un facteur de mélange et d'un facteur de déformation élastique. Le facteur de mélange a été rapproché, à l'aide de l'expression de Flory-Huggins, d'un paramètre d'interaction, obtenu de mesures osmotiques sur un dérivé, qui a été préparé par la réaction de l'acétate de cellulose avec un excès de diisocyanate, évitant ainsi la formation d'un réseau. En s'appuyant sur les différentes expressions théoriques connues pour le facteur de déformation élastique, les données de gonflement permettent de calculer le nombre de ponts dans les gels. Toutes les théories conduisent à un pontage beaucoup plus bas que nous fournit l'analyse chimique. Ceci n'a jamais été observé dans la même proportion auparavant, mais peut être spécifique pour des gels obtenus par pontage en solution. Nous sommes forcés de conclure qu'aucune des théories n'est applicable. Les données peuvent cependant être expliquées, en postulant que les configurations des chaînes entre les ponts ne suivent pas une distribution gaussienne, mais sont au contraire données par:

$$\omega(\mathbf{r})d\mathbf{r} = \omega_x(x)\omega_y(y)\omega_z(z) dx dy dz \text{ où } \omega_x(x) = C|x|^n \exp \{-bx^2\}$$

Une distribution pareille non-gaussienne peut provenir des restrictions topologiques, qui peuvent inclure celles dues au volume exclu. Comme valeur de l'énergie libre d'une déformation élastique nous trouvons, selon le raisonnement de James et Guth, mais se basant sur la nouvelle fonction de distribution:

$$\Delta F_{el}/kT = \nu[(n+1)/2][\lambda_x^2 + \lambda_y^2 + \lambda_z^2 - 3] - \nu n \ln \lambda_x \lambda_y \lambda_z$$

dans laquelle  $\nu$  représente le nombre de chaînes dans le réseau et  $\lambda_x \lambda_y$  et  $\lambda_z$  sont les rapports de déformation par rapport à l'état non-tendu. Dans les théories gaussiennes bien

connues le facteur  $n + 1$  est absent, et devant le log. au lieu de  $n$  se trouve plutôt  $0.2/f$  ou  $1$  ( $f$  = fonctionnalité du pontage) selon le cas où les résultats de James et Guth, de Flory et Wall, ou de Hermans sont employés, respectivement.

### Zusammenfassung

Gängige Theorien für verschiedene Polymere weisen Unstimmigkeiten auf, die dann besonders klar werden, wenn man die dreidimensionale Deformation (Quellung) von Netzwerken betrachtet, welche durch Vernetzung eines Polymeren in Lösung dargestellt werden. Eine Überprüfung dieser Theorien kann erhalten werden bei genauer Kenntnis der Zahl der Vernetzungen im Netzwerk und wenn das Netzwerk einem ganzen Deformationsbereich (Quellungsverhältnissbereich) unterworfen wird. Zu diesem Zweck wurde eine Reihe von sieben Gelen durch Vernetzung von sekundärem Zelluloseacetat (D.S. = 2,42) in Dioxanlösung (5-10%) mit Dianisidindiiocyanat hergestellt. Die Zahl der chemischen Vernetzungen wurde durch Reaktion der unverbrauchten Isocyanatgruppen mit  $^{14}\text{C}$ -markiertem Methanol bestimmt. Dann wurde die durch steigende Konzentration von Zelluloseacetat in den das Gel umgebenden Dioxan- und Methylacetatlösungen hervorgerufene Änderung der Quellung des Gels durch genaue Messung der Längenänderung von 2 cm langen Streifen unter einem Ablesemikroskop verfolgt. Beim Quellungs-gleichgewicht ist die Aktivität des Lösungsmittels innerhalb und ausserhalb des Gels gleich. Die Aktivität der äusseren Lösungen wurde osmometrisch bestimmt. Die Aktivität im Gelinneren besteht aus einem Mischungs- und einem elastischen Deformationsterm. Der Mischungsterm wurde aus dem Flory-Huggins-Ausdruck erhalten, wobei der Wechselwirkungsparameter durch osmometrische Messungen an einem Derivat erhalten wurde, das durch Reaktion von Zelluloseacetat mit einem Überschuss an Diisocyanat unter Vermeidung einer Vernetzung dargestellt wurde. Durch die verschiedenen bekannten theoretischen Ausdrücke für den elastischen Deformationsterm gestatten die Quellungsdaten die Berechnung der Zahl der Vernetzungen im Gel. Alle Theorien führen jedoch zu einer weit geringeren Zahl der Vernetzungen, als sich aufgrund der chemischen Analyse ergeben. Dies wurde nie vorher im selben Ausmass beobachtet, kann aber für durch Vernetzung in Lösung erhaltene Gele spezifisch sein. Der Schluss, dass keine bekannte Theorie anwendbar ist, liegt nahe. Andererseits können die Ergebnisse unter der Annahme, dass die Kettenkonfiguration zwischen den Vernetzungen keiner Gauss-Verteilung folgt, sondern durch  $\omega(\mathbf{r})d\mathbf{r} = \omega_x(x)\omega_y(y)\omega_z(z) dx dy dz$  mit  $\omega_x(x) = C|x|^n \exp\{-bx^2\}$  gegeben ist, erklärt werden. Eine solche nicht-Gaussische Verteilung kann durch topologische Beschränkungen, zu denen möglicherweise die auf das ausgeschlossene Volumen zurückzuführenden gehören, hervorgerufen werden. Für die freie Energie der elastischen Deformation finden wir nach den Überlegungen von James und Guth, aber unter Verwendung der neuen Verteilungsfunktion:

$$\Delta F_{el}/kT = \nu[(n + 1)/2][\lambda_x^2 + \lambda_y^2 + \lambda_z^2 - 3] - \nu n \ln \lambda_x \lambda_y \lambda_z$$

wo  $\nu$  = Zahl der Ketten im Netzwerk und  $\lambda_x$ ,  $\lambda_y$  und  $\lambda_z$  die Deformationsverhältnisse in bezug auf den unverformten Zustand sind. In den bekannten Gaussischen Theorien fehlt der Term  $n + 1$  und vor dem Logarithmus steht an Stelle von  $n$  entweder  $0,2/f$  oder  $1$  ( $f$  = Funktionalität der Vernetzung) abhängig davon, ob die Ergebnisse von James und Guth, Flory und Wall oder Hermans verwendet werden.

Received December 9, 1963

## Diffraction Study of Crystallite Orientation in a Stretched Polychloroprene Vulcanizate

W. R. KRIGBAUM and R.-J. ROE,\* *Department of Chemistry, Duke University, Durham, North Carolina*

### Synopsis

Crosslinked polychloroprene samples were allowed to crystallize from the melt at various fixed elongations. X-ray diffraction studies revealed that the  $c$  axis becomes oriented toward the stretching direction, while the  $a$  and  $b$  axes are randomly distributed about the  $c$  axis. The alignment of the crystallite  $c$  axes toward the drawing direction is much more perfect than that of the amorphous statistical chain segments prior to crystallization. This can be explained if we assume that the formation of a stable nucleus for crystallization requires the simultaneous alignment of  $\nu$  amorphous segments. Thus, such measurements offer a means by which the critical size of the crystallization nuclei can be determined. The sizes deduced for polychloroprene vary with elongation from a cube 30 Å. on a side at relative elongation  $\alpha = 1.45$  to a 17 Å. cube at  $\alpha = 7.40$ . Although our samples were not crystallized isothermally, these results are in qualitative agreement with nucleation theory. If the variation of  $\nu$  can, indeed, be estimated theoretically, then it will be possible to predict the entire crystallite orientation distribution in materials of this type from first principles. The orientation of crystallites formed in a sample at relative elongation  $\alpha = 2.92$  was found to be essentially independent of temperature from 24° C. to the melting point. For low degrees crystallinity,  $\omega$ , it is shown that a plot of  $1/T$  versus  $1/(1 - \omega)^2$  is linear, thus permitting an evaluation of the melting point by extrapolation. Finally, the crystallite orientations were compared for a sample crystallized from the melt at  $\alpha = 2.86$  and for the same sample after further drawing to  $\alpha = 3.50$  at room temperature. The distribution in the latter case was considerably broader, which demonstrates the primary role played by interactions between crystallites in the cold drawing of partially crystallized materials.

### I. INTRODUCTION

The anisotropic character of drawn polycrystalline materials is a factor of primary importance when one seeks an understanding of the mechanical properties of fibers and films. Although metals can also be made to show anisotropic properties by appropriate treatment, the long-chain nature of polymeric materials permits them to exhibit a wider spectrum of orientational behavior.

The usual commercial procedure for inducing orientation involves cold drawing of a partially crystallized polymer. Here the crystallites function as network tie points which inhibit relaxation, and during deforma-

\* Present address: Electrochemicals Department, E. I. du Pont de Nemours and Co., Inc., Niagara Falls, N.Y.

tion both the pre-existing crystallites and the amorphous chain sections are preferentially oriented. The mechanism of crystallite orientation in such a process is then greatly influenced by the interactions, such as cohesion and friction, between neighboring crystallites, with the result that the final state is not a simple function of the imposed strain, but depends also upon the rate of deformation and the temperature at which the sample is strained. Most of the previous studies of crystallite orientation have involved samples prepared by cold drawing; however, these have failed to exhibit clearly the important connection between the resulting crystallite orientation and that of the amorphous chains prior to crystallization.

For a better understanding of the latter relationship it is necessary to postpone all crystallization until the sample has attained its final state of strain. This can be effected by utilizing covalent crosslinks to prevent relaxation and by carrying out the deformation above the melting point, or by heating the sample to melt out all crystallites after the drawing operation. The use of a permanent network permits the orientation of the amorphous chains to be specified in terms of the known strains (the relative elongation  $\alpha$  in the case of uniaxial drawing). By following this procedure the state of crystallite orientation will be free from the effects of the previous sample history, and it can be made to approach the true thermodynamic equilibrium state more closely. The importance of ensuring crystallization from a completely amorphous deformed network was stressed previously by Flory<sup>1</sup> in connection with his study of the stress-strain relationship and the degree of crystallinity of deformed polymers. The same considerations obviously apply in the study of crystallite orientation.

In the present work we have investigated by x-ray diffraction the crystallite orientation in crosslinked polychloroprene films which had been stretched and rendered completely amorphous prior to recrystallization under conditions of fixed length. Stein and co-workers<sup>2</sup> earlier studied the crystallite orientation in drawn polyethylene samples which had been treated similarly. They were able to demonstrate a transition in the crystallite growth habit with increasing relative elongation. In the present work we wish to establish the relationship between the orientation distribution of the segments in the completely amorphous network chains and that of the crystallites which subsequently form as the strained network is cooled.

## II. EXPERIMENTAL

Neoprene film used for this study was prepared by casting on a mercury surface from a benzene solution containing Neoprene HC and 0.5% of its weight of a crosslinking agent NA-22. Both of these materials were kindly supplied by the Elastomer Chemicals Division of E. I. du Pont de Nemours and Co. After the solvent had been removed by slow evaporation, the film was transferred to a vacuum oven and cured by heating for 30 min. at 150° C. The film thus prepared showed no residual orientation when examined



by x-ray diffraction. The optimum sample thickness for  $\text{CuK}\alpha$  radiation is about 0.17 mm.,<sup>3</sup> and, since the thickness will decrease on stretching, the amount of polymer solution was adjusted to obtain a film thickness of 0.23 mm. A strip cut from the film was softened by a brief heating, elongated to the desired length, and mounted on a brass sample frame. The relative elongation  $\alpha$  was determined by measuring the distance between ink marks on the sample. Several samples drawn to different elongations were heated simultaneously to 80°C. for 20 min. under vacuum, and the temperature was slowly lowered to room temperature over a period of 10 hr. From the standpoint of approaching the equilibrium crystalline state more closely, it would have been preferable to have crystallized isothermally at a temperature as near the melting point as possible. However, the results of Kössler and Švob<sup>3</sup> indicate that polychloroprene undergoes very rapid degradation at elevated temperatures in the presence of air. Although our crystallization was performed under vacuum, discoloration and eventual darkening of the samples was observed after prolonged heating, so the heating schedule described above was adopted as an optimum compromise.

X-ray measurements were performed with an XRD-5 diffractometer fitted with a G. E. single crystal orienter. The source, detector, and the center of the sample all lie in a horizontal plane. The inclination of the draw axis from the horizontal plane is designated by the angle  $\chi$ , and rotation of the sample holder ( $\theta$  motion) and detector ( $2\theta$  motion) about the vertical axis are coupled so that the vertical plane containing the draw axis always bisects the angle formed by the source, sample center, and detector. X-rays from a copper target were passed through a  $\beta$  filter composed of two nickel foils, and the diffracted intensities, as measured with a scintillation counter and pulse height selector, were printed out by a digital recorder. Several collimating systems were investigated, and it was found that the one designed for single crystal analysis appeared to yield the best resolution without too great a sacrifice in intensity.

The three reflections listed in Table I were selected for the study of crystallite orientation. The unit cell of polychloroprene is orthorhombic with  $a = 8.84$  A.,  $b = 10.24$  A., and  $c = 4.79$  A. (see Bunn<sup>4</sup>). The reflection A gives information on the orientation of the  $c$  axis directly. The orientation of the  $a$  and  $b$  axes could also be directly obtained if reflections

TABLE I  
Reflections Selected for Measurement

	$2\theta$	Miller index	Intensity as calculated by Bunn <sup>4</sup>
A	37.60°	(002)	3.3
B	21.80°	(210)	18.6
C	19.90°	(120)	25.8
	19.90°	(200)	5.5

(200) and (020) were measurable, but the (200) peak unfortunately overlaps another stronger reflection (120), and the intensity from (020) is too weak to be useful. Hence, information on the orientation of the  $a$  and  $b$  axes had to be obtained indirectly from measurements of the reflection B (210) and the composite reflection C (120) + (200).

For each reflection the value of  $2\theta$  was fixed at the peak of the reflection profile and the intensity was measured at successive intervals of  $2^\circ$  to  $4^\circ$  in  $\chi$ . The plane-normal distribution function  $q(\chi)$  is obtained from the intensity function  $I_0(\chi)$  by normalization:

$$q(\chi) = I_0(\chi) / \int_0^\pi I_0(\chi) \sin \chi d\chi \quad (1)$$

This procedure involves the assumption that the peak intensity  $I(\chi)$  is directly proportional to the number of crystallites having the particular plane-normal in question in the direction  $\chi$ . For random assemblages of small crystallites, this assumption is probably justified (see Deas<sup>5</sup>), provided that the  $2\theta$  profile of the reflection does not change with  $\chi$ , so that the peak intensity is always proportional to the total intensity integrated over a  $2\theta$  range around the peak. A preliminary check was therefore made concerning this point. The  $2\theta$  profiles of reflection C were measured at several

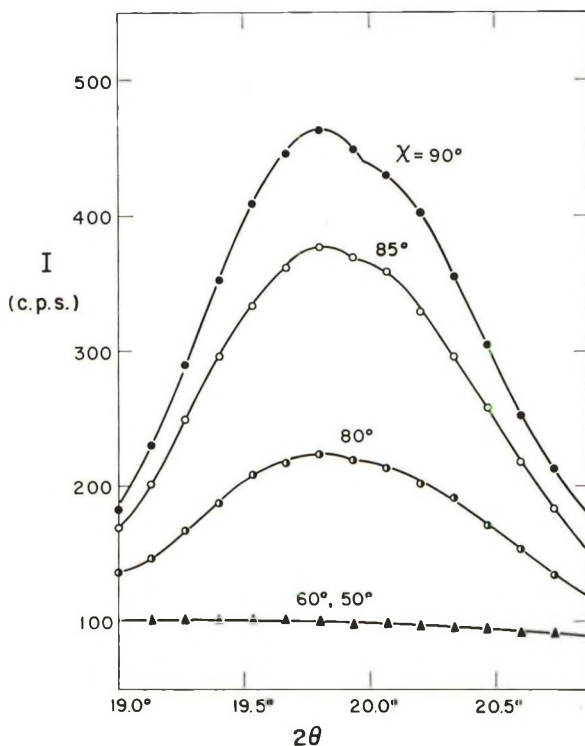


Fig. 1.  $2\theta$  scan of reflection C at the fixed  $\chi$  angles indicated for each curve.

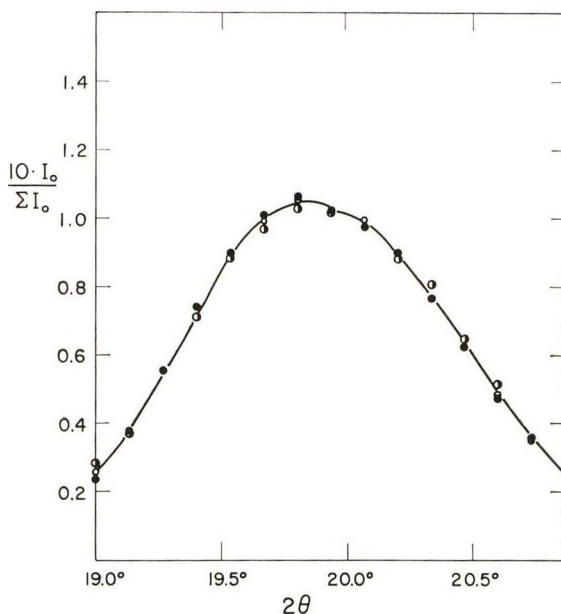


Fig. 2. The  $2\theta$  profiles of reflection C brought to a common scale by dividing the corrected intensity by the total area under the peak: (●) 90°C.; (○) 85°C.; (◐) 80°C.

different  $\chi$  values, as shown in Figure 1. After subtracting the background (amorphous) intensity, the corrected intensity  $I_0$  was divided by the integrated intensity for each profile and replotted, as shown in Figure 2. It is seen that the reduction into a single profile curve gives full justification for the procedure involving measurement of the peak intensity.

### III. RESULTS

#### A. Crystallite Orientation as a Function of Draw Ratio

##### 1. Diffraction Data

Orientation measurements were made on eight samples stretched to different relative lengths  $\alpha$ . Examples of the plane-normal distribution function  $q(\chi)$ , obtained from the measured intensity  $I(\chi)$  through use of eq. (1), are plotted in Figures 3-5. The shapes of the curves for the other samples are similar to these, since only the peak width varies with  $\alpha$ . The distribution function for reflection A (002) has a peak at  $\chi = 0^\circ$ , while the functions for reflections B and C have peaks at  $\chi = 90^\circ$ . Since the normals to the planes (210), (120), and (200) are all perpendicular to the  $c$  axis, which is the chain direction of the polychloroprene molecule, it is immediately apparent that as the polymer chains become aligned with extension of the sample, the crystallites also tend to line up with their  $c$  axes pointing more or less toward the stretching direction. Moreover, the curves for reflections B and C are very similar to each other, suggesting

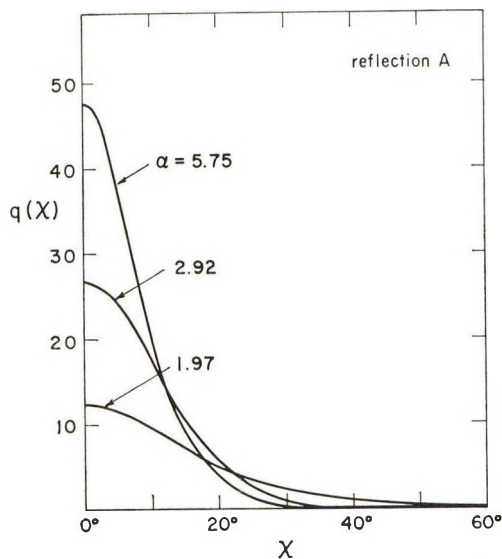


Fig. 3. The normalized plane-normal orientation distribution function  $q(\chi)$  of reflection A (002 plane) obtained for samples at the indicated relative elongations  $\alpha$ .

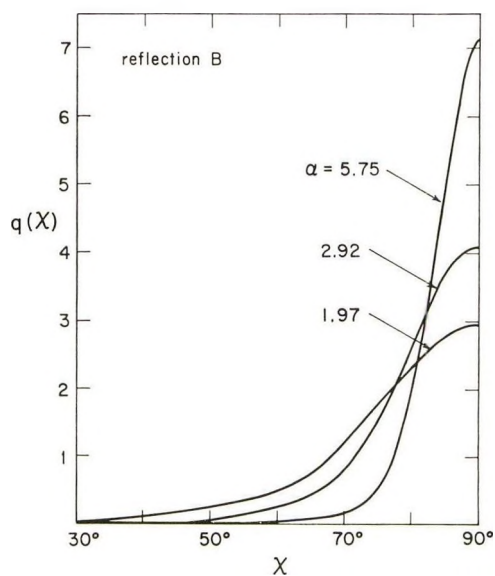


Fig. 4. The plane-normal distribution function of reflection B (210 plane) for the indicated elongations.

that the crystallites orient randomly around the  $c$  axis, without any tendency for either the  $a$  or  $b$  axis to align with the stretching direction.

Since the shapes of the orientation distribution functions are single-peaked, and all closely resemble a Gaussian function for the various samples, a single parameter, such as the average value of  $\cos^2 \chi$ , suffices for the pres-

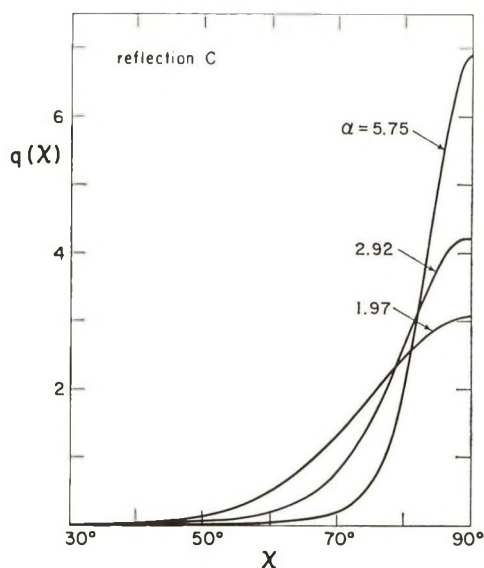


Fig. 5. The plane-normal distribution function of reflection C (120 and 200 planes).

ent purpose to characterize the degree of orientation as a function of  $\alpha$ . Averages of  $\cos^2 \chi$  were computed from the observed intensities according to the relation

$$\langle \cos^2 \chi \rangle = \frac{\int_0^\pi q(\chi) \cos^2 \chi \sin \chi d\chi}{\int_0^\pi I_0(\chi) \sin \chi d\chi} \quad (2)$$

These are listed in Table II for reflections A, B, and C under the columns headed "obs." For orthorhombic crystals,  $\langle \cos^2 \chi \rangle$  for any plane-normal can be calculated once  $\langle \cos^2 \chi \rangle$  values have been determined from experimental measurements for two planes.<sup>6,7</sup> In the present work  $\langle \cos^2 \chi \rangle$  values were obtained for three different reflections, and therefore the least-square method proposed by Sack<sup>6,7</sup> was employed in calculating the  $\langle \cos^2 \chi \rangle$  values for the (200) and  $\langle 020 \rangle$  planes. The same method also permits the calculation of  $\langle \cos^2 \chi \rangle$  values for the measured reflections A, B, and C. These calculated values are, in effect, corrected for the mutual geometric relationship among the three reflections, and thus should be more accurate than the original values of  $\langle \cos^2 \chi \rangle$ . Since the reflection C is composite, weights were assigned to the (120) and (200) reflections, for use in the least-square calculation, in proportion to the square of structure factors calculated by Bunn<sup>4</sup> for his proposed structure, and listed in Table I. The values of  $\langle \cos^2 \chi \rangle$  thus calculated are given in Table II.

The calculated values of  $\langle \cos^2 \chi \rangle$  for the three crystallographic axes,  $a$  (200),  $b$  (020), and  $c$  (002) also appear plotted in Figure 6 as a function of  $\alpha$ . We can immediately draw some qualitative conclusions from this plot.

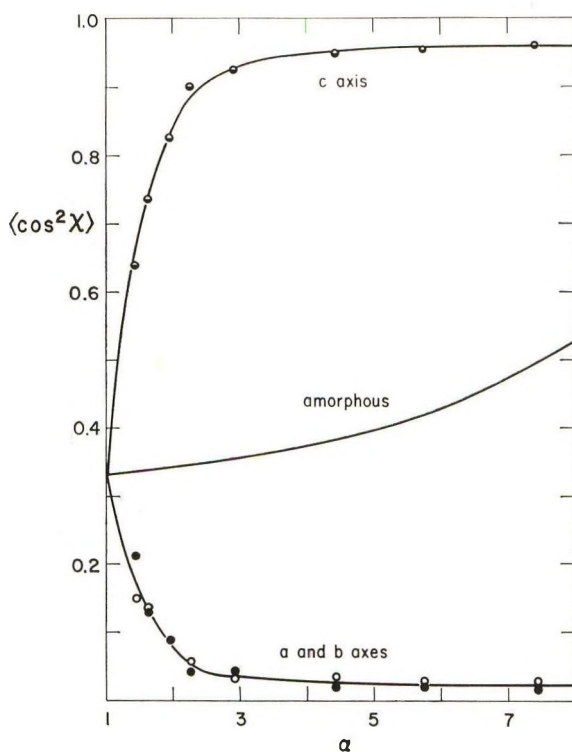


Fig. 6. The variation of  $\langle \cos^2 \chi \rangle$  with elongation  $\alpha$ . The points refer to the experimental values of  $\langle \cos^2 \chi \rangle$  for the following crystallographic axes: (●) *a* axis; (○) *b* axis; (◐) *c* axis. The curve labeled amorphous refers to the calculated values of  $\langle \cos^2 \chi \rangle$  for the amorphous segment orientation which existed prior to crystallization.

First, at low  $\alpha$  values the degree of orientation improves very rapidly with increasing  $\alpha$ , the value of  $\langle \cos^2 \chi \rangle$  for the *c* axis changing almost linearly from  $1/3$  (random orientation) at  $\alpha = 1$  to 0.9 at  $\alpha = 2.4$ . The *c* axis has

TABLE II  
Observed and Calculated Values of  $\langle \cos^2 \chi \rangle$

$\alpha$	$\cos^2 \chi$							
	A (002)		B (210)		C (120) + (200)		(200)	(020)
	Obs.	Calc.	Obs.	Calc.	Obs.	Calc.	Calc.	Calc.
1.45	0.671	0.638	0.220	0.203	0.223	0.174	0.213	0.149
1.64	0.740	0.736	0.131	0.129	0.139	0.133	0.128	0.136
1.97	0.814	0.826	0.083	0.089	0.070	0.088	0.090	0.085
2.27	0.898	0.902	0.042	0.044	0.046	0.051	0.041	0.057
2.92	0.928	0.925	0.043	0.042	0.040	0.036	0.043	0.032
4.44	0.943	0.949	0.017	0.020	0.019	0.028	0.018	0.034
5.75	0.949	0.945	0.016	0.019	0.017	0.024	0.017	0.029
7.40	0.952	0.958	0.013	0.015	0.014	0.023	0.014	0.029

already become quite well oriented at  $\alpha = 4$ , so that the corresponding  $\langle \cos^2 \chi \rangle$  value tends to level off at higher  $\alpha$ , although it still shows a definite tendency to increase slowly toward the limiting value unity (perfect orientation). Secondly, for a given value of  $\alpha$ , the  $\langle \cos^2 \chi \rangle$  values for the  $a$  and  $b$  axes are nearly the same, the small difference between them probably arising from experimental error. This confirms the assertion, drawn previously from comparison of the distribution curves for reflections B and C, that the crystallites exhibit needlelike behavior in assuming a random orientation around the  $c$  axis.

## 2. Characterization of the Network

A quantitative interpretation of the foregoing results on crystallite orientation requires a knowledge of the degree of orientation of the segments of the network chains which existed in the strained state before the onset of crystallization. We have previously shown<sup>8</sup> that the distribution of statistical segment orientations in a network polymer can be deduced if the average number of statistical segments per network chain,  $N$ , is known. Unfortunately, we can only obtain a rather crude estimate of  $N$  through the following procedure. According to the Gaussian theory of rubber elasticity,<sup>9</sup> the number of repeating units per chain,  $N_u$ , can be evaluated from measurement of the retractive force by use of the relation

$$N_u = \rho RT(\alpha - 1/\alpha^2)/M_u f \quad (3)$$

where  $\rho$  is the density of the sample,  $R$  the gas constant,  $M_u$  the molecular weight of the repeating unit, and  $f$  the retractive force per unit cross-sectional area. Force-elongation measurements were performed at 80°C. upon a strip of polychloroprene. The sample was enclosed in a glass tube through which nitrogen gas was passed continuously in order to prevent oxidation. The sample exhibited some creep and permanent set, and darkening was observed after a few days at 80°C., even in a nitrogen atmosphere. The length under load was therefore measured after 16 hr., and the recovered length was measured 8 hr. after removal of the load. The original and recovered lengths were averaged for the computation of the relative elongation  $\alpha$ . Using the values  $\rho = 1.24$  g./cc. and  $M_u = 88.5$ ,  $N_u$  was found to be 103 according to eq. (3). Moore and Watson,<sup>10</sup> Mullins,<sup>11</sup> and Treloar<sup>9</sup> have pointed out that  $N_u$  values obtained from modulus measurements are usually smaller than those estimated by chemical methods. The ratio of these  $N_u$  values varies somewhat with the degree of crosslinking, but is about 1.8 for a natural rubber network having a crosslink density comparable to our polychloroprene sample. This would suggest  $N_u \cong 180$ . Next, we need to divide  $N_u$  by the number,  $s$ , of repeating units per statistical segment. Even for natural rubber, which has been investigated rather thoroughly, there is considerable disagreement among the values for  $s$  reported by various workers.<sup>12</sup> A simple average of all of these gives  $s = 1.5$ .<sup>13</sup> There appears to be no information concerning the unperturbed

dimensions of the polychloroprene chain. In view of the larger C—Cl dipole, we will assume  $s = 3$ , to obtain  $N \cong 60$ . Due to the numerous uncertainties, this estimate could be in error by a factor of two. The quantitative results to be derived in the following sections will be affected correspondingly; however, the principal conclusions are believed to be valid in spite of this uncertainty.

### *3. Comparison of the Orientation Distributions of Crystallites and Statistical Chain Segments*

In a previous paper<sup>8</sup> we have derived the orientation distribution function  $w(\cos \chi)$  for statistical segments in a strained amorphous network, making use of the Kuhn-Grün-Treloar<sup>14</sup> model of a network of flexibly linked chains. Here  $\chi$  is the angle specifying the orientation of a statistical segment with respect to the stretching direction. The distribution function was obtained in series form, the first terms of which are

$$w(\cos \chi) = (1/2) + (1/4N) (\alpha^2 - 1/\alpha) (3 \cos^2 \chi - 1) + 0(1/N^2) \quad (4)$$

Terms through the fourth, which contains the factor  $(1/N^3)$ , are evaluated in the paper.<sup>8</sup> Upon substituting  $N = 60$  and the appropriate  $\alpha$  values for the samples examined, it becomes strikingly evident that the distribution of crystallite  $c$ -axis orientations is much sharper than that of the statistical segments prior to crystallization. For the purpose of comparison, the curve labeled "amorphous" in Figure 6 shows the values of  $\langle \cos^2 \chi \rangle$  calculated for statistical segments using the expression including four terms. One sees that there is no resemblance between the shapes of the curves representing the variation of  $\langle \cos^2 \chi \rangle$  with  $\alpha$  for the amorphous segments and the crystallite  $c$  axis. In order to understand this gross difference, we must consider more carefully the crystallization process in strained polymers.

Kinetic studies of polymer crystallization have established that the mechanism of crystallization involves two rate-determining steps: primary and secondary nucleation. Thus, once the growth process is initiated by primary (homogeneous or heterogeneous) nucleation, the rate of growth of a crystallite, or an aggregate of crystallites, depends almost entirely upon the rate of secondary nucleation, the deposition of additional segments on the growing secondary nuclei being much faster than the nucleation step.

In a stretched polymer, the rates of both primary and secondary nucleation are expected to be orientation-dependent and to be most rapid along the drawing direction. In the subsequent process of depositing additional segments, the orientation of the latter cannot be different from that of the nucleus upon which growth occurs. Although the rate of growth may also be orientation-dependent to some extent, it is always much more rapid than nucleation, with the result that the orientation distribution of all the crystalline segments at a given time will be roughly the same as the orientation distribution of the nuclei which have been formed up to that moment.



In other words the orientation of crystallites, as well as their rate of growth, is determined almost entirely by the nucleation process.

The rate of nucleation as a function of orientation can be deduced from the following simplified picture of the nucleation process. An embryo or a nucleus can become stable only when its volume exceeds a certain critical value which depends on the relative magnitudes of the surface free energy and the bulk free energy change due to the phase transition. If this critical volume contains  $\nu$  statistical segments, then the formation of such an aggregate requires the simultaneous alignment of all  $\nu$  segments in the same direction. Let  $P(\Omega)d\Omega$  be the probability of finding a statistical segment in an amorphous chain with its axis oriented within the range of solid angles  $(\Omega, \Omega + d\Omega)$ . Then the rate  $R(\Omega)$  of formation of nuclei having the particular orientation in question will be proportional to the  $\nu$ th power of the probability  $P(\Omega)$  pertaining to the orientation of a single statistical segment; that is,

$$R(\Omega) = \text{const. } [P(\Omega)]^\nu \quad (5)$$

In the case of a secondary (surface) nucleation, the availability of crystal surfaces having the correct orientation can influence  $R(\Omega)$  somewhat, but when  $\nu$  is large the availability of amorphous segments having the proper orientation should be the factor of overwhelming importance.

For the probability  $P(\Omega)$  we take the orientation distribution function  $w(\chi)$  of the statistical segments existing before the onset of crystallization.<sup>8</sup> Then invoking the assumption that the nucleation process controls the overall crystallite orientation distribution in the sample, we obtain the function  $q_c(\chi)$  describing the orientation distribution of the crystallite  $c$  axes, and the average  $\langle \cos^2 \chi \rangle$  of the square of the cosine of the angle between the  $c$  axis and the stretching direction:

$$q_c(\chi) = \frac{[w(\chi)]^\nu}{\int_0^\pi [w(\chi)]^\nu \sin \chi \, d\chi} \quad (6)$$

$$\langle \cos^2 \chi \rangle = \int_0^\pi \cos^2 \chi \, q_c(\chi) \sin \chi \, d\chi \quad (7)$$

The second column of Table III lists the values of  $\nu$  which give agreement between  $\langle \cos^2 \chi \rangle$  as calculated according to eqs. (6) and (7) and the value obtained for reflection A (002) as listed in the third column of Table II. These  $\nu$  values vary smoothly over the range 90–20 as  $\alpha$  is increased from 1.45 to 7.40 (with the exception of one sample at  $\alpha = 2.27$ , which appears to involve an experimental error). In Figures 7–9 the  $c$  axis orientation distribution functions  $q_c(\chi)$  calculated according to eq. (6) are shown as full curves, while the circles represent the same functions measured experimentally. In calculating  $q_c(\chi)$  the values of  $\nu$  were again adjusted independently to obtain a best fit between the theoretical and experimental curves; however, these fitted values of  $\nu$  are seen to be very nearly the same

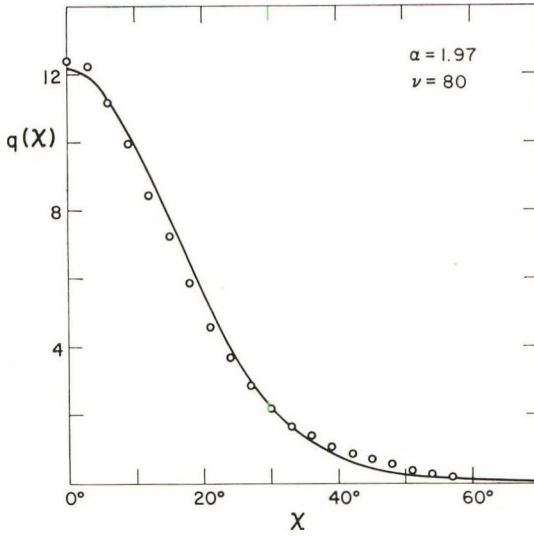


Fig. 7. The experimental distribution function  $q(\chi)$  of the (002) plane-normal for a sample elongated to  $\alpha = 1.97$ . The full curve represents the  $q(\chi)$  function derived theoretically (see text).

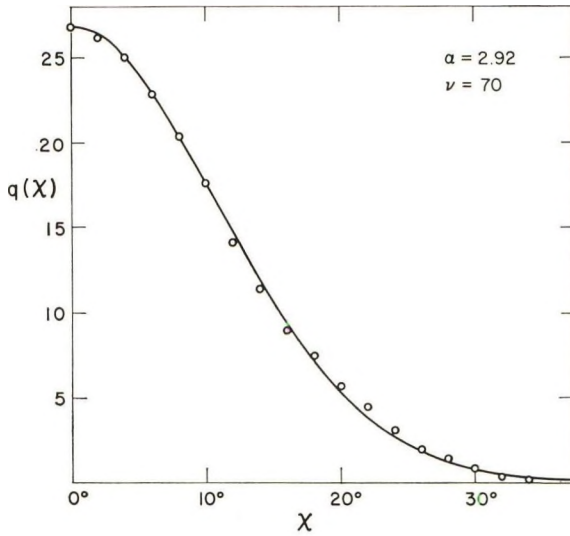


Fig. 8. See legend to Fig. 7.

as those listed in Table III. Although there may be some minor deviations, the agreement between the theoretical and experimental crystallite orientation distributions is quite satisfactory.

The  $c$  axis orientation distribution function  $q_c(\chi)$  given by eq. (6) actually has to be compared with the experimental distribution obtained for a sample having a very low crystallinity, since  $w(\chi)$  in eq. (6) refers to the

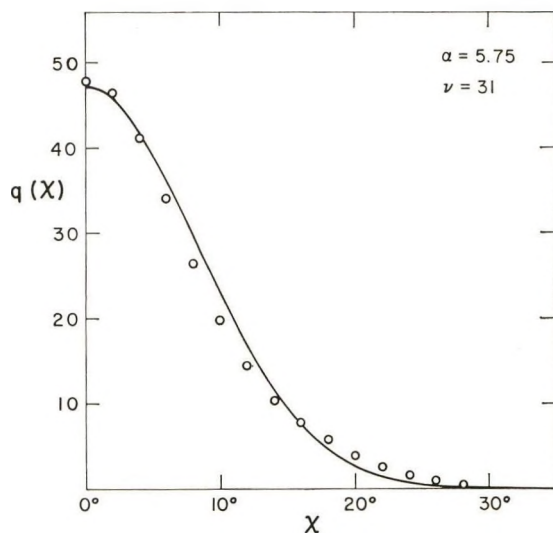


Fig. 9. See legend to Fig. 7.

orientation of statistical segments prior to crystallization. As crystallization proceeds, the orientation distribution of the remaining amorphous chains may gradually depart from  $w(\chi)$ . In the present study the crystallinities were confined to about 30%. Within this range the resulting change in the amorphous segment orientation distribution is believed to be small, since as the more highly oriented segments are depleted, a new equilibrium with respect to the segment orientation is established in the amorphous phase. Also, although the formation of further nuclei is equivalent to addition of new crosslinks to the network, these are introduced into the sample in the strained state, and therefore their effect on  $w(\chi)$  is negligible.

From  $\nu$  we can calculate the volume of a crystallite nucleus. Recalling that a statistical segment was assumed to consist of three chloroprene units, the volume is given by  $(3\nu/4)$  times the unit cell volume, where the factor

TABLE III  
Variation of the Secondary Nucleus Size

$\alpha$	$\nu$ (from orientation)	Melting temp. $t_M$ , °C.	Estimated crystallization temp. $t_c$ , °C.
1.45	89	51.3	39.9
1.64	86	51.4	39.7
1.97	78	51.9	39.6
2.27	92	52.5	41.2
2.92	70	54.1	41.1
4.44	44	60.0	43.3
5.75	24	67.3	44.1
7.40	19	79.8	52.8

$1/4$  arises from the fact that a unit cell, according to Bunn,<sup>4</sup> contains four chloroprene units. For the  $\nu$  values 90 and 20, the volume of the nucleus turns out to be 29,000 A.<sup>3</sup> (30 A. cube), and 6,500 A.<sup>3</sup> (17 A. cube), respectively. Although both the primary and secondary nuclei play a role in determining the crystallite orientation distribution, the fact that the number of the latter greatly exceeds that of the former suggests that the values given above probably refer to the volume of the secondary nuclei.

If the variation of  $\nu$  with  $\alpha$  can be estimated from nucleation theory, then the entire crystallite orientation distribution in polychloroprene and similar materials can be calculated from first principles. Our data are not sufficiently extensive to afford a quantitative test of this point; however, we can at least demonstrate that the effects observed are of the order of magnitude predicted by nucleation theory. It is well known that the melting point of a network polymer is raised by deformation.<sup>15,16</sup> On the other hand, all of the samples received the same cooling schedule from the melt, so that we may expect that the crystallization temperatures for these samples should not vary strongly with  $\alpha$ . Hence, the degree of supercooling at the time of crystallization would have increased in a regular fashion with strain. According to nucleation theory the critical nucleus size in the case of surface nucleation is approximately proportional to  $1/\Delta T$ , where  $\Delta T$  is the difference between the melting and crystallization temperatures. The observed decrease in  $\nu$  with  $\alpha$  is thus in the expected direction.

We may therefore attempt a more quantitative comparison with nucleation theory. Hirai<sup>17</sup> has treated a model involving spherical segments having a coordination number six. The number  $\nu$  of such segments in the critical secondary nucleus is given by

$$\nu^{1/2} = (1/3) (T_M/\Delta T) \quad (8)$$

where  $T_M$  is the melting point of the sample. On the other hand, Hoffman, Weeks, and Murphy<sup>18</sup> have obtained an expression for the critical radius  $\rho_0$  of a cylindrical secondary nucleus of fixed height  $\lambda_0$ :

$$\rho_0 \cong (\sigma/\Delta h_f) (T_M/\Delta T) \quad (9)$$

where  $\sigma$  and  $\Delta h_f$  are the lateral surface free energy and the heat of fusion per cubic centimeter, respectively. If we consider the polymer segment to be cylindrical with radius  $r_0$ , and identify  $\lambda_0$  with the length of a segment, then we obtain

$$\nu^{1/2} = (\sigma/r_0\Delta H_f) (T_M/\Delta T) \quad (10)$$

The lateral surface free energy  $\sigma$  is not known for polychloroprene. For polyethylene, Hoffman and Weeks<sup>19</sup> give the values  $\sigma = 12.2$  erg/cm.<sup>2</sup> and  $\Delta h_f = 2.8 \times 10^9$  erg/cm.<sup>3</sup>. From the dimensions of the unit cell of polyethylene the radius of a segment is calculated as  $r_0 = 1.7$  Å. Substitution of these values into eq. (10) leads to

$$\nu^{1/2} = (1/3.9) (T_M/\Delta T) \quad (11)$$

The near agreement between this relation and eq. (8) may be taken as a justification for our use of the latter relation.

The melting point was measured for one sample, as described in the following section, yielding  $t_M = 54.1^\circ\text{C}$ . for  $\alpha = 2.92$ . Melting temperatures corresponding to the other elongations were calculated according to eq. (10A) given in the Appendix. For this purpose the  $t_M$  value given above, and the elastic force  $f$  measured at  $80^\circ\text{C}$ . (see section IIIA2), were required. The values of  $t_M$  thus obtained are listed in the third column of Table III. The fourth column gives the values of the crystallization temperature  $t_c$  which, according to eq. (8), would yield the observed  $\nu$  values. Since it is known that crystallization occurred above  $35^\circ\text{C}$ ., the theoretical values of  $t_c$  are of the correct magnitude. Furthermore, the slow increase with  $\alpha$  predicted for  $t_c$  is entirely reasonable in view of the slow increase in  $t_M$  with elongation. It therefore appears likely that the nucleation treatments can be applied without modification to strained samples; however, conclusive proof will require a more extensive study employing samples crystallized isothermally.

## B. Crystallite Orientation and the Degree of Crystallinity as a Function of Temperature

The crystallite orientation and the degree of crystallinity were measured for one sample at a relative elongation  $\alpha = 2.92$  as the temperature was raised stepwise from room temperature to a temperature very near the sample melting point. The sample holder attached to the x-ray apparatus was fitted with a four-junction copper-constantan thermocouple to measure the sample temperature, a thermistor probe for regulating the temperature, and a nitrogen gas inlet. In order to minimize complications due to recrystallization, the measurements had to be performed fairly rapidly at each temperature. Since reflection C of Table I has the highest intensity, and since it was shown in section IIIA1 that the orientation parameter determined from this reflection can readily be interpreted in terms of the  $c$  axis orientation, the measurements are performed only upon this reflection.

The degree of crystallinity  $\omega$  may be computed from the x-ray intensity  $I_0(\chi)$ , measured as a function of  $\chi$  and corrected for background, by

$$\omega = \text{const.} \int_0^{\pi/2} I_0(\chi) \sin \chi \, d\chi \quad (12)$$

Instead of attempting to evaluate the constant in the above equation, we have obtained from the diffraction data only relative values of the crystallinity. These were placed on an absolute scale by an independent measurement of the density of the sample at room temperature by a flotation method. Using the values of one density given by Maynard and Mochel<sup>20</sup> for the crystalline and amorphous polymers, 1.35 and 1.236 g./cc., respectively, we obtain from the measured density, 1.270 g./cc.,  $\omega = 0.30$ . Values

TABLE IV  
The Orientation Parameter of Reflection C and the Degree of Crystallinity  
Measured for Relative Elongation  $\alpha = 2.92$

Temp. $t$ , °C.	$\langle \cos^2 \chi \rangle$	$\omega$
24.0	0.038	0.300
29.8	0.038	0.296
32.5	0.037	0.297
37.4	0.039	0.293
39.5	0.038	0.280
41.2	0.039	0.272
43.6	0.039	0.245
45.9	0.037	0.196
47.6	0.040	0.124
48.2	0.040	0.110
50.4	0.040	0.090
52.8	(0.080)	(0.037)

observed at various temperatures for the average of  $\cos^2 \chi$  for reflection C, and the degree of crystallinity  $\omega$ , appear in Table IV.

It is seen that over a fairly broad range of temperature and degree of crystallinity the distribution of crystallite orientations remains invariant. The sudden increase in  $\langle \cos^2 \chi \rangle$  at 52.8°C. is probably not significant because the experimental error is quite large at this temperature due to the very small amount of crystallinity remaining. The observed invariance implies that the thermodynamic stability of a crystallite formed under these conditions is independent of its particular orientation with respect to the drawing direction.

The temperature dependence of the degree of crystallinity observed experimentally may be compared with that calculated according to the treatment of Flory.<sup>1</sup> By assuming that crystallites in a strained polymer network are perfectly aligned toward the stretching direction, and that the amorphous chains connecting the crystallites still obey Gaussian statistics, he obtained the following expression for  $\omega$  as a function of  $T$  and  $N$

$$1 - \omega = \{ [3/2 - \varphi(\alpha)] / (3/2 - \Theta) \}^{1/2} \quad (13)$$

where

$$\varphi(\alpha) = \sqrt{\frac{6}{\pi}} \frac{\alpha}{\sqrt{N}} - \left( \frac{\alpha^2}{2} + \frac{1}{\alpha} \right) \frac{1}{N} \quad (14)$$

and

$$\Theta = \frac{\Delta H_f}{R} \left( \frac{1}{T_M^0} - \frac{1}{T} \right) \quad (15)$$

where  $T_M^0$  is the melting point of the unstrained sample. Upon combining eqs. (13) and (15) and rearranging, we obtain:

$$\frac{1}{T} = \frac{1}{T_M^0} - \frac{3}{2} \frac{R}{\Delta H_f} + \frac{R}{\Delta H_f} [3/2 - \varphi(\alpha)] / (1 - \omega)^2 \quad (16)$$

Thus, a plot of  $1/T$  against  $1/(1 - \omega)^2$  should yield a straight line with a slope equal to  $(R/\Delta H_f)[3/2 - \varphi(\alpha)]$ . The present data appear plotted in the manner in Figure 10. The eight points corresponding to lower degrees of crystallinity lie fairly well on a straight line, the slope of which is  $1.45 \times 10^{-4} \text{ deg.}^{-1}$ . If we use a value of 6.0 kcal./mole for the heat of fusion per statistical segment, then the slope expected from the theory for  $\alpha = 2.92$  and  $N = 60$  is  $3.52 \times 10^{-4}$ . Although the observed and calculated slopes differ by a factor of about two, this agreement is perhaps satisfactory in view of the uncertainty in the magnitude of  $N$ . The melting point of the strained sample,  $T_M$ , may be evaluated from the ordinate corresponding to  $\omega = 0$  (i.e.,  $1/(1 - \omega)^2 = 1$ ), and is found to correspond to 54.1°C. The experimental points in Figure 10 representing lower temperatures ( $1/T > 3.2 \times 10^{-3}$ ) deviate considerably from the linear behavior

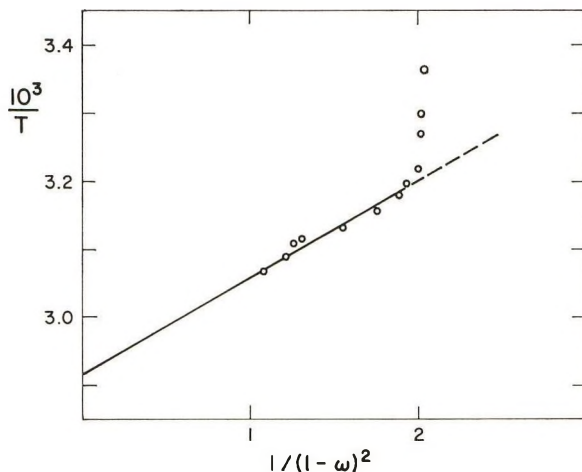


Fig. 10. Variation of the degree of crystallinity  $\omega$  with temperature  $T$  for  $\alpha = 2.92$  plotted in accordance with eq. (16).

predicted theoretically. In order to find possible causes for this deviation, we must first examine the physical reason behind the linear relationship between  $1/T$  and  $1/(1 - \omega)^2$ . In his theoretical treatment, Flory calculated the entropy change associated with the additional constraints imposed upon the amorphous chains as perfectly aligned crystallites grow in the strained network. However, Roe, Smith, and Krigbaum<sup>21</sup> have shown that even when crystallization occurs in an isotropic polymer there is an important contribution from the deformation entropy of the remaining amorphous chains connecting the crystallites. This deformation entropy prevents crystallization from proceeding to completion. On this basis they deduced expressions for the equilibrium degree of crystallinity  $\omega$  at any temperature for folded chain and single pass (bundlelike) crystallite models. For either model the theoretical relation also depends upon whether Gaussian or inverse Langevin statistics are assumed in computing the deforma-

tion entropy. Their expression based upon Gaussian statistics may be rearranged into the form:<sup>22</sup>

$$1/T = A + B(R/\Delta H_f)[1/(1 - \omega)^2] \quad (17)$$

the parameters  $A$  and  $B$  depending to some extent upon the crystallite model. However, it can be shown quite generally, without recourse to a specific crystallite growth model, that eq. (17) is a direct consequence of the assumption that the broad melting range of polymers is due to the deformation entropy of the remaining amorphous chains, and that the latter is given to a sufficient approximation by Gaussian statistics. Calculations show that the chains in an initially isotropic sample approach full extension rather rapidly as  $\omega$  increases, so that the more precise inverse Langevin statistics must be employed for higher  $\omega$  values.<sup>21</sup> Thus, crystallinity data for polyethylene and polypropylene are found<sup>22</sup> to obey eq. (17) closely when  $\omega$  is small, but to exhibit deviations when  $\omega$  exceeds 0.2 to 0.3. On the other hand, Roe, Smith, and Krigbaum<sup>21</sup> were able to fit the temperature dependence of the degree of crystallinity for polyethylene over the entire observed range by the more precise relation based on inverse Langevin statistics. The deviation from linearity found in Figure 10 is therefore believed to be chiefly due to the non-Gaussian behavior of the highly extended amorphous chains. A second possible contributing factor in the present case is the 10–15% of noncrystallizable 1,4-*cis* units in our polychloroprene sample.

### C. Effect of Further Drawing upon the Orientation of Preformed Crystallites

As stressed in the introduction, the samples used in the present study were all crystallized from the completely amorphous, stretched state. To assess the importance of this precaution, we have studied the crystallite orientation of one sample which was stretched at room temperature in the presence of crystallites.

Curve 1 of Figure 11 represents the orientation distribution function  $q(\chi)$  of reflection C as measured for a sample stretched to  $\alpha = 2.86$  and crystallized from the melt. When the sample was further stretched at room temperature to  $\alpha = 3.50$  and the distribution function again measured, the result represented by curve 2 of Figure 11 was obtained. The extent of broadening is surprisingly large, the corresponding change in  $\langle \cos^2 \chi \rangle$  being from 0.041 to 0.129. If the crystallites behaved as isolated inclusions imbedded in a network, their orientation would have improved with further drawing. The observed broadening therefore stresses the fact that the complicated interactions between crystallites are of primary importance in such a drawing process. It seems advisable to obtain a firm understanding of the behavior of samples crystallized from the amorphous strained state before undertaking a study of the additional complications arising from cold drawing.



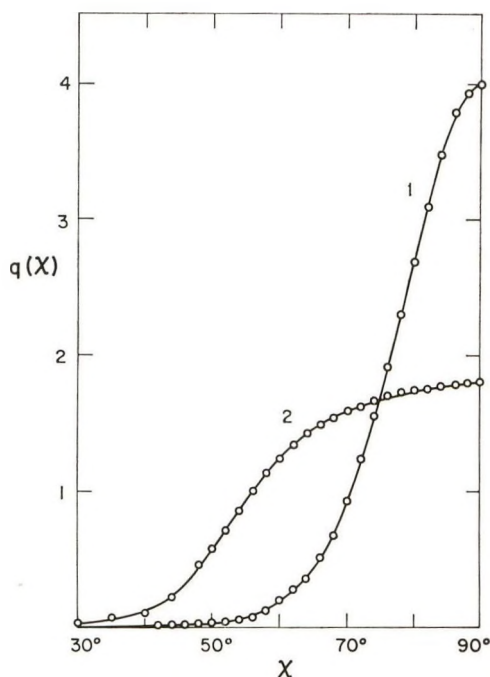


Fig. 11. The change in the plane-normal distribution function  $q(\chi)$  for reflection C with cold drawing: (1) sample crystallized from the melt at  $\alpha = 2.86$  and (2) drawn further to  $\alpha = 3.50$  at room temperature.

Earlier, Arlman and Goppel<sup>23</sup> reported results of their study on crystallite orientation in natural rubber which directly contradict many of our observations on polychloroprene. They reported the orientation distribution to be nearly independent of elongation in the range  $\alpha = 4.5$ – $7.0$ , while a sharpening of the crystallite distribution was observed as the temperature was raised. They did not describe their drawing procedure, but in view of the observations on cold drawing described in the preceding paragraph, these differences could be reconciled if we assume that their samples contained considerable crystallinity before they were drawn. Further support for this conjecture is given by a preliminary result obtained for natural rubber in this laboratory. When a strip of radiation crosslinked rubber was stretched to  $\alpha = 6.04$  and crystallized overnight at room temperature, the (002) reflection gave an angular breadth of the distribution curve at half-peak height equal to  $8.6^\circ$  in  $\chi$ . A second sample was stretched to  $\alpha = 5.00$  and allowed to crystallize in the same manner. The angular breadth in  $\chi$  was now  $9.8^\circ$ . When this sample was further stretched to  $\alpha = 6.04$ , the angular breadth as measured immediately after stretching was still  $9.8^\circ$ , but it decreased to  $9.0^\circ$  after the sample was allowed to stand overnight at fixed elongation. The narrowing of the distribution with increasing temperature which was reported by Arlman and Goppel may be ascribed, at least in part, to recrystallization. We have found that natural

rubber is very prone to recrystallize above room temperature, and in fact their data also clearly indicate an increase in the degree of crystallinity between 70 and 80°C.

#### IV. CONCLUSIONS

In crosslinked polychloroprene networks which were stretched and crystallized from the melt, the  $c$  axis of the crystallites becomes oriented toward the stretching direction, while the  $a$  and  $b$  axes are randomly distributed around the  $c$  axis.

The  $c$  axis orientation distribution is much sharper than the orientation distribution of amorphous statistical segments which existed before crystallization. The sharper distribution of the crystallite orientation can be explained in terms of the joint probability of finding  $\nu$  segments in the appropriate orientation,  $\nu$  being the critical number of statistical segments required for the formation of a nucleus for crystal growth. If this interpretation is correct, then comparison of amorphous and crystalline orientation distributions offers a method for estimating the critical size of the crystallite nuclei.

Contrary to a previous observation for natural rubber, the crystallite orientation in stretched polychloroprene does not change as the degree of crystallization  $\omega$  is decreased progressively by increasing the temperature. A linear relationship between  $1/T$  and  $1/(1 - \omega)^2$  is obeyed when  $\omega$  is small, thus demonstrating that crystallization causes a deformation of the remaining amorphous chains, and that it is this deformation which is responsible for the broad melting range exhibited by polymers.

When the sample was stretched further in the presence of crystallites, the orientation distribution became very much broader, which demonstrates the primary importance of interactions between crystallites in such a process. The crystallization of a strained sample from the melt is inherently a simpler process, and therefore it would seem to be profitable to seek a detailed understanding of this process before attempting a study of cold-drawing phenomena.

#### APPENDIX

An expression will be derived relating the melting point  $T_M$  of a stretched polymer network to the extent of elongation  $\alpha$ . The melting point is the temperature at which the chemical potentials of the solid and liquid phases are equal. Since we are here dealing with a one-component system, the chemical potential is equal to the molar Gibbs free energy  $F$  in each phase. For a constant pressure process the molar free energy  $F_a(\alpha, T)$  of the amorphous phase is a function of  $T$  and  $\alpha$ , while we assume that the molar free energy  $F_c(T)$  of the crystalline phase is a function of  $T$ , but does not depend on  $\alpha$ . We are thus neglecting the free energy change associated with the orientation of the crystallites formed in a stretched network.

The condition for phase equilibrium at the melting point  $T_M$  of the stretched network under isobaric conditions is given by

$$F_c(T_M) = F_a(\alpha, T_M) \quad (\text{A1})$$

If  $T_{M^0}$  is the melting point of an unstretched isotropic sample ( $\alpha = 1$ ), we have

$$F_c(T_{M^0}) = F_a(1, T_{M^0}) \quad (\text{A2})$$

Subtracting eq. (A2) from eq. (A1) we obtain

$$F_c(T_M) - F_c(T_{M^0}) = F_a(\alpha, T_M) - F_a(1, T_{M^0}) = [F_a(\alpha, T_M) - F_a(1, T_M)] + [F_a(1, T_M) - F_a(1, T_{M^0})]$$

which can be rewritten as

$$\int_{T_{M^0}}^{T_M} \left[ \frac{\partial F_c(T)}{\partial T} - \frac{\partial F_a(1, T)}{\partial T} \right] dT = F_a(\alpha, T_M) - F_a(1, T_M) \quad (\text{A3})$$

Since

$$(\partial F / \partial T)_p = -S$$

the left-hand member of eq. (A3) becomes

$$- \int_{T_{M^0}}^{T_M} \Delta S(T) dT$$

where  $\Delta S$  is the difference in entropy between the crystalline and isotropic amorphous phases, i.e.,

$$\Delta S(T) = S_c(T) - S_a(1, T) \quad (\text{A4})$$

If we neglect the temperature variation of  $\Delta S(T)$ , and use the relation

$$\Delta H_f = -T_{M^0} \Delta S(T_{M^0}) \quad (\text{A5})$$

where  $\Delta H_f$  is the molar heat of fusion, we have for the left-hand member of eq. (A3)

$$\text{l.h.m. of eq. (A3)} = \Delta H_f \frac{T_M - T_{M^0}}{T_{M^0}} \quad (\text{A6})$$

The right-hand member of eq. (A3) represents the free energy change (or the stored free energy, see Treloar<sup>9</sup>) on elongation to  $\alpha$  at temperature  $T_M$ . The force per unit cross-sectional area,  $f(\alpha, T_M)$  which is required at temperature  $T_M$  to maintain the network at elongation  $\alpha$  is related to the stored free energy by

$$F_a(\alpha, T_M) - F_a(1, T_M) = V_0(T_M) \int_1^\alpha f(\alpha, T_M) d\alpha \quad (\text{A7})$$

where  $V_0(T_M)$  is the molar volume of the sample. Combining eqs. (A6) and (A7) we obtain

$$\frac{1}{T_M} = \frac{1}{T_M^0} - \left( \frac{V_0}{\Delta H_f} \right) \left( \frac{1}{T_M} \right) \int_1^\alpha f(\alpha, T_M) d\alpha \quad (\text{A8})$$

Equation (A8) shows that the measurement of the elastic force  $f$  as a function of  $\alpha$  and  $T$  can furnish an estimate of  $T_M$ . According to the theory of rubber elasticity in the Gaussian approximation

$$f(\alpha, T) = \gamma T (\alpha - 1/\alpha^2) \quad (\text{A9})$$

where the constant  $\gamma$  is the temperature coefficient of the modulus of rigidity. Thus, to the same approximation we have

$$\frac{1}{T_M} = \frac{1}{T_M^0} - \frac{V_0 \gamma}{2\Delta H_f} (\alpha^2 + 2/\alpha - 3) \quad (\text{A10})$$

The constant  $\gamma$  can, if required, be related to the number  $N$  of statistical segments per chain by use of eq. (3). Equation (A10) then becomes

$$\frac{1}{T_M} = \frac{1}{T_M^0} - \frac{R}{2\Delta H_f' N} (\alpha^2 + 2/\alpha - 3) \quad (\text{A11})$$

where  $\Delta H_f'$  now refers to the heat of fusion per mole of statistical segments.<sup>24</sup>

This investigation was supported by Chemstrand Research Center, Inc.

## References

1. Flory, P. J., *J. Chem. Phys.*, **15**, 397 (1947).
2. Judge, J. T., and R. S. Stein, *J. Appl. Phys.*, **32**, 2357 (1961); T. T. Li, R. J. Volungis, and R. S. Stein, *J. Polymer Sci.*, **20**, 199 (1956).
3. Kössler, I., and L. Švob, *J. Polymer Sci.*, **54**, 17 (1961).
4. Bunn, C. W., *Proc. Roy. Soc. (London)*, **A180**, 40 (1942).
5. Deas, H. D., *Acta. Cryst.*, **5**, 542 (1952).
6. Sack, R. A., *J. Polymer Sci.*, **54**, 543 (1961).
7. Roe, R.-J., and W. R. Krigbaum, *J. Chem. Phys.* in press.
8. Roe, R.-J., and W. R. Krigbaum, *J. Appl. Phys.* in press.
9. Treloar, L. R. G., *The Physics of Rubber Elasticity*, 2nd Ed., Oxford Univ. Press, London, 1958.
10. Moore, C. G., and W. F. Watson, *J. Polymer Sci.*, **19**, 237 (1956).
11. Mullins, L., *J. Polymer Sci.*, **19**, 225 (1956).
12. Mullins, L., *J. Appl. Polymer Sci.*, **2**, 257 (1959).
13. Smith, K. J., Jr., A. Greene, and A. Ciferri, paper presented at the International Conference on Rheology, Providence, R. I., August 1963.
14. Treloar, L. R. G., *Trans. Faraday Soc.*, **50**, 881 (1954).
15. Wildshut, A. J., *J. Appl. Phys.*, **17**, 51 (1946).
16. Roberts, D. E., and L. Mandelkern, *J. Res. Natl. Bur. Std.*, **54**, 167 (1955).
17. Hirai, N., *J. Polymer Sci.*, **42**, 213 (1960).
18. Hoffman, J. D., J. J. Weeks, and W. M. Murphy, *J. Res. Natl. Bur. Std.*, **63A**, 67 (1959).

19. Hoffman, J. D., and J. J. Weeks, *J. Chem. Phys.*, **37**, 1723 (1962).
20. Maynard, J. T., and W. E. Mochel, *J. Polymer Sci.*, **13**, 235 (1954).
21. Roe, R.-J., K. J. Smith, Jr., and W. R. Krigbaum, *J. Chem. Phys.*, **35**, 1306 (1961).
22. W. R. Krigbaum and I. Umatsu, paper submitted for publication in *J. Polymer Sci.*
23. Arlman, J. J., and J. M. Goppel, in *X-ray Crystallography*, Part C, J. Bouman, Ed., Interscience, New York, 1951.
24. Smith, K. J., Jr., Ph.D. Thesis, Duke University, 1961.

### Résumé

Des échantillons de polychloroprène pontés ont été cristallisés à partir du polymère fondu sous différentes élongations fixées. Des études de diffraction des rayons-X ont révélé que l'axe  $c$  s'oriente dans la direction de l'élongation tandis que les axes  $a$  et  $b$  sont distribués autour de l'axe  $c$ . La direction des axes  $c$  des cristallites par rapport à la direction d'étirement est beaucoup plus parfaite que celle des segments statistiques amorphes de chaîne avant la cristallisation. Ceci peut être expliqué en admettant que la formation d'un noyau stable pour la cristallisation exige l'alignement simultané de  $\nu$  segments amorphes. Donc de telles mesures donnent un moyen par lequel la forme critique du noyau de cristallisation peut être déterminé. Les formes obtenues pour le polychloroprène varient avec l'élongation d'un cube de 30 Å, à une élongation relative  $\alpha = 1.45$  à un cube de 17 Å. avec  $\alpha = 7.40$ . Bien que nos échantillons ne soient pas cristallisés isothermiquement, ces résultats sont en accord qualitatif avec la théorie de nucléation. Si la variation de  $\nu$  peut, en effet, être estimée par la théorie, il sera possible de prédire la distribution complète de l'orientation des cristallites des matériaux de ce type au départ de ces premiers principes. L'orientation des cristallites fermés dans un échantillon à élongation  $\alpha = 2.92$  a été trouvée essentiellement indépendante de la température depuis 24°C jusqu'au point de fusion. Pour les bas degrés de cristallinité,  $\omega$ , nous trouvons un rapport linéaire entre  $1/T$  et  $1/(1 - \omega)^2$  ce qui permet une évaluation du point de fusion par extrapolation. Finalement les orientations des cristallites d'un échantillon cristallisé d'un polymère fondu à  $\alpha = 2.86$  et/du même échantillon après une élongation jusque  $\alpha = 3.50$  à température ambiante ont été comparées. La distribution dans le second cas était considérablement plus large, ce qui démontre le rôle primaire joué par les interactions entre cristallites pendant l'étirement à froid des matériaux partiellement cristallisés.

### Zusammenfassung

Vernetzte Poly(chloropren)proben wurden bei verschiedenen festgehaltenen Dehnungen aus der Schmelze zur Kristallisation gebracht. Röntgenbeugungsuntersuchungen ergaben, dass sich die  $c$ -Achse in die Dehnungsrichtung orientiert, während die  $a$ - und  $b$ -Achsen statistisch um die  $c$ -Achse verteilt sind. Die Orientierung der Kristallit- $c$ -Achsen zur Zugrichtung ist viel vollkommener als die der amorphen statistischen Kettensegmente vor der Kristallisation. Dies kann unter der Annahme erklärt werden, dass die Bildung eines stabilen Kristallisationskeimes gleichzeitige Orientierung von  $\nu$  amorphen Segmenten erfordert. So bieten solche Messungen ein Mittel zur Bestimmung der kritischen Grösse der Kristallisationskeime. Die für Poly(chloropren) bestimmten Grössen schwanken mit der Dehnung von einem Würfel mit 30 Å. Seitenlänge bei einer relativen Dehnung von  $\alpha = 1,45$  bis zu einer Seitenlänge von 17 Å.  $\alpha = 7,40$ . Obwohl unsere Proben nicht isotherm kristallisiert waren, stimmen diese Ergebnisse qualitativ mit der Keimbildungstheorie überein. Wenn die Schwankung von  $\nu$  theoretisch berechnet werden kann, so wird es möglich sein, die gesamte Kristallorientierungsverteilung von Materialien dieser Art aus elementaren Gesetzen vorherzusagen. Die in einer Probe bei einer Relativdehnung  $\alpha = 2,92$  im Temperaturbereich von 24°C bis zum Schmelzpunkt gebildete Kristallorientierung zeigte sich im wesentlichen von der Temperatur unabhängig. Für geringen Kristallinitätsgrad  $\omega$  ergibt sich eine lineare Abhängigkeit

von  $1/T$  gegen  $1/(1 - \omega)^2$  und damit eine Möglichkeit der Berechnung des Schmelzpunktes durch Extrapolation. Schliesslich wurde die Kristallitorientierung für eine aus der Schmelze bei  $\alpha = 2,86$  kristallisierte Probe und für dieselbe Probe nach Weiterer Dehnung zu  $\alpha = 3,50$  bei Raumtemperatur verglichen. In letzterer Probe war die Verteilung beträchtlich breiter, was die wichtige Rolle der Wechselwirkung zwischen Kristalliten beim kalten Dehnen von teilweise kristallisierten Materialien zeigt.

Received December 9, 1963

## Homopolymers and Terpolymers of 5,7-Dimethyl-1,6-octadiene\*

J. M. WILBUR, JR.,† and C. S. MARVEL, *Department of Chemistry,  
University of Arizona, Tucson, Arizona*

### Synopsis

Polymerization of 5,7-dimethyl-1,6-octadiene with a 2/1 molar ratio of triisobutylaluminum/vanadium oxychloride, triisobutylaluminum/titanium tetrachloride or triisobutylaluminum/vanadium tetrachloride affords an elastic homopolymer. Attempted polymerization of the isomeric 3,7-dimethyl-1,6-octadiene under the same conditions failed. Elastomeric terpolymers of ethylene, propylene, and 5,7-dimethyl-1,6-octadiene have been prepared with these same coordination catalysts.

### INTRODUCTION

Recent publications<sup>1-3</sup> have indicated that desirable elastomeric properties and remarkable oxidation and ozone resistance are characteristic of ethylene-propylene copolymers. The practical utilization of these copolymers has been slightly retarded by the special vulcanization procedures they required. This disadvantage has been overcome by incorporating appropriate amounts of nonconjugated dienes into the ethylene-propylene polymer.<sup>4-7</sup> The resulting product is a terpolymer comprising flexible polymethylene chains having alkyl groups attached at frequent intervals and much less frequently, pendant unsaturated hydrocarbon groups in sufficient amounts to impart sulfur curability. The terpolymerization can be accomplished with coordination catalysts in a manner similar to that described by Gladding, Fisher, and Collette.<sup>6</sup> Under the conditions used, only the terminal double bond of the nonconjugated diene is active in the polymerization. The internal double bond is inactive and remains as a side-chain cure site in the interpolymer. In this respect, it was of interest to investigate 5,7-dimethyl-1,6-octadiene and 3,7-dimethyl-1,6-octadiene as nonconjugated dienes for terpolymerization with ethylene and propylene. This paper also describes some homopolymerization experiments with these octadienes.

\* This is a partial report of work done under contract with the Utilization Research and Development Divisions, Agricultural Research Service, U. S. Department of Agriculture, and authorized by the Research and Marketing Act. The contract was supervised by Dr. J. C. Cowan of the Northern Division.

† Present address: Science Department, Southwest Missouri State College, Springfield, Missouri.

The available commercial dimethyl octadiene is a mixture of the 5,7-dimethyl-1,6-octadiene (5,7-isomer), 3,7-dimethyl-1,6-octadiene (3,7-isomer) and other unidentified compounds. This mixture could not be fractionated into its pure components. However, sufficiently pure monomer for polymerizations could be prepared by two distillations with a spinning band column having 45 theoretical plates. Monomer obtained in this manner contains at least 86% of the 5,7-isomer and up to 10% of the 3,7-isomer. This mixture also contains an unidentified compound which may comprise up to 7% of the mixture.

Polymerization of the 5,7-isomer can be accomplished with a 2/1 molar ratio of triisobutylaluminum (TIBA) vanadium oxychloride, or triisobutylaluminum/vanadium tetrachloride or triisobutylaluminum/titanium tetrachloride in an inert solvent such as heptane or tetrachloroethylene. The use of TIBA/TiCl<sub>4</sub> catalyst affords a significantly improved yield (70%) of polymer with  $\eta_{inh}^{30} = 1.86$  (0.4%, benzene). The other catalysts afford polymer in yields of 13% and 16%, respectively, and an inherent viscosity of 1.3–1.5.

The TIBA/TiCl<sub>4</sub> catalyst affords a polymer in 26% yield,  $\eta_{inh}^{30} = 1.01$  (0.4%, benzene), from mixtures of the 5,7-isomer containing about 50% of the 3,7-isomer. This same catalyst under identical conditions failed to produce polymer with samples of the 3,7-isomer (89% pure by vapor-phase chromatography) containing about 5–6% of the 5,7-isomer. Thus, the 3,7-isomer will not polymerize under the same conditions as the 5,7-isomer and its presence will not interfere with polymerization of the 5,7-isomer.

Terpolymers of ethylene-propylene 5,7-dimethyl-1,6-octadiene are conveniently prepared in heptane or tetrachloroethylene solution with a 2/1 molar ratio of TIBA/VOCl<sub>3</sub> or TIBA/TiCl<sub>4</sub>. These terpolymers have identical infrared spectra and show characteristic absorption at 850, 980, and 1160 cm.<sup>-1</sup>. Infrared absorption at 840–850 cm.<sup>-1</sup> is characteristic of a trisubstituted olefinic bond and is present in the spectra of the monomer, homopolymer, and terpolymer.

## EXPERIMENTAL

### Materials

Samples of 5,7-dimethyl-1,6-octadiene and 3,7-dimethyl-1,6-octadiene were furnished by the Glidden Company. Ethylene and propylene were Matheson C. P. grade and these were used directly after drying with Davison Tel-Tale silica gel. The tetrachloroethylene was Matheson, Coleman, and Bell spectral grade dried with silica gel. Heptane, Phillips 99 mole-%, was purified by the method of Harold and Wolf.<sup>8</sup> Triisobutylaluminum and diisobutylaluminum chloride (Texas Alkyls), vanadium trichloride, vanadium tetrachloride, and vanadium oxychloride (Anderson Chemicals), titanium tetrachloride (Matheson, Coleman and Bell, 99.5%), and vanadium acetylacetonate (MacKenzie Chemical Co.) were all used directly without further purification.



**2,7-Dimethyl-1,6-octadiene.** Crude octadiene (3600 ml.) was washed five times with 200 ml. of a 10% solution of sodium bisulfite and once with 200 ml. of water. After two more washings with 200 ml. of 20% sodium bisulfite solutions and three washings with 200 ml. of water, the octadiene was dried with anhydrous magnesium sulfate, and some 2,6-di-*tert*-butyl-*p*-cresol was added as an antioxidant. Two distillations from calcium hydride under reduced pressure in a nitrogen atmosphere using a spinning band column (36 in.  $\times$  10 mm.) afforded 169.2 g. (31% yield of a fraction boiling at 89–90°C./100 mm.,  $n_D^{30}$  1.4340. Vapor-phase chromatographic analysis\* shows the presence of 5,7 isomer (86%) and 3,7-isomer (7%); the remainder is an unidentified substance. This material is sufficiently pure for use in polymerization. In other cases the sample of octadiene with boiling point at 88–89°C./99–100 mm., and refractive index at 30°C. in the range 1.4320–1.4343 was sufficiently pure for use. In a similar example, purification by such a procedure afforded an analytical sample (92% 5,7-isomer by vapor-phase chromatography), b.p. 88.5°C./102 mm.,  $n_D^{30}$  1.4323. The infrared spectrum shows absorption at 845  $\text{cm.}^{-1}$  which is characteristic of C–H out-of-plane bending associated with a trisubstituted olefinic bond. Other characteristic absorption at 915 and 990  $\text{cm.}^{-1}$  ascribed to the vinyl group is also present.

ANAL. Calcd. for  $\text{C}_{10}\text{H}_{16}$ : C, 86.88%; H, 13.12%. Found: C, 86.80%; H, 13.11%.

**Purification of 3,7-Dimethyl-1,6-octadiene.** A sample of the 3,7-isomer (125 g.) having  $n_D^{30}$  1.4326 was distilled over calcium hydride under reduced pressure in a nitrogen atmosphere with the use of aforementioned spinning band column. A fraction (31.3 g., 25% yield), b.p. 94°C./99 mm.,  $n_D^{30}$  1.4324, shown by vapor-phase chromatographic analysis to contain about 88.6% 3,7-isomer and 4.8% 5,7-isomer was used for polymerization.

### General Procedure for the Preparation of Homopolymers of 5,7-Dimethyl-1,6-octadiene

The polymerization mixtures were prepared and catalyst transfers were conducted in a dry box under a dry nitrogen atmosphere. A 4-oz. bottle was charged with a measured volume of solvent and a weighed amount of aluminum alkyl was added first and then a weighed amount of transition metal halide was added. The bottle was sealed with a rubber serum cap and aged 30 min. at room temperature before adding the monomer by means of hypodermic syringe. In other cases (Table I, runs 1, 2, 3), the solvent and monomer were mixed first, the bottle was capped, and the aluminum alkyl was added by means of hypodermic syringe through the serum cap as a solution in heptane or tetrachloroethylene. Finally, the

\* These values are not corrected for thermal conductivity and represent relative peak heights. Measurements were made with a Perkin-Elmer vapor fractometer (Model No. 154) with the use of a 2-m. UCON LB-550-X column at 150°C. and a helium flow.

TABLE I  
 Polymerization of 5,7-Dimethyl-1,6-Octadiene

Run no.	Solvent, and amt., ml.	Monomer, moles	Aluminum alkyl and amt., moles	Transition metal halide and amt., moles	Al/V molar ratio	Time, hr.	Temp., °C.	Yield, % <sup>a</sup>	Polymer viscosity data	
									Concn., g./100 ml. benzene	$\eta_{inh}^{30}$
1	Heptane, 25	0.022	TIBA, <sup>b</sup> 0.005	VOCl <sub>3</sub> , 0.0025	2	24	45	18	0.4028	1.33
2	TCE, <sup>c</sup> 25	0.022	TIBA, 0.005	VOCl <sub>3</sub> , 0.0025	2	24	45	16	0.5400	0.94
3	Heptane, 25	0.022	TIBA, 0.005	VOCl <sub>3</sub> , 0.0025	2	24	-25	0	—	—
4	Heptane, 25	0.03	TIBA, 0.010	VCl <sub>3</sub> , 0.0022	8.5	24	45	0	—	—
5	Heptane, 30	0.025	TIBA, 0.0088	VCl <sub>3</sub> , 0.0022	4	87.5	25	0	—	—
6	TCE, 30	0.03	DIBAC, <sup>d</sup> 0.0079	V(acac) <sub>3</sub> , <sup>e</sup> 0.0016	5	87.5	25	Trace	—	—
7	TCE, 30	0.022	DIBAC, 0.0079	V(acac) <sub>3</sub> , 0.002	4	87.5	25	Trace	—	—
8	Heptane, 20	0.021	TIBA, 0.005	VCl <sub>3</sub> , 0.0025	2	18	45-50	16	0.4144	1.39
9	Heptane, 20	0.021	TIBA, 0.005	TiCl <sub>4</sub> , 0.0025	2	18	45-50	70	0.4128	1.86

<sup>a</sup> Only the benzene-soluble portion is recorded.

<sup>b</sup> Triisobutylaluminum.

<sup>c</sup> Tetrachloroethylene.

<sup>d</sup> Diisobutylaluminum chloride.

<sup>e</sup> Vanadium acetylacetonate.

addition of the transition metal halide was accomplished in the same manner. Changing the order of mixing the catalyst and monomer did not markedly affect the polymerization. After the reaction had proceeded the specified time and at the temperature noted, the polymer was isolated by pouring into methanol (250 ml.) containing some 2,6-di-*tert*-butyl-*p*-cresol as an antioxidant. Purification was accomplished by dissolving the polymer in benzene containing some antioxidant and precipitating by pouring into excess methanol. This was repeated until a colorless product was obtained. Finally, the benzene solution was filtered, and removal of the benzene from the filtrate by freeze-drying afforded the pure polymer. The experimental results are summarized in Table I.

### Polymerization of a Mixture of 5,7-Dimethyl-1,6-octadiene and 3,7-Dimethyl-1,6-octadiene

A 4-oz. bottle was charged with 20 ml. of heptane in a dry box in a nitrogen atmosphere. A heptane solution of TIBA (2.88 ml., 0.005 mole) and  $\text{TiCl}_4$  (0.80 ml., 0.0025 mole) was added to the bottle by means of hypodermic syringe. The bottle was capped with a rubber serum cap and allowed to age at room temperature for 30 min. A mixture containing 5,7-dimethyl-1,6-octadiene (3 ml., 0.014 mole) and 3,7-dimethyl-1,6-octadiene (3 ml., 0.014 mole) was added by means of hypodermic syringe. The mixture was heated 18 hr. at 45–50°C. with occasional shaking. The polymer was isolated and purified in the same manner as described for the homopolymer of the 5,7-isomer. This afforded 0.5 g. (26% yield) of a polymer with  $\eta_{inh}^{30} = 1.01$  (0.4048 g./100 ml.  $\text{C}_6\text{H}_6$ ).

### Attempted Polymerization of 3,7-Dimethyl-1,6-octadiene

The same procedure as described for the homopolymerization of 5,7-dimethyl-1,6-octadiene was used. The reaction was carried out exactly as before with the exception of the use of 5 ml. (0.024 mole) of 3,7-dimethyl-1,6-octadiene (88.6% pure by V.P.C.), b.p. 94°C./99 mm.,  $n_D^{30}$  1.4324. There was no evidence of polymer formation when the reaction mixture was poured into methanol (250 ml.).

### General Procedure for Preparation of Ethylene-Propylene-Octadiene Terpolymers

A flask of appropriate size was equipped with a mechanical stirrer, thermometer, gas addition tube dipping below the surface of the solvent, an inlet tube fitted with a rubber serum cap for introduction of catalyst and octadiene by means of a hypodermic syringe, and a silica gel drying column (12 × 1 in.). This drying column was connected to an addition funnel which was protected from the atmosphere by a drying tube and bubbler trap. After vigorously drying the apparatus and flushing it with nitrogen, the solvent was charged to the flask by passage under nitrogen through a column containing 200 mesh silica gel (Davison No. 923). The silica gel

column was then replaced with a long tube containing Davison Tel-Tale silica gel and traces of oxygen were removed by passing a stream of nitrogen through the vigorously agitated solvent for 15 min. In some cases a condenser was placed between the flask and the drying column to reduce the loss of solvent during the reaction. After this was completed, the solution was saturated with a stream of ethylene and propylene for 10–15 min. and then the octadiene was added by means of a hypodermic syringe. In some cases the octadiene was added before saturating with ethylene and propylene. Matheson C. P. grade ethylene and propylene were used after drying by passage over Tel-Tale silica gel. The catalyst was added by means of a hypodermic syringe as a solution in heptane or tetrachloroethylene. The TIBA was added first, and then  $\text{VOCl}_3$  or  $\text{TiCl}_4$  was added after a few minutes. Three solutions were prepared in a dry box under nitrogen by adding weighed amounts of coordination catalyst to the appropriate amount of solvent in 4-oz. bottles which were then capped with a rubber serum cap.

At this stage a solution of TIBA was injected into the reaction mixture followed by a solution of  $\text{VOCl}_3$  or  $\text{TiCl}_4$ . An exothermic reaction started, and the temperature rose to 30–40°C. The flow of ethylene and propylene was continued for the desired time. The polymer was isolated by pouring the reaction mixture into about 1500 ml. of methanol containing a small amount of antioxidant (2,6-di-*tert*-butyl-*p*-cresol). The polymer was collected and washed with methanol in a Waring Blendor and then redissolved in 200 ml. of benzene (to which had been added 100 ml. of methanol containing some anti-oxidant). The polymer was then precipitated by adding this solution to excess methanol in a Waring Blendor. The polymer workup varied slightly from this point and will be described under each experiment.

**Terpolymer A-124.** This polymer was prepared in 450 ml. of tetrachloroethylene from 9.2 ml. of 5,7-dimethyl-1,6-octadiene (b.p. 88–89°C./99 mm.,  $n_D^{30}$  1.4320; vapor phase chromatography indicated the presence of about 4% of the 3,7-dimethyl isomer and 2–3% of an unknown compound). Polymerization was carried out for about 40 min. (30 min. flow of ethylene at a rate of 0.25–0.5 l./min. and propylene at a rate of 3–3.5 l./min. with 10 min. final stirring). After isolation of this polymer, 3.5 g. of benzene soluble and 1.2 g. of benzene insoluble material was obtained. The latter insoluble fraction was not further investigated. The soluble fraction was isolated from the benzene by freeze drying and was a tough, rubbery product with an inherent viscosity of 1.03 (0.4636 g. of polymer in 100 ml. of benzene) at 30°C. In tetrachloroethylene the viscosity was 1.94 (0.1% solution).

Analysis shows this polymer contains approximately 62.5% propylene and 7% diene. The propylene content was estimated on films from the ratio of absorbances A<sub>8.7</sub>/A<sub>2.3</sub>. The diene content was estimated by bromine titration. The infrared spectrum shows absorption at 845  $\text{cm.}^{-1}$  which is characteristic of the trisubstituted double bond structure found

in the 5,7-dimethyl-1,6-octadiene. Other characteristic absorption occurs at 1160 and 980  $\text{cm.}^{-1}$ .

**Terpolymer B-4-2.** This polymer was prepared in 1 l. of tetrachloroethylene. The solvent was saturated with ethylene (1 l./min.) and propylene (3 l./min.) before adding 0.03 mole of 5,7-dimethyl-1,6-octadiene followed by 0.005 mole of TIBA and 0.0025 mole of  $\text{VOCl}_3$ . At the end of the first and second hours a new charge of octadiene and catalyst mixture was added. At the end of  $2\frac{3}{4}$  hr. the product was isolated, and 15 g. of terpolymer was obtained by drying under reduced pressure.

A portion of this material (3.9 g.) was purified for analysis by dissolving in 200 ml. of benzene, filtering the solution through a glass wool plug, and removing the benzene by freeze drying. This afforded 3.0 g. of terpolymer containing 71 wt.-% propylene ( $\pm 10\%$ ), 85.54% C, 14.07% H,  $\eta_{\text{inh}}^{30} = 1.88$  (0.4732 g./100 ml. tetrachloroethylene). The infrared spectrum had characteristic absorption at 845, 980, and 1160  $\text{cm.}^{-1}$ .

**Terpolymer B-24-1.** This polymer was prepared in 2 l. of tetrachloroethylene which was saturated by a 10 min. flow of ethylene (0.5–1 l./min.) and propylene (2.5–3 l./min.) before the addition of 0.46 mole of 5,7-dimethyl-1,6-octadiene. (This sample had  $n_D^{30}$  1.4326 and was roughly 89% pure by vapor-phase chromatography). Then 0.01 mole of TIBA followed by 0.005 mole of  $\text{TiCl}_4$  was added. A flow of ethylene (0.5–1.0 l./min.) and propylene (2.5–3 l./min.) was passed into the stirred mixture continuously. An additional charge of the same amount of octadiene and catalyst mix then was added after 30 min., 60 min., 90 min., and 240 min. The reaction was stopped after 5.5 hr. The terpolymer isolated amounted to 94.3 g. It contained 84 wt.-% propylene ( $\pm 10\%$ );  $\eta_{\text{inh}}^{30} = 0.25$  (0.4392 g./100 ml. benzene). The infrared spectrum had the same characteristic absorption at 850, 980, and 1160  $\text{cm.}^{-1}$  as was present in the previously mentioned terpolymers. Analysis showed 85.71% C and 14.56% H.

**Terpolymer B-36-1.** This polymer was prepared in 1500 ml. of tetrachloroethylene from 0.2 mole of 5,7-dimethyl-1,6-octadiene. (Vapor phase chromatography indicated it to be 86% 5,7-isomer and 7% 3,7-isomer. Ethylene flow was at a rate of 1 l./min. and propylene flow at 3 l./min. The catalyst was 0.1 TIBA and 0.5 mole of  $\text{TiCl}_4$ . The reaction was allowed to proceed for  $2\frac{3}{4}$  hr., and the polymer was isolated as before. The yield was 46 g. of an elastic terpolymer with  $\eta_{\text{inh}}^{30} = 0.732$  (0.4292 g./100 ml. benzene). This material showed the same characteristic infrared absorption at 845, 980, and 1160  $\text{cm.}^{-1}$  as was present in the other terpolymers. Analysis showed 85.72% C and 14.52% H.

**Terpolymer B-41-1.** This polymer was prepared in 2 l. of tetrachloroethylene. There was added 0.18 ml. of 5,7-dimethyl-1,6-octadiene; the ethylene flow was 1 l./min. and propylene flow was 3 l./min. The catalyst was 0.1 mole of TIBA and 0.05 mole of  $\text{VOCl}_3$ . After 3 days the polymer was isolated as before to yield 78.5 g. of terpolymer,  $\eta_{\text{inh}}^{30} = 0.88$  (0.4580 g./100 ml. benzene). The infrared spectrum of the product showed the same characteristic absorptions as in previous examples. Analysis showed

TABLE II  
 Evaluation of Terpolymers as Rubbers

Properties	Polymer		Nordel (control)
	B-36-1	B-41-1	
$T_g$ (DTA), °C.	-57	-52	—
Bromine equiv., (wt.-% diene) <sup>a</sup>	9.4	4.1	—
Inherent viscosity (0.1% solution in perclene at 30°C.)	1.28	1.82	2.7-2.8
Propylene content, wt.-%	63	70.5	40-44
Curing results <sup>b</sup>			
$M_{300}$ , psi	680	750	2400
$T_B$ , psi	680	1370	3770
$E_B$ , %	300	560	400
Permanent set, % at break	20	55	5
Yerzley resilience (25°C.), %	36.7	35.1	62.5
Shore hardness, A	61	64	65
Compression set (22 hr./70°C.)	30	33	10
Heat build-up ( $3/16$ in.)	Blew 4.5 min.	Blew 1.3 min.	Okay <sup>c</sup>
Temperature, C.	47	74	48
Change in compression	81	228	11
Final center temperature, °C.	164	158	159
Mill behavior	Good at 25°C.		Good at 25°C.

<sup>a</sup> Bromine equivalent is a measure of total unsaturation. Very poor results are obtained when double bonds are trisubstituted.

<sup>b</sup> Same recipe for all cures: polymer 100, HAF black 50, stearic acid 1, zinc oxide 5, sulfur 1, thionex 1.5, MET 0.5; temp. 150°C. for 60 min.

<sup>c</sup> 20-min. cycle.

85.67% C and 14.32% H. The benzene-insoluble fraction was worked up in a similar manner and afforded 25.0 g. of a soft, non-elastic solid.

### Evaluation of Some Terpolymers as Rubbers

In Table II are collected a few data on two of the terpolymers reported here which have been vulcanized and evaluated as rubbers. These data show that at this time optimum compositions for good rubbery properties have not been achieved.

The authors are grateful to Dr. J. L. Nyce of du Pont Elastomers Research Department for the determination of the propylene content of the terpolymers and the evaluation of two terpolymers as rubbers. Other analyses were performed by Micro-Tech Laboratories, Skokie, Illinois. We are also indebted to Dr. Carl Bordenca, Manager of Research and Development, the Glidden Company, Jacksonville, Florida, for a generous supply of 5,7-dimethyl-1,6-octadiene and the 3,7-dimethyl isomer.

### References

1. Natta, G., paper presented at International Synthetic Rubber Symposium, London, 1957.
2. Natta, G., *Rubber Plastics Age*, **38**, 495 (1957).
3. *Rubber Plastics Age*, **40**, 437 (1959).
4. E. I. du Pont de Nemours and Co., U. S. Pat. 2,933,480 (April 19, 1960).
5. Montecatini, Austral. Pat. 29,377 (July 8, 1957).

6. Gladding, E. K., B. S. Fisher, and J. W. Collette, *Ind. Eng. Chem. Product Res. Devel.*, **1**, 65 (1962).

7. *Chem. Eng. News*, **40**, No. 47, 25 (1962).

8. Harold, W., and K. L. Wolf, *Z. Physik. Chem.*, **12B**, 194 (1931).

### Résumé

La polymérisation de 5,7-diméthyl-1,6-octadiène avec un rapport molaire 2/1 de triisobutylaluminium/oxychlorure de vanadium, triisobutyl aluminium/tétrachlorure de titanium ou bien triisobutylaluminium/tétrachlorure de vanadium donne un homopolymère élastique. On a essayé en vain la polymérisation de l'isomère 3,7-diméthyl-1,6-octadiène dans les mêmes conditions. On a préparé des terpolymères élastomériques d'éthylène, propylène et 5,7-diméthyl-1,6-octadiène en présence des mêmes catalyseurs de coordination.

### Zusammenfassung

Die Polymerisation von 5,7-Dimethyl-1,6-octadien mit einem 2:1-Molverhältnis von Triisobutylaluminium/Vanadiumoxychlorid, Triisobutylaluminium/Titantetrachlorid oder Triisobutylaluminium/ Vanadiumtetrachlorid gibt ein elastisches Homopolymeres. Ein Versuch zur Polymerisation des isomeren 3,7-Dimethyl-1,6-Octadien unter denselben Bedingungen schlug fehl. Elastomere Terpolymere von Athylen, Propylen und 5,7-Dimethyl-1,6-octadien wurden mit denselben Koordinationkatalysatoren hergestellt.

Received December 26, 1963

## Epoxidation of Poly-2-methyl-6-allyl-1,4-phenylene Oxide and Copolymer of 2-Methyl-6-allyl-4-bromophenol and 2,6-Dimethyl-4-bromophenol\*

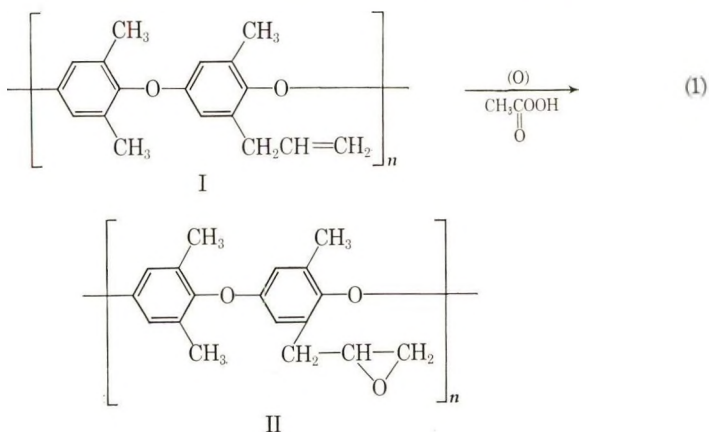
K. C. TSOU,† H. E. HOYT, and B. D. HALPERN, *Central Research Laboratory, The Borden Chemical Company, Philadelphia, Pennsylvania*

### Synopsis

Epoxidized homopolymer of 2-methyl-6-allyl-4-bromophenol and its copolymers with 2,6-dimethyl-4-bromophenol have been prepared. When more than theoretical amount of peracetic acid was used, chain degradation occurred. This chain degradation was also demonstrated by the reduction in viscosity of poly-(2,6-dimethyl-1,4-phenylene oxide when treated with peracetic acid under similar conditions.

### INTRODUCTION

In a previous report,<sup>1</sup> copolymers of 2,6-dimethyl-4-bromophenol and 2-methyl-6-allyl-4-bromophenol were prepared for thermosetting polyphenylene oxides. In order to provide sites with greater polarity so as to enhance the adhesion of the copolymer, it was considered desirable to epoxidize the allyl side chain of the copolymer to a glycidyl group as in eq. (1).



The epoxidation of the homopolymer, poly-(2-methyl-6-allyl)-1,4-phenylene oxide was likewise studied. This paper presents our experience in the

\* This work was done under Army Contract No. DA-36-034-ORD-3501-RD.

† Present address: Ravdin Institute, Hospital of the University of Pennsylvania, Philadelphia, Pennsylvania.



epoxidation of these polymers and observations on the epoxidized product.

## EXPERIMENTAL

Peracetic acid was obtained from Becco Division, FMC Corporation. Homopolymer of 2-methyl-6-allyl-4-bromophenol and copolymer of this phenol with 2,6-dimethyl-4-bromophenol were prepared by methods described in the previous paper.<sup>1</sup>

### Epoxidation of Poly-(2-Methyl-6-allyl)-1,4-phenylene Oxide

To 24 g. of poly-(2-methyl-6-allyl)-1,4-phenylene oxide ( $[\eta] = 0.34$  in benzene at 30°C.) in 120 ml. of chloroform was added 6.0 g. of a 40% peracetic acid (equivalent to 21% of the available allyl group by bromine titration). The flask was warmed and vigorously stirred for 2 hr. at 40°C. The reaction mixture was cooled, transferred to a separatory funnel, washed twice with 25 ml. water and once with 5 g. sodium bisulfite in 30 ml. water, and then twice with 25 ml. water. The washed solution was evaporated on a steam bath to a syrup which was redissolved in 250 ml. benzene. The resulting solution was then added dropwise into four volumes of methanol, kept cold by addition of dry ice. The precipitated polymer was filtered, washed with methanol, and vacuum-dried at 40°C. for 2 hr.; yield 23.5 g.; epoxy value 0.78 meq./g.; intrinsic viscosity  $[\eta] = 0.335$  at 30°C. in benzene.

### Epoxidation of Copolymer of 2,6-Dimethyl-4-bromophenol and 2-Methyl-6-allyl-4-bromophenol

The epoxidation of the copolymer was carried out under the same conditions. If more than one equivalent of peracetic acid is used per allylic double bond, degradation of the polymer occurs to some degree as shown by reduction in intrinsic viscosity. For example, when a 92% stoichiometric excess of peracetic acid over the available allyl group, as determined by bromine addition was used, the intrinsic viscosity of a 50:50 copolymer was reduced from 0.297 to 0.135.

### Reaction of Peracetic Acid with Poly-(2,6-dimethyl)-1,4-phenylene Oxide

A 6-g. sample of poly-(2,6-dimethyl)-1,4-phenylene oxide ( $[\eta] = 0.54$ , % Br, 0.90) was refluxed in a solution of 60 ml. chloroform containing 6 g. of 40% peracetic acid for 2 hr. The oxidized polymer was recovered as described above; yield 3.5 g. The intrinsic viscosity was found to be 0.11; bromine content 1.48%; infrared spectrum identical to that of the original material.

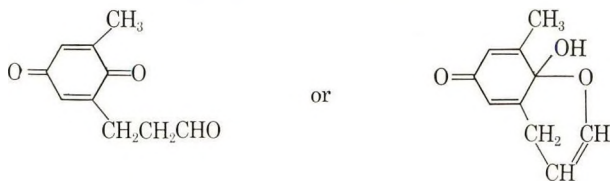
From the solution following polymer precipitation, 1.5 g. of a characteristic pungent yellow crystalline material was recovered, m.p. 62–63°C.

Sublimation of the crystals gave a sublimate melting at 69–70°C. The infrared spectrum gave characteristic quinone bands (6.05 and 6.2  $\mu$ ).

## RESULTS AND DISCUSSION

While the epoxidation of polymers containing unsaturation is well known, our initial attempts to epoxide poly-(2-methyl-6-allyl)-1,4-phenylene oxide were unsuccessful. This difficulty was soon resolved when it was obvious that in spite of the expected stability of poly(2,6-disubstituted)-1,4-phenylene oxide towards many other oxidation reactions, this type of polymer can be degraded with peracetic acid as shown in the experimental section.

In initial trials the reaction was carried out at 60°C. by refluxing a chloroform solution of the polymer with peracetic acid at about 100% excess over the calculated allyl group present. Epoxidized polymers were obtained in 75–80% yield, which showed infrared spectra almost identical to those of the original polymers, except for a reduction of the intensity of the allyl band at 11  $\mu$  and the appearance of a weak epoxide band at 9.3  $\mu$ . However, the intrinsic viscosity was substantially reduced. There was also obtained a yellow, pungent-smelling by-product which gave a positive Tollen's test, and therefore suggested its structure as



In further work it was found that by conducting the reaction at 40°C. and by using a deficiency of peracetic acid relative to the allyl group present, very little degradation in molecular weight was encountered, with almost quantitative yield of epoxidized polymer. It thus became possible to prepare polymers of predictable epoxy value without reduction in viscosity. The epoxidation conditions for a series of copolymer 50 and poly-(2-methyl-6-allyl)-1,4-phenylene oxide, and their effect on yields and on the chemical and physical properties of the products are summarized in Table I.

The precursor allyl polymers themselves crosslink on heating to give insoluble, stiff materials. One would expect the cure rate and degree of curing to be proportional to the degree of unsaturation and that this might be measurable by a test based on the stroke cure principle used for phenolic resins.<sup>4</sup> As reported elsewhere,<sup>1</sup> it was found that the relationship did indeed hold when the test was carried out at a controlled surface temperature of 500°F. As can be seen from the data in Table I, conversion of allyl to epoxy further shortened the cure time in proportion to the found epoxy value. Incorporation of compatible diamines, such as *m*-phenylenediamine, further reduced the cure times.

TABLE I  
 Epoxidation of Copolymer 50<sup>a</sup> and Poly-(2-methyl-6-allyl)-1,4-phenylene Oxide

Sample no.	Precursor		Epoxy			Epoxidation conditions			Low molecular fraction yield, % <sup>f</sup>		
	$[\eta]$ (benzene, 30°C.)	Double bonds, meq./g. <sup>b</sup>	Cure time at 500°F., sec. <sup>c</sup>	$[\eta]$ (benzene, 30°C.)	Epoxy, meq./g. <sup>d</sup>	Double bonds, meq./g. <sup>e</sup>	Cure time at 500°F., sec.	Peracetic acid, mole/double bond		Temp., °C.	Time, hr.
40	0.29	3.00	38	0.26	0.72	2.28	16	0.48	42	2	97.2
102	0.29	3.00	38	0.26	0.90	2.10	2	1.12	42	2	91.5
135	0.28	3.00	35	0.23	1.16	1.84	—	1.12	42	4	—
6	0.30	3.00	43	0.11	1.32	1.68	—	1.92	60	4	81.6
99	0.30	3.00	43	0.14	1.69	1.31	1	1.92	46	2	82.6
118	0.37	3.00	—	0.35	0	3.00	—	1.12	25	72	95.0
38 <sup>e</sup>	0.34	5.71	3	0.33	0.78	4.93	2	0.21	43	2	92.0
134 <sup>e</sup>	0.34	5.71	3	—	0	—	—	<sup>h</sup>	—	—	—

<sup>a</sup> The number refers to mole-% of 2-methyl-6-allyl-4-bromophenol used in the preparation of the copolymer.

<sup>b</sup> Determined by bromine addition on precursor polymer.<sup>3</sup>

<sup>c</sup> Time to lose Newtonian flow on hot plate by the "stroke cure" method.<sup>4</sup>

<sup>d</sup> Pyridine-HCl method.<sup>7</sup>

<sup>e</sup> Calculated value from double bond content of precursor minus epoxy content.

<sup>f</sup> Unprecipitated material recovered from methanol-benzene liquor.

<sup>g</sup> Poly-(2-methyl-6-allyl)-1,4-phenylene oxide.

<sup>h</sup> By *tert*-butyl peroxide method of Yang and Finnegan.<sup>5</sup>

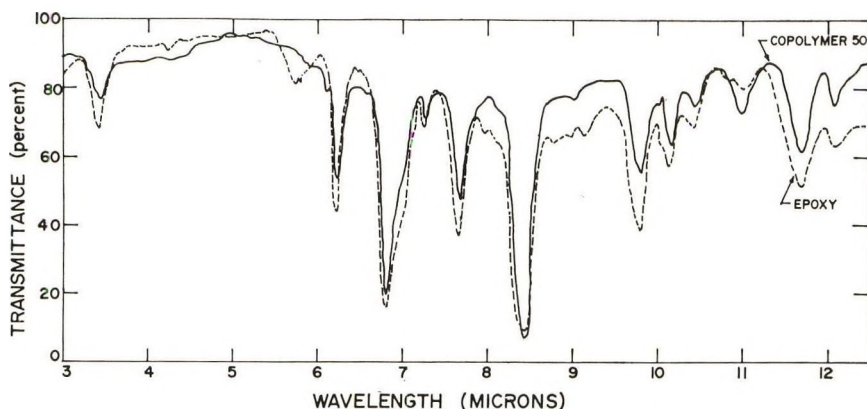


Fig. 1. Infrared spectra of copolymer 50 and epoxy derivative.

The infrared spectra before and after epoxidation (Fig. 1) show that the predominant changes were in the reduction of the allyl bands at 6.1 and 11.0  $\mu$ , appearance of a weak ether band at 9.3  $\mu$ , and increase in the bands at 5.8–6.0  $\mu$ , indicating some oxidation to carbonyl.

TABLE II  
Solubility of Poly-(2,6-disubstituted)-1,4-phenylene Oxides

Sample no.	Polymer type	$[\eta]_{\text{benzene}}^{30^\circ\text{C.}}$	Solubility	
			Acetone	Methyl ethyl ketone (10%)
56	Poly-(2,6-dimethyl)-1,4-phenylene oxide	0.54	Insol.	Insol.
96	Poly-(2,6-dimethyl)-1,4-phenylene oxide	0.32	Insol.	Insol.
62	Copolymer 10 <sup>a</sup>	—	Insol.	Sl. swollen
66	Copolymer 20 <sup>b</sup>	—	Insol.	Sl. swollen
29	Copolymer 50 <sup>c</sup>	0.29	Swell	Partly sol. <sup>d</sup>
41	Copolymer-70 <sup>c</sup>	—	Swell	Partly sol. <sup>d</sup>
31	Poly-(2-methyl-6-allyl)-1,4-phenylene oxide (PMAP)	0.35	Swell to dough	Soluble
40	Epoxidized copolymer 50	0.255	Swell	Soluble
102	Epoxidized copolymer 50	0.26	Swell	Soluble
38	Epoxidized PMAP	0.335	Swell to soft dough	Soluble

<sup>a</sup> From 10 mole-% 2-methyl-6-allyl-4-bromophenol, 90 mole-% 2,6-dimethyl-4-bromophenol.

<sup>b</sup> From 20 mole-% 2-methyl-6-allyl-4-bromophenol, 80 mole-% 2,6-dimethyl-4-bromophenol.

<sup>c</sup> From 50 mole-% 2-methyl-6-allyl-4-bromophenol, 50 mole-% 2,6-dimethyl-4-bromophenol

<sup>d</sup> From 70 mole-% 2-methyl-6-allyl-4-bromophenol, 50 mole-% 2,6-dimethyl-4-bromophenol.

<sup>e</sup> Initially formed complete solution, then polymer partly precipitated.

The effect of epoxidation was noted by an appreciable change in the solubility behavior of the polymer as shown in Table II. For example, copolymer 50 was partially soluble in methyl ether ketone, but when 20% of the allyl groups were epoxidized, the resulting polymer was found to be completely soluble in methyl ethyl ketone. The solubility of related polyphenylene oxides are also included for comparison in this table. That substitution of the allyl group for methyl in the copolymer series greatly enhances the solubility in ketonic solvent can presumably be attributed to an increase in the randomness of the polymer structure.

### Reaction of Peracetic Acid with Poly-(2,6-Dimethyl)-1,4-phenylene Oxide

The decrease in intrinsic viscosity of the copolymer suggested a chain degradation. It was therefore considered to be of importance to carry out the peracetic acid experiments on poly-(2,6-dimethyl)-1,4-phenylene oxide in order to ascertain whether this was true, since in the allyl-containing polymer the degradation of the allyl group itself might conceivably contribute to the lowering in viscosity.

When the peracetic oxidation was carried out under rigorous conditions, on a poly-(2,6-dimethyl)-1,4-phenylene oxide sample with an intrinsic viscosity  $[\eta] = 0.54$ , the viscosity of the product was reduced to 0.110. A partially reddish-yellow crystalline solid was isolated from the mother liquor after reprecipitation. The structure of the product remains to be elucidated, but the infrared spectrum bears close resemblance to that of 2,6-dimethyl-1,4-benzoquinone (6.05, 6.20  $\mu$  pair quinone band but also 2.90  $\mu$  OH). The melting point was found to be 69–70°C., whereas the literature value for 2,6-dimethyl-1,4-benzoquinone is 72–73°C. A mixed melting point from an authentic sample however produces no depression in melting point.

### Alternative Epoxidation Methods

The use of *tert*-butyl peroxide along with benzyltrimethylamine according to the method of Yang and Finnegan<sup>5</sup> was attempted in one of the preparations (No. 134) of Table I and was not successful.

Addition of hypobromous acid to the allyl group by a modified method of Controulis<sup>6</sup> was also attempted. The reaction of bromine with the polymer was evident from the decoloration of the bromine water. However, the product showed no OH in its infrared spectra, although the intensity of the allyl band at 6.1 and 11.0  $\mu$  was reduced. There was also a new band at 5.85  $\mu$ . The intrinsic viscosity was reduced from 0.30 to 0.20, and the polymer had very high bromine content (33.04%). Apparently, bromination of the double bond had occurred, and to a smaller extent there was some bromine substitution on the alkyl side chains as shown by the HBr formed during the reaction. Treatment of this product with sodium hydroxide gave a polymer which contained no glycidyl group by analysis.

### References

1. Hoyt, H. E., B. D. Halpern, K. C. Tsou, M. Bodnar, and W. Tannar, *J. Appl. Polymer Sci.*, **8**, 1631 (1964).
2. Hodgman, C. D., R. C. West, and S. M. Selby, *Tables for Identification of Organic Compounds*, Chemical Rubber Publishing Co., Cleveland, Ohio, 1960, p. 105.
3. Snell, F. D., and F. M. Bilfen, *Commercial Methods of Analysis*, McGraw-Hill, New York, 1944, p. 345.
4. D'Alelio, C. F., *Experimental Plastics*, Wiley, New York, 1946, p. 165.
5. Yang, N. C., and R. A. Finnegan, *J. Am. Chem. Soc.*, **80**, 5845 (1958).
6. Controulis, J., M. C. Rebstock, H. M. Crooks, Jr., and Q. R. Bartz, *J. Am. Chem. Soc.*, **71**, 2463 (1949).
7. Siggia, S., *Quantitative Organic Analysis*, Wiley, New York, 1959, p. 157.

### Résumé

On a préparé un homopolymère époxydé du 2-méthyl-6-allyl-4-bromophénol et ses copolymères avec le 2,6-diméthyl-4-bromophénol. Lorsqu'on utilise une quantité d'acide peracétique supérieure à la théorie, il s'en suit une dégradation de chaîne. Par la réduction de viscosité du (2,6-diméthyl)-1,4-poly-phénylène oxyde traité avec de l'acide peracétique dans les mêmes conditions, on a montré qu'une dégradation de chaîne, analogue avait lieu.

### Zusammenfassung

Das epoxidierte Homopolymere von 2-Methyl-6-allyl-4-bromphenol und seine Copolymeren mit 2,6-Dimethyl-4-bromphenol wurden dargestellt. Bei Anwendung von mehr als der theoretischen Menge von Peressigsäure trat Kettenabbau ein. Ein solcher Kettenabbau konnte auch durch die Viskositätsverminderung von Poly-(2,6-dimethyl)-1,4-phenylenoxyd bei der Behandlung mit Peressigsäure unter ähnlichen Bedingungen nachgewiesen werden.

Received August 13, 1963

Revised January 16, 1964

## Endgroup Studies in Persulfate-Initiated Vinyl Polymer by Dye Techniques. Part I. Initiation by Persulfate Alone

PREMAMOY GHOSH, SUBHASH CHANDER CHADHA, ASISH R. MUKHERJEE, and SANTI R. PALIT, *Indian Association for the Cultivation of Science, Calcutta, India*

### Synopsis

Quantitative determination of endgroups of poly(methyl methacrylate), polystyrene and poly(vinyl acetate) obtained by aqueous initiation with  $K_2S_2O_8$  under varied conditions have been made by the application of two sensitive dye techniques, called the dye partition technique and the dye interaction technique. The description of the dye techniques are given in detail. Sulfate ( $OSO_3^-$ ) and hydroxyl (OH) endgroups are generally found to be incorporated in the polymers to an average total of 1.5 to 2.5 endgroups per polymer chain. Hydroxyl endgroups are always present to a fairly large extent. The proportion of sulfate endgroups in polymers is highly dependent on the pH of the polymerizing medium; it increases with the alkalinity of the medium and sharply decreases under acid conditions.

There have been rather conflicting reports.<sup>1-4</sup> mostly based on a very limited number of experiments, regarding the nature of endgroups in vinyl and related polymers formed by initiation with persulfates. Systematic investigations have therefore been made with the help of two sensitive dye techniques, called the dye partition technique<sup>5</sup> and the dye interaction technique,<sup>6</sup> developed in this laboratory. The present paper reports the results for initiation by persulfate alone in aqueous media. The dye techniques are also described herein in detail.

### EXPERIMENTAL

#### Materials

Monomers (methyl methacrylate, styrene, and vinyl acetate) were purified by the usual procedures and stored in a refrigerator. Potassium persulfate (E. Merck, analytical grade) was used as the initiator.

#### Preparation and Purification of Polymers

Aqueous polymerization of the various monomers is carried out with persulfate initiator under nitrogen atmosphere by following a procedure described elsewhere.<sup>7</sup> The polymers obtained are then filtered, washed,

dried at 45–50°C., and finally purified by a method of repeated precipitation.<sup>6</sup>

### Dye Partition Method for Determination of Sulfate and Other Anionic Sulfoxy Endgroups

A known amount of the purified polymer dissolved in 10 ml. of chloroform in a 25 ml., well-stoppered centrifuge tube is well shaken for 1–2 hr. with an equal volume of an aqueous methylene blue dye reagent which is prepared by dissolving 20 mg. of purified methylene blue (chloride) dye in 1 liter of aqueous 0.01*M* hydrochloric acid solution. The biphasic system is then allowed to stand for about 2 hr. A distinct blue color in the chloroform layer indicates the presence of anionic sulfate endgroup in the polymer. This dye partition test is specific only for all anionic sulfoxy endgroups (strong acid endgroups), and weak acidic endgroups, such as carboxyl (COOH), fail to give any response.

The chloroform layer is then separated from the aqueous layer and then centrifuged, if necessary, to get a clear solution, and the color developed is measured in a Hilger spectrophotometer at 660  $m\mu$  with the use of 1-cm. cells. The quantity of anionic sulfoxy endgroup present in the polymer is obtained by comparing the experimental optical density values with a calibration curve of pure sodium lauryl sulfate (NaLS), obtained by following a similar procedure.<sup>8</sup>

### Distinction between Sulfate ( $\text{OSO}_3^-$ ) and Sulfonate ( $\text{SO}_3^-$ ) Endgroups

The above technique can be utilized to distinguish between sulfate and sulfonate endgroups; this depends on the fact that the former are easily hydrolyzable. The hydrolysis is carried out by refluxing with phthalic anhydride in pyridine medium (see section on determination of hydroxyl endgroup below). For polymers bearing only sulfate endgroups, the original response to methylene blue reagent becomes negative, indicating that the sulfate endgroups have been destroyed during this treatment, evidently due to hydrolysis<sup>3,9</sup> of the relatively easily hydrolyzable sulfate ( $\text{OSO}_3^-$ ) endgroups. Polymers bearing sulfonate endgroups and the like (obtained by aqueous initiation with bisulfite, sulfite, hydrosulfite, etc.), however, after similar treatment give an almost unchanged response to the dye partition test, indicating the nonhydrolyzable nature of the sulfonate and similar sulfoxy endgroups.

### Dye Interaction Method for Determination of Sulfate, Sulfonate, and Carboxyl Endgroups

The dye interaction test is carried out in a single phase, usually in benzene solution. A sensitive dye reagent<sup>9</sup> is prepared by quick extraction of an aqueous solution (pH 10) of calcozine rhodamine 6GX conc. dye with benzene. The orange yellow extract of the dye is a reagent which changes its color to pink or pink with greenish fluorescence when treated with near



micronormal to micronormal solutions of organic acids and salts soluble in benzene and with benzene solution of polymers containing anionic endgroups, such as sulfate and carboxyl. The test for acidic endgroups in polymers is carried out in the following manner. Equal volumes of a polymer solution of known concentration in benzene and the sensitive rhodamine reagent are mixed together, and a change in the color of the reagent indicates the presence of anionic endgroups in the polymer. A measure of the color change gives the amount of anionic endgroups present and is carried out in a Hilger spectrophotometer at  $515\text{ m}\mu$  with the use of 1-cm. cells. The optical density of the blank dye is maintained at  $0.40 \pm 0.005$  for convenience in comparison.

For sulfate endgroup estimation it is difficult to obtain a calibration curve with NaLS by this method because of some uncertainty regarding its solubility in benzene. A calibration curve has, however, been obtained indirectly with the help of methyl methacrylate polymers bearing sulfate endgroups, the sulfate content of which has been determined by the dye partition method. For carboxyl endgroup estimation in polymers, formic acid has been found to be a suitable basis of comparison, and the suitability of this basis has been checked by quantitative study of carboxyl groups in a large number of copolymers<sup>6</sup> in which one of the reactant monomers is a carboxylic monomer. It has generally been found that if a polymer contains only sulfate endgroups, their estimations by the dye interaction method made on the basis of NaLS and formic acid are in reasonably good agreement.

### Determination of Hydroxyl (OH) Endgroups

Hydroxyl endgroups have been usually determined after transforming them to carboxyl groups by the phthalic anhydride-pyridine technique<sup>7,10</sup> described elsewhere.<sup>11</sup> Sulfate endgroups are destroyed by hydrolysis during this process and are converted to carboxyl groups by the phthalic anhydride present.

### Determination of Intrinsic Viscosity and Molecular Weight of Polymers

The intrinsic viscosity  $[\eta]$  for each polymer was obtained by the usual method of extrapolation. Number-average molecular weights ( $\bar{M}_n$ ) for poly(methyl methacrylate), poly(vinyl acetate), and polystyrene were calculated from the respective  $[\eta]$  values by use of eqs. (1)–(3) all viscosity measurements being made at  $35 \pm 0.1^\circ\text{C}$ .

For poly(methyl methacrylate) in benzene:<sup>12</sup>

$$\bar{M}_n = 2.81 \times 10^5 [\eta]^{1.32}$$

For polystyrene in benzene:<sup>13</sup>

$$\bar{M}_n = 1.84 \times 10^5 [\eta]^{1.40}$$

TABLE I  
Endgroups in Poly(Methyl Methacrylate) Initiated by Potassium Persulfate (Monomer Concentration: 0.094 mole/l.)

K <sub>2</sub> S <sub>2</sub> O <sub>8</sub> concn., mmole/l.	Conditions of polymerization	[ $\eta$ ]	Dye test for endgroups						Average number of sulfate + hydroxyl endgroups/chain	
			Dye interaction test with rhodamine reagent		Dye partition test with methylene blue reagent		Corre- sponding normality of NaLS, $N \times 10^{-6}$	SO <sub>4</sub> <sup>-</sup>	OH	Total
			O.D. of 0.1% polymer solution at 515 m $\mu$	Corre- sponding normality of HCOOH, $N \times 10^{-6}$	O.D. of 0.1% polymer solution at 660 m $\mu$					
3.7	25°C., dark	2.45	0.45	1.0	0.11	1.3	1.2	0.7	1.9	
18.5	"	1.8	0.49 <sup>a</sup>	1.8	0.00 <sup>a</sup>	0.0	2.1	0.0	2.1	
37	"	1.2	0.598	3.8	0.30	3.5	—	—	—	
3.7	35°C., dark	2.3	0.60 <sup>a</sup>	3.8	—	—	1.57	0.5	2.07	
18.5	"	1.65	0.625	4.2	0.39	4.4	1.6	0.7	2.3	
37	"	1.4	0.69 <sup>a</sup>	5.6	—	—	1.8	0.35	2.15	
110	"	0.9	0.50	2.0	0.16	1.9	2.1	0.22	2.32	
3.7	60°C., dark	1.36	0.55 <sup>a</sup>	2.9	0.01 <sup>a</sup>	0.0	2.08	0.00	2.08	
			0.56	3.1	0.29	3.3	2.2	0.0	2.2	
			0.60 <sup>a</sup>	3.8	—	—	5.4	—	—	
			0.64	4.5	0.45	5.0	—	—	—	
			0.67 <sup>a</sup>	5.0	—	—	—	—	—	
			0.80	7.8	0.71	8.0	—	—	—	
			0.80 <sup>a</sup>	7.8	0.005 <sup>a</sup>	0.0	—	—	—	
			0.70	5.7	0.48	5.4	—	—	—	
			0.68 <sup>a</sup>	5.3	—	—	—	—	—	

<sup>a</sup> The same polymer as above after phthalic anhydride treatment.

TABLE II  
Endgroups in Poly(Methyl Methacrylate) Initiated by Potassium Persulfate (Monomer Concentration: 0.094 mole/l.)

K <sub>2</sub> S <sub>2</sub> O <sub>8</sub> concn., mmole/l.	Conditions of polymerization	[ $\eta$ ]	Dye test for endgroups						Average number of COOH groups per polymer chain (due to hydrolysis)
			Dye interaction test with rhodamine reagent		Dye partition test with methylene blue reagent		Average number of endgroups per polymer chain		
			O.D. of 0.05% polymer solution at 515 m $\mu$	Corre- sponding HCOOH normality, $N \times 10^{-6}$	O.D. of 0.1% polymer solution at 660 m $\mu$	Corre- sponding NaIS normality, $N \times 10^{-6}$			
9.25	Strong sunlight	0.8	2.5	0.40	4.6	0.9 (SO <sub>4</sub> <sup>-</sup> )	0.9 (SO <sub>4</sub> <sup>-</sup> )		
18.5	"	0.7	4.75	—	—	0.9 (OH)	0.9 (OH)		
3.7	UV light	1.5	4.0	0.62	7.0	1.2 (SO <sub>4</sub> <sup>-</sup> )	1.2 (SO <sub>4</sub> <sup>-</sup> )		
18.5	0.01M HCl, dark, 30°C.	1.75	5.75	—	—	0.6 (OH)	0.6 (OH)		
18.5	0.1M HCl, dark, 30°C.	1.35	1.25	0.16	1.9	0.93 (SO <sub>4</sub> <sup>-</sup> )	0.93 (SO <sub>4</sub> <sup>-</sup> )		
18.5	0.01M NaOH, dark, 30°C.	1.4	2.50	—	—	1.2 (OH)	1.2 (OH)		
18.5	0.01M NaOH, dark, 30°C.	1.4	0.25	0.04	0.5	0.29 (SO <sub>4</sub> <sup>-</sup> )	0.29 (SO <sub>4</sub> <sup>-</sup> )	0.0 (COOH)	
18.5	0.01M NaOH, dark, 30°C.	1.4	1.05	—	—	0.94 (OH)	0.94 (OH)		
18.5	0.01M HCl, dark, 30°C.	1.35	2.2	0.01	0.1	0.04 (SO <sub>4</sub> <sup>-</sup> )	0.04 (SO <sub>4</sub> <sup>-</sup> )	1.79 (COOH)	
18.5	0.01M NaOH, dark, 30°C.	1.4	3.25	—	—	0.88 (OH)	0.88 (OH)		
18.5	0.01M NaOH, dark, 30°C.	1.4	2.8	0.29	3.2	1.4 (SO <sub>4</sub> <sup>-</sup> )	1.4 (SO <sub>4</sub> <sup>-</sup> )	1.05 (COOH)	
18.5	0.01M NaOH, dark, 30°C.	1.4	3.5	—	—	0.61 (OH)	0.61 (OH)		

\* The same polymer as above after phthalic anhydride treatment.

TABLE III  
Endgroups in Polystyrene and Poly(Vinyl Acetate) (Obtained by Aqueous Persulfate Initiation (Monomer Concentration: 1%, v/v)

Monomer	K <sub>2</sub> S <sub>2</sub> O <sub>8</sub> concn., mmole/l.	Conditions of polymerization	[ $\eta$ ]	Dye test for endgroups			
				Dye interaction test with rhodamine reagent		Dye partition test with methylene blue reagent	
				O.D. of 0.1% polymer solution at 515 m $\mu$	Corre- sponding HCOOH normality, $N \times 10^{-6}$	O.D. of 0.1% polymer solution at 660 m $\mu$	Corre- sponding NaLS normality, $N \times 10^{-6}$
Styrene	7.4	35°C. (emulsion) <sup>a</sup>	4.3	1.0	0.05	0.6	0.85 (SO <sub>4</sub> <sup>-</sup> )
"	7.4	60°C. (emulsion) <sup>a</sup>	1.5	4.8	0.22	2.5	0.82 (SO <sub>4</sub> <sup>-</sup> )
"	3.7	Sunlight	1.3	2.0	0.22	2.6	0.7 (SO <sub>4</sub> <sup>-</sup> )
"	18.5	"	0.7	3.0	0.29	3.3	0.36 (SO <sub>4</sub> <sup>-</sup> )
"	37	"	0.5	11.0	—	—	1.15 (OH)
"	3.7	"	0.88	4.5	0.53	4.8	0.34 (SO <sub>4</sub> <sup>-</sup> )
"	3.7	"	0.88	18.0	—	—	1.26 (OH)
"	3.7	"	0.88	12.0	1.06	12.0	1.94 (SO <sub>4</sub> <sup>-</sup> )
Vinyl acetate	3.7	+0.01M NaOH Sunlight	1.1	1.0	0.18	2.1	0.81 (SO <sub>4</sub> <sup>-</sup> )
"	3.7	"	1.15	3.0	0.33	3.8	1.48 (SO <sub>4</sub> <sup>-</sup> )
"	3.7	+0.01M NaOH 60°C., dark	1.24	4.0	0.26	3.0	1.35 (SO <sub>4</sub> <sup>-</sup> )
"	3.7	"	1.25	7.3	0.35	4.0	1.80 (SO <sub>4</sub> <sup>-</sup> )
"	3.7	+0.01M NaOH 0.1M, HCl + UV	1.2	—	0.00	0.00	0.00 (SO <sub>4</sub> <sup>-</sup> )
"	3.7	0.01M, HCl + UV	1.1	—	0.02	0.25	Negligible (SO <sub>4</sub> <sup>-</sup> )

<sup>a</sup> Sodium laurate (0.5%) was used in emulsion polymerization.

<sup>b</sup> The same polymer as above after phthalic anhydride treatment.

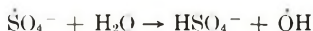
For poly(vinyl acetate) in acetone:<sup>14</sup>

$$[\eta] = 1.76 \times 10^{-4} (\bar{M}_n)^{0.68}$$

## RESULTS AND DISCUSSION

The results of endgroup analysis are presented in Tables I, II, and III. All the polymer samples exhibit a positive response, faint or intense to methylene blue reagent in the dye partition test, indicating the presence of at least some sulfate endgroups ( $\text{OSO}_3^-$ ). This is in direct contradiction to our previous results.<sup>4</sup> This error has now been traced to the inadvertent use of some drastic method of purification which hydrolyzed out the sulfate endgroups. The response to the dye interaction test is in confirmation of the dye partition test, and the quantitative results based on the two methods on the same sample are in good agreement (Table I).

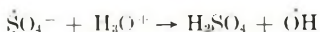
Examination of phthalated samples clearly indicates the presence of OH endgroup (transformed to  $\text{COOH}$ ). This is direct evidence of the presence in the polymerization system of hydroxyl radicals, probably generated by the reaction between sulfate ion radicals and surrounding water molecules:<sup>15</sup>



However, all the phthalated polymers show a negative response to methylene blue reagent indicating that the  $\text{SO}_3^-$  endgroups have been destroyed by hydrolysis in course of phthalation. This easy hydrolyzability of sulfate distinguishes it from sulfonate and confirms the presence of only sulfate endgroups in the present samples with complete exclusion of sulfonate endgroups.

In duplicate experiments (not shown in the Tables), it is found that the amounts of  $\text{SO}_4^-$  and OH endgroups in the polymers may vary to certain extents but their total always amounts to about 2 per polymer chain. This is ascribable to the heterogeneous nature of the polymerization process wherein it is difficult to control the local conditions.

Photo-initiation of polymerization reduces the induction period and yields polymers of lower molecular weight; however, but endgroup content remains more or less the same. Polymers obtained in alkaline media give good response for the  $\text{SO}_4^-$  endgroup, while those obtained in acid conditions give rather poor response for the same (Table II). It appears that the sulfate radicals react very fast with water under acid conditions:<sup>16</sup>



The major role is played by  $\dot{\text{O}}\text{H}$  radicals under such conditions, as is shown by some experiments with MMA under acid conditions (Table II). The total amount of endgroups (predominantly OH) under such conditions has been found to be about 1 per chain. Under alkaline conditions, however, total endgroup content remains at nearly 2 per chain. A fairly intense response to the dye interaction test given by polymers prepared in acid and

alkaline conditions is evidently due to the hydrolysis of some ester units of MMA to carboxyl.

Endgroup studies of aqueous persulfate-initiated polymers of styrene and vinyl acetate show that these polymers conform more or less to the same pattern (Table III) as the PMMA samples. Examination of OH endgroups of vinyl acetate polymers could not be done due to difficulties in purification after phthalation.

### References

1. Mochel, W. E., and J. H. Peterson, *J. Am. Chem. Soc.*, **71**, 1426 (1949).
2. Smith, W. V., *J. Am. Chem. Soc.*, **71**, 4077 (1949).
3. Bartlett, P. D., and K. Nozaki, *J. Polymer Sci.*, **3**, 216 (1948).
4. Palit, S. R., *Makromol. Chem.*, **36**, 89 (1959); *ibid.*, **38**, 96 (1960).
5. Palit, S. R., and P. Ghosh, *Microchem. J. Symp. Ser.*, **2**, 663 (1961).
6. Palit, S. R., and P. Ghosh, *J. Polymer Sci.*, **58**, 1225 (1962).
7. Palit, S. R., and A. R. Mukherjee, *J. Polymer Sci.*, **58**, 1243 (1962).
8. Mukerjee, P., *Anal. Chem.*, **28**, 870 (1956).
9. Berry, K. L., and J. H. Peterson, *J. Am. Chem. Soc.*, **73**, 5195 (1951).
10. St.-Pierre, L. E., and C. C. Price, *J. Am. Chem. Soc.*, **78**, 3432 (1956).
11. Ghosh, P., A. R. Mukherjee, and S. R. Palit, *J. Polymer Sci.*, **A2**, 2807 (1964).
12. Baxendale, J. H., S. Bywater, and M. G. Evans, *J. Polymer Sci.*, **1**, 237 (1946).
13. Johnson, D. H., and A. V. Tobolsky, *J. Am. Chem. Soc.*, **74**, 938 (1952).
14. Wagner, R. H., *J. Polymer Sci.*, **2**, 21 (1947).
15. Bartlett, P. D., and J. D. Cotman, *J. Am. Chem. Soc.*, **71**, 1419 (1949).
16. Dainton, F. S., private communication (1962).

### Résumé

On a fait la détermination quantitative des groupes terminaux de poly(méthacrylate de méthyle, styrène et acétate de vinyle) obtenus par initiation en milieu aqueux par le  $K_2S_2O_8$  dans des conditions variables. La détermination se fait par application de deux techniques à colorant sensible: la technique de partition du colorant et la technique d'interaction du colorant. La description des techniques au colorant est donnée en détails. Finalement on a trouvé les groupes terminaux de sulfate ( $OSO_3^-$ ) et hydroxyle (OH) incorporés dans la chaîne polymérique jusqu'à un total moyen de 1.5 à 2.5 de groupes terminaux par chaîne. On trouve toujours des groupes hydroxyliques présents à un taux assez élevé. La proportion de groupes sulfates dans les polymères dépendent fortement du pH du milieu de polymérisation. Cette proportion augmente avec l'alcalinité du milieu et diminue fort dans des conditions acide.

### Zusammenfassung

Eine quantitative Bestimmung der Endgruppen von Polymethylmethacrylat, Polystyrol und Polyvinylacetat, das durch Start mit wässrigem  $K_2S_2O_8$  unter verschiedenen Bedingungen erhalten worden war, wurde mit zwei empfindlichen Anfärbemethoden, dem sogenannten Farbstoffverteilungsverfahren und dem Farbstoffwechselwirkungsverfahren durchgeführt. Die Anfärbemethoden werden genau beschrieben. Sulfat- ( $OSO_3^-$ )- und Hydroxyl-(OH)-Endgruppen sind im allgemeinen zu einem Gesamtmittelwert von 1,5 bis 2,5 Endgruppen pro Polymerkette eingebaut. Hydroxylendgruppen sind immer in ziemlich grossem Ausmass vorhanden. Der Anteil an Sulfatendgruppen im Polymeren ist in hohem Ausmass vom pH des Polymerisationsmediums abhängig: er nimmt mit der Alkalinität des Mediums zu und fällt unter sauren Bedingungen scharf ab.

Received September 5, 1963

Revised January 2, 1964

## Endgroup Studies in Persulfate-Initiated Vinyl Polymer by Dye Techniques. Part II. Initiation by Redox Persulfate Systems

PREMAMOY GHOSH, SUBHASH CHANDER CHADHA, and SANTI R. PALIT, *Indian Association for the Cultivation of Science, Calcutta, India*

### Synopsis

Poly(methyl methacrylate) samples obtained by aqueous redox initiation with persulfate in conjunction with reducing sulfoxy compounds such as  $\text{HSO}_3^-$ ,  $\text{SO}_3^-$ ,  $\text{S}_2\text{O}_3^{2-}$ ,  $\text{S}_2\text{O}_4^{2-}$ , and  $\text{S}_2\text{O}_5^{2-}$  are found by dye techniques to contain both hydrolyzable sulfate endgroups (derived from persulfate) and nonhydrolyzable sulfonate endgroups or the like (derived from the activator) to an average total of about 2 endgroups per polymer molecule. Sulfide ( $\text{S}^{2-}$ ) is unique as an activator, as only sulfate endgroups (no sulfonate or hydroxyl) have been found in the polymers. Persulfate used in conjunction with other activators (such as  $\text{Ag}^+$ ,  $\text{Fe}^{++}$  hydrazine and hydroxylamine, aliphatic amines, alcohols, reducing acids and their salts, etc.) produce polymers with both sulfate and hydroxyl endgroups. Incorporation of sulfate endgroups is favored under basic conditions and tends to be suppressed under acid conditions.

The results of our investigations on endgroups in vinyl polymers initiated in aqueous media by thermal and photochemical decomposition of potassium persulfate have been reported in Part I of this series.<sup>1</sup> The present paper reports the results of investigations on endgroups in methyl methacrylate polymers obtained by aqueous redox initiation with persulfate ( $\text{K}_2\text{S}_2\text{O}_8$ ) using a large variety of activators such as, reducing sulfoxy compounds ( $\text{NaHSO}_3$ ,  $\text{Na}_2\text{SO}_3$ ,  $\text{Na}_2\text{S}_2\text{O}_3$ ,  $\text{Na}_2\text{S}_2\text{O}_4$ ,  $\text{Na}_2\text{S}_2\text{O}_5$ ), sodium sulfide, silver nitrate, ferrous sulfate, formic acid, sodium formate, oxalic acid, aliphatic amines, hydrazine, hydroxylamine, and alcohols.

### EXPERIMENTAL

#### Materials

Methyl methacrylate (MMA) monomer was purified by the usual procedure<sup>1</sup> and was stored in a refrigerator. Reagent grade Merck or equivalent (B.D.H.) products were used as far as possible.

#### Preparation and Purification of Polymers

Aqueous redox polymerization of methyl methacrylate (with the use of persulfate initiator and an activator) and subsequent isolation and purification of the polymers were carried out by the usual procedures.

TABLE I  
Endgroups in Poly(methyl Methacrylate) Obtained by Redox Persulfate Initiation in Aqueous Media  
(Methyl methacrylate = 0.094 mole/l.; Temperature 30°C.)

Activator	Activator concn. $\times 10^2$ , mole/l.	$K_2S_2O_8$ concn. $\times 10^2$ , mole/l.	$[\eta]$	Dye interaction test with rhodamine reagent		Dye partition test with methylene blue reagent		Average number of endgroups per polymer chain					
				Polymer solution concn., %	O.D. at 515 $m\mu^a$	Sulfoxy or COOH end-content, $N \times 10^{-6}$	Polymer solution concn., %	O.D. at 660 $m\mu$	Sulfoxy end-group content, $N \times 10^{-6}$	Sulfoxy, hydrolyzable	Sulfoxy, nonhydrolyzable	OH	Total
NaHSO <sub>4</sub>	0.2	0.37	0.65	0.05	0.75	6.5	0.05	0.54	6.2	1.05	0.92	0.0	1.97
				0.05 <sup>b</sup>	0.73	6.2	0.05 <sup>b</sup>	0.25	2.9				
	1.0	0.37	0.40	0.05	1.01	11.3	0.05	0.95	10.7	0.57	1.24	0.0	1.81
				0.05 <sup>b</sup>	0.96	10.6	0.05 <sup>b</sup>	0.66	7.4				
	5.0	0.37	0.15	0.01	0.97	10.8	0.01	0.75	8.5	0.65	1.32	0.0	1.97
				0.01 <sup>b</sup>	0.82	8.0	0.01 <sup>b</sup>	0.53	6.0				
Na <sub>2</sub> SO <sub>4</sub>	0.2	1.85	0.58	0.05	0.75	6.5	0.05	0.59	6.8	0.83	1.01	0.0	1.84
				0.05 <sup>b</sup>	0.70	5.8	0.05 <sup>b</sup>	0.33	3.7				
	0.16	0.37	2.2	0.1	0.82	8.0	0.2	0.38	4.3	0.92	0.80	0.0	1.72
				0.1 <sup>b</sup>	0.79	7.2	0.2 <sup>b</sup>	0.18	2.0				
	0.8	0.37	2.0	0.1	0.88	9.0	0.2	0.46	5.2	1.01	0.81	0.0	1.82
				0.1 <sup>b</sup>	0.84	8.2	0.2 <sup>b</sup>	0.20	2.3				
Na <sub>2</sub> SO <sub>4</sub>	4.0	0.37	1.50	0.025	1.04	12.1	0.1	0.31	3.6	0.96	0.77	0.0	1.73
				0.025 <sup>b</sup>	1.00	11.3	0.1 <sup>b</sup>	0.15	1.7				
	0.16	1.85	0.90	0.1	0.84	8.2	0.1	0.70	8.0	1.09	0.99	0.0	2.08
				0.1 <sup>b</sup>	0.76	6.8	0.1 <sup>b</sup>	0.33	3.8				



$\text{Na}_2\text{S}_2\text{O}_3$	0.13	0.37	0.80	0.1	0.79	7.2	0.1	0.58	6.6	0.90	0.48	0.30	1.68
	0.65	0.37	0.70	0.1 <sup>b</sup>	0.86	8.6	0.1 <sup>b</sup>	0.20	2.3	1.38	0.80	0.0	2.18
	3.25	0.37	0.40	0.1 <sup>b</sup>	0.96	10.6	0.1	1.10	12.4	1.34	0.67	0.0	2.01
	0.13	1.85	0.54	0.05 <sup>b</sup>	0.92	9.9	0.1 <sup>b</sup>	0.41	4.7	0.55	0.45	0.64	1.64
	0.12	0.37	0.59	0.1	0.95	11.1	0.05 <sup>b</sup>	0.36	4.0	0.86	0.88	0.0	1.74
$\text{Na}_2\text{S}_2\text{O}_4$	0.60	0.37	0.50	0.1 <sup>b</sup>	0.77	7.0	0.1	0.70	8.0	0.60	1.23	0.0	1.83
	3.0	0.37	0.40	0.05 <sup>b</sup>	1.04	12.1	0.1 <sup>b</sup>	0.32	3.6	0.51	1.5	0.0	2.01
	0.12	1.85	0.36	0.05 <sup>b</sup>	0.75	6.5	0.05	0.53	6.0	0.67	1.18	0.0	1.85
	0.1	0.37	0.79	0.05 <sup>b</sup>	0.70	5.8	0.05 <sup>b</sup>	0.27	3.1	1.42	0.88	0.0	2.3
	0.5	0.37	0.50	0.05 <sup>b</sup>	0.82	8.0	0.05 <sup>b</sup>	0.73	8.3	0.9	1.34	0.0	2.24
$\text{Na}_2\text{S}_2\text{O}_6$	2.5	0.37	0.25	0.05 <sup>b</sup>	0.76	6.8	0.05 <sup>b</sup>	0.50	5.6	0.75	1.45	0.0	2.2
	0.1	0.37	0.51	0.05 <sup>b</sup>	1.05	12.6	0.05	1.06	12.1	0.70	1.30	0.0	2.0
	0.2	0.37	0.50	0.05 <sup>b</sup>	1.01	11.5	0.05 <sup>b</sup>	0.79	8.9	1.86	0.0	0.0	1.86
	0.1	1.85	0.51	0.025 <sup>b</sup>	1.06	12.5	0.05	1.12	12.7	1.68	0.0	0.0	1.68
	0.2	0.74	0.40	0.05 <sup>b</sup>	0.95	10.4	0.05 <sup>b</sup>	0.71	8.1	1.68	0.0	0.0	1.68
$\text{Na}_2\text{S}$	0.2	0.37	0.50	0.05 <sup>b</sup>	0.72	6.0	0.05 <sup>b</sup>	0.19	2.2	1.68	0.0	0.0	1.68
	0.2	0.37	0.50	0.05 <sup>b</sup>	1.00	11.2	0.05	0.95	10.7	1.68	0.0	0.0	1.68
	0.2	0.74	0.40	0.05 <sup>b</sup>	0.99	11.0	0.05 <sup>b</sup>	0.53	6.0	1.68	0.0	0.0	1.68
	0.2	1.85	0.35	0.025 <sup>b</sup>	1.06	12.5	0.02	0.89	10.0	1.68	0.0	0.0	1.68
	0.2	1.85	0.35	0.05 <sup>b</sup>	0.95	10.4	0.02 <sup>b</sup>	0.58	6.6	1.68	0.0	0.0	1.68

<sup>a</sup> The optical density of blank rhodamine reagent is  $0.40 \pm 0.005$ .

<sup>b</sup> The respective polymers after phthalation.

### Detection and Estimation of Endgroups

The purified polymers were then tested for endgroups present by the application of the dye partition technique<sup>2</sup> and the dye interaction technique<sup>3,4</sup> as described in Part I. Detection and estimation of anionic sulfoxy endgroups, such as sulfate ( $\text{OSO}_3^-$ ) and sulfonate ( $\text{SO}_3^-$ ), were better carried out by the dye partition method, which is specific only for this type of endgroup.<sup>1</sup>

Hydroxyl endgroups in polymers were usually converted to carboxyl endgroups by refluxing pyridine solution of the polymers with phthalic anhydride on a water bath for a period of 6 hr.<sup>1</sup> Sulfate endgroups, being hydrolyzable in nature, are also transformed to carboxyl endgroups during this treatment. The polymers thus treated were then properly purified and tested for endgroups by the above two dye techniques. The quantity of various endgroups, such as sulfate, sulfonate, and the like, hydroxyl, and carboxyl, in the polymers was obtained by the methods described in Part I.<sup>1</sup>

### Determination of Molecular Weight

Number-average molecular weights ( $\bar{M}_n$ ) of poly(methyl methacrylate) samples were obtained viscometrically in benzene solution at  $35 \pm 0.1^\circ\text{C}$ ., as described in Part I, with the help of the following equation,<sup>5</sup>

$$\bar{M}_n = 2.81 \times 10^5 [\eta]^{1.32}$$

## RESULTS AND DISCUSSION

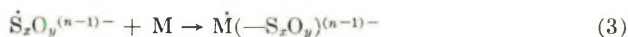
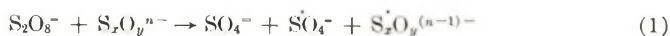
The results of endgroup analysis in poly(methyl methacrylate) obtained by aqueous redox initiation with persulfate with the use of reducing sulfoxy compounds and sodium sulfide as activators are presented in Table I. Representative data obtained by using other activators are shown in Table II.

### Reducing Sulfoxy Compounds as Activators

The reducing sulfoxy compounds used as activators were sodium bisulfite ( $\text{HSO}_3^-$ ), sodium sulfite ( $\text{SO}_3^{=}$ ), sodium thiosulfate ( $\text{S}_2\text{O}_3^{=}$ ), sodium hydrosulfite ( $\text{S}_2\text{O}_4^{=}$ ), and sodium metabisulfite ( $\text{S}_2\text{O}_5^{=}$ ). Both the persulfate and the activator concentrations were varied over a fairly wide range.

All the polymer samples were found to contain anionic strong acid endgroups, both hydrolyzable and nonhydrolyzable. The hydrolyzable part is presumably sulfate ( $\text{OSO}_3^-$ ) endgroups and the nonhydrolyzable part is presumably sulfonate ( $\text{SO}_3^-$ ) or similar endgroups. An approximate average total of 1.7–2.0 endgroups per polymer chain has been obtained for the  $\text{S}_2\text{O}_8^{=}$ – $\text{HSO}_3^-$  initiator system, 1.6–2.1 for the  $\text{S}_2\text{O}_8^{=}$ – $\text{SO}_3^{=}$  system, 1.5–2.2 for the  $\text{S}_2\text{O}_8^{=}$ – $\text{S}_2\text{O}_3^{=}$  system, 1.6–2.2 for the  $\text{S}_2\text{O}_8^{=}$ – $\text{S}_2\text{O}_4^{=}$  system, and 2.0–2.3 for the  $\text{S}_2\text{O}_8^{=}$ – $\text{S}_2\text{O}_5^{=}$  system (Table I). This picture envisages the

termination process to be mainly due to primary radicals or mutual combination of the growing radicals. The general initiation reaction in these systems may be schematically represented as shown in eqs. (1)–(4).



This shows that the electron exchange reaction between persulfate and a reducing sulfoxy compound generates sulfate ion radicals ( $\dot{S}O_4^-$ ) and sulfoxy ion radicals of the type  $(\dot{S}_xO_y)^{(n-1)-}$  in solution,<sup>6</sup> and these ion radicals give rise to initiation of polymerization. It is relevant to point out that all reducing sulfoxy compounds with the exception of thiosulfate used herein have also been found to be capable of initiating aqueous polymerization of methyl methacrylate by themselves, and the sulfoxy endgroups incorporated in the polymers have been found to be nonhydrolyzable in all cases.<sup>7</sup> It may, therefore, be concluded that in the redox initiation with persulfate and reducing sulfoxy compounds, the hydrolyzable sulfoxy endgroups are sulfate endgroups derived from persulfate molecules and the nonhydrolyzable sulfoxy endgroups are sulfonate endgroups or the like, evidently derived from the activator molecules. Reports in the literature<sup>8–11</sup> suggest that in redox initiation involving persulfate and a reducing sulfoxy compound, incorporation of sulfoxy endgroups in the polymer from both the redox components is possible, and this has been further confirmed and quantitatively examined herein.

### Hydroxyl Endgroups

In sharp contrast with initiation by persulfate alone,<sup>1</sup> hydroxyl endgroups are practically nonexistent in polymers obtained by using these redox initiator systems, persulfate–thiosulfate system being the only exception. In the latter case, OH appears only when the  $S_2O_8^{2-}/S_2O_3^{2-}$  mole ratio is higher than 1. In all the other redox systems, however, if the concentration of the reducing sulfoxy compounds is lowered to about  $0.5 \times 10^{-3}M$  or even less, some hydroxyl endgroups are found to appear in the polymers (not shown in the table). The incorporation of hydroxyl endgroup is probably due to the generation of hydroxyl radicals in solution by reaction of sulfate ion radicals with water molecules<sup>1,12</sup> according to eq. (4), which is helped by the high active mass of water and a long life of OH radicals in water due to regenerative transfer reaction. The general absence of OH endgroups in these polymers, except when the activator ( $HSO_3^-$ ,  $S_2O_4^{2-}$ ,  $SO_3^{2-}$ , etc.) concentration is very low, is probably due to the fact that the reducing sulfoxy compounds or radicals derived from them are very good scavengers of  $\dot{O}H$  radicals. Taking for example, the persulfate–bisulfite ( $S_2O_8^{2-}$ – $HSO_3^-$ ) redox system, the ready consumption of  $\dot{O}H$  radicals by bisulfite ions

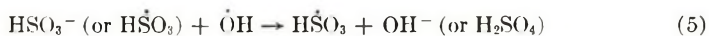


N <sub>2</sub> H <sub>4</sub> ·H <sub>2</sub> SO <sub>4</sub>	0.04	1.8	0.1	0.61	4.0	0.2	0.20	2.3	0.71	0.60	1.6
			0.1 <sup>b</sup>	0.66	5.0	—	—	—	—	—	—
NH <sub>2</sub> OH·H <sub>2</sub> SO <sub>4</sub>	0.8	1.6	0.1	0.65	4.8	0.2	0.18	2.0	0.52	0.42	1.04
			0.1 <sup>b</sup>	0.69	5.6	—	—	—	—	—	—
HCHO	1.0	2.4	0.1	0.43	0.8	0.2	0.18	2.0	0.89	1.06	—
			0.1 <sup>b</sup>	0.50	2.0	—	—	—	—	—	—
CH <sub>3</sub> OH	2.0	2.8	0.1	0.48	1.5	0.2	0.18	2.0	1.1	0.97	—
			0.1 <sup>b</sup>	0.52	2.3	—	—	—	—	—	—
C <sub>2</sub> H <sub>5</sub> OH	2.0	2.7	0.1	0.48	1.5	0.2	0.20	2.3	1.14	0.81	—
			0.1 <sup>b</sup>	0.52	2.3	—	—	—	—	—	—
HCOONa	2.0	2.0	0.1	0.49	1.7	0.2	0.29	3.3	1.15	0.70	—
			0.1 <sup>b</sup>	0.54	2.7	—	—	—	—	—	—
HCOOH	2.0	1.8	0.1	0.44	1.0	0.2	0.12	1.4	0.43	0.61	—
			0.1 <sup>b</sup>	0.50	2.0	—	—	—	—	—	—
H <sub>2</sub> C <sub>2</sub> O <sub>4</sub>	1.0	2.5	0.1	0.47	1.4	0.2	0.12	1.4	0.60	0.50	0.6
			0.1 <sup>b</sup>	0.50	2.0	—	—	—	—	—	—
(C <sub>2</sub> H <sub>5</sub> ) <sub>2</sub> NH	0.9	1.4	0.05	0.60	3.8	0.2	0.80	9.0	1.98	0.0	2.7
			0.05 <sup>b</sup>	0.54	2.8	—	—	—	—	—	—
(C <sub>2</sub> H <sub>5</sub> ) <sub>3</sub> N	0.4	2.4	0.1	0.70	5.8	0.2	0.26	3.0	1.4	0.58	3.8
			0.1 <sup>b</sup>	0.74	6.5	—	—	—	—	—	—
	1.0	1.6	0.05	0.65	4.8	0.2	0.62	7.0	1.82	0.0	3.2

<sup>a</sup> The optical density of blank rhodamine reagent is  $0.40 \pm 0.005$ .

<sup>b</sup> The respective polymers after phthalation.

(HSO<sub>3</sub><sup>-</sup>) or by sulfonic acid radicals (H<sup>•</sup>SO<sub>3</sub>) already present in the medium may be represented as shown in eq. (5)



leading to oxidation of the activator or the radical derived from it.

A much stronger response to the dye interaction test as compared with that given by the dye partition test, was obtained for some polymers prepared with redox initiation involving Na<sub>2</sub>SO<sub>3</sub>. A similar observation was also made for MMA polymers obtained by aqueous initiation with Na<sub>2</sub>SO<sub>3</sub> alone. This is evidently due to the fairly alkaline nature of the medium, whereby some of the ester units of methyl methacrylate are hydrolyzed to carboxyl units; this effect has been found to be more pronounced with the use of a higher concentration of Na<sub>2</sub>SO<sub>3</sub> and longer duration of contact of the polymer in the alkaline medium. Since the results of the dye partition test are unaffected by carboxyl groups in polymers, endgroup results obtained on this basis are, therefore, more consistent and dependable.

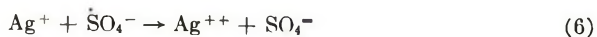
### Sodium Sulfide as Activator

Use of Na<sub>2</sub>S as activator in redox persulfate initiation of MMA polymerization leads to incorporation of only hydrolyzable sulfoxy endgroups in the polymers. Sulfoxy endgroups incorporated are, therefore, all sulfate and no sulfonate. Hydroxyl endgroups are not found in the polymers. It is not possible on the basis of dye tests to say anything about the incorporation of sulfide endgroups in the polymers, since organic sulfides are not generally sensitive to the dye tests. Sulfate endgroups are incorporated in the polymers to an average of 1.7–1.9 per polymer chain (Table I) and, therefore, it may be said that to a fair approximation sulfide endgroups are either non-existent in these polymers or they are present in rather small amounts.

### Ag<sup>+</sup> and Fe<sup>++</sup> Ions as Activators

Polymerization is catalyzed markedly when Ag<sup>+</sup> and Fe<sup>2+</sup> ions are used to activate persulfate decomposition, and polymers obtained give responses for both sulfate and hydroxyl endgroups. The Ag<sup>+</sup>-S<sub>2</sub>O<sub>8</sub><sup>=</sup> system has been found to lead to incorporation of an average total of 0.5–0.6 endgroups per polymer molecule; and the polymers obtained are of fairly low molecular weights. With FeSO<sub>4</sub> as activator, an average total of about 1 endgroup per polymer chain has been obtained.

The comparatively low sulfate endgroup content in polymers initiated by the Ag<sup>+</sup>-S<sub>2</sub>O<sub>8</sub><sup>=</sup> system is probably due to the fact that Ag<sup>+</sup> ion is a good scavenger of sulfate ion radicals,<sup>13</sup> e.g.,

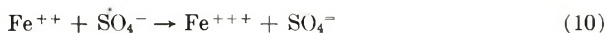


Incorporation of hydroxyl endgroups may be explained, at least in part, by the generation of hydroxyl radicals due to reactions between higher valent silver ions and water molecules,<sup>13</sup> e.g.,

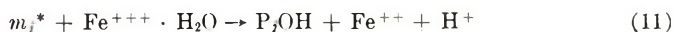


With a trivalent silver complex as initiator of polymerization in an aqueous medium, incorporation of OH endgroups in the resulting polymer has recently been confirmed in this laboratory.<sup>14</sup> The silver ions in the various oxidation states probably play important roles in the polymerization process resulting in an overall decrease in the average endgroup content of the polymers. In any case, it is very difficult to explain the very small endgroup content (0.5–0.6) of these polymers, and the whole thing requires closer observation.

Similarly, in the  $\text{Fe}^{++}\text{-S}_2\text{O}_8^{=}$  redox system, scavenging of  $\dot{\text{S}}\text{O}_4^-$  radicals by  $\text{Fe}^{++}$  ion is also probable:<sup>15</sup>



Hydroxyl endgroups incorporated in the polymer may possibly be due to the generation of  $\dot{\text{O}}\text{H}$  radicals by reaction (4), or by a mechanism involving ferric ions in solution, as shown in eq. (11):



Dainton et al.,<sup>16,17</sup> however, remarked that for poly(methyl methacrylate), termination of the latter type by  $\text{Fe}^{+++}$  ion is very slow and insignificant. An average total of one endgroup per polymer chain in this system indicates that the termination probably takes place predominantly by disproportionation.

### Hydrazine and Hydroxylamine as Activators

The prominent effect of acidic conditions on the nature and extent of endgroups incorporated in persulfate initiated polymers is demonstrated by the use of hydrazine hydrate ( $\text{N}_2\text{H}_4 \cdot \text{H}_2\text{O}$ ) and hydrazine sulfate ( $\text{N}_2\text{H}_4 \cdot \text{H}_2\text{SO}_4$ ) as activators (Table II). In the former case endgroups incorporated are mainly sulfate to the extent of about 1.7–1.8 per chain, response to OH endgroups being either negative or very faint; but in the latter case (under acidic conditions), incorporation of sulfate endgroups is suppressed markedly (to about 0.5–0.7 per chain). Polymerization with hydroxylamine sulfate ( $\text{NH}_2\text{OH} \cdot \text{H}_2\text{SO}_4$ ) as activator also conforms to the same pattern as with ( $\text{N}_2\text{H}_4 \cdot \text{H}_2\text{SO}_4$ ). Some hydroxyl endgroups (0.4–0.6 per chain) are also found in these polymers prepared with acidic activators. Average total endgroup content in the range of 1–1.3 per chain suggests the termination mechanism to be primarily due to disproportionation under acidic conditions.<sup>1</sup>

### Other Activators

As expected for acidic conditions, use of formic acid and oxalic acid as activators produces polymers bearing an average total of about one endgroup per chain ( $\text{SO}_4^-$  and OH combined), sulfate content being in the range of 0.4–0.6 per chain. With the use of some nonacidic activators, viz., sodium formate, formaldehyde, and methyl and ethyl alcohol, an average total of about 1.6–2.1 endgroup ( $\text{SO}_4^-$  and OH) per chain is obtained, of which sulfate endgroups are present to the extent of nearly 1 per chain. From endgroup analysis it, therefore, appears almost certain that termination in persulfate-initiated aqueous polymerization of MMA is mainly due to primary radicals or mutual combination in neutral or basic conditions (about 2 endgroups/chain), and to disproportionation in acidic conditions (nearly 1 endgroup/chain).

### Amines as Activators

Use of diethylamine and triethylamine as activators has yielded polymers giving good response for sulfate endgroups, these endgroups being present to the extent of 1.5–2 per polymer chain. Hydroxyl endgroups are found to occur at a relatively low concentration of the amines to an extent of about 0.2–0.4 per chain. No basic amino endgroup has, however, been found in these polymers, the test being carried out by a highly base sensitive eosin dye reagent in benzene.<sup>4</sup> Amines, being basic in nature, generate some carboxyl groups in the polymers due to hydrolysis of ester units of MMA and this is evidenced by the results of dye interaction test (Table II).

### References

1. Ghosh, P., S. C. Chadha, A. R. Mukherjee, and S. R. Palit, *J. Polymer Sci.*, **A2**, 4435 (1964).
2. Palit, S. R., *Makromol. Chem.*, **36**, 89 (1959); *ibid.*, **38**, 96 (1960).
3. Palit, S. R., *Chem. Ind. (London)*, **1960**, 1531.
4. Palit, S. R., and P. Ghosh, *Microchem. Tech. Symp. Ser.*, **2**, 663 (1961).
5. Baxendale, J. H., S. Bywater, and M. G. Evans, *J. Polymer Sci.*, **1**, 237 (1946).
6. Bunn, D., *Trans. Faraday Soc.*, **42**, 190 (1946).
7. Mukherjee, A. R., P. Ghosh, S. C., Chadha, and S. R. Palit, to be published.
8. Sully, B. D., *J. Chem. Soc.*, **1950**, 1498.
9. Firsching, F. H., and I. Rosen, *J. Polymer Sci.*, **36**, 305 (1959).
10. Tsuda, Y., *J. Appl. Polymer Sci.*, **5**, 104 (1961).
11. Berry, K. L., and J. H. Peterson; *J. Am. Chem. Soc.*, **73**, 5195 (1951).
12. Bartlett, P. D., and J. D. Cotman, *J. Am. Chem. Soc.*, **71**, 1419 (1949).
13. Morgan, L. B., *Trans. Faraday Soc.*, **42**, 140 (1946).
14. Ghosh, P., A. R. Mukherjee, and S. R. Palit, *J. Polymer Sci.*, **A2**, 2817 (1964).
15. Kolthoff, I. M., A. I. Medalia, and H. P. Raaen, *J. Am. Chem. Soc.*, **73**, 1733 (1951).
16. Dainton, F. S., and D. G. L. James, *Trans. Faraday Soc.*, **54**, 649 (1958).
17. Collinson, E., and F. S. Dainton, *Nature*, **177**, 1224 (1956).



### Résumé

On a trouvé au moyen de techniques de coloration, que des échantillons de polyméthacrylate de méthyle, obtenus par initiation réductrice avec le persulfate en milieu aqueux, en conjonction avec des composés sulfoxy réducteurs tels que  $\text{SO}_3^-$ ,  $\text{SO}_3^{2-}$ ,  $\text{S}_2\text{O}_3^{2-}$  et  $\text{S}_2\text{O}_5^{2-}$ , contiennent des groupements terminaux sulfate, hydrolysables (provenant du persulfate) et des groupements terminaux sulfonates, non hydrolysables, ou semblables (provenant de l'activant), en une moyenne totale d'environ deux groupements terminaux par molécule. L'ion sulfure ( $\text{S}^{2-}$ ) est le seul activant puisqu'on ne trouve dans les polymères que des groupements terminaux sulfate (pas de sulfonate ou d'hydroxyle). Le persulfate, employé simultanément avec d'autres activateurs (comme les ions  $\text{Ag}^+$ ,  $\text{Fe}^{2+}$ , l'hydrazine et l'hydroxylamine. Des amines aliphatiques, les alcools, les acides réducteurs, et leurs sels etc.) forment des polymères contenant des groupements terminaux sulfates et hydroxyles. L'incorporation de groupements terminaux sulfate est favorisée en milieu basique et tend à être supprimée en milieu acide.

### Zusammenfassung

In Polymethylmethacrylatproben, die durch Redoxstart in wässrigem Persulfat mit reduzierenden Sulfoxyverbindungen wie  $\text{HSO}_3^-$ ,  $\text{SO}_3^{2-}$ ,  $\text{S}_2\text{O}_3^{2-}$ ,  $\text{S}_2\text{O}_4^{2-}$  und  $\text{S}_2\text{O}_5^{2-}$  erhalten worden waren, konnten mit dem Anfärbeverfahren sowohl hydrolysierbare Sulfatendgruppen (vom Persulfat stammend) als auch nicht hydrolysierbare Sulfonatendgruppen oder ähnliche (vom Aktivator stammend) in einem Gesamtmittelwert von etwa 2 Endgruppen pro Polymermolekül nachgewiesen werden. Sulfid ( $\text{S}^{2-}$ ) verhält sich als Aktivator insofern eigenartig als nur Sulfatendgruppen (kein Sulfonat oder Hydroxyl) im Polymeren gefunden wurden. Mit anderen Aktivatoren (wie  $\text{Ag}^+$ ,  $\text{Fe}^{2+}$ , Hydrazin und Hydroxylamin, aliphatische Amine, Alkohole, reduzierende Säuren und ihre Salze etc.) bildet Persulfat Polymere mit Sulfat- und Hydroxylendgruppen. Im basischen Milieu ist der Einbau von Sulfatendgruppen begünstigt, im sauren wird er unterdrückt.

Received September 5, 1963

Revised January 2, 1964

## Some Calculations of Intrinsic Viscosity and Molecular Weight Distribution for Trifunctional, Randomly Branched Polymers

G. E. MYERS\* and J. R. DAGON, *Union Carbide Corporation, Plastics  
Division, Bound Brook, New Jersey*

### Synopsis

Computations have been performed of the intrinsic viscosity of trifunctional, randomly branched whole polymers. Both the Thurmond-Zimm and the Zimm-Kilb treatments of the viscosity of branched polymers have been combined with the Beasley molecular weight distribution function. The Beasley distribution function has also been compared with a function derived by Flory for trifunctionally branched condensation polymers. The two functions are in good agreement at low extents of branching, but at higher branch contents the former function extends to significantly higher molecular weights.

### INTRODUCTION

In connection with studies of the long-chain branching and molecular weight distribution of poly(hydroxy ether)<sup>1</sup> and of high pressure polyethylene we have had occasion to carry out machine computations for the intrinsic viscosity of trifunctional, randomly branched polymers. To perform the calculations we have combined both the Thurmond-Zimm<sup>2</sup> and the Zimm-Kilb<sup>3</sup> treatments of the viscosity of branched polymers with the Beasley<sup>4</sup> molecular weight distribution. We have also had machine computations carried out of the Flory distribution function<sup>5</sup> for trifunctionally branched condensation polymers in order to compare this distribution with that derived by Beasley for a free radical polymerization involving chain transfer to polymer.

We present here the results of both calculations with the feeling that they may well be of interest and use to others.

### THEORY

#### Viscosity Relationships

We assume first the applicability of the Mark-Houwink relation to all molecular weight species of a linear (unbranched) polymer. In particu-

\* Present address: Lockheed Propulsion Company, Redlands, California.

lar, we assume the intrinsic viscosity,  $[\eta]_{i,l}$ , of the  $i$ th linear species to be given by

$$[\eta]_{x,i} = K x^a \quad (1)$$

where  $x$  represents the degree of polymerization.

The intrinsic viscosity,  $[\eta]_{x,b}$ , of a branched species of the same chemical structure and molecular weight has been related to  $[\eta]_{x,l}$  by the following eqs. (2) and (3).

$$[\eta]_{x,b} = g_x^{3/2} (m) [\eta]_{x,l} \quad (2)$$

or

$$[\eta]_{x,b} = g_x^{1/2} (m) [\eta]_{x,l} \quad (3)$$

Here,  $g_x$  is, of course, the ratio of the mean square radii of branched and linear molecules and depends upon the number  $m$  of trifunctional branch points according to eq. (4).<sup>6</sup>

$$g_x = \left[ \left( 1 + \frac{m}{7} \right)^{1/2} + \frac{4m}{9\pi} \right]^{-1/2} \quad (4)$$

Most of the evidence indicates that eq. (2) overestimates the effect of branching upon viscosity for low branch contents and that eq. (3) is to be preferred in such cases.<sup>3,7-10</sup> We shall employ eq. (3) in the remainder of the derivation here but will present results calculated by use of both relationships since some experimental evidence indicates that eq. (2) may be more realistic at high branch contents.<sup>1,11</sup>

Equations (1) and (3), therefore, yield\*

$$[\eta]_{x,b} = K g_x^{1/2} (m) x^a \quad (5)$$

If the normalized weight distribution function of the branched whole resin is  $w(x)$ , then the viscosity of that whole resin is

$$[\eta]_b = K \int_0^\infty w(x) g_x^{1/2} (m) x^a dx \quad (6)$$

where the subscript  $x$  is employed with  $g$  to indicate that  $m$ , and hence  $g$ , may vary with  $x$ .

Defining the normalized variable  $t$  as

$$t \equiv x/\bar{x}_w \quad (7)$$

\* It should perhaps be made clear that there are two assumptions implicit in the present use of equations (4) and (5). The first is that the quantity  $g$ , defined by Zimm and Stockmayer<sup>6</sup> as

$$g_x = \frac{\sum_m g(m) w(m,x)}{\sum_m w(m,x)} = \left[ \left( 1 + \frac{m}{7} \right)^{1/2} + \frac{4m}{9\pi} \right]^{-1/2}$$

should be the same for fractions derived from their "random" distribution polymer as for fractions from the Beasley or Flory distributions. The second assumption is that  $g_x^{1/2} = \bar{g}_x^{1/2}$ . These points have been discussed by Zimm and Stockmayer and Kilb<sup>14</sup> for related situations, and it would appear that any effects in the present case would be relatively minor.

where  $\bar{x}_w$  is, of course, the weight-average degree of polymerization, converts eq. (6) into

$$[\eta]_b = K \bar{x}_w^a \int_0^\infty w(t) g t^{1/2} t^a dt \quad (8)$$

Similarly, eq. (5) becomes

$$[\eta]_b = K \bar{x}_w^a g t^{1/2} t^a \quad (9)$$

### Distribution Function

As noted previously, we have used for  $w(t)$  the function derived by Beasley for a free radical polymerization which involves termination by disproportionation, by transfer to monomer, and by transfer to polymer.<sup>4</sup> The chain transfer to polymer, of course, results in long chain branching, and its probability is assumed to be proportional to the number of monomer units present in the given polymer molecule, i.e., random branching occurs. In the absence of branching the distribution reduces to the "most probable" one; the length distribution of the branches themselves is also the "most probable" distribution. Beasley's function is given by

$$w(t)dt = \frac{4(1 - \beta)tdt}{(1 - 2\beta)^2 \left[ 1 + \frac{2\beta t}{(1 - 2\beta)} \right]^{1 + 1/\beta}} \quad (10)$$

where  $\beta$  is a branching parameter which lies between zero and unity and is 1/2 at the point corresponding to incipient gelation.

The average number of branch points for all molecules having a particular  $x$  or  $t$  was also shown by Beasley to be

$$m(t) = \frac{2t}{(1 - 2\beta)} - \frac{1}{\beta} \ln \left[ 1 + \frac{2\beta t}{(1 - 2\beta)} \right] \quad (11)$$

This relation, along with eqs. (4) and (10), permits the calculation of  $[\eta]_b$  from eq. (8).

## RESULTS AND DISCUSSION

### Viscosity Calculations

Values of  $[\eta]_b/K\bar{x}_w^a$  were computed from eq. (8) with an IBM 1620 machine for nine values of  $\beta$  and four values of  $a$ . (It is perhaps unnecessary to point out that if  $K$  is defined for monodisperse samples, the quantity  $[\eta]_b/K\bar{x}_w^a$  is equivalent to  $\bar{x}_v^a/\bar{x}_w^a$ .) The calculations were carried out by employing both eqs. (2) and (3) for the dependence of  $[\eta]_b$  upon  $g$  and also by assuming  $g$  to be unity, the last case corresponding to a sample which is unbranched yet still follows the Beasley molecular weight distribution. Since the function  $w(t)$  is normalized to unity, the summation in eq. (8) has the value unity under the conditions:  $g = 1$ ,  $a = 1$ , and  $g = 1$ ,  $a = 0$ . These conditions were employed to determine both the upper limit of summation and the number and size of the steps in the summation.

TABLE I  
 Values of  $[\eta]_b/K\bar{x}^a$ 

$\beta$	$[\eta]_b/K\bar{x}_w^a$															
	$a = 0.50$				$a = 0.73$				$a = 0.765$				$a = 0.800$			
	$g^{3/2}$	$g^{1/2}$	$g = 1$	$g$	$g^{3/2}$	$g^{1/2}$	$g = 1$	$g$	$g^{3/2}$	$g^{1/2}$	$g = 1$	$g$	$g^{3/2}$	$g^{1/2}$	$g = 1$	$g$
0.05	0.900	0.922	0.933	0.934	0.908	0.934	0.948	0.948	0.912	0.938	0.952	0.952	0.916	0.943	0.957	0.957
0.10	0.856	0.901	0.926	0.913	0.859	0.913	0.942	0.942	0.862	0.917	0.947	0.947	0.865	0.922	0.953	0.953
0.15	0.808	0.876	0.915	0.885	0.804	0.885	0.933	0.933	0.806	0.890	0.939	0.939	0.808	0.894	0.945	0.945
0.20	0.755	0.847	0.903	0.854	0.743	0.854	0.924	0.924	0.744	0.858	0.930	0.930	0.745	0.863	0.938	0.938
0.25	0.694	0.809	0.885	0.812	0.673	0.812	0.908	0.908	0.672	0.816	0.915	0.915	0.672	0.821	0.924	0.924
0.30	0.625	0.763	0.861	0.761	0.598	0.761	0.887	0.887	0.592	0.765	0.896	0.896	0.590	0.769	0.906	0.906
0.35	0.544	0.700	0.822	0.689	0.499	0.689	0.851	0.851	0.495	0.692	0.862	0.862	0.492	0.696	0.875	0.875
0.40	0.447	0.612	0.757	0.586	0.387	0.586	0.786	0.786	0.381	0.587	0.800	0.800	0.376	0.590	0.817	0.817
0.45	0.315	0.465	0.619	0.413	0.242	0.413	0.633	0.633	0.234	0.411	0.649	0.649	0.225	0.408	0.666	0.666

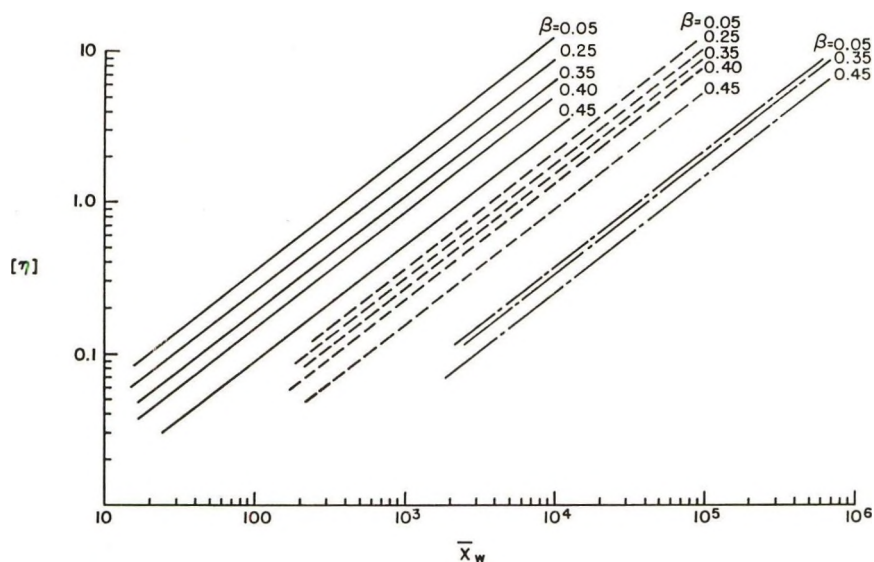


Fig. 1. Calculated viscosities for Beasley whole resins using  $K$  and  $a$  for poly(hydroxy ethers):<sup>1</sup> (—)  $[\eta]_b$ , Zimm-Stockmayer; (---)  $[\eta]_b$ , Zimm-Kilb,  $\bar{x}_w$  scale shifted one decade; (- - -)  $[\eta]_b$ ,  $\bar{x}_w$  scale shifted two decades.

The resultant values of  $[\eta]_b/K\bar{x}_w^a$  are given in Table I. Figure 1 presents a log-log plot of the calculated  $[\eta]_b$  versus  $\bar{x}_w$  for whole resins possessing  $K$  and  $a$  parameters applicable to linear fractions of poly(hydroxyether).<sup>1</sup> From Table I and Figure 1 the following generalizations are warranted, all of which are consistent with our prior understanding.

(1) Note first that constant  $\beta$  necessitates constant  $\bar{x}_w/\bar{x}_n$ . Therefore, at constant  $\beta$  and at given  $a$  the reduction in  $[\eta]$  brought about by breadth of distribution alone ( $g = 1$ ) is of the same magnitude as that caused by long chain branching, particularly, of course, for  $g^{1/2}$ . Naturally, any such comparison of the effects of distribution breadth and branching upon viscosity is dependent upon the particular distribution function employed and it happens that the Beasley distribution even in the absence of branching has abnormally two low values of  $\bar{x}_v/\bar{x}_w$ . This is demonstrated in Table

TABLE II  
Comparison of  $\bar{x}_v/\bar{x}_w$  for Various Distributions for  $a$  Value of 0.73

$\bar{x}_w/\bar{x}_n$	$x_v/\bar{x}_w$		
	Beasley (unbranched)	Schulz-Zimm <sup>12</sup>	Wesslau <sup>13</sup>
2	0.94	0.94	0.92
3	0.88	0.92	—
4	0.82	0.91	0.83
6	0.72	0.91	0.79
8	0.62	0.90	0.75
10	0.56	0.90	0.74

II, where  $\bar{x}_v/\bar{x}_w$  is compared at various values of  $\bar{x}_v/\bar{x}_n$  for the unbranched Beasley,<sup>4</sup> the Schulz-Zimm,<sup>12</sup> and the Wesslau<sup>10</sup> distribution functions.

(2) Keeping in mind that the tabulated numbers in Table I depend upon  $\bar{x}_w^a$  we see that at constant  $\beta$  an increase in  $a$  produces an increase in  $[\eta]$  at constant  $\bar{x}_v$ . This is in agreement with the approach of  $\bar{x}_v$  to  $\bar{x}_w$  as  $a$  approaches unity.

(3) At constant  $a$  an increase in  $\beta$ , i.e., an increase in distribution breadth and/or branching, yields a lower  $[\eta]$  for a given  $\bar{x}_w$ .

### Comparison of Flory and Beasley Distributions

Flory has derived an expression for the molecular weight distribution in a random, trifunctionally branched condensation polymer.<sup>5</sup> His expression is shown in eq. 12.

$$w(x) = 2(1 - \alpha)^2(1 - q)^2q^{(x-1)} \sum_{m=0}^{\infty} \frac{h^m x(x-1) \dots (x-2m)}{(m+2)!m!} \quad (12)$$

where  $h = \alpha(1 - \alpha)(1 - q)^2/q^2$  and  $\alpha$  and  $q$  are related, respectively, to Beasley's  $\beta$  and  $x_0$ , where  $x_0$  is the average number of monomer units per chain. Beasley's equations were first employed for our purposes because of their far greater mathematical simplicity. Subsequently, however, computer calculations of eq. (12) were carried out to determine the equivalence of the two distributions.

Plots of the computed integral distribution,  $I(x)$ , are shown in Figure 2 for various values of Flory's branching parameter  $\alpha$  and one value of  $q$ .

The correctness of the calculations of eq. (12) was checked first by a comparison with the published curves of Flory<sup>5</sup> and second by applying

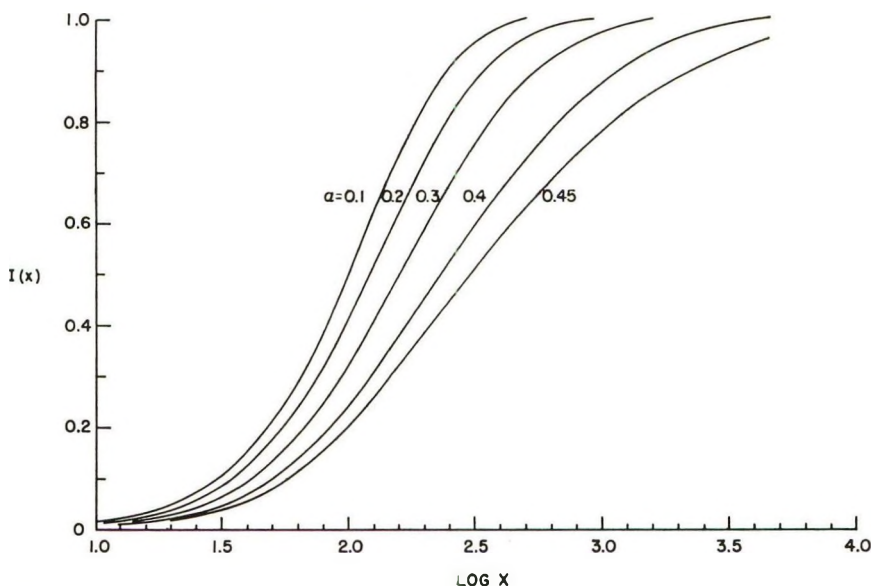


Fig. 2. Flory distribution for random, trifunctionally branched polymers at  $q = 0.98$ .

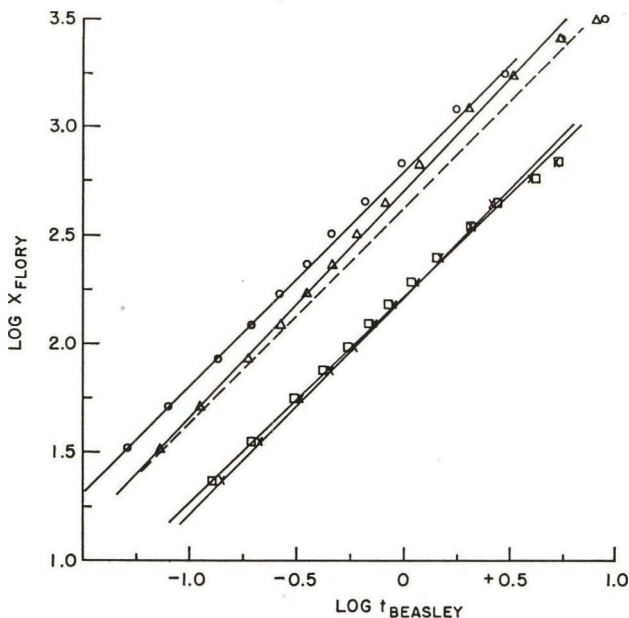


Fig. 3. Comparison of Beasley and Flory distributions: ( $\times$ )  $\alpha = 0.20$ ,  $q = 0.98$ ,  $\beta = 0.15$ , slope = 1.00,  $(\bar{x}_w)_F = 160$ ,  $[\eta]_F = 0.44$ ,  $(\bar{x}_w)_B = 166$ ,  $[\eta]_B = 0.45$ ; ( $\square$ )  $\alpha = 0.20$ ,  $q = 0.98$ ,  $\beta = 0.40$ , slope = 0.96,  $(\bar{x}_w)_F = 160$ ,  $[\eta]_F = 0.44$ ,  $(\bar{x}_w)_B = 166$ ,  $[\eta]_B = 0.45$ ; ( $\circ$ )  $\alpha = 0.40$ ,  $a = 0.98$ ,  $\beta = 0.40$ , slope = 1.00,  $(\bar{x}_w)_F = 426$ ,  $[\eta]_F = 0.43$ ,  $(\bar{x}_w)_B = 615$ ,  $[\eta]_B = 0.58$ ; ( $\triangle$ )  $\alpha = 0.40$ ,  $q = 0.98$ ,  $\beta = 0.35$ , slope = 1.05,  $(\bar{x}_w)_F = 506$ ,  $[\eta]_F = 0.56$ ,  $(\bar{x}_w)_B = 506$ ,  $[\eta]_B = 0.64$ ; (---) slope = 1.00,  $(\bar{x}_w)_F = (\bar{x}_w)_B$ ,  $[\eta]_B = [\eta]_F$ . Points taken at  $I$  values of 0.05, 0.10, 0.20, . . . , 0.90, 0.95, 0.98, 0.99.

different criteria for the convergence of the series over  $m$  and noting the effect upon meeting the normalization conditions. The two distributions are compared in Figure 3, where  $\log x_{\text{Flory}}$  is plotted against  $\log t_{\text{Beasley}}$  at identical values of the respective integral weight distributions,  $I(x)$  and  $I(t)$ . For exact equality of the two functions such a plot should yield a straight line of unit slope and the value of the ordinate at the point where the abscissa is zero should give the weight-average degree of polymerization of the Beasley sample. This average is designated  $(\bar{x}_w)_B$  in Figure 3, whereas  $(\bar{x}_w)_F$  is the weight-average degree of polymerization computed for the Flory distribution at the particular  $\alpha$  and  $q$ . The quantities  $[\eta]_F$  and  $[\eta]_B$  are the viscosities corresponding to  $(\bar{x}_w)_F$  and  $(\bar{x}_w)_B$  and were picked off the solid lines in Figure 1 at the appropriate values of  $\beta$ .

Within the usual experimental error involved in measuring distributions the straight line condition is indeed met up to an  $I$  of at least 0.95 and probably higher, whereas above that point the Beasley distribution extends to greater molecular weights.

For some purposes, therefore, it would appear that these two functions could be used interchangeably. This is particularly true at the lower extents of branching, since the functions do become identical when no branching occurs. When  $\alpha$  is 0.20, for example,  $(\bar{x}_w)_B$  and  $(\bar{x}_w)_F$  are very close,



as are their respective  $[\eta]$ 's. At higher branch contents (broader distribution), however, the equivalence of the two functions is significantly lessened for properties sensitive to the upper end of the distribution. For  $\alpha = 0.40$ , the  $\bar{x}_w$ 's and  $[\eta]$ 's differ rather drastically and the dashed line, which was deliberately drawn with unit slope such that  $(\bar{x}_w)_B$  equals  $(\bar{x}_w)_F$ , deviates widely from the calculated points.

None of the results reported here would have been possible without the aid of Mr. J. H. Webb and Mrs. D. J. Fenichel in programming for the computer and in carrying out the computing.

### References

1. Myers, G. E., and J. R. Dagon, *J. Polymer Sci.*, in press.
2. Thurmond, C. D., and B. H. Zimm, *J. Polymer Sci.*, **8**, 477 (1952).
3. Zimm, B. H., and R. W. Kilb, *J. Polymer Sci.*, **37**, 19 (1959).
4. Beasley, J. K., *J. Am. Chem. Soc.*, **75**, 6123 (1953).
5. Flory, P. J., *J. Am. Chem. Soc.*, **63**, 3901 (1941).
6. Zimm, B. H., and W. H. Stockmayer, *J. Chem. Phys.*, **17**, 1301 (1949).
7. Stockmayer, W. H., and M. Fixman, *Ann. N. Y. Acad. Sci.*, **57**, 334 (1953).
8. Wenger, F., *J. Polymer Sci.*, **57**, 481 (1962).
9. Hobbs, L. M., G. C. Berry, and V. C. Long, paper presented at International Symposium on Macromolecular Chemistry, Montreal, Canada, July 27–Aug. 1, 1961.
10. Cantow, M., G. Meyerhoff, and G. V. Schulz, *Makromol. Chem.*, **49**, 1 (1961).
11. Guillet, J. E., paper presented at 141st National Meeting, American Chemical Society, Washington, D. C., March 20–29, 1962.
12. Booth, C., and L. R. Beason, *J. Polymer Sci.*, **42**, 92 (1960).
13. Chiang, R., *J. Polymer Sci.*, **36**, 91 (1959).
14. Kilb, R. W., *J. Polymer Sci.*, **38**, 403 (1959).

### Résumé

On a opéré des calculs sur la viscosité intrinsèque de polymères trifonctionnels statistiquement ramifiés. On a combiné et le traitement de Thurmond-Zimm et celui de Zimm-Kilb relatifs à la viscosité de polymères branchés, avec la fonction de Beasley pour la distribution des poids moléculaires. On a également fait la comparaison entre la fonction de distribution de Beasley et une fonction dérivée de la théorie de Flory se rapportant aux polymères polycondensés trifonctionnels et ramifiés. Les deux fonctions sont en bon accord pour des taux faibles de ramification, mais pour des taux plus élevés, la première rend compte de poids moléculaires significativement plus élevés.

### Zusammenfassung

Berechnungen über die Viskositätszahl trifunktioneller, statistisch verzweigter, unfraktionierter Polymerer wurden angestellt. Die Behandlung der Viskosität verzweigter Polymerer sowohl nach Thurmond-Zimm als auch nach Zimm-Kilb wurde mit der Molekulargewichtsverteilungsfunktion von Beasley kombiniert. Die Verteilungsfunktion von Beasley wurde auch mit einer von Flory für trifunktionell verzweigte Kondensationspolymere abgeleiteten Funktion verglichen. Die beiden Funktionen stimmen bei niedrigem Ausmass der Verzweigung gut überein, bei höherem Verzweigungsgehalt erstreckt sich aber erstere Funktion zu wesentlich höheren Molekulargewichten.

Received September 27, 1963

Revised January 16, 1964

## Polymers Containing the Cyclopentyl and Cyclohexyl Groups

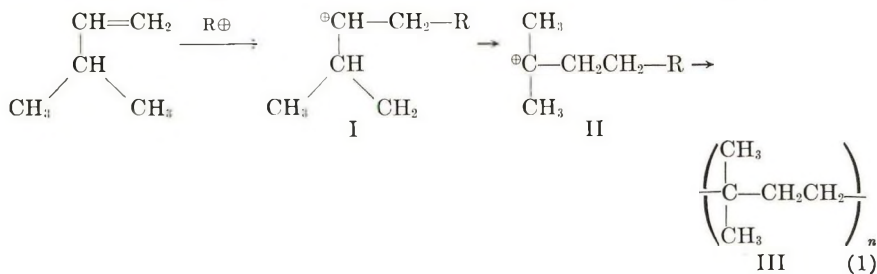
A. D. KETLEY and R. J. EHRIG, *W. R. Grace & Company, Washington Research Center, Clarksville, Maryland*

### Synopsis

Polymers have been prepared from a group of monomers containing the cyclohexyl and cyclopentyl groups. These monomers were of the type  $(C_6H_{11})-(CH_2)_n-CH=CH_2$  (where  $n = 0-3$ ) and  $(C_5H_9)-(CH_2)_n-CH=CH_2$  (where  $n = 0-1$ ). Both Ziegler-Natta and Friedel-Crafts catalysts were used. By comparison of the infrared spectra of corresponding polymers prepared with the two types of catalysts, it has been shown, for the cyclohexyl compounds, that intramolecular hydride transfers take place to a significant extent during the propagation step of the Friedel-Crafts polymerizations. These hydride transfers result in the formation of a tertiary carbonium-ion end which, on propagation, leads to a polymer in which cyclohexyl groups are part of the main chain. The cyclopentyl compounds, however, do not behave in this way. In this case, the relative reactivities of the tertiary and secondary carbonium ions are such that propagation through the latter is favored. Attempts to polymerize 2,4-spiroheptane and 2,5-spirooctane to give model compounds for the "rearranged" polymers are also reported.

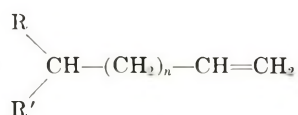
The polymerization of  $\alpha$ -olefins by Lewis acids generally yields very complex products quite different from the simple, linear polymers obtained with Ziegler-Natta catalysts.<sup>1</sup> Recently, the structures of the products from the Lewis acid-catalyzed polymerization of propylene and butene-1 were described, and it was shown that they resulted from the occurrence of several possible hydride transfers in the propagation step of the reaction.<sup>2</sup>

These results led us to investigate polymerizations in which the propagating carbonium ion might rearrange, in the propagation step, to one other more stable ion rather than to several other carbonium ions as in the case of propylene and butene-1. An apparently ideal example was 3-methylbutene-1, since the initially formed secondary carbonium ion (I) could irreversibly rearrange to the more stable tertiary carbonium ion (II).

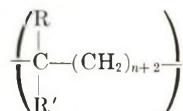


In an independent study, Kennedy<sup>3,4</sup> has shown that hydride transfer does indeed take place to give a polymer having either partially or exclusively the structure III. The NMR and infrared data of Kennedy are in agreement with results obtained in this laboratory and with our observation that the infrared spectrum of the 3-methylbutene-1 polymer is almost identical to that of the polymer obtained by the reaction of 1,1-dimethylcyclopropane with aluminum bromide.<sup>5</sup>

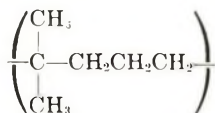
For polymers having this "rearranged" structure to be formed, it is necessary that the rate of rearrangement be much greater than the rate of propagation. This is apparently the case for the hydride transfer between adjacent carbon atoms in 3-methylbutene-1, at least below  $-100^{\circ}\text{C}$ . If it were also true for hydride transfers between nonadjacent carbon atoms, then olefins of the structure



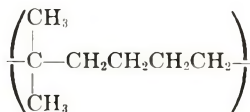
Would yield polymers having the repeat unit:



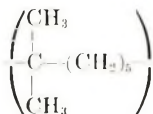
Edwards and Chamberlain have shown that 4-methylpentene-1 can be polymerized to a polymer containing 90% of units:<sup>6</sup>



For 5-methylhexene-1 the percentage of

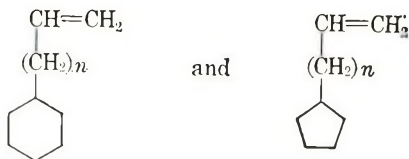


units in the polymer falls sharply to 50% or less. A possible reason for this is that, in one conformation, the tertiary hydrogen in the 4-methylpentene-1 carbonium ion is favorably placed for a direct 1,3-hydride shift to take place, whereas for 5-methylhexene-1, two consecutive hydride transfers may have to occur. Good evidence for such 1,3-hydride shifts has recently been obtained by Karabatsos and Orzech for the nitrous acid deamination of the perchlorate salt of 1-propylamine-1,2,2,2*d*,<sup>7</sup> and by Skell in the deoxidations of 1,1-dideutero-1-propanol and 2-methyl-1-butanol.<sup>8,9</sup> The NMR spectrum of a polymer of 6-methylheptene-1 prepared by us showed no evidence of the structure:

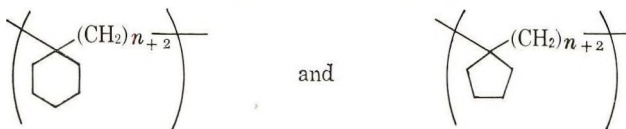


While hydride transfers undoubtedly occur in this case also, they are apparently stepwise and do not proceed far enough to give the tertiary carbonium ion before another monomer unit adds to the chain.

The polymerization of the monomers:

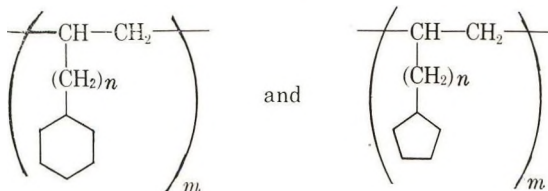


where  $n = 0-3$ , by Friedel-Crafts catalysts to give "rearranged" polymers is an unusually interesting case, since the expected products would contain structural units in which the cyclohexyl or cyclopentyl rings would be integral parts of the chain rather than pendant groups:



By analogy with the acyclic systems discussed above, vinyl cyclohexane and vinyl cyclopentane would be expected to yield the most highly rearranged products. However, the cyclopentyl polymers might possibly rearrange more than their acyclic analogs due to the driving force of ring strain favoring formation of the tertiary carbonium ion.

In this paper the preparation and properties of linear polymers:



by Ziegler-Natta catalysts and of "rearranged" polymers by Friedel-Crafts catalysts from the corresponding monomers is described. Infrared data from both classes of polymers are used to assign structures to the "rearranged" materials.

## RESULTS

### Polymers Prepared with Friedel-Crafts Catalysts

Table I gives the properties of polymers prepared with  $\text{AlBr}_3$  in ethyl chloride solvent at temperatures between  $-50$  and  $-113^\circ\text{C}$ .

TABLE I  
 Polymerization of Cyclohexyl and Cyclopentyl Alkenes by Friedel-Crafts Catalysts

Compound	Polymerization temp., °C.	M.W. <sup>a</sup>	Softening temp., °C.
Vinylcyclohexane	-50	10,500	110
Vinylcyclohexane	-113		120
Allylcyclohexane	-78	13,100	90
Vinylcyclopentane	-78	906	55
Vinylcyclopentane	-110	950	58
Allylcyclopentane	-78	1,270	78
5-Cyclohexylpentene-1	-78		—

<sup>a</sup> Measured by a Mechrolab vapor pressure osmometer.

The x-ray patterns of the first five materials are unusual. The pattern of polyvinylcyclohexane prepared at  $-113^{\circ}\text{C}$ . is typical. While the pattern does not resemble that of the crystalline material, the relatively sharp single peak suggests that the chains are more highly ordered than is usually the case for amorphous polymers. Attempts to anneal these materials did not, however, result in any apparent increase in crystallinity.

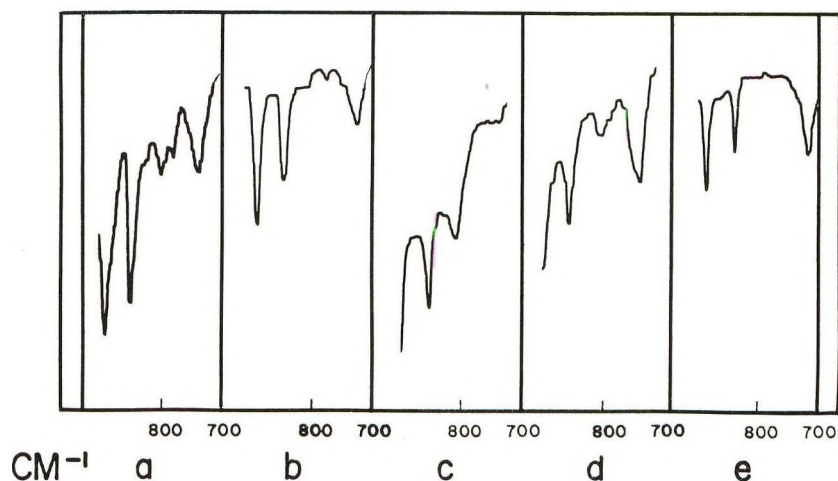


Fig. 1. Infrared spectra of the Friedel-Craft polymers of: (a) vinylcyclohexane; (b) allylcyclohexane; (c) vinylcyclopentane; (d) allylcyclopentane; (e) 5-cyclohexylpentene-1.

The first six materials in Table I can be pressed into clear, brittle films. Poly-5-cyclohexylpentene-1 is elastomeric.

An infrared spectrum of the polymer of vinyl cyclohexane prepared with a Friedel-Crafts catalyst at  $-113^{\circ}\text{C}$ . is shown in Figure 1a. The spectra of the polymers prepared at  $-78^{\circ}\text{C}$ . are shown in Figures 1b-1d.

#### Polymers Prepared with Ziegler-Natta Catalysts

Table II shows the properties of polymers prepared with a  $\text{TiCl}_3/\text{Al}(\text{C}_2\text{H}_5)_2\text{Cl}$  catalyst at  $40^{\circ}\text{C}$ .

TABLE II  
 Polymerization of Cyclohexyl and Cyclopentyl Alkenes by Ziegler-Natta Catalysts

Compound	Melting temp. $T_m$ , °C. <sup>a</sup>	$\eta_{sp}/c$ <sup>b</sup>	Crystallinity	Insoluble in ether, %	Insoluble in pentane, %
Vinylcyclohexane	383	5.02	+	93.2	90.3
Allylcyclohexane	214	2.50	+	68.4	6.8
Vinylcyclopentane	292		+	100.0	91.2
Allylcyclopentane	210	1.94	+	74.3	53.1
4-Cyclohexylbutene-1	138	3.73	-	94.0	92.4
5-Cyclohexylpentene-1	123		-	85.0	51.6

<sup>a</sup> Determined with a duPont 900 differential thermal analyzer.

<sup>b</sup> Measured in 1% solutions in chloroform or toluene at 25°.

Infrared spectra of these polymers are shown in Figure 2.

The melting points determined by DTA are in fair agreement with the crystalline melting points obtained by other workers.<sup>10-12</sup> Overberger et al. have observed that vinylcyclopentane decomposed without melting at 260°C. We could not confirm this observation. Poly-5-cyclohexylpentene-1 has been previously prepared by Dunham, et al., but they did not record a first-order transition for this polymer.

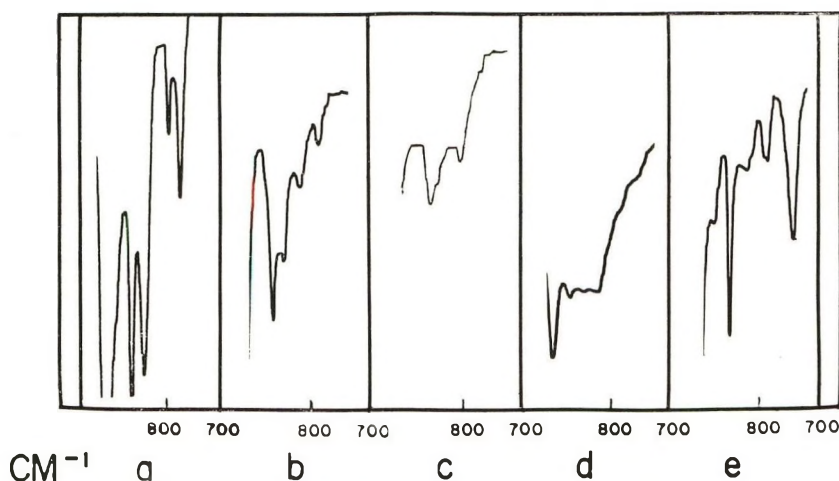


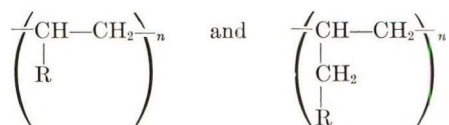
Fig. 2. Infrared spectra of the Ziegler-Natta polymers of: (a) vinylcyclohexane; (b) allylcyclohexane; (c) vinylcyclopentane; (d) allylcyclopentane; (e) 5-cyclohexylpentene-1.

### Infrared Spectra

The "normal" Ziegler-Natta polymers of these cyclohexyl and cyclopentyl monomers have only one methylene group per monomer unit in the backbone. The Friedel-Crafts polymers, if they have the postulated rearranged structures, should have two or more methylene groups. This should give rise to significant differences between the spectra of the two

sets of polymers in the methylene rocking region of the infrared (700–800  $\text{cm}^{-1}$ ). Thus Kennedy has assigned the band at 752  $\text{cm}^{-1}$  in cationic poly-3-methylbutene-1 to the skeletal rocking mode of the  $\text{-(CH}_2\text{CH}_2\text{-)}$  group.<sup>4</sup> This band is completely absent in the Ziegler-Natta polymer. A similar assignment has been made by van Schooten and Mostert for this band in ethylene-propylene copolymers.<sup>13</sup> The same workers assign a band at 730  $\text{cm}^{-1}$  to  $\text{-(CH}_2\text{-)}_3$  sequences. Methylene rocking vibrations in side-chains and end groups have somewhat higher frequencies; for example, the  $\text{-(CH}_2\text{CH}_2\text{CH}_2\text{-)}$  in the terminal propyl group of polypropylene absorbs at 740  $\text{cm}^{-1}$ ,<sup>14,15</sup> while bands at 760–770  $\text{cm}^{-1}$  have been assigned at the  $\text{-(CH}_2\text{-)}_2$  group in the side chains of several polymers.<sup>14</sup>

Neither the vinyl nor allyl cycloalkane polymers prepared with Ziegler-Natta catalysts show any absorption between 775 and 720  $\text{cm}^{-1}$ . This is true of both the heptane-insoluble and heptane-soluble fractions of the polymers. This agrees with the expected structures



of these materials. The Ziegler-Natta polymers of 4-cyclohexylbutene-1 and 5-cyclohexylpentene-1, however, have bands at 745 and 730  $\text{cm}^{-1}$ , respectively, due to  $\text{-(CH}_2\text{CH}_2\text{-)}$  and  $\text{-(CH}_2\text{CH}_2\text{CH}_2\text{-)}$  groups in the side chains.

The infrared absorptions in the methylene rocking region of polymers prepared with Friedel-Crafts catalysts are shown in Table III, together with assignments of these bands.

TABLE III  
Methylene Rocking Absorptions of Polycyclohexyl and Cyclopentyl Alkenes Prepared with Friedel-Crafts Catalysts

Compound	Infrared absorption, $\text{cm}^{-1}$	Assignment
Polyvinylcyclohexane	748	$\text{-(CH}_2\text{-)}_2$
Polyallylcyclohexane	725	$\text{-(CH}_2\text{-)}_3$
Polyvinylcyclopentane	None	—
Polyallylcyclopentane	750	$\text{-(CH}_2\text{-)}_2$
Poly-5-cyclohexylpentene-1	721	$\text{-(CH}_2\text{-)}_5$
Polyallylcyclohexane- $d_{11}$	680, 695, 722	$\text{-(CH}_2\text{CHDC}_2\text{-)}$

Also included in Table III are the infrared methylene rocking vibrations of the polymer obtained by cationic polymerization of allylcyclohexane- $d_{11}$  in which all ring hydrogen atoms are substituted by deuterium (Fig. 3). The spectrum between 800 and 1400  $\text{cm}^{-1}$ , due primarily to the cyclohexyl ring, is shifted drastically to lower frequencies. However, the 725  $\text{cm}^{-1}$  band in the nondeuterated polymer is split into three bands at 680, 695,

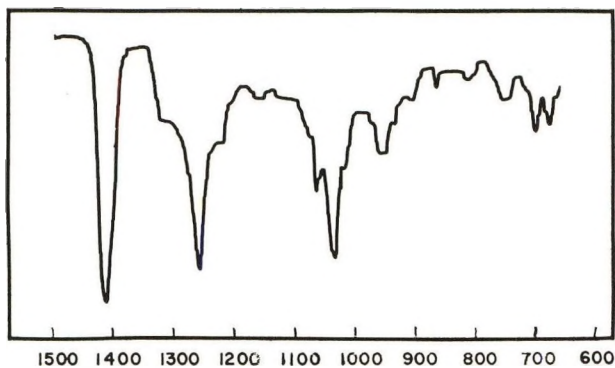


Fig. 3. Infrared spectrum of polyallylcyclohexane- $d_{11}$ .

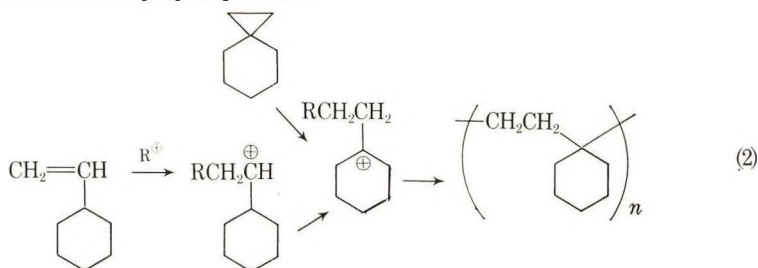
and  $722\text{ cm.}^{-1}$ , probably indicative of the  $-(\text{CH}_2\text{CHDCH}_2)-$  backbone unit.

### Nuclear Magnetic Resonance Studies

Attempts to confirm the structures of the Friedel-Crafts polymers by NMR were not successful. The NMR spectra of all these polymers have only one very broad absorption from  $\tau = 7.5$  to  $\tau = 9.5$ . Also, the NMR spectrum of the polymer from allylcyclohexane- $d_{11}$ , in which all the ring protons are replaced by deuterium, showed no better resolution. It is probable that the NMR spectra of these polymers cannot be resolved due to their having stiff, inflexible chains.

### Model Polymers from Cyclopropyl Compounds

The identity of the polymers from the rearrangement polymerization of 3-methylbutene-1 and the polymerization of 1,1-dimethylcyclopropane suggests that the ring opening of the cyclopropyl compounds might be a general method for preparing polymers having  $(-\text{CH}_2\text{CH}_2-)$  sequences in the backbone. These, in turn, could be model polymers for those obtained by rearrangement polymerization of vinyl compounds. Polymers from 2,5-spirooctane and 2,4-spiroheptane should, for example, have the same structure as polymers from the rearrangement polymerization of vinylcyclohexane and vinylcyclopentane:





Polymerization of both 2,5-spirooctane and 2,4-spiroheptane by  $\text{AlBr}_3$  proceeds much less readily than that of 1,1-dimethylcyclopropane under similar conditions. Whereas the latter compound polymerizes rapidly at  $-50^\circ\text{C}$ ., the spiro compounds must be heated to  $35\text{--}40^\circ\text{C}$ . before a rapid, exothermic polymerization takes place. The infrared spectra of the two polymers do not resemble those of polyvinylcyclohexane or polyvinylcyclopentane, respectively, whether prepared with Friedel-Crafts or Ziegler Natta catalysts (Fig. 4).

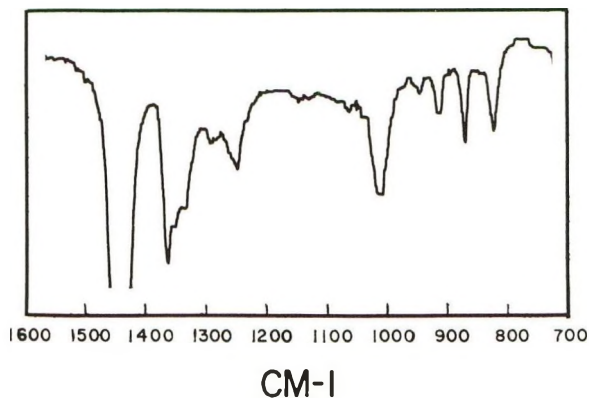


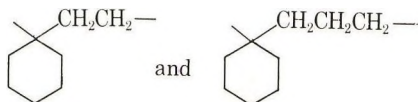
Fig. 4. Infrared spectrum of the Friedel-Crafts polymer obtained from spiro-2,5-octane.

Attempted polymerization of 2,5-spirooctane by  $\text{TiCl}_4$  gave no polymer at any temperature but instead a good yield of a colorless liquid, boiling point  $56^\circ\text{C}/37\text{ mm}$ . This agrees with the boiling point given by Reppe for bicyclo[4.2.0]octane.<sup>16</sup>

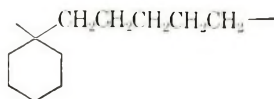
Presumably, the reaction of 2,5-spirooctane with Friedel-Crafts reagents results in ring expansion because the hydride transfer to the spiro carbon from the adjacent methylene group leaves a relatively stable secondary carbonium ion. With 1,1-dimethylcyclopropane, hydride transfer would have to take place from a methyl group, leaving the energetically unfavorable primary carbonium ion. The polymerization of the spiro compounds at  $35\text{--}40^\circ\text{C}$ . by  $\text{AlBr}_3$  probably takes place through the intermediate formation of the bicyclo compounds, followed by opening of the cyclobutyl ring to give complex products.

## DISCUSSION

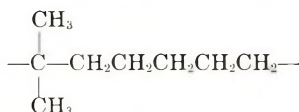
The presence of methylene rocking bands arising from  $\text{—}(\text{CH}_2\text{CH}_2)\text{—}$  sequences in cationic polyvinylcyclohexane and from  $\text{—}(\text{CH}_2\text{CH}_2\text{CH}_2)\text{—}$  in cationic polyallylcyclohexane, together with the absence of these bands in the Ziegler Natta polymers, indicates that hydride shifts do occur in the propagation steps of the cationic polymerizations to give materials containing the structures:



However, the failure of the materials to crystallize suggests that rearrangement is not complete and that the product is a "copolymer" of rearranged and unrearranged units. Surprisingly, the strong band at  $721\text{ cm.}^{-1}$  in cationic poly-5-cyclohexylpentene-1 indicates that this polymer has predominantly the structure:<sup>14</sup>

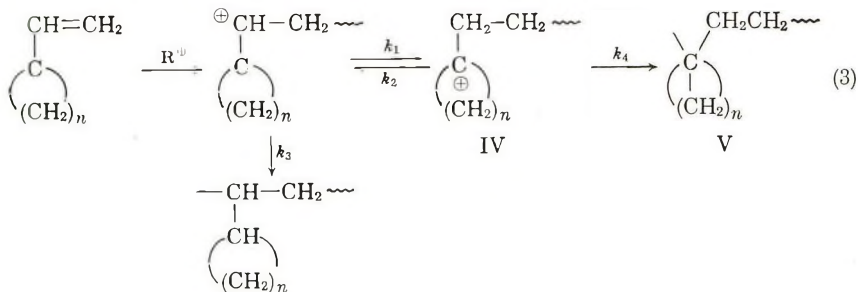


This is in contrast to the acyclic analog, cationic poly-6-methylheptene-1, which shows no contribution from the structure:



Ziegler-Natta poly-5-cyclohexylpentene-1 has a methylene rocking absorption at  $730\text{ cm.}^{-1}$  which arises from the  $-(\text{CH}_2\text{CH}_2\text{CH}_2)-$  sequence in the pendant cyclohexylpropyl groups.

The cationic polymers of vinyl cyclopentane, prepared both at  $-78^\circ$  and at  $-110^\circ\text{C.}$  show no absorption at  $740\text{--}745\text{ cm.}^{-1}$ . It appears, therefore, that these polymers are not rearranged. This observation, that cationic polymerization proceeds predominantly with rearrangement in the case of vinylcyclohexane and without rearrangement in the case of vinylcyclopentane is unexpected. In the general scheme:

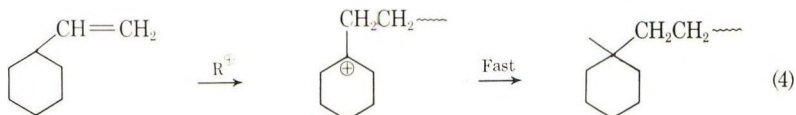


$k_3$  must almost certainly be approximately the same for both the cyclohexyl and cyclopentyl compounds. Therefore, either the initially formed ion in the vinylcyclopentane polymerization does not rearrange or, if it does, the resulting rearranged carbonium ion is much less reactive than in the case of vinyl cyclohexane.

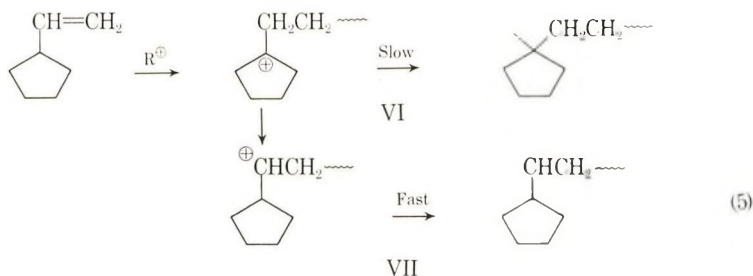
H. C. Brown has pointed out that reactions involving a change of coordination number of a ring carbon atom from 3 to 4 proceed slowly in five-

membered rings and rapidly in six-membered rings, due primarily to an increase in *I* strain in the former case.<sup>19</sup> For example, cyclohexanone reacts with semicarbazide 10 times as fast as cyclopentanone<sup>20</sup> and  $\delta$ -valerolactone hydrolyzes in acid solution 170 times as fast as  $\gamma$ -butyrolactone.<sup>19</sup> Consequently, since the propagation step IV  $\rightarrow$  V involves a change in a ring carbon from  $sp_2$  to  $sp_3$ , one would expect  $k_1$  for the cyclopentyl compound to be considerably less than for the cyclohexyl compound. However, by the same reasoning, when  $n = 4$ ,  $k_2$  should be less than when  $n = 5$ . Hence the lower reactivity of *I* when  $n = 4$  should be compensated for by a higher concentration of the rearranged carbonium ion.

An alternative scheme to that outlined above involves synchronous addition of monomer and hydride transfer. In the polymerization of vinyl cyclohexane, the rearranged carbonium ion might be reactive enough to be removed by reaction with monomer as soon as it was formed:

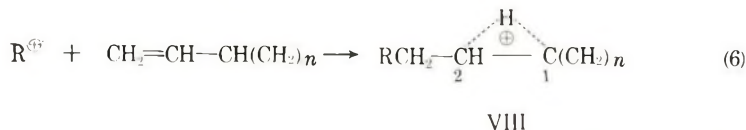


whereas for vinylcyclopentane, the lower reactivity of the rearranged carbonium ion might allow it to equilibrate with the more reactive secondary ion through which propagation would proceed:



Again it is difficult to see why the operation of *I* strain on the rate of addition of monomer to VI should not also inhibit the rearrangement of VI to VII.

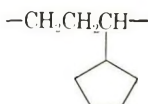
The results may be rationalized by assuming propagation takes place through the intermediate VIII; as shown in eq. (6).



Intermediates of this kind have been suggested in the hydration of isobutylene<sup>21</sup> and the cationic polymerization of propylene.<sup>2</sup> When  $n = 4$ , *I* strain will inhibit addition of monomer to ring carbon 1, but will not affect addition to carbon 2 if carbon-carbon bond formation with monomer

is considerably advanced in the transition state before bond formation between the hydrogen and carbon 1 has advanced appreciably. Since the addition of monomer to carbon 1 will not be inhibited by *I* strain when  $n = 5$ , vinylcyclohexane gives the rearranged product even from the intermediate VIII.

Polyallylcyclopentane prepared with Friedel-Crafts catalysts is anomalous also, in that its principal absorption in the methylene rocking region is more reasonably ascribed to  $\text{-(CH}_2\text{CH}_2\text{)-}$  than to  $\text{-(CH}_2\text{CH}_2\text{CH}_2\text{)-}$ . The repeat unit in the polymer appears, therefore, to be predominantly



In this case also, propagation must proceed most favorably through the secondary carbonium ion adjacent to the ring.

It appears, therefore, that the occurrence of rearrangement polymerization such as is observed with 3-methylbutene-1 or vinylcyclohexane depends upon both the ease with which the hydride shift occurs, the stability of the resulting tertiary carbonium ion, and its reactivity towards another monomer unit.

## EXPERIMENTAL

### Materials

**Aluminum Bromide.**  $\text{AlBr}_3$  was Fisher Pure Grade. It was stored in nylon sealed ampules in a vacuum desiccator when not in use.

**Titanium Trichloride.**  $\text{TiCl}_3$  was A.A. grade purchased from Stauffer Chemical Co.

**Diethylaluminum Chloride.** This was obtained from Texas Alkyls and used as a 25% solution in *n*-heptane.

**Ethyl Chloride.** Matheson U.S.P. grade was dried by passage through an Air Dry Comp. G4060 MS desiccant cartridge.

**Vinylcyclohexane.** Vinylcyclohexane was obtained from Beacon Chemical Company. It was dried over calcium hydride and used without further purification.\*

**Allylcyclohexane.** Allylcyclohexane was prepared by the reaction of cyclohexylmagnesium bromide (from fractionated, Eastman White Label cyclohexyl bromide) with allyl bromide (Eastman Yellow Label). After conventional work-up and removal of ether, the product was fractionated over sodium through a 1-m. Goodloe column; boiling point  $550^\circ\text{C./24 mm.}$ \*

**Vinylcyclopentane.** Cyclopentyl ethanol was prepared by reacting ethylene oxide with cyclopentylmagnesium bromide (boiling point  $81\text{--}82^\circ$

\* All olefins used in this work were tested for purity by using a Perkin-Elmer Model 154 vapor fractometer with a diisodecyl phthalate column.

C./12 mm. (general procedures for all the Grignard reactions listed here follow Vogel<sup>22</sup>).<sup>\*</sup> The acetate of this alcohol was prepared and pyrolyzed at 500°C. through a glass wool-packed column. The crude vinylcyclopentane was fractionated from sodium; boiling point 98°C./758 mm.

**Allylcyclopentane.** Cyclopentylmagnesium bromide (from fractionated Eastman Yellow Label cyclopentyl bromide) was reacted with allyl bromide. The crude product was fractionated over sodium; boiling point 124–125°C./760 mm.

**4-Cyclohexylbutene-1.** Cyclohexylmethyl bromide (Beacon Chemical Company) was converted to cyclohexylmethylmagnesium bromide and the Grignard reagent reacted with allyl bromide. The product was distilled from sodium; boiling point 62°C./14 mm.

**5-Cyclohexylpentene-1.** 1-Cyclohexyl-2-bromoethane (Aldrich Chemical Company) was converted to the Grignard reagent which was then reacted with allyl bromide. The product was distilled from sodium; boiling point 80°C./12 mm.

**Allylcyclohexane-*d*<sub>11</sub>.** A 10.3-g. portion of cyclohexanol *d*<sub>12</sub> (Volk Lot 251.9) was allowed to react for 36 hr. with 25 ml. of concentrated HCl and 8 g. of calcium chloride at 100°C. A 96% yield of chlorocyclohexane-*d*<sub>11</sub> was obtained. This was converted to the Grignard reagent and reacted with allyl bromide. After conventional work-up and fractionation, a 40% yield (based on cyclohexanol-*d*<sub>12</sub>) of allylcyclohexane-*d*<sub>11</sub> was obtained; boiling point 55°C./24 mm.

**Spiro-2,5-octane.** Cyclohexylmethanol (boiling point 85°C./22 mm.) was prepared by the reaction of anhydrous formaldehyde with cyclohexylmagnesium bromide. The acetate of this alcohol (boiling point 83°C./14 mm.) was pyrolyzed by passage through a glass wool-packed column at 500°C. to give methylene cyclohexane (boiling point 101–102°C./755 mm). Methylene cyclohexane was converted to the spiro compound by reaction in refluxing ether with methylene iodide and Zn/Cu couple<sup>18</sup> for 48 hr. Unreacted olefin was removed by extraction with concentrated silver nitrate solution. The residual spiro-2,5-octane was fractionated. The fractional boiling at 73°C./96 mm. was shown by gas chromatography to be substantially pure material.

**Spiro-2,4-heptane.** Cyclopentyl carbinol (boiling point 61°C./22 mm.) was prepared by the reaction of formaldehyde with cyclopentylmagnesium bromide. The carbinol was converted to the acetate (boiling point 90°C./40 mm.), which was then pyrolyzed by passage through a glass wool column at 500°C. Spiro-2,4-heptane was then prepared from methylene cyclopentane (boiling point 75°C./755 mm.) by the Simmons method as described for spiro-2,5-octane. The product was distilled and a pure fraction boiling at 35°C./80 mm. obtained.

<sup>\*</sup> The boiling points reported here for cyclopentylethanol, cyclopentyl carbinol, cyclohexyl carbinol, and their acetates are all approximately 5% higher than those reported by Yahevina and Mezentsova.<sup>17</sup>

### Polymerizations

**Friedel-Crafts Polymerizations.** A 5-ml. portion of olefin was dissolved in 35 ml. of ethyl chloride in a 100-ml. stirred microreactor and cooled to the reaction temperature.  $\text{AlBr}_3$  (0.25 g.) was weighed into a Fischer-Porter aerosol tube in a nitrogen-filled dry box and then 20 ml. of ethyl chloride added. When the  $\text{AlBr}_3$  was completely dissolved, the solution was cooled to the reaction temperature and pressured into the nitrogen-flushed reactor. After completion of the polymerization, the polymer was washed with excess methanol and dried in a vacuum oven at  $40^\circ\text{C}$ .

**Ziegler-Natta Polymerizations.** All polymerizations were conducted in the same general manner with only minor variations. A typical example is given.

To a Fischer-Porter aerosol tube which had been properly pretreated was added 'AA'  $\text{TiCl}_3$  (0.5 g.), diethylaluminum chloride solution (1.5 ml.), and 15 ml. of heptane (mole ratio Ti/Al of 1/1). After the catalyst solution had been aged for 15 min. at room temperature, 0.5 mole of allylcyclohexane was added and the monomer allowed to polymerize overnight at  $40^\circ\text{C}$ . Methanol was then added to deactivate the catalyst, and the polymer was treated with a dilute HCl-methanol mixture.

The authors wish to thank Professor C. G. Overberger, Drs. F. X. Werber and W. C. Overhults for helpful discussions and K. Chan, D. Daniels, R. Daffin, L. Fisher, and E. Gorman who carried out the experimental work.

### References

1. Meier, R. L., *J. Chem. Soc.*, **1950**, 3656.
2. Ketley, A. D., and M. C. Harvey, *J. Org. Chem.*, **26**, 4649 (1961).
3. Kennedy, J. P., and R. M. Thomas, *Makromol. Chem.*, **53**, 28 (1962).
4. Kennedy, J. P., private communication.
5. Ketley, A. D., *J. Polymer Sci.*, **B1**, 313 (1963).
6. Edwards, W. R., and N. F. Chamberlain, *J. Polymer Sci.*, **A1**, 2299 (1963).
7. Karabatsos, G. J., and C. E. Orzech, *J. Am. Chem. Soc.*, **84**, 2838 (1962).
8. Skell, P. S., and L. Starer, *J. Am. Chem. Soc.*, **84**, 3962 (1962).
9. Skell, P. S., and R. J. Maxwell, *J. Am. Chem. Soc.*, **84**, 3964 (1962).
10. Campbell, T. W., and A. C. Haven, Jr., *J. Appl. Polymer Sci.*, **1**, 73 (1959).
11. Dunham, K. R., J. Van DenBerghe, J. W. H. Faber, and L. E. Contors, *J. Polymer Sci.*, **A1**, 751 (1963).
12. Overberger, C. G., A. E. Borchert, and A. Katchman, *J. Polymer Sci.*, **44**, 491 (1960).
13. van Schooten, J., and S. Mostert, *Polymer*, **4**, 135 (1963).
14. Harvey, M. C., and A. D. Ketley, *J. Appl. Polymer Sci.*, **5**, 247 (1961).
15. Natta, G., *J. Polymer Sci.*, **34**, 533 (1959).
16. Reppe, W., W. Schichting, K. Kloger, and T. Torpel, *Ann.*, **560**, 1 (1948).
17. Yahevina, R., and N. N. Mezentsova, *Uch. Zap. Mosk. Gos. Univ.*, No. **132**, **7**, 241 (1950).
18. Simmons, H. E., and R. D. Smith, *J. Am. Chem. Soc.*, **81**, 4256 (1959).
19. Brown, H. C., J. H. Brewster, and H. Shechter, *J. Am. Chem. Soc.*, **76**, 467 (1954).
20. Price, F., and L. P. Hammett, *J. Am. Chem. Soc.*, **63**, 2387 (1941).
21. Levy, J. B., R. W. Taft, and L. P. Hammett, *J. Am. Chem. Soc.*, **75**, 1253 (1953).
22. Vogel, A. I., *Practical Organic Chemistry*, Longmans, London, 1959.

### Résumé

On a préparé des polymères de quelques monomères contenant des groupes cyclohexyle et cyclopentyle. Ces monomères étaient du type:  $(C_6H_{11})-(CH_2)_n-CH=CH_2$  ( $n = 0-3$ ) et  $(C_5H_9)-(CH_2)_nCH=CH_2$  ( $n = 0-1$ ). On a employé des catalyseurs Ziegler-Natta et Friedel-Crafts. En comparant les spectres infra-rouges des polymères correspondants mais préparés avec les deux types de catalyseurs, on a trouvé que pour les dérivés cyclohexyliques, il y a, au cours de la propagation avec le catalyseur Friedel-Crafts, transfert intramoléculaire important d'hydrure. Les transferts d'hydrure entraînent la formation d'un ion carbonium tertiaire à la fin de la chaîne qui, en se propageant, forme un polymère dans lequel les groupes cyclohexyliques font partie de la chaîne. Les dérivés cyclopentyles ne se comportent pas de la même façon. Dans ce cas, les réactivités relatives des ions carbonium tertiaires et secondaires sont telles que la propagation via le dernier est favorisée. On rapporte aussi des essais pour polymériser les 2,4-spiroheptane et 2,5-spirooctane pour donner un produit-modèle des polymères réarrangés.

### Zusammenfassung

Aus Monomeren mit Zylohexyl- und Zyklopentylgruppen wurden Polymere hergestellt. Diese Monomeren waren vom Typ  $(C_6H_{11})-(CH_2)_n-CH=CH_2$  ( $n = 0-3$ ) und  $(C_5H_9)-(CH_2)_nCH=CH_2$  ( $n = 0-1$ ). Sowohl Ziegler-Natta- als auch Friedel-Crafts-Katalysatoren wurden verwendet. Durch Vergleich der Infrarotspektren entsprechender mit den beiden Katalysatorgruppen hergestellter Polymerer wurde für die Zyklohexylverbindungen gezeigt, dass die intramolekulare Hydridübertragung in einem beträchtlichen Ausmass während des Wachstumsschritts der Friedel-Crafts-Polymerisation stattfindet. Die Hydridübertragung führt zur Bildung einer tertiären Carboniumionengruppe, die bei Wachstum zu einem Polymeren mit Zyklohexylgruppen in der Hauptkette führt. Die Zyklopentylverbindungen verhalten sich jedoch nicht so. In diesem Fall ist die relative Reaktivität des tertiären und sekundären Carboniumions dergestalt, dass das Wachstum durch letzteres begünstigt wird. Weiters werden auch Versuche zur Polymerisation von 2,4-Spiroheptan und 2,5-Spirooctan zu Modellverbindungen für die umgelagerten Polymeren mitgeteilt.

Received September 16, 1963

Revised January 2, 1964

## Copolymerization of 4-Cyclopentene-1,3-dione with Acrylonitrile and Methyl Methacrylate\*

F. LYNN HAMB† and ANTHONY WINSTON, *Department of Chemistry,  
West Virginia University, Morgantown, West Virginia*

### Synopsis

The copolymerization of acrylonitrile and methyl methacrylate with 4-cyclopentene-1,3-dione ( $M_2$ ) is reported. The copolymers were prepared by heating the monomer feeds in sealed tubes with  $\alpha, \alpha'$ -azobisisobutyronitrile. Infrared bands for both the  $\beta$ -diketone and the nitrile, in the case of acrylonitrile, or ester, in the case of methyl methacrylate, indicated that copolymerization had occurred. The acrylonitrile copolymers were insoluble in the common solvents and swelled on treatment with dimethylformamide and dimethylsulfoxide. The methyl methacrylate copolymers were partially soluble in the usual solvents with the solubility and gel content varying with the composition of the copolymers. Solution viscosities indicated high molecular weights. The reduced specific viscosity of the sodium salt of the 0.05 methyl methacrylate copolymer increased with decreasing concentration, a characteristic typical of polyelectrolytes. The compositions of the copolymers were determined from the nitrogen analyses for acrylonitrile copolymers, and the ultraviolet absorption of the  $\beta$ -diketone for the methyl methacrylate copolymers. The molar extinction coefficient of the  $\beta$ -diketone structural unit was estimated from a study of model compounds. The reactivity ratios were evaluated by the usual methods. For the acrylonitrile ( $M_1$ )-4-cyclopentene-1,3-dione ( $M_2$ ) system,  $r_1 = 3.67$ ,  $r_2 = 0.21$ . For the methyl methacrylate ( $M_1$ )-4-cyclopentene-1,3-dione ( $M_2$ ) system  $r_1 = 7.4$ ,  $r_2 = 0.083$ . For each system  $Q$  and  $e$  values for 4-cyclopentene-1,3-dione were evaluated. The average values are  $Q = 0.20$ ,  $e = 1.42$ . The behavior of 4-cyclopentene-1,3-dione is compared with maleic anhydride and *N*-butylmaleimide with respect to the reactivity of the monomer, the reactivity of the radical, and the effective polarity of the double bond.

### INTRODUCTION

It has long been recognized that radicals derived from 1,2-disubstituted ethylenes have a low order of reactivity toward their parent monomers, as illustrated by their extremely low copolymerization reactivity ratios.<sup>1</sup> Many of these monomers, although reactive in copolymerization, do not homopolymerize satisfactorily to give high polymers.<sup>2a</sup> Cyclic five-membered monomers are irregular in their reactivities. Although vinylene carbonate polymerizes readily under mild conditions,<sup>2a</sup> maleic anhydride is quite resistant, and the polymerization has only recently been satisfactorily

\* Taken in part from the Ph.D. dissertation of F. Lynn Hamb (1963), West Virginia University.

† N.D.E.A. Predoctoral Fellow, 1960-1963.



effected under rather severe conditions.<sup>3</sup> In contrast to the low reactivity of maleic anhydride in vinyl homopolymerization, maleimide, a closely related monomer, homopolymerizes rapidly under mild conditions.<sup>4</sup> Apparently the substitution of a —NH— group for the —O— group in the ring enhances the reactivity of the radical with its own monomer. Since maleic anhydride and maleimide are sterically and electronically similar, it becomes difficult to assign a specific cause to this difference in reactivity in free radical polymerization.

The recent availability<sup>5,6</sup> of 4-cyclopentene-1,3-dione, a monomer similar in structure to maleic anhydride and maleimide, but containing a —CH<sub>2</sub>— group in place of the —O— or —NH—, makes possible through homopolymerization and copolymerization studies further comparisons of the effects of various substituents in the ring on the reactivities of double bonds in cyclic structures. The dione is a very reactive dieneophile in the Diels-Alder reaction and, through its methylene group, readily undergoes acid-catalyzed condensation with aldehydes.<sup>7</sup> In base, polymerization occurs by a proposed anionic mechanism.<sup>7</sup>

The purpose of this paper is to report the free-radical copolymerization of 4-cyclopentene-1,3-dione with acrylonitrile and methyl methacrylate and to compare the reactivity of this monomer with other cyclic monomers, particularly maleic anhydride and maleimide, through reactivity ratios and the Alfrey-Price<sup>8</sup> *Q* and *e* values.

## EXPERIMENTAL

### Materials

A mixture of 3-cyclopentene-1,2-diol and 4-cyclopentene-1,3-diol was prepared by the peracetic acid oxidation of cyclopentadiene.<sup>9</sup> Oxidation with chromic acid afforded 4-cyclopentene-1,3-dione.<sup>7</sup> The compound was recrystallized three times from ethyl ether and dried before use.

Acrylonitrile (Eastman Organic Chemicals) was passed through a silica gel column just prior to use to remove the hydroquinone inhibitor.<sup>2b</sup>

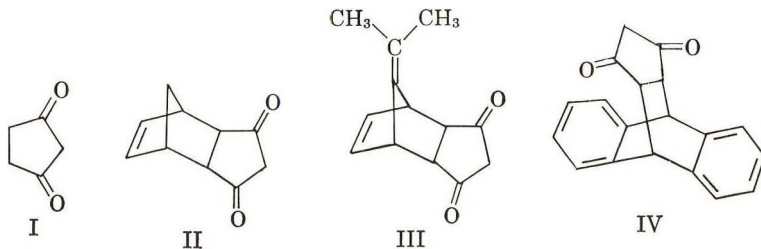
Methyl methacrylate (Matheson, Coleman and Bell) was washed with 5% sodium hydroxide, then with water, and was dried over anhydrous magnesium sulfate. The monomer was distilled at 50°C./125 mm. just prior to use.

$\alpha, \alpha'$ -Azobisisobutyronitrile (The Borden Chemical Company) was recrystallized from ethyl ether to give white needles, m.p. 94°C. (dec.).

Benzene was washed with sulfuric acid, then with water and was dried over calcium chloride. It was distilled through a 30-in. packed column, and the middle fraction was collected and stored over sodium.

### Model Compounds

Compounds I–IV were prepared for use in estimating the molar extinction coefficient of the  $\beta$ -diketone unit in methyl methacrylate copolymers.



Cyclopentane-1,3-dione (I) was prepared by reduction of 4-cyclopentene-1,3-dione with zinc dust in acetic acid.<sup>5</sup>

The Diels-Alder adducts II and IV were prepared by the condensation of 4-cyclopentene-1,3-dione with cyclopentadiene<sup>5</sup> and anthracene,<sup>5,10</sup> respectively.

Compound III was prepared by a Diels-Alder reaction between 2.0 g. (0.019 mole) of dimethylfulvene and 1.5 g. (0.015 mole) of 4-cyclopentene-1,3-dione in 4 ml. of benzene. After three days at room temperature the reaction mixture consisted of a mass of tacky solid. The solid (0.6 g.) was collected and recrystallized from chloroform to yield white crystals of the adduct, m.p. 200–201°C.

ANAL. Calcd.  $C_{13}H_{14}O_2$ : C, 77.20%; H, 6.98%. Found: C, 77.31%; H, 6.85%.\*

## Copolymerization with Acrylonitrile

### *Polymerization Procedure*

A homogeneous solution of the desired molar ratio of acrylonitrile and 4-cyclopentene-1,3-dione in benzene was charged into a thick-walled tube. The initiator,  $\alpha, \alpha'$ -azobisisobutyronitrile, was added in the amount of 0.015 mole-% of the total charge. The sample was degassed a minimum of three times by alternate cooling in liquid air and warming under low pressure. The tube was sealed under 0.1–0.2 mm. pressure of nitrogen and placed in a constant temperature bath at  $60 \pm 0.1^\circ\text{C}$ . The mixture was heated and stirred until reaction was estimated to have proceeded to 2 or 3% conversion, as evidenced by the precipitation of the polymer. Stirring was accomplished by the agitation of a small bar magnet in the tube by a magnetic stirrer placed outside the bath adjacent to the tube. The tube was opened, and the contents were poured into ethyl ether. After settling, the copolymers were filtered, washed with ether, dried in air, and weighed to determine the per cent conversion.

### *Characterization and Analysis*

In the infrared spectra of the copolymers a sharp band at  $2240\text{ cm}^{-1}$  (nitrile) and a broad band with its maximum at  $1590\text{ cm}^{-1}$  ( $\beta$ -diketone) are evidence that both monomers participate in the polymerization reaction.

\* Elemental analyses by Galbraith Laboratories, Inc., Knoxville, Tennessee.

The copolymers from all feed compositions have very similar solubility properties. The copolymers are swollen by dimethylformamide and dimethyl sulfoxide. They are insoluble in diethyl carbonate, methanol, benzene, acetone, chloroform, tetrahydrofuran, petroleum ether (30–60°C.), and ethyl ether. The general insolubility and the swelling of the copolymers in dimethylformamide and dimethyl sulfoxide may be indicative of crosslinking between polymer chains.

In the heat of a Bunsen flame the copolymers fuse into brittle pellets. Films of the copolymers, fabricated at 20,000 lb. and 140–150°C., are transparent, amber in color, hard, and very brittle.

TABLE I  
Reactivity Ratio Data for the Copolymerization of  
Acrylonitrile ( $M_1$ ) and 4-Cyclopentene-1,3-dione ( $M_2$ ) in Benzene

$f_1$ Mole fraction $M_1$ in feed	Time, min.	Conversion, %	N, %	$F_1$ mole fraction $M_1$ in polymer
0.90	90	2.79	24.01	0.94
0.80	120	1.62	23.63	0.93
0.60	160	1.85	19.92	0.85
0.40	185	1.63	14.89	0.70
0.25	195	2.06	13.49	0.65
0.15	225	1.64	11.08	0.57
0.05	440	2.30	1.73	0.11

The copolymers were ground to a finely divided state, washed repeatedly with ether, dried in air, and subsequently dried under high vacuum at 80°C. for 4–5 hr. The composition was determined from nitrogen analyses. The polymerization data are presented in Table I.

### Copolymerization with Methyl Methacrylate

#### *Polymerization Procedure*

To the desired ratio of methyl methacrylate and 4-cyclopentene-1,3-dione dissolved in pure dry benzene was added 0.5 mole-% of the total charge  $\alpha, \alpha'$ -azobisisobutyronitrile. The mixture was charged into a thick-walled tube and degassed twice under a low pressure of nitrogen by alternate warming and cooling in a Dry Ice-acetone bath. The tube was sealed and placed in a constant temperature bath at  $65 \pm 1^\circ\text{C}$ . The contents were stirred with a small bar magnet until the polymerization had proceeded to a 2–5% conversion, as evidenced by the increased viscosity. The polymer was precipitated by addition of the mixture to petroleum ether (30–60°C.) for feeds of high methyl methacrylate content or ethyl ether for feeds of low methyl methacrylate content. The precipitated polymers were collected by filtration, dried in air, and weighed. The polymerization data and conversions are reported in Table II.

TABLE II  
Conversion Data for Copolymerization of Methyl Methacrylate ( $M_1$ )  
and 4-Cyclopentene-1,3-dione ( $M_2$ ) in Benzene

$f_1$ Mole fraction $M_1$ in feed	Total feed, moles	Vol. benzene, ml.	Time, min.	Conversion %
1.00	0.040	5	210	30.0
0.95	0.0737	5	30	4.35 <sup>a</sup>
0.90	0.0778	5	30	3.61
0.80	0.100	10	50	6.54 <sup>b</sup>
0.70	0.121	10	35	2.76 <sup>c</sup>
0.60	0.100	5	50	6.61 <sup>d</sup>
0.50	0.0816	10	35	3.25
0.40	0.100	10	65	4.30
0.25	0.100	10	35	3.91
0.15	0.0807	10	35	1.14
0.10	0.0697	12	50	2.08
0.05	0.100	12	55	0.62

<sup>a</sup> Trace of gel.

<sup>b</sup> 12% gel.

<sup>c</sup> 47% gel.

<sup>d</sup> 65% gel.

The copolymers were purified by precipitation into petroleum ether from ethyl acetate solution after separation of any insoluble material. The copolymers from the 0.05, 0.10, 0.15 feeds were not reprecipitated, as these tended to form emulsions. The polymers were dried under reduced pressure over phosphorus pentoxide at 80°C.

#### *Characterization of the Copolymers*

**Spectra.** Infrared absorption bands at 1730  $\text{cm.}^{-1}$  (ester) and 1600  $\text{cm.}^{-1}$  ( $\beta$ -diketone) indicate the presence of both methyl methacrylate and 4-cyclopentene-1,3-dione structural units in the copolymers. Ultraviolet absorption, characteristic of  $\beta$ -diketones, occurs at 247  $m\mu$  for ethanol solutions of the copolymers or 255  $m\mu$  for chloroform solutions.

**Solubility.** In general, the copolymers from feeds above 0.25 mole fraction methyl methacrylate are either partially or completely soluble in ethyl acetate, benzene, chloroform, acetone, tetrahydrofuran, and methyl ethyl ketone, the solubility decreasing progressively with increasing concentration of the dione in the copolymer. On the other hand, the solubility in ethanol and aqueous sodium hydroxide increases with increasing dione content. In dimethylformamide and dimethyl sulfoxide the copolymers are partially soluble over the entire composition range.

In all of the copolymerizations gel was formed, Table II, which showed considerable swelling with various solvents. The occurrence of gel, the amount of which increased with increasing 4-cyclopentene-1,3-dione content, may be a result of crosslinking, possibly through the active hydrogens of the  $\beta$ -diketone unit.

**Softening Behavior.** Clear, flexible films of the copolymers could be cast from ethyl acetate or chloroform solution. The softening point of the films, as determined on a K $\ddot{o}$ ffler hot stage, decreased with increasing dione concentration. At higher temperatures the copolymers of low dione content melted to viscous oils (Table III).

TABLE III  
Melting and Softening Behavior of Methyl Methacrylate-  
4-Cyclopentene-1,3-dione Copolymers  
(Films Cast from Chloroform)

Feed composition, mole fraction MMA	Softening point, °C.	High temperature behavior
1.0	145	Viscous, rubbery
0.95	140	Viscous liquid at 290°C.
0.90	135	Viscous liquid at 280°C.
0.80	125	Darkens at 200°C., does not melt
0.70	125	Darkens at 200°C., does not melt

**Solution Viscosity.** The intrinsic viscosities of several of the copolymers and of poly(methyl methacrylate) prepared under similar conditions are compared in Table IV. Although the molecular weights of the copolymers are not known, the high intrinsic viscosities indicate a reasonably high degree of polymerization.

TABLE IV  
Intrinsic Viscosities of Methyl Methacrylate ( $M_1$ )-  
4-Cyclopentene-1,3-dione Copolymers in Chloroform at 30°C.

Feed ratio, mole fraction $M_1$	Intrinsic viscosity of copolymer
1.0	1.36 $\pm$ 0.05
0.95	2.11 $\pm$ 0.05
0.90	2.30 $\pm$ 0.05
0.80	1.36 $\pm$ 0.07
0.70	1.75 $\pm$ 0.05

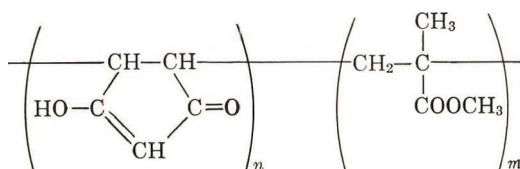
TABLE V  
Viscosity Data for Aqueous Solutions of  
the Sodium Salt of the 0.05  $M_1$  Copolymer

Concentration g./100 ml.	$\eta_{sp}$	$\eta_{sp}/c$
0.1267	0.094	0.742
0.0634	0.059	0.931
0.0422	0.045	1.06
0.0317	0.036	1.13
0.0253	0.031	1.22

The sodium salt of the copolymer from the 0.05 mole fraction feed was prepared by potentiometric titration with sodium hydroxide in 10% aqueous ethanol. The solvent was evaporated, and the copolymer salt was washed quickly with a small amount of water and dried. Viscosity measurements on aqueous solutions of the copolymer salt revealed that the reduced specific viscosity increases with decreasing concentration (Table V), a behavior consistent with the electrolytic nature of the copolymer salt.

#### Analysis of the Copolymers

**Methods.** Two methods of analysis are indicated by the structure (V) of the copolymer: titration of the  $\beta$ -diketone through its enolic hydrogen or ultraviolet measurements of the conjugated carbonyl.



V

Although potentiometric titration of several of the copolymers in aqueous ethanol provided some analytical data, the low solubility of many of the polymers in solvents suitable for titration prevented this method from being used to cover the entire range of copolymer composition. By using two solvents, ethanol and chloroform, however, it was possible to measure the composition of all but one (0.25 feed) of the copolymers by their ultraviolet absorption.

**Ultraviolet of Model Compounds.** The wavelength and the molar extinction coefficient for the  $\beta$ -diketone structural unit in the copolymer was estimated from the ultraviolet data for model compounds I-IV in two solvents, 95% ethanol and chloroform (Table VI).

From Table VI, the extinction coefficient of the  $\beta$ -diketone structural unit was assigned the values 9290 for ethanol solutions and 3555 for chloroform solutions. These values were taken as the average for compounds

TABLE VI  
Ultraviolet Absorption of Model Compounds

Compound	95% Ethanol			Chloroform		
	Concn., mole/l. $\times 10^6$	$\lambda_{\text{max}}$ , m $\mu$	$\epsilon$	Concn., mole/l. $\times 10^5$	$\lambda_{\text{max}}$ , m $\mu$	$\epsilon$
I	1.98	245	12,000	16.0	246	3,800
II	1.36	263	9,260	16.2	249	6,300
III	1.29	264	9,460	15.8	246	3,510
IV	1.75	265	9,140	16.0	248	3,600

II, III, and IV for ethanol solutions and III and IV for chloroform. Compound I, which lacks substitution at the 4 and 5 positions of the ring and is, therefore, not as closely related to the disubstituted structural unit of the copolymers as were compounds II–IV, was not included in the average. The cause of the high extinction coefficient for compound II in chloroform is not known at this time, but it may be due to a difference in solvent effect on the two possible forms, *exo* and *endo*, both of which might have been present. Minor variations in the wavelength and extinction coefficient with concentration<sup>11</sup> were minimized by maintaining reasonably constant concentrations.

**Copolymer Composition Analysis.** The analytical data for the copolymers are presented in Table VII. The absorbancy,  $A_{(\text{obs})}$ , of the copolymer at  $\lambda_{\text{max}}$  for the  $\beta$ -diketone unit was determined with a Beckman DU quartz spectrophotometer. For the copolymers of low dione content, it was necessary to correct the  $A_{(\text{obs})}$  values for the absorption of the methyl methacrylate units in order to obtain the absorbancy due solely to the dione. This was done in the following way. The extinction coefficient of the methyl methacrylate structural unit for poly(methyl methacrylate) in chloroform was determined at each of the reported wavelengths. These values varied in magnitude between 2 and 6. From the molar extinction coefficient of the dione, an approximate copolymer composition was calculated by assuming  $A_{(\text{obs})} = A_{(\text{M}_2)}$ . The absorbancy arising from the dione units,  $A_{(\text{M}_2)}$ , was then determined from the relationship

$$A_{(\text{M}_2)} = A_{(\text{obs})} - c_{(\text{M}_1)}\epsilon_{(\text{M}_1)}$$

The corrected copolymer composition was then calculated from  $A_{(\text{M}_2)}$ . For the copolymer of high dione content this correction is negligible.

TABLE VII  
Ultraviolet Analytical Data for Copolymers of Methyl Methacrylate ( $\text{M}_1$ ) and 4-Cyclopentene-1,3-dione ( $\text{M}_2$ )

$f_1$ Mole fraction $\text{M}_1$ in feed	Solvent	Concn., g./l.	$\lambda_{\text{max}}$	Absorbance			$F_1$ Mole fraction $\text{M}_1$ in polymer
				Obs.	MMA	$\text{M}_2$	
0.95	$\text{CHCl}_3$	0.8300	259	0.237	0.022	0.215	0.993
0.90	"	0.5600	250	0.250	0.032	0.218	0.990
0.80	"	0.4040	255	0.393	0.016	0.377	0.974
0.70	"	0.2180	252	0.388	0.006	0.382	0.953
0.60	"	0.2900	254	0.873	0.008	0.865	0.920
0.50	"	0.2650	251	1.070	0.009	1.061	0.892
0.40	"	0.0365	252	0.228	0.001	0.227	0.832
0.15	$\text{C}_2\text{H}_5\text{OH}$	0.0160	248	0.585	—	0.585	0.609
0.10	"	0.0200	247	0.905	—	0.905	0.520
0.05	"	0.0150	246	0.822	—	0.822	0.423

## RESULTS

## Copolymerization with Acrylonitrile

In Figure 1 the mole fraction acrylonitrile in the copolymer  $F_1$  is plotted against the mole fraction in the monomer feed  $f_1$ . Treatment of the copolymer equation by the method of Mayo and Lewis<sup>12</sup> provided the series of lines shown in Figure 2. Values of  $r_1$  and  $r_2$  were determined from the

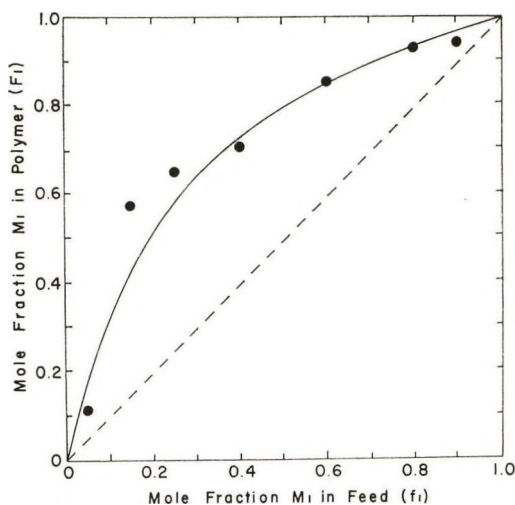


Fig. 1. Copolymerization of acrylonitrile ( $M_1$ ) with 4-cyclopentene-1,3-dione ( $M_2$ ). The solid curve was calculated for  $r_1 = 3.7$ ,  $r_2 = 0.20$ .

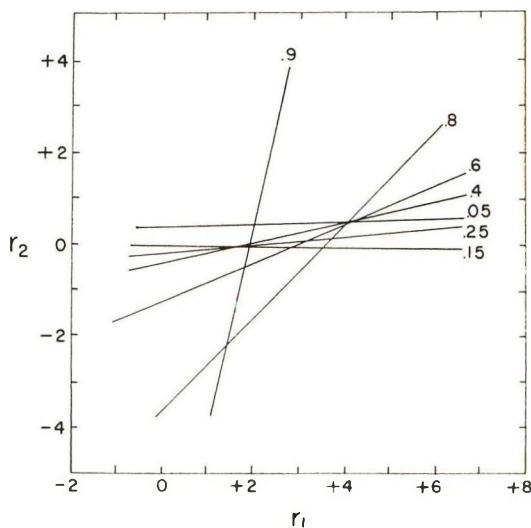


Fig. 2. Mayo-Lewis plot for determining reactivity ratios for the system acrylonitrile ( $M_1$ )–4-cyclopentene-1,3-dione ( $M_2$ ). The numbers at each line are the feed compositions.  $r_1 = 3.5 \pm 0.6$ ,  $r_2 = 0.2 \pm 0.2$ .



TABLE VIII  
Reactivity Ratios for the System  
Acrylonitrile ( $M_1$ ) and 4-Cyclopentene-1,3-dione ( $M_2$ )

No.	Method	$r_1$	$r_2$
1	Mayo and Lewis	$3.0 \pm 1.0$	$0.25 \pm 0.25$
2	Modified Mayo and Lewis, excluding 0.9 data	$3.5 \pm 0.6$	$0.2 \pm 0.2$
3	Fineman-Ross	3.80	0.24
4	Curve-fitting	3.70	0.20
5	Average of 2, 3, and 4	3.67	0.21

region of intersection bounded by the 0.9, 0.8, 0.05, and 0.15 feed lines, an area which includes all of the experimental data. If the somewhat uncertain 0.9 feed line is omitted, the area of intersection becomes bounded by the 0.8, 0.6, 0.15 feed lines, providing modified values of  $r_1$  and  $r_2$ . Although this operation has little effect on  $r_2$ ,  $r_1$  is changed to a significantly higher value (Table VIII).

The solution of the copolymer equation by the method of Fineman and Ross<sup>13</sup> is shown in Figure 3, where the solid line is the least-squares fit to the experimental data. In this case, in order to obtain a real solution it was necessary to exclude the 0.9 feed because its inclusion resulted in a positive intercept on the  $R(\rho - 1)/\rho$  axis giving an impossible negative value for  $r_2$ . The necessity for such an omission provides further justification for similar action in the Mayo-Lewis solution.

With the aid of the IBM 1620 digital computer appropriate values for  $r_1$  and  $r_2$ , taken within the intersection area of the Mayo-Lewis plot, Fig-

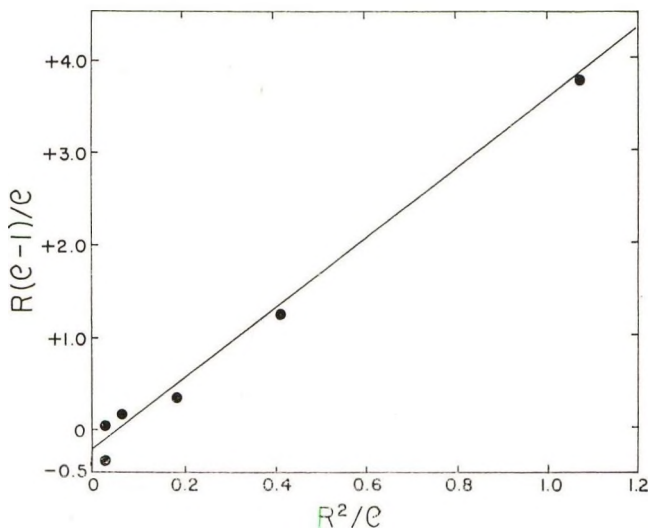


Fig. 3. Fineman-Ross plot for determining reactivity ratios for the system acrylonitrile ( $M_1$ )-4-cyclopentene-1,3-dione ( $M_2$ ).  $r_1 = 3.80$ ,  $r_2 = 0.24$ .

ure 2, were assigned, and  $F_1$  versus  $f_1$  curves were calculated. The solid curve in Figure 1 was judged to represent the best fit to the experimental data. The reactivity ratios as determined by the several methods are compared in Table VIII. The best value of the reactivity ratios is reported as the average of numbers 2, 3, and 4.

### Copolymerization with Methyl Methacrylate

The analytical data of Table VII are presented in Figure 4 as a graph of the mole fraction of methyl methacrylate in the copolymer  $F_1$  versus the

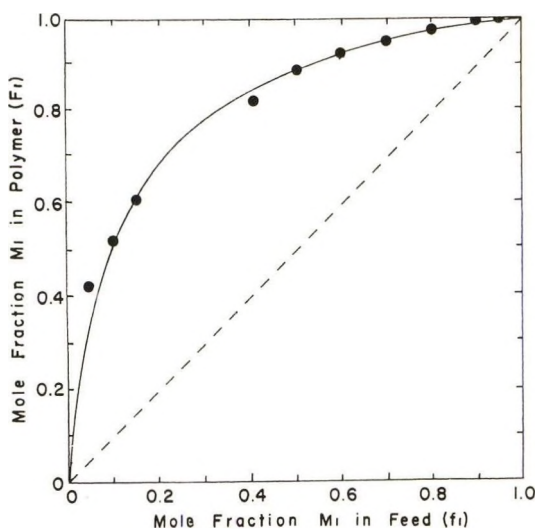


Fig. 4. Copolymerization of methyl methacrylate ( $M_1$ )-4-cyclopentene-1,3-dione ( $M_2$ ). The solid curve was calculated for  $r_1 = 7.35$ ,  $r_2 = 0.075$ .

mole fraction of methyl methacrylate in the monomer feed  $f_1$ . At all feed compositions the mole fraction of methyl methacrylate is greater in the copolymer than in the feed.

Treatment of the composition data by the method of Mayo and Lewis is shown in Figure 5. The reactivity ratios are taken as the center of the area where the maximum number of intersections occur, an assignment which omits the data for the 0.90, 0.80, and 0.70 feeds. Solution of the

TABLE IX  
Reactivity Ratios for the System Methyl  
Methacrylate ( $M_1$ ) and 4-Cyclopentene-1,3-dione ( $M_2$ )

No.	Method	$r_1$	$r_2$
1	Mayo and Lewis	$7.5 \pm 0.5$	$0.10 \pm 0.05$
2	Fineman-Ross	7.35	0.074
3	Curve-fitting	7.35	0.075
4	Average of 1, 2, and 3	7.4	0.083

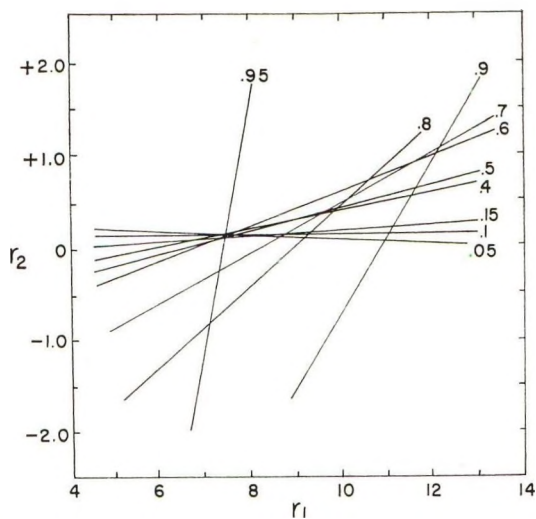


Fig. 5. Mayo-Lewis plot for determining reactivity ratios for the system methyl methacrylate ( $M_1$ )-4-cyclopentene-1,3-dione ( $M_2$ ). The numbers represent feed compositions.  $r_1 = 7.5 \pm 0.5$ ,  $r_2 = 0.10 \pm 0.05$ .

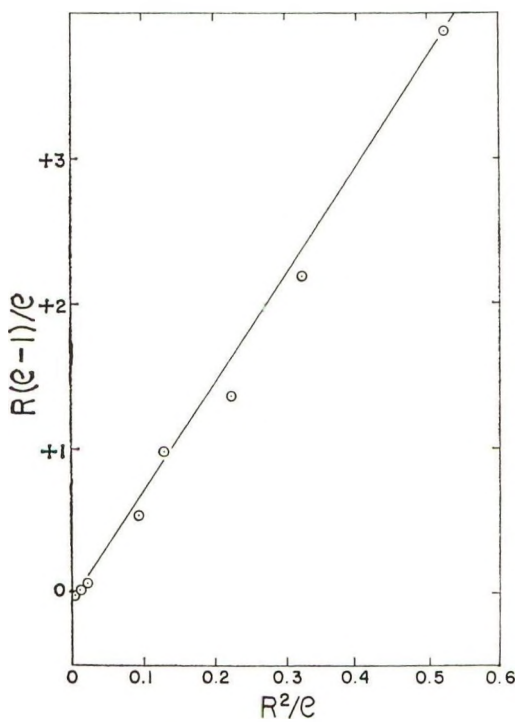


Fig. 6. Fineman-Ross plot for determining reactivity ratios for the system methyl methacrylate ( $M_1$ )-4-cyclopentene-1,3-dione ( $M_2$ ).  $r_1 = 7.35$ ,  $r_2 = 0.074$ .

copolymer equation by the method of Fineman and Ross is shown in Figure 6. Here it was necessary to omit the data for the 0.95 and 0.90 feeds since their inclusion resulted in a positive intercept on the  $R(\rho - 1)/\rho$  axis and a corresponding impossible negative value for  $r_2$ . In the solution by the curve-fitting method, the solid curve in Figure 4 was judged to give the best fit to the experimental data. The reactivity ratios obtained by the three methods are compared and averaged in Table IX.

## DISCUSSION

The  $Q$  and  $e$  parameters for 4-cyclopentene-1,3-dione were calculated by using the values  $Q = 0.50$ ,  $e = 1.23$  for acrylonitrile<sup>14</sup> and  $Q = 0.73$ ,  $e = 0.4$  for methyl methacrylate.<sup>15</sup> These results are compared in Table X and averaged to provide the best  $Q$  and  $e$  values.

TABLE X  
 $Q$  and  $e$  Values for 4-Cyclopentene-1,3-dione

	Copolymerization with		Average
	Acrylonitrile	Methyl methacrylate	
$Q$	0.26	0.13	0.20
$e$	1.74	1.10	1.42

The relative reactivities of acrylonitrile and 4-cyclopentene-1,3-dione with the two polymer radicals are tabulated in Table XI. The corresponding information for maleic anhydride, taken from copolymerization with acrylonitrile ( $M_1$ ) ( $r_1 = 6$ ,  $r_2 = 0$ ),<sup>17</sup> is included for comparison.

TABLE XI  
Relative Reactivities of Monomers with Polymer Radicals

Monomer	Radical	
	Acrylonitrile	4-Cyclopentene-1,3-dione
Acrylonitrile	1	4.8
4-Cyclopentene-1,3-dione	0.27	1
Maleic anhydride <sup>a</sup>	0.16	—

<sup>a</sup> Data of Mayo, Lewis, and Walling.<sup>16</sup>

Both radicals are more reactive toward acrylonitrile monomer than toward the dione. In reaction with the acrylonitrile radical the dione is about 1.7 times more reactive than maleic anhydride. In contrast with maleic anhydride, which resists adding its own kind, the dione radical does have a slight tendency to add dione monomer, as indicated by a reactivity ratio  $r_2$  greater than zero.

The relative reactivities of methyl methacrylate and 4-cyclopentene-1,3-dione with the two polymer radicals are given in Table XII and compared with corresponding information secured from copolymerization studies of methyl methacrylate with maleic anhydride ( $r_1 = 6.7$ ,  $r_2 = 0.02$ );<sup>17</sup> ( $r_1 = 3.5$ ,  $r_2 = 0.03$ );<sup>18</sup> and *N*-butylmaleimide ( $r_1 = 1.33$ ,  $r_2 = 0.12$ ).<sup>19</sup>

TABLE XII  
Relative Reactivities of Monomers with Polymer Radicals

Monomer	Radical			
	Methyl methacrylate	4-Cyclopentene-1,3-dione	Maleic anhydride	<i>N</i> -Butylmaleimide
Methyl methacrylate	1	12	50 <sup>a</sup> , 33 <sup>b</sup>	8.3 <sup>c</sup>
4-Cyclopentene-1,3-dione	0.14	1	—	—
Maleic anhydride	0.15, <sup>a</sup> 0.24 <sup>b</sup>	—	1	—
<i>N</i> -Butylmaleimide	0.75 <sup>a</sup>	—	—	1

<sup>a</sup> Data of de Wilde and Smets.<sup>17</sup>

<sup>b</sup> Data of Blackley and Melville.<sup>18</sup>

<sup>c</sup> Data of Coleman and Conrady.<sup>19</sup>

Comparison of the relative reactivities of methyl methacrylate and 4-cyclopentene-1,3-dione radicals (Table XII) shows that both of these radicals are considerably more reactive with methyl methacrylate monomer than with dione monomer. This behavior is very similar to that observed when acrylonitrile is the comonomer. Comparison of the three cyclic monomers with respect to their reactivity toward the methyl methacrylate radical indicates the following order of reactivity: *N*-butylmaleimide > maleic anhydride ≥ 4-cyclopentene-1,3-dione. The same order of reactivity of the monomers is indicated by their relative *Q* values (Table XIII).

Assuming almost equal reactivities of the dione and maleic anhydride monomers, it then appears that the dione radical is less discriminating than maleic anhydride radical (Table XII), and, hence, would have a greater intrinsic reactivity. The relative *e* values indicate the following order of electron attracting ability of the groups substituted on the double bond of

TABLE XIII  
*Q* and *e* Data for Cyclic Monomers

	4-Cyclopentene-1,3-dione	Maleic anhydride <sup>a</sup>	Maleic anhydride <sup>b</sup>	<i>N</i> -Butylmaleimide <sup>c</sup>
<i>Q</i>	0.20	0.19	0.38	0.94
<i>e</i>	1.42	1.8	1.9	1.75

<sup>a</sup> Data of de Wilde and Smets.<sup>17</sup>

<sup>b</sup> Data of Blackley and Melville.<sup>18</sup>

<sup>c</sup> Data of Coleman and Conrady.<sup>19</sup>

the cyclic monomers: maleic anhydride  $\geq$  *N*-butylmaleimide  $>$  4-cyclopentene-1,3-dione. This is the same order as would be expected from a consideration of the availability of the electrons on the —O—, the —NR—, or the —CH<sub>2</sub>— for participation in a resonance distribution of the charges between the carbonyl groups. The slightly lower *e* for the dione indicates less radical stabilization, resulting in lower reactivity of the monomer and a greater reactivity of the product radical.

These studies of the reactions of cyclic five-membered monomers are continuing, and in a future publication will be reported the copolymerization of 4-cyclopentene-1,3-dione with styrene.

We should like to express our appreciation to the West Virginia University Data Processing Center for computer service and to C. H. DePuy for information concerning the synthesis of 4-cyclopentene-1,3-dione prior to publication.

### References

1. Young, L. J., *J. Polymer Sci.*, **54**, 411 (1961).
2. Sorenson, W., and T. W. Campbell, *Preparative Methods of Polymer Chemistry*, Interscience, New York, 1961, (a) pp. 188–189; (b) p. 168.
3. Lang, J. L., W. A. Pavelich, and H. D. Clarey, *J. Polymer Sci.*, **A1**, 1123 (1963).
4. Tawney, P. O., R. H. Snyder, R. P. Conger, K. A. Leibbrand, C. H. Stiteler, and A. R. Williams, *J. Org. Chem.*, **26**, 15 (1961).
5. DePuy, C. H., and E. F. Zaweski, *J. Am. Chem. Soc.*, **81**, 4920 (1959).
6. Rasmusson, G. H., H. O. House, E. F. Zaweski, and C. H. DePuy, *Org. Syntheses*, **42**, 36 (1962).
7. DePuy, C. H., and P. R. Wells, *J. Am. Chem. Soc.*, **82**, 2909 (1960).
8. Alfrey, T., and C. C. Price, *J. Polymer Sci.*, **2**, 101 (1947).
9. Korach, M., D. R. Nielsen, and W. H. Rideout, *Org. Syntheses*, **42**, 50 (1962).
10. DePuy, C. H., and C. E. Lyons, *J. Am. Chem. Soc.*, **82**, 631 (1960).
11. Bastron, H., R. E. Davis, and L. W. Butz, *J. Org. Chem.*, **8**, 515 (1943).
12. Mayo, F. R., and F. M. Lewis, *J. Am. Chem. Soc.*, **66**, 1594 (1944).
13. Fineman, M., and S. D. Ross, *J. Polymer Sci.*, **5**, 259 (1950).
14. Lewis, F. M., F. R. Mayo, and W. F. Hulse, *J. Am. Chem. Soc.*, **67**, 1701 (1945).
15. Lewis, F. M., C. Walling, W. Cummings, E. R. Briggs, and F. R. Mayo, *J. Am. Chem. Soc.*, **70**, 1519 (1948).
16. Mayo, F. R., F. M. Lewis, and C. Walling, *J. Am. Chem. Soc.*, **70**, 1529 (1948).
17. de Wilde, M. C., and G. Smets, *J. Polymer Sci.*, **5**, 253 (1950).
18. Blackley, D. C., and H. W. Melville, *Macromol. Chem.*, **18/19**, 16 (1956).
19. Coleman, L. E., Jr., and J. A. Conrady, *J. Polymer Sci.*, **38**, 241 (1959).

### Résumé

On rend compte de la copolymérisation de l'acrylonitrile et du méthacrylate de méthyle avec la 4-cyclopentène-1,3-dione (M<sub>2</sub>). Les copolymères ont été préparés en chauffant les réactifs monomériques en tube scellé en présence d' $\alpha,\alpha,\alpha$ -azo-bis isobutyronitrile. La présence à l'infra rouge de bandes caractéristiques de la  $\beta$  dicétone et du nitrile (dans le cas de l'acrylonitrile) ou de l'ester (dans le cas du méthacrylate de méthyle) indiquent que la copolymérisation a bien eu lieu. Les copolymères d'acrylonitrile sont insolubles dans les solvants habituels et gonflent par traitement au diméthylformamide et au diméthylsulfoxyde. Les copolymères de méthacrylate de méthyle sont partiellement solubles dans les solvants usuels et la solubilité et le contenu en gal varient avec la composition des copolymères. La viscosité des solutions indique des poids moléculaires élevés. La viscosité spécifique réduite du sel sodique du copolymère 0.05 de méthacrylate de méthyle augmente avec la dilution, ce qui est caractéris-

tique des polyelectrolytes. Les compositions des copolymères ont été déterminées par analyse d'azote par les copolymères d'acrylonitrile et par l'absorption ultraviolette de la  $\beta$ -dicétone pour les copolymères de méthacrylate de méthyle. Le coefficient d'extinction molaire de l'unité structurale  $\beta$ -dicétone a été estimé sur la base d'un modèle. Les rapports de réactivité ont été calculés par la méthode ordinaire. Pour le système acrylonitrile ( $M_1$ )-4-cyclopentène-1,3-dione ( $M_2$ )  $r_1 = 3.67$   $r_2 = 0.21$ . Pour le système méthacrylate de méthyle ( $M_1$ )-4-cyclopentène-1,3-dione ( $M_2$ )  $r_1 = 7.4$  et  $r_2 = 0.083$ . Pour chaque système, les valeurs  $Q$  et  $e$  pour la 4-Cyclopentène-1,3-dione ont été calculées. La valeur moyenne de  $Q = 0.20$  et de  $e = 1.42$ . On compare le comportement de la 4-cyclopentène-1,3-dione avec celui de l'anhydride maléique et de la *N*-butylmaléimide en ce qui concerne la réactivité du monomère, celle du radical et le polarité effective de la double liaison.

### Zusammenfassung

Über die Copolymerisation von Acrylnitril und Methylmethacrylat mit 4-Cyclopenten-1,3-dion ( $M_2$ ) wird berichtet. Die Copolymeren wurde durch Erhitzen der Monomermischungen in zugeschmolzenen Röhren mit  $\alpha, \alpha$ -Azo-bisobutyronitril hergestellt, Infrarotbanden für sowohl  $\beta$ -Diketon und Nitril, im Fall von Acrylnitril, als auch Ester, im Fall von Methylmethacrylat, lassen das Eintreten der Copolymerisation erkennen. Die Acrylnitrilcopolymeren waren in üblichen Lösungsmitteln unlöslich und quollen bei Behandlung mit Dimethylformamid und Dimethylsulfoxyd. Die Methylmethacrylatcopolymeren waren teilweise in üblichen Lösungsmitteln löslich, wobei die Löslichkeit und der Gelgehalt von der Copolymerzusammensetzung abhängig waren. Die Lösungsviskosität zeigt ein hohes Molekulargewicht an. Die reduzierte spezifische Viskosität des Natriumsalzes des 0,05 Methylmethacrylatcopolymeren nahm mit abnehmender Konzentration zu, was ein für Polyelektrolyte typisches Merkmal ist. Die Copolymerzusammensetzung wurde für Acrylnitrilcopolymeren aus der Stickstoffanalyse und für Methylmethacrylatcopolymeren aus der Ultraviolettabsorption des  $\beta$ -Diketons bestimmt. Der molare Extinktionskoeffizient der  $\beta$ -Diketonstruktureinheit wurde durch eine Untersuchung an Modellverbindungen bestimmt. Die Reaktivitätsverhältnisse wurden mit den üblichen Methoden berechnet. Für das Acrylnitril- ( $M_1$ )-4-Cyclopenten-1,3-dion ( $M_2$ )-system ergab sich  $r_1 = 3,67$ ,  $r_2 = 0,21$ . Für das Methylmethacrylat ( $M_1$ )-4-Cyclopenten-1,3-dion ( $M_2$ )-system  $r_1 = 7,4$ ,  $r_2 = 0,083$ . Für jedes System wurden  $Q$ - und  $e$ -Werte von 4-Cyclopenten-1,3-dion berechnet. Der Mittelwert beträgt  $Q = 0,20$ ,  $e = 1,42$ . Das Verhalten von 4-Cyclopenten-1,3-dion wird in bezug auf die Reaktivität des Monomeren, die Reaktivität des Radikals und die Effektivpolarität der Doppelbindung mit Maleinsäureanhydrid und *N*-Butylmaleinimid verglichen.

Received November 4, 1963

Revised January 14, 1964

## Measurement of Membrane Potentials and Test of Theories

N. LAKSHMINARAYANAIHAH, *Department of Pharmacology, University of Pennsylvania, Philadelphia, Pennsylvania*, and V. SUBRAHMANYAN, *Department of Chemistry, A. C. College of Technology, Guindy, Madras, India*

### Synopsis

The emf's of the system Ag, AgCl/NaCl ( $m^I$ )/membrane/NaCl( $m^{II}$ )/AgCl, Ag containing phenol-formaldehyde sulfonate membrane have been measured at 30°C. The membrane phase has been analyzed for its electrolyte and water contents and in-tramembrane activity coefficients have been derived as a function of external electrolyte concentration. Transference numbers of Na<sup>+</sup> counterion and water have been measured as functions of both current density and external concentration. The data have been used to test the principal theories of membrane potential. The fixed-charge theory of Teorell and Meyer and Sievers did not give satisfactory agreement between observed and calculated emf's of membrane cells, whereas the Scatchard theory did.

### I. INTRODUCTION

Several theories proposed in recent years of electrical potentials arising across homogeneous ion-exchange membranes separating different salt solutions have been reviewed and reformulated.<sup>1</sup> The fixed-charge theory of Teorell<sup>2</sup> and Meyer and Sievers<sup>3</sup> (T.M.S. theory) contains some assumptions about single ion activity coefficients in the membrane phase which make its application unrealistic and neglects the effect of solvent transfer on membrane potential.<sup>4</sup> The thermodynamic theory of Scatchard<sup>5</sup> takes this effect into account and describes the potential of a membrane cell of the type Ag, AgCl/NaCl ( $a^I$ )/membrane/NaCl ( $a^{II}$ )/AgCl, Ag in terms of the equation

$$E = - \frac{2RT}{F} \int_I^{II} (\bar{l}_+ - 10^{-3} m_{\pm} M \bar{l}_w) d \ln a_{\pm} \quad (1)$$

where  $E$  is the emf of the membrane cell,  $F$  the Faraday,  $m_{\pm}$  the mean molality of the electrolyte solution of activity  $a_{\pm}$ .  $\bar{l}_+$  and  $\bar{l}_w$  are the transference numbers of counterion and solvent, respectively, in the membrane phase (barred terms refer to the membrane phase).  $M$  is the molecular weight of the solvent. Use of this equation, however, calls for experimental determinations of  $\bar{l}_+$  and  $\bar{l}_w$  as functions of  $m_{\pm}$ .

The above equation has also been derived by others<sup>1,6</sup> by applying the



principles of irreversible thermodynamics to transport phenomena in membranes.

Hills, Jacobs, and Lakshminarayanaiah<sup>4</sup> have attempted comprehensive tests of the theories using relevant data acquired for crosslinked polymethacrylic acid (PMA) membrane and find the agreement between calculated and observed emf very disappointing. In their work, transport numbers of counterion and water have been determined at one specified current density only. Recent work has shown that the values of  $\bar{t}_+$ <sup>7,8</sup> and  $\bar{t}_w$ <sup>9</sup> are controlled by the current densities used in their determinations. Unless the values of  $\bar{t}_+$  and  $\bar{t}_w$  which are used in the calculations of cell emf are free from the effects of current density and electrolyte diffusion (see results), the attempt at testing the various theories of membrane potentials loses its validity.

This paper therefore describes a series of measurements of membrane cell emf and of transference numbers of counterion and water as functions of current density and external electrolyte concentration in phenol-formaldehyde sulfonate membranes. The approach of Hills et al.<sup>4</sup> has been adopted for a complete reassessment of the adequacy of the theories of membrane potentials to describe the emf's of even those membrane cells in which there is incomplete ionic selectivity.

## II. EXPERIMENTAL

### Preparation of Membranes

Appropriate weights of phenolsulfonic acid, 38% formaldehyde solution and water in the ratio 2:1:0.67, respectively, were mixed, and the resulting solution was transferred into glass formers (two glass plates separated by pieces of microscope cover slips and sealed at three edges). The fourth edge was also sealed. Polymerization was carried out by immersing the formers for 6 hr. in a water bath at 85°C. After cooling, the plates were separated, and brown, transparent, tough sheets of phenolsulfonic acid (PSA) membranes were taken out. They were washed thoroughly with distilled water and conditioned in 1*N* HCl solution. After decanting the acid, they were rinsed with conductivity water and converted into the Na<sup>+</sup> form by treating with 1*N* NaCl solution. They were next equilibrated in the solution to be used in subsequent experiments. The membranes had a thickness of ~0.5 mm.

### Solutions and Water Content of Membranes

NaCl (A.R.) recrystallized from conductivity water and dried at 200°C. was used. Standard solutions were prepared in conductivity water.

Pieces of membrane equilibrated in various NaCl solutions were surface dried between the folds of a filter paper and placed in a weighing bottle and weighed. They were dried to constant weight in an air oven at 110°C.

### Capacity of Membranes

A known weight of surface-dried membrane was treated with exactly 25 ml. of 0.1*N* HNO<sub>3</sub> and allowed to stand in a shaking machine for 24 hr. The liquid was decanted carefully, and the membrane was washed a number of times with conductivity water by agitating it in the shaking machine. The washings were transferred into the vessel containing the decanted liquid and the whole was analyzed for its acid and chloride contents by titrating against 0.05*N* carbonate-free NaOH and 0.05*N* AgNO<sub>3</sub>, respectively, in the usual way. The acid uptake of the membrane is equivalent to the quantity of fixed charges, and the chloride content is equivalent to the concentration of the coion. These two quantities determined for various electrolyte solutions were used in the Donnan equation

$$\bar{\gamma}_{\pm} e^{\pi V/2RT} = m_{\pm} \gamma_{\pm} / (\bar{m}_{+} \bar{m}_{-})^{1/2} \quad (2)$$

(where  $\gamma_{\pm}$  is the mean activity coefficient of the electrolyte in the membrane phase,  $\pi$  the difference between the swelling pressure in the membrane and the pressure in the external electrolyte solution of mean molality  $m_{\pm}$ ,  $\gamma_{\pm}$  is the mean-activity coefficient of the electrolyte,  $\bar{m}_{+}$  and  $\bar{m}_{-}$  are the molalities of the counterion and coion in the membrane phase) to derive corresponding values for the activity coefficient terms in the membrane phase.

### Membrane Potentials

The Na<sup>+</sup> form of the membrane equilibrated in the stronger of the two solutions to be used in the experiment was clamped between two half-cells in the silicone-greased rubber gaskets, the flanges being ends of industrial glass piping held together by Bakelite connectors. The half-cells were of the type described by Hills et al.<sup>10</sup> The membrane assembly thus formed the connecting limb of the two half-cells which were fitted with two inlet tubes on the sides reaching almost the surfaces of the membrane. These were used for flow of the NaCl solutions over the membrane faces by hydrostatic pressure. In the absence of other forces, this flow of solutions served to disturb or displace the diffusion layers existing at the two membrane surfaces. Each half-cell carried a pair of Ag-AgCl electrodes which were prepared by the procedure described by Brown.<sup>11</sup> The whole assembly was placed in an air thermostat maintained at 30 ± 0.1°C.

The emf of the cell Ag, AgCl/NaCl (*a*<sup>I</sup>)/membrane/NaCl (*a*<sup>II</sup>)/AgCl, Ag was measured by means of a Leeds and Northrup K-1 potentiometer and a d'Arsonval galvanometer (Cambridge Instrument Co.). Steady potentials observed at a solution flow rate of 5-6 l./hr. were recorded with a few membranes. The agreement between the pairs of electrodes was better than 10 μv. Measured emf's were discarded when the agreement between the values obtained with different membranes was not within 1%.

A steady but lower "equilibrium" emf was observed when there was no flow of solutions over the membrane surfaces. This potential described

the steady state in which the membrane existed with the diffusion layers extending outwards from its surfaces. These "equilibrium" emf's were highly reproducible and, therefore, suggested the existence of the diffusion layers close to the membrane faces.

### Water Transport

An apparatus of the type described elsewhere<sup>4,12</sup> was used in a water thermostat maintained at  $30 \pm 0.1^\circ\text{C}$ . Reversible Ag-AgCl electrodes were used.

The transference number of water was determined by measuring the volume changes in the anode and cathode compartments when a known quantity of electricity was passed through the system, solution ( $m$ )  $\rightleftharpoons$  membrane  $\rightleftharpoons$  solution ( $m$ ). A significant change in height, about 1 cm. of the level of liquid in the precision bore capillary, was brought about by passage of a small quantity of electricity (about 10 coulombs). There was little change in the concentration of solution on either side of the membrane. The hydrostatic pressure built up on the cathode side was compensated by adding light petroleum to the anode.

For the passage of 1 Faraday of current, at the cathode 1 mole of AgCl disappears, 1 mole of Ag and  $\bar{l}_+$  moles of NaCl appear. If  $V_c$  is the actual volume of solvent transported, then

$$V_c = V_0 + \bar{V}_{\text{AgCl}} - \bar{V}_{\text{Ag}} - \bar{l}_+ \bar{V}_{\text{NaCl}} \quad (3)$$

where  $V_0$  is the observed volume change per Faraday, the  $\bar{V}$  is the respective partial molar volumes and  $\bar{l}_+$  is the transport number of  $\text{Na}^+$ . Substituting 25.77 and 10.28 for  $\bar{V}_{\text{AgCl}}$  and  $\bar{V}_{\text{Ag}}$ , respectively, eq. (3) becomes

$$V_c = V_0 + 15.49 - \bar{l}_+ \bar{V}_{\text{NaCl}}$$

$\bar{V}_{\text{NaCl}}$  values for different concentrations are evaluated by using the usual equation.<sup>13</sup>  $\bar{l}_+$  values are taken from the data given in Table II. The same procedure was followed for determining the decrease in volume on the anode side. The corresponding transport number of the solvent is given by

$$\bar{l}_w = V_c / \bar{V}_{\text{H}_2\text{O}} \quad (4)$$

### Counterion-Transport Number

All-glass, H-type cells of various capacities were used. The biggest cell contained half-cells of 350 ml. capacity and was used for electrolyte solutions  $< 0.1m$ . A medium size cell, each half-cell  $\sim 30$  ml. in capacity was used for concentrations of 0.1006–0.5066*m*. The smallest cell contained a cathode compartment  $\sim 13$  ml. and an anode chamber  $\sim 30$  ml. This was used for solutions  $\geq 1.024m$ . In experiments where the solutions were circulated through the anode compartment, a half-cell of the type used by Lakshminarayanaiah<sup>14</sup> was employed.

An equilibrated membrane blotted with filter paper was clamped as described above. Exactly known weights ( $\sim 300$  g. for dilute solutions,  $\sim 20$  g. for moderately strong solutions and  $\sim 10$  g. for concentrated solutions) of NaCl solution of the same concentration were transferred by weight burets into each compartment of the cell which was kept in an air thermostat at  $30 \pm 0.1^\circ\text{C}$ . Ag-AgCl electrodes were used.

A known quantity of electricity was passed through the cell and through the silver coulometer in series with it. A calibrated milliammeter and a variable resistor were also used in series to pass definite and steady currents through the system.

The contents of each half-cell were run into tared flasks, weighed, and analyzed by titration against standard  $\text{AgNO}_3$ .

The counterion transport number  $\bar{t}_+$  is given by

$$\bar{t}_+ = (\Delta n / \Delta Q) F \quad (5)$$

where  $\Delta n$  is the number of moles of electrolyte transported per  $\Delta Q$  coulombs passed through the cell and  $F$  is the Faraday.

### III. RESULTS

#### Mean Ion Activity Coefficient in the Membrane Phase

The results of chemical analysis of the membrane phase are presented in Table I as a function of the molality  $m$  or mean activity  $a_{\pm}$  of the external solution. They are water content  $w$ , of the resin phase (expressed as the weight of water per gram wet membrane), fixed charge  $X$  (moles per kilogram of water in the membrane) and total coion molality  $\bar{m}_-$  (also as moles

TABLE I  
Equilibrium Water Content  $w$ , Fixed-Charge Molality  $X$ , and the Activity Coefficient Term  $\bar{\gamma}_{\pm} e^{\pi V/2RT}$  in the Membrane Phase as Functions of Activity of External Solutions of NaCl

Molality $m$	Activity $a_{\pm}$	Water content $w$ , g. $\text{H}_2\text{O/g.}$ wet resin	$\bar{m}_-$	$X$	$\bar{\gamma}_{\pm} e^{\pi V/2RT}$	$\xi$
0.001004	0.000969	0.633	0.006	1.263	0.011	0.138
0.002004	0.001907	0.633	0.008	1.266	0.018	0.159
0.005005	0.004644	0.633	0.009	1.276	0.043	0.169
0.01005	0.00907	0.633	0.010	1.291	0.079	0.177
0.02005	0.01751	0.631	0.015	1.295	0.124	0.217
0.05006	0.04116	0.628	0.029	1.309	0.208	0.301
0.1006	0.0781	0.622	0.034	1.372	0.357	0.319
0.2026	0.1481	0.613	0.103	1.372	0.380	0.568
0.5066	0.3440	0.605	0.325	1.372	0.463	1.083
1.024	0.6738	0.602	0.675	1.372	0.573	1.714
2.089	1.414	0.567	1.477	1.379	0.688	2.977
5.700	5.444	0.540	5.213	1.481	0.921	7.980

per kilogram of water in the membrane). The counterion molality  $\bar{m}_+$  can be derived as the sum of  $X$  and  $\bar{m}_-$ . By using these values in the Donnan equation, eq. (2), the mean activity coefficient of the electrolyte in the membrane was calculated and the values are given in Table I. These values include the swelling pressure term  $e^{\pi v^*/2RT}$  which has been shown to contribute little to  $\bar{\gamma}_{\pm}$  values.<sup>15</sup> Elsewhere<sup>16</sup> similar values have been determined for the same membrane material but in rod form. The values obtained with membranes are consistently lower than those obtained with rods, but they are not so low as to conform to the theoretical predictions of the theory of Lazare, Sundheim, and Gregor,<sup>17</sup> except when the external concentrations are in the region of molalities one and above; and they deviate considerably from the theory of Mackie and Meares.<sup>15</sup> In view of this, in all the calculations involving  $\bar{\gamma}_{\pm}$  in this paper the values presented in Table I have been used.

TABLE II  
Transference Numbers of Water and Na<sup>+</sup> Ions in Crosslinked PSA Membranes as Functions of Current Density and External Molality at 30°C.

Molality <i>m</i>	$\bar{l}_w$ by eq. (4)	Current density, ma./cm. <sup>2</sup>	$\bar{t}_+$ by eq. (5)			
			(Ord)	(1)	(2)	(3)
0.005005	90.00	0.51	0.997			
		1.01	0.931			
		2.53	0.901			
		5.05	0.858			
		10.10	0.804			
0.01005	86.22	0.51	0.997			
		1.01	0.981			
		2.53	0.960			
		5.05	0.915			
		10.10	0.847			
0.1006	37.28	0.51	0.651		0.900	
		1.01	0.820			
		2.53	0.820		0.905	0.900
		5.05	0.909		0.900	0.906
		10.10	0.868			
0.5066	18.22	2.53	0.453		0.830	
		5.05	0.776			
		10.10	0.776		0.840	0.830
		20.20	0.820			
		30.30	0.834		0.836	0.833
1.024	11.11	5.05	0.529			
		10.10	0.755		0.800	0.796
		20.20	0.775			
		30.30	0.799		0.792	0.794
		40.40		0.800		
2.089	6.06	30.30		0.721		
3.210	3.94	30.30		0.695		
4.450	2.89	30.30		0.675		
5.700	2.11	30.30		0.574		

The last column of Table I was computed by using the relation  $\xi = 2a_{\pm}/(X\bar{\gamma}_{\pm}e^{\pi V/2RT})$ . The values of  $\xi$  increase with increase in the activity of the external electrolyte solution. These data were useful in the calculation of the emf's of membrane cells to test the T.M.S. theory.

### Water-Transport Number

It is observed from a preliminary report already published<sup>18</sup> concerning the present system that the volume of water transport per Faraday of current is governed by both current density and external concentration. At concentrations  $>0.1006m$ ,  $\bar{l}_w$  is independent of current density, whereas at external concentrations  $<0.1006m$ , the volume of transport is dependent on the density of current flowing through the system. In these dilute solutions, there seems to be an asymptotic rise in the transport of water when very small currents are passed.

As ions move under the influence of an electric field water molecules surrounding these ions also move by gaining momentum from the moving ions. It may be anticipated from the value of the interstitial molality of the membrane at  $m = 0.01005$  (viz. 1.301) that there must be a maximum of 769 ml. of water transported for the transport of 1 g.-atom of  $\text{Na}^+$  ions. Actual transport being double this quantity (see Table II), suggests that water is moving faster than  $\text{Na}^+$  ions or in other words nearly  $1/2$  g.-atom of  $\text{Na}^+$  counterions is immobile. It is possible as suggested elsewhere<sup>9</sup> that this large transport of solvent is due to selective transfer through uncharged or slightly charged pores present in the membrane. A detailed report about solvent transfer through different ion-exchange membranes will be published elsewhere.<sup>19</sup> The data concerning  $\bar{l}_w$  relevant to this paper presented in Table II are taken from that report.

### Counterion-Transport Number

The essential experimental results are given in Table II. When the external concentrations are below  $0.1006 m$ , values of  $\bar{l}_+$  increase as the current density is decreased and at any given current density, the values are larger the higher the concentration of the solution. At every current density with the exception of  $0.51 \text{ ma./cm.}^2$ ,  $\bar{l}_+$  values with  $m = 0.01005$  are higher than corresponding values with  $m = 0.005005$ .

When the membrane system containing the same solution of  $\text{NaCl}$  on either side of the membrane is electrolyzed, depletion of electrolyte at the membrane surface facing the anode (so called Bethe-Toropoff effect<sup>20</sup>) takes place. The rate at which  $\text{Na}^+$  ions move in the membrane phase is controlled by their transport number which is unity under normal conditions due to membrane being selective to cations; however, the cations enter the liquid layer near the membrane-solution interface at a rate controlled by the transport number of  $\text{Na}^+$  ions in aqueous  $\text{NaCl}$  solution. This value is nearly 0.4. Thus the rate of removal of counterions is greater than the rate of their replacement in the membrane phase. As there is no forced convection such as stirring provided in the cell, higher currents

produce  $\text{H}_3\text{O}^+$  ions which take part in transport through the membrane replacing  $\text{Na}^+$  ions (membrane polarization) and as a result  $\bar{t}_+$  decreases. However, if the current densities employed are such that the rate of removal of  $\text{Na}^+$  ions from the membrane phase is equal to the rate of their entry into the membrane interface facing the anode, the correct value of  $\bar{t}_+$  would be obtained even when no stirring is employed to eliminate concentration polarization at the electrodes and membrane interfaces. This is realized at very low current densities ( $0.51 \text{ ma./cm.}^2$ ) as reflected by the high value of 0.997 for  $\bar{t}_+$  which is close to the value of unity expected of a perfect cation exchanger. The reproducibility of this value was very good and, therefore, suggested that the membrane and not the liquid films existing at the membrane-solution interfaces control electrolyte transfer through the membrane when very low currents are used.

It is further seen from Table II, that when  $m = 0.1006$  values of  $\bar{t}_+$  increase, reach a maximum, and then decrease as the current strength is decreased. Kressman and Tye<sup>7</sup> have observed similar results with commercial membranes using  $0.1N$  solution in multicompartiment cells. Their explanation points to the desirability of planning the experiments carefully to obtain meaningful values for  $\bar{t}_+$ . They have demonstrated what has been described above. When high currents were used ( $7-43 \text{ ma./cm.}^2$ ) the liquid layer near the membrane surface facing the anode became acidic, but at low currents there was no change in pH. As a consequence, it is inferred that high current densities produced membrane polarization which caused low values for  $\bar{t}_+$ .

Electrolysis in our membrane cell causes electrolyte accumulation in the cathode compartment and depletion in the anode chamber. The concentration difference between the two solutions controls electrolyte diffusion through the membrane and this diffusion counteracts electrical transference and hence reduces the values of  $\bar{t}_+$ . The period of electrolysis and the current densities used in electrolysis become very important in deriving meaningful values for  $\bar{t}_+$ . Very high current densities cannot be employed as they cause membrane polarization, whereas low current densities can only be used provided measurable concentration differences can be produced within reasonable time. If a longer period of time (i.e., very low current density) is used, electrolyte transfer by diffusion would be great, and as a result  $\bar{t}_+$  would decrease with decrease with current density. This type of decrease in  $\bar{t}_+$  is absent at  $m = 0.005005$  or  $0.01005$ . In these electrolyte environments the membrane by excluding coions (see Table I) completely prevents diffusion of salt from the high concentration side to the low concentration side. Similar behavior is noticed when the external concentrations are greater than  $0.1006m$ . In these cases the effect of concentration polarization (membrane polarization) is not realized in the range of current densities employed and the interfering factor influencing the actual values of  $\bar{t}_+$  is only diffusion. This must be eliminated to realize meaningful values for  $\bar{t}_+$ . The following possible approaches may be made to eliminate diffusion. (1) Slight change in concentration,

enough to get a significant titer value, is brought about by electrolysis in as short a time as possible. This can be done by passing a high current for a short time which can be conveniently determined by some preliminary experiments. (2) Initial concentrations in the two half cells are so chosen that on completing the experiment the concentrations in the two compartments are reversed.<sup>21</sup> The mean concentration difference between the two chambers during the period of the experiment is nearly zero. (3) A solution whose concentration is close to that on the cathode side is circulated through the anode chamber.<sup>8</sup>

Repeated runs were made with 0.1006*m* by means of each of the three methods and they all produced (except method 1) a value of 0.91 for  $\bar{t}_+$  of the Na<sup>+</sup> ion. The reproducibility of the results under any particular set of experimental conditions was always less than 1%. This value of  $\bar{t}_+$  agreed with the value obtained by ordinary electrolysis (Ord, Table II) at a current density of 5.1 ma./cm.<sup>2</sup>

Similar repeated trials with 0.5006 and 1.024*m* solutions also gave concordant values. These and other results of ordinary electrolysis are presented in Table II. Due to simplicity of operation, method (1) was used in all experiments with concentrated solutions. A current density of 30.30 ma./cm.<sup>2</sup> was used for about 10 min. in all experiments with solutions of molalities in the range 2.089–5.700. The use of even higher current densities and correspondingly shorter periods of time gave results which agreed with the values presented in Table II. The variation here also was within the limits of experimental error which was less than 1%.

Use of method (1) calls for patience in analytical work. The concentration changes being small, the results were always checked by another independent method. The solutions before and after electrolysis were passed through a column of cation exchange resin in H<sup>+</sup> form and the HCl in the effluent was titrated.

#### IV. DISCUSSION

The cmf of the membrane cell Ag,AgCl/NaCl (*m*<sup>I</sup>)/membrane/NaCl (*m*<sup>II</sup>)/AgCl,Ag at 30°C. for different molalities of the external solutions are given in Table III. These values are compared with  $E_{\max}$  values (last column), which are the maximum possible values of electrical potentials arising across an ideally permselective membrane through which little transport of coion or solvent takes place. It is given by

$$E_{\max} = - (2RT/F) \ln (a_{\pm}^{\text{II}}/a_{\pm}^{\text{I}}) \quad (6)$$

A gradual decrease of selectivity with increase in the mean molality of the external solution is observed. The causes of this decrease are twofold: (1) uptake of electrolyte as the external concentration is increased and (2) transport of water caused by osmosis and electroosmosis.

The T.M.S. theory attributes the decrease in selectivity to uptake of electrolyte and neglects the effect of solvent transfer. How well this theory



TABLE III  
Emf's of the cell Ag,AgCl/NaCl ( $m^I$ )/membrane/NaCl ( $m^{II}$ )/AgCl, Ag at 30°C.

Cell number	$m^I$	$m^{II}$	$E_{\text{obs}}$ , mv.	$E/E_{\text{max}}$
1	0.002004	0.001004	34.79	0.984
2	0.005005	0.002004	45.85	0.985
3	0.01005	0.005005	34.57	0.990
4	0.02005	0.01005	33.80	0.984
5	0.05006	0.02005	42.00	0.941
6	0.1006	0.05006	30.00	0.896
7	0.2026	0.1006	28.00	0.839
8	0.5066	0.2026	32.30	0.734
9	1.024	0.5066	22.19	0.632
10	2.089	1.024	20.74	0.533
11	5.700	2.089	32.00	0.455

accounts for the observed data may be examined. In this attempt and in testing the Scatchard equation, all the assumptions and calculations used by Hills et al.<sup>4</sup> are followed.

By equating the terms  $\bar{\gamma}_+$ ,  $\bar{\gamma}_-$ , and  $e^{\tau V/2RT}$  to unity in eq. (10) of the previous paper<sup>1</sup> and calculating  $U$  on the basis of the limiting mobilities of  $\text{Na}^+$  and  $\text{Cl}^-$  ions observed in aqueous solution, the emf's of membrane cells 1-11 were calculated and they are shown in Table IV as  $E'$ . At mean external molalities  $<0.015$  (cells 1-4), the agreement between calculated and measured emf's ( $E' - E_{\text{obs}} < 0.6$ ) is good but at  $m > 0.015$  calculated values are higher than the observed values. Addition of  $\psi_w$ , the emf due to water transport, calculated by using the equation

$$\psi_w = -(RT/F) \int_1^{II} \bar{t}_w d \ln a_w \quad (7)$$

improves the agreement except for cell 11, where the calculated value is lower than the observed value. Studies with PMA membranes gave good agreement.

The procedure adopted above is not in keeping with the observed fact that the mean ion activity coefficients in the membrane phase are far from unity. So, experimentally determined values of  $\bar{\gamma}_{\pm}$  and  $\xi$  given in Table I and  $\bar{t}_+$  values presented in Table II were used to test the T.M.S. theory in the same way as Hills, Jacobs, and Lakshminarayanaiah.<sup>4</sup> The outcome was as disappointing as their results with PMA membranes.

Equation (1) given above may be integrated, provided the variations of  $\bar{t}_+$  and  $\bar{t}_w$  with external electrolyte concentrations are known. Experimental values of  $\bar{t}_+$  and  $\bar{t}_w$  corresponding to particular values of  $m$  are given in Table II. These data were interpolated graphically to derive suitable values of  $\bar{t}_+$  and  $\bar{t}_w$  for the required values of  $m$ . With the values so obtained, integration of eq. (1) was carried out numerically by means of Simpson's rule. The results are given in Table IV. Further, interpolation of transport data was also made assuming a linear variation of  $\bar{t}_+$

TABLE IV  
Membrane Cell Emf's Calculated From the T.M.S. Theory  
and from the Scatchard Equation

Cell number	Diffusion potential	$E'$ , mv.	$E' - E_{\text{obs}}$ , mv.		$E$ , mv.	$E - E_{\text{obs}}$ , mv.
			$E_{\text{obs}}$ , mv.	$\psi_w$		
1	-0.01	35.37	+0.58	-0.32	35.29	+0.50
2	-0.04	46.25	+0.40	-0.50	46.14	+0.29
3	-0.06	34.50	-0.07	-0.54	34.43	+0.14
4	-0.02	34.26	+0.46	-0.99	33.36	-0.44
5	-0.07	44.30	+2.30	-1.56	41.51	-0.49
6	-0.28	31.91	+1.91	-1.94	29.06	-0.94
7	-0.11	33.05	+5.50	-2.86	27.03	-0.97
8	-0.59	42.21	+9.91	-6.77	31.77	-0.53
9	-1.43	30.40	+8.21	-6.86	21.92	-0.27
10	-2.95	27.58	+6.84	-7.80	20.65	-0.09
11	-6.99	36.93	+4.93	-16.34	32.56	+0.56

and  $\bar{l}_w$  with  $m$  between the experimentally determined values, i.e., linear variation of  $\bar{l}_+$  (and  $\bar{l}_w$ ) with  $m$  between  $\bar{l}_{+(1)}$  [and  $\bar{l}_{w(1)}$ ] determined at  $m_{(1)}$  and  $\bar{l}_{+(2)}$  [and  $\bar{l}_{w(2)}$ ] determined at  $m_{(2)}$ . Use of these values in the numerical integration of the equation gave results which were not significantly different from those given in Table IV. These emf's agree very well with the observed values ( $E - E_{\text{obs}} \gtrsim 1$  mv.).

In the study with PMA membranes,<sup>4</sup> a number of possibilities existing to cause the disagreement between observed and theoretical values of emf have been discussed. It is now apparent that the observed discrepancy is not due to any shortcomings of the theory but simply due to the neglect of the effects of current density on the values of  $\bar{l}_+$  and  $\bar{l}_w$ . So it must be concluded that the thermodynamic theory of Scatchard and the treatments of others based on the thermodynamics of irreversible processes which are equivalent for isothermal electrical potentials, are satisfactory in describing the emf's of membrane cells even in high concentration ranges in which there is incomplete ionic selectivity.

The writing of this work has been supported in part by grant NB-03322-03 from the National Institute of Neurological Diseases and Blindness and in part by grant GB 865 from the National Science Foundation.

### References

- Hills, G. J., P. W. M. Jacobs, and N. Lakshminarayanaiah, *Proc. Roy. Soc. (London)*, **A262**, 246 (1961).
- Teorell, T., *Proc. Soc. Exptl. Biol., N. Y.*, **33**, 282 (1935); *Proc. Natl. Acad. Sci., U. S.*, **21**, 152 (1935).
- Meyer, K. H., and J. F. Sievers, *Helv. Chim. Acta*, **19**, 649, 665, 987 (1936).
- Hills, G. J., P. W. M. Jacobs, and N. Lakshminarayanaiah, *Proc. Roy. Soc. (London)*, **A262**, 257 (1961).
- Scatchard, G., *J. Am. Chem. Soc.*, **75**, 2883 (1953).
- Lorimer, J. W., E. I. Boterenbrood, and J. J. Hermans, *Discussions Faraday Soc.*, **21**, 141 (1956).

7. Kressman, T. R. E., and F. L. Tye, *Discussions Faraday Soc.*, **21**, 185 (1956).
8. Subrahmanyam, V., and N. Lakshminarayanaiah, *Current Sci. (India)*, **31**, 146 (1962).
9. Lakshminarayanaiah, N., *Proc. Indian Acad. Sci.*, **A55**, 200 (1962).
10. Hills, G. J., J. A. Kitchener, and P. J. Ovenden, *Trans. Faraday Soc.*, **51**, 719 (1955).
11. Brown, A. S., *J. Am. Chem. Soc.*, **56**, 646 (1934).
12. Despic', A., and G. J. Hills, *Discussions Faraday Soc.*, **21**, 150 (1956).
13. Harned, H. S., and B. B. Owen, *The Physical Chemistry of Electrolyte Solutions*, Reinhold, New York, 1943.
14. Lakshminarayanaiah, N., *J. Polymer Sci.*, **46**, 529 (1960).
15. Mackie, J. S., and P. Meares, *Proc. Roy. Soc. (London)*, **A232**, 485 (1955).
16. Lakshminarayanaiah, N., *J. Polymer Sci.*, **A1**, 139 (1963).
17. Lazare, L., B. R. Sundheim, and H. P. Gregor, *J. Phys. Chem.*, **60**, 641 (1956).
18. Subrahmanyam, V., and N. Lakshminarayanaiah, *Current Sci. (India)*, **29**, 307 (1960).
19. Hills, G. J., P. W. M. Jacobs, N. Lakshminarayanaiah, and V. Subrahmanyam, to be published.
20. Bethe, A., and T. Toropoff, *Z. Physik. Chem.*, **88**, 686 (1914).
21. Hale, D. K., and D. J. McCauley, *Trans. Faraday Soc.*, **57**, 135 (1961).

### Résumé

On a mesuré à 30°C la force électromotrice des systèmes Ag, AgCl/NaCl ( $m^1$ )/membrane/NaCl( $m^{11}$ )/AgCl, Ag contenant une membrane de phénol-formaldéhyde sulfonate. On a analysé la phase membrane pour sa teneur en électrolyte et en eau et on a déduit les coefficients d'activité intramembrane en fonction de la concentration externe en électrolyte. On a mesuré les nombres de transfert du contre-ion sodium et de l'eau en fonction des densités de courant et de la concentration externe. Ces données ont été utilisées pour tester les théories principales du potentiel de membrane. La théorie de la charge fixe de Teorell et Meyer et Sievers ne donnent pas un accord satisfaisant entre les forces électromotrices observées et calculées pour la cellule "membrane" contrairement à la théorie de Scatchard.

### Zusammenfassung

Die EMK des eine Phenol-Formaldehydsulfonatmembran enthaltenden Systems Ag, AgCl/NaCl( $m^1$ )/Membran/NaCl( $m^{11}$ )/AgCl, Ag wurde bei 30°C gemessen. Die Membranphase wurde auf ihren Elektrolyt- und Wassergehalt analysiert, und die Intramembranaktivitätskoeffizienten wurden als Funktion der äusseren Elektrolytkonzentration abgeleitet. Die Überföhrungszahl von Na<sup>+</sup>-Gegenionen und Wasser wurde sowohl als Funktion der Stromdichte als auch der äusseren Konzentration gemessen. Die Ergebnisse wurden zur Überprüfung der wichtigsten Theorien über Membranpotentiale verwendet. Die Theorie der fixierten Ladung von Teorell, Meyer und Sievers ergab im Gegensatz zu der Theorie von Scatchard keine befriedigende Übereinstimmung zwischen der beobachteten und der berechneten EMK der Membranzellen.

Received November 21, 1963

Revised January 16, 1964

## Chain Folding in Amylose Crystals

R. ST. J. MANLEY, *Physical Chemistry Division, Pulp and Paper Research Institute of Canada, and Department of Chemistry, McGill University, Montreal, Canada*

### Synopsis

Crystals of amylose were prepared by precipitation from aqueous solution with *n*-butanol. The crystals are rectangular platelets, and crosses or rosettes formed by the intergrowth of single platelets. In the electron microscope they are seen to consist of layers 75 Å. in thickness. Distinct spiral terrace growths related to screw dislocations were not observed, but the presence of dislocation edges suggests that the crystals thicken by a dislocation mechanism. Low-angle, x-ray measurements on aggregates of the crystals reveal a long spacing in good agreement with that calculated from shadow lengths. However, in contrast with other polymers, the long spacing appears to be invariant with crystallization temperature. Electron diffraction spot patterns show that the platelets are single crystals and indicate that the chain molecules are folded within the lamellae.

### INTRODUCTION

This paper forms part of a study of the growth and structure of single crystals of carbohydrate polymers and their derivatives. The immediate aim in this work is to ascertain whether chain folding occurs in those polymers, and whether there are any features distinguishing these crystals from those of the linear synthetic polymers. Ultimately it is hoped to relate the single crystal observations to the problem of the molecular morphology of native cellulose fibers. In a recent paper<sup>1</sup> it was shown that cellulose acetate can be crystallized from dilute solution as well-defined single crystals having many features in common with those of linear synthetic polymers.<sup>2-7</sup> Thus it was demonstrated that the crystals are composed of lamellae about 180 Å. in height and that thickening takes place through the development of spiral growths centered on screw dislocations. The cellulose acetate chain molecules are oriented perpendicular to the lamellae and, in spite of their known inflexibility, assume folded configurations within the lamellae. In this paper a similar study of amylose is described.

Amylose is a linear polysaccharide which occurs in starch. It is composed of anhydroglucose residues and is thus chemically similar to cellulose from which it differs, however, in the details of its chain structure. Whereas in cellulose the glucose residues are joined by 1 → 4β glycosidic bonds, in amylose they are linked by 1 → 4α glycosidic bonds. As a result the

chain configuration of the two polymers is quite different. In cellulose successive glucose residues follow a 2-fold helicoidal path while in amylose the molecule is constrained to assume a 3-fold helical conformation. The amylose molecule is therefore considerably more flexible than that of cellulose.

It has long been known that amylose forms water-insoluble crystalline complexes with *n*-butanol,<sup>8</sup> and Rundle and co-workers<sup>9,10</sup> have determined their crystal structure. The unit cell is orthorhombic with the dimensions  $a = 13.7$  Å,  $b = 23.8$  Å,  $c = 8.05$  Å. (chain axis) when monohydrated and  $a = 13.0$  Å,  $b = 23.0$  Å,  $c = 8.05$  Å. (chain axis) when anhydrous.<sup>11</sup> The chain molecules assume a helical configuration with 6 glucose units per turn and each unit cell contains two helices in an antiparallel arrangement.

The purpose of the present paper is to present the results of a study of amylose crystals by electron microscopy and electron and x-ray diffraction. Various aspects of the crystal growth are described, and it will be shown that the amylose molecules fold within thin lamellae.

## EXPERIMENTAL

### A. Materials and Methods

The material used in this investigation was a commercially prepared amylose (Superlose) obtained from Stein, Hall, and Co., Inc., New York. The intrinsic viscosity in dimethyl sulfoxide at 25°C. was 1.10 dl./g. and corresponds to an approximate molecular weight of 510,000 as obtained from the viscosity-molecular weight relation derived by Cowie.<sup>12</sup>

The first problem was to obtain crystals suitably thin for electron microscopy and electron diffraction. From a series of preliminary experiments it was established that this could be accomplished by the following procedure. Amylose was dissolved in 1*N*-sodium hydroxide to give a concentration of 0.2–0.5%. The solution was neutralized to pH 7, heated to about 90°C., and then saturated with hot *n*-butanol. Crystallization of the amylose was then effected at 45°C. with gentle stirring. The precipitate was separated by centrifugation, washed thoroughly with methanol, and stored under methanol. Crystals could be grown at considerably lower concentrations, but they were not as large or as well formed as those obtained at the high concentrations. Although amylose is known to be highly susceptible to chain scission, it was established from viscosity measurements that there was no degradation of the polymer under these conditions of dissolution and crystallization.

For examination of the crystals in the electron microscope drops of the methanol suspension were dried down on a glass slide previously coated with an evaporated carbon film. The specimens were then shadowed with gold-palladium. Subsequently, the films were floated off on water and mounted on electron microscope specimen grids. The specimens were examined by direct transmission in a JEM 6A electron microscope, in which

also selected area diffraction experiments were performed. As with other polymers,<sup>13</sup> diffraction patterns could only be obtained by working at very low beam currents. The diffracting power of the crystals is almost instantaneously destroyed at normal beam intensities. Internal calibration of the diffraction patterns was achieved with the aid of a thin evaporated layer of thallium chloride.

### B. Observations

A preparation of crystals obtained as described above always contained three types in approximately equal proportion. These are (a) single rectangular platelets having a length approximately twice the width, (b) cross-shaped crystals consisting of two platelets intersecting at an angle of about  $60^\circ$ , and (c) rosette-shaped crystals consisting of three platelets with a  $60^\circ$  angle of intersection. The single rectangular platelets and the rosettes have been described by Kerr<sup>14</sup> and Schoch.<sup>15</sup>

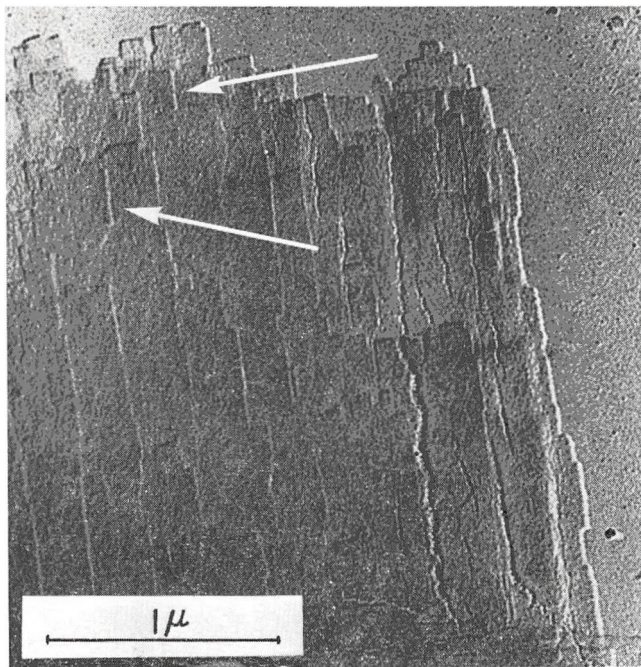


Fig. 1. Electron micrograph of an amylose crystal. Dislocation edges are indicated by the arrows; Au-Pd shadowed.  $\times 30,000$ .

The micrographs shown in Figures 1, 2, and 3 are representative of the results obtained in the electron microscope examination of the crystals. They are built up of thin rectangular-shaped layers whose thickness, as determined from shadow length measurements is about 75 Å. Generally the crystals contained so many intergrown layers in compact formation that it was difficult to trace the edges of the layers and thereby ascertain whether

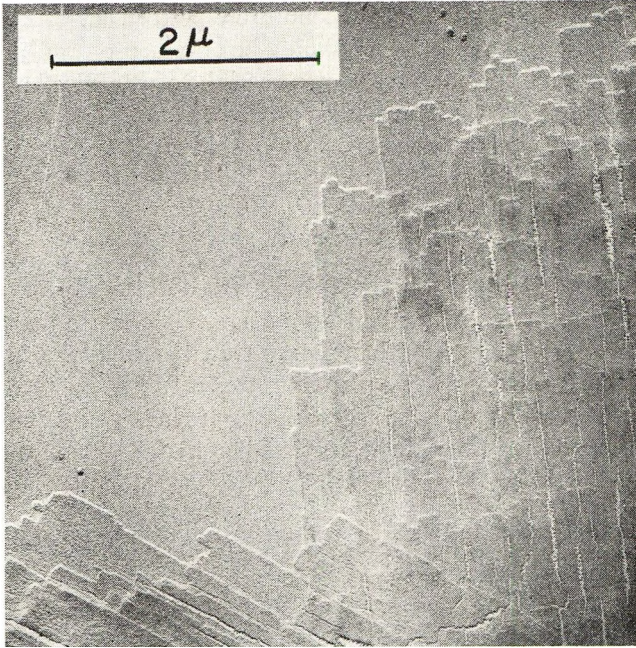


Fig. 2. Electron micrograph of an amylose crystal; Au-Pd shadowed.  $\times 17,000$ .

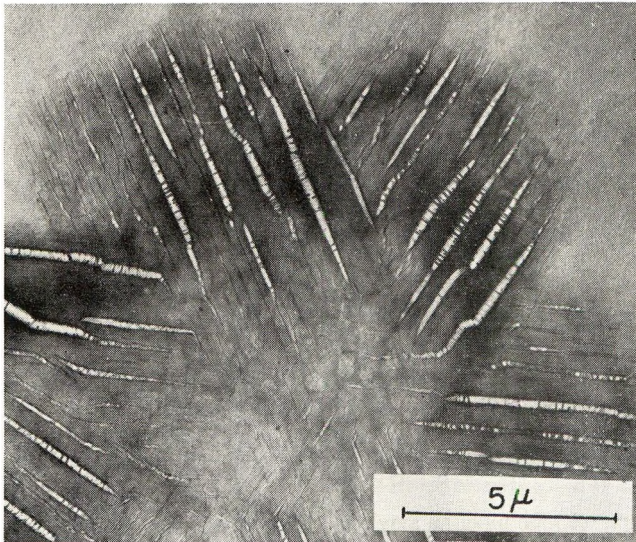
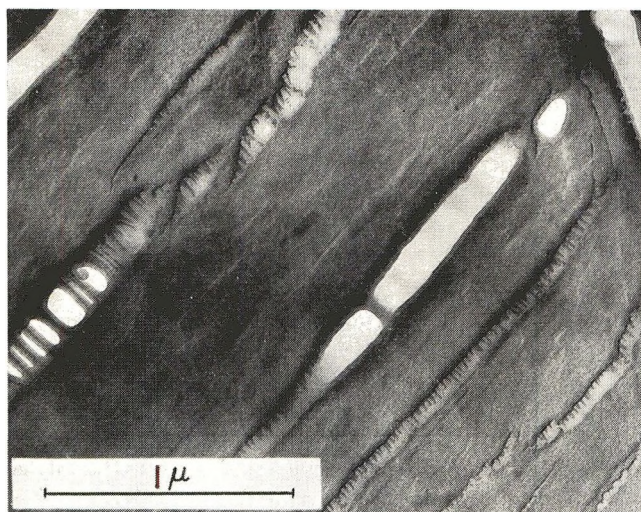
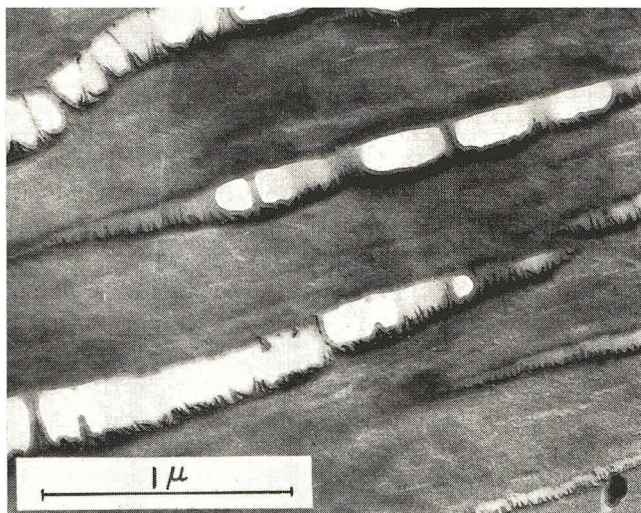


Fig. 3. Electron micrograph of a rosette-shaped amylose crystal. There are numerous cracks parallel to the long axes of the component platelets. Au-Pd shadowed.  $\times 5,500$ .

dislocation centered spiral growth is involved in the thickening of the crystals. In some photographs dislocation edges were observed on some of the layers. Two of these are indicated by the arrows in Figure 1. This suggests that the crystals do thicken by the usual spiral dislocation type mechanism.



(a)



(b)

Fig. 4. Details of a crystal as in Fig. 3 showing fractures with fibers pulled out across them. Electron micrograph.  $\times 20,800$ .

Figure 3 shows a rosette-shaped crystal. Examination of the central portion suggests that such crystals develop by the interpenetrant growth of three of the rectangular platelets, the angle between their axes being  $60^\circ$ . It seems likely that this form of growth is due to complex twinning. Another manifestation of twinning is found in the observation that near the edges of the single platelets there are frequently re-entrant corners associated with growth faces which have a different orientation from the main crystal. In Figure 1 such a set of lamellae can be seen protruding from the long edge of a platelet crystal.



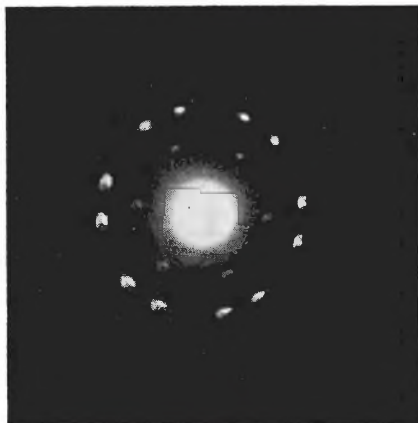


Fig. 5. Electron-diffraction pattern given by amylose crystals with the beam perpendicular to the plane of crystal. The rings are due to thallos chloride used as an internal standard.

All the crystals examined showed elongated cracks along the direction of the larger dimension. These are probably associated with stresses due to shrinkage which occurs either when the crystals are dehydrated by washing with methanol or on being dried down on the carbon substrate from methanol. It was observed that threads are pulled out across the cracks as illustrated in Figure 3. A structure appears to be present in the center of each thread. Similar observations have been made by Keller,<sup>16</sup> Reneker and Geil,<sup>17</sup> and Hirai et al.<sup>18</sup> in torn polyethylene crystals. Figure 4 shows details of the cracks. It can be seen that the cracks are not propagated through all the crystal layers simultaneously. It appears that the uppermost layers rupture first pulling cut fibers across the crack, and subsequently the same process occurs in the lower lamellae. As will be seen later the amylose chain molecules are folded along the (010) and (100) faces, and the cracks are elongated in the  $\langle 010 \rangle$  direction. The development of threads between the fracture surfaces is probably related to the pulling out of the folded molecules, a process which can probably be explained on the basis of a dislocation mechanism.<sup>19</sup>

In the electron diffraction experiments, sharply defined spot patterns were obtained. Figure 5 shows a typical diffraction pattern obtained with the plane of the platelets normal to the electron beam. The pattern represents the reciprocal lattice net of the  $(hk0)$  reflections of the crystals. All crystals examined, whether single rectangular platelets, crossed crystals or rosettes (or portions thereof), gave the same diffraction pattern. The spots are disposed on three Debye-Scherrer circles; the outermost contains twelve spots while the two inner circles contain six spots each. The innermost spots are rather close to the main beam and although quite clear on the original plates, are not easily seen in the reproduction. The spots have been indexed as (150), (200), and (110) and the corresponding spacings are 4.28, 6.61, and 11.5 Å, respectively. The axial lengths in the basal

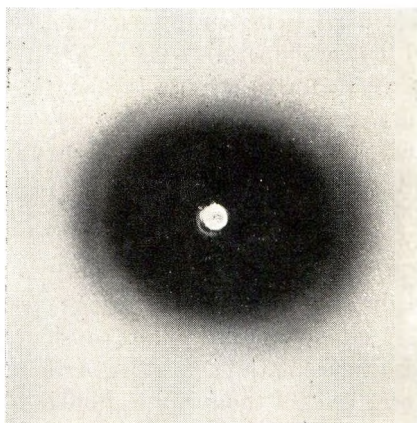


Fig. 6. Low-angle x-ray pattern given by an aggregate of amylose crystals.

plane of the crystals then have the dimensions 13.2 and 23.3 Å. These values are in good agreement with the dimensions given by Rundle for the *ab* projection of the orthorhombic cell in the anhydrous material. It follows that the *c* axis, and hence the chain molecules, are oriented perpendicular to the plane of the crystal lamellae.

On the basis of the indices given above it can readily be shown that the observed electron diffraction patterns contain more spots than would be expected for a single amylose crystal. As will be seen subsequently this type of pattern may be due to the superposition of the diffraction patterns of three single orthorhombic lattices.

For x-ray examination the crystals were slowly filtered from methanol suspension to form a tablet which was dried under vacuum at 50°C. Wide-angle diffraction patterns were obtained in a flat-film camera using nickel filtered  $\text{CuK}_\alpha$  radiation. With the beam perpendicular to the plane of the tablet the pattern showed continuous rings with spacings characteristic of Rundle's anhydrous V amylose.<sup>11</sup> When the beam was parallel to the plane of the tablet the pattern showed preferred orientation. The positions of the intensity maxima on the arcs indicated, in agreement with the electron diffraction evidence, that the molecular chain axis is perpendicular to the plane of the crystals.

The low-angle, x-ray observations were made on the same tablets with the beam parallel to the plane of the tablet. A Kiessig vacuum camera<sup>20</sup> was used with a collimating system which permitted a resolution of about 300 Å. A low-angle pattern is shown in Figure 6. In addition to a strong continuous scattering in the immediate vicinity of the central beam, the pattern showed well defined arcs in two orders. The first of these is strong, while the second is very weak and does not appear in reproduction. From the Bragg equation the calculated long spacing is 75 Å., in excellent agreement with the thickness of the lamellae as determined from the electron micrographs. It is accordingly evident that the long spacing gives a measure of the thickness of the layers in the crystals.

The variation of the long spacing with temperature was also investigated for crystals prepared in the temperature range 30–60°C. Contrary to expectation no change could be observed in the long spacing as determined by low-angle, x-ray diffraction. This is in contrast to the case of the linear synthetic polymers, where the long spacing increases with temperature.<sup>5, 21, 22</sup> Further reference will be made to this point later.

## DISCUSSION

Attention has already been drawn to the extra spots in the electron diffraction diagrams. It is now of interest to consider the origin and significance of these. In Figure 7, three single orthorhombic lattices are projected on the  $c$  axis zero level of the reciprocal lattice. They have a common origin, and the angle between their axes is 60°. On each lattice the (150), (200), and (110) spots are shown. This construction leads to a common reciprocal lattice showing a number of extra reflections due to twinning. The relative positions of the reflections is the same as they might appear in the electron diffraction patterns obtained from crystals whose (001) plane is normal to the electron beam. It is clear that as a result of twinning the reflections are disposed on (150), (200), and (110) circles having respectively 12, 6, and 6 spots. On the (110) circle there should actu-

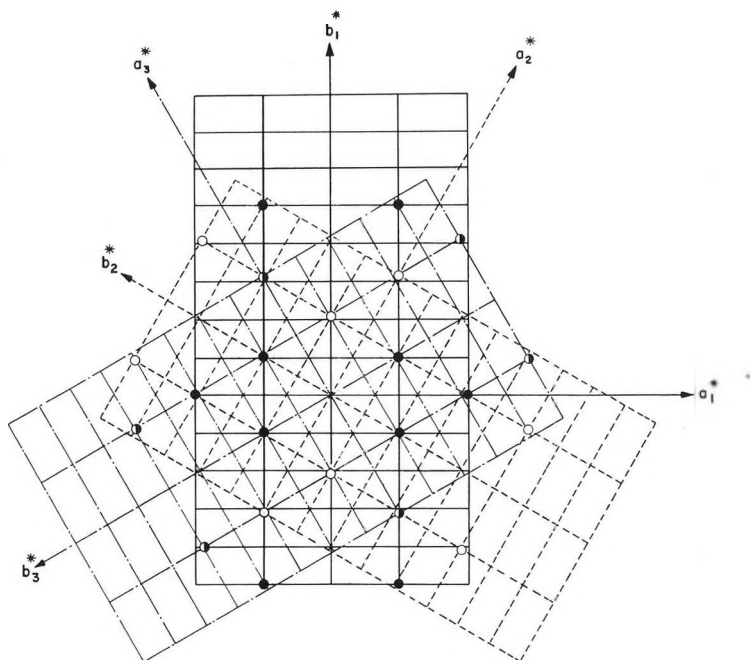


Fig. 7. Computed electron diffraction pattern obtained by the projection of three single lattices onto the (001) plane of the reciprocal lattice. The angle between the axes of the member lattices is 60°. Filled, open, and half-filled circles represent reflections from  $a_1^*b_1^*$ ,  $a_2^*b_2^*$ , and  $a_3^*b_3^*$  lattices, respectively.

ally be 12 spots, but due to an almost perfect registry of a number of the reciprocal lattice points only 6 spots appear. It thus seems possible that the amylose crystals contain elements of repeated micro twinning of a type commonly known as trilling. The angle of tilt between the lattices is  $60^\circ$  as measured on the observed diffraction patterns. Taking the  $b/a$  axial ratio to be 1.77 for the dry crystals the angle of tilt for (110) twinning is calculated to be  $60^\circ 32'$ . Twinning would thus take place by reflection across the (110) plane.

In the above, the diffraction spots in the 4.28, 6.61, and 11.5 Å. Debye-Scherrer rings have been indexed as reflections arising only from  $\{150\}$ ,  $\{200\}$ , and  $\{110\}$  planes, respectively. However, if other reflections are taken into consideration the interpretation of the diffraction effects is less straightforward. According to Rundle's anhydrous V amylose orthorhombic (pseudo-hexagonal) unit cell,<sup>11</sup>  $d_{150} \cong d_{210} \cong d_{310}$ ;  $d_{200} \cong d_{130}$ ;  $d_{110} \cong d_{020}$ ; furthermore, it can be readily demonstrated that the disposition of the  $\{110\}$  and  $\{020\}$ ;  $\{200\}$  and  $\{130\}$ ; and  $\{130\}$ ,  $\{240\}$ , and  $\{310\}$  points in the zero layer of the reciprocal lattice of a single amylose crystal will coincide (or very nearly so) with the disposition of the  $\{110\}$ ,  $\{200\}$ , and  $\{150\}$  points in the zero layer of the composite reciprocal lattice of the three  $\{110\}$  twinned orthorhombic lattices shown in Figure 7. Accordingly, if the diffraction spots falling on the 4.28, 6.61, and 11.5 Å. Debye-Scherrer rings in the diffraction patterns are indexed only as  $\{150\}$ ,  $\{200\}$  and  $\{110\}$  reflections, respectively, then the diffraction patterns from single crystals and twinned crystals are distinct. If, however, the  $\{240\}$ ,  $\{310\}$ ,  $\{130\}$ , and  $\{020\}$  reflections are taken into consideration, then the situation is more complicated since both single and twinned crystals give rise to similar diffraction patterns. Thus, if the intensities of the reflections with identical  $d$  spacings are similar (as well they might be because of the pseudo-hexagonal nature of anhydrous V amylose crystals), then the incidence of twinning cannot be based unambiguously on a consideration of the diffraction effects only. This feature would appear to provide an explanation for the rather puzzling observation mentioned earlier, that all crystals, whether single platelets, crosses, or rosettes or portions of them, yield the same apparently twinned diffraction pattern.

The electron diffraction spot diagrams indicate that when amylose is precipitated from aqueous solutions with *n*-butanol the material obtained consists of single crystals. As seen earlier, the analysis of the patterns also indicates that the molecular chain axis is oriented perpendicular to the plane of the lamellae. This is in accord with Rundle's deductions from optical observations.<sup>9</sup>

We also know from the work of Rundle<sup>10</sup> that the amylose molecules assume a helical configuration with a pitch of about 8 Å. and that each unit cell contains 6 glucose residues per turn of the helix. The observed lamella thickness of 75 Å. thus corresponds to about 9 unit cell lengths. Accordingly it follows that each layer should contain 54 glucose residues per chain, corresponding to a chain length of about 280 Å. if the length of

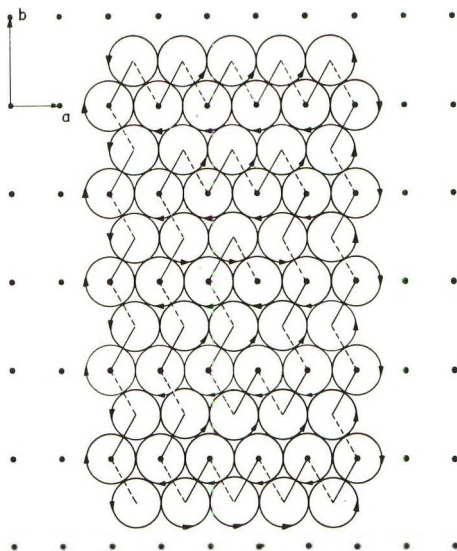


Fig. 8. A projection parallel to the  $c$  axis of a single amylose platelet showing the proposed arrangement of the folds. The helices, represented by the circles, are 13 Å. in diameter. Arrows on the circles indicate the direction of the amylose chains. The solid and dashed lines represent, respectively, the folds on the upper and lower lamellar surfaces.

the glucose unit is taken at 5.15 Å. On the other hand, our viscosity measurements indicate that the average degree of polymerization of the amylose molecules in the crystals is about 3000 and corresponds to a molecular length of about 15,000 Å. This is greatly in excess of the chain length that can be accommodated within the lamellae while standing straight. Accordingly, by analogy with other polymer crystals, it is reasonable to conclude that the molecules must be sharply folded within the lamellae.

It is now of interest to consider how the folded molecules are arranged in the crystal layers. The lamellae may be considered to consist of helical tubes 13 Å. in diameter arranged in a pseudo-hexagonal close-packed array. Figure 8 shows a  $c$  axis projection of the  $ab$  plane of the lattice. As mentioned earlier, the  $a$  and  $b$  axes lie in the plane of the lamellae, and the long and short bounding faces correspond, respectively, to the  $\langle 010 \rangle$  and  $\langle 100 \rangle$  directions. As these are the growing faces it is presumed that the chains will fold along them. A possible mode of fold packing can then be visualized as is illustrated in Figure 8. The chain molecules are oriented along the  $c$  axis, i.e., normal to plane of the figure, and are designated by circles with an arrow to indicate the sense of the helix. The folds on the upper and lower  $(001)$  surfaces are indicated by solid and dashed lines respectively. The helices joined by folds are those at the corner and centre of adjacent unit cells. The folds are thus situated in  $(110)$  planes. This arrangement of the folds would account for the antiparallel arrangement of the two chains in each unit cell as proposed by Rundle.

Another mode of fold packing is that in which the helices connected by folds are those at the corners of adjacent unit cells. Here the folds lie in the (010) and (100) planes. This arrangement is, however, considered to be unlikely as it must of necessity lead to discontinuities of the fold structure. In Figure 8, if it is imagined that the folds are in the (010) and (100) planes, it can be readily seen that after a molecule completes a loop around the crystal a (110) fold must be introduced to permit occupancy of the next succeeding layer of lattice sites. It is interesting to note the difference in fold packing with respect to polyethylene which also has (110) folds. In polyethylene the fold plane is (110), whereas in amylose it is (100) and (010).

The question may be asked whether the helix is maintained within the fold. No information on this point is available from the experiments described above, but certain further experiments now in progress may have a bearing on this question. In a study of the dilute acid hydrolysis of amylose crystals prepared as described above, it was found that the course of the hydrolysis is very similar to that observed in the case of cellulose fibers.<sup>23</sup> Initially the molecular chain length was found to decrease rapidly with time and eventually a constant or "leveling-off" value was reached. To explain this, it may be supposed that the hydrolysis leads to cleavage of the glycosidic bonds within the chain folds. The "leveling-off" chain length would then be expected to bear a simple relationship to the length of the molecule contained between the folds. This would thus appear to be an interesting system for studying the relation between molecular morphology and chemical reactivity in carbohydrate polymers. Among other things, such a study might throw new light on the related problem of the acid hydrolysis of cellulose fibers. Further experiments are in progress to elucidate this problem. At any rate, the hydrolysis of the amylose chains would be expected to be influenced by the configuration of the component glucose residues. The presumed preferential rapid attack on bonds contained in the folds would therefore suggest that the helical chain configuration may not be maintained in the folds.

As mentioned earlier, the step height of the amylose crystals was found to be invariant with crystallization temperature. On the other hand, in the case of polyethylene the step height is known to increase markedly with temperature, there being a change from 90 to 150 Å. for crystallization temperatures in the range 50–90°C.<sup>5,21,22</sup> Existing theories<sup>24–26</sup> on the growth of polymer crystals from dilute solutions predict this change on the assumption that the fold length is determined by the size of critical nucleus which in turn is related to the degree of supercooling. For the amylose crystals the constancy of the step height with change in crystallization temperature is therefore surprising. At the present time we are unable to suggest a mechanism that would convincingly account for this behavior.

Finally, it may be of interest to speculate on the possibility that chain folding may play a role in the molecular organization of the starch granule. It is known that starch grains are built of concentric layers and that the

molecular chain direction is perpendicular to the layers. Recently Frey-Wyssling and Buttrose<sup>27</sup> showed that the layers of potato starch, as seen in the light microscope, can be resolved into much finer submicroscopic lamellae. It has also been shown<sup>28</sup> that starch granules of many different types give x-ray reflections at low angles corresponding to spacings of about 100 Å. Thus, it is tempting to identify this periodicity with the thickness of the finest layers within the granule. In the light of our results on amylose crystals it seems reasonable to suggest that this periodicity might result from the regular folding of the chain molecules within the layers. It is, of course, realized that great care must be exercised in extending the concept of chain folding in lamellar crystals grown in isotropic media to the rather more complex case of the starch granule comprised not only of linear amylose molecules but also of the branched isomer amylopectin. Further work would be required to prove or disprove these speculations.

The author is greatly indebted to Dr. F. A. Khoury for valuable comments on the origin of the "twin" reflections. Thanks are also due to Drs. D. C. Bassett, E. Passaglia, and P. H. Geil for kindly reading the manuscript and making helpful suggestions, and to Mr. C. P. Henry for assistance with the experimental work.

The work was supported under the Pioneering Research Program administered by the Institute of Paper Chemistry, Appleton, Wisconsin, to whom grateful acknowledgment is hereby made.

### References

1. Manley, R. St. J., *J. Polymer Sci.*, **A1**, 1875 (1964).
2. Till, P. H., *J. Polymer Sci.*, **24**, 301 (1957).
3. Keller, A., *Phil. Mag.*, **2**, 1171 (1957).
4. Fischer, E. W., *Z. Naturforsch.*, **12a**, 753 (1957).
5. Keller, A., and A. O'Connor, *Discussions Faraday Soc.*, **25**, 114 (1958).
6. Geil, P. H., N. K. J. Symons, and R. G. Scott, *J. Appl. Phys.*, **30**, 1516 (1959).
7. Geil, P. H., *J. Polymer Sci.*, **44**, 449 (1960).
8. Schoch, T. J., *Cereal Chem.*, **18**, 121 (1941).
9. Rundle, R. E., and D. French, *J. Am. Chem. Soc.*, **65**, 558 (1943).
10. Rundle, R. E., and F. C. Edwards, *J. Am. Chem. Soc.*, **65**, 2200 (1943).
11. Rundle, R. E., *J. Am. Chem. Soc.*, **69**, 1769 (1947).
12. Cowie, J. M. G., *Makromol. Chem.*, **42**, 230 (1961).
13. Keller, A., *J. Polymer Sci.*, **36**, 361 (1959).
14. Kerr, R. W., and G. M. Severson, *J. Am. Chem. Soc.*, **65**, 193 (1943).
15. Schoch, T. J., *J. Am. Chem. Soc.*, **64**, 2957 (1942).
16. Keller, A., *Phil. Mag.*, **2**, 1171 (1957).
17. Reneker, D. H., and P. H. Geil, *J. Appl. Phys.*, **31**, 1916 (1960).
18. Hirai, N., H. Kiso, and T. Yasui, *J. Polymer Sci.*, **61**, S1 (1962).
19. Passaglia, E., and H. D. Keith, to be published.
20. Kiessig, H., *Kolloid-Z.*, **152**, 62 (1957).
21. Price, F. P., *J. Chem. Phys.*, **35**, 1884 (1961).
22. Rånby, B. G., F. F. Morehead, and N. M. Walter, *J. Polymer Sci.*, **44**, 349 (1960).
23. Battista, O. A., *Ind. Eng. Chem.*, **42**, 502 (1950).
24. Price, F. P., *J. Polymer Sci.*, **42**, 49 (1960).
25. Lautritzen, J. I., Jr., and J. C. Hoffman, *J. Res. Natl. Bur. Std.*, **64A**, 73 (1960).
26. Frank, F. C., and M. P. Tosi, *Proc. Roy. Soc. (London)*, **A263**, 323 (1961).
27. Frey-Wyssling, A., and M. S. Buttrose, *Makromol. Chem.*, **44-46**, 173 (1961).
28. Sterling, C., *J. Polymer Sci.*, **56**, S10 (1962).

### Résumé

Des cristaux d'amylose ont été préparés par précipitation à partir d'une solution aqueuse au moyen de *n*-butanol. Les cristaux sont des plaques rectangulaires et des croix ou des rosettes formées par croissance de simples plaques. Au moyen du microscope électronique, on peut voir que ces cristaux sont constitués par des couches de 75 Å d'épaisseur. On n'a pas observé de croissance en palier spiralé distinct en relation avec les dislocations, mais la présence de bords de dislocation suggère que les cristaux s'épaississent par un mécanisme de dislocation. Les mesures effectuées par rayons X à angle faible sur les agrégats de cristaux révèlent une grande distance en bon accord avec celle calculée à partir des longueurs d'ombre. Cependant, en contraste avec d'autres polymères, la grande distance semble être invariable avec la température de cristallisation. Les diagrammes de diffraction électronique montrent que les plaques sont de simples cristaux et indique que les molécules de la chaîne sont repliées à l'intérieur des lamelles.

### Zusammenfassung

Amylosekristalle wurden durch Fällung aus wässriger Lösung mit *n*-Butanol hergestellt. Die Kristalle bilden rechteckige Plättchen und durch Ineinanderwachsen verschiedener Plättchen Kreuze oder Rosetten. Im Elektronenmikroskop wurde festgestellt, dass sie aus Schichten von 75 Å Dicke bestehen. Es wurde kein charakteristisches Spiralterrassenwachstum als Folge von Schraubenversetzungen beobachtet, die Gegenwart von Versetzungslinien spricht aber für ein Kristalldickenwachstum durch einen Versetzungsmechanismus. Röntgen-Kleinwinkelmessungen an Kristallaggregaten ergaben Langperioden in guter Übereinstimmung mit den aus Schattenlängen berechneten. Im Gegensatz zu anderen Polymeren scheinen jedoch die Langperioden gegen die Kristallisationstemperatur unempfindlich zu sein. Elektronenbeugungspunktogramme zeigen, dass die Plättchen Einkristalle sind, und lassen annehmen, dass die Kettenmoleküle innerhalb der Lamellen gefaltet sind.

Received November 12, 1963

Revised December 27, 1963



## Molecular Configuration and Hydrodynamic Behavior of Poly-*N-tert*-butylacrylamide in Methanol

B. R. JENNINGS and H. G. JERRARD, *Department of Physics, University of Southampton, Southampton, England*

### Synopsis

The results of a light-scattering study of six samples of poly-*N-tert*-butylacrylamide in methanol are presented. Some confirmatory results have been obtained with the use of an ultracentrifuge. The derivation of molecular parameters from Zimm plots and centrifugation data is briefly described. Methanol is found to be a good solvent for poly-NTBA, in which it behaves as a stiff molecule expanded beyond random flight predictions. The effect of the stiffness on the Zimm plots and on the interpretation of the results is discussed. Values of the weight-average and number-average molecular weights ( $\bar{M}_w$  and  $\bar{M}_n$ ), the  $z$ -average and number-average radii of gyration  $(\overline{\rho_z^2})^{1/2}$  and  $(\overline{\rho_n^2})^{1/2}$  and the corresponding end-to-end distances  $(\overline{r_z^2})^{1/2}$  and  $(\overline{r_n^2})^{1/2}$  are found.  $\overline{r^2} = 161\bar{N}$ , where  $N$  is the degree of polymerization and  $\bar{r}$  is measured in Angstroms. Values are also obtained for the length of the statistical element, the Kratky-Porod persistence length, the coiling factor, the molecular expansion factor, the second osmotic virial coefficient, ( $A_2$ ), and the Flory constants  $\Phi$  and  $K_V$ . Equations for the variation of  $(\overline{\rho_n^2})^{1/2}$  and of  $A_2$  with molecular weight are derived: they are  $(\overline{\rho_n^2})^{1/2} = 3.76 \times 10^{-9} \bar{M}_n^{-0.515}$  and  $A_2 = 0.082 \bar{M}_w^{-0.515}$ , respectively. The value of  $\Phi$  is considerably less than that normally predicted, and possible reasons for this are suggested. Empirical relations involving the excluded volume effect are mentioned.

### I. INTRODUCTION

Light scattering can be used to determine size and configuration of polymer molecules and to get information on polymer-solvent interaction. In the present paper the results of a study made on poly-*N-tert*-butylacrylamide (poly-NTBA) are presented. The light-scattering observations have been used to determine weight-average and number-average molecular weights and have been employed to find radii of gyration and to test the validity of some theoretical predictions. Molecular weights have also been determined in a few cases by ultracentrifuge measurements using the approach to equilibrium method of Archibald.<sup>1</sup> The purpose of making the latter measurements was essentially to confirm the values obtained from the light scattering observations.

The preparation of the polymer and the method of measurement of the scattered light have been described elsewhere.<sup>2,3</sup> Six samples were investigated by this technique. Sedimentation equilibrium runs were made on two samples. The ultracentrifuge used was a Spinco analytical Model

E instrument and a schlieren optics system was employed. The cells used, 12 mm. in length, were about three quarters filled with the solution and were run at 4609 rpm (1,544*g*). This speed was chosen because preliminary experiments showed that over a period of 12 hr. there was no sign of a sedimentation velocity peak developing so that true or near equilibrium conditions were assumed to prevail.

## II. TREATMENT OF OBSERVATIONS

### A. Light Scattering

The observations may conveniently be presented in the form of Zimm plots.<sup>4</sup> A theoretical plot for a polydisperse system is shown in Figure 1.

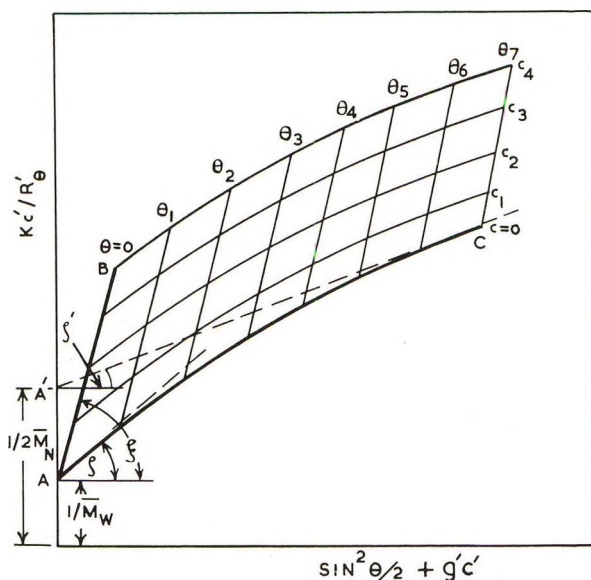


Fig. 1. Theoretical Zimm plot and derived parameters. AB zero angle line, AC zero concentration line.

It consists of a number of curves of  $Kc'/R'_\theta$  plotted against  $\sin^2\theta/2 + g'c'$  for different concentrations  $c'$  (g./cm.<sup>3</sup>) and scattering angles  $\theta$ . In this plot  $R'_\theta = R_\theta/(1 + \cos^2\theta)$ , where  $R_\theta$  is the Rayleigh scattering ratio,  $K$  an optical constant, and  $g'$  a numerical constant chosen to make  $g'c'$  of the same order of magnitude as  $\sin^2\theta/2$ . The lines AB, of zero angle ( $\theta = 0$ ), and AC, of zero concentration ( $c' = 0$ ) are extrapolated curves. From such a plot information is obtained as follows<sup>5</sup>: The common intercept A of AB and AC on the ordinate axis gives the reciprocal of the weight-average molecular weight  $\bar{M}_w$ . The initial slope  $\zeta$  of AC is given by

$$\zeta = 16\pi^2 \bar{\rho}_z^2 \bar{n}^2 / 3\lambda_0^2 \bar{M}_w$$

where  $(\overline{\rho_z^2})^{1/2}$  is the Z-average radius of gyration,  $n$  the refractive index of the solution, and  $\lambda_0$  the wavelength *in vacuo*, so that  $(\overline{\rho_z^2})^{1/2}$  may be found. The intersection on the ordinate of the asymptote to AC for high-angle data gives half the reciprocal of the number-average molecular weight  $\overline{M}_n$ . The slope  $\zeta'$  of this asymptote is given by

$$\zeta' = 8\pi^2 \overline{\rho_n^2} n^2 / \lambda_0^2 \overline{M}_n$$

where  $(\overline{\rho_n^2})^{1/2}$  is the number-average radius of gyration which may thus be determined. The initial slope  $\xi$  of AB gives twice the second osmotic virial coefficient ( $A_2$ ). The radii of gyration  $(\overline{\rho^2})^{1/2}$  are related to the corresponding end-to-end distances ( $r$ ) by equations dependent on the molecular model assumed. For Gaussian coils  $\overline{\rho^2} = r^2/6$ , and the distribution of molecular weights may be expressed by the formula

$$W(M)dM = \frac{y^{Z+1} M^Z e^{-yM}}{\Gamma(Z+1)} dM \quad (1)$$

where  $W(M)$  is that weight fraction of the polymer having a molecular weight in the range  $M$  to  $M + dM$  and  $Z$  and  $y$  are parameters of the width of the distribution such that

$$y = Z/\overline{M}_n = (Z+1)/\overline{M}_w = (Z+2)/\overline{M}_z \quad (2)$$

and  $\Gamma$  denotes the gamma function. For  $Z = 1$ ,

$$1/\overline{M}_n = 2/\overline{M}_w = 3/\overline{M}_z \quad (3)$$

and in this case the Zimm plots would be rectilinear rather than curved so the asymptote A'C and the curve AC coincide. whence  $\zeta = \zeta'$ . Curvature of a Zimm plot is also brought about by coil stiffness<sup>6,7</sup> and spurious scattering by dust which is more noticeable at low angles. These may

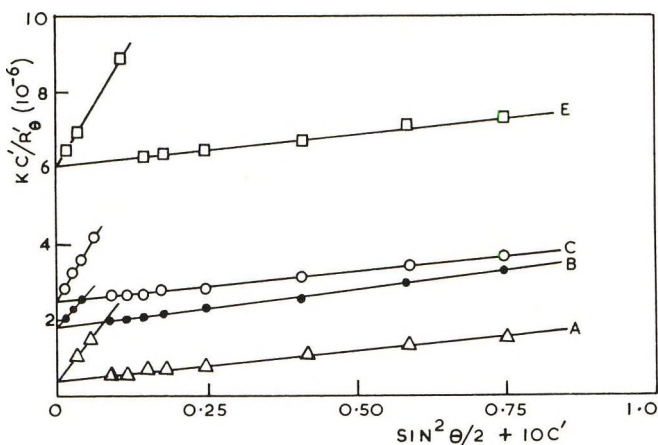


Fig. 2. Initial slopes of rectilinear Zimm plots for samples A, B, C, and E at 20°C. and at 4358 Å.

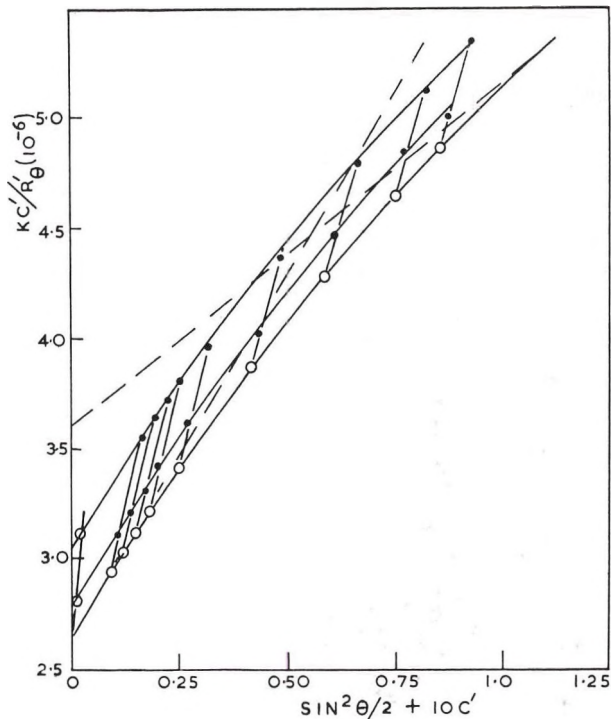


Fig. 3. Zimm plot for sample D at 20°C. and at 4358 Å.

change the curvature due to polydispersity so that care must be taken in the interpretation of the plots.

In the present studies four rectilinear plots (Fig. 2) and two curved plots (samples D and F), one of which is shown in Figure 3, were obtained. With sample F difficulty was experienced in cleaning the material, with the result that the curvature downward at low angles ( $\theta < 45^\circ$ ) due to polydispersity was enhanced by dust. High-angle values, however, were reliable, giving a curve similar to that obtained for sample D and values for  $\bar{M}_n$  and  $(\bar{\rho}^2_n)^{1/2}$  were obtained from the asymptote. A distribution the same as for D was assumed so that a value of  $\bar{M}_w$  was also found. It was further assumed that poly-NTBA molecules in methanol obey random flight conditions so that

$$\bar{\rho}_z^2/\bar{\rho}_n^2 = \bar{r}_z^2/\bar{r}_n^2 = \bar{M}_z/\bar{M}_n = (Z + 2)/Z \quad (4)$$

and

$$\bar{\rho}_w^2/\bar{\rho}_n^2 = \bar{r}_w^2/\bar{r}_n^2 = \bar{M}_w/\bar{M}_n = (Z + 1)/Z \quad (5)$$

For sample F the value of  $\bar{r}_z^2$  was calculated from eq. (4). From Eq. 5 values of  $\bar{\rho}_w^2$  and  $\bar{r}_w^2$  may be found for all samples. In practice high polymers seldom satisfy random flight conditions because any polymer solvent interaction or excluded volume effects will make the coil exceed random

TABLE I  
 Experimental Values from Light-Scattering Data<sup>a,c</sup>

Parameter	Sample A	Sample B	Sample C	Sample D	Sample E	Sample F
$\bar{M}_w \times 10^4$	245	54.6	40.4	37.9	16.5	8.8 <sup>b</sup>
$(\bar{\rho}_z^2)^{1/2}$ , A.	880	463	360	506	230	230
$\bar{M}_n \times 10^4$	122	27.3	20.2	13.9	8.3	3.2
$(\bar{\rho}_n^2)^{1/2}$ , A.	507	245	207	171	132	77
$A_2 \times 10^{-5}$	10.1	10.2	13.1	9.5	13.5	22.8
$(\bar{r}_z^2)^{1/2}$ , A.	2,155	1,040	883	1,240	563	560 <sup>b</sup>
$(\bar{r}_n^2)^{1/2}$ , A.	1,240	600	507	419	323	189
$\bar{M}_n \times 10^2$	95.9	21.4	15.9	10.9	6.5	2.5

<sup>a</sup> Molecular weight of monomer ( $M_0$ ) = 127.2.

<sup>b</sup> Denotes calculated values.

<sup>c</sup> For samples A B C D values of  $A_2$  are accurate to about 15% and the other parameters to about 6%. For samples D and F the corresponding accuracies are about 20% and 10%.

flight limitations but eqs. (4) and (5) give sufficiently good approximations. The values of  $\bar{M}_n$ ,  $\bar{M}_w$ ,  $(\bar{r}_n^2)^{1/2}$ ,  $(\bar{r}_z^2)^{1/2}$ , and  $A_2$  are given in Table I.

Poly-NTBA is a long chain molecule with bulky side groups so that rotation of the individual bonds forming the chain will probably experience appreciable steric hindrance giving rise to stiffness. The effect of this must be considered before the reliability of the results (Table I) obtained from the Zimm plots is established. The stiffness of the coil may be characterized by a parameter  $x$  which varies from infinity to zero according to whether the coil is flexible or stiff. Peterlin<sup>6,7</sup> gives values of the variation of the reciprocal of the particle scattering factor  $P(\theta)$  with  $\sin^2\theta/2$  for values of  $x$ , and shows that only for values of  $P(\theta)^{-1}$  greater than about 2 do the values of  $x$  for flexible and stiff coils begin to differ appreciably. Thus in Zimm plots, where  $Kc'/R_\theta'$  is proportional to  $P(\theta)^{-1}$ , the effect of stiffness will be negligible either for values of  $P(\theta)^{-1} < 2$  or for  $P(\theta)^{-1} > 2$  when  $x$  is large.  $x$  is identical with the limiting value of  $\bar{N}(1 - \overline{\cos \beta'})$ , in which  $\bar{N}$  is the degree of polymerization and  $\beta'$  is the supplement of the equivalent valence angle, where the latter is the valence angle for a molecule having the same bond length  $l$ , the same number of bonds and the same dimensions as poly-NTBA but without rotational hindrance. It is related to  $l$ , to the length  $b$  of the statistical element and the root-mean-square end-to-end distance  $(\bar{r}^2)^{1/2}$  of the coils by the relationship

$$\bar{r}^2 = Nl^2 \left( \frac{1 + \overline{\cos \beta'}}{1 - \overline{\cos \beta'}} \right) = Nb^2 \quad (6)$$

Taking  $l$ , the carbon bond length, as 1.54 Å. and the values of  $b$  (Table II) calculated from  $(\bar{r}_n^2)/N_n$ , it was found that the magnitude of  $\overline{\cos \beta'}$  was 0.97 and the values of  $x$  as in Table II. The small values of  $x$  correspond to values of  $P(\theta)^{-1} < 2$  so that for all samples the curvature of the Zimm plots can be attributed to polydispersity.

TABLE II  
 Stiffness Parameters

Parameters	Sample A	Sample B	Sample C	Sample D	Sample E	Sample F
Statistical element $b$	12.7	12.9	12.7	12.7	12.7	11.9
Kratky-Porod persistence length $a$	55.0	64.4	57.0	63.3	62.8	53.9
Coiling factor $\bar{r}_{\max}/(\bar{r}_n^2)^{1/2}$	9.7	4.5	3.9	3.3	2.5	1.7
Stiffness criterion $x$	288	64	48	33	19.5	8.5

### B. Sedimentation

True sedimentation equilibrium may take days to attain but in the approach to true equilibrium, solute cannot leave the solution at the bottom of the cell, nor at the liquid meniscus and so must be in equilibrium at these two positions. The normal equilibrium equation is thus applicable and for a polydisperse system, the weight average molecular weight is given by:

$$\bar{M}_w = \frac{RT(\partial c/\partial x)_i}{(1 - V\rho_0)\omega^2 x_i c_i} \quad i = m, b \quad (7)$$

where  $m$  and  $b$  refer to meniscus and cell bottom respectively,  $c$  is the concentration at a distance  $x$  from the axis of rotation,  $V$  is the partial specific volume,  $\rho_0$  is the solvent density,  $\omega$  is the angular velocity of the rotor, and  $R$  and  $T$  have their usual meanings.

According to Klainer and Kegles,<sup>8</sup> provided a plateau region exists and no schlieren velocity peaks occur, then

$$c_m = c_0 - \frac{1}{x_m^2} \int_{x_m}^X x^2 (\partial c/\partial x) dx \quad (8)$$

and

$$c_b = c_0 + (1/x_b^2) \int_X^{x_b} x^2 (\partial c/\partial x) dx \quad (9)$$

where  $c_0$  is the initial concentration of the solution and the distance  $X$  is measured to a point within the plateau region.

Sedimentation runs were made on samples B and D. Molecular weights were calculated from measurements made on a pattern taken 140 min. from the commencement of the sedimentation run (Fig. 4). The initial concentrations  $c_0$  of the two samples studied were determined by auxiliary sedimentation velocity runs at a speed of 29,500 rpm (63,240g) with a double-sector cell containing the solution in one sector and the solvent in the other. The schlieren angles, temperature, and cell sizes were identi-

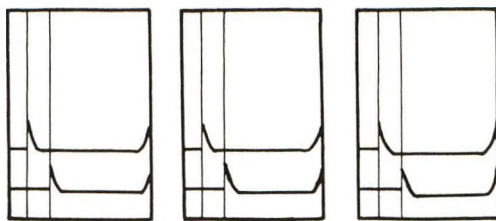


Fig. 4. Typical ultracentrifuge approach to equilibrium patterns after 92, 140, and 172 min. for samples B (top) and D. Schlieren angle  $70^\circ$ . Temperature  $20^\circ\text{C}$ .

cal with those of the equilibrium run. Photographs were taken at different times and the areas under the peaks were measured using a planimeter. By extrapolating these values, the area corresponding to the initial concentration was found. The method used to calculate  $\int x^2(\partial c/\partial x)dx$  at the bottom and meniscus of the cell and hence  $c_b$  and  $c_m$  was as described by Schachman.<sup>9</sup> From these observations, two values for the molecular weight were determined. The average value of these for the two samples were  $(54.8 \pm 0.7) \times 10^4$  and  $(35.3 \pm 0.5) \times 10^4$ , respectively. Some corrections to these values might be necessary because they have been made at a temperature different from the  $\theta$  value. At this value the net interaction between segments of a pair of polymer molecules becomes zero and the molecules can overlap freely rendering the centrifuge values more accurate. Hence these results cannot be taken as exact but they confirm those obtained by light scattering (Table I).

### III. APPLICATION AND DISCUSSION OF RESULTS

#### A. Calculation of Length $b$ of Statistical Element and of Steric Hindrance or Stiffness

Several authors<sup>10-13</sup> have shown that for a molecule obeying Gaussian statistics in which the individual bonds are freely jointed and for which the volume effect is negligible, eq. (6) may be replaced by

$$\bar{r}^2 = Nl^2 \left( \frac{1 + \overline{\cos \beta}}{1 - \overline{\cos \beta}} \right) \left( \frac{1 + \overline{\cos \psi}}{1 - \overline{\cos \psi}} \right) = Nb^2 \quad (10)$$

in which  $\overline{\cos \psi}$  is a parameter which is a measure of the degree of restriction placed upon the rotation of the bonds, i.e., the stiffness of the coil, and  $\beta$  is the supplement of the true valence angle and is related to the equivalent angle  $\beta'$  of eq. (6) by the equation

$$\frac{1 + \overline{\cos \beta'}}{1 - \overline{\cos \beta'}} = \frac{(1 + \overline{\cos \beta})(1 + \overline{\cos \psi})}{(1 - \overline{\cos \beta})(1 - \overline{\cos \psi})} \quad (11)$$

The angle  $\psi$  is the statistical average of the angle made by a chosen bond with the plane containing two previous bonds. If there is no polymer-solvent interaction ( $A_2 = 0$ ), this angle is a measure of the skeletal steric

hindrance of the molecule. Even in cases where the conditions for the validity of eq. (10) do not apply exactly, the determination of  $b$  and  $\psi$  are still of value because, provided the molecule is large enough, they give a measure of the size of the molecule for a given value of  $N$ . The value of  $b$  for the samples used is essentially constant at 12.7 Å. (Table II). The lower value of 11.9 Å. for the low molecular weight sample F is to be expected, for  $b$  would decrease as the coil dimensions decrease. The constancy of  $b$  over the molecular weight range shown signifies that all samples favor the same statistical configuration and leads to a value of  $\cos \psi$  of 0.95 ( $\psi = 18^\circ 20'$ ). Such a value indicates a high degree of restriction within the molecular configuration.

Another parameter which characterizes the stiffness of a chain is the Kratky-Porod persistence length<sup>14,15</sup>  $a$ , which is defined as the projection of an infinitely long chain along the direction of the first bond, and is given by<sup>16</sup>

$$\overline{\rho^2} = a^2 \alpha^2 [x/3 - 1 + (2/x) - 2/x^2 (1 - e^{-x})] \quad (12)$$

In this equation  $x = \bar{r}_{\max}/a$ , where  $\bar{r}_{\max}$  is the extended length of the molecule (i.e.,  $\bar{r}_{\max} = \bar{N}l \cos \beta/2$ ), and  $\alpha$  is the expansion factor which is a measure of the increase in molecular dimensions beyond those for the unperturbed system when the interactions are zero or cancel out. For the range of values of  $x$  (8.5–288) used here, eq. (12) can be reduced to

$$\overline{\rho^2} = \bar{r}_{\max}^2 \alpha^2 a/3$$

From the determined values of  $\overline{\rho_n^2}$ ,  $\bar{r}_{\max}$ , and  $\alpha$  (see below), the number-average values of  $a$  were calculated (Table II). The values obtained for  $a$  are quite high. This is shown by a consideration of the Kuhn and Kuhn theory<sup>17,18</sup> in which a molecular model of the random coils is considered to be built up of a number of statistical segments, of length  $A_m = 2a$ . No valence restrictions were placed on the model, so that for flexible coils,  $A_m$  should not be high. Taking the average value of  $a$  as 59.5 Å. gives a value of  $A_m$  of 119 Å., so that with a bond length of 1.54 Å. the segments would be equivalent to 77 monomer units.

### B. Variation of Radius of Gyration with Molecular Weight

The equation relating the apparent limiting viscosity number to the molecular weight has been determined previously<sup>2</sup> to be

$$[\eta] = 8.87 \times 10^{-4} \bar{M}_w^{0.525}$$

The viscosity number relates to zero concentration and a gradient  $G$  of 760 sec.<sup>-1</sup>.

The exponent value of 0.525 indicates that the molecule in this solvent is not freely draining and the finite positive values of  $A_2$  (Table I) determined in the present study indicate that polymer-solvent interaction is present so that it is not expected that the polymer will obey random flight conditions. Radii of gyration  $(\overline{\rho_n^2})^{1/2}$ , determined directly from the Zimm plots so that there was no necessity to assume any particular molecular model,



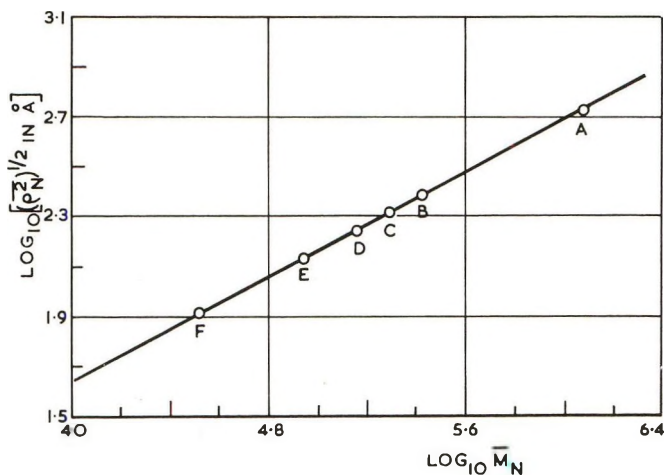


Fig. 5. Variation of radius of gyration  $(\overline{\rho_n^2})^{1/2}$  with number-average molecular weight  $\overline{M}_n$  for samples A-F.

are plotted as a function of  $\overline{M}_n$  in Figure 5. From this line it was found by use of the method of least squares that

$$(\overline{\rho_n^2})^{1/2} = 3.76 \times 10^{-9} \overline{M}_n^{0.515} \quad (13)$$

or

$$(\overline{\rho_n^2})^{1/2} = 3.76 \times 10^{-9} \overline{M}_n^{1+\epsilon} \quad (14)$$

where  $\epsilon = -0.485$ . This confirms that the molecule has expanded beyond random flight predictions and that methanol is a good solvent.

### C. Variation of Second Osmotic Virial Coefficient $A_2$ with Molecular Weight and Determination of the Expansion Factor

According to the dilute solution theory of Krigbaum and Flory,<sup>19</sup>  $A_2$  should decrease as  $\overline{M}$  increases. A linear dependence has been found for certain molecular weight ranges by some authors. In the present study an approximate linear relationship has been found for five samples (Fig. 6) and by use of the method of least squares it is found that  $A_2 = 0.082 \overline{M}_w^{-0.515}$ . Sample A has an inexplicably high value.

The second virial coefficient is a guide to the expansion of the polymer arising from nonideal systems. An equation connecting the molecular expansion factor  $\alpha$  and  $A_2$  has been derived by Orofino and Flory:<sup>20</sup> it is

$$A_2 = \left[ \frac{16\pi N_A}{3^{3/2} \overline{M}^2} (\overline{\rho^2})^{3/2} \right] \ln \left[ 1 + \frac{\pi^{1/2}}{2} (\alpha^2 - 1) \right] \quad (15)$$

where  $N_A$  is Avogadro's number. Using the number-average values of  $\overline{M}$  and  $(\overline{\rho^2})^{1/2}$ , values of  $\alpha$  have been found (Table III). For all samples the values are very close to unity, suggesting that long-range interactions

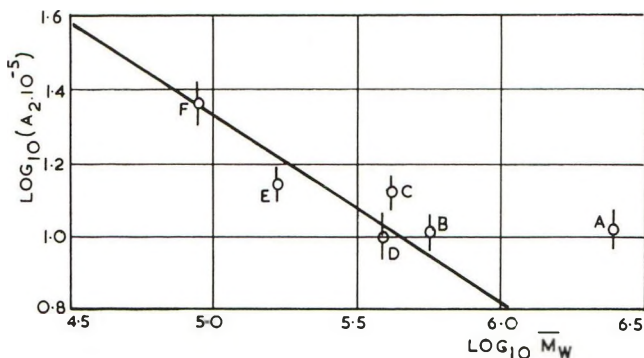


Fig. 6. Variation of second osmotic virial coefficient  $A_2$  with weight-average molecular weight  $\bar{M}_w$  for samples A-F.

are not important, and that most of the polymer extension arises from skeletal (or internal) effects.

TABLE III  
Flory Expansion Factor  $\alpha$ , and constants  $K_V$  and  $\Phi$

Sample	Expansion factor $\alpha$	Flory constants		
		$K_V \times 10^{-3}$	$\Phi \times 10^{21}$	
			Gaussian	Lansing-Kraemer
A	1.11	1.30	0.93	1.47
B	1.05	1.55	0.88	1.39
C	1.09	1.32	0.87	1.37
D	1.04	—	0.98	2.22
E	1.04	1.44	0.85	1.35
F	1.05			
Average values		1.40	0.90	1.56

#### D. Determination of the Flory Universal Constant $\Phi$

If an impermeable or partially permeable molecule is considered to act hydrodynamically in the solvent like a sphere then, for a monodisperse medium, according to Flory and Fox,<sup>21</sup>

$$\Phi = [\eta]M/(\bar{r}^2)^{3/2} \quad (16)$$

and

$$K_V = \Phi(\bar{r}_0^2/M)^{3/2} \quad (17)$$

so that

$$[\eta] = K_V M^{1/2} \alpha^3 \quad (18)$$

$[\eta]$  is the limiting viscosity number referred to zero concentration and zero gradient,  $\Phi$  is a universal constant, and applies to any randomly coiling

polymer in any solvent, whereas  $K_V$  is a particular constant for a polymer in any solvent.  $\alpha$  is the molecular expansion factor and  $r_0$  is the root-mean-square separation between the ends when the second osmotic virial coefficient is zero. The value of  $\Phi$  was predicted as  $3.6 \times 10^{21}$  from the Kirkwood-Riseman<sup>22</sup> treatment, where the hydrodynamic configuration of the molecule is considered as similar to a cloud of independent beads, but the greater part of the experimental data gives values in the range 2.0 to  $2.2 \times 10^{21}$ , so that 2.1 is the figure often used.

For a polydisperse system,<sup>23</sup> the number-averages of the quantities  $\bar{M}$  and  $[(\bar{r}^2)^{3/2}]$  and not just  $(\bar{r}_n^2)^{3/2}$  must be used in eqs. (16) and (17). Light-scattering data give  $\bar{M}_w$  and  $\bar{r}_z^2$ , and in order to employ these values directly a factor  $q$  is introduced such that

$$\Phi = [\eta] \bar{M}_w q / (\bar{r}_z^2)^{3/2} \quad (19)$$

For a Gaussian distribution of molecular weights<sup>24</sup>

$$q = \frac{(Z + 2)^{3/2} \Gamma(Z + 2)}{(Z + 1)^2 \Gamma(Z + 3/2)} \quad (20)$$

in which  $\Gamma$  denotes the gamma function, while according to Newman et al.<sup>23</sup> a Lansing-Kraemer<sup>25</sup> distribution gives

$$q = (\bar{M}_w / \bar{M}_n)^{13/8} \quad (21)$$

From previous viscosity measurements<sup>2</sup> and the present data, values of  $\Phi$  have been calculated from eqs. (19), (20), and (21); they are tabulated in Table III. The values are low even for high molecular weight samples. A possible explanation is as follows. The results above (Sects. IIIA-III C) seem to suggest that the poly-NTBA molecule is very extended in methanol, mainly because of steric hindrance within the molecule. Newman et al.<sup>23</sup> have suggested the criterion that the coiling factor  $\bar{r}_{\max} / (\bar{r}^2)^{1/2}$  must be greater than 10 for a true random coil. If this ratio is not exceeded, as is here the case (Table II), the spatial distribution will no longer be spherically symmetric and the Flory theory cannot be expected to apply, so that although the molecular weights are high these large extensions may give rise to low values of  $\Phi$ . Another explanation or an additional reason for low  $\Phi$  values could be attributed to the measured quantities  $\bar{M}_w$ ,  $\bar{r}_z^2$ , and  $[\eta]$ . The values of  $\bar{M}_w$  and  $\bar{r}_z^2$ , however, are most probably correct since the values of  $\bar{M}_w$  are in satisfactory agreement with the values obtained by ultracentrifugation and the  $\bar{r}_z^2$  values have been checked by using the dissymmetry light-scattering technique. The values of  $[\eta]$  were obtained<sup>2</sup> by using capillary viscometers and by extrapolation of the graph of reduced viscosity against concentration to zero concentration. Since, however, the graph at low concentrations showed a pronounced curvature which varies with the velocity gradient used, the use of the value  $[\eta]_{c=0}^{G=760}$  instead of  $[\eta]_{c=0}^{G=0}$  to calculate  $\Phi$  may introduce an error.

Experiments with a concentric cylinder viscometer have shown that poly-

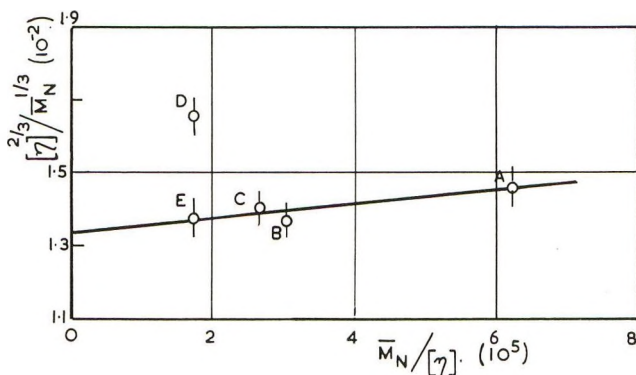


Fig. 7. Variation of  $[\eta]^{2/3} / \bar{M}_n^{1/3}$  with  $\bar{M}_n / [\eta]$  for samples A-E.

NTBA in methanol exhibits rheopecty, i.e., an increase in viscosity with gradient following an initial fall while conditions of laminar flow still prevail. This gives the possibility that the value  $[\eta]_{c=0}$   $G=760$  may be somewhat lower than  $[\eta]_{c=0}$   $G=0$ ; a twofold increase, which would give values of  $\Phi$  nearer that usually accepted, is not to be excluded.

#### E. Determination of the Flory Constant $K_V$

Equation (18) may be rearranged to read

$$([\eta]^{2/3} / \bar{M}_n^{1/3})^{3/2} = K_V^{3/2} \alpha^2 = K_V^{3/2} (1 + \gamma K_V \bar{M}_n / [\eta]) \quad (22)$$

where

$$\gamma = (\alpha^5 - \alpha^3) / \bar{M}_n^{1/2}$$

so that if, as Flory<sup>10</sup> suggests,  $\gamma$  is a constant, a graph of  $[\eta]^{2/3} \bar{M}_n^{-1/3}$  against  $\bar{M}_n / [\eta]$  would be a straight line of intercept  $K_V^{3/2}$  on the ordinate axis and slope  $\gamma K_V^{3/2}$ . The graph plotted for five samples is shown in Figure 7. Excluding sample D a linear curve results from which, using the method of least squares,  $K_V$  was found to be  $(1.53 \pm 0.20) \times 10^{-3}$ . This value is high in comparison with those of the order of  $10^{-3}$  listed by Flory which is incompatible with the fact that possibly  $[\eta]$  and  $\Phi$  are low. However from eq. (17) it can be seen that  $K_V$  is proportional to  $\bar{r}_0^3$ , and extra large values of  $r_0$  might be expected from consideration of the large degree of hindrance to bond rotations.

Equation (18) has also been used to calculate values for  $K_V$  by use of the values of  $\alpha$  and  $\bar{M}_n$  given in Tables I and III. The average value is  $1.40 \times 10^{-3}$  and agrees well with that of  $(1.53 \pm 0.20) \times 10^{-3}$  above.

#### F. The Excluded Volume Effect

The volume excluded to polymer molecules because of the finite volumes occupied by other molecules which is known as the excluded volume has

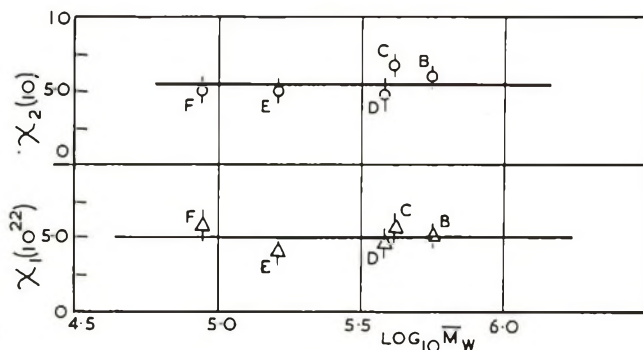


Fig. 8. Variation of  $\chi_1 = A_2 \bar{M}_w^2 / (\bar{r}_w)^{3/2}$  and  $\chi_2 = A_2 \bar{M}_w / [\eta]$  with molecular weight for samples B-F.

been included in at least two empirical relationships.<sup>20,26</sup> If it be assumed that the radius of the equivalent sphere in the Flory-Fox theory<sup>21</sup> is proportional to  $(\bar{r}^2)^{1/2}$ , then the excluded volume would be proportional to  $(\bar{r}^2)^{3/2}$ . One such empirical relationship is that for high molecular weight polymers in thermodynamically good solvents

$$A_2 \bar{M}_w^2 / (\bar{r}_w^2)^{3/2} = \chi_1 \quad (23)$$

where  $\chi_1$  is a constant. Since  $M / (\bar{r}^2)^{3/2}$  is proportional to  $1/[\eta]$  according to eq. (16), substitution in eq. (23) gives

$$A_2 \bar{M}_w / [\eta] = \chi_1 / \Phi = \chi_2 \quad (24)$$

where  $\chi_2$  is another constant.

Constant values of  $\chi_1$  and  $\chi_2$  have been reported for a number of polymer systems and are seen here to hold for five samples of poly-NTBA in methanol (Fig. 8) over the molecular weight range  $8.8 \times 10^4$  to  $2.45 \times 10^6$ . The values obtained are  $4.93 \times 10^{22}$  and 54 for  $\chi_1$  and  $\chi_2$ , respectively. The values for sample A were  $11.4 \times 10^{22}$  and 127, which although inexplicable are consistent with the high value for  $A_2$  shown in Figure 6.

#### IV. CONCLUSIONS

Most hydrodynamic theories for polymers are based upon the molecules assuming configurations represented by Gaussian statistics. Strictly, however, because of the effect of both short- and long-range interactions, these statistics seldom apply to polymer solutions. Short-range interactions are steric and energetic hindrances to bond rotation within the molecules, while long-range interactions consist of the excluded volume effect and polymer-polymer and polymer-solvent interactions. The theories only apply to monodisperse systems, which are rarely found in practice. Generally, polymers of a high degree of polymerization behave very similarly to random coils, especially at or near the  $\Theta$ -temperature of the solution. Poly-NTBA in methanol, however, is expanded well beyond

random flight conditions even for very high degrees of polymerization ( $\approx 9,500$ ) as is shown by high values of the statistical element  $b$ , of the Kratky-Porod persistence length  $a$  and of the Kuhn statistical segment  $A_m$ . The molecular size of poly-NTBA may be found from eqs. (6) and (10); for  $\bar{N} \geq 650$ , if  $r$  is obtained in Angstroms,  $\bar{r}^2 = 161\bar{N}$ . The dimensions and viscosity of the polymer in solution show that long range interactions partly account for this molecular extension. However the small values of the expansion factor  $\alpha$  show that stiffness of the coil does not arise mainly from the long-range effects, but rather from the hindrances by the bulky substituents of the chain to bond rotation. This is confirmed by the high values of the parameter  $\cos \psi$ . The stiffness is further reflected in the coiling factor,  $r_{\max}/(\bar{r}^2)^{1/2}$ , having a value less than ten, so that the system cannot be expected to conform to the value of  $2.1 \times 10^{21}$  for the Flory-Fox constant  $\Phi$ . Except for sample D, values obtained for  $\Phi$  appear to increase slightly with molecular weight, an anomalous behavior which has been experienced with other stiff bulky polymers, especially cellulose and its derivatives. The authors suggest therefore that care must be taken before a value for  $\Phi$  of  $2.1 \times 10^{21}$  is assumed, and then used to calculate molecular dimensions from a knowledge of  $M$  and  $[\eta]$ . The criterion that the molecular weight is high is not in itself enough. It is suggested that the factor  $\Phi^{1/3}P^{-1}$  from the theory of Flory and Mandelkern<sup>27</sup> might be a more reliable constant, where  $P$  is a universal parameter obtained by considering the frictional coefficient ( $f_0$ ) of the polymer in a solvent of viscosity ( $\eta_0$ ). By analogy with  $\Phi$ ,

$$f_0/\eta_0 = P(\bar{r}_0^2/M)^{1/2}M^{1/3} \alpha = P(\bar{r}^2)^{1/2}$$

Little work seems to have been reported on the use of this factor. It is also noted that few of the workers reporting values of  $2.1 \times 10^{21}$  for  $\Phi$  have used a value of  $[\eta]$  appertaining to zero velocity gradient.

The values of the expansion factor  $\alpha$  obtained by using the Orofino and Flory equation which relates the second osmotic virial coefficient  $A_2$  to  $\alpha$  lead to values of the Flory constant  $K_V$  which are in good agreement with that obtained from the Flory-Fox equations. This suggests that the equation is at worst a very good approximation for these systems.

The poly-NTBA samples were prepared by Dr. E. A. S. Cavell and Mr. I. T. Gilson of the Department of Chemistry both of whom the authors wish to thank. The viscosity values were determined by Mr. Gilson, and the rheopectic behavior investigated by Mr. D. J. Groves of the Department of Physics who made measurements with a concentric cylinder viscometer. The ultracentrifuge was purchased from a grant made by the Department of Scientific and Industrial Research (D.S.I.R.) for special researches. The authors acknowledge the facilities provided by the Department of Physics where this work was carried out. One of us (B. R. J.) thanks the D.S.I.R. for a research award during the tenure of which this work was performed.

## References

1. Archibald, W. J., *J. Phys. Chem.*, **51**, 1204 (1947).
2. Cavell, E. A. S., I. T. Gilson, B. R. Jennings, and H. G. Jerrard, *J. Polymer Sci.*, **A2**, 3615 (1964).
3. Jerrard, H. G., and D. B. Sellen, *Appl. Optics*, **1**, 243 (1962).
4. Zimm, B. H., *J. Chem. Phys.*, **16**, 1099 (1948).
5. Benoit, H., A. M. Holtzer, and P. Doty, *J. Phys. Chem.*, **58**, 635 (1954).
6. Peterlin, A., *Makromol. Chem.*, **9**, 244 (1953).
7. Peterlin, A., *J. Polymer Sci.*, **10**, 425 (1953).
8. Klainer, S. M., and G. Kegeles, *J. Phys. Chem.*, **59**, 952 (1955).
9. Schachman, H. K., *Methods in Enzymology*, **4**, 32 (1957).
10. Flory, P. J., *Principles of Polymer Chemistry*, Cornell Univ. Press, Ithaca, N. Y., 1953.
11. Kuhn, H., *J. Chem. Phys.*, **15**, 843 (1947).
12. Benoit, H., *J. Chim. Phys.*, **44**, 18 (1947).
13. Taylor, W. J., *J. Chem. Phys.*, **16**, 257 (1948).
14. Kratky, O., *Monatsh.*, **80**, 251 (1949).
15. Kratky, O., and G. Porod, *Rec. Trav. Chim.*, **68**, 1106 (1949).
16. Benoit, H., and P. Doty, *J. Phys. Chem.*, **57**, 958 (1953).
17. Kuhn, H., *J. Colloid Sci.*, **5**, 331 (1950).
18. Kuhn, H., and W. Kuhn, *J. Polymer Sci.*, **5**, 519 (1950).
19. Krigbaum, W. R., and P. J. Flory, *J. Am. Chem. Soc.*, **75**, 1775 (1953).
20. Orofino, I. A., and P. J. Flory, *J. Chem. Phys.*, **26**, 1067 (1957).
21. Forry, P. J., and T. G. Fox, *J. Am. Chem. Soc.*, **73**, 1904 (1951).
22. Klikwood, J. G., and J. Riseman, *J. Chem. Phys.*, **16**, 565 (1948).
23. Newman, S., W. R. Krigbaum, C. Langier, and P. J. Flory, *J. Polymer Sci.*, **14**, 451 (1954).
24. Krigbaum, W. R., and L. H. Sperling, *J. Chem. Phys.*, **64**, 99 (1960).
25. Lansing, W. D., and E. O. Kraemer, *J. Am. Chem. Soc.*, **57**, 1369 (1935).
26. Schultz, A. R., *J. Am. Chem. Soc.*, **76**, 3422 (1954).
27. Mandelkern, L., and P. J. Flory, *J. Chem. Phys.*, **20**, 212 (1952).

## Résumé

On présente les résultats d'une étude par diffusion lumineuse de six échantillons de poly-*N*-tertiaire butyle acrylamide dans le méthanol. Certains résultats confirmatifs ont été obtenus par ultra-centrifuge. On décrit brièvement la dérivation des paramètres moléculaires à partir des diagrammes de Zimm et des résultats de la centrifugation. On a trouvé que le méthanol est un bon solvant pour le poly-N.T.B.A., dans lequel il se comporte comme une molécule rigide dépolymérisée au delà des prévisions statistiques. On discute l'influence de la rigidité sur les diagrammes de Zimm et sur l'interprétation des résultats. On a trouvé les valeurs des poids moléculaires moyens en poids et en nombre ( $\bar{M}_w$  et  $\bar{M}_n$ ), la moyenne  $z$  et les rayons de gyration  $(\bar{p}_z^2)^{1/2}$  et  $(\bar{p}_n^2)^{1/2}$  et les distances quadratiques moyennes correspondantes  $(\bar{r}_z^2)^{1/2}$  et  $(\bar{r}_n^2)^{1/2}$ .  $\bar{r}_z = 161 \bar{N}$  où  $N$  est le degré de polymérisation et  $\bar{r}$  est mesuré en Angstroms. On a également obtenu des valeurs pour la longueur de l'élément statistique, la longueur de persistance de Kratky-Porod, le facteur d'enroulement, le facteur d'expansion moléculaire, le second coefficient viriel osmotique,  $(A_2)$  et les constantes de Flory  $\Phi$  et  $K_V$ . On déduit des équations pour la variation de  $(\bar{p}_n^2)^{1/2}$  et de  $A_2$  avec le poids moléculaire: ce sont  $(\bar{p}_n^2)^{1/2} = 3.76 \times 10^{-9} \bar{M}_n^{-0.515}$  et  $A_2 = 0.082 \bar{M}_w^{-0.515}$  respectivement. La valeur de  $\Phi$  est beaucoup plus petite que celle prévue normalement et on suggère des raisons possibles. On mentionne des relations empiriques impliquant l'effet du volume exclu.

### Zusammenfassung

Die Ergebnisse einer Lichtstreuungsuntersuchung von sechs Poly-*N-tertiar*-butylacrylamidproben in Methanol werden mitgeteilt. Einige übereinstimmende Ergebnisse wurden mit einer Ultrazentrifuge erhalten. Die Ableitung der Molekülparameter aus dem Zimm-Diagramm und den Zentrifugenergebnissen wird kurz beschrieben. Methanol ist ein gutes Lösungsmittel für Poly-N.T.B.A., in dem es sich als steifes, über die Irrflugdimension hinaus expandiertes Molekül verhält. Der Einfluss der Steifigkeit auf das Zimm-Diagramm und die Interpretation der Ergebnisse wird diskutiert. Werte für das Gewichts- und Zahlenmittel des Molekulargewichts ( $\bar{M}_w$  und  $\bar{M}_n$ ), das  $z$ -Mittel und Zahlenmittel des Gyrationradius  $(\overline{\rho_z^2})^{1/2}$  und  $(\overline{\rho_n^2})^{1/2}$  und die entsprechenden End-zu-Endabstände  $(\overline{r_z^2})^{1/2}$  und  $(\overline{r_n^2})^{1/2}$  werden bestimmt.  $\bar{r}^2 = 161 \bar{N}$ , wenn  $N$  der Polymerisationsgrad ist und  $\bar{r}$  in Angström gemessen wird. Weiters werden Werte für die Länge des statistischen Elements, die Kratky-Porod-Persistenzlänge, den Knäuelungsfaktor, den Molekülexpansionsfaktor, den zweiten osmotischen Virialkoeffizienten ( $A_2$ ) und die Flory-Konstanten  $\Phi$  und  $K_V$  erhalten. Gleichungen für die Abhängigkeit von  $(\overline{\rho_n^2})^{1/2}$  und  $A_2$  vom Molekulargewicht werden abgeleitet, sie lauten:  $(\overline{\rho_n^2})^{1/2} = 3,76 \times 10^{-9} \bar{M}_n^{-0,515}$  und  $A_2 = 0,082 \bar{M}_w^{-0,515}$ . Der Wert von  $\Phi$  ist beträchtlich geringer als der normalerweise erwartete; mögliche Gründe dafür werden angegeben. Empirische Beziehungen unter Verwendung des Effekts des ausgeschlossenen Volumens werden erwähnt.

Received December 16, 1963



## Synthesis of Low Molecular Weight Polystyrene by Anionic Techniques and Intrinsic Viscosity-Molecular Weight Relations Over a Broad Range in Molecular Weight\*†

T. ALTARES, JR., D. P. WYMAN, and V. R. ALLEN, *Mellon Institute, Pittsburgh, Pennsylvania*

### Synopsis

Anionic polymerization techniques have been used to prepare low molecular weight ( $M \leq 10,000$ ) polystyrene of  $\bar{M}_w/\bar{M}_n \leq 1.1$ . The preparation and characterization of polymers are described. Good agreement with results reported by others was obtained for the viscosity-molecular weight relation in benzene at 25°C., viz.  $[\eta] = 1.0 \times 10^{-3} \bar{M}_n^{0.5}$ , for  $500 < \bar{M}_n \leq 10,000$ . For high molecular weight fractions ( $2.5 \times 10^4 < M \leq 1.5 \times 10^6$ ) of anionically prepared polystyrene, the expression,  $[\eta]_{\text{benzene}} = 8.5 \times 10^{-5} M^{0.75}$ , was found to be applicable and in agreement with relations given in the literature. Under theta conditions—cyclohexane as solvent at 34.5°C.—a single expression,  $[\eta] = 8.4 \times 10^{-4} M^{0.5}$ , was found to apply over the entire molecular weight range,  $500 < M \leq 1.5 \times 10^6$ .

### INTRODUCTION

Low molecular weight ( $\bar{M} < 10,000$ ) polystyrene can be synthesized readily via cationic polymerization methods.<sup>2,3</sup> However, molecular weight distributions are generally quite broad. Because certain programs in progress in these laboratories required low molecular weight polymer having narrow distributions in molecular weight, anionic polymerization techniques were used to prepare these hitherto undescribed materials. The experimental methods used in their synthesis and characterization are described herein. Correlations are included on the dilute solution properties of fractions of anionic polystyrene covering a wide range in molecular weights.

\* Synthesis studies supported in part by the Office of Naval Research under Contract No. Nonr 2693(00). Dilute solution viscosity studies supported in part by Aeronautical Systems Division, Wright-Patterson Air Force Base under Contract No. AF 33(657)-10661.

† Paper presented at the 145th Meeting, American Chemical Society, New York, September 1963.<sup>1</sup>

## EXPERIMENTAL

### Materials

Styrene was purified by fractional distillation at reduced pressure under nitrogen. Middle cuts were collected in calibrated, ball-type breakseal ampules, degassed, and stored under vacuum at Dry Ice temperatures until used. Benzene was distilled from a solution of butyllithium and styryllithium. Tetrahydrofuran (THF) was fractionally distilled from a sodium biphenyl solution. Analysis by gas chromatography showed that the THF thus obtained was pure and free of biphenyl.

### Polymerizations

All polymerizations were conducted under high vacuum with the use of the kinds of apparatus described in the literature.<sup>4,5</sup> In a typical example of the preparation of a low molecular weight polymer, 20 g. of styrene, 0.0513 mole of butyllithium in hexane, 0.120 mole of tetrahydrofuran, and 0.1 mole of methanol were placed in breakseal ampules equipped with magnetic hammers and these were sealed about the periphery of a 500 cc. flask attached to the vacuum line. Approximately 200 cc. of benzene and the styrene were distilled into the flask, the solution which was obtained was frozen, and the reactor was sealed off from the vacuum line. When the solution was about one-half thawed, the butyllithium was admitted and all surfaces of the reactor were thoroughly washed with the slurry in the flask. This step was carried out as rapidly as possible ( $\sim 25$  sec.), and the color of the reaction mixture at this point was a faint yellow. The THF was then introduced into the rapidly stirred slurry which immediately became dark red and evolved sufficient heat to melt most of the solid benzene. After  $1/2$  hr. of stirring at room temperature, the reaction was terminated by addition of methanol. The colorless solution which was obtained was washed thoroughly with water and then freeze dried. This polymer was a colorless, viscous liquid, and the yield was quantitative.

All of the polymers with  $M < 30,000$  were prepared in this manner, with the exception that those with  $M > 1500$  were isolated by precipitation in an excess (tenfold) of cold methanol before freeze drying.

### Molecular Weight Determinations

Number-average molecular weights  $\bar{M}_n$  were determined by one or more of the following means: cryoscopy and ebulliometry; vapor pressure osmometry; nuclear magnetic resonance (NMR) spectroscopy.

Cryoscopic and ebulliometric measurements were made by the Schwartzkopf Microanalytical Laboratories, Woodside, New York, on camphor and benzene solutions, respectively. Vapor pressure osmometry measurements were made by the Mellon Institute Research Services Group using a Mechrolab instrument with benzene as solvent. Nuclear magnetic resonance (NMR) spectra were obtained with a Varian A-60 spectrometer.

The solvent was carbon tetrachloride, and tetramethylsilane was the internal reference.

### Intrinsic Viscosity

Solution flow times were measured in Cannon-Ubbelohde viscometers which had been calibrated for kinetic energy effects. Benzene solutions were measured at  $25$  and  $30 \pm 0.01^\circ\text{C}$ . and cyclohexane solutions at  $34.5 \pm 0.01^\circ\text{C}$ . ( $\theta$ ). The concentration was expressed in grams/dl. Density corrections were applied to solutions containing polymers of  $M < 5 \times 10^4$  by using the specific volume data of Fox and Flory.<sup>6</sup>

### Molecular Weight Distributions

When applicable, i.e., polymers with  $\bar{M} > 5000$ , conventional solution fractionation techniques were used to obtain  $w_i - \bar{M}_i$  data for the computation of molecular weight distributions.

The very low molecular weight ( $\bar{M} < 1500$ ) polymers proved to be extremely difficult to fractionate by precipitation techniques, due to the difficulty encountered in the separation of the homogenous and precipitated phases. Therefore, elution chromatography was used. The substrate was chromatographic-grade silica gel. The polymer was placed on the column in a minimum amount of carbon tetrachloride. It was eluted, first with petroleum ether (b.p.  $30-60^\circ\text{C}$ .), then with petroleum ether- $\text{CCl}_4$ , and, finally, a mixture of methanol-benzene was used to desorb the remaining polymer.

The lowest molecular weight polymers ( $\bar{M}_n \simeq 540$  and  $800$ ) were partially analyzed by gas chromatography (VPC). A 6-in. column composed of Apiezon L on Celite was used. This column was temperature programmed at  $15^\circ\text{C}/\text{min}$ . up to  $300^\circ\text{C}$ . and helium was used as the carrier gas.

Kinetic molecular weights were predicted by the equation  $\bar{M}_{\text{predicted}} = \text{grams monomer}/(\text{moles BuLi} - X)$ . The parameter,  $X$ , was the number of moles of BuLi used to purge the reactor and reagents of the final traces of impurities. Since the reactor and quantities of reagents used throughout these preparations, e.g., as described above, were essentially the same in each case,  $X$  was found to be a relatively constant factor, ca.  $10^{-3}$  mole.

## RESULTS

The polymerization data for all of the low molecular weight polymers are compiled in Table I. In every case the yield of polymer was virtually quantitative, and the molecular weights obtained were in good agreement with the predicted kinetic molecular weights.

As shown in Table II, a polymer with  $M = 6000$  prepared by use of the styrene-butyllithium-benzene THF system had  $\bar{M}_w/\bar{M}_n = 1.04$ . Thus, polymers with narrow molecular weight distributions and molecular weights  $\geq 5000$  can be prepared by this method.

TABLE I  
 Low Molecular Weight Polystyrenes Prepared by Anionic Initiation

Polymer	BuLi, moles $\times 10^{-4}$	Wt. mono- mer, g.	$\bar{M}_{kinetic}^a$	$\bar{M}_{n(exp)}^b$	$[\eta],^c$ dl.	$[\eta]_{\theta}^d$ g.	$\bar{M}_w/\bar{M}_n$
1	513	20	400	540	0.025		1.07
2	496	40	810	820	0.032	0.024	1.09
3	126	22.7	1,960	1800	0.041	0.037	1.08
4	102	22.3	2,400	2260	0.045		1.07
5	23.5	10.0	7,400	6000	0.080		1.04
6	30.6	20.4	9,900	7200	0.085		1.03

<sup>a</sup>  $\bar{M}_{kinetic}$  = g. monomer/(moles BuLi -  $1 \times 10^{-3}$ ).

<sup>b</sup> These are the average experimental values obtained from a number of independent determinations. The data used are shown in Table IV.

<sup>c</sup> Measured in benzene at 25°C.

<sup>d</sup> Measured in cyclohexane at  $T_{\theta}$  (34.5°C.).

 TABLE II  
 Solution Fractionation of Polymer.  $\bar{M}_v = 6000^{a,b}$ 

Fraction	$w_i$	$[\eta],$ dl g	$M_i^c$
1	0.078	0.088	7750
2a	0.123	0.084	7100
2b	0.076	0.077	5900
3a	0.125	0.084	7100
3b	0.097	0.077	5900
4	0.082	0.081	6600
5	0.100	0.078	6600
6	0.086	0.077	5900
7	0.059	0.074	5700
8	0.073	0.073	5400
9	0.062	0.074	5700
10	0.040	0.053	2800

<sup>a</sup> Acetone solvent, H<sub>2</sub>O-methanol precipitant.

<sup>b</sup>  $\bar{M}_w = \sum w_i M_i = 6200$ ;  $\bar{M}_n = 1/\sum w_i/M_i = 5990$ ;  $\bar{M}_w/\bar{M}_n = 1.04$ .

<sup>c</sup>  $\bar{M}_v = 1.0 \times 10^{-3} \bar{M}_n^{1/2}$ .

The very low molecular weight polymers, i.e.,  $M < 1500$ , were fractionated by elution chromatography. The lowest molecular weight polymer,  $M = 540$ , was fractionated by elution chromatography (Table III). Most of the sample was eluted in one large fraction (fraction 6). It was necessary, therefore, to determine whether this was due to homogeneity or poor separation. For this reason fraction 6, as well as the whole polymer, was examined via vapor-phase chromatography (VPC). Fraction 6 showed a major peak with a retention time (RT) of 21.6 min. A much smaller but still measurable (ca. 3%) peak with RT = 13.1 min. as well as four trace peaks with lower retention times were also detected. The first of these, RT = 5.4 min., was shown to be *n*-hexylbenzene by comparison with this compound. It was assumed that the six peaks were due

to polymers with  $\bar{P}_n = 1-6$ , i.e., for RT = 5.4 min.,  $\bar{P}_n = 1$  (*n*-hexylbenzene); RT = 7 min.,  $\bar{P}_n = 2$ ; RT = 9 min.,  $\bar{P}_n = 3$ ; RT = 11.4 min.,  $\bar{P}_n = 4$ ; RT = 13.1 min.,  $\bar{P}_n = 5$ ; RT = 21.6 min.,  $\bar{P}_n = 6$ . Indeed, these were the only peaks detected in any of the polymers, including those with molecular weights greater than the sample in Table III. Apparently polymers with  $P_n > 6$  were retained on the column.

TABLE III  
Column Fractionation of Polymer,  $\bar{M}_n = 540^a$

Frac- tion	Solvent	Vol. solvent, ml.	Wt. polymer recovered,		$\Sigma w_i$	$M_i^b$
			g.	$w_i$		
1	PE <sup>c</sup>	100	0.008	0.002	0.002	
2	75% PE, 25% CCl <sub>4</sub>	100	0.002	0.006	0.008	
3	50% PE, 50% CCl <sub>4</sub>	100	0.034	0.011	0.019	
4	25% PE, 75% CCl <sub>4</sub>	100	0.084	0.026	0.045	210 <sup>d</sup>
5	CCl <sub>4</sub>	100	0.220	0.069	0.114	440
6	10% CH <sub>3</sub> OH, 90% C <sub>6</sub> H <sub>6</sub>	100	2.322	0.733	0.847	631
7	50% CH <sub>3</sub> OH, 50% C <sub>6</sub> H <sub>6</sub>	100	0.496	0.157	1.00	695
8	C <sub>6</sub> H <sub>6</sub>	500	0.000	0.000		

<sup>a</sup> Silica gel substrate.

<sup>b</sup> Vapor pressure osmometer.

<sup>c</sup> Petroleum ether, b.p. 30–60°C.

<sup>d</sup> Value for total fractions 1–4; estimated from gas chromatography:  $\bar{M}_w = \Sigma w_i M_i$   
= 611;  $\bar{M}_n = 1/\Sigma w_i/M_i = 569$ ;  $\bar{M}_w/\bar{M}_n = 1.07$ .

The VPC data could not be used for rigorous calculations of heterogeneity because sufficiently pure standards for  $\bar{P}_n = 2, 3, 4, 5$ , and 6 were not available for the calibration of the detector system. (The detector system uses a thermal conductivity cell for detection, and consequently only with light or low boiling materials can one measure quantitatively the amounts of compounds examined, i.e., obtain 100% mass balances.) In this case mass balances were not achieved. A mass balance could have been achieved, however, if pure standards had been used and a factor for each component could have been obtained experimentally. With *n*-hexylbenzene as a standard and on observing that the  $\bar{P}_n = 6$  peak comprised 97% of the area on the chromatogram (that for  $\bar{P}_n = 5$  about 3% and the peaks for  $\bar{P}_n = 2-4$  hardly more than background irregularities, having no measurable area), and  $\bar{M}_n = 631$ , determined experimentally for fraction 6, calculations of  $\bar{M}_n$  for the unfractionated sample indicate that within the experimental limits the lower homologs,  $\bar{P}_n = 1-4$ , are essentially absent.

Although polymers with  $\bar{P}_n > 6$  were not detectable via vapor-phase chromatography and fractions 6 and 7 of Table III may indeed contain materials with  $\bar{P}_n > 6$ , calculations of  $\bar{M}_w$  and  $\bar{M}_n$  indicate, for example, that the results obtained could not accommodate more than 5% of a

TABLE IV  
Determination of Molecular Weights of Low Molecular  
Weight Anionic Polystyrenes

Sample	Molecular weight $M$				$\bar{M}_n$ (avg.)	$\bar{P}_n$ (avg.)
	From VO <sup>a</sup>	From B.P. <sup>b</sup>	From F.P. <sup>c</sup>	From NMR		
1	542	531		550	541	4.65
1a <sup>d</sup>	655	638		600	631	5.5
2	798	888	802	787	819	7.35
2a <sup>d</sup>		1018		995	1107	10
3	1767	1734		1888	1796	17
4	2200	2324			2262	21
5	5400				5400	52

<sup>a</sup> Determined by means of the Mechrolab vapor pressure osmometer.

<sup>b</sup> Determined by boiling point elevation in benzene.

<sup>c</sup> Determined by freezing point depression in camphor.

<sup>d</sup> The main fractions (~70%) from elution chromatography.

homolog with  $\bar{P}_n = 8$ . Similar combinations of analytical techniques for the other polymers in Table I, save for the one with  $\bar{M}_n = 6000$ , which was characterized by conventional fractionation from acetone solution (Table II), gave identical results. Therefore, it is concluded that the synthetic methods described herein do indeed yield low molecular weight polymers with narrow molecular weight distributions.

A variety of methods were used to determine the number-average molecular weights of the low molecular weight polymers (Table IV). These included osmometry, ebullioscopy, cryoscopy, and nuclear magnetic resonance spectroscopy (NMR). The results were in good agreement and, in most cases, differed by less than 10% between any two.

A log-log plot of the intrinsic viscosities versus  $\bar{M}_n$  of the low molecular weight polymers is shown in Figure 1. Three different sets of data are

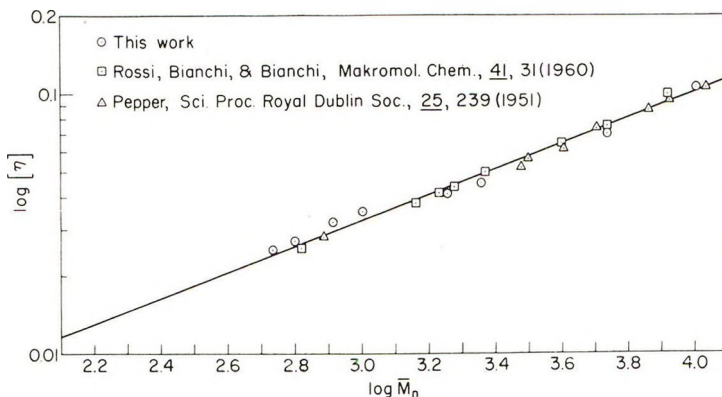


Fig. 1. Plot of  $\log [\eta]$  vs.  $\log \bar{M}_n$  for low molecular weight polymers for this work and data of Rossi et al.<sup>2</sup> and Pepper.<sup>3</sup>

shown on this plot; those of the present study, those of Rossi, Bianchi, and Bianchi<sup>2</sup> and those of Pepper.<sup>3</sup> Density corrections were applied to the last data before plotting. In agreement with Bianchi et al.,<sup>2</sup> the expression

$$[\eta] = 1.0 \times 10^{-3} \bar{M}_n^{0.5} \quad (1)$$

was found to be an excellent approximation to the experimental data over the molecular weight range under consideration ( $\bar{M}_n = 500$ – $10,000$ ).

## DISCUSSION

The use of NMR as a method of obtaining number-average molecular weights was possible because the butyllithium initiator resulted in the incorporation of a butyl endgroup in the polymer. Consequently, the ratio of aliphatic to aromatic protons asymptotically approached a value of 0.6 as  $\bar{P}_n$  increased. However, for polymers with  $\bar{P}_n < 10$ , a plot of the number of aliphatic protons/number aromatic protons versus molecular weight or  $\bar{P}_n$  is reasonably steep, and, as shown in Table IV, these determinations are in very good agreement with more conventional methods of obtaining number average molecular weights.

The three sets of data plotted in Figure 1 ( $\log [\eta]$  versus  $\log \bar{M}_n$ ) fall on the same line, despite the fact that the polymers and solvents used in the measurements of  $[\eta]$  were different. For example, the polymers prepared here have narrow molecular weight distributions, butyl and proton end groups, and  $[\eta]$  measured in benzene. The polymers studied by Bianchi, Rossi, and Rossi<sup>2</sup> and Pepper<sup>3</sup> were fractions of cationically polymerized styrene and presumably contained olefin and proton endgroups. Also, the viscosities were measured in toluene. Since all the data can be represented by one line despite these differences, it would appear that  $[\eta]$  is independent of the endgroups when hydrocarbon structures are involved, and for low  $M$  that  $[\eta]$  is independent of solvent. This behavior is consistent with the hydrodynamic theories<sup>7-9</sup> in that, as  $\bar{P}_n$  becomes very small, the long-range intramolecular interactions would vanish.

If we look now at the higher molecular weight range, where  $[\eta]/[\eta]_\theta$  is considerably greater than unity, the viscosity-molecular weight behavior of polystyrene in benzene, as well as in many other solvents, has received much attention. Of the many Mark-Houwink type relations,  $[\eta] = KM^a$ , reported for this system, five of these<sup>10-14</sup> appear to be quite similar, with values of  $K$  and  $a$  in the range  $(0.8-1.1) \times 10^{-4}$  and  $0.73-0.76$ , respectively. In the practical molecular weight range, ca.  $(3-5) \times 10^5$ , values of  $M$  computed from  $[\eta]$  using these relations are in excellent agreement (within 5%). However, for the extremes in molecular weight, at which it is sometimes necessary to make measurements, computed values of  $M$  can differ by as much as 15%. Further, a discrepancy as large as 15% was found between molecular weights computed using these relations when compared with that obtained from  $[\eta]$  measured in cyclohexane by using

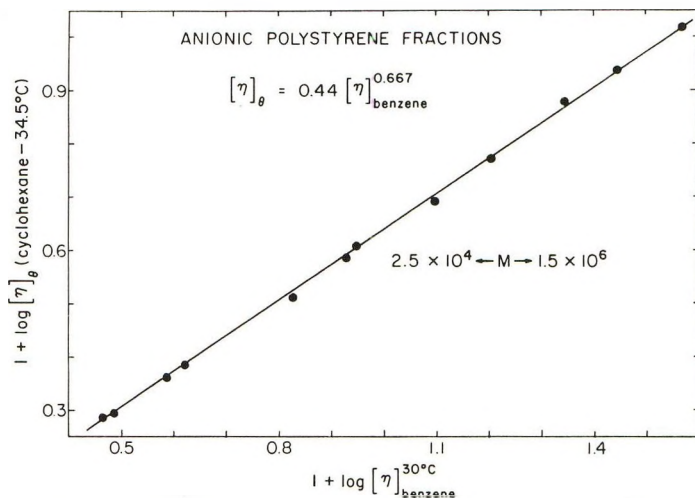


Fig. 2. Logarithms of the intrinsic viscosities measured on the same sample in cyclohexane at 34.5°C. ( $\theta$ ) and in benzene at 30°C. The samples were fractions of anionic polystyrene having  $M_w/M_n < 1.1$ . The linear relation (solid line) was obtained by using method of least squares.

the well-known Flory-Krigbaum<sup>15</sup> relation  $[\eta]_{\theta} = 8.2 \times 10^{-4} M^{0.5}$ . Thus, in order to make the results more self-consistent, we have investigated the viscosity-molecular weight relations for polystyrene making use of a supply of fractions of "anionic" polystyrenes covering a wide range in molecular weight.

Viscosities measured on the same samples in benzene at 30°C. and in cyclohexane at 34.5°C., are listed in Table V along with values of the Huggins parameter,  $k'$ , obtained. The samples used were fractions of anionic polystyrene<sup>16</sup> for which  $\bar{M}_w/\bar{M}_n < 1.1$ . A log-log plot of the data is shown in Figure 2, from which it can be seen that a linear dependence is obeyed over the range  $2.5 \times 10^4 \leq M \leq 1.5 \times 10^6$ . The straight line in Figure 2, obtained by the method of least squares, can be expressed by the relation

$$[\eta]_{\theta} = 0.44 [\eta]_{benzene}^{0.667} \quad (2)$$

This expression was used to correlate  $[\eta]_{\theta}$  (cyclohexane)- $M$  data, both obtained in this laboratory and reported by others, Table VI, with  $[\eta]$  (benzene)- $M$  relations from the literature in the following way. The  $[\eta]_{\theta}$ - $M$  data for polystyrene fractions of  $\bar{M}_w \simeq \bar{M}_n$ , plotted logarithmically in Figure 3, can be approximated by the expression

$$[\eta]_{\theta} = 8.4 \pm 0.2 \times 10^{-4} M^{0.5} \quad 8 \times 10^2 \leq M \leq 2 \times 10^6 \quad (3)$$

in excellent agreement with the Flory-Krigbaum relation<sup>15</sup>  $[\eta]_{\theta} = 8.2 \times 10^{-4} M^{0.5}$ . Combining eqs. (2) and (3) yields

$$[\eta]_{benzene}^{30^{\circ}C.} = 8.5 \times 10^{-5} M^{0.75} \quad 2.5 \times 10^4 \leq M \leq 2 \times 10^6 \quad (4)$$



TABLE V  
Intrinsic Viscosities of Fractions of Anionic Polystyrene in  
Benzene and in Cyclohexane

Fraction	$M \times 10^{-3a}$	Benzene at 30.0°C.		Cyclohexane at 34.5°C.	
		$[\eta]$ , dl./g.	Huggins constant $k'$	$[\eta]_{\theta}$ , dl./g.	Huggins constant $k'$
A-5-1	1530	3.72	0.35	1.04	0.70
A-16-1	1090	2.80	0.32	0.866	0.67
A-16-5	820	2.21	0.35	0.760	0.65
A-14-A	500	1.60	0.35	0.592	0.67
L-14-M	345	1.25	0.36	0.492	0.62
S-108 <sup>b</sup>	235	0.90	0.38	0.408	0.62
S-111-5	210	0.85	0.37	0.386	0.60
S-105-1	150	0.67	0.36	0.325	0.64
A-20 <sup>b</sup>	83	0.42	0.39	0.242	0.63
S-102 <sup>b</sup>	75	0.387	0.41	0.230	0.59
A-12-B	55	0.305	0.40	0.197	0.62
A-25-C	45	0.276	0.42	0.178	0.60

<sup>a</sup> Computed from eq. (3).

<sup>b</sup> Unfractionated,  $\bar{M}_w/\bar{M}_n \cong 1.1$ . Samples designated by S- were kindly furnished by Dr. H. W. McCormick of the Dow Chemical Company (cf. ref. 21).

which is represented by the broken line in Figure 3. This expression is nearly an average of the five relations reported<sup>10-14</sup> for this system. Though neither eq. (3) nor (4) is very different from the previously reported rela-

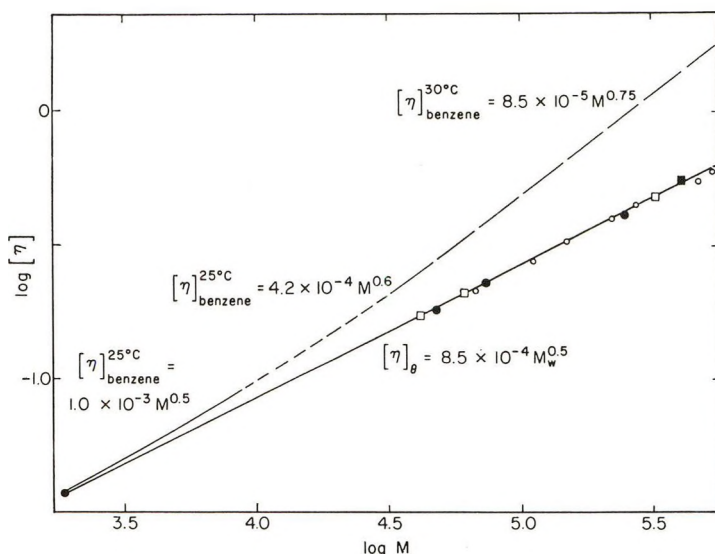


Fig. 3. Viscosity molecular weight relations for polystyrene in benzene (upper curve) and in cyclohexane (lower line) at 34.5°C. ( $\theta$ ). Symbols on lower line are data from (●) this work, (□) Krighaum and Flory,<sup>15</sup> (○) Hahn et al.,<sup>17</sup> and (■) Orofino and Mickey.<sup>16</sup> Sections of upper curve approximated within 3% by equations given.

tions, both offer the advantage that they are internally self-consistent, i.e., for a polystyrene sample having  $\bar{M}_w/\bar{M}_n \leq 1.2$ , the molecular weight calculated from the measured viscosities in both solvents is the same, within 3%. Further, this provides a quick method for estimation of chain length polydispersity in a sample of polystyrene by simple comparison of viscosity-average molecular weights,  $\bar{M}_v = (w_i M_i^a)^{1/a}$ , computed by using eqs. (3) and (4). Thus, according to Frisch and Lundberg<sup>19</sup>

$$(\bar{M}_w/\bar{M}_n) - 1 = 8[(\bar{M}_v, \text{eq. (4)}/\bar{M}_v, \text{eq. (3)}) - 1] \quad (5)$$

This approach should give reliable results for polystyrene samples with  $\bar{M}_w/\bar{M}_n > 2$ . For  $\bar{M}_w/\bar{M}_n \leq 2$  the error inherent in the  $[\eta]$  measurements would be comparable to the differences in  $[\eta]$  caused by the heterogeneity.

TABLE VI  
Viscosity-Molecular Weight Data for Polystyrene

Sample designation	$[\eta]$ , dl./g. Cyclohexane, 34.5°C.	$M \times 10^{-3}$	Method of obtaining $M$	Reference
S-108	0.408	254 <sup>a</sup>	Light scattering	Present work
A-20	0.242	84	" "	"
A-25-C	0.178	49	" "	"
A-43	0.037	1.85	" "	"
L-5	0.473	322	Osmotic pressure	Krigbaum and Flory <sup>15</sup>
O-4	0.215	61	" "	"
L-4	0.173	41.6	" "	"
—	0.59	542	Osmotic pressure	Hahn, Müller, and Webber <sup>17</sup>
—	0.55	480	" "	"
—	0.45	277	" "	"
—	0.40	224	" "	"
—	0.33	151	" "	"
—	0.275	112	" "	"
—	9.215	68	" "	"
—	0.552	404	Osmotic pressure	Orofino and Mickey <sup>18</sup>
		406	Light scattering	"

<sup>a</sup> An average of  $\bar{M}_w = 251,000$  and  $256,000$  obtained independently by Drs. T. A. Orofino and G. C. Berry, respectively, of this laboratory. Other values for this polymer were reported by Cowie et al.,<sup>21</sup>  $\bar{M}_w = 230,000$  from light scattering and by H. W. McCormick (private communication),  $\bar{M}_w = 267,000$  from sedimentation.

It is interesting from a practical standpoint, at least, that the relation, eq. (3) for polystyrene in cyclohexane (theta) is applicable over more than a thousandfold range in molecular weight, from  $M = 500$  to  $1.5 \times 10^6$ . From a theoretical standpoint, it is surprising that the square root dependence, predicted for an impermeable random coil chain,<sup>20</sup> is (apparently) obeyed in the very low molecular weight range.

The three relations for polystyrene in benzene can be represented by a smoothly increasing function, shown as the upper curve in Figure 3 (solid, dashed, and broken lines) in accord with theory.<sup>7-9</sup> When the data of Tables I and V were treated according to the theories of Flory and Fox<sup>7</sup> and of Fixman,<sup>9</sup> it was not possible to choose between them; the data were approximated equally well by both. Clearly, very precise measurements at low shear viscosity on higher molecular weight samples,  $\bar{M} \geq 10^6$ , are needed in order to distinguish between the theories by this approach.

The authors are indebted to Mr. Carl Lindemann for the gas chromatographic results and to Dr. G. C. Berry for many helpful discussions concerning this work. The encouragement and advice of Dr. T. G. Fox is gratefully acknowledged.

### References

1. Altares, T., Jr., D. P. Wyman, and V. R. Allen, *Polymer Division Preprints*, **4**, 343 (1963).
2. Rossi, C., U. Bianchi, and E. Bianchi, *Makromol. Chem.*, **41**, 31 (1960).
3. Pepper, D. C., *Sci. Proc. Roy. Dublin Soc.*, **25**, 239 (1951).
4. Worsfold, D. J., and S. Bywater, *Can. J. Chem.*, **38**, 1891 (1960).
5. Wenger, F., and S.-P. S. Yen, *Makromol. Chem.*, **43**, 1 (1961).
6. Fox, T. G., and P. J. Flory, *J. Appl. Phys.*, **21**, 581 (1950).
7. Fox, T. G., Jr., and P. J. Flory, *J. Am. Chem. Soc.*, **73**, 1904 (1951).
8. Kurata, M., W. H. Stockmayer, and A. Roig, *J. Chem. Phys.*, **33**, 151 (1960).
9. Fixman, M., *J. Chem. Phys.*, **36**, 3123 (1962).
10. Orofino, T. A., and F. Wenger, *J. Phys. Chem.*, **67**, 566 (1963).
11. Cowie, J. M. G., and S. Bywater, *Trans. Faraday Soc.*, **57**, 705 (1961).
12. Ewart, R. H., and H. C. Tingey, paper presented at 111th Meeting, American Chemical Society, Atlantic City, 1947.
13. Flory, P. J., *Principles of Polymer Chemistry*, Cornell Univ. Press, Ithaca, N. Y., 1953, p. 312.
14. Bawn, C. E. H., R. F. J. Freeman, and A. R. Kamaliddin, *Trans. Faraday Soc.*, **46**, 1107 (1950).
15. Krigbaum, W. R., and P. J. Flory, *J. Polymer Sci.*, **11**, 37 (1953).
16. Allen, V. R., and T. G. Fox, *J. Chem. Phys.*, in press.
17. Hahn, W., W. Müller, and R. V. Webber, *Makromol. Chem.*, **21**, 131 (1956).
18. Orofino, T. A., and J. W. Mickey, *J. Chem. Phys.*, **38**, 2512 (1963).
19. Frisch, H. L., and J. L. Lundberg, *J. Polymer Sci.*, **37**, 123 (1959).
20. Kirkwood, J. G., and J. Riseman, *J. Chem. Phys.*, **16**, 565 (1948).
21. Cowie, J. M., D. J. Worsfold, and S. Bywater, *Trans. Faraday Soc.*, **57**, 705 (1961).

### Résumé

On a employé des techniques de polymérisation anionique pour préparer du polystyrène de bas poids moléculaire ( $M \leq 10.000$ ) dont  $M_w/M_n \leq 1.1$ . On décrit la méthode de préparation et de caractérisation de ces polymères. On obtient un bon accord avec les résultats rapportés par d'autres auteurs pour la relation viscosité-poids moléculaire dans le benzène à 25°C., notamment  $[\eta] = 1.0 \times 10^{-3} M_n^{0.5}$ , pour  $500 < M_n \leq 10.000$ . Pour les fractions de poids moléculaire élevé du polystyrène préparé anioniquement ( $2.5 \times 10^4 < M \leq 1.5 \times 10^6$ ) on trouve que l'expression  $[\eta]_{\text{benzene}} = 8.5 \times 10^{-5} \bar{M}^{0.75}$  est applicable et en accord avec les relations données dans la littérature. Dans des conditions  $\theta$ , soit le cyclohexane comme solvant à 34.5°C., une expression unique  $[\eta] = 8.4 \times 10^{-4} M^{0.5}$ , est applicable dans tout le domaine de poids moléculaire  $500 < M \leq 1.5 \times 10^6$ .

### Zusammenfassung

Anionische Polymerisationsverfahren wurden zur Herstellung von niedrigmolekularem ( $M \leq 10.000$ ) Polystyrol mit  $M_w/M_n \leq 1,1$  verwendet. Herstellung und Charakterisierung dieser Polymeren werden beschrieben. Für die Viskosität-Molekulargewichtbeziehung in Benzol bei 25°C. wurde gut Übereinstimmung mit den von anderen Autoren mitgeteilten Ergebnissen erzielt, nämlich  $[\eta] = 1,0 \times 10^{-3} M_n^{0,5}$  für  $500 < M_n \leq 10.000$ . Bei hochmolekularen Fraktionen ( $2,5 \times 10^4 < M \leq 1,5 \times 10^6$ ) von anionisch hergestelltem Polystyrol zeigte sich der Ausdruck  $[\eta]_{\text{benzol}} = 8,5 \times 10^{-5} M^{0,75}$  anwendbar und in Übereinstimmung mit Literaturangaben. Unter Theta-Bedingungen —Cyklohexan als Lösungsmittel bei 34,5°C.—war ein einziger Ausdruck,  $[\eta] = 8,4 \times 10^{-4} M^{0,5}$  im ganzen Molekulargewichtsbereich  $500 < M \leq 1,5 \times 10^6$  anwendbar.

Received December 26, 1963

## Reaction of Polystyryllithium with Carbon Dioxide\*

D. P. WYMAN, V. R. ALLEN, and T. ALTARES, JR., *Mellon Institute, Pittsburgh, Pennsylvania*

### Synopsis

A benzene solution of polystyryllithium of narrow chain length distribution was found to react with carbon dioxide to form (upon acidification) not only the corresponding polystyrene carboxylic acid but also significant amounts of di-polystyryl ketone and tri-polystyryl carbinol. The amounts of the latter two products were somewhat dependent on the rate at which carbon dioxide could be added to the system. Thus, the yields of di-polystyryl ketone and tri-polystyryl carbinol were 28% and 12%, respectively, if termination was accomplished by allowing gaseous carbon dioxide to diffuse into the system, but the total yield of these products was only 22% if the termination was carried out by pouring the polystyryllithium solution onto crushed, solid Dry Ice. Lithium polystyrene carboxylate was found to be partly associated in benzene and cyclohexane, but the free acid was not.

The polymerization of styrene by anionic techniques gives polymers of narrow chain length distribution and of predictable molecular weights.<sup>1,2</sup> Because there is no termination step,<sup>3</sup> a solution of polystyryllithium obtains which can be made to react further as in the formation of model branched polymers.<sup>4,5</sup> Also, controlled termination provides a means of introducing different endgroups into the polymer, and it is of interest to preparative and physical polymer chemists alike to determine what, if any, influence such substituents would have on the polymer properties.

It has been shown that polystyryllithium in moderately concentrated benzene solutions is associated,<sup>2</sup> as evidenced by marked lowering of the viscosity on termination. We have found that similar, though less extensive, association is exhibited by dilute solutions of the lithium salt of polystyrenecarboxylic acid in benzene and in cyclohexane. The corresponding polymeric carboxylic acid did not give any evidence of association.

A sample of polystyryllithium, terminated with gaseous carbon dioxide, was found to contain not only the polystyrenecarboxylic acid but also di-polystyryl ketone and branched tripolystyryl carbinol in ca. 60, 28, and 12% yield, respectively. This unexpected result is discussed in terms of the reactions described by Gilman<sup>6</sup> between carboxylates and organolithium compounds.

\* This work was supported in part by the Office of Naval Research under Contract No. Nonr 2693(00).

### Experimental

Polystyryllithium was prepared by means of conventional high vacuum techniques<sup>1,2</sup> in benzene solution with butyllithium as initiator. The terminated polymer was precipitated in methanol, washed with water, and vacuum dried. The polymers were fractionated by one-step precipitation from benzene solution at 30°C. with methanol.

Intrinsic viscosity measurements were made in benzene at 30°C. and in cyclohexane at 34.5°C. ( $\theta$ ). The viscosity-average molecular weight,  $\bar{M}_v$ , was computed from the relation<sup>7</sup>

$$[\eta]_{(\text{benzene})} = 8.5 \times 10^{-5} \bar{M}_v^{0.75} \quad (1)$$

The number-average molecular weight was computed from osmotic pressure measurements on toluene solutions at 25°C. Ultracentrifugal sedimentation patterns (schlieren optics) were obtained on cyclohexane solutions at 35°C.

The polystyrenecarboxylic acid was reduced with lithium aluminum hydride, used in excess. The reducing agent was added to a 1% solution of the acid in tetrahydrofuran and the mixture stirred for 1 hr. at room temperature. Excess hydride was reacted with isopropanol, the slurry acidified, and the polymer recovered by precipitation in methanol.

A qualitative measure of the carboxylic acid content was determined by the colorimetric procedure developed by Palit and Ghosh<sup>8</sup> based on a rhodamine-carboxyl complex formation.

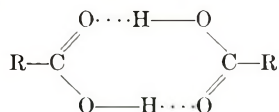
### Results and Discussion

A sample of polystyrene which had been terminated accidentally in a methanol-Dry Ice mixture gave intrinsic viscosities of 0.205 in cyclohexane and 0.300 in benzene. These values were not consistent with the relation<sup>7</sup>

$$[\eta]_{(\text{cyclohexane}, 34.5^\circ\text{C.})} = 0.44 [\eta]_{(\text{benzene}, 30^\circ\text{C.})}^{0.667} \quad (2)$$

This polymer, after reduction with lithium aluminum hydride and acidification, gave viscosities of 0.182 in cyclohexane and 0.276 in benzene, values which are in better agreement with eq. (2).

It was felt initially that this effect was probably due to hydrogen bonding between terminal carboxylic acid groups, viz.,



where  $R$  = polystyryl.

To test this hypothesis, a sample of polystyryllithium was prepared and the solution divided into two parts. One part, designated S-36-H, was terminated conventionally by addition of pure degassed methanol. The other, designated S-36-CO<sub>2</sub>, was terminated by diffusion of carbon dioxide into the system and precipitated in acidified methanol.

The higher viscosity for S-36-CO<sub>2</sub> (Table I) would be expected if appreciable hydrogen bonding occurred in benzene solvent. However, the viscosity was unchanged after reduction, although the rhodamine test indicated that the carboxylic acid concentration had been decreased from ca. 10<sup>-5</sup> to <10<sup>-7</sup> moles/g. of polymer. Thus, the higher viscosity of S-36-CO<sub>2</sub> did not appear to be caused by hydrogen bonding. Examination of these polymers in the ultracentrifuge revealed two interesting results: (1) the pattern of S-36-H showed a single sharp sedimentation profile, found to be characteristic of polystyrene with  $\bar{M}_w/\bar{M}_n < 1.1$ , and (2) S-36-CO<sub>2</sub> showed definite triplet profiles indicative of three molecular weight species. The main peak corresponded to that of S-36-H while the other two appeared as shoulders toward the higher molecular weight field. Although accurate analysis was not possible, the molecular weights were in the approximate ratios of 1:2:3.

TABLE I  
Composition and Viscosities of Anionic Polystyrene  
Terminated with Carbon Dioxide (S-36-CO<sub>2</sub>)

Fraction	Wt.-%	$[\eta]^a$ , dl./g.	$\bar{M}_v \times 10^{-3}^b$	$\bar{M}_n \times 10^{-3}^b$
Precursor (methanol- terminated)		0.333	62	
Whole polymer		0.420	83	
1	7.5	0.562	126 (150) <sup>d</sup>	
2	5.4	0.564	126 (150) <sup>d</sup>	135
3	11.5	0.508	110	
4	12.6	0.471	100	
5	4.4	0.454	93	
6	8.0	0.365	71	
7	23.0	0.330	62	
8	25.0	0.317	58	

<sup>a</sup> Measured in benzene at 30°C.

<sup>b</sup> From  $[\eta] = 8.5 \times 10^{-5} \bar{M}_v^{0.75}$  (data of Altares et al.<sup>7</sup>).

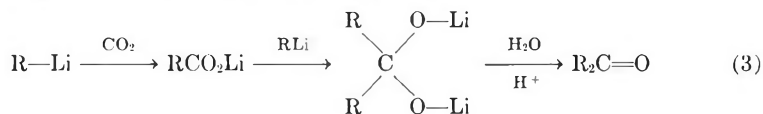
<sup>c</sup> From osmotic pressure measurements in toluene at 25°C.

<sup>d</sup> Assumed branched structure; computed from  $[\eta]_{\text{branched}}/[\eta]_{\text{linear}} = g'$  with  $g' = 0.87$  (data of Wenger and Yen<sup>8</sup>).

The three components were separated by fractional precipitation and the fractions characterized by intrinsic viscosity and osmotic pressure measurements (Table I). From these data it is possible to describe the composition of S-36-CO<sub>2</sub> as follows: (a) ca. 60% of the polymer is comprised of the expected polystyrenecarboxylic acid of  $\bar{M} = 62,000$  (fractions 6, 7, and 8); (b) ca. 28% is made up of dipolystyryl ketone of  $\bar{M} = 126,000$ ; (c) the rest, ca. 12%, is composed of tripolystyryl carbinol of  $\bar{M} \sim 150,000$ . Fractions 6, 7, and 8 appear to be the expected polystyrenecarboxylic acid because of the agreement of their (average) viscosity with that of the precursor. Fractions 3, 4, and 5 have an (average) viscosity corresponding to twice the molecular weight of the precursor. Fractions 1 and 2 exhibit a number-

average molecular weight, computed from osmotic pressure measurements, of  $\bar{M}_n = 135,000$ , and intrinsic viscosities which give an apparent  $\bar{M}_v = 126,000$ , computed from eq. (1). However, it is known<sup>9,10</sup> that the viscosity of a star-type branched polymer is lower than that of a linear sample of the same molecular weight. Using the value of  $[\eta]_{\text{branched}}/[\eta]_{\text{linear}} = g' = 0.87$  reported by Orofino and Wenger,<sup>10</sup> we compute  $\bar{M}_v = 150,000$  for fractions 1 and 2. Thus, although an exact ratio of molecular weights of 3:1, compared with precursor, is not obtained, the indication is strong that these two fractions are predominantly a branched tripolystyryl product.

The infrared analysis of a low molecular weight analog of S-36-CO<sub>2</sub>, prepared by reacting styrene with butyllithium under nitrogen with appropriate concentrations to yield a degree of polymerization of ca. four and terminating with carbon dioxide, showed the presence of a significant amount of a ketone, as was observed by Gilman<sup>6</sup> using simple molecules. The most obvious path of ketone formation involves attack of the organolithium compound on the lithium carboxylate, viz.,



where R = polystyryl. The mode of formation of the higher molecular weight, apparently branched product is less obvious, but most likely involves, as the final intermediate (before hydrolysis) R<sub>3</sub>-C-OLi (*vide infra*).

One possible check of this proposed scheme for the formation of the higher molecular weight components is based on the dependence of these species on the concentration of CO<sub>2</sub>. According to eq. (3), a high concentration of CO<sub>2</sub> would favor RCO<sub>2</sub>Li formation and thus remove RLi from the system. Hence, the probability of the second step, leading to the higher molecular weight components, would be lowered. This was accomplished experimentally by separating a solution of polystyryllithium into three portions. One, designated S-50-H, was terminated with methanol as in the case of S-36-H. Another, S-50-CO<sub>2</sub>-D, comparable to S-36-CO<sub>2</sub>, was terminated by diffusion of CO<sub>2</sub> into the system. The final portion, S-50-CO<sub>2</sub>-HC (high concentration) was terminated by slowly pouring the polystyryllithium solution, under an atmosphere of nitrogen, onto granulated solid carbon dioxide. For the latter two polymers the rhodamine test was positive, both giving  $[-\text{CO}_2\text{H}] \sim 10^{-5}$  moles/g. of polymer, indicating that termination (of S-50-CO<sub>2</sub>-HC) by moisture from the nitrogen (or the air) was negligible.

The data in Table II are clearly in accord with the hypothesis above. The molecular weight of S-50-CO<sub>2</sub>-HC is only 9% higher than for S-50-H, indicating the absence of the higher molecular weight species, while that for S-50-CO<sub>2</sub>-D is 23% higher (compared with 34% higher for the S-36 series). Indeed, a rough fractionation of the latter (Table II) showed the presence of the higher molecular weight components in ca. 22% yield.

The formation of these high molecular weight adducts removes the need for assumed hydrogen bonding. However, some form of association is



TABLE II  
Effect of Carbon Dioxide Concentration During Termination on the  
Composition and Viscosities of Anionic Polystyrene

Termination	Sample	Wt.-%	$[\eta]_{\text{benzene}}^{30^\circ}$	$\bar{M}_v \times 10^{-3}^a$
Control (MeOH-terminated)	S-50-H	—	0.393	78
High concentration CO <sub>2</sub>	S-50-CO <sub>2</sub> -HC	—	0.411	85
Diffusion of CO <sub>2</sub>	S-50-CO <sub>2</sub> -D	—	0.443	96
	Fraction 1	22	0.560	126
	Fraction 2	56	0.410	85
	Fraction 3	15	0.385	

<sup>a</sup> Computed from eq. (1).

still necessary to explain the anomalous viscosity behavior of the polystyryllithium terminated with the mixture of methanol and Dry Ice. The significant factor is that this polymer had not been precipitated in acidified methanol; consequently, the product was the lithium salt of polystyryl carboxylate, and not the free acid. Thus, as suggested by the work of Brody, Richards, and Szwarc,<sup>11</sup> the metal gegenion is apparently necessary for association through ion-pair formation, and hydrogen bonding of the polymeric free acid in these nonpolar solvents is not significant.

The authors would like to thank Mr. R. E. Kerwin who carried out the osmotic pressure measurements and conducted the ultracentrifugal sedimentation studies.

### References

1. Wenger, F., and S.-P. S. Yen, *Makromol. Chem.*, **43**, 1 (1961).
2. Worsfold, D. J., and S. Bywater, *Can. J. Chem.*, **38**, 1891 (1960).
3. Szwarc, M., M. Levy, and R. Milkovich, *J. Am. Chem. Soc.*, **78**, 2656 (1956).
4. Morton, M., T. E. Helminiak, S. D. Gadkary, and F. Bueche, *Conference on High Temperature Polymer and Fluid Research, Dayton, Ohio, May 1962*, Vol. I, p. 165.
5. Wenger, F., and S.-P. S. Yen, paper presented at 141st Meeting, American Chemical Society, Washington, D. C., March 1962, Polymer Division; *Preprints*, **3**, No. 1, 162 (1962).
6. Gilman, H., and P. R. Van Ess, *J. Am. Chem. Soc.*, **55**, 1258 (1933).
7. Altares, T., Jr., V. R. Allen, and D. P. Wyman, *J. Polymer Sci.*, **A2**, 4533 (1964).
8. Palit, S. R., and P. Ghosh, *J. Polymer Sci.*, **58**, 1225 (1962).
9. Zimm, B. H., and R. W. Kilb, *J. Polymer Sci.*, **37**, 19 (1959).
10. Orofino, T. A., and F. Wenger, *J. Phys. Chem.*, **67**, 566 (1963).
11. Brody, H., D. H. Richards, and M. Szwarc, *Chem. Ind. (London)*, **1958**, 1473.

### Résumé

Une solution benzénique de polystyryl-lithium ayant une dispersion de poids moléculaire peu marquée, réagit avec l'anhydride carbonique pour donner (après acidification) non seulement le "polystyrène acide carboxylique" correspondant, mais aussi des quantités importantes de di-polystyryl-cétone et de tri-polystyryl-carbinol. La quantité des deux derniers produits dépend de la vitesse d'addition de l'anhydride carbonique. Donc, les rendements en di-polystyryl-cétone et en tri-polystyryl-carbinol sont de 28% et 12% respectivement, si la terminaison est réalisée en faisant diffuser de l'anhydride carbonique gazeux dans le système, mais le rendement total de ces produits n'est que de

22% si la terminaison est réalisée en versant la solution de polystyryl-lithium sur de la glace pilée. On a trouvé que le lithium polystyrène carboxylate est partiellement associé dans le benzène et dans le cyclohexane, ce qui n'est pas le cas pour l'acide libre.

### Zusammenfassung

Eine Benzollösung von Polystyrollithium mit enger Kettenlängenverteilung reagierte mit Kohlendioxyd unter Bildung (bei Säurezusatz) nicht nur der entsprechenden Polystyrolcarbonsäure sondern auch beträchtlicher Mengen von Dipolystyrylketon und Tripolystyrylcarbinol. Die Menge der zwei letzteren Produkte war etwas von der Zusatzgeschwindigkeit des Kohlendioxyds zum System abhängig. Die Ausbeute an Dipolystyrylketon und Tripolystyrylcarbinol war 28% bzw. 12%, wenn der Abbruch durch Eindiffundieren von gasförmigem Kohlendioxyd in das System bewerkstelligt wurde, bei Abbruch durch Eingießen der Polystyrollithiumlösung auf gemahlenes festes Trockeneis betrug die Gesamtausbeute nur 22%. Lithiumpolystyrolcarboxylat war in Benzol und Cyclohexan teilweise assoziiert, die freie Säure jedoch nicht.

Received January 3, 1964

Revised January 24, 1964

## Polymerization of *tert*-Butyl Crotonate\*

M. L. MILLER and J. SKOGMAN, *Exploratory Research Department,  
Central Research Division, American Cyanamid Company,  
Stamford, Connecticut*

### Synopsis

Lithium alkyls and phenylmagnesium bromide, in toluene, and lithium-naphthalene, in dimethoxyethane, polymerize *tert*-butyl crotonate. Sodium naphthalene produces only low polymer ( $M_n < 3000$ ), and potassium naphthalene gives no polymer. Even lithium naphthalene, which polymerized *tert*-butyl crotonate readily, fails to polymerize *tert*-butyl tiglate. Free radicals polymerize neither *tert*-butyl crotonate nor *tert*-butyl tiglate. Poly(*tert*-butyl crotonate) formed in the presence of lithium naphthalene is noncrystalline, in the presence of lithium alkyls, either noncrystalline or partly crystalline, and in the presence of phenylmagnesium bromide, highly crystalline. Poly(crotonic acid) was prepared from poly(*tert*-butyl crotonate).

The reluctance of 1,2-disubstituted olefins to homopolymerize, under conditions ordinarily used for polymerization, is so general that the failure of this class of monomers to homopolymerize is almost a rule of polymer chemistry<sup>1,2</sup> but a rule with exceptions. Maleic anhydride,<sup>3</sup> maleimide,<sup>4</sup> vinylene carbonate,<sup>5</sup> and esters of fumaric acid<sup>6</sup> have been polymerized by free radical initiator, and  $\beta$ -chlorovinyl ethers,<sup>7</sup> alkenyl ethers<sup>8-10</sup> indene,<sup>11</sup> benzofurane,<sup>12</sup> acenaphthylene,<sup>13</sup> and  $\beta$ -nitrostyrene<sup>14</sup> have been polymerized by ionic or ionic coordination catalysts. Also, Natta stated in a review<sup>8</sup> that Farina had polymerized crotonates but gave no details. This communication is concerned with the polymerization of *tert*-butyl crotonate.

*tert*-Butyl crotonate, like most 1,2-disubstituted ethylenes and like ethyl and methyl crotonates, resists polymerization by free radical initiators. This resistance is shown by the experiments listed in Table I. These experiments used initiators which were chosen because they polymerize vinyl monomers at low and at high temperatures. Experiments at low temperatures were considered necessary because *tert*-butyl crotonate is a bulky monomer which may form polymer with a low ceiling temperature.

In the first experiment, monomer was exposed to 20 Mrad of 3 Mev x-rays at  $-45^\circ\text{C}$ . In the second experiment, which was carried out at room temperature, sunlight was allowed to fall on monomer sensitized by benzoin. The third experiment subjected monomer to a massive dose of

\* Paper presented before the 145th Meeting of the American Chemical Society, New York, New York, September 12, 1963.

free radicals, supplied by 2% azobisisobutyronitrile at 100°C., followed by 400 hr. heating at 100°C. These treatments—rigorous as some of them were—produced only a trace of gum.

In some earlier work with ionic and ionic-coordination catalysts<sup>15</sup> we

TABLE I  
Attempts to Polymerize *tert*-Butyl Crotonate by Free Radical Initiation

Initiation	Temp., °C.	Time, hr.	Per cent polymerization
Radiation <sup>a</sup>	-40	4.5	~0
Sunlight (benzoin)	room temp.	~50	~0
Free radical and thermal <sup>b</sup>	100	400	0.9

<sup>a</sup> 20 Mrad of 3 Mev x-rays, dose rate 9 Mrad/hr.

<sup>b</sup> Azobisisobutyronitrile, 2%.

found that *tert*-butyl acrylate could be polymerized under conditions where methyl acrylate is not polymerized. Therefore, it seemed possible that *tert*-butyl crotonate could be polymerized under conditions where ethyl crotonate is not polymerized. This turned out to be true. *tert*-Butyl crotonate can be polymerized by three distinct initiators: lithium alkyls, the charge transfer complex between lithium and naphthalene, and phenylmagnesium bromide. Under conditions where these initiators polymerize *tert*-butyl crotonate readily, ethyl crotonate is not polymerized, nor is the related monomer *tert*-butyl tiglate, which differs from *tert*-butyl crotonate by having a methyl group on both the  $\alpha$  and the  $\beta$  carbons.

## EXPERIMENTAL

### Preparation of Monomers

*tert*-Butyl crotonate and *tert*-butyl tiglate were prepared by the reaction of isobutylene with the appropriate acid in the presence of sulfuric acid.<sup>16</sup> Monomers were fractionated, dried over calcium hydride and distilled, under vacuum, into ampules in which they were sealed. The properties of the monomers are listed in Table II.

Ethyl crotonate was obtained from the Monomer-Polymer Laboratory of the Borden Company.

TABLE II  
Properties of Monomers

Ester	Boiling point, °C. (760 mm.)	Index of refraction $n_D$	Specific gravity $d_4^{25}$
Tiglate	164-168	1.4295 (20°C.)	0.8762
Crotonate	153-155	1.4217 (26°C.)	0.8387

### Polymerization in the Presence of Alkyl Lithium

*n*-Butyllithium was supplied by the Foote Mineral Company as a 15.3% solution in hexane. 2-Methylbutyllithium was prepared from 2-methylbutyl chloride and lithium and was used as a 1.43*M* solution in petroleum ether. Polymerization in the presence of alkyl lithium was carried out in a flask provided with two side-arms and a center neck. The tube containing initiator was attached to one side-arm and the tube containing monomer to the other. Pure dry toluene was distilled into the center neck under vacuum. The flask was sealed from the vacuum line and brought to the polymerization temperature, which was  $-45^{\circ}\text{C}$ . for work with alkyl lithium. At the end of the period of polymerization, the contents of the flask were treated with methanol containing enough water to precipitate the polymer. The polymer was washed several times with a water-methanol mixture and dried under vacuum at  $55^{\circ}\text{C}$ .

When the straight-chain alkyl, *n*-butyllithium was used as initiator, polymerization was sluggish unless a few milligrams of heated lithium hydride was added. Then polymerization was rapid—60% conversion in 1 hr. However, polymer formed under these conditions always contained gel. The increase in rate of polymerization in the presence of heated lithium hydride is attributed to the presence of finely divided lithium formed when powdered lithium hydride was heated while flaming the polymerization flask under vacuum.<sup>17</sup> This finely divided lithium accelerated polymerization in the presence of *n*-butyllithium and, apparently, also removed an occasional hydrogen atom from the  $\alpha$ -methyl of the monomer, thereby producing gel. When *n*-butyl lithium was replaced by the branched alkyl lithium, 2-methylbutyllithium, polymerization was rapid without added lithium hydride. With this initiator conversions were 40–60% in 1 hr., depending on concentration of initiator. Polymers formed under these conditions were completely soluble in chloroform and heptane and swelled strongly in acetone. Intrinsic viscosities of different preparations ranged from 0.75 to 0.95 dl./g. in chloroform at  $30^{\circ}\text{C}$ . Light scattering showed one sample to have a molecular weight of 50,000, and x-ray diffraction showed the polymers to be amorphous or, in one instance, partly crystalline.

### Polymerization in the Presence of Lithium and Naphthalene

Polymerization in the presence of lithium and naphthalene was carried out in a flask provided with a wide-bore vacuum stop-cock which was used for removing aliquots and for adding monomer. The solvent was dimethoxyethane, dried over sodium and naphthalene. At the beginning of a run, the flask was charged with lithium and naphthalene, solvent was distilled into the flask under vacuum, and the flask was sealed from the vacuum line and shaken until the green color of the initiator solutions was well developed. Then an aliquot of the solution was removed by use of a syringe provided with a long hypodermic needle which was introduced

through the bore of the stop-cock. This aliquot was added to aqueous ethanol and titrated with 0.1*N* HCl. The tube leading from the stop-cock was flamed, cooled under nitrogen, and a sealed ampule containing monomer was attached with plastic tubing. Polymerizations in the presence of lithium and naphthalene were carried out at  $-45^{\circ}\text{C}$ . and at  $+26^{\circ}\text{C}$ . Polymerizations were not run at  $-78^{\circ}\text{C}$ . because monomer crystallizes from solution at low temperatures. As soon as monomer was added to initiator solution, polymerization started and the polymerizing mixture turned a light red-brown color. Conversions obtained under a variety of conditions are listed in Table III.

TABLE III  
Polymerization of Crotonates in the Presence of Alkali Metals and  
Naphthalene Dissolved in Dimethoxyethane

Monomer	Metal	Initiator, concn., moles/l.	Tem- perature of polymer- ization, $^{\circ}\text{C}$ .	Time, hr.	Amt. monomer poly- merized, %
<i>tert</i> -Butyl crotonate	Lithium	0.37	$-45$	1.0	75
	"	0.09	$-45$	1.0	47
	"	$\sim 0.1$	$-45$	0.5	50
	"	$>0.1$	26	5.0	70
	"	0.12	26	19	49
	Sodium	0.12	26	19	oil
	"	$>0.1$	$-45$	1.5	22 <sup>a</sup>
Ethyl crotonate	"	$>0.1$	$-45$	0.5	$\sim 0$
	Potassium	0.12	26	19	0
	" <sup>b</sup>	$>0.1$	$\sim -40$	0.5	0
Ethyl crotonate	Lithium	0.2	26	72	0
	"	$\sim 0.6$	$-20$	2	0

<sup>a</sup>  $\bar{M}_n < 3,000$  (estimated by Barger's method<sup>18</sup>).

<sup>b</sup> In liquid ammonia, no naphthalene.

The first three entries in Table III refer to polymerizations at  $-45^{\circ}\text{C}$ . The second and third runs used 10% monomer and close to 0.1*N* initiator, but polymerizations were allowed to continue for different lengths of time, 0.5 and 1.0 hr. Nevertheless, in spite of the different polymerization time, conversions were the same. This showed that the polymerization which occurred, took place in less than 0.5 hr. The first run used initiator and monomer in the same ratio as in the two succeeding runs but at a higher concentration. The higher concentration raised the conversion from 50% to 75% but at the same time reduced the intrinsic viscosity from 0.4 to 0.2 dl./g. These experiments showed that chains were terminated and that the polymer was not living. The fourth and fifth entries in Table III refer to polymerizations carried out at  $+26^{\circ}\text{C}$ . These experiments showed that equally good conversions can be obtained at  $26^{\circ}\text{C}$ . and at

-45°C. This means that, if poly(*tert*-butyl crotonate) has a low ceiling temperature, this temperature is higher than 26°C.

When lithium was replaced by sodium, *tert*-butyl crotonate did not form high polymer in the presence of naphthalene, but instead 22% of the monomer was converted to an oil with a number-average molecular weight of less than 3000. When lithium was replaced by potassium, *tert*-butyl crotonate formed no polymer in the presence of naphthalene. However, these same initiators, sodium naphthalene and potassium naphthalene, produced 100% conversion to polymer in 0.5 hr. when the isomeric monomer, *tert*-butyl methacrylate, was used.

Even lithium naphthalene, which polymerized *tert*-butyl crotonate readily, failed to polymerize ethyl crotonate and failed to polymerize *tert*-butyl tiglate.

*tert*-Butyl crotonate can also be polymerized by phenylmagnesium bromide. A Belgian patent,<sup>19</sup> which came to our attention after the completion of this work, disclosed the preparation of crystalline polymer from *tert*-butyl and isopropyl crotonate in the presence of phenylmagnesium bromide. In an experiment which is typical of our work, 0.02*M* phenylmagnesium bromide produced 55% conversion of *tert*-butyl crotonate to polymer in 2 hr. at 27°C. when the monomer was used as a 5% solution in toluene. The polymer had an intrinsic viscosity in chloroform at 30°C. of 0.06 dl./g. and was highly crystalline. The x-ray diffraction pattern contained seven distinct lines with *d* spacings of 10.6, 8.34, 6.32, 5.53, 4.64, and 3.93 Å. The fact that polymer formed in the presence of phenylmagnesium bromide was highly crystalline, shows that, if this polymer is isotactic, it consists entirely of a single one of the two types of isotactic polymer that can form from 1,2-disubstituted ethylenes.<sup>7</sup>

The Ziegler-type catalyst formed by the reaction of *n*-butyllithium with titanium tetrachloride, which polymerizes *tert*-butyl acrylate readily,<sup>15</sup> was unsuccessful with *tert*-butyl crotonate. The only product was a small mass of hard, insoluble matter which contained polymer and inorganic catalyst residues. Neither the Ziegler catalyst nor phenylmagnesium bromide polymerized *tert*-butyl tiglate.

### Properties of Poly(*tert*-butyl Crotonate)

Poly(*tert*-butyl crotonate) is a white solid which, like other *tert*-butyl esters, decomposes to isobutylene and the corresponding acid at 250°C. When molding temperatures are kept below 250°C., clear moldings can be made.

Examination of the crystalline polymer with differential thermal analysis disclosed no sharp first-order transition below the decomposition temperature. Examination of the amorphous polymer showed a glass transition at 86°C. This transition temperature was confirmed, to within 4°C., by a study of the dynamic mechanical properties of the polymer by the torsional braid method<sup>20</sup> which showed a glass transition at 82°C. when the

frequency was 1 cycle/sec. This transition temperature is higher than the glass transition temperature of atactic poly(*tert*-butyl acrylate), 39°C.<sup>21</sup>

The infrared spectrum of poly(*tert*-butyl crotonate) shows the absorption bands expected for a polymer of this composition, but there are minor differences in the spectra of polymers made in the presence of different initiators due to differences in tacticity. These differences occur, for the most part, in the region of the spectrum between 700 and 1000 cm.<sup>-1</sup>.

Poly(*tert*-butyl crotonate) can be converted to poly(crotonic acid) by refluxing a solution of the polymer in chloroform in the presence of sulfuric acid. Poly(crotonic acid) formed in this way shows the expected infrared spectrum and the expected elemental analysis. (C, H, O, observed 56.90%, 7.42%, 36.37%; calculated 55.81%, 7.03%, 37.17%). Poly(crotonic acid) is a white solid which is insoluble in water but dissolves in alkali metal hydroxides. Titration with lithium hydroxide in the presence of lithium chloride shows that, when titrated under the same conditions, poly(crotonic acid) is a weaker acid than poly(acrylic acid) and that its acid strength is close to, but greater than the acid strength of poly(methacrylic acid).

## DISCUSSION

The reluctance of 1,2-disubstituted ethylenes to homopolymerize is not well understood. A number of explanations for this reluctance have been proposed. They include: a low stabilization energy between monomer and free radicals in the transition state,<sup>22</sup> excessive chain transfer,<sup>23</sup> termination by cyclization,<sup>14</sup> and steric factors.<sup>1,2</sup> There are a number of observations in this study which point to the importance of steric factors. The effect of these factors can be looked for in initiation, in propagation, and in termination. Certainly the failure of *tert*-butyl tiglate to polymerize under any of the conditions tested must be attributed to the effect of a bulky group on initiation. Also, it seems likely that the difference in the ability of different alkali metals to polymerize *tert*-butyl crotonate in the presence of naphthalene is due to steric factors since only lithium, the smallest of the alkali metals, produced high polymer. Bhattacharyya, Lee, Smid, and Szwarc<sup>24</sup> showed that the copolymerization of styrene and  $\alpha$ -methylstyrene proceeded faster when lithium ions were counterions than when the counterions were larger alkali metal ions. This reduced rate of copolymerization in the presence of large counterions was attributed to steric crowding during propagation. The spectacular differences in the abilities of the alkali metals to polymerize *tert*-butyl crotonate in the presence of naphthalene shows that steric restrictions to the polymerization of *tert*-butyl crotonate are severe.

It is also possible to explain the polymerization of *tert*-butyl crotonate under conditions where ethyl crotonate does not polymerize, by steric factors—this time by their effect on termination. Bockman and Schuerch<sup>14</sup> showed that ethyl crotonate does not polymerize in the presence of anionic initiators because it forms cyclic dimer so readily. Apparently, the bulk



of the *tert*-butyl group in *tert*-butyl crotonate impedes dimerization and permits high polymer to form.

The authors wish to acknowledge the assistance of Mrs. J. Sutherland who carried out the polymerizations with Grignard reagent, of Miss E. C. Eberlin, Mr. J. R. Murry, and Dr. A. F. Lewis who measured glass transition temperatures, and Dr. L. A. Siegel and Mr. W. R. Doughman who measured x-ray diffractions.

### References

1. Alfrey, T., Jr., J. J. Bohrer, and H. Mark, *Copolymerization*, Interscience, New York, 1952, p. 49.
2. Mayo, F. R., F. M. Lewis, and C. Walling, *Discussions Faraday Soc.*, **2**, 285 (1947).
3. Lang, J. L., W. A. Pavelich, and H. D. Clarey, *J. Polymer Sci.*, **55**, S31 (1961).
4. Tawney, P. O., R. H. Snyder, P. P. Conger, K. A. Leibbrand, C. H. Stiteler, and A. R. Williams, *J. Org. Chem.*, **26**, 15 (1961).
5. Newman, M. S., and R. W. Addor, *J. Am. Chem. Soc.*, **75**, 1263 (1953); *ibid.*, **77**, 3789 (1955).
6. Brit. Patent 389,467 (1933); Ger. Patent 699,445 (1940).
7. Natta, G., Peraldo, M. Farina, and G. Bressan, *Makromol. Chem.*, **55**, 139 (1962).
8. Natta, G., *Chim. Ind. (Milan)*, **42**, 1207 (1960).
9. Natta, G., M. Farina, M. Peraldo, P. Corradini, G. Bressan, and P. Ganis, *Atti. Accad. Nazl. Lincei. Rend. Classe Sci. Fis. Mat. Nat.*, **28**, 442 (1960).
10. Natta, G., M. Farina, and M. Peraldo, *Chim. Ind. (Milan)*, **42**, 255 (1960).
11. Sigwalt, P., *J. Polymer Sci.*, **52**, 15 (1961).
12. Natta, G., M. Farina, M. Peraldo, and G. Bressan, *Makromol. Chem.*, **43**, 68 (1961).
13. Imoto, M., and I. Soematsu, *Bull. Chem. Soc. Japan*, **34**, 26 (1961).
14. Bockman, O. C., and C. Schuerch, *Polymer Letters*, **1**, 145 (1963).
15. Hopkins, E. A. H., and M. L. Miller, *Polymer*, **4**, 75 (1963).
16. McCloskey, A. L., G. S. Fonken, R. W. Kluiber, and W. S. Johnson, *Organic Syntheses*, **34**, 26 (1954).
17. Hüttig, G. H., and A. Krajewski, *Z. Anorg. Allgem. Chem.*, **141**, 133 (1924).
18. Barger, G., *J. Chem. Soc.*, **1904**, 286.
19. Natta, G., Belg. Pat. 599,833 (Nov. 10, 1961).
20. Lewis, A. F., and J. K. Gillham, *J. Appl. Polymer Sci.*, **6**, 422 (1962).
21. Miller, M. L., and C. E. Rauhut, *J. Polymer Sci.*, **38**, 63 (1959).
22. Hayashi, K., T. Yonezawa, C. Nagata, S. Okamura, and K. Fukui, *J. Polymer Sci.*, **20**, 537 (1956).
23. Joshi, R. M., *Makromol. Chem.*, **53**, 33 (1962).
24. Bhattacharyya, D. N., C. L. Lee, J. Smid, and M. Szwarc, *J. Am. Chem. Soc.*, **85**, 533 (1963).

### Résumé

Les alcoyle-lithiums et le bromure de phényl-magnésium dans le toluène, et le lithium-naphtalène dans le diméthoxyéthane, polymérisent le crotonate de *tert*-butyle. Le sodium naphtalène produit seulement des polymères de bas poids moléculaire ( $M_n < 3000$ ) et le potassium naphtalène ne donne pas de polymère. Même le lithium naphtalène, qui polymérise aisément le crotonate de *tert*-butyle, ne polymérise pas le tiglato de *tert*-butyle. Les radicaux libres ne polymérisent ni le crotonate ni le tiglato de *tert*-butyle. Le polycrotonate de *tert*-butyle formé en présence de lithium-naphtalène n'est pas cristallin, en présence d'alcoyl-lithium il est soit noncristallin soit partiellement cristallin, et en présence de bromure de phényl-magnésium est hautement cristallin. L'acide polycrotonique a été préparé à partir de polycrotonate de *tert*-butyle.

### Zusammenfassung

Lithiumalkyle und Phenylmagnesiumbromid in Toluol und Lithiumnaphthalin in Dimethoxyäthan polymerisieren *tert*-butylcrotonat. Natriumnaphthalin ergibt nur niedrige Polymere ( $M_n < 3000$ ), Kaliumnaphthalin ergibt kein Polymeres. Sogar Lithiumnaphthalin, das *tert*-butylcrotonat leicht polymerisiert, kann *tert*-butyltiglat nicht zur Polymerisation bringen. In Gegenwart von Lithiumnaphthalin gebildetes Poly-*tert*-butylcrotonat ist nicht kristallin, im Gegenwart von Lithiumalkylen entweder nicht kristallin oder teilweise kristallin und in Gegenwart von Phenylmagnesiumbromid hochkristallin. Freie Radikale polymerisieren weder *tert*-butylcrotonat noch *tert*-butyltiglat. Polycrotonsäure wurde aus Poly-*tert*-butylcrotonat dargestellt.

Received January 15, 1964

## Glass Transformation Temperatures of Poly(vinyl Alkyl Ethers) and Poly(vinyl Alkyl Sulfides)

JOGINDER LAL and G. S. TRICK, *The Goodyear Tire & Rubber Company, Research Division, Akron, Ohio*

### Synopsis

A number of poly(vinyl alkyl ethers) and poly(vinyl alkyl sulfides) of reasonably high molecular weight were prepared. Glass transformation temperatures  $T_g$  of the various polymers were measured dilatometrically. In general, the  $T_g$  value decreased with increasing length of the  $n$ -alkyl group. Data relating  $T_g$  values of poly(vinyl  $n$ -alkyl ethers) with length of  $n$ -alkyl group were treated in terms of free volume concepts of the liquid state. Branching on the alkyl group of the polymer increased the  $T_g$  value. Poly(vinyl  $n$ -alkyl sulfides) had  $T_g$  values about 35°C. higher than their oxygen analogs. A comparison of poly(vinyl  $n$ -alkyl ethers) and polymers of normal  $\alpha$ -olefins showed that the ether group and methylene group in side chains were equivalent in influencing the glass transformation temperatures. From a comparison of poly(vinyl  $n$ -alkyl ethers) and poly( $n$ -alkyl methacrylates) it is concluded that the nature of the backbone is important in determining the ease with which side chain crystallization takes place.

### INTRODUCTION

The influence of pendant groups on the glass transformation temperature  $T_g$  of polymers has been reported in the literature for several series of polymers. The chemical nature, length, and size of the groups were varied without altering the backbone polymer structure. Rogers and Mandelkern<sup>1</sup> have determined dilatometrically the  $T_g$  values for several poly( $n$ -alkyl methacrylates). They found that as the number of carbon atoms in the ester side chain is increased,  $T_g$  for the polymers decreases continuously, reaching -65°C. for poly( $n$ -dodecyl methacrylate). They have interpreted their results in terms of free volume concepts of the liquid state and the partitioning of the specific volume into its various components.  $T_g$  values for a few poly(vinyl alkyl ethers) have been determined by Schmieder and Wolf<sup>2</sup> using a torsion pendulum method. Some low temperature properties on the same series have also been reported by Fishbein and Crowe.<sup>3</sup> In the present study, we prepared several poly(vinyl alkyl ethers) and measured dilatometrically their  $T_g$  values.  $T_g$  values of three poly(vinyl alkyl sulfides) were also determined and compared with the values of their corresponding oxygen analogs. In addition, several poly( $n$ -alkyl methacrylates) were examined to supplement the data of Rogers and Mandelkern.<sup>1</sup>

## EXPERIMENTAL

## Materials

**Vinyl Alkyl Ethers and Their Polymers.** Ethyl, *n*-butyl, isobutyl, and 2-ethylhexyl vinyl ethers were obtained from Union Carbide Chemical Company. A sample of vinyl *n*-pentyl ether was kindly supplied by H. M. Teeter of Northern Regional Research Laboratory, U.S.D.A. The remaining vinyl alkyl ethers used in our studies were synthesized by transesterification of the corresponding high purity alcohols (Eastman) with a suitable vinyl alkyl ether in the presence of mercuric acetate catalyst according to the procedure of Watanabe and Conlon.<sup>4</sup> For preparing isopropyl, *n*-hexyl, *n*-octyl, *n*-decyl, and *n*-dodecyl vinyl ethers the corresponding alcohols were transesterified with vinyl *n*-butyl ether, whereas for vinylating *sec*-butyl alcohol the latter was reacted with vinyl 2-ethylhexyl ether. These monomers were carefully distilled through a 1-liter helices-packed column equipped with a constant temperature distillation head. All monomers were freed from contaminating alcohols by distilling them two or three times over sodium wire. In a few cases involving higher vinyl alkyl ethers this purification was preceded by washing of the monomer with an aqueous solution of calcium chloride and then drying over potassium hydroxide pellets. Some physical constants of the monomers are given in Table I.

TABLE I  
Physical Constants of Vinyl Alkyl Ethers, CH<sub>2</sub> = CHOR

R group	Refractive index		Literature values	
	$n_D^{30}$	Boiling point, °C.	Refractive index $n_D^{20}$	Boiling point, °C.
Ethyl	1.3718	35.5	1.3768, <sup>a</sup> 1.3767, <sup>b</sup> 1.3778 <sup>c</sup>	36-37, <sup>a</sup> 35.5 <sup>b,c</sup>
Isopropyl	1.3792	55	1.3850, <sup>a,b</sup> 1.3848 <sup>d</sup>	55.5, <sup>b,d</sup> 54-56 <sup>a</sup>
<i>n</i> -Butyl	1.3968	94	1.4022, <sup>b</sup> 1.4017 <sup>d</sup>	93.8 <sup>b,d</sup>
<i>sec</i> -Butyl	1.3920	81	1.3970 <sup>b,e</sup>	81, <sup>b</sup> 81-81.5 <sup>e</sup>
Isobutyl	1.3912	83	1.3965, <sup>b</sup> 1.3966 <sup>d</sup>	83.2, <sup>b</sup> 83 <sup>d</sup>
<i>n</i> -Pentyl	1.4105	119	—	111 <sup>b</sup>
<i>n</i> -Hexyl	1.4125	143	1.4171 <sup>b,f</sup>	143.5 <sup>b,f</sup>
<i>n</i> -Octyl	1.4220	75/12 mm.	1.4268 <sup>a,b</sup> 1.4270 <sup>f</sup>	63-64/5 mm., <sup>a</sup> 58/4 mm., <sup>b</sup> 186-187 <sup>f</sup>
2-Ethylhexyl	1.4220	67/7 mm., 178	—	177.7 <sup>e</sup>
<i>n</i> -Decyl	1.4296	72/0.65 mm.	1.4346, <sup>b</sup> 1.4347 <sup>f</sup>	101/10 mm. <sup>b</sup> 224.2-225 <sup>f</sup>
<i>n</i> -Dodecyl	1.4335	84/0.65 mm., 72/0.15 mm.	—	—

<sup>a</sup> Data of Watanabe and Conlon.<sup>4</sup>

<sup>b</sup> Data of Schildknecht et al.<sup>5</sup>

<sup>c</sup> Data of Shostakovskii et al.<sup>8</sup>

<sup>d</sup> Data of Voronkov.<sup>9</sup>

<sup>e</sup> Data of Shostakovskii et al.<sup>7</sup>

<sup>f</sup> Data of Shostahovskii et al.<sup>6</sup>

<sup>g</sup> Manufacturers' data.<sup>10</sup>

Poly(vinyl methyl ether) was obtained from Putnam Chemical Company. It was dissolved in acetone and the higher molecular weight fraction used in this work was precipitated with heptane. The isolated polymer was stabilized with a little phenyl  $\beta$ -naphthylamine and dried under vacuum. All other poly(vinyl alkyl ethers) investigated by us were obtained by polymerizing the monomers in pentane solution. Vinyl isobutyl ether was polymerized with triisobutylaluminum-titanium tetrachloride system<sup>11</sup> at  $-78^{\circ}\text{C}$ . Vinyl isopropyl ether and vinyl 2-ethylhexyl ether were polymerized by boron trifluoride-diethyl ether complex at  $-78^{\circ}\text{C}$ . The remaining vinyl alkyl ethers were polymerized by aluminum hexahydrosulfate heptahydrate catalyst<sup>12</sup> at  $5$ – $25^{\circ}\text{C}$ . The last mentioned catalyst was found to be quite convenient in preparing reasonably high molecular weight polymers. Generally, methanol containing a little phenyl  $\beta$ -naphthylamine was used for precipitating these polymers. The isolated polymers were dissolved in benzene and reprecipitated. They were then dried at  $40^{\circ}\text{C}/2$  mm. pressure for 72 hrs. In the case of poly(vinyl ethyl ether) precipitation was carried out with water.

**Isopropenyl Methyl Ether and Polymer.** A sample of isopropenyl methyl ether was kindly supplied by Dow Chemical Company. The monomer was distilled over sodium wire. It was polymerized in pentane solution at  $-78^{\circ}\text{C}$ . with  $\text{BF}_3$ -diethyl ether.

**Vinyl Alkyl Sulfides and Their Polymers.** Vinyl methyl sulfide was obtained from Monomer-Polymer Laboratories, The Borden Chemical Company. It was distilled, and the middle cut was used for polymerization.

Vinyl ethyl sulfide was obtained in 80% yield by the dehydration of  $\beta$ -hydroxyethyl ethyl sulfide over KOH at  $270^{\circ}\text{C}$ . according to the procedure of Price and Gillis.<sup>13</sup> Redistillation gave a material having b.p.  $91.5^{\circ}\text{C}/750$  mm.,  $n_{\text{D}}^{30.5}$  1.4733,  $d_{30}^{30}$  0.8711 (lit.:<sup>14</sup> b.p.  $91.9$ – $92.2$ ,  $n_{\text{D}}^{20}$  1.4756).

ANAL. Calcd. for  $\text{C}_4\text{H}_8\text{S}$ : C, 54.49%; H, 9.15%; S, 36.36%. Found: C, 54.75%; H, 9.08%; S, 36.30%.

$\beta$ -Hydroxyethyl ethyl sulfide b.p.  $74.5^{\circ}\text{C}/13$  mm.,  $n_{\text{D}}^{30}$  1.4844,  $d_{30}^{30}$  1.0144, was obtained in 90% yield by reacting sodium ethyl mercaptide and  $\beta$ -chloroethanol.

ANAL. Calcd. for  $\text{C}_4\text{H}_{10}\text{OS}$ : C, 45.25%; H, 9.43%; S, 30.19%. Found: C, 44.85%; H, 8.85%; S, 30.07%.

A considerable amount of difficulty was experienced in preparing vinyl *n*-butyl sulfide of high purity by the dehydration of  $\beta$ -hydroxyethyl *n*-butyl sulfide. The yields were also low, presumably due to the degradation of the monomer formed. A sample of vinyl *n*-butyl sulfide,  $n_{\text{D}}^{30}$  1.4690 (lit.:<sup>14</sup>  $n_{\text{D}}^{20}$  1.4722), kindly supplied by Rohm and Haas Company, was used for polymerization.

Vinyl methyl sulfide on slow polymerization for several months in a sealed tube under fluorescent light gave a solid material having an inherent viscosity value of 0.55 dl./g. Vinyl ethyl sulfide and vinyl *n*-butyl sulfide

were bulk polymerized with azobisisobutyronitrile at 60°C. in a sealed tube to give viscous liquids having inherent viscosity values of 0.2 dl./g. For ease of handling during dilatometric  $T_g$  determination, these liquids were crosslinked with 4% by weight of dicumyl peroxide and 1% by weight of finely divided sulfur in a sealed tube at 155°C. The crosslinked materials were extracted with benzene and finally dried at 40°C. and 2 mm. pressure for 72 hrs.

***n*-Alkyl Methacrylates and Their Polymers.** *n*-Dodecyl, *n*-tetradecyl, and *n*-hexadecyl methacrylates were synthesized by direct esterification of the corresponding high purity alcohols (Eastman) with glacial methacrylic acid with the use of *p*-toluenesulfonic acid as a catalyst and a small amount of phenothiazine as an inhibitor.

They were purified by fractional distillation. The middle cuts, the physical constants of which are given in Table II, were polymerized in bulk at 60°C. with benzoyl peroxide initiator. The polymerized materials were dissolved in benzene and precipitated in methanol. This was repeated twice. The purified polymers were dried at 40°C./2 mm. pressure for 64 hr.

TABLE II  
Physical Characteristics of *n*-Alkyl Methacrylates and Their Polymers

Alkyl group in methacrylate	Monomer refractive index		Polymer		
	$n_D^{30}$	Literature values	$n_D^{30}$	$T_g$ , °C. (dilatometer)	$T_g$ , °C. (literature)
<i>n</i> -Dodecyl	1.4422	$n_D^{35}$ 1.4430 <sup>a</sup> $n_D^{20}$ 1.4452 <sup>b</sup>	1.4740	-55	-65 <sup>a</sup>
<i>n</i> -Tetradecyl	1.4457	$n_D^{30}$ 1.4480 <sup>b</sup> $n_D^{20}$ 1.4495 <sup>b</sup>	1.4746	-72	-9 <sup>c</sup>
<i>n</i> -Hexadecyl	1.4490	$n_D^{20}$ 1.4515 <sup>b</sup>	1.4750	$T_m = 22^d$	

<sup>a</sup> Data of Rogers and Mandelkern.<sup>1</sup>

<sup>b</sup> Data of Rehberg and Fisher.<sup>15</sup>

<sup>c</sup> Data of Wiley and Brauer.<sup>16</sup>

<sup>d</sup>  $T_m$  = melting temperature (side chain crystallization), °C.

### Physical Properties

Inherent viscosities were determined at 30°C. on 0.1% solution of the polymer in benzene. These values are expressed in units of deciliters/gram.

Densities of the polymers were measured by the displacement method in methanol and by the use of a density gradient column.

The low temperature torsion flex test on the various polymers was carried out according to ASTM D 1053-54T. For ease of handling of the polymers of vinyl *n*-octyl, vinyl *n*-decyl and vinyl *n*-dodecyl ethers they were lightly crosslinked with 1 wt.-% of dicumyl peroxide at 155°C. in a suitable rectangular mold under pressure. The inflection temperatures<sup>17</sup>

TABLE III. Physical Characteristics of Poly(vinyl Alkyl Ethers) and Poly(vinyl Alkyl Sulfides)

Alkyl group in (CH <sub>2</sub> CHOR) <sub>n</sub> or (CH <sub>2</sub> CHSR) <sub>n</sub>	Density, g./cc.				Molar refractivity	<i>T<sub>g</sub></i> , °C. (dila- tomeric)	Inflection temp., °C.	Low temperature stiffening, °C.	Solubility parameter, <sup>a</sup> cal. <sup>1/2</sup> /cc. <sup>1/2</sup>
	Inherent viscosity, dl./g.	Alcohol immersion (at 27°C.)	Density gradient tube (at 30°C.)	<i>n</i> <sub>D</sub> <sup>30</sup>					
Vinyl alkyl ethers									
Methyl	0.8	—	—	—	—	—34	-20	-10, <sup>b</sup> -31 <sup>c</sup>	7.94
	1.8	1.037	—	1.4700	15.54	-31	-15	—	—
Ethyl	1.9	—	—	—	—	-42	-23	-17, <sup>b</sup> -10 <sup>d</sup>	7.54
<i>n</i> -Butyl	4.7	0.968	0.951	1.4540	20.53	-43	-21	—	—
<i>n</i> -Pentyl	4.3	0.927	0.926	1.4563	29.50	-55	-41	-32 <sup>b</sup>	7.85
<i>n</i> -Hexyl	3.4	—	0.918	1.4581	33.94	-66	-54	—	7.86
<i>n</i> -Octyl	2.2	0.925	0.902	1.4591	38.86	-77	-61	—	7.81
	2.6	0.914	—	—	—	-80	-63	—	—
	4.2	—	0.893	1.4613	48.03	-79	-62	—	7.87
<i>n</i> -Decyl	1.0	—	—	—	—	—	-33	—	—
	2.1	0.88	0.883	1.4628	57.48	<i>T<sub>m</sub></i> = 7 <sup>o</sup>	-32	—	7.88
<i>n</i> -Dodecyl	1.9	0.892 <sup>f</sup>	0.892 <sup>f</sup>	1.4640	67.74	<i>T<sub>m</sub></i> = 30 <sup>o</sup>	0	—	8.02
Isopropyl	2.2	—	0.924	—	—	-3	6	—	—
<i>sec</i> -Butyl	0.8	—	0.924	—	—	-20	-5	—	—
Isobutyl	4	—	0.916	1.4740	30.42	-19	-7	-1, <sup>b</sup> < -10 <sup>d</sup>	7.50
2-Ethylhexyl	1.2	0.904	0.897	1.4626	47.94	-66	-55	-24 <sup>e</sup>	—
Poly(isopropenyl Methyl Ether)	2.5	—	—	—	—	+67	—	—	—
Vinyl alkyl sulfides									
Methyl	0.6	1.184	—	—	—	-1	15	—	9.66
Ethyl	0.2	—	—	—	—	-7	—	—	—
<i>n</i> -Butyl	0.2	0.984	—	—	—	-20	—	—	8.5

<sup>a</sup> From Small.<sup>19</sup> <sup>b</sup> Data of Schmieder and Wolf.<sup>2</sup> <sup>c</sup> Data of Fishbein and Crowe.<sup>3</sup> <sup>d</sup> Data of Jenckel.<sup>18</sup> <sup>e</sup> *T<sub>m</sub>* = melting temperature (side chain crystallization), °C. <sup>f</sup> In the amorphous state after melting and quenching.

of the twist angle versus temperature curves of the polymers are indicated in Table III. For comparison purpose, these curves were adjusted<sup>17</sup> so as to have a twist reading of about  $160^\circ$  at  $25^\circ\text{C}$ .

Glass transformation temperatures of the polymers were measured dilatometrically by using mercury or silicone oil as the confining fluid. The rate of heating was about  $10^\circ\text{C./hr}$ .

## RESULTS

### Poly(vinyl Alkyl Ethers)

In Figure 1, the dependence of specific volume, refractive index, and molar refractivity on the length of alkyl group of poly(vinyl *n*-alkyl ether) is shown. As expected, the molar refractivities increase linearly as the alkyl group is increased from  $\text{C}_1$  to  $\text{C}_{12}$ .

In Figures 2 and 3 are plotted typical experimental data showing the change in dilatometer reading with temperature. No attempt was made to standardize the amount of polymer and mercury or silicone oil used in each experiment. Consequently, the absolute changes in dilatometer reading with temperature are of no quantitative significance. In those polymers which exhibited a sharp change in coefficient of thermal expansion, the temperature at which this occurred was taken as the glass transformation temperature. In Figure 3 are also shown typical results for a polymer exhibiting a first-order transition. Data of this type were obtained by slowly cooling the sample until crystallization was indicated. The sample was then slowly heated and the temperature at which the

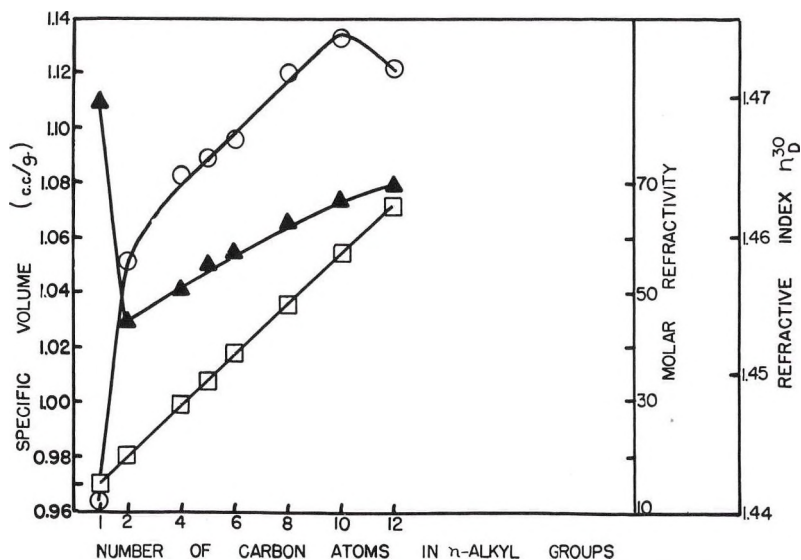


Fig. 1. The dependence of (O) specific volume, (▲) refractive index  $n_D^{30}$ , and (□) molar refractivity on the length of *n*-alkyl group in poly(vinyl *n*-alkyl ethers).



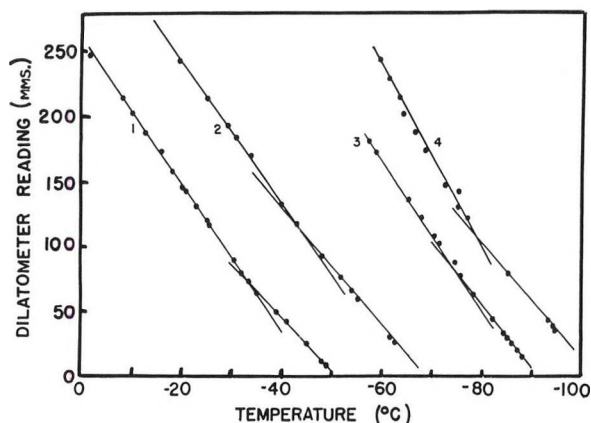


Fig. 2. Typical dilatometric data used to determine glass transformation temperatures of poly(vinyl alkyl ethers): (1) methyl; (2) ethyl; (3) *n*-hexyl; (4) *n*-octyl.

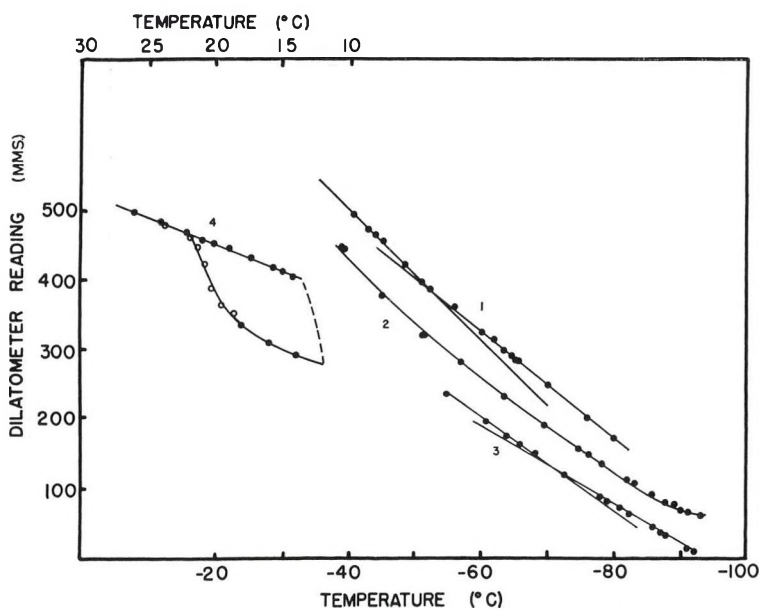


Fig. 3. Further typical dilatometric data used to determine polymer transitions: (1) *n*-dodecyl methacrylate (lower temperature scale); (2) *n*-decyl vinyl ether (lower temperature scale); (3) *n*-tetradecyl methacrylate (lower temperature scale); (4) *n*-hexadecyl methacrylate (upper temperature scale), (●) cooling curve, (○) warming curve.

warming and cooling curves intersected was taken as the melting temperature.

In Tables II and III are recorded the dilatometric glass transformation values for all the samples examined. A few of the samples that exhibited side chain crystallization with an associated first-order transition require special comment. The poly(*n*-hexadecyl methacrylate) and the poly-

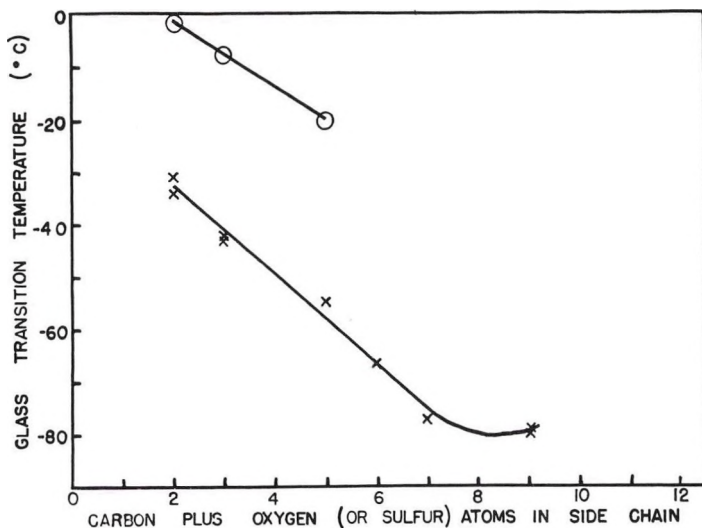


Fig. 4. Variation of glass transformation temperature with length of side chain for (X) poly(vinyl *n*-alkyl ethers) and (O) poly(vinyl *n*-alkyl sulfides).

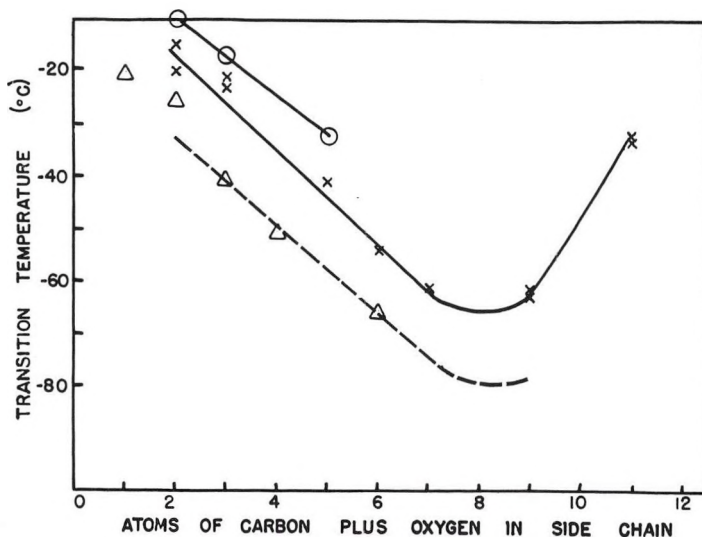


Fig. 5. Variation of transition temperatures of poly(vinyl *n*-alkyl ethers) and poly-*n*- $\alpha$ -olefins with length of side chain: (---) best line from points (X) in Fig. 4; ( $\Delta$ ) poly-*n*- $\alpha$ -olefins, data of Dannis;<sup>21</sup> (X) inflection temperatures for poly(vinyl *n*-alkyl ethers); (O) softening temperatures of poly(vinyl *n*-alkyl ethers) by torsional pendulum, data of Schmieder and Wolf.<sup>2</sup>

(vinyl *n*-dodecyl ether) both exhibited rapid crystallization below the melting point and it was not possible to quench completely these materials. Consequently, no valid glass transformation temperature for the completely amorphous material could be obtained. In the case of poly-

(vinyl *n*-decyl ether) it appeared to be possible to quench this material to low temperature. As shown in Figure 3, the dilatometric measurements on the quenched sample indicated a continuous change in the thermal coefficient of expansion in the region of  $-90^{\circ}\text{C.}$  to  $-40^{\circ}\text{C.}$ , and it was impossible to obtain two linear intersecting lines. The crystalline material and a lightly crosslinked quenched material exhibited similar behavior, with the crystalline material exhibiting a first-order transition at  $+7^{\circ}\text{C.}$  when warmed slowly. Consequently, no dilatometric glass transformation temperature could be established.

In Tables II and III are also recorded literature data on the low temperature transition of some of these polymers. The marked difference between our results for poly(*n*-tetradecyl methacrylate) and those of Wiley and Brauer<sup>16</sup> might be due to the occurrence of a small amount of crystallization under the conditions used by these investigators.

In Figure 4 are plotted the dilatometric glass transformation temperatures as a function of the length of the alkyl group of the poly(vinyl *n*-alkyl ethers). In the same graph are plotted the more limited data for poly(vinyl *n*-alkyl sulfides).

In Figure 5 the best line from the points in Figure 4 for poly(vinyl alkyl ethers) has been plotted together with the inflection temperatures from Table III. Softening temperature values reported by Schmieder and Wolf<sup>2</sup> by the torsional pendulum method are also plotted for comparison purposes. The relation between dilatometric glass transformation temperature and inflection temperature of several polymers has been reported<sup>17</sup> and is further supported by the data in Figure 5. The softening temperature values of Schmieder and Wolf are higher than our dilatometric  $T_g$  values, presumably due to the higher frequency used in the torsional pendulum measurements.

## DISCUSSION

It is interesting to compare the low temperature properties of poly(vinyl alkyl ether) with those of polymers of *n*  $\alpha$ -olefins. Slichter and Davis<sup>20</sup> have shown by NMR relaxation studies of polymers of *n*  $\alpha$ -olefins that increase in the length of the *n*-alkyl side chain contributes to increased segmental mobility in the polymer. The glass transformation temperatures of various  $\alpha$ -olefin polymers have been determined by Dannis<sup>21</sup> from measurements of the linear coefficient of expansion. His results are plotted in Figure 5 and show that the low temperature properties remain essentially unaltered by substituting the ether group by a methylene group. An associated comparison has been made by Natta et al.,<sup>22</sup> who showed that crystalline poly(vinyl isobutyl ether) and poly-5-methyl-1-hexene have similar isotactic helical structure, i.e., the ether and methylene groups behave quite similarly in determining the crystal structure of these polymers.

From Table III, some conclusions may be drawn regarding the influence of substitution in the alkyl group on the  $T_g$  values of poly(vinyl alkyl

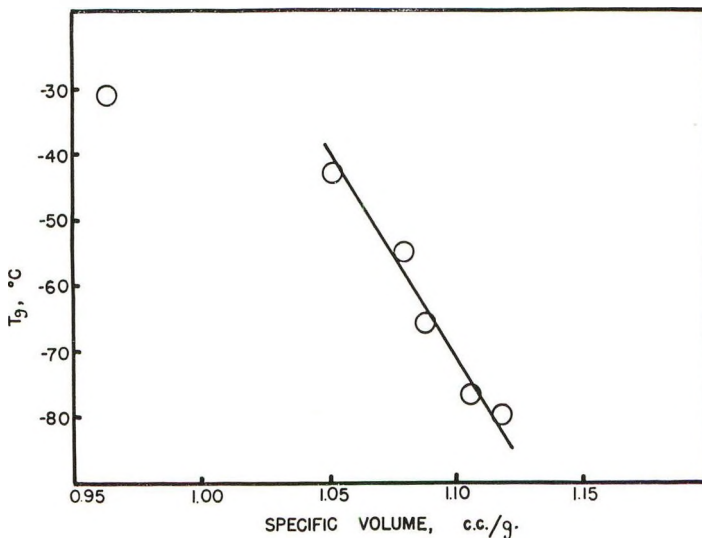


Fig. 6. Plot of dilatometric  $T_g$  and specific volume (at 30°C.) of poly(vinyl *n*-alkyl ethers.)

ethers). Poly(vinyl isopropyl ether), where substitution occurs on the carbon atom adjacent to the ether linkage, has a  $T_g$  about 40°C. higher than the linear poly(vinyl ethyl ether). Similarly, poly(vinyl *sec*-butyl ether) has a  $T_g$  29°C. higher than the estimated value for poly(vinyl *n*-propyl ether). Poly(vinyl 2-ethylhexyl ether) in which the substitution is two carbon atoms away from the ether group has a  $T_g$  11°C. higher than poly(vinyl *n*-hexyl ether).

The influence of branching in the alkyl group on the  $T_g$  values can also be seen by comparing the  $T_g$  value of  $-55^\circ\text{C}$ . for poly(vinyl *n*-butyl ether) with the value of  $-20^\circ\text{C}$ . for poly(vinyl *sec*-butyl ether) and  $-19^\circ\text{C}$ . for poly(vinyl isobutyl ether). Similarly, the  $T_g$  value of  $-66^\circ\text{C}$ . for poly(vinyl 2-ethylhexyl ether) is 14°C. higher than the  $T_g$  value of  $-80^\circ\text{C}$ . for poly(vinyl *n*-octyl ether).

Poly(isopropenyl methyl ether) has a  $T_g$  value of 67°C. compared to  $-31^\circ\text{C}$ . for poly(vinyl methyl ether). Thus the presence of a methyl group on the methoxy-bearing carbon atom of the backbone elevated the  $T_g$  value by about 100°C. A difference of this magnitude is also observed between the  $T_g$  values of poly(methyl methacrylate) and poly(methyl acrylate).

Any quantitative treatment of glass transformation data is hampered by the lack of any clear understanding of the factors that are of significance in determining the value of the glass transformation. Rogers and Mandelkern<sup>1</sup> were successful in treating their data on poly(*n*-alkyl methacrylates) by partitioning the specific volume into two components: a free volume and an occupied volume. Both of these volumes were considered to vary with temperature and composition. By using as a criterion for glass formation that the fractional free volume of all polymers at this glass trans-

formation temperature is the same, then from a plot of  $T_g$  versus specific volume and from the change in volume-temperature coefficient at the  $T_g$  it was concluded that as the length of the alkyl group in the ester side chain was increased, about 15% of the volume increase became free volume. This increase in free volume was considered to account for the decrease in  $T_g$ .

We have treated our data for the poly(vinyl *n*-alkyl ethers) in a similar way. The plot of  $T_g$  versus specific volume (from the density gradient tube) is shown in Figure 6. The value for poly(vinyl methyl ether) does not fit the curve, but the other five points yield a reasonably straight line. An average change in volume-temperature coefficient of approximately  $2.2 \times 10^{-4}$  cc./g. °C. was obtained for the methyl, ethyl, *n*-butyl, and *n*-hexyl polymers at their respective  $T_g$ . Combining this value with the slope from Figure 5, it may be calculated<sup>1</sup> that on lengthening the side chain 14% of the volume increase becomes free volume, i.e., within experimental error the same value as was found<sup>1</sup> for poly(*n*-alkyl methacrylates). From the density value in Table III and an extrapolation of the linear portion of the curve in Figure 6, it would be estimated that poly(vinyl *n*-decyl ether) would have a  $T_g$  of about  $-90^\circ\text{C}$ . Although precise volume-temperature measurements were not made below  $-95^\circ\text{C}$ . the fact, as stated previously, that a gradually curving line was obtained above  $-90^\circ\text{C}$ . makes it impossible to determine  $T_g$  by a dilatometric method. In Table III are recorded solubility parameter values calculated according to the method of Small.<sup>19</sup> It may be seen that the values fall within a narrow range and in contrast with the case of poly(*n*-alkyl methacrylates)<sup>1</sup> there is no systematic decrease in cohesive energy density as the length of the side chain is increased.

Dimarzio and Gibbs<sup>23</sup> have derived the expression

$$B_A (T_2 - T_{2A}) + B_B (T_2 - T_{2B}) = 0$$

for estimating the second-order transition or glass transformation temperature of a copolymer composed of monomers A and B. In this expression,  $B_A$  is the fraction of rotatable bonds of type A in the copolymer and  $B_B$  is the fraction of rotatable bonds of type B,  $T_{2A}$  and  $T_{2B}$  are the glass transformation temperatures of the homopolymers of A and B, respectively, and  $T_2$  is the glass transformation temperature of the copolymer. Visualizing poly(methyl methacrylate) onto which segments of polymethylene have been grafted, they estimated  $T_g$  values of several higher poly(*n*-alkyl methacrylates) which are in fair agreement with the values reported by Rogers and Mandelkern.

The above expression may be rewritten in the form

$$T_2 = T_{2A} + B_B (T_{2B} - T_{2A})$$

Following Dimarzio and Gibbs, we view poly(vinyl *n*-alkyl ethers) as poly(vinyl methyl ethers) on to which segments of polymethylene have been grafted. We have used the values of  $153^\circ\text{K}$ .<sup>21</sup> for  $T_{2A}$  and  $242^\circ\text{K}$ . for

$T_{2B}$  for polyethylene and poly(vinyl methyl ether), respectively. If poly(vinyl methyl ether) is assigned four flexible bonds and each methylene group added in the pendant group is assigned  $\frac{2}{3}$  of a flexible bond, the calculated  $T_2$  values are found to be in reasonable agreement with our experimental dilatometric values (Table IV).

TABLE IV

Alkyl group in poly(vinyl alkyl ether)	$B_B$	$T_g, ^\circ\text{K.}$	
		Experimental	Calculated
Ethyl	6/7	230	229
<i>n</i> -Butyl	2/3	218	212
<i>n</i> -Pentyl	3/5	207	206
<i>n</i> -Hexyl	6/11	196	201.5
<i>n</i> -Octyl	6/13	194	193.4

### Poly(vinyl Alkyl Sulfides)

The  $T_g$  values for the three poly(vinyl alkyl sulfides) reported in Table III are 30–35°C. higher than their corresponding oxygen analogs. This might be associated with the corresponding higher cohesive energy density values recorded in Table III.

### Poly(*n*-alkyl Methacrylates)

The values of the glass transformation temperature recorded in Table II supplement the results of Rogers and Mandelkern.<sup>1</sup> The value of  $-55^\circ\text{C.}$  obtained for poly(*n*-dodecyl methacrylate) is significantly different from their value of  $-65^\circ\text{C.}$  but does not affect any of their conclusions. The results also establish that poly(*n*-hexadecyl methacrylate) is the first member of this series to exhibit side chain crystallization.

### First-Order Transitions

Some comments may be made regarding the occurrence of crystallization and the melting points of the crystalline materials. The crystallization is presumed to be of the side chain variety. It may be noted that the nature of the backbone governs the ease with which side chain crystallization takes place; poly(vinyl *n*-decyl ether) is the first member of the poly(vinyl alkyl ether) series to show measurable side chain crystallization but it is necessary to go to a longer alkyl side chain ( $\text{C}_{16}$ ) in the methacrylate series. In addition, the melting point depends on both the length of the side chain and the nature of the backbone. From Table II, poly(*n*-hexadecyl methacrylate) has a melting point  $T_m$  of  $22^\circ\text{C.}$  while poly(vinyl *n*-hexadecyl ether) has a reported melting point<sup>24</sup> of  $53^\circ\text{C.}$  Similarly, a melting point of  $37.5^\circ\text{C.}$  is reported<sup>1</sup> for poly(*n*-octadecyl methacrylate) while poly(vinyl *n*-octadecyl ether) has  $T_m = 50\text{--}52^\circ\text{C.}$ <sup>25</sup> The sample of poly(vinyl *n*-dodecyl ether) crystallized fairly readily with a half time of crystallization of 30 min. at  $0^\circ\text{C.}$

The authors wish to express their thanks to the Goodyear Tire & Rubber Company for permission to publish these results, to Dr. K. W. Scott for valuable discussions and to Mr. J. E. McGrath, Mr. D. J. Zimmerman, and Mr. J. M. Ryan for a portion of the experimental work.

### References

1. Rogers, S. S., and L. Mandelkern, *J. Phys. Chem.*, **61**, 985 (1957).
2. Schmieder, K., and K. Wolf, *Kolloid Z.*, **134**, 149 (1953).
3. Fishbein, L., and B. F. Crowe, *Makromol. Chem.*, **48**, 221 (1961).
4. Watanabe, W. H., and L. E. Conlon, *J. Am. Chem. Soc.*, **79**, 2828 (1957).
5. Schildknecht, C. E., A. O. Zoss, and C. McKinley, *Ind. Eng. Chem.*, **39**, 180 (1947).
6. Shostakovskii, M. F., B. I. Mikhant'ev, and V. A. Neterman, *Izv. Akad. Nauk SSSR, Otdel. Khim. Nauk*, **1952**, 485.
7. Shostakovskii, M. F., B. I. Mikhant'ev, and N. N. Ovchinnikova, *Izv. Akad. Nauk SSSR, Otdel. Khim. Nauk*, **1952**, 1099.
8. Shostakovskii, M. F., F. P. Sidel'kovakaya, and V. A. Gladyshevskaya, *Zhur. Priklad. Khim.*, **25**, 102 (1952).
9. Voronkov, M. G., *Zhür. Obshch. Khim.*, **20**, 2060 (1950).
10. Brochure from Union Carbide Chemical Company.
11. Lal, J., *J. Polymer Sci.*, **31**, 179 (1958).
12. Mosley, S. A., U. S. Pat. 2,549,921 (April 24, 1951).
13. Price, C. C., and R. G. Gillis, *J. Am. Chem. Soc.*, **75**, 4750 (1953).
14. Shostakovskii, M. F., E. N. Prilezhaeva, and N. I. Uvarova, *Izv. Akad. Nauk SSSR, Otdel. Khim. Nauk*, **1955**, 906.
15. Rehberg, C. E., and C. H. Fisher, *Ind. Eng. Chem.*, **40**, 1429 (1948).
16. Wiley, R. H., and G. M. Brauer, *J. Polymer Sci.*, **3**, 647 (1948).
17. Trick, G. S., *J. Appl. Polymer Sci.*, **3**, 253 (1960).
18. Jenckel, E., *Kolloid-Z.*, **100**, 163 (1942).
19. Small, P. A., *J. Appl. Chem.*, **3**, 71 (1953).
20. Slichter, W. P., and D. D. Davis, *Bull. Am. Phys. Soc.* [2], **8**, 240 (1963).
21. Dannis, M. L., *J. Appl. Polymer Sci.*, **1**, 121 (1959).
22. Natta, G., I. Bassi, and P. Corradini, *Makromol. Chem.*, **18-19**, 455 (1956).
23. Dimarzio, E. A., and J. H. Gibbs, *J. Polymer Sci.*, **40**, 121 (1959).
24. Fort, T., and A. E. Alexander, *J. Colloid Sci.*, **14**, 190 (1959).
25. Schneider, W. J., L. E. Gast, E. H. Melvin, C. A. Glass, and H. M. Teeter, *J. Am. Oil Chemists Soc.*, **34**, 244 (1957).

### Résumé

On a préparé un certain nombre d'éthers polyvinyl-alcoyle et des sulfures de polyvinyl-alcoyle d'un poids moléculaire raisonnablement élevé. On a mesuré dilatométriquement les points de transition vitreuse de ces différents polymères. En général, les valeurs de  $T_g$  diminuent lorsque croît la longueur des groupes  $n$ -alcoyles. Les résultats lient les points de transition vitreuse des éthers de polyvinyl- $n$ -alcoyles avec la longueur des groupements  $n$ -alcoyles sont traités en faisant usage du concept de volume libre à l'état liquide. La ramification du groupement alcoyle du polymère augmente la valeur du point de transition vitreuse. Les sulfures de polyvinyle  $n$ -alcoyles sont caractérisés par des valeurs du point de transition vitreuse qui sont inférieures d'environ 35° C à celles de leurs homologues oxygénés. Lorsqu'on compare les éthers de polyvinyle- $n$ -alcoyles avec les polyoléfines normales, on s'aperçoit que les groupes éthers et méthylènes des chaînes latérales ont des effets équivalents sur la température de transition vitreuse. La comparaison des éthers de polyvinyl- $n$ -alcoyle et des polyméthacrylates de  $n$ -alcoyle permet de conclure que la nature du squelette est importante parce qu'elle détermine l'aisance avec laquelle la cristallisation des chaînes latérales se produit.

### Zusammenfassung

Eine Anzahl von Polyvinylalkyläthern und Polyvinylalkylsulfiden mit genügend hohem Molekulargewicht wurde dargestellt. Die Glasumwandlungstemperatur  $T_g$  der verschiedenen Polymeren wurde dilatometrisch bestimmt. Im allgemeinen nimmt der  $T_g$ -Wert mit zunehmender Länge der  $n$ -Alkylgruppe ab. Die Beziehung zwischen den  $T_g$ -Werten von Polyvinyl- $n$ -alkyläthern und der Länge der  $n$ -Alkylgruppe wurde auf Grundlage des Freivolumskonzepts des flüssigen Zustandes behandelt. Mit einer Verzweigung der Alkylgruppe des Polymeren nimmt  $T_g$  zu. Polyvinyl- $n$ -alkylsulfide haben einen um etwa 35°C höheren  $T_g$ -Wert als ihr Sauerstoffanalogon. Ein Vergleich von Polyvinyl- $n$ -alkyläthern mit Polynormal- $\alpha$ -olefinen zeigt, dass in bezug auf die Beeinflussung der Glasumwandlungstemperatur die Äther- und Methylengruppen in den Seitenketten gleichwertig sind. Aus einem Vergleich von Polyvinyl- $n$ -alkyläther mit Poly- $n$ -alkylmethacrylat wird auf die Wichtigkeit der Hauptkette zur Bestimmung der Leichtigkeit der Seitenkettenkristallisation geschlossen.

Received January 15, 1964



## Polymerization of Acetaldehyde. Part V. Polyaldol Condensation of Acetaldehyde by Alkali Metal Amalgam as Catalyst. II.

TATSUYA IMOTO and TSUTOMU MATSUBARA,\* *Faculty of  
Engineering, Osaka City University, Kita-ku, Osaka, Japan.*

### Synopsis

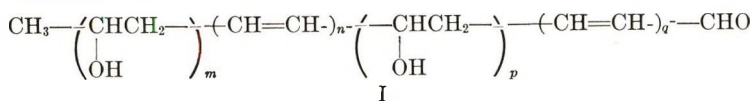
In a previous paper, it was reported that an acetaldehyde polymer of the poly(vinylalcohol) type was obtained by polymerization of acetaldehyde with sodium amalgam as catalyst. In the present, more detailed investigation, it was found that the catalyst concentration, the reaction time, the reaction temperature, and the solvent concentration have certain effects on the molecular weight and the yield of polymer. At the early stage of this polymerization, the yield is proportional to the square root of the reaction period. So, at this stage, the reaction may be assumed to be diffusion-controlled. Several solvents and the two-stage polymerization have influences upon this polymerization.

### INTRODUCTION

Many reports of polyether-type polymerization of acetaldehyde have been published, but few reports have appeared in the literature on the poly(vinyl alcohol) type polymerization.

In a previous communication,<sup>1</sup> it was reported that an aldehyde polymer of the poly(vinyl alcohol) type was obtained by polymerization of acetaldehyde with the use of sodium amalgam as catalyst. Degering and Stoudt<sup>2</sup> polymerized acetaldehyde using organic amines as catalyst in a nitrogen bomb; however, this was not reported in detail. Some reports have been referred to by Leipuuskii and Reinov<sup>3</sup> concerning some high pressure polyaldol condensation of acetaldehyde, but we have not yet been able to find these. Another communication on low molecular weight acetaldehyde resins of the aldol type is reported to have been issued by BASF.

T. Imoto et al.<sup>4</sup> previously polymerized acetaldehyde by triethylamine under high pressure and considered the polymerization mechanism to involve repeated aldol condensation reactions; the polymer was supposed to have the following structure:



\* Present address: New Japan Nitrogenous Fertilizer Co. Ltd., Chiyoda-ku, Tokyo, Japan.

Thus, the reaction may involve concurrent partial dehydration and introduction of a double bond which is reflected in coloring of the product. Furthermore, similar results were obtained in the case of polymerization of crotonaldehyde.<sup>5</sup> In order to confirm the above reaction mechanism, a study of the kinetics of this reaction was performed.<sup>6</sup>

However, in this polymerization with alkali metal amalgam as catalyst, very little dehydration took place. Moreover, this method gave a poly-(vinyl alcohol) type of polyacetaldehyde which contains few double bonds and which was colorless to pale yellow in color. Although the polymer obtained by this method had very high viscosity, its molecular weight was not very high.

In this paper, the effects of catalyst concentration, duration of the reaction, reaction temperature, and solvent concentration are studied, and the processes of polymerization are reported.

## EXPERIMENTAL

The acetaldehyde monomer (AcH) was obtained by distillation of acetaldehyde which was prepared by pyrolysis of purified paraldehyde with anhydrous sodium sulfate. Solvents were purified by common methods, and amalgams were also prepared by common procedure.

The polymerization was carried out in a four-necked 500-ml. flask fitted with a thermometer and stirrer, monomer input tube, and necks for input and output of dry N<sub>2</sub> gas; transfer of all reactants to the reaction flask avoided any contact with air. Solvent was added into the flask before the acetaldehyde monomer. The reaction mixture was stirred at a moderate rate and cooled to -50 or -60°C. with an acetone-Dry Ice (or methanol-Dry Ice) bath. After the previously weighed amalgam was quickly added as catalyst, the temperature of the reaction system was raised slowly until the desired reaction temperature was attained, at which the system was then left for the specified reaction time.

After the polymerization, the reaction mixture was added to water and the solvent was decanted off. The mercury was then decanted from the residue, and the alkali metal was removed by ion exchange. The effluent was concentrated at reduced pressure (about 75°C./10 mm. Hg) by use of a boiling water bath. The polymer thus obtained was a highly viscous liquid or semi-solid, colorless to pale yellow in color. The molecular weight of the polymer was measured by a cyroscopic method with benzene as solvent. Element analysis, infrared spectral analysis, and the measurement of solubility of the polymer were carried out for a few samples. These results were consistent with a structure of the same type as described above.

## RESULTS AND DISCUSSION

### 1. Effect of Catalyst Concentration

The procedure was carried out by varying the concentration of catalyst at definite reaction conditions, i.e., temperature 0°C. and reaction time 20

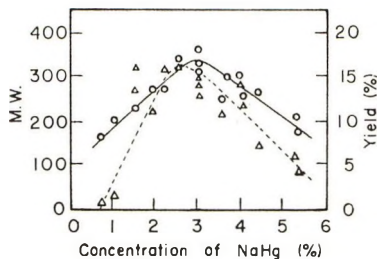


Fig. 1. Effects of catalyst concentration with 3.0% Na-Hg as catalyst: (—○—) M.W.; (---Δ---) yield. Temp., 0°C.; time, 20 hr.

hr. Figure 1 shows that there is a single optimum catalyst concentration at which a maximum molecular weight and maximum yield of the polymer are obtained. This optimum value lies at about 2-3% catalyst concentration. At concentrations over 3%, however, the yield of reaction products of low molecular weight increases; these materials may be removed during polymer purification by concentrating under reduced pressure, so as a result, the yield of polymer decreases.

## 2. Effects of Reaction Time

At 3.0% catalyst concentration and a reaction temperature of 0°C., the relation of the molecular weight of polymer to the reaction time is as shown in Figure 2. The molecular weight approaches a constant (ca. 350) value after about 20 hr. under these conditions.

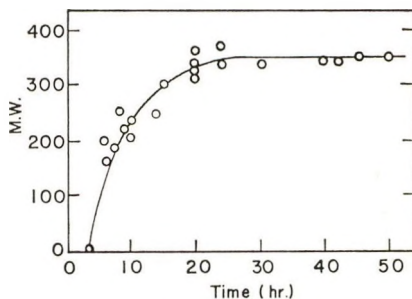


Fig. 2. Effects of reaction time with 3.0% Na-Hg as catalyst; temp., 0°C., cat. 3.0%.

## 3. Effects of Reaction Temperature

Figure 3 shows the results of reaction at 3.0% catalyst concentration for 20 hr. The molecular weights increase with the reaction temperature up to about 0°C. This phenomenon may be due to the fact that some of the acetaldehyde monomer in the reaction system evaporates at such a reaction time on account of some failure in the apparatus.

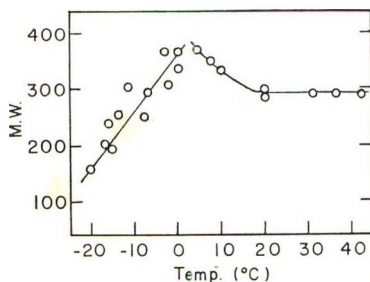


Fig. 3. Effect of reaction temperature with 3.0% Na-Hg as catalyst; time, 20 hr., cat. 3.0%.

#### 4. Effects of Reaction Period at Early Stage

In these experiments, polymers larger than dimer have been obtained owing to the concentrating of reaction products under reduced pressure (Table I).

TABLE I  
Polymerization of Acetaldehyde with Sodium Amalgam as Catalyst

No.	AcH, g.	3.0% Na-Hg, g.	Reaction time, t. min.	Temp., °C.	Yield, %	$t^{1/2}$
53	78.8	0.82	0	~0	0	0
54	"	"	5	"	8.2	2.24
55	"	"	10.5	"	14.9	3.86
56	79.9	0.83	15	"	18.4	3.89
57	79.0	0.82	20	"	20.8	4.48
58	78.8	"	25	"	17.5	5.00
59	79.3	0.83	30	"	25.6	5.48
60	79.0	0.82	45	"	27.3	6.72
61	78.8	"	60	"	28.2	7.75
62	"	1.64	0.5	"	3.2	0.71
63	79.1	"	1	"	5.2	1.00
64	78.8	"	2	"	12.9	1.42
65	78.9	"	8	"	14.2	2.83
66	78.8	"	12.5	"	15.9	3.54
67	79.4	1.65	17	"	27.1	4.13
68	79.1	"	22.5	"	27.6	4.75
69	79.5	"	27.5	"	26.3	5.25
70	"	"	42	"	34.4	5.85
71	78.8	1.64	57	"	32.8	7.55
72	83.9	3.49	0.5	"	7.3	0.71
73	80.4	3.35	2.5	"	18.0	1.58
74	79.2	3.30	8.5	"	25.5	2.92
75	79.0	3.29	18	"	25.3	4.24
76	"	"	27.5	"	31.1	5.24

Figure 4, in which the polymer yield is plotted versus the reaction time, i.e., the reaction rate curve, also indicates that the yield of the polymer

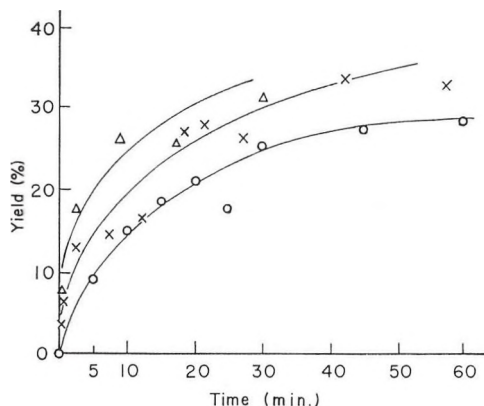


Fig. 4. Relation between the yield and the reaction time at early stage. Temp., 0°C.: (O) cat. concentration 1.04%; (X) cat. concentrated 2.08%; (Δ) cat. concentration 4.16%.

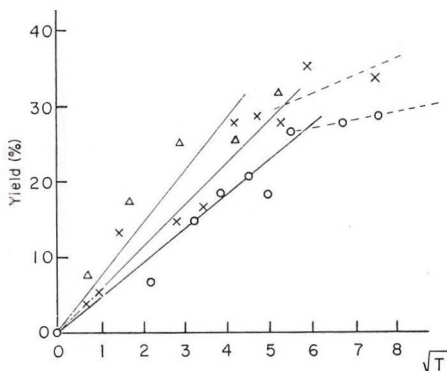
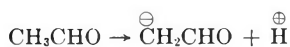


Fig. 5. Relation between the yield and the reaction time at early stage. Temp., 0°C.: (O) cat. concentration 1.04%; (X) cat. concentration 2.08%; (Δ) cat. concentration 4.16%.

increases with increase in catalyst concentration. However, a kinetic study of this reaction system is unsatisfactory.

Bell and McTigue<sup>7</sup> reported the rate-determining step to be the reaction:



Although this should be first-order with respect to monomer, experimental plots of the square root of the reaction time versus the yield show a nearly linear relation at the early stage (Fig. 5). It may, therefore, be assumed that this reaction is diffusion-controlled, because it obeys a parabolic law, i.e., Fick's first law. The diffusion of sodium from the amalgam to the solution should control the reaction rate of this polymerization. Some scatter existing in the data of Figure 5 may be attributed to fluctuations in the rate of stirring.

### 5. Effects of the Solvent

The results of the experiments carried out at 0°C. for 20 hr. in several solvents are given in the Table II and are shown in Figures 6-9. From these

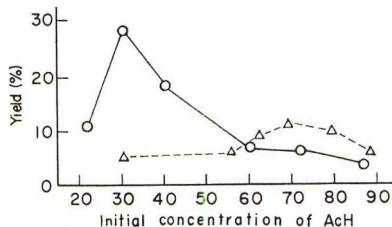


Fig. 6. Effects of solvent on yield at varying concentrations of AcH: (O) diethyl ether; (Δ) petroleum ether. 3.2% Na-Hg; 0°C., 20 hr.

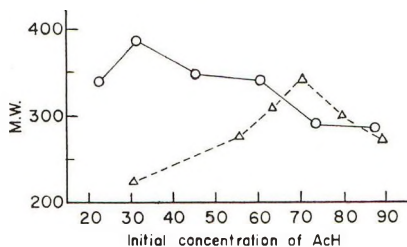


Fig. 7. Effects of solvent on M.W. at varying concentrations of AcH: (O) diethyl ether (Δ) petroleum ether. 3.2% Hg-Na; 0°C.; 20 hr.

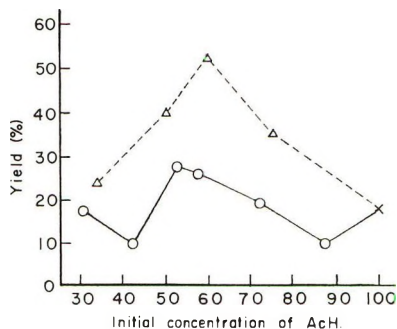


Fig. 8. Effects of solvent on yield at varying concentrations of AcH: (O) toluene; (Δ) n-hexane. 1.0% Li-Hg; 0°C.; 20 hr.

data, it may be assumed that optimum concentrations of each solvent exist for this polymerization system, and that the yields and molecular weights of polymers are larger than those in bulk polymerization.

### 6. Effects of Two-Stage Polymerization

Results of a two-stage polymerization are given in the Table III and Figures 10 and 11. The two-stage polymerization means that the reac-

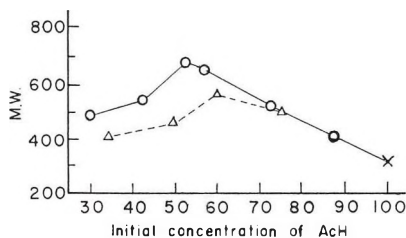


Fig. 9. Effects of solvent on M.W. at varying concentrations of AcH: (O) toluene; ( $\Delta$ ) *n*-hexane. 1.0% Li-Hg; 0°C.; 20 hr.

tion products obtained in the polymerization are further heated to 60–70°C. for about 1 hr. without removal of the catalyst ion. The product of the two-stage polymerization is indeed the same as that obtained in the one-stage polymerization. Figures 10 and 11 show that this two-stage polymerization results in larger yields and higher molecular weight products than the one-stage polymerization.

TABLE II  
Solution Polymerization of Acetaldehyde with Sodium or Lithium Amalgam  
(Time, 20 hr.; Temp., 0°C.)

No.	Solvent		Catalyst		Yield, %	M.W.	
	AcH, g.	Kind	Amount, g.	Kind			
77	79	Petroleum ether	186	3.0% Na-Hg	2.4	5.1	226
78	158	"	124	"	4.6	6.3	271
79	"	"	93	"	"	8.9	304
80	205	"	"	"	6.2	10.7	348
81	236	"	62	"	7.0	10.2	302
82	"	"	31	"	"	6.8	278
83	79	Diethyl ether	180	"	2.5	28.8	387
84	118	"	144	"	3.8	19.4	341
85	158	"	108	"	5.0	7.6	338
86	197	"	72	"	6.3	"	295
87	237	"	36	"	7.5	5.5	292
88	63	"	216	"	1.9	10.5	336
89	193	Toluene	170	5.6% Li-Hg	2.0	27.6	676
90	158	"	218	"	1.6	9.9	540
91	118	"	262	"	1.2	17.8	487
92	237	"	87	"	2.4	19.1	530
93	292	"	44	"	3.0	10.0	408
94	213	"	157	"	2.2	26.0	662
95	193	<i>n</i> -Hexane	66	"	2.0	34.5	512
96	"	"	132	"	"	54.6	572
97	158	"	162	"	1.6	40.1	463
98	118	"	231	"	1.2	23.7	408
99	556	"	"	"	5.0	18.0	302

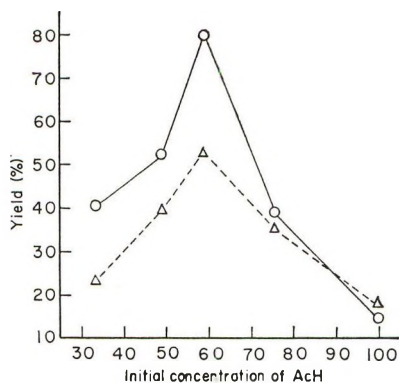


Fig. 10. Effects of two-stage polymerization on yield at varying concentrations of AcH. *n*-Hexane; 1.0% Li-Hg; 0°C., 20 hr.; (—○—) two-stage polymerization; (—△—) one-stage polymerization.

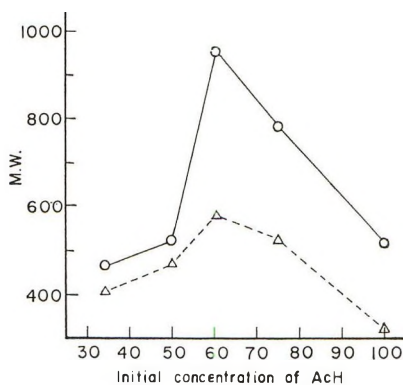


Fig. 11. Effects of the two-stage polymerization on M.W. at varying concentrations of AcH. *n*-Hexane; 1.0% Li-Hg; 0°C.; 20 hr.; (—○—) two-stage polymerization; (—△—) one-stage polymerization.

TABLE III  
Effects of Two-Stage Polymerization in *n*-Hexane  
(Time, 20 hr.; Temp., 0°C.)

No.	Type <sup>a</sup>	AcH, g.	<i>n</i> -Hexane, g.	5.5% Li-Hg, g.	Yield, %	M.W.
95	A	193	66	2.0	34.5	512
	B	193	66	2.0	39.4	789
96	A	193	132	2.0	54.6	572
	B	193	132	2.0	81.1	960
97	A	158	162	1.6	40.1	463
	B	158	162	1.6	52.5	567
98	A	118	231	1.2	23.7	408
	B	118	231	1.2	41.0	452
99	A	556		5.0	18.0	302
	B	556		5.0	15.0	517

<sup>a</sup> A = one-stage polymerization; B = two-stage polymerization.



### References

1. Imoto, T., and T. Matsubara, *J. Polymer Sci.*, **56**, S4 (1962).
2. Degering, E. E., and T. Stoudt, *J. Polymer Sci.*, **7**, 653 (1951).
3. Leipunskii and Reinov, *Compt. Rend. Acad. Sci., URSS*, **30**, 624 (1948).
4. Imoto, T., T. Oota, and J. Kambara, *Nippon Kagaku Zasshi*, **82**, 492 (1961).
5. Imoto, T., T. Oota, and T. Matsubara, *Nippon Kagaku Zasshi*, **82**, 378 (1961).
6. Ooiwa, M., To. Matsubara, and T. Imoto, *Nippon Kagaku Zasshi*, **84**, 887 (1963).
7. Bell, R. P., and P. T. McTigue, *J. Chem. Soc.*, **1950**, 2983.

### Résumé

Dans un article précédent, on a rapporté qu'un polymère de l'acétaldéhyde du type alcool polyvinylique avait été obtenu par polymérisation de l'acétaldéhyde en utilisant l'amalgame de sodium comme catalyseur. Actuellement on a trouvé que la concentration en catalyseur, le temps de réaction, la température de réaction et la concentration en solvant exercent un certain effet sur le poids moléculaire et le rendement en polymère. Au début de cette polymérisation, le rendement est proportionnel à la racine carrée du temps de réaction. Ainsi à partir de ce degré d'avancement, la réaction peut être contrôlée par diffusion. Plusieurs solvants, de même la polymérisation en deux étapes, accélèrent cette polymérisation.

### Zusammenfassung

In einer früheren Arbeit wurde über die Herstellung von Acetaldehydpolymerem vom Polyvinylalkoholtyp durch die Polymerisation von Acetaldehyd unter Verwendung von Natriumamalgam als Katalysator berichtet. Nun wurden folgende Aspekte gefunden. Die Katalysatorkonzentration, die Aufenthaltsdauer, die Reaktionstemperatur und die Lösungsmittelkonzentration haben auf das Molekulargewicht und die Polymerausbeute einen gewissen Einfluss. Im frühen Stadium dieser Polymerisation ist die Ausbeute der Quadratwurzel aus der Reaktionszeit proportional. Daher kann in diesem Stadium angenommen werden, dass die Reaktion diffusionskontrolliert ist. Einige Lösungsmittel sowie die Zweistufenpolymerisation haben auf diese Polymerisation einen günstigen Einfluss.

Received October 28, 1963

Revised January 24, 1964

## A Study of the Statistical Character of Anionic Polymers\*

V. S. NANDA,† *Institute of Theoretical Science, University of Oregon,  
Eugene, Oregon*, and R. K. JAIN, *Physics Department, University of Delhi,  
Delhi, India*

### Synopsis

The effect of initiation and propagation rate constant ratio on the statistical character of termination-free anionic polymers is discussed. For obtaining the expressions for the size distribution and the averages, we have followed a mathematical procedure which might prove useful in the treatment of more complicated problems. The conditions under which the ultimate polymer has an appreciable or negligible inhomogeneity are clearly stated.

The effect of initiation and propagation rate constant ratio on anionic polymers, in the absence of any termination reaction, was discussed theoretically by Gold.<sup>1</sup> Later Glusker et al.,<sup>2</sup> in an essentially experimental paper, quoted some relevant theoretical results. The purpose of the present communication is to bring out clearly some interesting characteristics of the polymer and determine a suitable criterion for the ultimate inhomogeneity. However, we have considered it worthwhile to rederive expressions for the size distribution and the averages by procedures which not only seem mathematically elegant but also could prove useful in the solution of more complicated problems.

The customary notation in setting up the kinetic scheme is followed here. The initiator species  $I$  undergoes first order reaction with the monomer  $M$  according to the rate constant  $k_i$ , to give rise to an active center with a degree of polymerization one. This in turn can propagate indefinitely according to the rate constant  $k_p$ . The following kinetic scheme, which is the same as in Gold's paper, can then be put down.

$$dM/dt = -k_iMI - k_pM \sum_x N_x \quad (1)$$

\* Work supported in part by the National Science Foundation (G19518) and the Division of General Medical Sciences, Public Health Service (GM09153-02).

† Present address: Chemistry Department, University of Southern California, Los Angeles, California.

$$\left. \begin{aligned} dI/dt &= -k_iMI \\ dN_1/dt &= k_iMI - k_pMN_1 \\ dN_2/dt &= k_pMN_1 - k_pMN_2 \\ \dots\dots\dots \\ dN_x/dt &= k_pMN_{x-1} - k_pMN_x \\ \dots\dots\dots \end{aligned} \right\} \quad (2)$$

where  $N_1, N_2, \dots, N_x, \dots$  denote the concentration of the active species of degree of polymerization 1, 2,  $\dots, x, \dots$ , respectively. These equations are subject to the initial conditions

$$\begin{aligned} M(0) &= M_0 \\ I(0) &= I_0 \\ N_x(0) &= 0 \end{aligned} \quad (3)$$

and the constraints

$$\left. \begin{aligned} \sum N_x &= I_0 - I \\ \sum_x xN_x &= M_0 - M \end{aligned} \right\} \quad (4)$$

Introducing the modified time  $\tau$ , which is related to the actual time  $t$  by the relation

$$t = \int_0^\tau d\tau/k_iM(\tau) \quad (5)$$

eq. (1) and the set of eqs. (2) can be linearized.<sup>3</sup> For the monomer and the initiator, we find easily on integration

$$M = M_0 - I_0(1 - r)(1 - e^{-\alpha\tau}) - I_0\tau \quad (6)$$

and

$$I = I_0e^{-\alpha\tau} \quad (7)$$

where  $r = k_p/k_i$  and  $\alpha r = 1$ . The set of eqs. (2), after linearization can be put in the convenient matrix form

$$d(\nu)/d\tau = [\mu](\nu) \quad (8)$$

Here  $(\nu)$  is a column vector with elements  $I, N_1, N_2, \dots, N_x, \dots$ , and  $[\mu]$  is a square matrix of the form

$$[\mu] = \begin{bmatrix} -\alpha & 0 & 0 & 0 & \dots \\ \alpha & -1 & 0 & 0 & \dots \\ 0 & 1 & -1 & 0 & \dots \\ 0 & 0 & 1 & -1 & \dots \\ \dots\dots\dots \end{bmatrix} \quad (9)$$

Following the steps given in the Appendix, one gets as a solution of eq. (8), eq. (7) for the initiator concentration and

$$N_x = I_0\alpha e^{-\tau} q^x \sum_{k=x}^\infty \frac{u^k}{k!} \quad x \geq 1 \quad (10)$$

for the  $x$ -mer concentration, where  $u = \tau/q$ , and  $q = (1 - \alpha)^{-1}$ . It may be mentioned that the foregoing expression for  $N_x$  is valid for all  $\alpha$ , whereas Gold in his analysis had to consider the cases  $\alpha = 0$ ,  $\alpha = 1$  and  $\alpha > 1$  separately. It can be easily verified that all his results follow as special cases from eq. (10).

We now give a rigorous procedure for obtaining various averages of interest. The  $s$ th moment of the distribution is defined by the relation

$$Q_s = \frac{\sum_{x=1}^{\infty} x^s N_x}{\sum_{x=1}^{\infty} N_x} \quad s = 0, 1, 2, \dots \quad (11)$$

whence the averages can be written, e.g., the  $s$ th average is

$$\bar{i}_s = Q_s / Q_{s-1} \quad (12)$$

For finding an expression for  $Q_s$ , we first consider the double summation in the expression

$$\sum_{x=1}^{\infty} N_x = \alpha I_0 e^{-\tau} \sum_{x=1}^{\infty} q^x \sum_{k=x}^{\infty} u^k / k! \quad (13)$$

The procedure followed by Gold<sup>1</sup> for evaluating this sum is valid only for  $q < 1$ , as otherwise the series (C2) in his paper would be divergent.\* In the present treatment we change the order of summation in eq. (13) and, taking care of the limits, obtain

$$\begin{aligned} \sum_{x=1}^{\infty} N_x &= \alpha I_0 e^{-\tau} \sum_{k=1}^{\infty} \frac{u^k}{k!} \sum_{x=1}^k q^x \\ &= \alpha I_0 e^{-\tau} \sum_{k=1}^{\infty} \frac{u^k}{k!} \left( \frac{q - q^{k+1}}{1 - q} \right) \end{aligned}$$

It should be noted that the summation over  $x$ , carried out here, is finite and hence applicable for all  $q$ . The infinite summation over  $k$  can now be carried out safely as the series to be summed has an infinite radius of convergence. We obtain

$$\sum_{x=1}^{\infty} N_x = \alpha I_0 e^{-\tau} \left( \frac{q}{1 - q} \right) (e^u - e^{qu}) \quad (13a)$$

From the form of eq. (10) for  $N_x$ , it is easily seen that the expressions for the higher moments can be built up from eq. (13a) by the successive use of the operator  $q\partial/\partial q$ .

Having deduced the moments, the following expressions for the number-average chain length  $\bar{i}_n$  ( $\equiv i_1$ ) and the weight-average chain length  $\bar{i}_w$  ( $\equiv i_2$ ) can be written by the help of eq. (12) as

$$\bar{i}_n = [\alpha\tau - 1 + \alpha + e^{-\alpha\tau}(1 - \alpha)] / [\alpha(1 - e^{-\alpha\tau})] \quad (14)$$

$$\bar{i}_w = \frac{\alpha^2\tau^2 - 2\alpha\tau + 2 + 3\alpha^2\tau - 3\alpha + \alpha^2 - e^{-\alpha\tau}(2 - 3\alpha + \alpha^2)}{\alpha[\alpha\tau - 1 + \alpha + e^{-\alpha\tau}(1 - \alpha)]} \quad (15)$$

\* Fortunately, the results obtained by him with the invalid procedure are nevertheless correct as will be seen in the sequel.

These results should be compared with the corresponding ones obtained by an idealized statistical treatment<sup>4</sup> which has been shown to be a good approximation for the case of long chains.

We now take up the consideration of the statistical characteristics of the polymer. For the stage of the reaction characterized by  $\alpha\tau \ll 1$  one obtains from eqs. (14) and (15) the series expansions

$$i_n = (\tau/2) \frac{\left[ \left( 1 + \frac{2}{\tau} \right) - \frac{\alpha\tau}{3} + \dots \right]}{\left[ 1 - \frac{\alpha\tau}{2} + \dots \right]} \quad (14a)$$

$$i_w = (2\tau/3) \frac{\left[ \left( 1 + \frac{9}{2\tau} + \frac{3}{\tau^2} \right) - \frac{\alpha\tau}{4} + \dots \right]}{\left[ \left( 1 + \frac{2}{\tau} \right) - \frac{\alpha\tau}{3} + \dots \right]} \quad (15a)$$

in which the succeeding terms involve square and higher powers of  $(\alpha\tau)$  only. If simultaneously  $\tau \gg 1$ , these results show\* that the inhomogeneity

$$\zeta = [(i_w/i_n) - 1] \rightarrow (1/3) \quad \begin{array}{l} \alpha\tau \ll 1 \\ i_n \gg 1 \end{array} \quad (16)$$

Next we consider the stage of the reaction when both  $\tau$  and  $\alpha\tau \gg 1$ . It is seen from eqs. (14) and (15) that now  $i_n$  and  $i_w$  have nearly the same value. Thus

$$\zeta \rightarrow 1 \quad \alpha\tau \gg 1 \quad (17)$$

and the polymer formed must be highly homogeneous.

One might ask for the highest value of the inhomogeneity that could be observed during the course of the reaction. It is easily verified that for a given  $\tau$  the ratio  $i_w/i_n$  and hence  $\zeta$ , has the highest value for  $\alpha \rightarrow 0$ . Dropping terms involving  $\alpha\tau$ , one may determine from eqs. (13a) and (14a) that  $\zeta_{\max} = 0.375$  for  $\tau = 6$ , which according to eq. (14a) corresponds to  $i_n = 4$ .

The foregoing considerations are likely to give the impression that inhomogeneity is appreciable only for the earlier stages and disappears at the completion of the reaction when the monomer is ultimately consumed.† On the other hand, the results quoted by Glusker et al. indicate that for  $\alpha \ll 1$ ,  $(i_w/i_n) \rightarrow 4/3$  (which implies  $\zeta \rightarrow 1/3$ ) at the end of the reaction. Actually both the conclusions are special cases of a general result as will be seen in the sequel.

\* Gold<sup>1</sup> has given in his paper extensive tables and figures to show the variation of  $i_w/i_n$  with  $u$  ( $= \tau/q$ ). It may be pointed out here that his calculations in Table I for  $r = 10^6$  and the corresponding plot in Fig. 3, which suggest that  $\zeta$  is zero for  $u < 10^4$ , are obviously incorrect as will be seen from eq. (16) of our paper.

† In fact, Gold in the concluding remarks on p. 97 of his paper<sup>1</sup> has actually drawn such a conclusion.

For the following discussion, the relation between the actual time  $t$  and the modified time  $\tau$  is crucial. For any given value of  $\alpha$ , one can determine  $\tau_m$ , the value of  $\tau$  at the end of the reaction ( $t = \infty$ ), from eq. (6) for different  $M_0/I_0$  ratios. It can be verified that values of  $\tau_m$  satisfying both the conditions  $\alpha\tau_m \ll 1$  and  $\alpha\tau_m \gg 1$  are obtainable. As an example of  $\alpha\tau_m \ll 1$ , for  $\alpha = 10^{-4}$ ,  $(M_0/I_0) = 48.48$ , we get  $\tau_m = 10^3$ . On the other hand, with  $\alpha = 10^{-2}$ ,  $(M_0/I_0) = 911.1$ , we get  $\tau_m = 10^3$  which corresponds to the case  $\alpha\tau_m \gg 1$ . In view of the foregoing remarks, it follows from eqs. (16) and (17) that the ultimate polymer can have the inhomogeneity characteristic of a rectangular distribution on the one extreme or can be highly homogeneous on the other. Quantitative conditions in this connection will now be put down. From eq. (7) we have

$$\tau_m \approx (2M_0/I_0\alpha)^{1/2} - 1 \quad \alpha\tau_m \ll 1 \quad (18a)$$

and

$$\tau_m \approx (M_0/I_0) + (1 - \alpha)/\alpha \quad \alpha\tau_m \gg 1 \quad (18b)$$

These results, in association with eqs. (16) and (17), give for long chains the conditions

$$\zeta \rightarrow (1/3) \quad \text{when } (2M_0\alpha/I_0)^{1/2} \ll 1 \quad (19a)$$

and

$$\zeta \rightarrow 0 \quad \text{when } (\alpha M_0/I_0) \gg 1 \quad (19b)$$

for the cases of Glusker et al. and Gold, respectively.

A detailed picture of the statistical character of the polymer for a very wide range of conditions can be obtained from Figs. 1 and 2. The values of  $\zeta$  can be read from these diagrams as a function of conversion  $(M_0 - M)$  for  $r = 10^6, 10^4, 10^2, 10, 1$ , and 0. The same set of curves also gives the value of  $\zeta$  at the end of the reaction as a function of the initial monomer concentration  $M_0$  [cf. eq. (6)].

Considering first the variation of  $\zeta$  with  $M_0 - M$ , it is noted that so long as  $r$  is not large as compared to unity the inhomogeneity is appreciable only over a small range of conversion. In all cases it rises rather fast when the reaction has advanced to the stage that  $r(M_0 - M)/I_0$  is of the order of unity. For higher conversions it quickly reaches its maximum value, which lies below 0.375. The location of the position of the maximum could be of some practical importance. For  $\alpha$  very small so that  $\alpha\tau \ll 1$ , we can write using eq. (7)

$$i_n = (M_0 - M)/(I_0 - I) \simeq (M_0 - M)/I_0\alpha\tau \quad (20)$$

Since the maximum value of  $\zeta$ , as indicated earlier, occurs for  $\tau = 6$ ,  $i_n = 4$ , the maximum in the  $\zeta$  versus conversion plot corresponds to  $[(M_0 - M)/I_0] = 24\alpha$ . The values of  $\alpha$  should thus be obtainable from the foregoing study in an actual experiment.

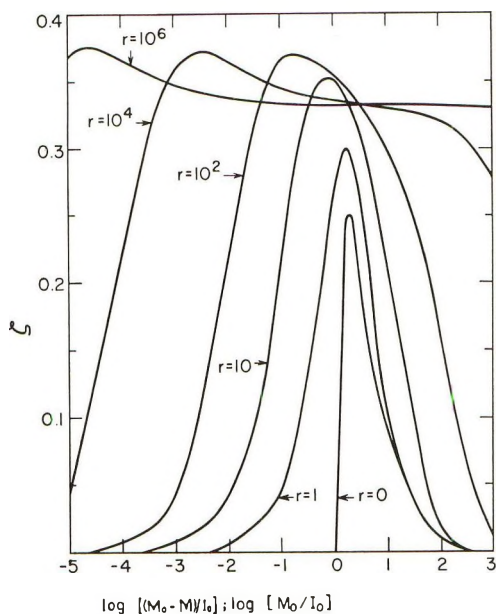


Fig. 1. The variation of  $\zeta$  with conversion ( $M_0 - M$ ). The variation of the ultimate value of  $\zeta$  with the starting monomer concentration  $M_0$  represented by the same set of curves.

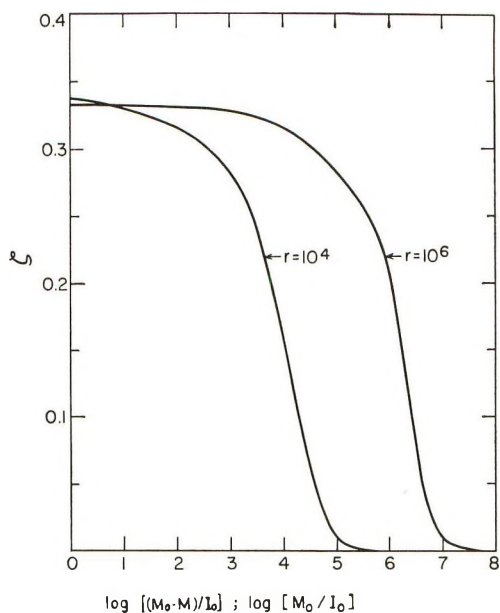


Fig. 2. The variation of  $\zeta$  with conversion ( $M_0 - M$ ). The variation of the ultimate value of  $\zeta$  with the starting monomer concentration  $M_0$  represented by the same set of curves.

Considering now the variation of the ultimate value of  $\zeta$  with the initial monomer concentration, it may be noted from Figure 1 that when  $r$  is not large as compared to unity, the inhomogeneity is negligible for  $(M_0/I_0) > 10^2$  which also implies here  $i_n > 10^2$  [cf. eq. (14)]. When, however,  $r \gg 1$ ,  $\zeta$  has the value  $1/3$ , over the practical range of interest  $\log(M_0/I_0) > 0$ , so long as the condition  $\alpha M_0/I_0 \ll 1$  is satisfied. The transition to the homogeneous state occurs for values of  $M_0/I_0$  in the neighborhood of  $1/\alpha$ . The decrease in  $\zeta$  is slower at first but becomes rapid as  $\zeta$  approaches the value  $1/\alpha$  from below. When  $M_0/I_0 > (10/\alpha)$ , the inhomogeneity becomes negligible. This result applies for long chains irrespective of the value of  $\alpha$ .

### APPENDIX

Here we give the intermediate steps for obtaining the expression (10) for the size distribution quoted in the text. Since the elements of the matrix  $[\mu]$  are all constant, the solution of equation (8) can be written as\*

$$(\nu) = e^{[\mu]\tau} (\nu)_0 \quad (\text{A1})$$

Here  $(\nu)_0$  is the row vector  $(\nu)$  at  $\tau = 0$  and

$$e^{[\mu]\tau} = [U] + [\mu]\tau + [\mu]^2 (\tau^2/2!) + \dots \quad (\text{A2})$$

where  $[U]$  is the unit matrix. We define a matrix  $[\mu']$  by the relation

$$[\mu'] = [\mu] + [U] \quad (\text{A3})$$

where

$$[\mu'] = \begin{bmatrix} q^{-1} & 0 & 0 & 0 & \dots \\ \alpha & 0 & 0 & 0 & \dots \\ 0 & 1 & 0 & 0 & \dots \\ 0 & 0 & 1 & 0 & \dots \\ \dots & \dots & \dots & \dots & \dots \end{bmatrix}$$

Noting that

$$e^{-[U]\tau} (\nu)_0 = e^{-\tau} (\nu)_0$$

eq. (A1) for  $(\nu)$  could be written in the alternative form

$$(\nu)e^\tau = e^{[\mu']\tau} (\nu)_0 \quad (\text{A4})$$

For obtaining the expressions for the various elements of  $(\nu)$  one requires the evaluation of  $[\mu']^x$  for a general  $x$ . The following form is readily established by induction.

\* See, for instance, Pipes.<sup>5</sup> It may be indicated that we have also been able to treat successfully some difficult problems in polymer kinetics for which the elements of the matrix  $[\mu]$  are not time-independent. Details will be reported in a subsequent publication.



$$[\mu']^x = \begin{bmatrix} q^{-x} & 0 & 0 & 0 & \dots \\ \alpha q^{-x+1} & 0 & 0 & 0 & \dots \\ \dots & \dots & \dots & \dots & \dots \\ \alpha q^0 & 0 & 0 & 0 & \dots \\ 0 & 1 & 0 & 0 & \dots \\ 0 & 0 & 1 & 0 & \dots \\ \dots & \dots & \dots & \dots & \dots \end{bmatrix} \quad (\text{A5})$$

By using eqs. (A4) and (A5) one gets after some simple algebra both relations (6) and (10) of the text.

One of us (V. S. N.) is thankful to Prof. Fixman for his interest and to Prof. Simha for making some valuable comments. The second author (R. K. J.) was in receipt of a fellowship from the Directorate of Scientific and Industrial Research (India) during the course of this work.

### References

1. Gold, L., *J. Chem. Phys.*, **28**, 91 (1958).
2. Glusker, D. L., I. Lysloff, and E. Stiles, *J. Polymer Sci.*, **49**, 315 (1961).
3. Ginell, R., and R. Simha, *J. Am. Chem. Soc.*, **65**, 706 (1943).
4. Nanda, V. S., and R. K. Jain, *J. Chem. Phys.*, **39**, 1363 (1963).
5. Pipes, L. A., *Applied Mathematics for Engineers and Physicists*, McGraw-Hill, New York, 1958, p. 101.

### Résumé

On discute de l'effet du rapport des constantes de vitesses a'initiation et de propagation sur le caractère statistique des polymères anioniques sans terminaison. Pour obtenir les expansions de la distribution du degré de polymérisation et les moyennes, on a suivi une procédé mathématique, qui peut être employé également pour des problèmes plus compliqués. On a exposé clairement les conditions dans lesquelles le dernier polymère a une inhomogénéité appréciable ou négligeable.

### Zusammenfassung

Der Einfluss des Verhältnisses der Start- und Wachstumsgeschwindigkeitskonstanten auf den statistischen Charakter des Abbruchs freier anionischer Polymerer wird diskutiert. Um die Ausdrücke für die Grössenverteilung und die Mittelwerte zu erhalten, wurde eine mathematische Methode angewendet, die zur Behandlung schwieriger Probleme nützlich sein könnte. Die Bedingungen, unter denen das Endpolymere nennenswerte oder vernachlässigbare Inhomogenität besitzt, werden eindeutig festgestellt.

Received January 3, 1964

## Polymerization of Higher Aldehydes. III. Elastomeric Polyacetaldehyde\*†

O. VOGL, *Plastics Department, E. I. du Pont de Nemours and Company, Inc., Wilmington, Delaware*

### Synopsis

Amorphous elastomeric polyacetaldehyde was prepared in bulk and in solution using cationic initiators. This polymer is the same as Letort's polyacetaldehyde. The acetaldehyde polymerization must be conducted at  $-40^{\circ}\text{C}$ . or lower in order to overcome the competitive trimerization or tetramerization. The reactivity of a number of initiators can be modified by using different solvents. The influence of temperature and type of initiator and solvent on the polymerization was studied.

### INTRODUCTION

The commercialization of formaldehyde<sup>2,3</sup> high polymers has significantly stimulated the exploration of the relatively neglected field of aldehyde polymers.

The first investigators<sup>4,5</sup> prepared polyacetaldehyde by a technique sometimes called "crystallization polymerization" which reportedly required as its essential feature the crystallization of the monomer without additional initiator. Polyacetaldehyde obtained by this method is a non-crystalline elastomer quite different from the high melting and highly crystalline polyformaldehyde. Subsequent studies<sup>6-8</sup> more than a decade later revealed that acetaldehyde crystallization polymerization must be carried out under very accurately controlled conditions. Ultraviolet irradiation of the monomer in the presence of small amounts of oxygen appeared to have a beneficial effect.<sup>9,10</sup>

### EXPERIMENTAL

#### Materials

##### *Preparation of Pure Acetaldehyde*

Acetaldehyde, obtained from Eastman in a sealed vial, was distilled twice in a low temperature still from an antioxidant (0.1% of AgeRite

\* Part of this paper was presented at the Gordon Conference on Polymers, New London, N. H., July 1962.

† This is the third paper on polymerization of higher aldehydes. For parts I and II, see ref. 1.

White,  $\beta,\beta'$ -dinaphthylphenylenediamine) in a nitrogen atmosphere. The receiver was kept at  $-78^{\circ}\text{C}$ . and the purified sample was used immediately. Acetaldehyde was transferred with a flamed-out hypodermic syringe.

The distillation apparatus was rinsed with soap solution or dilute NaOH solution after each distillation to eliminate acid build-up in the distillation column. Acidic cleaning solutions, particularly for the Dry Ice condenser, should be avoided. Acidity on the glass surface causes rapid polymer formation and plug up in the condenser.

#### *Determination of Impurities*

The impurities found to be present in acetaldehyde samples were primarily acid and water, and in addition small amounts of other impurities.

**Acid.** Acid was determined by titration of 10 ml. or 20 ml. samples in oxygen-free ice water with 0.02*N* NaOH solution (Bromothymol Blue as indicator). Acid content was, in most cases, 20–30 ppm. The acid content was determined routinely in every sample purified for polymerization.

**Water.** Water was estimated by gas chromatography, because Karl Fischer titration for traces of water (less than 0.1%) does not operate with aldehydes.<sup>11</sup>

**Other Impurities.** Small amounts of ethanol and paraldehyde, and probably, ethyl acetate were present also in the original acetaldehyde as determined by gas chromatography. Double distillation reduced these impurities and water to an undetectable level.

#### *Solvents*

The ethylene and propylene used as solvents were polymerization grade. Tetrahydrofuran was purified as usual, distilled from lithium aluminum hydride and stored over sodium. All other solvents were of the best grade available and were taken from freshly opened bottles without further purification.

### **Polymerization**

Two kinds of apparatus were found suitable for polymerizations.

**A.** For the more qualitative studies of initiators and solvents a test tube-like apparatus equipped with stirrer, thermometer, nitrogen supply and exit, closed by a bubbler (filled with mineral oil) was used.

The polymerization was carried out as follows. The tube was flamed out and cooled in a dry box under nitrogen; initiator and solvent were added. The apparatus was closed and cooled in a Dewar flask while nitrogen was being passed through the solution. Cold acetaldehyde ( $-78^{\circ}\text{C}$ .) was then added with a hypodermic syringe while stirring, and the solution stirred until well mixed.

After completion of the reaction, the initiator was deactivated by adding a small amount of pyridine or tripropylamine, and the viscous solution was evaporated under reduced pressure.

B. For preparative runs, a three-necked flask with two additional openings for a thermometer and serum stopper was used.

In a typical polymerization, ethylene (300 ml.) was condensed with a 1-liter round-bottomed flask equipped with a paddle-type stirrer, nitrogen supply and exit, and thermometer. Acetaldehyde (55 ml.) was then injected with a hypodermic syringe and the stirrer started. The reaction mixture was then brought to the desired temperature and the initiator added. After an induction period of 15–20 min., the polymerization proceeded rapidly and the reaction mixture became very viscous. The mixture was allowed to stand for 2 hr. Pyridine (100 ml.) was then added to deactivate the initiator and dissolve the polymer. The temperature during this addition of pyridine was kept below the boiling point of ethylene ( $-104^{\circ}\text{C}.$ ) in order to avoid excessive boiling. At this temperature pyridine solidifies immediately, and the reaction was left overnight at  $-78^{\circ}\text{C}.$  in order to permit the ethylene to evaporate slowly. On agitation at room temperature, the polymer dissolved completely in the residual pyridine.

If desired, the polymer could be isolated at this stage by pouring the pyridine solution into water.

For the end capping a solution of 20 ml. of pyridine and 200 ml. of acetic anhydride was added to the pyridine solution of polymer, and the mixture was shaken under nitrogen for 1–2 hr. The viscous solution was poured into an excess of ice and water, thereby precipitating the polymer. The polymer was then kneaded by hand in several changes of water in order to destroy the acetic anhydride completely. (Rubber gloves should be worn during this operation.)

Further removal of impurities was effected by dissolving the polymer in ether and extracting the solution several times with distilled water. The solution was then dried and filtered, and the ether evaporated under reduced pressure at room temperature. Removal of the last traces of solvent required good vacuum.

## Characterization of the Polymer

### *Viscosity Measurements*

Viscosity measurements of polyacetaldehyde were carried out in an Ostwald viscometer at  $25^{\circ}\text{C}.$  in 0.5% butanone solutions. The viscosity-molecular weight relationship<sup>12,45</sup> was used to calculate the molecular weight.

### *Infrared Spectra*

Infrared spectra were taken on solutions of the polymer in  $\text{CCl}_4$  or on compression-molded samples of approximately 0.2 mm. thickness (Fig. 1). The film showed very strong absorption between 8.3 and  $9.7\ \mu$  and between 10.2 and  $11\ \mu$ , as well as a considerable amount of overtone absorption between 2 and  $6.5\ \mu$ . There was only a trace of a carbonyl band at  $5.73\ \mu$  (acetate ends). The solution spectrum showed a sharp doublet band at

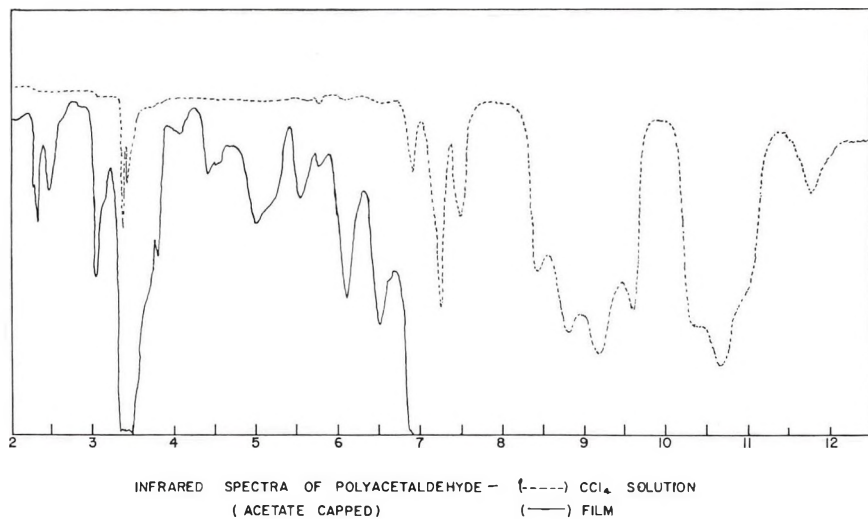


Fig. 1. Infrared spectra of polyacetaldehyde (acetate capped): (---) CCl<sub>4</sub> solution; (—) film.

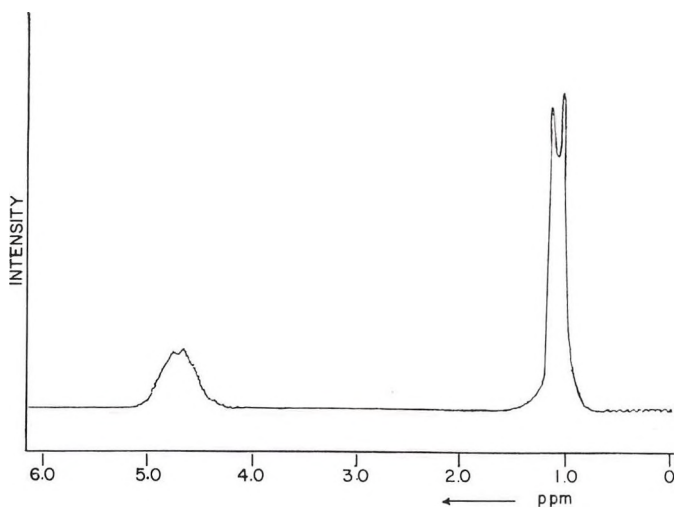


Fig. 2. Elastomeric polyacetaldehyde (10% CCl<sub>4</sub> solution), Varian A-60.

3.37 and 3.43  $\mu$ , as well as C-H frequencies at 6.91, 7.24, and 7.48  $\mu$ . A strong band of four absorption peaks was present at 8.42, 8.80, 9.20, and 9.60  $\mu$ , and another strong band with two shoulders was centered at 10.65  $\mu$ . One further band occurred at 11.80  $\mu$ .

Hydroxyl absorption was missing completely, and a very minute absorption of the acetate endgroups was noticeable. This is consistent with a high molecular weight polymer.

These results are in good agreement with the structure of polyacetaldehyde as a polyacetal.<sup>13-15</sup>

### Nuclear Magnetic Resonance Spectrum

The nuclear magnetic resonance spectrum has been determined on 4% solutions (in  $\text{CCl}_4$ ) of both low and very high molecular weight polyacetaldehyde (Fig. 2). The methyl groups produced a band that was split into a doublet.

### X-Ray Analysis

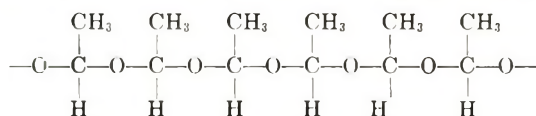
The x-ray pattern showed a typical amorphous spacing of approximately 3.9 and 7.2 Å,<sup>1a</sup> which is identical with the results of Letort's polymer.<sup>6</sup>

## RESULTS

In this paper the word "polymerization" (of aldehydes) denotes the addition polymerization across the carbon-oxygen double bond to give linear polyacetals of reasonable *molecular weight*. The formation of the cyclic trimer (paraldehyde) and the cyclic tetramer (metaldehyde) are designated trimerization and tetramerization, respectively. We also suggest that formation of polymeric products from acetaldehyde and other aldehydes by aldol condensation should be called polyaldol condensation.

### Cationic Solution Polymerization of Acetaldehyde

Polymerization of acetaldehyde to give linear polymer (I)



requires low temperatures. At room temperature a competitive reaction—the trimerization of acetaldehyde to paraldehyde—supervenes. Paraldehyde is the sole product of the acid-catalyzed acetaldehyde "polymerization" at temperatures down to  $-10^\circ\text{C}$ ., while from  $-10$  to about  $-30^\circ\text{C}$ . some of the tetrameric metaldehyde is also formed.

The following conditions were considered necessary for the formation of the linear polymer: The rate of propagation at the third and fourth propagation step of the acetaldehyde polymerization should be greater than the rate of ring closure to form the six- or eight-membered ring. Once the fifth monomer unit is added, chain propagation would be strongly favored over medium-sized or larger ring formation.

The formation of linear high acetaldehyde polymer instead of the cyclic trimer was achieved by the proper combination of the following variables: (1) temperature; (2) initiator; and (3) solvents.

In general, the formation of linear polyacetaldehyde is favored by the use of low temperatures, less active initiators and poorer solvents. The relationship between these factors is quite intricate, however, and the influence of each will be discussed below.

*Temperature*

Polymerization has been observed at as low as  $-150^{\circ}\text{C}.$ ; above  $-40^{\circ}\text{C}.$  we have not been able to obtain high molecular weight polyacetaldehyde. All polymerization initiators that are active initiators in this temperature range cause trimer formation above  $-40^{\circ}\text{C}.$  However, some initiators form paraldehyde even at temperatures lower than  $-40^{\circ}\text{C}.$

*Initiators*

**Nature of the Initiator.** We have divided the initiators for the acetaldehyde polymerization into three groups: (1) very active initiators (paraldehyde formation); (2) moderately active initiators (polymer formation); and (3) inactive compounds.

1. *Very Active Initiators.* These initiators do not favor polymer formation at an initial temperature of  $-78^{\circ}\text{C}.$  (Table I); instead, a very exothermic reaction occurs and paraldehyde (with some metaldehyde) is

TABLE I  
Very Active Initiators  
(Initial Reaction Temperature  $-65^{\circ}\text{C}.$ , Reaction Time 5 Hr.)  
Paraldehyde Formation

Initiator		Initiator concentration, wt.-% based on monomer	Monomer: solvent ratio	Remarks <sup>a</sup>
H <sub>2</sub> SO <sub>4</sub>	Diethyl ether	0.1	2:1	⊕ ( $-20^{\circ}\text{C}.$ ) <sup>b</sup>
Phosphomolybdic acid	Diethyl ether	0.1	2:1	⊕ ( $-15^{\circ}\text{C}.$ ) <sup>b</sup>
Phosphotungstic acid	Diethyl ether	0.1	2:1	⊕
P <sub>2</sub> O <sub>5</sub>	Diethyl ether	0.05	2:1	⊕
Al sulfate	Diethyl ether	0.15	2:1	⊕
BF <sub>3</sub> etherate	Diethyl ether	0.1, 0.02	2:1	⊕ ( $-10^{\circ}\text{C}.$ ) <sup>b</sup>
FeCl <sub>3</sub>	Diethyl ether	0.2, 0.05	10:1, 2:1	⊕ (boiled over) <sup>b</sup>
	Pentane (1% THF)	0.2	1:1	⊕ ( $+15^{\circ}\text{C}.$ ) <sup>b</sup>
	CH <sub>2</sub> Cl <sub>2</sub>	0.2	1:1	⊕ ( $+10^{\circ}\text{C}.$ ) <sup>b</sup>
	Diethylpentane	0.2, 0.05	1:1	⊕ ( $+20^{\circ}\text{C}.$ ) <sup>b</sup>
SnCl <sub>4</sub>	Diethyl ether	0.1, 0.02	2:1	⊕
TiCl <sub>4</sub>	Diethyl ether	0.1, 0.02	2:1	⊕
TiF <sub>4</sub>	Diethylpentane	0.05	2:1	⊕
ZrCl <sub>4</sub>	Diethyl ether	0.05	2:1	⊕
PCl <sub>3</sub>	Diethyl ether	0.5	2:1	⊕
SbCl <sub>3</sub>	Diethyl ether	0.5	2:1	⊕
TiCl <sub>3</sub>	CH <sub>2</sub> Cl <sub>2</sub> <sup>c</sup>	1	1:8	⊕ (10%)
VCl <sub>3</sub>	CH <sub>2</sub> Cl <sub>2</sub>	0.5	1:8	⊕ (3%)

<sup>a</sup> ⊕ denotes paraldehyde formation in all cases; if not noted otherwise, the yield was close to quantitative.

<sup>b</sup> Indicates the temperature to which the system rose during polymerization.

TABLE II  
Moderately Active Initiators  
(Initial Reaction Temperature  $-65^{\circ}\text{C}$ ., Reaction Time 5 Hr.)  
Polymer Formation<sup>a</sup>

Initiator	Solvent	Initiator concentration, wt.-% based on monomer	Monomer:- solvent ratio	Remarks <sup>a</sup>
$\text{H}_3\text{PO}_4$ 85%	Ether	0.5	10:1	$(-40^{\circ}\text{C}.)^{\text{b}}$
	Pentane	0.5	1:1	
HCl (conc. aqueous)	Ether	0.2	2:1	$\eta = 0.16$
$\text{HNO}_3$ (conc.)	Ether	0.2	2:1	
$\text{CF}_3\text{COOH}$	Ether	0.1	2:1	
Phosphomolybdic acid	Pentane	0.1	1:1	
$\text{AsF}_3$	Ether	0.1	2:1	
$\text{AsCl}_3$	Ether	0.15	2:1, 10:1	
$\text{SbF}_3$	Ether	0.05	2:1	$\eta = 0.33$
$\text{AlCl}_3$	Ether	0.1	2:1	
Al sulfate	Pentane	0.01	2:1:1	$(-15^{\circ}\text{C}.)^{\text{b}}$
	$\text{CH}_2\text{Cl}_2$			
Adipoyl chloride	Ether	0.2	2:1	$\eta = 0.28$

<sup>a</sup> All polymer yields greater than 50%.

<sup>b</sup> Temperature rise during reaction.

TABLE III  
Moderately Active Initiators  
(Initial Reaction Temperature  $-65^{\circ}\text{C}$ ., Reaction Time 5 Hr.)  
Polymer Formation

Initiator	Solvent	Initiator concentration, wt.-% based on monomer	Monomer:- solvent ratio	Remarks <sup>a</sup>
$\text{ZrCl}_2$	Ether	0.5	2:1	++
$\text{TiF}_4$	Pentane	0.1	1:1	++
$\text{SbF}_3$	Pentane	0.15	1:1	++
$\text{SbF}_3$	$\text{CH}_3\text{Cl}_2$	0.15	1:1	++, ⊕
$\text{CCl}_3\text{COOH}$	Ether	0.1	1:1	+
Phosphotungstic acid	Pentane	0.1	1:1	+
$\text{ZrCl}_4$	Ether	0.015	2:1	+
$\text{TiCl}_3$	Ether	0.2	2:1	+
$\text{FeCl}_3/\text{Pyridine}$	Pentane	0.2/1%	1:1	+, ⊕

<sup>a</sup> ++ denotes polymer yield of 10-50%; + denotes traces of polymer formed; ⊕ denotes paraldehyde formation.



produced in essentially quantitative yield. Most of the common cationic initiators, such as  $\text{BF}_3$ ,  $\text{TiCl}_4$ ,  $\text{SnCl}_4$ ,  $\text{FeCl}_3$ , and  $\text{H}_2\text{SO}_4$ , belong to this group. When the solubility of the initiator was low, the yield of paraldehyde was lowered ( $\text{TiCl}_3$ ,  $\text{VCl}_3$ ).

However, if the polymerization temperature is prevented from rising (e.g., by use of refluxing ethylene as a solvent), these initiators will give rise to polymer.

*2. Moderately Active Initiators.* This group contains the initiators that form polymer at  $-60$  to  $-80^\circ\text{C}$ . in high yield (Table II). Brønsted acids with a  $\text{p}K$  of 2 and lower, such as phosphoric acid and trifluoroacetic acid, are included in this group, as are some of the less active Lewis acids. In Table III, polymerizations are listed that give polymers in 50% yield or less.

*3. Inactive Compounds.* A number of metal halides and organic acids considered as potential initiators have been tried with ether as the solvent; they were found to give no polymerization of acetaldehyde at  $-60^\circ\text{C}$ . (Table IV).

TABLE IV  
Inactive Compounds (Reaction Temperature  $-65^\circ\text{C}$ .,  
Reaction Time Overnight, Solvent Ether, Initiator Concentration 0.5%)  
No Polymer Formation

Acetic acid	$\text{TiCl}_2$
Chloroacetic acid	$\text{TiF}_3$
Bromoacetic acid	$\text{VCl}_3$
Cyanoacetic acid	$\text{CoF}_2$
Acrylic acid	$\text{CrF}_3$
Oxalic acid	$\text{PbF}_2$
$\text{AlF}_3$	$\text{ZrF}_4$
$\text{BeCl}_2$	$\text{NH}_4\text{Cl}$
$\text{SbOCl}$	$\text{NH}_4\text{HF}_2$
$\text{BiOCl}$	$\text{Ph}_3\text{P}$
$\text{BiF}_3$	$(\text{BuO})_3\text{P}$
$\text{CdCl}_2$	Silica
$\text{B}(\text{Ac})_3$	LiAc

Some of them, like acetic acid and even chloroacetic acid, are not strong enough acids to cause polymerization under these conditions. Others, such as  $\text{AlF}_3$ ,  $\text{ZrF}_4$ , and  $\text{NH}_4\text{HF}_2$ , might be active, but are not sufficiently soluble in the reaction medium.

**Complexes of Lewis Acids as Initiators.** Complexes of Lewis acids with ethers, as well as with amines, have been investigated. Essentially no difference was observed in the reactivity when either the free Lewis acid or its etherate was used as initiator of the acetaldehyde polymerization. Amines (pyridine or tripropylamine) or amides (dimethylformamide) completely inhibit the reactivity of Lewis acids toward acetaldehyde.

**Initiator Concentration.** It must be noted at this point that the type of initiator activity exerted by any given initiator is not only determined by

its chemical nature, but also by its concentration. Hence, if one takes a series of initiators which are all type 1 (very active) at a concentration of 2% and repeats the runs using a tenfold decrease in the concentration, the initiators again subdivide into types 1, 2, 3 (See Table V).

TABLE V  
Change of Reaction Products with Initiator Concentration  
(Reaction Temperature  $-65^{\circ}\text{C}$ ., Reaction Time 5 Hr., Solvent Ether)

Initiator	Initiator concentration, wt.-%	Result <sup>a</sup>
ZrCl <sub>4</sub>	0.25	⊕
	0.015	+
Al sulfate	0.15	⊕
	0.01	No reaction
BF <sub>3</sub> , TiCl <sub>4</sub>	0.20	⊕
SnCl <sub>4</sub> , FeCl <sub>3</sub>	0.02	⊕

<sup>a</sup> ⊕ denotes paraldehyde formation; + denotes traces of polymer formed.

From Table V it can be seen that BF<sub>3</sub>:etherate, TiCl<sub>3</sub>, SnCl<sub>4</sub>, and FeCl<sub>3</sub> are still type 1 catalysts, even at the 0.02% level. However, ZrCl<sub>3</sub> has changed to type 2, and aluminum sulfate has become inactive.

#### Solvents

Under otherwise equal conditions, solvents with higher dielectric constant cause enhanced solvation of the carbonium ion chain end. Formation of paraldehyde is favored by the use of solvents having a higher dielectric constant.

It can be seen from Table VI that the reaction product changes from paraldehyde to elastomeric polyacetaldehyde with aluminum sulfate, phosphomolybdic acid, phosphotungstic acid, and TiF<sub>4</sub> upon substituting pentane or toluene for ether as the solvent. SbCl<sub>3</sub>, VCl<sub>3</sub>, and TiCl<sub>3</sub> give no

TABLE VI  
Change of Reaction Products with Acetaldehyde Concentration  
(Reaction Temperature  $-60^{\circ}\text{C}$ ., Reaction Time 16 Hr., Solvent Ether, Initiator Al Sulfate<sup>a</sup>)

Acetaldehyde concentration in toluene, %	Results <sup>b</sup>
100 (pure acetaldehyde)	⊕ <sup>c</sup>
90	⊕, polymer
80	Polymer, some ⊕
70	Polymer
60	Polymer
50	Polymer

<sup>a</sup> 0.5% with respect to monomer.

<sup>b</sup> ⊕ denotes paraldehyde formation.

<sup>c</sup> Paraldehyde with some metaldehyde.

polymer in hydrocarbon solvents, possibly because of their lack of solubility.

Other initiators show less solvent dependence;  $\text{SbF}_3$ ,  $\text{H}_3\text{PO}_4$ , and  $\text{CF}_3\text{-COOH}$  give polymer, while  $\text{FeCl}_3$  and  $\text{BF}_3$  give only paraldehyde, regardless of whether the polymerization is carried out in ether or pentane.

It is necessary to maintain the temperature below  $-78^\circ$  in order to obtain polymer with  $\text{BF}_3$  in hydrocarbon solvents.

The influence of solvation on the course of the reaction is well illustrated by the aluminum sulfate-initiated runs with various concentrations of acetaldehyde in toluene (Table VI). Pure acetaldehyde gives paraldehyde as the sole product with no polymer formation. The acetaldehyde-toluene mixture (9:1) gives paraldehyde and polymer, while in mixtures containing higher percentages of toluene (4:1 to 1:1) only polymer was found.

#### Other Variables

In our hands the most convenient system for the preparation of larger amounts of polyacetaldehyde is the  $\text{BF}_3$ -initiated polymerization in ethylene; propylene was also used but this system was more difficult to control.

Yields and molecular weight are consistently good in these polymeri-

TABLE VII  
 $\text{BF}_3$ -Initiated Acetaldehyde Polymerization

Wt. acetaldehyde, g.	Solvent, ml.	Initiator	Temperature, $^\circ\text{C}$ .	Time, hr.	Yield, g.	$\eta_{inh}^a$
32	Ethylene 250	$\text{BF}_3$ (gas, 10 cc.)	-130	1	26	3.73
28	Ethylene 200 Isobutylene 30	$\text{BF}_3$ (gas, 10 cc.)	-125	2	17.5	2.45
48	Ethylene 250	$\text{BF}_3$ etherate (5 drops)	-130	1	44 <sup>b</sup>	3.67
40	Ethylene 400	$\text{BF}_3$ etherate (2 drops in 8 ml. toluene)	-65	2	+++ <sup>b</sup>	
40	Ethylene 200	$\text{BF}_3$ etherate (1 drop in 3 ml. ether)	-125	1.5	+++ <sup>b</sup>	
40	Propylene 250	$\text{BF}_3$ etherate (1.5 drops in 5 ml. ether)	-65 <sup>c</sup>			

<sup>a</sup> In 0.1% butanone solution,  $25^\circ\text{C}$ .

<sup>b</sup> Few insoluble particles of isotactic polymer also obtained.

<sup>c</sup> After 4 drops of the initiator solution was added, paraldehyde is formed in a violent reaction.

zations; the molecular weight ( $1.5 \times 10^6$ ) of polyacetaldehyde is one of the highest ever observed. Some of the experiments are recorded in Table VII.

It is worth noting that acetaldehyde can also be polymerized with isobutylene as the solvent. No polymerization of the isobutylene occurred, nor have we observed any incorporation of isobutylene into the polymer. Isobutylene by itself very readily polymerizes under similar conditions.

Another interesting observation was made when  $\text{BF}_3$  etherate was used as the initiator. When acetaldehyde was added to the ethylene suspension of  $\text{BF}_3$  etherate ( $\text{BF}_3$  diethyl ether crystallizes at temperatures below  $-65^\circ\text{C}$ .), 0.2–0.5% of the polymer obtained was insoluble in acetone and ether. It proved to be crystalline isotactic polyacetaldehyde, identical with polymer prepared by anionic polymerization.

### Letort's Polymer

Polyacetaldehyde prepared by cationic solution polymerization is, according to x-ray, infrared, and other data, the same polymer as obtained by Letort's crystallization polymerization.

The literature procedure for "crystallization polymerization" with oxygen addition and controlled ultraviolet irradiation was followed as closely as possible.<sup>8,10</sup> We have confirmed most of the experimental results of Letort and other authors as far as yield and properties of the polymer were concerned. In general, yields ranged from 15 to 35%, and the reaction was erratic and poorly reproducible.

However, we have found one important variable in the crystallization polymerization technique which previous investigators heretofore had not recognized; namely, the condition of the surface of the glass vessel in which the polymerization is carried out. We made the following observations.

If the reaction vessel is simply rinsed with water and acetone and flamed out between polymerizations, polymer yields are obtained as reported in the literature (15–35%) as mentioned above. If the reaction flask is washed with diluted sodium hydroxide solution or an alkaline detergent, the yield is reduced to 1–2%. Frequently no polymerization took place. If the reaction flask is washed with an acidic cleaning solution, or if the flask is exposed for 5 min. to gaseous  $\text{BF}_3$  followed by evacuation of the flask at 0.1 mm. for  $1/2$  hr., the yield (25–40%) is slightly increased and the reproducibility greatly improved.

These experiments support the cationic mechanism for the crystallization polymerization without the necessity of assuming a radical initiation and chain propagation, and confirm independently Letort's latest results.<sup>16–18</sup>

After we had obtained crystalline isotactic polyacetaldehyde from runs in which solid  $\text{BF}_3$  etherate was present, we investigated carefully a number of acetaldehyde polymer samples obtained by crystallization polymerization for traces of crystalline polyacetaldehyde. In our hands, however, this technique did not produce crystalline polyacetaldehyde, even in trace amounts.

### Stabilization

Polyacetaldehyde has been reported to have fairly low thermal and oxidative stability compared with other polymers.<sup>19</sup> This was one of the main reasons for the lack of interest in this polymer.

It is well known that the stability of polyacetals depends in general upon the purity of the polymer, the nature of the end groups, and the presence of stabilizers. All three points are important for the stabilization of polyacetaldehyde.

Satisfactory purity was achieved by kneading the elastomer in water until monomer, initiator residue, acetic acid, and pyridine were removed.

The hydroxyl end groups were etherified and esterified in order to prevent chain "unzipping," and further stabilization was obtained by the addition of polyamide stabilizers and aromatic amine antioxidant.

The thermal stability was measured under nitrogen at 111°C. and 138°C. The above samples had a  $k_{111}$  of 0.01%/min. and a  $k_{138}$  of 0.1%/min.<sup>2</sup> A more detailed description is published elsewhere.<sup>20</sup>

### Mechanical Properties

Some mechanical properties of solvent cast films<sup>12</sup> of uncapped polyacetaldehyde have been recorded previously. Our measurements are in agreement with these results. We have also studied compression-molded films in order to eliminate the possibility of any residual solvent remaining in the films. In making such films only Teflon (Du Pont's registered trademark for its fluorocarbon resin) and poly(vinyl alcohol) sheeting were

TABLE VIII  
Mechanical Properties of Elastomeric Polyacetaldehyde

Temperature, °C.	Tensile strength, psi	Ultimate elongation, %
23	25-27	580
-10	170	15
-40	990	11

found to be useful as shim covers. The compression molding operations were carried out at 105°C. at 5,000-10,000 psi for 1 min. followed by a 5-min. interval at room temperature. Unstabilized polyacetaldehyde showed degradation and bubble formation under these conditions while films of stabilized polyacetaldehyde were bubble free.

The tensile strength and ultimate elongation of the samples were measured at different temperatures as seen in Table VIII. The recovery was good even at high elongations. The internal friction\* and torsion modulus

\* The internal friction measurements were carried out by M. G. McCrum of this department.

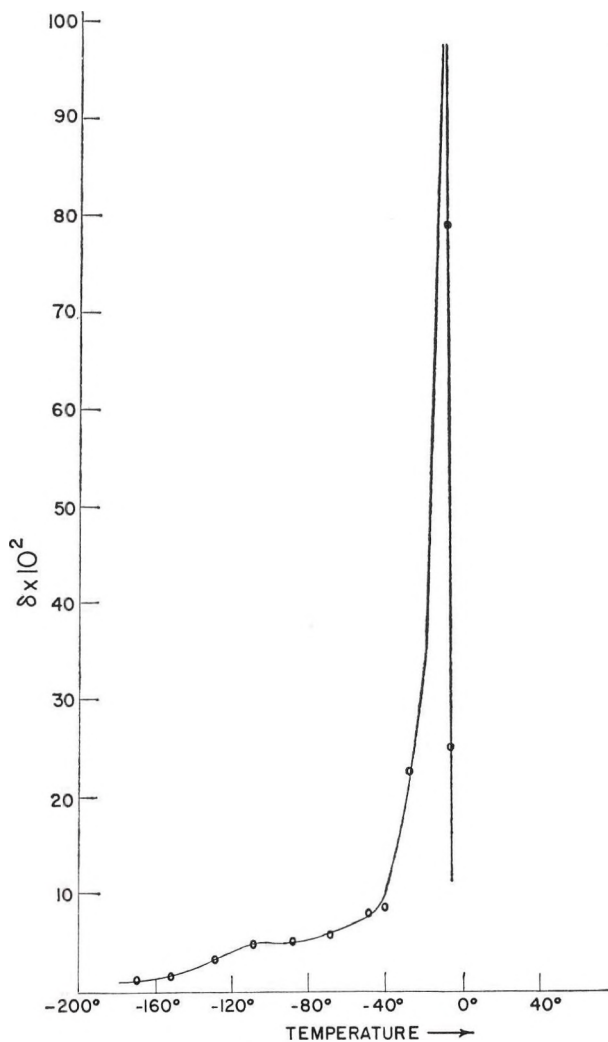


Fig. 3. Internal friction of polyacetaldehyde.

measurements showed a main amorphous transition at  $-18^{\circ}\text{C}$ . (0.6 cycles/sec.) and a small transition at about  $-100^{\circ}\text{C}$ . (Fig. 3).

## DISCUSSION

A considerable amount of effort<sup>3-9,16,19,21-30</sup> has been expended on the study of acetaldehyde polymerization over the past 25 years, but polyacetaldehyde had remained a laboratory curiosity until quite recently.<sup>43</sup> Recent investigations have shown that acid-initiated polymerization of acetaldehyde is giving high molecular weight elastomeric polymer.

Acid initiation occurs in both Letort's crystallization polymerization<sup>16</sup> and solution<sup>1,20</sup> and bulk polymerizations<sup>1,20,31,32</sup> above the melting point.

Formerly, crystallization polymerization<sup>4,5</sup> was the only known method of acetaldehyde polymerization, but it has now become apparent that it is only a special case of acid-initiated acetaldehyde polymerization.

Furukawa has developed a method of polymerization that requires condensation of acetaldehyde on  $\gamma$ -alumina<sup>31,32,44</sup> and other metal oxides at low temperatures *in vacuo* in order to achieve high yields. This polymerization utilizes the strongly acidic sites in the  $\gamma$ -alumina, and better results are obtained when the alumina\* is acid-washed.<sup>33</sup> Furukawa found that adding liquid acetaldehyde to  $\gamma$ -alumina results in very low yields. This would seem to indicate that the liquid acetaldehyde does not penetrate into the interstitial pores of the initiator.

The first suggestion of a cationic ( $\text{BF}_3$ -initiated) acetaldehyde polymerization is contained in a patent of Smyers.<sup>36</sup> He described some of the polymer properties, such as solubility, but did not give the details for its preparation. The properties are in agreement with those of elastomeric acetaldehyde, but he claimed the polymer to be poly(vinyl alcohol). Thus the true value of this preparation was not appreciated. Smyers' patent also mentioned the copolymerization of acetaldehyde with isobutylene and other comonomers, and the homopolymerization of acetone; however, our attempts along these lines have been entirely unsuccessful.

In the last two years a number of papers have appeared concerning the polymerization of acetaldehyde to the elastomer with  $\gamma$ -rays<sup>37</sup> and x-rays.<sup>38</sup> These results are not inconsistent with a cationic polymerization mechanism.

In a recent paper<sup>39</sup> aliphatic phosphines were reported to be initiators. We believe that the basicity of phosphines is not the reason for their activity as initiators since amines of similar or even higher  $\text{p}K$  are not initiators, but rather that the phosphorus atom is capable of utilizing a suborbital to accept an electron pair from the carbonyl oxygen. This results in a positive polarization of the carbonyl carbon.

Copolymers of acetaldehyde have not been reported previously. The Consortium für Electrochemie has now been able to copolymerize acetaldehyde with a number of other aliphatic aldehydes,<sup>40</sup> using the solution technique with  $\text{BF}_3$  as the initiator.

In the following papers<sup>41,42</sup> we will discuss in more detail the isotactic form of polyacetaldehyde briefly mentioned in this paper.

We wish to thank Drs. F. C. McGrew and C. E. Schweitzer for continued interest and encouragement and Drs. D. Funck, R. Thamm, and D. M. Simons for many stimulating discussions. The skillful assistance of Mr. J. F. Mansure is greatly appreciated.

\* The acidic sites in a number of oxides ( $\text{TiO}_2$ ,  $\text{Al}_2\text{O}_3$ ,  $\text{SiO}_2$ , etc.) are known to cause acid-catalyzed carbonium ion rearrangements at higher temperatures.<sup>34,35</sup>

## References

1. Vogl, O., (a) *J. Polymer Sci.*, **46**, 261 (1960) (Part I); (b) *Chem. Ind. (London)* **1961**, 748 (Part II).
2. MacDonald, R. N., U. S. Pat. 2,768,994 (1956).
3. Schweitzer, C. E., R. N. MacDonald, and J. O. Punderson, *J. Appl. Polymer Sci.*, **1**, 164 (1959) and following papers.
4. Letort, M., *Compt. Rend.*, **202**, 767 (1936).
5. Travers, M. W., *Trans. Faraday Soc.*, **32**, 246 (1936).
6. Rigby, H. A., C. J. Danby, and C. N. Hinselwood, *J. Chem. Soc.*, **1948**, 234.
7. Bevington, J. C., R. G. W. Norrish, *Proc. Roy. Soc. (London)*, **A196**, 363 (1949).
8. Bevington, J. C., *Quart. Rev. (London)*, **6**, 141 (1952).
9. Letort, M., and J. Petry, *J. Chim. Phys.*, **48**, 594 (1951).
10. Brit. Pat. 696,105 (1953).
11. Oemler, A., private communication.
12. Bovey, F. A., and R. C. Wands, *J. Polymer Sci.*, **14**, 113 (1953).
13. Staudinger, H., *Trans. Faraday Soc.*, **32**, 249 (1936).
14. Sutherland, G. B. B. M., A. R. Philpotts, and G. H. Twigg, *Nature*, **157**, 257 (1946).
15. Novak, A., and Whalley, *Can. J. Chem.*, **37**, 1710 (1959).
16. Letort, M., and P. Mathis, *Compt. Rend.*, **241**, 651, 1765 (1955).
17. Letort, M., and A. J. Richard, *Compt. Rend.*, **249**, 274 (1959).
18. Letort, M., and A. J. Richard, *J. Chim. Phys.*, **57**, 752 (1960).
19. Delzenne, G., and G. Smets, *Makromol. Chem.*, **18/19**, 82 (1956).
20. Funck, D. L., and O. Vogl, U. S. Pat. 3,001,966 (1961), U. S. Application, 8/18/58.
21. Letort, M., and X. Duval, *Compt. Rend.*, **216**, 58, 608 (1943).
22. Duval, X., and M. Letort, *Bull. Soc. Chim. France*, **1946**, 580.
23. Letort, M., X. Duval, and Y. Rollin, *Compt. Rend.*, **224**, 50 (1947).
24. Letort, M., and J. Petry, *Compt. Rend.*, **231**, 519, 545 (1950).
25. Letort, M., and A. J. Richard, *Compt. Rend.*, **240**, 86 (1955).
26. Letort, M., and P. Mathis, *Compt. Rend.*, **242**, 371 (1956).
27. Petry, J., and M. Letort, Ger. Pat. 933,785 (1955).
28. Letort, M., and J. Petry, French Pat. 1,020,456 (1952).
29. Letort, M., *J. Chim. Phys.*, **54**, 728 (1957).
30. Letort, M., *Bull. Soc. Chim. France*, **1957**, 763.
31. Furukawa, J., T. Saegusa, and H. Fujii, Ger. Pat. 1,154,627 (1963), Brit. Pat. 864,997 (1961), Jap. Appl., 1/6/59.
32. Furukawa, J., T. Saegusa, T. Tsuruta, H. Fujii, and T. Tatano, *J. Polymer Sci.*, **36**, 546 (1959).
33. Furukawa, J., T. Tsuruta, T. Saegusa, H. Fujii, and T. Tatano, (a) Jap. Pat. 22,743 (1961); (b) Jap. Pat. 22,742 (1961).
34. Pines, H., and A. W. Shaw, *J. Am. Chem. Soc.*, **79**, 1474 (1957).
35. Rondestvedt, C. S., *J. Am. Chem. Soc.*, **84**, 3319 (1962).
36. Smyers, W. H., U. S. Pat. 2,274,749 (1942).
37. Chachaty, C., *Compt. Rend.*, **251**, 385 (1960).
38. Pshezhetskii, V. S., V. A. Kargin, and N. A. Bakh, *Vysokomol. Soedin.*, **3**, 925 (1961).
39. Koral, J. N., and B. W. Song, *J. Polymer Sci.*, **54**, S34 (1961).
40. Belg. Pat. 592,462 (1960); Brit. Pat. 876,956 (1961); Germ. Appl. 6/30/59.
41. Vogl, O., *J. Polymer Sci.*, **A2**, 4609 (1964).
42. Vogl, O., *J. Polymer Sci.*, **A2**, 4623 (1964).
43. *Chem. Eng.*, **66**, No. 7, 72 (1959).
44. Furukawa, J., T. Saegusa, T. Tsuruta, H. Fujii, A. Kawasaki, and T. Tatano, *Makromol. Chem.*, **33**, 32 (1960).
45. Muthana, M. S., and H. Mark, *J. Polymer Sci.*, **4**, 91 (1949).



### Résumé

On a préparé du polyacétaldéhyde élastomère amorphe en solution et en bloc, en employant des initiateurs cationiques. Ce polymère est identique au polyacétaldéhyde de Letort. Pour éviter la trimérisation ou la tétramérisation compétitive il faut travailler à  $-40^{\circ}$  ou plus bas. On peut changer la réactivité d'un certain nombre d'initiateurs en employant différents solvants. L'influence de la température, de type d'initiateur et de solvant sur la polymérisation a été étudiée.

### Zusammenfassung

Amorpher, elastomerer Polyacetaldehyd wurde in Substanz und in Lösung mit kationischen Startern hergestellt. Dieses Polymere ist mit dem Letort'schen Polyacetaldehyd identisch. Die Acetaldehydpolymerisation muss, um die auftretende Tri- oder Tetramerisation hintanzuhalten, bei  $-40^{\circ}\text{C}$  oder weniger ausgeführt werden. Die Reaktivität einer Anzahl von Startern kann durch Verwendung verschiedener Lösungsmittel modifiziert werden. Der Einfluss der Temperatur, des Startertyps und des Lösungsmittels auf die Polymerisation wurde untersucht.

Received November 22, 1963

Revised January 13, 1964

## Polymerization of Higher Aldehydes. IV. Crystalline Isotactic Polyaldehydes: Anionic and Cationic Polymerization\*

O. VOGL, *Plastics Department, E. I. du Pont de Nemours and Company, Inc., Wilmington, Delaware*

### Synopsis

Low temperature polymerization of aldehydes in solvents of low dielectric constants yields crystalline isotactic polyaldehydes. Alkali metal alkoxides were found to be the best initiators; but alkali metals, alkali metal alkyls, Grignard reagents, lithium aluminum hydride, and aluminum organic compounds also work effectively. Isotactic polyaldehydes were also obtained by cationic initiation (stannic bromide, solid  $\text{BF}_3$  etherate). The stereoregularity increases with the increase of the space requirements of the side chain.

### INTRODUCTION

The concept of stereoregularity has revolutionized the field of addition polymerization. Since the first announcement of stereoselective olefin polymers by Natta and his school,<sup>1</sup> a large number of papers and patents has appeared which reflect the scientific and commercial interest in stereoregular olefin polymers and stereoselective polymerizations.

Olefins with aliphatic and aromatic substituents, and even some with polar substituents, undergo stereoselective polymerization.<sup>2-4</sup> In the case of methyl methacrylate, both isotactic and syndiotactic polymers have been identified.<sup>3,4</sup> With the exception of propylene oxide,<sup>5,6</sup> stereoselective polymerizations had been limited to monomers containing a carbon-carbon double bond.

Other unsaturated compounds giving rise to polymers with asymmetric C atoms should be capable of undergoing stereoregular polymerization. Aldehydes appeared to us to be particularly attractive and suitable monomers. We announced the preparation of stereoregular crystalline polyaldehydes several years ago.<sup>7</sup>

Later, Furukawa<sup>8-10</sup> and Natta<sup>11-16</sup> also succeeded in preparing crystalline polyaldehydes.

Natta and his co-workers<sup>12</sup> established the isotactic structure of the crystalline polyaldehydes by x-ray investigations.

\* Part of this paper was presented at the Gordon Conference on Polymers, New London, New Hampshire, July 1962, and at the meeting on Mechanism of Stereospecificity, Moretonhampstead, Devon, England, May 1962.

Anionic initiators were used in most of our work. Several cationic initiators also gave stereoregular aldehyde polymers. Isotactic polyaldehydes appear to be the first example in which the same stereoregular polymer was prepared by typical anionic as well as cationic initiators.

## EXPERIMENTAL

### Materials

#### *Aldehydes*

Commercial aldehydes<sup>17</sup> of the best available grade were stored over sodium carbonate monohydrate under nitrogen for at least 2 hr. prior to distillation, in order to remove acid impurities. Other acid scavengers, such as anhydrous sodium carbonate, sodium bicarbonate, calcium carbonate, and molecular sieves proved ineffective or caused side reactions.

After filtration under nitrogen, about 0.1% of  $\beta,\beta'$ -dinaphthylphenylenediamine was added, and the aldehydes were distilled twice under dry nitrogen. The center cut, amounting to about half of the charge, was collected. A low temperature still was used for the distillation of the lower boiling aldehydes. Higher aldehydes were distilled through a spinning band column; those boiling higher than *n*-valeraldehyde were distilled under reduced pressure. The aldehydes were 99.8% plus pure as determined by gas chromatography.

The purity of the aldehydes was checked routinely by titration of the acid content, using Cresol Red as an indicator. If the aldehyde was insufficiently soluble in water isopropyl alcohol was used as the solvent.

#### *Solvents*

Reagent grade diethyl ether and tetrahydrofuran were distilled from lithium aluminum hydride and stored over sodium wire.

Aliphatic hydrocarbons were dried by being passed through a silica gel column (water was reduced from 29 ppm to 2 ppm) before being added to the reaction vessel. Reagent grade toluene was dried in the polymerization vessel by azeotropic distillation.

Polymerization grade ethylene and propylene were used without further purification.

#### *Initiators*

**Alkali Metals.** Lithium, sodium, and potassium sand in heptane suspension were from Orgmet, Hampstead, N.H.

**Metal Alkyls.** Commercial butyllithium in heptane, methyl- and phenylmagnesium bromides in ether, and triethylaluminum in cyclohexane were used as purchased.

**Alkali Alkoxides.** All the alkoxides were prepared from alkali metals and stoichiometric amounts of alcohol in a hydrocarbon solvent. Lithium triphenylmethoxide was also prepared from butyllithium and triphenyl-

methanol. Lower aliphatic alkoxides were prepared in pentane solution with alkali metal sand; a toluene solution was employed for less reactive alcohols, and heating was sometimes required.

One example illustrates the preparation of a less common alkoxide (potassium triphenylmethoxide). Potassium sand (about 2.2 g.) in heptane (10 ml.) was diluted with 50 ml. of benzene (nitrogen dry box). To this suspension a solution of triphenylmethanol (13 g.) in benzene (250 ml.) was added dropwise with magnetic stirring over a 2-hr. period. (Note: Air and moisture must be carefully excluded when working with finely divided potassium.)

The reaction mixture was boiled for  $1/2$  hr. (the original blue color became tan), and the reaction was set aside overnight. The yellow solution of potassium triphenylmethoxide (0.125*M*) was then filtered under nitrogen into a dry flask to remove a small amount of insoluble material.

The lower aliphatic alkoxides were insoluble in pentane, although the reaction proceeded smoothly in this solvent. They were filtered under nitrogen and used as solids. Benzoxides and cyclohexoxides were prepared in toluene, in which they are partially soluble; they were used either as solids or as toluene suspension.

**Alkali Metal Ketyls and Dimethylformamide Compounds.** Sodium and potassium benzophenone ketyls<sup>18</sup> and sodium and potassium dimethylformamide (DMF) compounds were prepared from the alkali metal and benzophenone or DMF in stoichiometric quantities in toluene. The preparation of the corresponding lithium compounds in ether solvents has been reported, but we were unable to prepare the lithium derivatives in aromatic solvents.

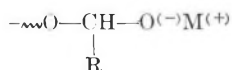
Potassium acetylacetonate was prepared similarly from potassium sand and acetylacetone in toluene.

**Lewis Acids.**  $\text{BF}_3 \cdot \text{O}(\text{C}_2\text{H}_5)_2$ ,  $\text{SnCl}_4$ ,  $\text{SnBr}_4$  (all from Eastman), and triethylaluminum (Hercules Powder Company) were used as received.

## Polymerization

### *Anionic Polymerization*

Alkali alkoxides are excellent initiators for aldehyde polymerization. This is not surprising since an anionically growing polyaldehyde chain is itself an alkoxide, namely an alkoxy substituted alkoxide:



Initiation with an alkali alkyl may be looked upon as alkoxide initiation. For example, butyllithium first reacts with acetaldehyde to yield lithium 2-hexoxide, which then proceeds to initiate polymerization of the excess acetaldehyde. Similar consideration holds for Grignard compounds.

Some observations were made of the catalytic activity of several alkoxides in *n*-butyraldehyde polymerizations. Judged by the rate of initiation and

polymer formation, the activity increases from primary to tertiary alkoxide in the order: ethoxide < isopropoxide < tertiary butoxide, and *n*-butoxide < secondary butoxide < tertiary butoxide; similarly, benzoxide < diphenyl methoxide < triphenyl methoxide, and also ethoxide < *n*-butoxide. Thus, increasing either the chain branching or the chain length enhances the initiator activity.

The same general method with only minor modifications was used for all aldehyde polymerizations; the following procedure for the polymerization of isobutyraldehyde should illustrate the technique.

A 500 ml., three-necked round-bottomed flask was equipped with a thermometer, a paddle-type stirrer, and a short extension tube capped with a rubber serum stopper. The apparatus was continuously swept with nitrogen which was exhausted through a bubbler filled with paraffin oil.

After immersing the reaction flask in a Dry Ice-acetone bath, sufficient nitrogen was admitted to keep the oil in the bubbler from backing up. Pentane (250 ml.) was added, and when the temperature reached  $-75^{\circ}\text{C}.$ , 10 ml. of 0.125*N* potassium triphenyl-methoxide in benzene was added with a hypodermic syringe. While maintaining vigorous stirring, isobutyraldehyde (40 ml.) was added with a hypodermic syringe; a white precipitate of polymer formed rapidly. (Polymerizations carried out in ether, toluene, and propylene gave more gelatinous polymer, and no supernatant liquid was noticeable.)

Polymerization was normally stopped by the addition of 200 ml. of cold acetone containing 0.5 ml. of acetic acid, and the polymer was collected after the reaction mixture had warmed to room temperature. Other work-up procedures, such as quenching with water, were not satisfactory. When an end-capped polymer was desired, acetic anhydride-pyridine was used as the quenching solvent, and the capping carried out by distilling off pentane and then refluxing the suspension.

**Reverse Addition.** In most cases the monomer was added to the initiator solution. A few attempts to add the initiator solution to the monomer solution resulted in low yields, because the rapid polymerization (particularly in the case of chloral) coated and inactivated the initiator as it entered the solution.

**Extent of Polymerization.** Attempts to measure the rate of polymerization by periodically withdrawing samples for gas chromatographic analysis failed. Low temperature filtration of the aliquot to remove the polymer was required since partial depolymerization occurred if the sample was allowed to warm to room temperature. The physical characteristics of the swollen polymer allowed it to pass through a loose filter, but it frequently plugged finer filter pores. The high polymerization rate compounded these difficulties. Nevertheless, a few successful attempts established that the unpolymerized monomer is not evenly distributed in the solution, but is mainly adsorbed on the polymer. At about 60% conversion, about one third of the residual monomer was found in solution by gas chromatography.

**Yields.** When quenched with acetone-acetic acid, the pentane suspen-

sion of the polymer is easily filtered, and yields were determined by drying and weighing of the polymer samples. The monomer remaining in the filtrate was determined by gas chromatography. The yield of isolated polymer and the yield calculated from unreacted monomer agreed closely, showing that the monomer is displaced quantitatively from the polymer by the quenching agent.

#### *Cationic Polymerization*

**Polyacetaldehyde.** Polymerization with  $\text{BF}_3$  etherate initiator and end capping have been described previously.<sup>19,20</sup> In order to separate the insoluble, isotactic polymer from the soluble, elastomeric polymer, the capped polyacetaldehyde (44 g.) was dissolved in 2 liters of reagent grade acetone by agitating the mixture at room temperature for several hours under nitrogen. Swollen globular particles remained undissolved and were removed by filtration through a 200 mesh, stainless steel screen. The insoluble part was washed three times by shaking it with 100 ml. of fresh acetone and screening as before. Finally, it was extracted overnight in a Soxhlet extractor with acetone under nitrogen, with the use of a thimble of nylon cloth in order to avoid contamination of the polymer. The polymer was then dried at 0.1 mm. at 25°C. in an oil vacuum (yield 0.25 g., 0.55%).

**Poly-*n*-butyraldehyde.** Batch polymerization of *n*-butyraldehyde with  $\text{Al}(\text{C}_2\text{H}_5)_3$  was carried out in the same manner as the anionic polymerization; the polymerization started immediately when 0.5 mole-% of pure triethylaluminum was used, but with lower quantities of initiator there was an induction period of up to 1.5 hr.

In semicontinuous polymerization, a 500-ml., round bottomed flask equipped with a paddle-type stirrer, a nitrogen sweep and two burets was cooled to -60°C. Purified *n*-butyraldehyde (60 ml.) was distilled into one buret, and 200 ml. of pentane, dried by passing it through a silica bed with nitrogen pressure, was added to the other buret; a pentane solution of stannic bromide (12 ml., 0.1*M*) was added to the pentane in the buret by means of a hypodermic syringe. The stirrer was started, and monomer and initiator solvent were simultaneously added to the polymerization flask at such a rate that the temperature was kept between -60 and -63 °C. The average rate of addition for monomer was 1.5 ml./min. After 40 min. the addition was complete. To cap the polymer, acetic anhydride/pyridine (8:1) were added, and the mixture was allowed to warm up slowly to room temperature. The pentane was removed by distillation and the pot residue heated to 135°C. The temperature was held at this point for 10 min. in order to allow the capping reaction to go to completion. (The polymer is not in solution during the capping reaction but is present as a highly swollen suspension. The capping proceeds more readily, the less the crystallinity of the polymer, because the polymer imbibes the reagents more readily.) The mixture was cooled and the residue filtered, washed with acetone and dried; yield: 20 g. of somewhat rubbery polymer.

TABLE I  
Extraction of Poly-*n*-butyraldehyde<sup>a</sup>

	Extraction time, hr.	Extract, g.	Extract, %
	20	16.8	57
	24	5.5	18.7
	26	1.1	3.9
	40	1.0	3.4
	34	0.1	0.3
Total	144	24.5	83.3
Crystal residue		3.6	12.2

<sup>a</sup> Solvent, pentane; initiator, SnBr<sub>4</sub>; original sample weight, 29.5g.

SnBr<sub>4</sub>-initiated polybutyraldehyde consists of a mixture of insoluble isotactic polymer chains and increasingly soluble, less crystalline polymer chains; some essentially amorphous material is present. The polymer softens at about 100°C. and can be cold-pressed or compression-molded at 105°C. into a translucent, rather tough and flexible sheet. Unlike amorphous polyacetaldehyde, it is not very elastic.

The polymer partially dissolves in aromatic and aliphatic hydrocarbons and methylene chloride, but is not very soluble in acetone, *n*-propyl alcohol, or the capping mixture, even at the boiling point. It is completely insoluble in acetonitrile, pyridine, ethanol, or water.

The polymer was extracted in a Soxhlet apparatus with pentane (Table I) until no more soluble polymer could be extracted. About 12% of the polymer in the batch was insoluble. This portion gave an x-ray pattern with

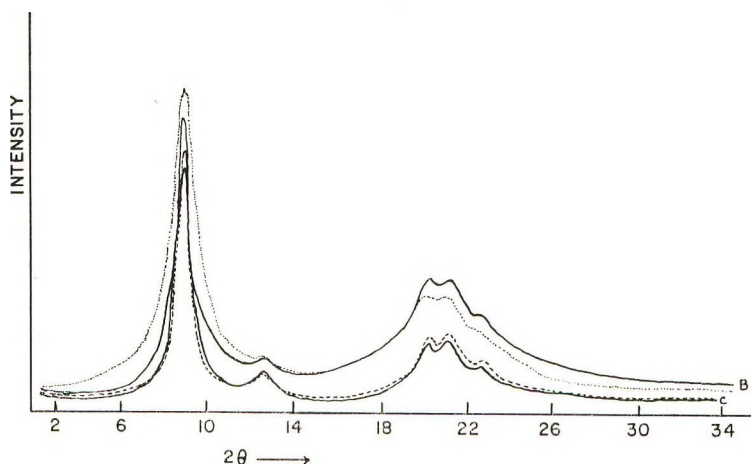


Fig. 1. Poly-*n*-butyraldehyde x-ray diffraction patterns: (---) anionic, whole polymer; (—B) cationic, whole polymer; (—C) cationic, insoluble fraction; (...) cationic, soluble fraction.

the same crystallinity and other properties as anionically initiated poly-*n*-butyraldehyde (Fig. 1).

## RESULTS

### Anionic Polymerization

#### *Crystalline Isotactic Polyacetaldehyde*

The first crystalline polyacetaldehyde was obtained by polymerizing acetaldehyde in ether with lithium aluminum hydride. The physical properties of the white, solid polymer were quite different from those of the known elastomer. It was insoluble in common solvents at room temperature but was quantitatively degraded to monomer by acidic 2,4-dinitrophenylhydrazine solution. (This method is recommended for the chemical determination of a polyacetal structure.<sup>21</sup>) Its infrared spectrum supported the polyacetal structure, and x-ray studies revealed a high degree of crystallinity.<sup>7</sup>

#### *Polymers of Higher Aldehydes*

Subsequently, a number of higher aldehydes were polymerized with anionic initiators at low temperatures. Yields of polymer from most aldehydes were high (Table II). In order to avoid degradation, the polymer was quenched at reaction temperature.

Anionic polymerization of aldehydes with long side chains (*n*-heptaldehyde) gave an essentially completely crystalline polymer, while acetalde-

TABLE II  
Polymerization of Aldehydes to Crystalline Isotactic Polymers<sup>a</sup>

Aldehyde	Solvent	Yield, % <sup>b</sup>	Remarks
Acetaldehyde	Propylene	+++	72% Total; 45% crystalline
Propionaldehyde	Propylene	+++	
<i>n</i> -Butyraldehyde	Propylene	+++	
	Pentane	+++	
Isobutyraldehyde	Propylene	+++	
	Pentane	+++	
<i>n</i> -Valeraldehyde	Propylene	+++	
<i>n</i> -Heptaldehyde	Propylene	+++	
<i>n</i> -Octaldehyde	Propylene	++	
Chloral	Propylene	+++	
3- <i>H</i> -Perfluoro- propionaldehyde	Propylene	+++	
Phenylacetaldehyde	Propylene	+++	
3-Methoxypropion- aldehyde	Propylene	+++	
Cyclohexaldehyde	Propylene	+	

<sup>a</sup> Initial reaction temperature,  $-75^{\circ}\text{C}$ .; initiator, 5 ml. of 0.13*M* potassium triphenylmethoxide; solvent:monomer ratio, 4:1.

<sup>b</sup> +++ = >75% yield; ++ = 20-50% yield; + = traces.



hyde polymerized under the same conditions always contained a sizable, soluble fraction, which could be extracted with acetone. These results point out, as known from other polymerizations, that bulkiness of the side chain improves the stereoregularity of the polyaldehyde.

Some aldehydes do not polymerize under the conditions described in this paper. Several reasons may be responsible for this failure.

**Solubility.** Monomer is insufficiently soluble at reaction temperature (*n*-decylaldehyde, m.p.  $-3^{\circ}\text{C}.$ ) and crystallizes before polymerization can occur.

**Steric Effects.** Aldehydes with  $\alpha$ -methyl-substitution (isobutyraldehyde) polymerized like linear ones. However,  $\alpha$ -ethyl groups prevented polymerization (2-ethylbutyraldehyde, 2-ethylhexaldehyde). Cyclohexanal polymerized only in meager yields.

**Electronic Effects.** Resonance stabilization of the carbonyl group by a conjugated double bond, by an aromatic ring, by hyperconjugation, or by an additional methyl group is reflected in a decrease of the infrared frequency of the carbonyl double bond to less than  $1725\text{ cm.}^{-1}$  (acrolein, benzaldehyde, acetone). Polymerization of these carbonyl compounds has not yet been achieved under the described conditions.

#### *Polymerization Variables*

**Initiators.** A large number of anionic initiators or potentially anionic initiators were tried for the polymerization of aldehydes (0.05–1 mole-%). The results are given in Table III. Three conditions important for initiator effectiveness are: sufficient solubility in the reaction medium (Na and Li methoxide are insoluble); ability to add to the carbonyl double bond (metal

TABLE III  
Alkali Metal Initiators Used in This Work<sup>a</sup>

Anion	Lithium	Sodium	Potassium	Cesium
Methoxide	×(0)	×(0)	—	—
Ethoxide	×	—	—	—
Isopropoxide				
<i>N</i> -Butoxide	×	—	—	—
<i>sec</i> -Butoxide	×	×	×	—
<i>tert</i> -Butoxide	×	×	×	—
Cyclohexoxide	—	×	×	—
Benzoxide	—	×	×	—
Diphenylmethoxide	—	×	×	—
Triphenylmethoxide	×	×	×	×
Phenoxide	—	×(0)	—	—
Benzophenone ketyl	—	×	×	—
DMF	—	×	×	—
Acetylacetonate	—	—	×	—
Butyl	×	—	—	—
Alkali metal	×	×	×	—

<sup>a</sup> × = used as initiator, polymerization occurred; ×(0) = used as initiator, no polymerization; — = was not prepared.

alkyls, alkali alkoxides, alkali ketyls, and others) and ability of the carbonyl addition product to propagate polymerization.

*Metal Alkyls.* The butyllithium-acetaldehyde system was examined extensively. The polymerization was fast and, in good solvents, gave mostly soluble polymers. The most stereoregular polyacetaldehyde was obtained in propylene solvent: 45% crystalline, 30% soluble portion.

Methyl and phenyl Grignards polymerized *n*-butyraldehyde to crystalline polymer. Aluminum alkyls were slower initiators and appeared to follow a cationic polymerization as judged by the fairly high portion of soluble polymer produced; the cationic process will be discussed later.

When typical coordination initiator combinations such as triethyl aluminum with  $\text{TiCl}_4$  or tetraisopropyl titanate (ratio 3:1) are used (initiators for ethylene polymerization), highly crystalline poly-*n*-butyraldehyde was formed immediately in high yield, indicating an anionic polymerization.

Tributylboron and tetrabutyltin were inactive.

*Metal Alkoxides.* The activity of Li, Na, K, and Cs alkoxides were compared. With any given alkoxide ion only minor differences in polymerization rate were observed as the alkali metal "gegenion" was changed. We wish to emphasize this fact because, in discussing anionic polymerization of aldehydes, one is inclined to compare this polymerization, at least formally, with the anionic polymerization of olefins, where alkali metal or metal alkyl initiators are used. A large difference exists between the ionic character of the carbon-lithium bond and that of carbon-sodium or carbon-potassium bond; therefore, remarkable differences have been observed in diene polymerizations with Li or Na as the alkali metal ion.<sup>22</sup> The difference in the ionic character of an oxygen-alkali metal bond of the growing polyaldehyde chain seems to be marginal and variations in polymerization rate are barely noticeable.

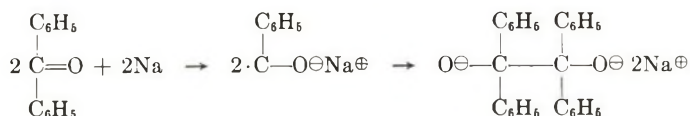
The most useful of the alkali alkoxide initiators was potassium triphenylmethoxide. It was soluble in toluene even at  $-78^\circ\text{C}$ ., and the solutions were stable. Consequently, a good part of this work was done with this initiator.

*Alkali Metals and Hydrides.* Alkali metals react with carbonyl compounds at  $-80^\circ\text{C}$ . to give the enolate ( $\text{R}_2\text{C}=\text{CH}-\text{O}^-$ ).<sup>23</sup> When lithium or potassium sand was used as initiator for the *n*-butyraldehyde polymerization, the metal dissolved and rapid polymerization took place. The enolate was probably the actual initiator.

Ionic metal hydrides ( $\text{NaH}$ ,  $\text{TiH}_2$ ) were ineffective because of poor solubility; a trace of polymer was obtained with  $\text{LiH}$ . The more soluble lithium aluminum hydride was a good initiator.

*Quaternary Ammonium Compounds.* Neither tetramethylammonium, triphenylmethoxide, nor dibenzyl dimethylammonium ethoxide polymerized *n*-butyraldehyde.

*Miscellaneous Initiators.* Na benzophenone ketyl and Na-DMF have been used previously as initiators for the polymerization of vinyl monomers:<sup>24</sup>



These compounds were excellent initiators for the polymerization of *n*-butyraldehyde. The polymerization is undoubtedly anionic, and, at least, in the case of the benzophenone ketyl, the actual initiator is probably the dianion, the chain growing from both ends as observed in styrene polymerization.<sup>25</sup>

Attempted modification of the initiator by solvation of the cation was thought to be a useful tool for the preparation of a more versatile initiator. Unreactive electron donating compounds (such as tertiary amines or amides) were added to potassium triphenylmethoxide in a molar ratio of 1:1. The results in Table IV show that the conversion is influenced considerably by this modification, but the molecular weight of the polymer<sup>26</sup> is not altered significantly.

Strong complexing agents, such as tertiary aliphatic amines and acetylacetone, inhibit the polymerization completely: some amides and tertiary heterocyclic amines influence the polymerization; ethers have little effect.

Modification of sodium benzophenone ketyl by tributylamine inhibits the polymerization, while THF, DMF, and symmetrical collidine exert little influence.

**Solvents.** Stereoselective polymerization of isoprene and copolymerization of methyl methacrylate with styrene illustrate ionic polymerizations in which product composition is strongly influenced by solvent.<sup>27</sup> In our work, the fastest, most complete polymerization was observed in solvents of low dielectric constant (Table V). For this reason aliphatic hydrocarbons, if miscible, were the "best" solvents and gave the highest crystallinity of polymer. However, good polymerizations were also carried out in

TABLE IV  
Modified Initiators<sup>a</sup>

Modifier	Yield, %	Endgroup ratios
None	95	2.05
Ethylene glycol dimethyl ether	95	—
Tetrahydrofuran	81	2.22
Dimethylformamide	87	—
Dimethylacetamide	49	2.50
<i>sym.</i> -Collidine	18.5	—
<i>N</i> -Methyl-2-pyrrolidone	8	—
<i>N,N'</i> -Ethylene-bis(2-pyrrolidone)	0	—
Acetylacetone <sup>b</sup>	0	—
Tributylamine	0	—

<sup>a</sup> Initial reaction temperature, 75°C.; initiator, potassium triphenylmethoxide, modifier n 1:1 molar ratio, 0.1 mole-% with respect to monomer; solvent, pentane; solvent: *n*-butyraldehyde ratio, 4:1.

<sup>b</sup> However, K-acetylacetonate was an active catalyst.

TABLE V  
 Influence of Solvents upon the Polymerization of *n*-Butyraldehyde<sup>a</sup>

Solvent	Dielectric constant, $\epsilon$ at 52°C. <sup>b</sup>	Initiator, mole-%	Time, min.	Yield, %	Remarks
Pentane	1.8	0.12	30	79	
Propylene	1.9	0.12	16 hr.	88.5	
Toluene	2.4	0.19	36	65	
Diethyl ether	4.3	0.12	30	38	
Tetrahydrofuran	7.4	0.10	65	32	Work-up by evaporation
Ethylene glycol dimethyl ether	10	0.10	35	1	-61°C. <sup>c</sup>
Trimethyl orthoformate	12	0.10	35	0	-58°C. <sup>c</sup>
Dimethylformamide	37.6	0.20	30 <sup>d</sup>	0	-48°C. <sup>c</sup>
Acetonitrile	37.5	0.20	40	0	
None ( <i>n</i> -butyraldehyde)	13.4	0.1	65	ca. 50	

<sup>a</sup> Initial reaction temperature, -75°C.; initiator, potassium triphenylmethoxide, 0.13*M* in toluene; solvent:*n*-butyraldehyde ratio, 4:1; work-up by acetone quench unless otherwise noted.

<sup>b</sup> Data of *Handbook of Chemistry and Physics*.<sup>28</sup>

<sup>c</sup> Above the melting point of the solvent.

<sup>d</sup> After 30 min., 0.2 mole-% of Na benzophenone ketyl was added; no reaction occurred.

aromatic hydrocarbons and monoethers. In ethylene glycol dimethyl ether, the yield of polymer was poor. Although the conversion was very dependent on the dielectric constant of the solvent, the degree of polymerization appeared to be independent as judged by the solution viscosity. Solvents with very high dielectric constant such as acetonitrile, dimethylformamide, and trimethyl orthoformate prevented polymerization.

**Temperature.** Polymerization of aldehydes can only be accomplished at low temperatures. Temperatures of -60 to -80°C. were chosen for most polymerizations because they can be easily obtained with Dry Ice-acetone mixtures. Lower temperatures sometimes gave erratic results in the case of *n*-butyraldehyde in pentane because of phase separation (about -90°C.).

The influence of temperature on aldehyde polymerization initiated by potassium triphenyl methoxide is shown in Figure 2. The optimum temperature for the polymerization is -80°C. Extrapolation of the curve locates the equilibrium temperature at -18°C.; the actual ceiling temperature is a few degrees higher, possibly -16°C. We believe that the ceiling temperatures of other aldehyde polymers lie in the same vicinity—certainly they are below room temperature.<sup>29</sup>

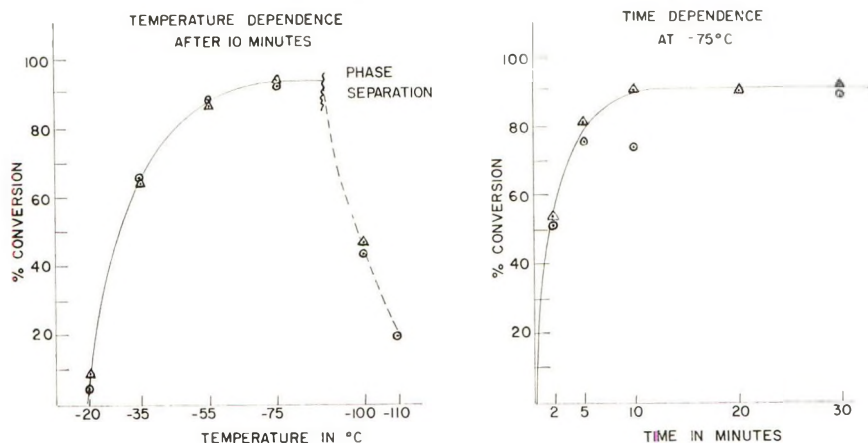


Fig. 2. *n*-Butyraldehyde polymerization, KTPM as initiator: (Δ) by gas chromatography; (○) isolated and weighed.

**Rate of Polymerization.** Rate of aldehyde polymerization was studied at  $-75^{\circ}\text{C}$ . It can be seen in Figure 1 that polymerization commences rapidly and is  $2/3$  complete in 5 min.; in 10 min. equilibrium is reached at around 95–97% conversion.

## Cationic Polymerization

### *Polyacetaldehyde*

While most cationic initiators gave the amorphous elastomeric polyacetaldehyde, under certain conditions with solid  $\text{BF}_3$  etherate, trace amounts of highly crystalline polyacetaldehyde were obtained. This polymer proved to be identical (x-ray, infrared spectrum) with isotactic polyacetaldehyde formed by anionic polymerization of acetaldehyde.

### *Poly-*n*-butyraldehyde*

The preparation of amorphous poly-*n*-butyraldehyde has been reported by Conant, et al.<sup>30–32</sup> and by Novak and Whalley,<sup>33</sup> but it has not been studied as extensively as polyacetaldehyde. In our work, anionic polymerization gave highly crystalline isotactic poly-*n*-butyraldehyde.

We also studied the cationic polymerization of *n*-butyraldehyde as a typical higher aldehyde. When stannic bromide was used as the initiator in pentane solution at  $-65^{\circ}\text{C}$ ., rapid polymerization occurred, and polymer different from the highly crystalline isotactic poly-*n*-butyraldehyde prepared anionically was isolated. However, x-ray diffraction studies showed it to contain some crystallinity.<sup>34,35</sup> The total polymer was therefore Soxhlet-extracted with pentane, and several fractions were investigated. A highly insoluble portion (12%) was identified as isotactic poly-*n*-butyraldehyde, since its infrared spectrum and x-ray pattern\* were identical

\* The x-ray study in this work was carried out by J. Whitney and J. Thomas.

with those of the anionically produced material (Fig. 2). The other fractions also revealed some crystallinity, decreasing as the solubility increased, but even the most soluble fraction showed some crystallinity.

*n*-Butyraldehyde polymerized with triethylaluminum exhibited a similar pattern of polymer composition as that obtained by stannic bromide initiation. About 20% of isotactic poly-*n*-butyraldehyde was isolated from the total polymer. The similarity of the products obtained from triethylaluminum and stannic bromide (an unquestionable cationic initiator) suggests strongly that triethylaluminum is functioning as a cationic initiator.

When stannic chloride is used as the initiator, a completely soluble polymer with no apparent crystallinity is formed. The use of solvents which swell poly-*n*-butyraldehyde to a greater extent than does pentane results in a decrease in the amount of the crystalline portion found in the final polymer.

We wish to thank Drs. F. C. McGrew and C. E. Schweitzer for their continued interest and encouragement. We are indebted to Dr. D. M. Simons for many enlightening discussions. The conscientious and skillful assistance of Mr. J. F. Mansure is greatly appreciated.

### References

1. Natta, G., P. Pino, P. Corradini, F. Danusso, E. Mantica, G. Mazzanti, and G. Moraglio, *J. Am. Chem. Soc.*, **77**, 1708 (1955).
2. Schildknecht, C. E., S. T. Gross, H. R. Davidson, J. M. Lambert, and A. O. Zoss, *Ind. Eng. Chem.*, **40**, 2104 (1948).
3. Fox, T. G, B. Garrett, W. E. Goode, S. Gratch, J. F. Kincaid, A. Spell, and D. Stroupe, *J. Am. Chem. Soc.*, **80**, 1768 (1958).
4. Gall, W. G., and N. G. McCrum, *J. Polymer Sci.*, **50**, 489 (1961).
5. Pruitt, M. E., and J. B. Baggatt, U. S. Pat. 2,706,181 (1955).
6. Price, C. E., and M. Osgan, *J. Am. Chem. Soc.*, **78**, 690 (1956).
7. Vogl, O., Belg. Pat. 580,553 (1959), Priority USA, 8/18/58; *J. Polymer Sci.*, **46**, 261 (1960).
8. Furukawa, J., T. Saegusa, T. Tsuruta, and H. Fujii, French Pat. 1,268,322 (1961), Priority Japan, 11/6/59.
9. Furukawa, J., T. Saegusa, T. Tsuruta, and H. Fujii, French Pat. 1,268,191 (1961), Priority Japan, 12/29/59.
10. Furukawa, J., T. Saegusa, H. Fujii, A. Kawasaki, H. Imai, and Y. Fujii, *Makromol. Chem.*, **37**, 149 (1960).
11. Natta, G., P. Chini, G. Mazzanti, and A. Brizi, Belg. Pat. 597,373 (1961), Priority Italy, 11/24/59.
12. Natta, G., G. Mazzanti, P. Corradini, and I. W. Bassi, *Makromol. Chem.*, **37**, 156 (1960).
13. Natta, G., G. Mazzanti, P. Corradini, P. Chini, and I. W. Bassi, *Atti Accad. Nazl. Lincei, Rend. Classe Sci. Fis. Mat. Nat.*, **28**, 8 (1960).
14. Natta, G., G. Mazzanti, P. Corradini, A. Valvassori, and I. W. Bassi, *Atti Accad. Nazl. Lincei, Rend. Classe Sci. Fis. Mat. Nat.*, **28**, 18 (1960).
15. Natta, G., P. Corradini, and I. W. Bassi, *Atti Accad. Nazl. Lincei, Rend. Classe Sci. Fis. Mat. Nat.*, **28**, 284 (1960).
16. Natta, G., P. Corradini, and I. W. Bassi, *J. Polymer Sci.*, **51**, 505 (1960).
17. Bayer, O., in *Methoden der Organischen Chemie*, Vol. VII, Part I, Sauerstoffverbindungen II, Fourth Ed., Houben-Weyl, Ed., Georg Thieme Verlag, Stuttgart, 1954, p. 502.

18. Bachmann, W. H., *J. Am. Chem. Soc.*, **55**, 1179 (1935).
19. Vogl, O., *J. Polymer Sci.*, **A2**, 4593 (1964). D. L. Funck and O. Vogl, U. S. Pat. 3,001,966 (1961), Applications, 8/18/58.
20. Vogl, O., Brit. Pat. 894,399 (1962); O. Vogl, *Chem. Ind. (London)*, **1961**, 748.
21. Vogl, O., unpublished results.
22. Ziegler, K., H. Grimm, and R. Willer, *Ann.*, **542**, 90 (1939); *Chem. Eng. News*, **33**, 3716 (1956).
23. Germ. Pat. 287,933 (1915) in *Friedl.*, Part 12, Julius Springer, Berlin, 1917, p. 48.
24. Zilkha, A., P. Nata, and M. Frankel, *Proc. Chem. Soc.*, **1959**, 364.
25. Szwarc, M., *Nature*, **178**, 1168 (1956).
26. Vogl, O., *J. Polymer Sci.*, **A2**, 4623 (1964).
27. Tobolsky, A. V., D. J. Kelley, K. F. O'Driscoll, and C. E. Rodgers, *J. Polymer Sci.*, **28**, 425 (1958).
28. *Handbook of Chemistry and Physics*, 43rd Ed., Chemical Rubber Publishing Co., Cleveland, 1961-1962.
29. Vogl, O., and W. M. D. Bryant, *J. Polymer Sci.*, **A2**, 4635 (1964).
30. Bridgeman, P. W., and J. B. Conant, *Proc. Natl. Acad. Sci. U. S.*, **15**, 680 (1929).
31. Conant, J. B., and C. O. Tongberg, *J. Am. Chem. Soc.*, **52**, 1659 (1930).
32. Conant, J. B., and W. R. Peterson, *J. Am. Chem. Soc.*, **54**, 628 (1932).
33. Novak, A., and E. Whalley, *Can. J. Chem.*, **37**, 1710, 1718 (1959).
34. Sobue, H., and H. Kubota, *Bull. Chem. Soc. Japan*, **34**, 883 (1961).
35. Ishida, S., *Kobunshi Kagaku*, **18**, 187 (1961).

### Résumé

La polymérisation d'aldéhydes à basse température dans des solvants de constantes diélectriques faibles donne des polyaldéhydes cristallins isotactiques. On trouve que des alcoolates de métaux alcalins sont les meilleurs initiateurs, mais les métaux alcalins, les métaux alcalins alcoylés, les réactifs de Grignard, l'hydrure de lithium-aluminium et des composés organiques d'aluminium sont aussi effectifs. On a obtenu des polyaldéhydes par l'initiation cationique (bromure d'étain, le  $\text{BF}_3$  étherate solide). La stéréolarité augmente en même temps que les exigences spatiales de la chaîne latérale.

### Zusammenfassung

Tieftemperaturpolymerisation von Aldehyden in Lösungsmitteln mit niedriger Dielektrizitätskonstante ergibt kristalline isotaktische Polyaldehyde. Alkalimetallalkoxyde sind die besten Starter. Alkalimetalle, Alkalimetallalkyle, Grignard-Reagenzien, Lithiumaluminiumhydrid und aluminiumorganische Verbindungen sind jedoch auch wirksam. Isotaktische Polyaldehyde wurden auch durch kationische Starter (Zinnbromid, festes  $\text{BF}_3$ -Ätherat) erhalten. Die Stereoregularität nimmt mit steigender Raumbeanspruchung der Seitenkette zu.

Received November 22, 1963

Revised January 13, 1964

## Polymerization of Higher Aldehydes. V. End-Capped Crystalline Isotactic Polyaldehydes: Characterization and Properties

O. VOGL, *Plastics Department, E. I. du Pont de Nemours and Company, Inc., Wilmington, Delaware*

### Synopsis

End-capped, isotactic polyaldehydes were characterized by the determination of the solution viscosities, melting points, the gel points and solubilities in a number of solvents. Relative endgroup molecular weights were estimated from infrared spectra. The stability of end-capped polyaldehydes is discussed.

### INTRODUCTION

In contrast to uncapped and unstabilized high molecular weight polyoxymethylene, which is comparatively stable even above 200°C.,<sup>1</sup> uncapped higher polyaldehydes<sup>2-4</sup> degrade readily at room temperature. However, end-capping<sup>5,6</sup> provides adequately stabilized polymers for the study of solubility, gel points, melting points, and for the determination of molecular weight (solution viscosity and endgroup analysis).

### EXPERIMENTAL

#### Materials

##### *Polymers*

Polyaldehydes were prepared as described previously<sup>2</sup> and were acetate end-capped with pyridine-acetic anhydride.<sup>5,6</sup>

##### *Solvents*

Tetrahydronaphthalene was boiled with sodium for 2 hr., distilled (nitrogen bleed), and stored under nitrogen.

Reagent grade or spectral grade solvents were used as such from freshly opened bottles. Other solvents were distilled once before use.

##### *Refining*

Polymers were refined by dissolving in tetrahydronaphthalene and then heating for 10-20 min. under nitrogen atmosphere. The polymers precipitated upon cooling and were filtered and washed with acetone; finally they



were extracted overnight with acetone in a Soxhlet apparatus (nitrogen atmosphere) to remove any residual tetrahydronaphthalene.

### Characterization

#### *Gel Points*

Gel points are determined on 2% polymer solution.

#### *Solution Viscosities*

Viscosities of the polymer solutions in tetrahydronaphthalene were determined in an Ostwald viscometer (No. 75). The viscosity measurements on poly-*n*-butyraldehyde solutions were run at 140°C.; those on polypropionaldehyde, poly-*n*-valeraldehyde, and poly-*n*-heptaldehyde solutions were made at 100°C.

#### *Infrared Spectra*

For the initial assignment of the structure, a combination of Nujol mull and KBr pellet techniques was found fruitful. However, the spectra shown in Figure 1 are those of cold-pressed films ( $0.25 \pm 0.025$  mm.). Relative number-average molecular weights were estimated for poly-*n*-butyraldehyde samples by comparing endgroup intensities of the acetyl carbonyl absorption band at  $5.72 \mu$ , the  $4.75 \mu$  band being used as an internal standard. The ratio ( $R = \text{intensity of } 5.72 \mu / \text{intensity of } 4.75 \mu$ ) was used for comparison.

#### *Melting Points*

The melting points of cold-pressed films were determined in a Fisher-Jones melting point apparatus; special care was taken to keep the samples under a nitrogen blanket. Prior to the pressing of the samples, unstable fractions were removed from the polymers by solution degradation in tetrahydronaphthalene as described previously. In the case of the higher melting polyaldehydes, the thermal stability was still not adequate after this treatment, therefore, thermal stabilizers (up to 1%)<sup>7</sup> and a trace of antioxidants (AgeRite White, 0.1%) were added to counteract the oxygen adsorbed on the surface of the polymer. It is believed that the melting points are accurate to  $\pm 5^\circ\text{C}$ .

#### *2,4-Dinitrophenylhydrazone Test*

The following technique was developed as a fast method to determine chemically the polyacetal structure of aldehyde polymers. A known amount of polyacetal was degraded in an acidic solution of 2,4-dinitrohydrazine, the monomeric aldehyde formed reacting immediately with the 2,4-dinitrophenylhydrazine to form the hydrazone. The applicability of the technique was tested on acetals of known structure such as polyformaldehyde, paraldehyde, metaldehyde I and II, and elastomeric polyacetaldehyde and found to be very suitable.

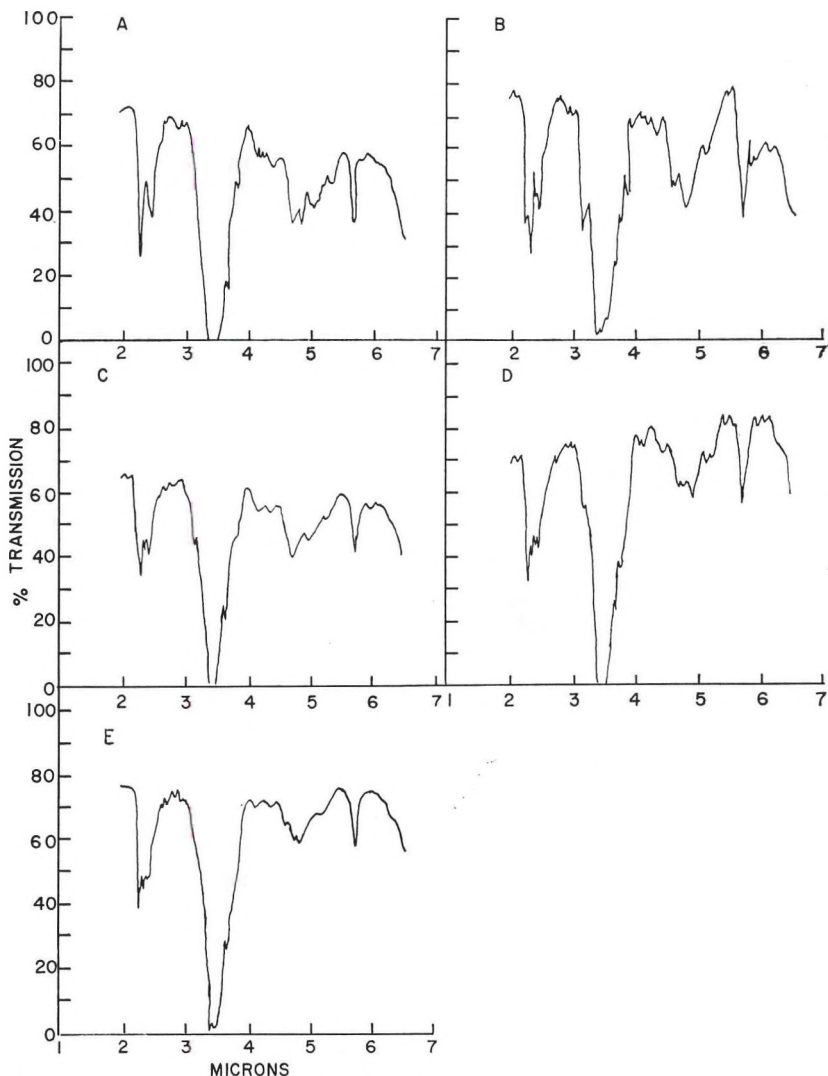


Fig. 1. Infrared film spectra of crystalline acetate end-capped polyaldehydes: (A) polypropionaldehyde; (B) polyisobutyraldehyde; (C) poly-*n*-butyraldehyde; (D) poly-*n*-valeraldehyde; (E) poly-*n*-heptaldehyde.

The procedure was as follows (see also Vogel<sup>8</sup>). To a suspension of 2,4-dinitrophenylhydrazine (0.22 g.) in concentrated sulfuric acid (1 ml.), distilled water (1.5 ml.) and ethyl alcohol (3 ml.) were added with cooling and stirring. The solution was added to 1 mmole of the polymer, preferably pretreated with 0.5 ml. of ethyl alcohol. The polymer sample dissolved rapidly, and the 2,4-dinitrophenylhydrazone started to precipitate immediately. It was found advantageous to let the reaction proceed for at least 2 hr., or better, overnight. The mixture was chilled, filtered, washed with water and dried. The melting points found for the derivatives

TABLE I  
2,4-Dinitrophenylhydrazone Test

Aldehyde polymer or oligomer	2,4-Dinitrophenylhydrazone recovered, %
Paraldehyde	97
Metaldehyde	92.5
Elastomeric polyacetaldehyde	96.5
Polyformaldehyde	98
Polyacetaldehyde	97.3
Poly- <i>n</i> -butyraldehyde	95.5
Poly- <i>n</i> -valeraldehyde	93.7
Poly- <i>n</i> -heptaldehyde	94
Polyisobutyraldehyde	96.8

were within 5°C. of the literature melting points. Results are shown in Table I.

When the sample is a copolymer, paper chromatographic separation can be used for the isolation and identification of the components.

## RESULTS AND DISCUSSION

The infrared spectra of the polyaldehydes and their chemical degradation by acidolysis in the presence of 2,4-dinitrophenylhydrazine to give 2,4-dinitrophenylhydrazones show beyond any reasonable doubt that the polyaldehydes possess an acetal structure. Additional characterizations have been carried out on acetyl end-capped polymers.

### Solubility and Gel Points of Polyaldehydes

Crystalline, isotactic polyaldehydes are insoluble in all known solvents at room temperature. Polyacetaldehyde, for example, is insoluble in alcohols (methanol, ethanol, *n*-butanol), phenol, acetone, butanone, acetonitrile, diethyl ether, dioxane, and ethyl acetate. It swells slightly in dimethylformamide and dimethylacetamide and somewhat more in tetrahydrofuran, toluene and chlorinated hydrocarbons. Likewise, we uncovered no room temperature solvent for isotactic poly-*n*-butyraldehyde. However, a number of organic compounds are solvents at elevated temperatures (Table II) and swell the polymer to a certain extent at room temperature.

The gel point is a good measure of solvent power. Aromatic hydrocarbons with aliphatic side chains of a certain chain length are good solvents for poly-*n*-butyraldehyde as are partially or completely hydrogenated cyclic hydrocarbons and higher boiling halogenated olefins. Some aromatic nitriles dissolve the polymer at the boiling point, but solvents with ether, ester, or ketone groups are of little value; phenols degrade the polymer completely.

Table III gives the characteristic gel points for a series of polyaldehydes dissolved in tetrahydronaphthalene.

The gel point is the temperature at which the first definite opalescence was observed when the polymer solution was cooled slowly; it was found to be quite independent of the concentration (solutions of 0.5–10% concentration were studied). However, gel point is a function of crystallinity and molecular weight, necessitating the use of polymer samples of comparable degrees of crystallinity and molecular weight.

TABLE II  
Solvents for Acetate End-Capped Poly-*n*-Butyraldehyde

Solvent	Temperature, °C.	
	Polymer in solution (2%)	Gel point
Norbornene	b.p.	m.p.
<i>p</i> -Diethylbenzene	105	55
<i>tert</i> -Butylbenzene	140	70
Tetrachloroethylene	b.p.	70
Decahydronaphthalene	165	80
Dihydrocyclopentadiene	140	80
Trichloroethylene	b.p.	80
<i>p</i> -Cymene	170	100
Dibenzyl	150	120
<i>p</i> -Xylene	b.p. (138)	130
Tetrahydronaphthalene	160	130
Naphthalene	b.p.	150

TABLE III  
Gel Points of Isotactic Aldehyde Polymers in Tetralin (5% Solids)

Polymer	Gel point, °C.
Formaldehyde	200
Propionaldehyde	85
<i>n</i> -Butyraldehyde	130
Isobutyraldehyde	185
<i>n</i> -Valeraldehyde	85
<i>n</i> -Heptaldehyde	30
<i>n</i> -Octaldehyde	<20
<i>n</i> -Butyraldehyde/isobutyraldehyde	150

<sup>a</sup> This sample was of distinctly lower crystallinity.

As may be seen in Table III, the gel points parallel the solubility and the melting point of the polymer. Polyisobutyraldehyde has a much higher gel point and melting point than poly-*n*-butyraldehyde, although both have a C<sub>3</sub> side chain. For the series of unbranched polyaldehydes, the gel point decreases with increased length of the side chain. (Not enough data are available for polypropionaldehyde, but the discrepancy is probably caused by lower crystallinity.)

The crystalline copolymer of *n*-butyraldehyde and isobutyraldehyde exhibited a gel point between the values for the homopolymers. (This co-

polymer is easily prepared in a 1:1 molar ratio. However, neither  $C_6H_{13}\cdot CHO-CH_3CHO$  nor  $PrCHO-(CH_3)_2CO$  could be anionically copolymerized.)

Of the polyaldehydes studied, polyformaldehyde has the highest gel point observed, namely, about 200°C. The gel point increases slightly with increasing molecular weight of the polyformaldehyde (Table IV).

TABLE IV  
Influence of Molecular Weight upon the Gel Point

Polyformaldehyde MW <sup>a</sup>	Gel point in tetrahydronaphthalene (2%), °C.
27,400	Not completely in solution
17,200	b.p.
12,500	200
6,700	195
3,400	190

<sup>a</sup>  $\bar{M}_n$  by acetate end group determination.

### Solution Degradation of the Unstable Fraction

Solution degradation in tetrahydronaphthalene was adopted for purification of polyaldehydes. Those polyaldehyde chains with only one stable endgroup (alkyl or acyl) or with two unstable (hemiacetal) ends degraded completely, but chains capped on both ends were stable under these conditions. The polymer samples were heated for 10 min. at the boiling point in tetrahydronaphthalene (2–5% solids) under an inert atmosphere. The solution was then cooled, diluted with a fourfold volume of acetone, filtered, washed, and dried. Polymers so treated showed no hydroxyl absorption in the infrared spectrum.

It is interesting to note that even polyaldehydes which had not been treated with acetic anhydride–pyridine gave 3–6% of stable fractions when subjected to the solution degradation procedure. This indicates that raw polyaldehydes have not only unstable hemiacetal endgroups but also stable ester end groups and probably ether endgroups; 3–6% of the polymer chains have such groups on both ends. These stable ends seem to be formed by a hydride ion transfer mechanism.

### Melting Points

It is interesting to compare melting points of end-capped polyaldehydes with those of the corresponding olefins (Table V).<sup>9,10</sup> The polyaldehydes melt at a somewhat higher temperature, particularly in the higher members of the homologous series. The melting points of isotactic normal polyaldehydes pass through a maximum at poly-*n*-butyraldehyde and decrease slowly thereafter. Methyl branching, particularly in the  $\alpha$ -position, raises the melting point as is the case for the isotactic olefin polymers.

TABLE V  
 Melting Points of Crystalline Isotactic Polyaldehydes

Monomer	Melting point, °C.	
	Polyaldehyde (X = O)	Polyolefin (X = CH <sub>2</sub> )
CH <sub>3</sub> CH=X	165 <sup>a</sup>	165
CH <sub>3</sub> CH <sub>2</sub> CH=X	185 <sup>b</sup>	125
CH <sub>3</sub> (CH <sub>2</sub> ) <sub>2</sub> CH=X	225 <sup>b</sup>	75
CH <sub>3</sub> (CH <sub>2</sub> ) <sub>3</sub> CH=X	155 (85) <sup>d</sup>	None
CH <sub>3</sub> (CH <sub>2</sub> ) <sub>5</sub> CH=X	150 (75) <sup>d</sup>	None
CH <sub>3</sub> (CH <sub>2</sub> ) <sub>6</sub> CH=X	35	None
(CH <sub>3</sub> ) <sub>2</sub> CHCH=X	>260 (dec.)	310
HCH=X <sup>c</sup>	178	137

<sup>a</sup> Uncapped sample.

<sup>b</sup> With some decomposition.

<sup>c</sup> Added for comparison.

<sup>d</sup> Transitions below the melting point of polymers.

The reasons for the differences between polyolefins and polyaldehydes could be found in: (a) difference in bond length (C—O is 1.41 Å. compared to 1.54 Å. in C—C); (b) different packing in the helical chain (fourfold compared to threefold) of the polymer; (c) differences in backbone chain polarity.

Poly-*n*-valeraldehyde and poly-*n*-heptaldehyde have a noticeable transition temperature below their melting points. This characteristic temperature is indicated in parentheses in Table V. Above this temperature samples of the polymers can be extruded through an orifice in the melt indexer or can be molded into various shapes. This phenomenon has not been observed in crystalline polyaldehydes with a side chain of less than C<sub>3</sub>, and we believe it is associated with the "melting" of the paraffinic side chains.

### Molecular Weights: Infrared Endgroup Analysis and Solution Viscosity

Most of our work was done with polyaldehyde samples of moderate molecular weight ( $\eta = 0.10$ – $0.35$ ). These molecular weights are easily obtained and are adequate for initial characterizations. Higher polymers with a viscosity up to  $\eta = 0.83$  have been prepared with the use of alkali metal dimethylformamide compounds or benzophenone ketyls.

A relative number-average molecular weight was estimated by correlating the infrared determination of the ester end group with solution viscosity measurements. This permitted the use of the ratio  $R = \text{intensity at } 5.72 \mu / \text{intensity at } 4.75 \mu$  for comparison of polymer samples—a technique adequate for our purpose (Fig. 2). We have not attempted to relate this ratio  $R$  to an absolute value which could be obtained, for example, by acetyl determination. We have, however, determined methoxyl endgroups of alkyl-capped samples of poly-*n*-butyraldehyde.<sup>5</sup>

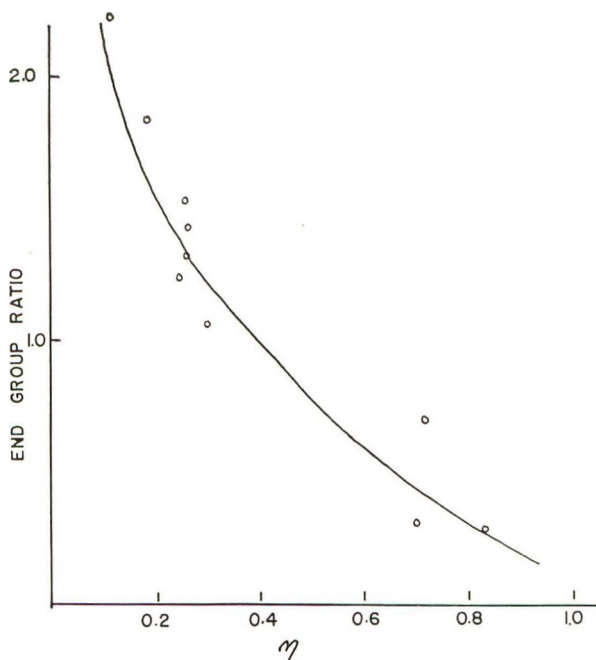


Fig. 2. Solution viscosity vs. endgroup relationship for poly-*n*-butyraldehyde.

Solution viscosities were determined in a constant temperature bath. When purified poly-*n*-butyraldehyde and poly-*n*-heptaldehyde were kept at 140 and 100°C., respectively, in tetrahydronaphthalene solution in the Ostwald viscometer for 2–3 hr., no change in viscosity occurred; thus the polymers were thermally stable under the conditions of the viscosity measurements.

Lower polyaldehydes showed a good correlation between the inherent viscosity and the relative molecular weight obtained from the infrared end group estimation: A value of  $\eta = 0.3$  corresponds to  $R = 1.1$ . A discrepancy between the measurements was observed with poly-*n*-heptaldehyde, however, in that a sample with a similar carbonyl intensity gave an  $\eta = 0.57$ , about twice the expected value. This abnormally high solution viscosity may result from some influence of the long polymer side chains.

#### Internal Friction

The internal friction of poly-*n*-butyraldehyde was determined by N. G. McCrum using the torsion pendulum method. The polymer possessed moderate crystallinity. Figure 3 shows a transition point at room temperature and a shoulder at about  $-30^\circ\text{C}$ .

#### Stability

The thermal degradation rate of polyoxymethylene is immeasurably low at 138°C. and is reportedly less than 0.01%/min. at 222°C.<sup>5,6</sup> End-capped higher aldehydes have been stabilized to give  $k_{138} < 0.1\%/min$ .

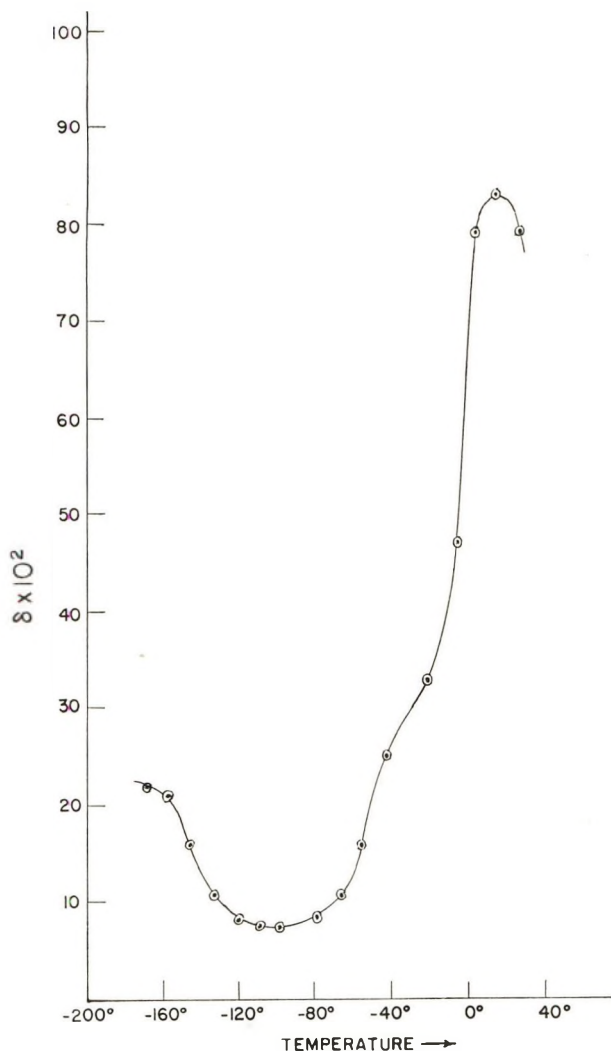


Fig. 3. Internal friction of polybutyraldehyde.

Stability of the polymers of higher aldehydes depends to a great extent upon the purity of the polymer. Among the detrimental impurities are: initiator residue (particularly acids or electrophiles in general), monomer residue (or unstable polymer fraction), and presence of peroxides. Stability is also somewhat dependent upon the length of the side chain and increases significantly with a  $C_4$  side chain. This may result from the hydrophobic side groups shielding the backbone chain against electrophilic attack.

The ceiling temperature of the polymer is below room temperature and spontaneous degradation may be observed upon standing if end-capping of the polymer ends is incomplete. In Figure 4 the degradation of uncapped



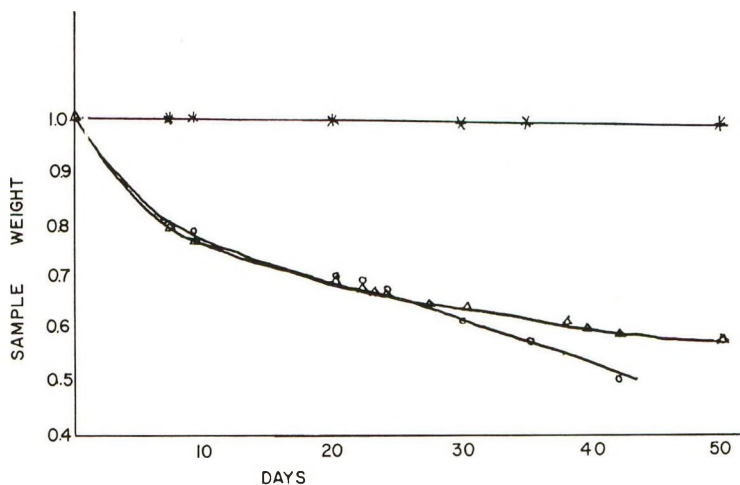


Fig. 4. Room temperature stability of poly-*n*-butyraldehyde: (\*) acetate end-capped, in air; (Δ) uncapped, in air; (O) uncapped, in nitrogen. These experiments were carried out by H. Marder.

polymer is compared with that of an acetate-capped sample. While 50% of uncapped polymer was degraded in 40 days even under nitrogen, acetate-capped polymer was virtually unchanged.

#### *Initiator Residue*

The removal of initiator residue is one of the most desirable but most difficult tasks in polyaldehyde work. Although only 0.1% of initiator or less is used in aldehyde polymerization, all the initiator remains in the polymer. In fact, even when polymerization is run to lower conversions, and even though substantial losses occur during capping and refining steps, all of the initiator is still found in the polymer. (Although most of our polymer samples contained only 0.02–0.2% ash, occasionally samples were found that contained as much as 0.8–1.0% of ash). The initiator cannot be removed by recrystallization of the polymer from tetrahydronaphthalene (although a perfectly clear solution is obtained), nor by washing the polymer with acetone. The best procedure found was to wash the polymer with alcohol, but the removal of initiator was still incomplete.

#### *Monomer Residue and Autooxidation*

Monomer is often generated from small unstable fractions and from oxidative degradation of the polymer. Monomeric higher aldehydes are not very volatile and remain adsorbed on the polymer chain. They are easily autooxidized to peroxides, which in turn oxidize the tertiary hydrogen on the polymer chain, further contributing to instability. As is the case with simple acetals,<sup>11</sup> the polyaldehydes are rather susceptible to autooxidation because of their tertiary C atoms flanked by two ether oxygens.

Unrefined, acetate-capped poly-*n*-butyraldehyde depolymerized completely overnight when placed in a closed container in the presence of air. About 8% of butyric acid and a sizable amount of peroxides were present in the degradation product. When the same sample was exposed to oxygen under conditions where the monomer could escape (open container) or when stored under an inert atmosphere, very little degradation was observed.

A detailed account of the stabilization of aldehyde polymers is given elsewhere.<sup>5,6</sup>

We wish to thank Drs. F. C. McGrew and C. E. Schweitzer for their continued interest and encouragement. We are indebted to Dr. D. M. Simons for many enlightening discussions. The conscientious and skillful assistance of Mr. J. F. Mansure is greatly appreciated.

### References

1. McDonald, R. N., U. S. Pat. 2,768,994 (1956).
2. Vogl, O., **A2**, 4609 (1964).
3. Vogl, O., Belg. Pat. 580,553 (1959).
4. Vogl, O., *J. Polymer Sci.*, **46**, 261 (1960).
5. Vogl, O., *Chem. Ind. (London)*, **1961**, 748.
6. Vogl, O., Brit. Pat. 894,399 (1962); A. U. Appln. 27668/59 (Serial 870,775).
7. Funck, D. L., and O. Vogl, U. S. Pat. 3,001,966 (1961).
8. Vogel, A., *Practical Organic Chemistry*, Third Ed., Longmans, Green, and Co., London, 1956, p. 4.
9. Natta, G., *Angew. Chem.*, **68**, 393 (1956).
10. Campbell, T. W., and A. C. Haven, *J. Appl. Polymer Sci.*, **1**, 73 (1959).
11. Criegee, R., in *Methoden der Organischen Chemie*, Vol. VIII, Sauerstoffverbindungen III, Houben-Weyl, Ed., Georg Thieme Verlag, Stuttgart, 1952, p. 23.

### Résumé

Des polyaldéhydes isotactiques stabilisés en fin de chaîne ont été caractérisés par la détermination des viscosités en solution, des points de fusion, de points de gélification et des solubilités dans un certain nombre de solvants. Des poids moléculaires relatifs (par détermination des groupements terminaux) ont été estimés à l'aide des spectres infra-rouges. La stabilité des polyaldéhydes stabilisés en fin de chaîne est discutée.

### Zusammenfassung

End-stabilisierte, isotaktische Polyaldehyde wurden durch die Bestimmung von Lösungsviskosität, Schmelzpunkt, Gelpunkt und Löslichkeit in einer Reihe von Lösungsmitteln charakterisiert. Relative Endgruppenmolekulargewichte wurden aus Infrarotspektren bestimmt. Die Stabilität end-stabilsierter Polyaldehyde wird diskutiert.

Received November 22, 1963

Revised January 13, 1964

## Polymerization of Higher Aldehydes. VI. Mechanism of Aldehyde Polymerization\*

O. VOGL and W. M. D. BRYANT, *Plastics Department, E. I. du Pont de Nemours and Company, Inc., Wilmington, Delaware*

### Synopsis

On the basis of results presented in previous papers possible mechanisms of polymerization of higher aldehydes are considered. The influence of solvents, temperature, initiator, and monomer upon the polymerization is discussed with particular emphasis on the stereoregularity of the resulting polymer. It is proposed that more than one monomer unit is involved in the propagation step. Both the stereoselective addition of monomer to the growing chain and the chain transfer reaction are thought to take place in a concerted manner. Chain transfer results in termination with the formation of hydroxyl, ester and probably ether end groups; growing chains which do not undergo transfer remain as "living" ends after the monomer supply is exhausted. Some thermodynamic values for carbonyl polymerizations are estimated.

### INTRODUCTION

In the preceding papers<sup>1-5</sup> we have described the catalytic polymerization of higher aldehydes, and some general conclusions about its mechanism can now be drawn. Aldehyde polymerization is a striking example of ionic polymerization. Not only are aldehydes polymerized by both cationic and anionic catalysts, but also stereoregular, isotactic polymers can be prepared by both types of polymerization. Some of the conclusions drawn from the aldehyde polymerization studies may be applicable to ionic polymerizations in general.

The consecutive steps in aldehyde polymerization: initiation, propagation, transfer, and termination, will be discussed separately and their importance for the overall process considered.

### RESULTS AND DISCUSSION

#### Polymerizability of Aldehydes

The polymerizability of aldehydes seems to correlate with the polarization of the carbonyl double bond as reflected by its infrared frequency. Aldehydes with a carbonyl frequency higher than  $1750\text{ cm.}^{-1}$  (chloral,

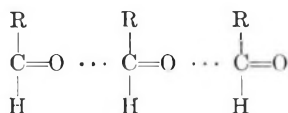
\* Part of this paper was presented at the Gordon Conference on Polymers, New London, New Hampshire, July 1962, and at the meeting on Mechanism of Stereospecificity, Moretonhampstead, Devon, England, May 1962.

formaldehyde) polymerize readily with rather weak nucleophiles such as pyridine. Alkali alkoxides are needed for the polymerization of saturated aldehydes ( $1750\text{--}1725\text{ cm.}^{-1}$ ), while special methods will be required for the polymerization of carbonyl compounds with a frequency of less than  $1725\text{ cm.}^{-1}$ . The decrease of the carbonyl frequency also parallels an increase in the electron density at the carbonyl carbon, which tends to hinder the polymerization of the carbonyl double bond (acrolein, acetone). In order to polymerize such carbonyl compounds, means of reducing the electron density on the carbonyl carbon will have to be developed. It may prove possible to correlate directly the infrared frequency of the carbonyl double bond of the monomer with its heat of polymerization, and, assuming a constant entropy, to estimate ceiling temperature of the polymer.

Hydrate and hemiacetal formation from carbonyl compounds parallel polymerizability. Chloral and formaldehyde exist almost exclusively as hydrates in aqueous solution and as hemiacetals in alcohol; aliphatic aldehydes are in equilibrium with about 50% of their hydrates and hemiacetals, while acetone is less than 1% hydrated.<sup>6,7</sup>

### Condition of the Monomer Solution before Polymerization

Polymerization of aldehydes must be performed at low temperatures, most advantageously at  $-78^\circ\text{C}$ . Best results are obtained in solvents of low dielectric constant. Schneider has shown that aldehyde molecules are associated in aggregates because of their dipole-dipole interaction.<sup>8</sup>



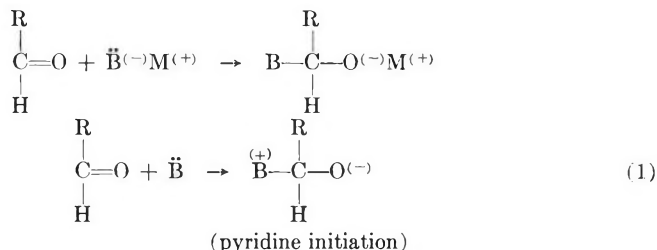
In changing from pentane to solvents with higher dielectric constants such as ethylene, toluene, or ether, the extent of aggregation will be decreased, although some molecular orientation doubtless remains. It should be pointed out that this orientation or "prearrangement" of the monomer in solution, or even in the crystalline state, is not alone sufficient to insure the production of a stereoregular polymer. This was also observed by Letort,<sup>9,10</sup> who polymerized acetaldehyde but could not detect any stereoregularity in the polymer. Even more impressive is the fact that poly(methyl methacrylate) prepared by polymerization of crystalline poly(methacrylic acid) monomer, followed by esterification, is more atactic than that prepared from methyl methacrylate monomer in solution.<sup>11</sup>

### Anionic Polymerization

Polymerization consists of initiation, propagation, and termination (or transfer). Lack of polymerization may be caused by failure to initiate or by inability of the initiated species to propagate.

*Initiation*

Anionic initiation of aldehyde polymerization requires the addition of nucleophile to the carbonyl carbon [eq. (1)] and with the placement of a cationic "gegenion" at the carbonyl oxygen.



Recent infrared studies have established the existence of such complexes in several cases.<sup>12</sup> The resultant alkoxide is capable of propagation with the proper carbonyl compound. These additions are equilibrium reactions, and polymerization can occur only when the equilibrium lies to the right or the subsequent propagation step is very fast.

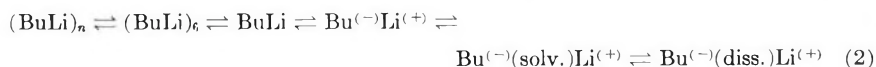
In the case of chloral and formaldehyde, tertiary amines are adequate nucleophiles, while alkali alkoxides, alkyls, and Grignard reagents are necessary for aliphatic aldehydes.

Polymerization of highly purified aldehyde has been accomplished with an initiator concentration as low as 0.05% of potassium triphenylmethoxide. If acid is present, one equivalent of the initiator is consumed to neutralize the acid.

*Propagation*

We prefer to separate propagation into two parts: the early propagation, where the rate of  $k_1$  to perhaps  $k_6$  is not constant, and the constant propagation rate,  $k_n$ .

**Nature of the Oxygen-Metal Bond.** Initiation and course of propagation in some olefin polymerizations (styrene, dienes) are greatly influenced by the nature of the metal-carbon bond. In particular, butyllithium initiation has been extensively studied. Butyllithium exists in numerous homopolar forms in solvents of low dielectric constants; in addition the following ionic species [eq. (2)] have either been demonstrated or postulated:<sup>13,14</sup> intimate ion-pair, solvated ion-pair, and dissociated ion-pair.<sup>15,16</sup>



The situation is much simpler in anionic aldehyde polymerization. Alkali alkoxides are the only important anionic catalysts, since other initiators, such as butyllithium or Grignard reagents immediately form alkoxides by addition to the monomeric aldehyde.

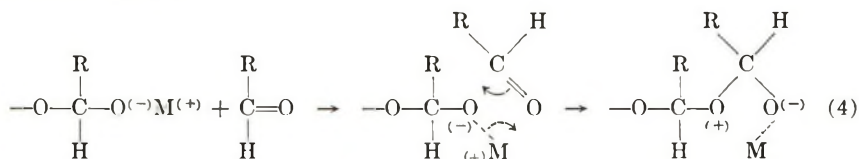
It is generally accepted that the oxygen-metal bond is for all practical purposes ionic. Therefore, we have to consider only the following species

[eq. (3)]: intimate ion-pair, solvated ion pair, dissociated ion-pair, and, for insoluble initiator, the crystal structure.



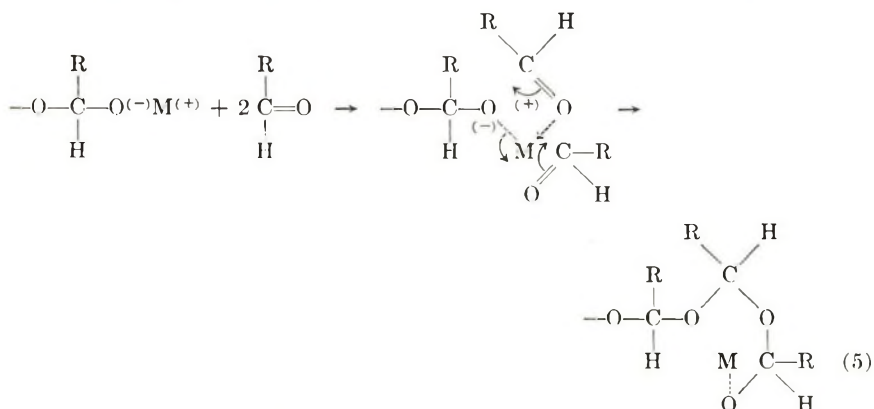
Intimate and solvated ion pairs might be considered as a single species in solvents of low dielectric constant ( $\epsilon$ ), where  $\epsilon_{\text{monomer}} > \epsilon_{\text{solvent}}$ , because the solvation is governed by the relatively polar monomer. The anionic polymerization of aldehydes requires solvents of low dielectric constant; solvents with a high dielectric constant (acetonitrile, trimethyl orthoformate, dimethylformamide) promote extensive dissociation of the oxygen metal ion pair and inhibit the polymerization.

**Method of Propagation.** As a first approximation, propagation of aldehyde polymerization presumably involves a four-center intermediate as shown in eq. (4):



However, three facts have to be added to this simple concept: (1) stereoregular polyaldehyde always precipitates during polymerization; (2) during polymerization less than half of the monomer is in solution, and the rest is adsorbed on the polymer chain;<sup>4</sup> (3) the metal cation is most likely tetra-coordinate, rather than dicoordinate, under these conditions.

We propose, therefore, a mechanism in which more than one monomer unit is involved in the transition state of propagation, as shown in eq. (5).



The fourth coordination is satisfied with an ether oxygen of the growing polymer chain; this "next neighbor" is probably the oxygen of the penultimate unit, but the metal ion could also coordinate with the oxygen one unit further back in the chain. This arrangement would assure the polymer's growing in a helical configuration.<sup>17</sup>

Until a few years ago stereoregularity in isotactic polymerizations was associated with insolubility of the initiator, and "lock and key" explanations were proposed which ascribed stereoregularity to particular surface arrangements in the crystal lattice of the initiator.<sup>18,19</sup> The discovery of soluble initiators for stereo-selective isotactic polymerizations has eliminated this concept as a necessary requirement.<sup>20,21</sup>

It might be argued that inhomogeneity is a necessary requirement for the propagation of isotactic polymerizations and, in fact, all known stereoselective aldehyde polymerizations become heterogeneous during polymerizations. However, we have no evidence whether the polymerization occurs at the precipitated polymer-solution boundary or in solution with subsequent precipitation of the polymer. In either case, however, the growing end can be in a helical conformation, supporting the recent idea advanced by Szwarc<sup>17</sup> and Ham<sup>22</sup> that stereoselective polymerization proceeds in such a way that the helix of the isotactic polymer is formed immediately.

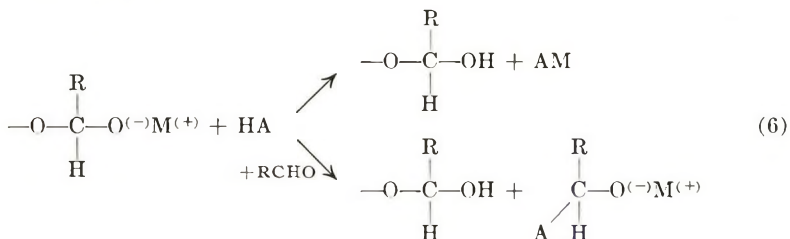
Another known fact of olefin polymerization seems to be true in aldehyde polymerizations: namely, that stereoregularity in the polymer increases with increased bulkiness of the side chain. Poly-*n*-heptaldehyde is completely crystalline, while polyacetaldehyde has rarely more than a 40% isotactic fraction.

We suggest that high stereoselectivity, at least in aldehyde polymerization, is caused by the attainment of the proper rate of polymerization. This can be achieved by proper combination of initiator, solvent (solvation), temperature, and structure of the monomer (size of the side chain).

#### Chain Transfer

When the average degree of polymerization in high conversion polymerization is lower than expected from the initiator concentration, chain transfer is suspected. Transfer during aldehyde polymerization could arise by: proton transfer from adventitious chain-transfer agents; proton transfer from monomer; and hydride transfer to monomer.

**Proton Transfer from Adventitious Chain-Transfer Agents.** Chain-transfer agents must be able to form an anion capable of initiating a new polymer chain [eq. (6)].



While one would normally expect hydroxylic compounds, such as water or alcohols, to function effectively as chain-transfer agents in anionic aldehyde polymerization, our experience indicates that this is not the case. The

deliberate addition of 1–3 mole-% of water or butanol to the system did not greatly reduce the molecular weight of the product. However, if the hydroxyl compound was present in the monomer prior to the addition of the catalyst the conversion to polymer dropped; this effect did not occur if a mixture of the hydroxyl compound and initiator solution was added to the monomer (see Table I). The data seem to indicate that the aldehyde hydrate or hemiacetal is capable of functioning as a chain terminator, with the former more effective than the latter.

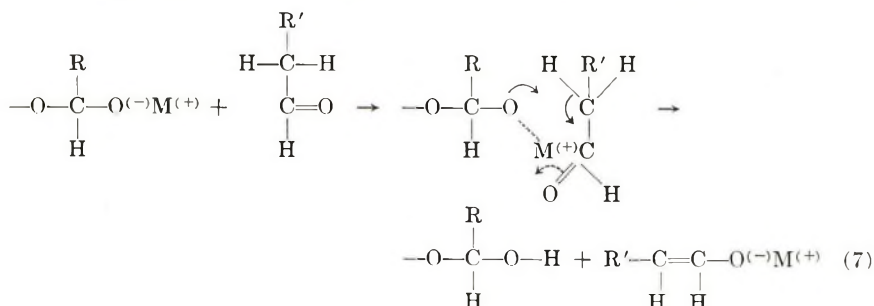
TABLE I  
Intentional Addition of Chain-Transfer Agents<sup>a</sup>

Chain transfer agent	Amt. chain transfer agent, mole-% based on monomer	Conversion, %
None	—	80–95
<i>n</i> -Butanol in pentane and initiator	0.8	86
<i>n</i> -Butanol in monomer	1	70
Water in pentane and initiator	4	89
Water in monomer	4	14
Phenol in pentane and initiator	0.8	2.6 <sup>b</sup>
Butyric acid in monomer (undistilled aldehyde)	1.7	2.5 <sup>b</sup>

<sup>a</sup> Initial reaction temperature,  $-75^{\circ}\text{C}.$ ; initiator, potassium triphenylmethoxide (0.15 mole-%); solvent, pentane, monomer; *n*-butyraldehyde (4:1).

<sup>b</sup> Some residual activity of the initiator is probably due to incomplete neutralization of the catalysts at low temperatures in low dielectric-constant solution.

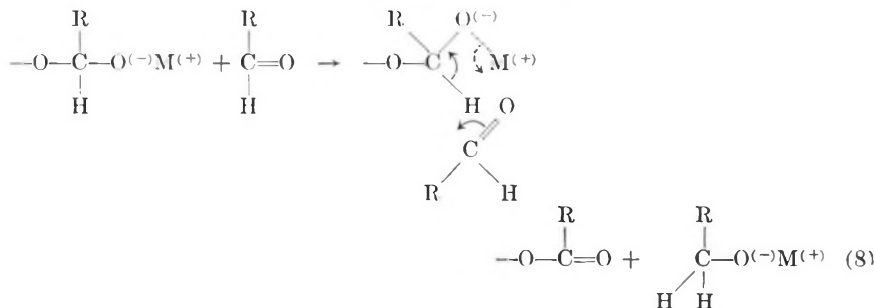
**Proton Transfer from Monomer.** Aliphatic aldehydes have a fairly acidic  $\alpha$ -hydrogen, and proton abstraction by the growing chain from the monomer is likely. Alternately, it is possible that the enol form of the aldehyde serves as a chain-transfer agent and this would give the same end result [eq. (7)]. Aldehyde enolates are claimed to be the active initiators in the polymerization of aldehydes with alkali metals.<sup>4</sup>



Unfortunately, chain transfer with the monomer has not been definitively established, since it is difficult to detect the vinyl ether ends resulting from enolate initiation in the infrared spectrum of aldehyde polymers.



**Hydride Transfer to Monomer.** Hydride transfer from the growing chain to the carbonyl carbon of the monomer results in the formation of an ester endgroup and the alkoxide corresponding to the monomer, capable of initiating a new chain, as shown in eq. (8). Since these ester-



capped chains are stable, we were able to isolate about 3–6% of the ester-capped crystalline polymer by allowing the uncapped polymer to depolymerize in hot tetrahydronaphthalene. A similar hydride transfer has been proved to be the important step in the Tishchenko and Cannizzaro reaction.

#### Termination

Termination is noticeable by decreased conversion. It occurs by reaction with "transfer agents" that produce anions incapable of initiating a new polymer chain. Examples are water, organic acids, phenols (see preceding section).

When chain ends are not terminated and chain growth can be revived by the addition of more monomer, the polymers are said to be "living."<sup>23,24</sup> The experimental evidence shows that a substantial portion of the polyaldehyde chain ends are "living."\* In the case of the polyaldehydes some difficulty arises because the polymer precipitates during the polymerization and a number of the "living" ends become occluded or "grown in." They cannot propagate further because monomer cannot reach the propagating site, but they can depolymerize upon heating (depropagate). Occluded ends apparently are responsible for erratic results and low yields during acetate end capping.

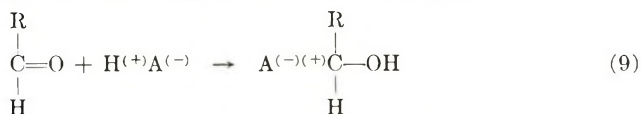
#### Cationic Polymerization

Cationic initiators may be conveniently placed into three groups. Some of them have been discussed in the past<sup>25,26</sup> but shall be included here for completeness.

\* We have carried out a normal polymerization of *n*-butyraldehyde with potassium triphenylmethoxide as the initiator. After the reaction was complete, it was kept for 4 hr. at reaction temperature and then an equal amount of *n*-butyraldehyde was added. After the normal work-up a yield of 135% (calculated for the original amount) of  $\eta_{inh} = 0.26$  was obtained. A control experiment under identical conditions, but without the second addition of monomer, gave a 78% yield of polymer with a  $\eta_{inh} = 0.24$ . Chain transfer according to eq. (7) seems to establish a "steady-state" molecular weight under these reaction conditions.

*Protic Acids*

Protic acids add across the double bond of the carbonyl compound leaving one hydroxyl endgroup and a growing carbonium ion [eq. (9)].



The initiation should be influenced only by the capability of the acid to protonate the carbonyl oxygen. The propagation requires low nucleophilicity of the counter ion  $\text{A}^-$  in order to avoid termination by recombination with the carbonium ion; such structures as



are unstable, even when A is moderately nucleophilic (e.g., when A is iodide).

*Carbonium or Acylium Ions*

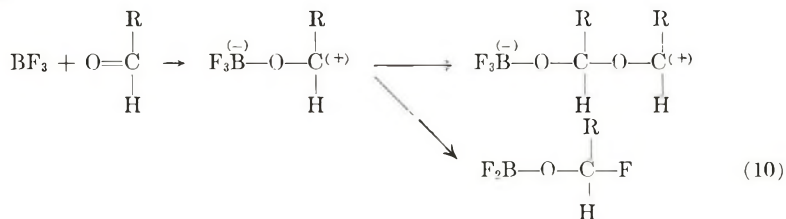
Alkylation or acylation of the carbonyl oxygen by stable carbonium ions<sup>27,28</sup> (acetyl tetrafluoroborate, triphenylmethyl perchlorate) is another convenient means of initiation for many types of polymerization.<sup>29-31</sup> Although it has not been tried in higher aldehyde polymerizations, these initiators should be very fast and should yield a polymer with one stable acyl or alkyl end-group instead of a hydroxyl.

*Lewis Acids*

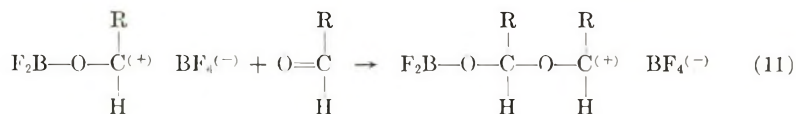
These initiators are perhaps the most widely used for cationic polymerization; they are also the most difficult to explain. Induction periods are observed with both olefin and aldehyde polymers.

In styrene polymerization it was demonstrated that a cocatalyst, such as water or alcohol, is necessary; and the actual polymerization initiator is a complex protic acid.<sup>30</sup> This scheme has also been adopted by some investigators for aldehyde polymerizations<sup>25,26</sup> by reasons of analogy.

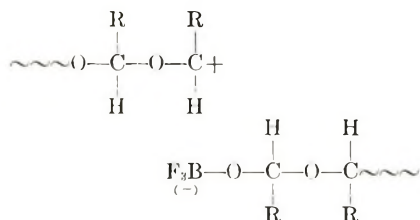
Another alternative mechanism for the initiation<sup>31</sup> of aldehyde polymerization which appears quite plausible has been offered [eq. (10)]. This involves addition of the Lewis acid ( $\text{BF}_3$ ) to the carbonyl compound, followed either by polymerization as such or by rearrangement of the dipolar adduct.



The compound formed in the "rearrangement" could in turn react with another molecule of  $\text{BF}_3$  as shown in eq. (11) to form a carbonium ion tetrafluoroborate, which is a possible initiator for the polymerization.



In the case of the mechanism shown in eq. (10) it is difficult to see charge separation beyond three monomer units, unless one suggests chain growth in two directions:

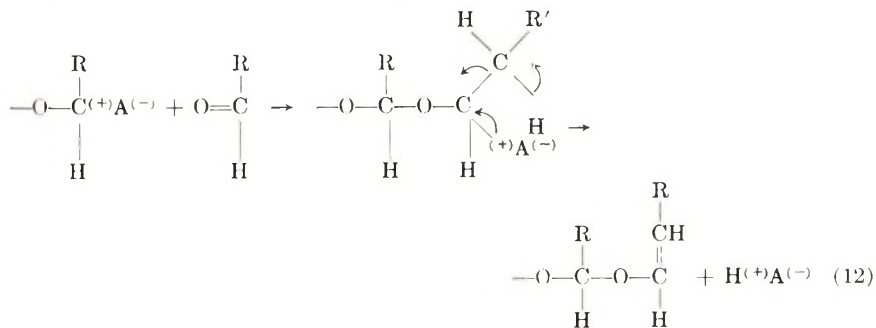


In the case of the mechanism of eq. (11) there are no data in the literature describing the reaction of  $\text{BF}_3$  with carbonyl compounds to form products of the type shown.<sup>32</sup>

At the present we can say only that the actual initiator is formed by the addition of the Lewis acid to the aldehyde solution at  $-78^\circ\text{C}$ .

Termination and transfer have been investigated more thoroughly in anionic aldehyde polymerization, and much less is understood about the cationic mechanism.

Lewis acid initiators often give mixtures of amorphous and isotactic polyaldehydes. Amorphous polyaldehydes so prepared have a very high molecular weight, indicating the absence of chain transfer. However, the amorphous polymers obtained from the higher more hindered aldehydes have lower molecular weights than expected. The isotactic poly-*n*-butyraldehyde fraction obtained by Lewis acid-initiated polymerization has the same order of molecular weight as the isotactic material prepared by anionic polymerization. This fact suggests an equal amount of chain transfer in the two reactions, a possible mechanism for the cationic chain transfer being as shown in eq. (12):



### Stereoregularity in Cationic Polymerization

Stereoregularity was noticed in acetaldehyde polymerization only when solid borontrifluoride-etherate was used as the initiator.<sup>4</sup> The initial rate of polymerization apparently is slow enough at the solid initiator surface to permit the formation of the helical chain, and a very small amount of isotactic polyacetaldehyde is thus formed. A chain-transfer reaction apparently occurs also, and the polymerization changes to a nonstereoselective mechanism, particularly when the aldehyde alkyl group is rather small.

The bulkier propyl side chain of the *n*-butyraldehyde facilitates formation of the helix during polymerization. Thus, the SnBr<sub>4</sub>-initiated polymerization of *n*-butyraldehyde yields a 1:6 ratio of isotactic/amorphous polymer, as compared to a 1:200 ratio obtained from acetaldehyde. (There is some evidence indicating that SnBr<sub>4</sub> gives a greater fraction of isotactic polymer than does BF<sub>3</sub> etherate. This might be expected in view of the ability of the large Sn atom to expand its valence shell to a coordination number of 6, enabling it to hold two monomer molecules in just the right position for isotactic propagation.)

### Stereoregularity and Degree of Polymerization

Cationic polymerization (BF<sub>3</sub>) of acetaldehyde gives amorphous polymer of very high molecular weight (DP ≈ 40,000). The reaction is almost explosive, even at very low temperatures. Anionically initiated stereoregular polymers are of lower degree of polymerization by about two magnitudes, and the rate of polymerization is slower. As the reactions were carried out under essentially the same environment with reagents of the same purity, the differences in molecular weight must be due to the relative rates of polymerization and chain transfer.

### Stereoblock Polymer

In our experimental work on isolating highly crystalline polyacetaldehyde (butyllithium-initiated polymerization) or poly-*n*-butyraldehyde (SnBr<sub>4</sub>-initiated polymerization) by extraction of the total polymer with acetone or ether, the polymer fractions obtained from successive extractions gave samples of varying consistency, ranging from soft and sticky polymers to firm and finally highly crystalline portions.<sup>4,33</sup> X-ray investigation showed that even the soluble fractions possessed low to moderate, but definite and increasing, crystallinity.

A similar extraction pattern was obtained with SnBr<sub>4</sub>-initiated *n*-butyraldehyde polymer. It seems reasonable to assume that these polymers are stereoblock polymers, and the crystallinity observed is due to some isotactic segments in the molecule.

### Side Reactions: Activation Energy of Aldehyde Polymerization

The reactions that aldehydes can undergo at room temperature and at higher temperatures in the presence of acids or bases are numerous. The

most important are the Tishchenko reaction, the aldol condensation, and, the Cannizzaro reaction. We may now ask why does polymerization occur at lower temperature and why was it not observed sooner? The answer is that the addition polymerization of aldehyde has the lowest activation energy of all aldehyde reactions and can thus proceed at quite low temperatures without interference. However, the uncapped polyaldehydes depolymerize in the temperature range  $-20$  to  $0^{\circ}\text{C}$ ., which thus represents the ceiling polymerization temperature. Therefore, polymerization does not compete with aldehyde reactions at room temperature and above.

In order to determine any side reaction of the monomer under polymerization conditions, we examined the nonpolymeric material remaining after polymerization at  $-75^{\circ}\text{C}$ . and found no trace of Tishchenko product by gas chromatography; at room temperature under the same conditions, butyl butyrate was formed rapidly in high yield.

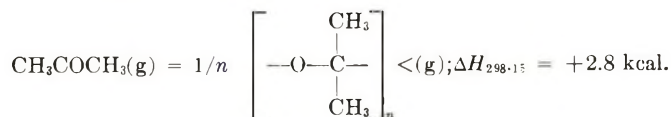
### Thermodynamics of Polymerization

Probably the only direct experimental value for the heat of polymerization of a higher aldehyde is that for the trimerization of acetaldehyde to paraldehyde measured by Cooper.<sup>34</sup> On the basis of the monomeric unit the enthalpy of polymerization,  $\Delta H$ , is  $-6.8$  kcal.

Although not yet realized experimentally, the polymerization of paraldehyde to polyacetaldehyde should involve an estimated heat effect,  $\Delta H$ , of  $0.0 \pm 0.5$  kcal./repeat unit.<sup>35</sup> This would result in a heat of polymerization ( $\Delta H^{\text{lc}}$ ) for acetaldehyde of about  $-6.8 \pm 0.5$  kcal. By analogy with 1-alkene polymers, higher aldehydes in the homologous series are expected to have a heat of polymerization only negligibly smaller than this value.

The temperature dependence of *n*-butyraldehyde polymerization has been studied. Extrapolation resulted in a value for the ceiling temperature<sup>36</sup> of  $-18^{\circ}\text{C}$ . Assuming the heat of polymerization of *n*-butyraldehyde is not different from that of acetaldehyde would permit calculation of an entropy of polymerization, ( $\Delta S_{255}^{\text{lc}}$ ) of  $-27.5$  e.u.

It is interesting to explore the degree of stability to be expected in polyacetone in view of recent claims that this material has been synthesized.<sup>37, 38</sup> The method of computing enthalpies of formation from structural increments of Andersen, Beyer, and Watson,<sup>39</sup> with appropriate revisions,<sup>40\*</sup> yields the following heat of polymerization:



With an allowance of 7.6 kcal. for the vaporization of acetone and an

\* Some revisions of the procedures of Andersen et al.<sup>39</sup> are included in the publication of Bryant.<sup>40</sup> In computing the enthalpy of the polymeric repeat unit, both the base and primary substitution contributions were omitted as these appear only once for the whole polymer molecule, and hence become negligible for the repeat unit.

estimated 4.7 kcal. for the polymeric unit, the heat of polymerization  $\Delta H_{298.15}^{\text{lc}}$  should be roughly  $+5.7 \pm 2.0$  kcal. The entropy change  $\Delta S_{298.15}^{\text{lc}}$  is estimated to be  $-28.8$  e.u., a reasonable value for the polymerization process.

Because the enthalpy is small, its endothermicity at  $25^\circ\text{C}$ . may possibly be reversed at quite low temperatures, since  $\Delta C_p$  becomes very important where  $\Delta H$  is small. However, our estimates of the heat capacities down to  $178^\circ\text{K}$ . suggest no change of sign above this temperature. Thus, it does not appear possible to compute a meaningful ceiling temperature for this reaction. At  $178^\circ\text{K}$ . the free energy change ( $\Delta F^{\text{lc}}$ ) is still  $+11.0$  kcal., well on the positive side of zero. However, the very marked changes in  $\Delta C_p$  expected below the glass temperatures of the components may introduce a short range of thermodynamic stability for this polymer.

We wish to thank Drs. F. C. McGrew and C. E. Schweitzer for their continued interest and encouragement. We are indebted to Dr. D. M. Simons for many enlightening discussions. The conscientious and skillful assistance of Mr. J. F. Mansure is greatly appreciated.

### References

1. Vogl, O., *J. Polymer Sci.*, **46**, 241 (1960).
2. Vogl, O., *Chem. Ind. (London)*, **1961**, 748.
3. Vogl, O., *J. Polymer Sci.*, **A2**, 4953 (1964).
4. Vogl, O., *J. Polymer Sci.*, **A2**, 4609 (1964).
5. Vogl, O., *J. Polymer Sci.*, **A2**, 4623 (1964).
6. Bayer, O., in *Methoden der Organischen Chemie*, Vol. VII, Part I, Sauerstoffverbindungen II, Fourth Ed., Houben-Weyl, Ed., Georg Thieme Verlag, Stuttgart, 1954, p. 416.
7. Bell, R. P., and A. O. McDougall, *Trans. Faraday Soc.*, **56**, 1281 (1960).
8. Schneider, W. G., and H. J. Bernstein, *Trans. Faraday Soc.*, **52**, 13 (1956).
9. Richard, A. J., *Acta Cryst.*, **1**, 645 (1954).
10. Letort, M., and A. J. Richard, *J. Chim. Phys.*, **1960**, 752.
11. Bovey, F., private communication.
12. Pestemer, M., and D. Lauerer, *Angew. Chem.*, **72**, 612 (1960).
13. Welch, F. J., *J. Am. Chem. Soc.*, **81**, 1345 (1959).
14. Bywater, S., and J. Worsfold, *Can. J. Chem.*, **38**, 1891 (1960).
15. Cram, D. J., A. Langemann, and F. Hauck, *J. Am. Chem. Soc.*, **81**, 5750 (1959).
16. Cram, D. J., K. P. Kopecky, F. Hauck, and A. Langemann, *J. Am. Chem. Soc.*, **81**, 5754 (1959).
17. Szwarc, M., *Chem. Ind. (London)*, **1958**, 1589.
18. Schildknecht, C. E., S. T. Gross, H. R. Davidson, J. M. Lambert, and A. O. Zoss, *Ind. Eng. Chem.*, **40**, 2104 (1948).
19. Natta, G., P. Pino, P. Corradini, F. Danusso, E. Mantica, G. Mazzanti, and G. Moraglio, *J. Am. Chem. Soc.*, **77**, 1708 (1955).
20. Breslow, D. S., and N. R. Newburg, *J. Am. Chem. Soc.*, **79**, 5072 (1955).
21. Patat, F., and H. Sinn, *Angew. Chem.*, **70**, 496 (1958).
22. Ham, G. E., *J. Polymer Sci.*, **46**, 475 (1960).
23. Szwarc, M., *Nature*, **178**, 1168 (1956).
24. Szwarc, M., M. Levy, and R. Milkovich, *J. Am. Chem. Soc.*, **78**, 2656 (1956).
25. Letort, M., and P. Mathis, *Compt. Rend.*, **249**, 274 (1959).
26. Furukawa, J., T. Saegusa, T. Tsuruta, H. Fujii, A. Kawasaki, and T. Tatano, *Makromol. Chem.*, **33**, 32 (1959).

27. Olah, G., and S. Kuhn, *Ber.*, **89**, 866 (1956).
28. Seel, F., *Z. Anorg. Allg. Chem.*, **250**, 331 (1943).
29. Evans, A. G., D. Holden, P. Plesch, M. Polanyi, H. Skinner, and M. A. Weinberger, *Nature*, **157**, 102 (1946).
30. Plesch, P. H., M. Polanyi, and H. A. Skinner, *J. Chem. Soc.*, **1947**, 257, 262.
31. Kern, W., H. Cherdron, and V. Jaacks, *Angew. Chem.*, **73**, 177 (1961).
32. Parshall, G., private communication.
33. Fujii, H., J. Furukawa, and T. Saegusa, *Makromol. Chem.*, **40**, 226 (1960).
34. Cooper, D. LeB., *Proc. Trans. Novu Scotian Inst. Sci.*, **17**, 82 (1927).
35. Dainton, F. S., K. J. Ivin, and D. A. G. Walmsley, *Trans. Faraday Soc.*, **56**, 1784 (1960) (See Table V).
36. Dainton, F. S., and K. J. Ivin, *Trans. Faraday Soc.*, **46**, 331 (1950).
37. Kargin, V. A., V. A. Kabanov, V. P. Zubov, and I. M. Papisov, *Dokl. Akad. Nauk SSSR*, **134**, 1098 (1960).
38. Furukawa, J., T. Saegusa, T. Tsuruta, S. Ohta, and G. Wasai, *Makromol. Chem.*, **52**, 230 (1962).
39. Andersen, J. W., G. H. Beyer, and K. M. Watson, *Natl. Petrol. News*, PR 476 (July 5, 1944).
40. Bryant, W. M. D., *J. Polymer Sci.*, **56**, 277 (1962).

### Résumé

Sur la base des résultats présentés antérieurement, on a examiné des mécanismes possibles de la polymérisation d'aldéhydes de haut poids moléculaire. On discute de l'influence des solvants de la température, de l'initiateur et du monomère sur la polymérisation en considérant surtout la stéréorégularité du polymère obtenu. On propose que plus qu'une unité de monomère prend part à l'étape de propagation. On admet que l'addition stéréosélective du monomère à la chaîne en croissance ainsi que la réaction de transfert de chaîne ont lieu d'une façon concertée. Le transfert de chaîne résulte dans la terminaison avec la formation de groupements terminaux hydroxyle, ester et probablement éther; des chaînes en croissance qui ne subissent pas de transfert forment des fins de chaînes vivantes lorsque tout le monomère a réagi. On a estimé quelques valeurs thermodynamiques pour les polymérisations de substances contenant une fonction carbonyle.

### Zusammenfassung

Auf Grundlage von in früheren Arbeiten mitgeteilten Ergebnissen werden mögliche Polymerisationsmechanismen höherer Aldehyde betrachtet. Der Einfluss von Lösungsmittel, Temperatur, Starter und Monomeren auf die Polymerisation wird mit besonderer Berücksichtigung der Stereoregularität des entstehenden Polymeren diskutiert. Die Beteiligung mehr als einer Monomereinheit beim Wachstumsschritt wird angenommen. Es wird angenommen, dass sowohl die stereoselektive Addition des Monomeren an die wachsende Kette als auch die Kettenübertragungsreaktion nach einem "Concerted"-Mechanismus verläuft. Die Kettenübertragung führt zur Bildung von Hydroxyl-, Ester- und möglicherweise Ätherendgruppen; wachsende Kettenenden, die keine Übertragung eingehen, bleiben nach Verbrauch des Monomeren als "lebende" Enden zurück. Einige thermodynamische Größen für die Carbonylpolymerisation werden bestimmt.

Received November 22, 1963

Revised January 13, 1964

## Electron Transfer Polymers. XXIII. Interactions of the Quinhydrone Type in Polyvinylhydroquinone Solutions

HIROYOSHI KAMOGAWA,\* YUEH-HUA CHEN GIZA,† and HAROLD G. CASSIDY, *Department of Chemistry, Yale University, New Haven, Connecticut*

### Synopsis

An investigation was made of the pink-orange color that reaches maximum intensity at the midpoint of the titration of homopolymers of vinylhydroquinone. It was shown that during oxidative titration the hydroquinone absorption at 295  $m\mu$  decreases in intensity while quinone absorption at 254  $m\mu$ , increases. At the midpoint of the titration absorption at approximately 455  $m\mu$ , the pink color, reaches its maximum intensity, with relatively low extinction coefficient. The position of the maxima does not change with extent of oxidation; the specific extinction coefficient is independent of concentration and degree of polymerization, but somewhat dependent on the nature of the solvent. When the functional groups were somewhat separated along the chain by copolymerization with an alternating comonomer, styrene,  $\alpha$ -methylstyrene, or acrylamide, there was no appreciable shift in the ultraviolet absorption peaks with oxidation, but in the visible region the intensity at 455  $m\mu$  was greatly decreased, compared with homopolymer, at all degrees of oxidation around the midpoint. Analysis of the spectroscopic data led to the conclusion that the number of quinhydrone-like interactions is low relative to the number of groups that are not interacting.

In the first paper explicitly on redox polymers<sup>1</sup> the term "electron exchange polymers" was used in the title because these substances were conceived in analogy to the proton-exchanging cation exchange resins. It was recognized that the analogy was not an exact one, and it was realized also that as an analogy becomes exact, it approaches an identity and then teaches us nothing new. That the term "electron exchange polymer" is not correctly descriptive of what occurs chemically with these polymers was discussed by Lange, Bonhoeffer, and Sansoni.<sup>2,3</sup> It was quite correctly pointed out that electrons are not exchanged in the redox process. Sansoni<sup>3,4</sup> suggested the generic name, "redox exchanger." He defined redox exchangers as solid and insoluble redox agents which are generally reversibly reducible-oxidizable and regenerable. He named two sub-

\* Present address: Textile Research Institute, 4 Sawatari, Kanagawa, Yokohama, Japan.

† Present address: Department of Chemistry, University of Notre Dame, Notre Dame, Indiana.



classes of redox exchangers: "redox ion exchangers," which are produced by bonding ionogenic redox systems to ion exchangers; and "redoxites," which are obtained by genuine chemical incorporation of reversible redox systems in a solid backbone,<sup>4</sup> "echten chemischen Einbau reversibler Redoxsysteme in ein festes Gerüst". Redoxites may be organic in nature, in which case they are named "redox resins," or inorganic in nature, in which case they are called "inorganic redoxites." Among the latter are the "redox minerals."

We have not taken to these names for two reasons. First, we wished to preserve the concept of an analogy, as embodied in "electron exchange polymer" until it could become familiar: and second, because we did not wish prematurely to forge a semantic cage for these substances. The name, redox exchanger, as defined by Sansoni excluded soluble polymers, with which we have chiefly worked, and it seemed to us that it would be better to wait to see how the field developed before proposing special names. At the same time we have from the very first used the general term "redox polymer" for these substances. It is a quite nonrestrictive term, and we included it as a subtitle to our first paper in the manuscript form. But a referee objected so strongly to this "Germanic" word, that we withdrew it from the final publication. (F. Helfferich is inadvertently in error on this matter.<sup>5</sup>)

Now we feel that the time has come to clarify nomenclature in a rational way—still using a minimum of special terms, but acknowledging that "electron exchange" is not nomenclaturally exact, even though it has a certain elegance.<sup>5</sup> We are, therefore, changing the name of our series of papers to "Electron Transfer Polymers" as a more formal title, and using the old name "redox polymers" informally for these substances. We will show in this and subsequent papers that the processes taking place with and within these polymers partake not only of electron transfer (explicit oxidation or reduction) but also of charge transfer (and perhaps of charge migration).

In the first paper on electron transfer polymers<sup>1</sup> it was reported that a polymerized vinylhydroquinone (later shown to be of low molecular weight) when oxidatively titrated took on a pinkish-orange coloration which reached maximum intensity at the midpoint of the titration and gave way, as the extent of oxidation increased, to the yellow color of the benzoquinone group. Various speculations were indulged in about the source of this color. We have come increasingly to the conclusion that the pink coloration is a manifestation of a quinhydrone-type interaction, brought about because donor (hydroquinonyl) and acceptor (quinonyl) groups can be held quite close together in their spacing along the flexible polymer chain, and thus be brought into position to interact.<sup>6</sup>

This conclusion was given some support by experiments in the titration of tetrahydroxybiphenyls.<sup>3</sup> When these 2,5,2',5'-tetrahydroxybiphenyls were oxidized, and when the resulting biquinones were reduced, orange, green, or bluish colors (depending on the substituents) appeared, waxed

in intensity to the midpoint and waned to the endpoint of the titration. Also, intensely colored crystalline quinhydrones could be isolated. The pink coloration was observed with low molecular weight material, with homopolymers of vinylhydroquinone, and with copolymers with  $\alpha$ -methylstyrene.<sup>1,6,8</sup>

It is known that hydroquinone and benzoquinone form an intensely colored complex in the solid state. When this substance is dissolved in polar solvents, for example water, the quinhydrone color disappears (to the eye) and what one sees is the yellow quinone color. Michaelis and Granick<sup>9</sup> concluded that in such solutions there must be less than 5% quinhydrone present. In nonaqueous solutions, free radical is present.<sup>10</sup> Apparently, the quinhydrone complex is dissociated strongly by aqueous and similar polar solvents. One would explain this as caused by solvation which is energetic enough to overcome the weak bonds of the quinhydrone complex, and which leads to bulky solvated molecules. These cannot easily approach each other closely enough to interact and yield evidence of charge transfer.

The polymer solutions which yield the pink-orange color upon titration are quite dilute—usually less than 0.1% concentration—and at such a dilution, quinhydrone itself does not give any visual evidence of color other than that of the quinone. Both polymer and quinhydrone give ultraviolet evidence of quinone and hydroquinone in equal amounts at the midpoint.<sup>8</sup> The color, therefore, must indicate some interaction that can be attributed to the fixing of the functional groups along the vinyl polymer chain. The recent development of a good method for the preparation of polyvinylhydroquinone in a high state of purity<sup>11</sup> has enabled us to present, in this paper, the results of a study of the effects of various factors upon color development, relations between ultraviolet spectra, and interactions. This development of color gives a new and potentially valuable method for studying the behavior of polymer chains in solution.

## EXPERIMENTAL

### Materials

**Polyvinylhydroquinone.** This polymer was obtained through lithium-initiated polymerization of vinyl-bis(1-ethoxyethyl)hydroquinone, followed by acid hydrolysis.<sup>11</sup> In a typical preparation, 50 g. of vinyl-bis(1-ethoxyethyl)hydroquinone was added to 150 ml. carefully purified tetrahydrofuran containing 1 g. lithium dispersion (Lithium Corp. of America; 30%). The round-bottomed flask, containing a magnetic stirring bar, was cooled in Dry Ice, evacuated to 0.1 mm., and sealed. The polymerization was allowed to continue for 72 hr. with stirring. During the first 30 min. it was necessary to cool the flask with water to moderate the violence of the initial reaction. The solution changed in color from light green through red-brown to light yellow. The flask was opened, the

highly viscous solution was diluted with a small amount of tetrahydrofuran and poured into a large quantity of methanol. The precipitated polymer was finally obtained in white, fluffy form by freeze-drying from benzene. A typical yield was 78%, with the intrinsic viscosity of the hydrolyzed polymer in 90% methanol 0.99 at 29.7°C.

For hydrolysis, 2 g. polymer were dispersed with vigorous stirring under nitrogen in 90 ml. absolute methanol to which had been added 10 ml. concentrated hydrochloric acid. Most of the polymer dissolved immediately, with development of a pink color. After stirring for 3 hr. at room temperature the solution was poured into concentrated aqueous sodium sulfate with rapid stirring to precipitate fine white polymer which was filtered and washed thoroughly with water. The hydrolyzed polymer was freeze-dried from *tert*-butyl alcohol containing about 5% water. A pale pink, fluffy polymer was obtained. It is fairly stable in the vacuum desiccator.

The yields of hydrolyzed polymer were almost quantitative, when the polymers were of relatively lower molecular weights ( $[\eta] = 0.3\text{--}0.5$ ). The higher molecular weight polymers were difficult to hydrolyze completely; also the amount of crosslinked and undissolved residue increased with molecular weight. With these materials, purified dioxane is recommended in place of methanol as solvent.

Polyvinylhydroquinone can be obtained, though in less pure form, from the dibenzoate. In earlier work we used alkaline hydrolysis for this preparation.<sup>6,8</sup> Another procedure was developed. A 1-g. portion of polyvinylhydroquinone dibenzoate<sup>12</sup> was suspended in a mixture of 10 ml. 60% perchloric acid and 20 ml. glacial acetic acid. Upon boiling for 5–10 min. the polymer dissolved completely to give a brownish solution. This was poured into a large amount of concentrated aqueous sodium sulfate to throw out a cloudy precipitate that could be separated by centrifugation. This precipitate was reduced with an aqueous hydrosulfite solution containing sodium bicarbonate, centrifuged down, and washed thoroughly with air-free water. Freeze-dried from 90% aqueous *tert*-butyl alcohol, it was obtained as a slightly brownish, fluffy material which gradually turned browner on exposure to air. It displays the characteristic ultraviolet and infrared spectra of polyvinylhydroquinone.

**Polyvinylquinone.** To 63.4 mg. of polyvinylhydroquinone ( $[\eta] = 0.42$ ) in 30 ml. 90% acetic acid was added dropwise, with vigorous stirring, 5 ml. of 0.181*N* bromine solution in the same solvent. This is one equivalent, based upon electrometric titration of the polymer, from which it is difficult to remove last traces of solvent. The resulting yellow precipitate was filtered, washed thoroughly with air-free water, and dried under reduced pressure. The oxidized polymer is soluble in cyclic ethers such as tetrahydrofuran and dioxane and in dimethylformamide; it is insoluble in aqueous alcohol or acetic acid. It is unstable in the sunlight and must be kept in the dark. The infrared spectrum (KBr) shows a sharp C=O absorption at 1650  $\text{cm.}^{-1}$  and its ultraviolet spectrum in a dioxane–90%

aqueous methanol (4:1 v/v) mixed solvent is characterized by a sharp absorption at  $254\text{ m}\mu$ .<sup>8</sup> Use of excess bromine in the titration broadens the ultraviolet band at  $254\text{ m}\mu$  and lessens the intensity of the absorption. It would be expected that substitution by bromine would occur as a reaction slower than the oxidation.

**Partially Oxidized Polyvinylhydroquinones.** Partially oxidized polymers were prepared by the same procedure as for polyvinylquinone. They were usually finely divided dark-brown materials and, especially in the case of the half-oxidized polymer, showed greatly decreased solubility—in some cases amounting to insolubility—in tetrahydrofuran and in dioxane-alcohol mixtures.

**Water-Soluble, Sulfonated Polyvinylhydroquinone and Its Copolymers.** These materials were prepared by treating polyvinylhydroquinone dibenzoate or its copolymers<sup>12</sup> with concentrated sulfuric acid for 30–50 min. at room temperature or slightly above, according to the procedure described elsewhere.<sup>8</sup> The resulting polymer solution, after dilution, was purified by dialysis against distilled water with the use of a cellophane bag.

## Methods

**Electronic Spectra.** The spectra of the polymer solutions were taken by means of a recording spectrophotometer, Spectronic 505 (Bausch & Lomb Co.). In the ultraviolet region 1 cm. cells were used exclusively; in the visible, 0.1 cm. cells were also used for the higher concentrations.

**Viscosity.** Viscosities were measured by means of a Cannon-Fenske-Ostwald type of viscometer at  $29.7^\circ\text{C}$ .

## RESULTS AND DISCUSSION

### Effect of Polymer Concentration on Color Intensity

In Tables I and II are shown values of the specific extinction coefficients ( $\epsilon_{sp}$ ) of partially oxidized polyvinylhydroquinones and of half-oxidized sulfonated polyvinylhydroquinones in relation to concentration.

The visible spectra of partially oxidized polyvinylhydroquinone in suitable solvents, such as dimethylformamide, tetrahydrofuran, and alcohol-dioxane mixtures, afford a distinct absorption band which has a maximum in the neighborhood of  $450\text{ m}\mu$ , and which shows much stronger absorption than is present in this region in the corresponding fully oxidized (quinone) polymer. The partially oxidized sulfonated polyvinylhydroquinones do not show any particular peak in the visible region because they are already somewhat discolored at the stage of acid treatment and subsequent dialysis.

The significant fact in these tables is that  $\epsilon_{sp}$  is independent of concentration within the measurable range in both cases. This relationship is independent of the degree of polymerization, but there are some differences among the solvents. The data may be interpreted to mean that

TABLE I  
Relation Between Polymer Concentration and Specific Extinction  
Coefficient in Partially Oxidized Polyvinylhydroquinone<sup>a</sup>

Polyvinyl- hydroquinone <sup>b</sup>	Concentration, g./l.	$\epsilon_{sp}$ <sup>c</sup>	
		455 m $\mu$	465 m $\mu$
A 50% Oxidized	0.111	1.31	
	0.221	1.33	
	0.443	1.24	
	0.886	1.22	
	1.39	—	1.24 <sup>d</sup>
	2.77	1.33	1.27
B 42.7% Oxidized	5.55	1.23	1.21
	0.150	1.07	
C 27.8% Oxidized	0.300	1.06	
	0.147	0.84	
	0.294	0.84	
	0.588	0.79	

<sup>a</sup> The solvent for spectroscopic measurements was dioxane-90% methanol = 4:1 (v/v).

<sup>b</sup> Viscosities of the polymers before oxidation, in 90% methanol at 29.7°C.; (A)  $[\eta] = 0.42$ ; (B), (C),  $[\eta] = 0.99$ .

<sup>c</sup>  $\epsilon_{sp} = D/lc$ , where  $D$  is optical density,  $l$  is length of path in cell in cm.; and  $c$  is concentration in g./l.

<sup>d</sup> The solvent was dimethylformamide.

TABLE II  
Relation Between Polymer Concentration and Specific Extinction Coefficient  
in Half-Oxidized Sulfonated Polyvinylhydroquinone<sup>a</sup>

Concentration, g./l. as polyvinyl hydroquinone dibenzoate	$\epsilon_{sp}$ <sup>b</sup>	
	370 m $\mu$	455 m $\mu$
1.37	0.617	0.303
0.685	0.680	0.365
0.392	0.638	0.314
0.229	0.623	0.297

<sup>a</sup> The polymer was oxidized with 0.1*N* ceric sulfate in 0.5*N* sulfuric acid. The inorganic ion was not removed, since cerous ion does not absorb appreciably in this region. The solvent was 0.5*N* sulfuric acid.

<sup>b</sup> No particular maxima were discerned in the visible region. For the definition of  $\epsilon_{sp}$ , see Table I.

interactions, if any, that are responsible for the color, are not intermolecular but intramolecular, at least below the concentration of 5 g./l., unless the polymer dissolves in some aggregated state, e.g., as micelles.

### Effect of Extent of Oxidation on Electronic Spectra

As shown in Figures 1 and 2 the absorption spectra of polyvinylhydroquinone in a suitable solvent undergo marked changes with extent of

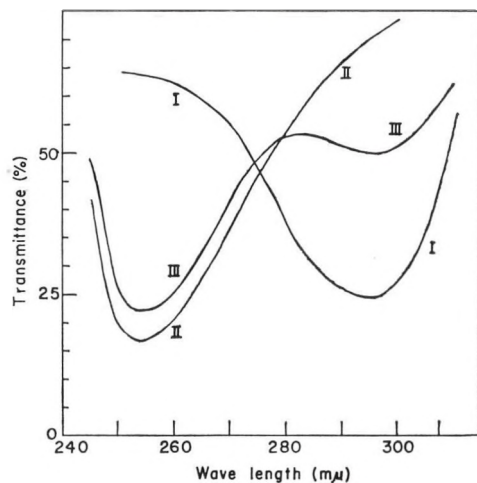


Fig. 1. Ultraviolet spectra of: (I) polyvinylhydroquinone (0.0240 g./l.); (II) polyvinylquinone (0.00620 g./l.); (III) polyvinylhydroquinone oxidized to the extent of 42.7% (0.0119 g./l.). The solvent is dioxane-90% methanol, 4:1. The transmittance is given in terms of the scale of the chart paper, and the curves cannot be compared quantitatively.

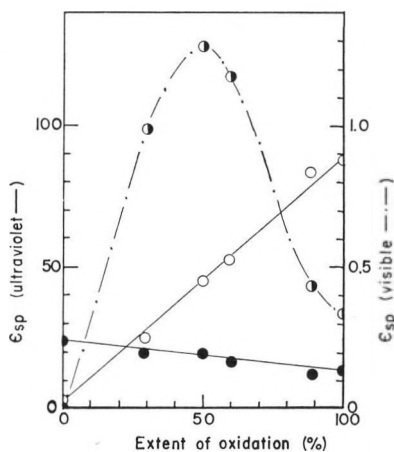


Fig. 2. Relationships between absorption intensities and extents of oxidation of polyvinylhydroquinone,  $[\eta] = 0.42$ , in dioxane-90% methanol, 4:1 solvent: (O) 254  $m\mu$  (quinone); (●) 295  $m\mu$  (hydroquinone); (⊙) 455  $m\mu$  ("quinhydrone"). The extent of oxidation is calculated from potentiometric data.  $\epsilon_{sp} = D/lc$ , where  $D$  represents optical density,  $l$ , internal length of cell in cm., and  $c$ , concentration in g./l.

oxidation. In Figure 1 is shown the change in ultraviolet absorption.<sup>8</sup> The absorption maximum at 295  $m\mu$  in dioxane-90% methanol (4:1 v/v), which is characteristic of the hydroquinone polymer, decreases in intensity as oxidation proceeds, and at the same time a new absorption at 254  $m\mu$  attributable to the quinone group appears and increases in intensity.

In the visible region, the pink-orange, or in more concentrated solutions, red-brown color attributable to some interaction of the functional groups of the polymer appears, intensifies with oxidation to about the midpoint, then decreases in intensity. The relationships are summarized in Figure 2. It is to be noted that in the ultraviolet spectra the two peaks (at 254 and 295  $m\mu$ ) did not shift in position, and that the relationship between  $\epsilon_{sp}$  and extent of oxidation is linear for both the quinone and the hydroquinone peaks. That there is no sharp isosbestic point in Figure 1 is attributable to the method of plotting. Only the shapes of the curves and the positions of the maxima are of interest; they are not corrected for shifts in 100% and 0% lines. The scale is that of the chart paper.

### Effect of Solvent on Extinction Coefficient

Since solvents for partially oxidized polyvinylhydroquinone are presently limited to those listed in Table III, we do not have available a wide variety of solvents for purposes of comparison. The available solvents are all polar, and may be assumed to interact with the functional groups of the polymer. The values of  $\epsilon_{sp}$  show some differences from each other among these solvents.

### Effect of Copolymerization with Inert Monomers

One way to isolate each functional group in vinylhydroquinone (VHQ) polymer is to copolymerize the monomer with an otherwise inert monomer that has the appropriate  $Q-e$  values.<sup>12</sup> This type of experiment was carried out, with the results given in Tables IV and V. Several kinds of copolymers obtained from vinylhydroquinone dibenzoate were halfoxidized and their ultraviolet spectra were compared with those of the completely oxidized polymer (the quinoid form) and the unoxidized polymer (substantially benzenoid form) as shown in Table IV. In no case was any appreciable shift in absorption peaks due to interactions between quinoid and benzenoid forms found. There was, however, an interesting result found in the behavior with respect to absorption intensities (Table V). With both vinylhydro-

TABLE III  
Dependence of Extinction Coefficient for 50% Oxidized Polyvinylhydroquinone  
Upon Kind of Solvent<sup>a</sup>

Solvent	$\epsilon_{sp}$ <sup>b</sup>	Absorption maximum, $m\mu$
Dioxane-90% methanol		
1:1	1.55	450
4:1	1.28	455
Tetrahydrofuran	1.30	450
Dimethylformamide	1.24	465

<sup>a</sup> The reduced polymer showed  $[\eta] = 0.42$  in 90% methanol at 29.7°C.

<sup>b</sup> For a definition of  $\epsilon_{sp}$  see Table I.

TABLE IV  
Relation Between Ultraviolet Maximum and Kind of Copolymer<sup>a</sup>

Polymer	VHQ, mole fraction	Absorption maximum, m $\mu$		
VHQ-styrene	0.0993		262	306
Half-oxidized	—	258	262	305
Completely oxidized	—	258		
VHQ- $\alpha$ -methylstyrene	0.418		263	305
Half-oxidized	—	258		304
Completely oxidized	—	258		
VHQ-acrylamide	0.130			304
Half-oxidized	—	258		304
Completely oxidized	—	258		
Polyvinylhydroquinone				300
Half-oxidized		258		300 <sup>b</sup>
Completely oxidized		258		
Isopropylhydroquinone				292
Completely oxidized		258		

<sup>a</sup> All polymers were of vinylhydroquinone dibenzoate origin and were sulfonated and dialyzed. Oxidation was with 0.1*N* ceric sulfate in 0.5*N* sulfuric acid. Optical measurements were made in 0.5*N* sulfuric acid.

<sup>b</sup> Only a shoulder present here.

TABLE V  
Relation Between Extinction Coefficient and Degree of Oxidation  
in Sulfonated Polymers<sup>a</sup>

Polymer	VHQ, mole fraction	Concentration, g./l. <sup>b</sup>	$\epsilon_{sp}$ (455 m $\mu$ )
VHQ-styrene	0.0993		
Half-oxidized		2.53	0.057
Completely oxidized		2.48	0.078
VHQ- $\alpha$ -methylstyrene	0.418		
Half-oxidized		0.0731	0.466 <sup>c</sup>
Completely oxidized		0.0730	1.23 <sup>c</sup>
Polyvinylhydroquinone			
Half-oxidized		0.444	0.678
Completely oxidized		0.437	0.232
Isopropylhydroquinone			
Half-oxidized		0.601	0.120
Completely oxidized		0.577	0.314

<sup>a</sup> Data are not to be compared quantitatively between polymers as all the materials were discolored somewhat by the acid treatment. The isopropylhydroquinone was given the same acid treatment.

<sup>b</sup> Concentrations were calculated for vinylhydroquinone dibenzoate copolymers and polymers in 0.5*N* sulfuric acid.

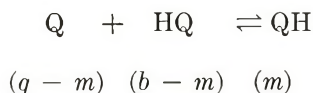
<sup>c</sup> Taken at 400 m $\mu$ .



quinone (VHQ)–styrene and VHQ– $\alpha$ -methylstyrene copolymers, the values of  $\epsilon_{sp}$  in the visible region are smaller for the half-oxidized polymers than for the fully oxidized polymers. This might be termed “noninteraction behavior,” since it is shown by isopropylhydroquinone. On the other hand, the  $\epsilon_{sp}$  in this region for half-oxidized VHQ homopolymer is larger than that for the fully oxidized polymer, thus indicating the presence of an interaction. The two copolymer systems are of alternating type<sup>12</sup> in which, on the average (especially since the comonomer was in excess), each VHQ moiety in the polymer chain is separated from the next by styrene or  $\alpha$ -methylstyrene, so that interactions between them are to this extent hindered. This might be the reason that there was no distinct color development in the half-oxidized copolymers, and might indicate that the color-producing interactions preferentially require immediately contiguous groups, that is, 1,3 or perhaps 1,5 along the polymer backbone, or close folding of the chain. Since no evidence for quinhydrone formation was observed with isopropyl-hydroquinone at a concentration as high as 0.6 g./l. (“noninteraction behavior”) there is here further support for the conclusion that the interactions shown by VHQ homopolymer are intramolecular.

### Correlation of Extent of Interaction with Polymer Composition

Since, as reported above, there was no appreciable effect of concentration within the measurable range upon extinction coefficient at the absorption maximum in the visible region, the possibility of the occurrence of interactions between two functional groups residing on two different polymer chains might be excluded. We can advantageously apply to the polymer results a formulation introduced by Michaelis and Granick.<sup>9</sup> Intramolecular associations (the postulated source of the color-producing interaction) which are affected by the ratios of quinoid and benzenoid components in the molecular chain are formulated on the assumption that a mass law holds:



where Q represents quinone, HQ hydroquinone, and QH quinhydrone;  $q$  and  $b$  are, respectively, the ratios of the initial quinoid and initial benzenoid components of the mixture, and  $m$  is the ratio of associated units. Then at equilibrium,

$$m/(q - m)(b - m) = k \quad (1)$$

The constant  $k$  might be expected to depend upon the kind of solvent, the temperature, the degree of polymerization in some cases, and the physical structure of the polymer.

If  $m$  were negligibly small as compared with  $q$  and  $b$ , then

$$m/qb \cong k \quad (2)$$

and  $m \propto \epsilon_a$ , where  $\epsilon_a = \epsilon_{sp} - \epsilon_q$ . Therefore, eq. (2) becomes

$$\epsilon_a/qb = k' \quad (3)$$

$\epsilon_a$  and  $\epsilon_q$  are specific extinction coefficients assignable to associated and quinoid components, respectively.  $\epsilon_{sp}$  is the measured extinction coefficient. The results based on this analysis are shown in Table VI.

TABLE VI  
Relation Between Extinction Coefficient and Polymer Composition

Experiment no. <sup>a</sup>	$q$ , Mole fraction	$b$ , Mole fraction	$\epsilon_{sp}$	$\epsilon_a$	$\epsilon_a/qb$	Difference from mean
1	0.50	0.50	1.28	1.11	4.45	+0.43
2	0.89	0.11	0.423	0.134	1.36	—
3	0.295	0.705	0.986	0.886	4.26	+0.24
4	0.59	0.41	1.17	0.97	4.02	0.0
5	0.28	0.72	0.822	0.929	3.63	-0.39
6	0.43	0.57	1.07	0.92	3.76	-0.26

<sup>a</sup> Experiments 1-4 were carried out with polyvinylhydroquinone polymer which, before oxidation, showed  $[\eta] = 0.42$  in 90% methanol at 29.7°C; experiments 5 and 6 with polymer  $[\eta] = 0.99$ . The optical measurements were made in dioxane-90% methanol (4:1 v/v).

It can be seen from this table that except for experiment 2, wherein the quinone component in the polymer is quite high, the values of  $\epsilon_a/qb$  are not too far from the mean of the results, 4.02, excluding that of experiment 2. Considering the experimental uncertainties, these results are conjectured to indicate, to a first approximation from the near constancy of  $k'$ , that the extent of interactions between the neighboring functional groups of the polymer chains under these conditions of solvent, and of incomplete equilibration, is fairly small. It should be remarked that these partially oxidized polymers were not equilibrated completely. This process would seem to require weeks of standing before equilibrium would be reached. What is provided is a provisional estimate of the extent of interaction: it is quite small. We have not considered it profitable to pursue with these data the more refined analyses of Rose and Drago.<sup>13</sup>

The small extent of interaction along the chain agrees with the observed low intensity of the pink coloration if it is also the case that this interaction is like other charge-transfer interactions in leading to an absorption band of high molecular extinction coefficient. That  $k'$  is not greatly affected by degree of polymerization endorses the conclusion that interactions take place between neighboring functional groups along the polymer molecule as described. The experiments with 2,5,2'5'-tetra-hydroxy-biphenyls<sup>7</sup> suggest that the rings may not have to be coplanar or stacked

one above the other for some interaction to occur, a conclusion arrived at by others.<sup>10,14</sup>

The conclusion that these interactions may not take place to a large extent can be supported by the linear relationships between  $\epsilon_{sp}$  of the ultraviolet spectra of hydroquinone and quinone peaks in the polymers, and the degree of oxidation (Fig. 2). It must be concluded that interactions take place only to the extent that they do not affect  $\epsilon_{sp}$  of, nor shift the positions of, the quinoid and hydroquinoid peaks.

Usually, charge-transfer interactions are recognized by the appearance of absorption bands of high intensity. We conjecture that the low absorption observed with these half-oxidized polymers is the result of low concentration of the interacting quinone and hydroquinone groups. When the half-oxidized material is isolated it is very dark in color, somewhat like quinhydrone. We think that if the polymer chains were prepared so that they could coil, there would be greater interaction of this kind. Molecular models show that while two groups in the 1,3 position along the chain can come quite close to each other, with the planes of the rings nearly parallel, that groups in the 1,5 position may fit much better. The question whether this contiguous relationship is requisite to the interaction is now under investigation.

We are pleased to acknowledge that this work has been supported by a PHS Research Grant GM 10864, National Institute of Arthritis and Metabolic Diseases, Public Health Service. We also thank Dr. Heinrich Hartmann and Mr. Robert E. Moser for providing some materials, and for giving advice during this work.

## References

1. Cassidy, H. G., *J. Am. Chem. Soc.*, **71**, 402 (1949).
2. Manecke, G., *Z. Elektrochem.*, **57**, 189 (1953); see the discussion on p. 194.
3. Sansoni, B., *Chem. Tech. (Berlin)*, **10**, 580 (1958).
4. Sansoni, B., *Anomalien Bei Ionenaustausch-Vorgängen*, vol. 1, 1961, p. 411.
5. Helfferich, F., *Ion Exchange*, McGraw-Hill, New York, 1962, see footnote to p. 551.
6. Ezrin, M., I. H. Updegraff, and H. G. Cassidy, *J. Am. Chem. Soc.*, **75**, 1610 (1953).
7. Giza, Y.-H. C., K. A. Kun, and H. G. Cassidy, *J. Org. Chem.*, **27**, 679 (1962).
8. Robinson, I. D., M. Fernandez-Refojo, and H. G. Cassidy, *J. Polymer Sci.*, **39**, 47 (1959).
9. Michaelis, L., and S. Granick, *J. Am. Chem. Soc.*, **66**, 1023 (1944).
10. Peover, M. E., *J. Chem. Soc.*, **1962**, 4540; Lindsey, A. S. M. E. Peover, and N. G. Savill, *J. Chem. Soc.*, **1962**, 4558.
11. Moser, R. E., H. Kamogawa, H. Hartmann, and H. G. Cassidy, *J. Polymer Sci.*, **A2**, 2401 (1964).
12. Kamogawa, H., and H. G. Cassidy, *J. Polymer Sci.*, **A1**, 1971 (1963).
13. Rose, N. J., and R. S. Drago, *J. Am. Chem. Soc.*, **81**, 6138 (1959); R. S. Drago and N. J. Rose, *J. Am. Chem. Soc.*, **81**, 6141 (1959).
14. Braude, E. A., *J. Chem. Soc.*, **1949**, 1902.

## Résumé

On a fait une étude de la couleur rose-orange, qui présente une intensité maximale au point d'équivalence de la titration des homopolymères de la vinylhydroquinone. On a

montré que pendant la titration par oxydation, l'intensité de l'absorption de l'hydroquinone à  $295\text{ m}\mu$  diminue, tandis que l'absorption de la quinone à  $295\text{ m}\mu$  augmente. Au point deéquivalence de la titration, l'absorption à environ  $455\text{ m}\mu$ , la "couleur rose" atteint son intensité maximale avec un coefficient d'extinction relativement bas. La position du maximum ne change pas avec l'avancement de l'oxydation; le coefficient spécifique d'extinction est indépendant de la concentration et du degré de polymérisation, mais est légèrement dépendant de la nature du solvant. Lorsque les groupements fonctionnels sont séparés le long de la chaîne par copolymérisation avec un comonomère comme le styrène, l'alpha-méthylstyrène, ou l'acrylamide, on n'observe presque pas de glissements des pics d'absorption dans l'ultraviolet avec l'oxydation, mais dans la région visible l'intensité à  $455\text{ m}\mu$  diminue fortement en comparaison avec l'homopolymère pour tous les degrés d'oxydation situés aux environs du point d'équivalence. L'analyse des données spectroscopiques fait conclure que le nombre des interactions du type quinhydrone est petit vis-à-vis du nombre des groupements qui ne présentent pas d'interaction.

### Zusammenfassung

Eine Untersuchung der rosa-orangen Farbe, die ihre Maximalintensität beim Umschlagpunkt der Titration von Vinylhydrochinonhomopolymeren erreicht, wurde angestellt. Es zeigt sich, dass die Intensität der Hydrochinonabsorption bei  $295\text{ m}\mu$  während der oxydativen Titration abnimmt, während die Chinonabsorption bei  $254\text{ m}\mu$  zunimmt. Beim Umschlagpunkt der Titration erreicht die Absorption der "rosa Farbe" bei ungefähr  $455\text{ m}\mu$  bei relativ niedrigen Extinctionskoeffizienten ihre Maximalintensität. Die Lage der Maxima ändert sich mit dem Oxydationsgrad nicht, der spezifische Extinktionskoeffizient ist von der Konzentration und dem Polymerisationsgrad unabhängig, dagegen etwas von der Art des Lösungsmittels abhängig. Wenn die funktionellen Gruppen durch Copolymerisation mit alternierenden Comonomeren, Styrol,  $\alpha$ -Methylstyrol oder Acrylamid entlang der Kette etwas separiert wurden, konnte keine merkliche Verschiebung der UV-Maxima mit der Oxydation beobachtet werden. Die Intensität bei  $455\text{ m}\mu$  im sichtbaren Bereich nahm jedoch im Vergleich zum Homopolymeren bei allen Oxydationsstufen um den Umschlagpunkt stark ab. Die Analyse der spektroskopischen Ergebnisse führt zu der Annahme, dass die Zahl der chinhydrontypigen Wechselwirkungen im Vergleich zu der Zahl der nicht wechselwirkenden Gruppen gering ist.

Received December 9, 1963

Revised January 22, 1964

## On the Theory of Divalent Ion Binding by Polyelectrolytes\*

ULRICH P. STRAUSS, *School of Chemistry, Rutgers, The State University, New Brunswick, New Jersey*, and SHNEIOR LIFSON, *Weizmann Institute of Science, Rehovoth, Israel*

### Synopsis

The problem of the binding of a divalent counterion by two adjacent binding sites of a uniform linear polyelectrolyte has been investigated for both finite and infinite chain lengths. Allowance has been made for interactions between adjoining ionized groups and for the presence of a univalent counterion which may also be bound. For the case of finite chain lengths, the partition function is obtained in terms of a  $3 \times 3$  matrix containing the conditional probabilities of the possible states of a polyelectrolyte group. By a novel method, the expression for the partition function is then simplified to a finite polynomial containing only the coefficients of the secular equation, but not its eigenvalues. From this expression for the partition function, the quasi-grand partition function for the infinitely long chain is calculated. It is shown that for both cases of finite and infinite chain length, closed explicit expressions relating the degrees of ionization and ion binding to the ion activities and the interaction parameter may be obtained from which the eigenvalues of the matrix have been eliminated. The applicability of the new method of calculation to other problems involving finite linear Ising lattices is briefly discussed.

### INTRODUCTION

In recent years the binding of divalent ions by polyelectrolytes has received increasing attention, both with synthetic<sup>1-6</sup> and biological<sup>7,8</sup> products. A general theoretical interpretation is made difficult by the complexity of the phenomenon. Thus, a divalent ion may be bound by one, two, or more fixed ionic groups of the macroion. These groups may be nearest neighbors, or, in the case of flexible polyelectrolytes, they may be widely separated along the chain. The latter case has been the basis of a number of treatments.<sup>1,2</sup> These treatments have necessarily been approximate; the problem is equivalent to that of the excluded volume effect in macromolecules which has not yet been solved rigorously. These treatments do not predict the general experimental observation that at high chain lengths of the macroion the binding results are independent of the chain length.<sup>6</sup> On the other hand, it is clear that the theoretical treat-

\* Part of this work was done while one of us (U. P. S.) was a National Science Foundation Senior Postdoctoral Fellow at the Centre de Recherches sur les Macromolécules, Strasbourg, France.

ments in terms of binding only by nearby groups must predict such an independence, besides avoiding the above-mentioned intrinsic difficulties in the mathematical technique. The nearest-neighbor approach has been employed by Irani and Callis,<sup>5</sup> who arbitrarily divided the chain into segments containing several binding groups, and by Hill,<sup>9</sup> who obtained a closed-form solution for the case involving two adjoining binding sites in the limit of infinite chain length and with the neglect of interactions between the fixed ionic groups.

In the present treatment we shall also limit ourselves to the case of a divalent ion being bound by two adjacent groups of a linear polyelectrolyte. However, we shall consider the coulomb interactions between adjoining ionized groups, and we shall treat both short- and long-chain polyelectrolytes. The techniques used include the matrix method<sup>9-13</sup> and the quasi-grand partition function which has recently been discussed and applied to the helix-coil transition in DNA.<sup>14</sup> It will be shown that despite the fact that the secular equation is cubic, closed-form solutions for the binding isotherms are obtained in both cases without the necessity of explicitly solving the cubic equation. The presence of univalent ions which may be bound to one polyelectrolyte site does not complicate the mathematics; we shall include one such species in our treatment.

## PARTITION FUNCTION AND BINDING PARAMETERS

### Case 1: Finite Chain Lengths

We consider a linear polyelectrolyte with  $P$  equally spaced identical ionizable groups assumed to be negative. The polyelectrolyte is immersed in and maintains equilibrium with an electrolyte solution containing both a species of univalent and one of divalent cations.

The following equilibria are considered:



where  $M$  denotes a univalent cation,  $D$  a divalent cation,  $(-)$  an ionized group,  $A$  a group associated with a univalent ion  $M$ , and  $C$  two adjacent groups associated with a divalent ion  $D$ . We shall use the letter  $a$  with the appropriate subscript to denote the activities of these ions and groups. We have then

$$a_A/a_-a_M = K_M \quad (3)$$

$$a_C/a_-^2a_D = K_D \quad (4)$$

where  $K_M$  and  $K_D$  may be considered as intrinsic binding constants of the uni- and divalent cations to one and two adjacent binding sites, respectively.\* The activities  $a_M$  and  $a_D$  refer to the immediate neighborhood of

\* While  $K_M$  does represent the binding constant of a monomer unit,  $K_D$  generally does not represent the binding constant of a dimer with  $D$ . We shall see later how the latter is related to  $K_D$  [see eq. (82)].

the macroion which is assumed to be at an electrostatic potential  $\psi$  with respect to the bulk of the solution. They are related to the corresponding activities in the bulk of the solution,  $a_M'$  and  $a_D'$  by

$$a_M = a_M' \exp \{-e\psi/kT\} \quad (5)$$

$$a_D = a_D' \exp \{-2e\psi/kT\} \quad (6)$$

where  $e$  is the positive electronic charge.

Each group on the polymer chain can exist in one of four states:  $(-)$ ,  $\overrightarrow{A}$ ,  $\overleftarrow{C}$ ,  $\overleftrightarrow{C}$ , where the latter two symbols denote the left and right partners, respectively, of a pair of adjacent groups associated with a divalent ion.\* As an example, a particular state of a chain with  $P = 5$  might be the following:  $(-)(-)\overrightarrow{A}\overleftrightarrow{C}\overleftarrow{C}$ . Its relative probability is given by the expression

$$a_- u a_- a_A a_C^{1/2} a_C'^{1/2} \quad (7)$$

where  $u = \exp(-E_{--}/kT)$ ,  $E_{--}$  being the energy of interaction between two adjoining ionized groups.† In order to avoid an excess of unknown parameters, the interactions between other groups which involve ion-dipole and dipole-dipole forces are neglected. Since  $E_{--}$  refers to a repulsion, the value of  $u$  must be between zero and unity.

Let us denote the partition function for the general case of  $P$  groups by  $Z_P$ . Since  $Z_P$  is the sum of terms like expression (7), we find the following equations for  $\theta_-$ , the degree of ionization, and for  $\theta_A$  and  $\theta_C$ , the degrees of binding of univalent and divalent ions, respectively.

$$\theta_-(P) = (a_-/P) (\partial \ln Z_P / \partial a_-) \quad (8)$$

$$\theta_A(P) = (a_A/P) (\partial \ln Z_P / \partial a_A) \quad (9)$$

$$\theta_C(P) = (a_C/P) (\partial \ln Z_P / \partial a_C) \quad (10)$$

It should be noted that  $\theta_C$  is the ratio of bound divalent ions to the number of binding sites and has a maximum value of  $1/2$ .

The partition function  $Z_P$  can be given in matrix notation as follows:

$$Z_P = \mathbf{wU(AU)}^{P-2}\mathbf{w}^+ \quad (11)$$

\* The endgroups can exist in only three states, since  $\overleftarrow{C}$  is impossible for the left end and  $\overrightarrow{C}$  for the right end. While because of the particular nature of the endgroups their activities might be different from those of the middle groups, any such differences are not considered here.

† Actually  $E_{--}$  has the meaning of a free energy of nearest-neighbor interactions averaged over all values of the internal rotation angles. For example, in a vinyl polymer we have

$$\exp\{-E_{--}/kT\} = (1/2\pi^2) \int_{\alpha} \int_{\psi} \exp\{-V(\varphi, \psi)\} d\varphi d\psi$$

where  $V$  is the electrostatic interaction between adjacent groups as a function of the two internal rotation angles between the bonds connecting the groups. For a more detailed discussion, see Lifson.<sup>15</sup>

where  $\mathbf{w}$  and  $\mathbf{w}^+$  are, respectively, the row and column vectors

$$\mathbf{w} = (a_-, a_A, a_C^{1/2}, 0) \quad \mathbf{w}^+ = (a_-, a_A, 0, a_C^{1/2})^* \quad (12)$$

and represent the chain end units. The asterisk is used to represent the transpose of a vector or matrix. The matrices  $\mathbf{A}$  and  $\mathbf{U}$  are given by the following scheme:

$$\mathbf{A} = \begin{pmatrix} a_- & 0 & 0 & 0 \\ 0 & a_A & 0 & 0 \\ 0 & 0 & a_C^{1/2} & 0 \\ 0 & 0 & 0 & a_C^{1/2} \end{pmatrix} \quad (13)$$

$$\mathbf{U} = \begin{array}{c|ccc} & \begin{array}{c} i+1 \\ \hline i \end{array} & \begin{array}{c} \vec{C} \\ \hline \vec{C} \end{array} & \begin{array}{c} \vec{C} \\ \hline \vec{C} \end{array} \\ \hline \begin{array}{c} \vec{C} \\ \hline \vec{C} \end{array} & \begin{array}{c} -A \\ \hline u \end{array} & \begin{array}{c} 1 \\ \hline 1 \end{array} & \begin{array}{c} 1 \\ \hline 1 \end{array} & \begin{array}{c} 0 \\ \hline 0 \end{array} \end{array} \quad (14)$$

where each term in  $\mathbf{U}$  represents the contribution of the interaction between the  $i$ th and  $(i + 1)$ st group to the corresponding term in the partition function.

With the similarity transformation

$$Z_P = [\mathbf{wUX}] [\mathbf{X}^{-1}\mathbf{AUX}]^{P-2} [\mathbf{X}^{-1}\mathbf{w}^+] \quad (15)$$

where

$$\mathbf{X} = \begin{pmatrix} 1 & 0 & 0 & 0 \\ 0 & 0 & -1 & a_A \\ 0 & 1 & 1 & -a_A \\ 0 & 0 & 0 & a_C^{1/2} \end{pmatrix} \quad (16)$$

$$\mathbf{X}^{-1} = \begin{pmatrix} 1 & 0 & 0 & 0 \\ 0 & 1 & 1 & 0 \\ 0 & -1 & 0 & a_A a_C^{-1/2} \\ 0 & 0 & 0 & a_C^{-1/2} \end{pmatrix}$$

the third rows and columns are reduced to 0, and the partition function is obtained in terms of a  $3 \times 3$  matrix,  $\mathbf{W}$ ,

$$Z_P = \mathbf{hW}^{P-2}\mathbf{h}^+ \quad (17)$$

where

$$\mathbf{h} = (ua_- + a_A, a_- + a_A, a_C) \quad (18)$$

$$\mathbf{h}^+ = (a_-, a_A, 1)^* \quad (19)$$

$$\mathbf{W} = \begin{pmatrix} ua_- & a_- & 0 \\ a_A & a_A & a_C \\ 1 & 1 & 0 \end{pmatrix} \quad (20)$$



It is convenient to define the row and column vectors

$$\begin{aligned} \mathbf{e} &= (1,1,0) \\ \mathbf{e}^+ &= (0,1,0)^* \end{aligned} \quad (21)$$

so that

$$\begin{aligned} \mathbf{h} &= \mathbf{eW} \\ \mathbf{h}^+ &= \mathbf{We}^+ \end{aligned} \quad (22)$$

Equation (17) now becomes

$$Z_P = \mathbf{eW}^P\mathbf{e}^+ \quad (23)$$

$Z_P$  is evaluated by transforming  $\mathbf{W}$  into the diagonal matrix

$$\Lambda = \mathbf{T}^{-1}\mathbf{WT} \quad (24)$$

so that

$$Z_P = \mathbf{eT}\Delta^P\mathbf{T}^{-1}\mathbf{e}^+ \quad (25)$$

The diagonal elements  $\lambda_1$ ,  $\lambda_2$ , and  $\lambda_3$  of  $\Lambda$  are the solutions of the secular equation of  $\mathbf{W}$

$$\lambda^3 = m\lambda^2 + n\lambda + q \quad (26)$$

where

$$m = ua_- + a_A \quad (27)$$

$$n = a_-a_A(1 - u) + a_C \quad (28)$$

$$q = a_-a_C(1 - u) \quad (29)$$

The columns of  $\mathbf{T}$  are right-hand eigenvectors of  $\mathbf{W}$  which satisfy the equations

$$\mathbf{W}\mathbf{t}_r^* = \lambda_r\mathbf{t}_r^* \quad r = 1, 2, 3$$

and the rows of  $\mathbf{T}^{-1}$  are left-hand eigenvectors of  $\mathbf{W}$  which satisfy the equations

$$\mathbf{s}_r\mathbf{W} = \lambda_r\mathbf{s}_r$$

We are free to choose proportionality factors for  $\mathbf{t}_r^*$  and  $\mathbf{s}_r$ , provided the condition  $\mathbf{TT}^{-1} = \mathbf{1}$  is satisfied. We choose them in such a way that  $\mathbf{t}_r^*$  and  $\mathbf{s}_r$  are given by

$$\begin{aligned} \mathbf{t}_r^* &= \{a_-/[\lambda_r + (1 - u)a_-], (a_A\lambda_r + a_C)/\lambda_r^2, 1/\lambda_r\}^* \\ \mathbf{s}_r &= C_r \{ \lambda_r/[\lambda_r + (1 - u)a_-], 1, a_C/\lambda_r \} \end{aligned} \quad (31)$$

where the  $C_r$  are the normalizing factors. This choice implies

$$\begin{aligned} \mathbf{eT} &= (1,1,1) \\ \mathbf{T}^{-1}\mathbf{e}^+ &= (C_1, C_2, C_3)^* \end{aligned} \quad (32)$$

and the normalizing factors  $C_r$  satisfying the equations

$$\sum_{r=1}^3 C_r = 1 \tag{33}$$

$$\sum_{r=1}^3 C_r/\lambda_r = 0 \tag{34}$$

$$\sum_{r=1}^3 C_r/\lambda_r^2 = 1/a_C \tag{35}$$

Equation (33) is obtained by forming the product of the two vectors in eq. (32) and noting that by eq. (21),  $\mathbf{e}^T \mathbf{T}^{-1} \mathbf{e}^+ = \mathbf{e} \mathbf{e}^+ = 1$ . Since  $\mathbf{T} \mathbf{T}^{-1} = \mathbf{1}$ , it is necessary that  $(\mathbf{T} \mathbf{T}^{-1})_{32} = 0$ , which leads to eq. (34), and that  $(\mathbf{T} \mathbf{T}^{-1})_{33} = 1$ , which leads to eq. (35).

With eq. (32), eq. (25) now becomes

$$Z_P = \sum_{r=1}^3 C_r \lambda_r^P \tag{36}$$

We shall obtain  $Z_P$  explicitly as a function of  $m$ ,  $n$ , and  $q$ , eliminating  $\lambda_r$  from eq. (36). We observe that by repeated application of the secular eq. (26), each value of  $\lambda_r$  must obey an equation of the form

$$\lambda_r^{P+2} = m_P \lambda_r^2 + n_P \lambda_r + q_P \quad r = 1, 2, 3 \tag{37}$$

for all values of  $P \geq 1$ , where the coefficients  $m_P$ ,  $n_P$ , and  $q_P$  are independent of  $r$ . Writing eq. (36) in the form

$$Z_P = \sum_{r=1}^3 (C_r/\lambda_r^2) \lambda_r^{P+2} \tag{38}$$

and applying successively eqs. (37) and (33)–(35), we obtain

$$Z_P = m_P + q_P/a_C \tag{39}$$

Recursion formulas for  $m_P$ ,  $n_P$ , and  $q_P$  can be obtained by multiplying eq. (37) by  $\lambda_r$  and applying eq. (26) to the right-hand side. Then

$$m_{P+1} = m m_P + n_P \tag{40}$$

$$n_{P+1} = n m_P + q_P \tag{41}$$

$$q_{P+1} = q m_P \tag{42}$$

which leads to

$$m_{P+1} = m m_P + n m_{P-1} + q m_{P-2} \tag{43}$$

Noting that by eqs. (26) and (37)

$$\begin{aligned} m_1 &= m \\ n_1 &= n \\ q_1 &= q \end{aligned} \tag{44}$$

we find by repeated applications of eqs. (40)–(43)

$$\begin{aligned} m_2 &= m^2 + n \\ m_3 &= m^3 + 2mn + q \\ m_4 &= m^4 + 3m^2n + n^2 + 2mq \\ m_P &= \sum_{t=0}^{[P/3]} \sum_{s=0}^{[(P-3t)/2]} \frac{(P-s-2t)!}{(P-2s-3t)!s!t!} m^{P-2s-3t} n^s q^t \end{aligned} \quad (45)$$

where the brackets indicate the integral part of the enclosed number.

Finally, on applying eqs. (42) and (29) to eq. (39) we have

$$Z_P = m_P + a(1-u)m_{P-1} \quad (46)$$

From this expression, both  $Z_P$  and the binding parameters  $\theta_-$ ,  $\theta_A$ , and  $\theta_C$  may now be obtained explicitly in terms of  $a_-$ ,  $a_A$ , and  $a_C$  by successive applications of eqs. (45), (27)–(29), and (8)–(10). While the computations involved become somewhat cumbersome as  $P$  increases, they are straightforward and need not be given here.

It is noteworthy that the procedure used here for eliminating  $\lambda_1$ ,  $\lambda_2$ , and  $\lambda_3$  from the partition function,  $Z_P$ , leads to expressions identical to those obtained by the combinatorial method and thus forms a bridge between the latter and the matrix method. The same procedure is also applicable to other Ising lattice problems involving linear polymers of finite chain length.

### Case 2: Large Chain Lengths

For large chain lengths it is inconvenient to use eqs. (45) and (46). Instead one may use two procedures: One involves the use of the largest eigenvalue of the matrix  $\mathbf{W}$ ,<sup>9-12</sup> the other the quasi-grand partition function.<sup>14</sup> We shall present here the latter method for the purpose of illustration. Following the procedure described by Lifson and Zimm<sup>14</sup>, we define the quasi-grand partition function

$$\Xi = \sum_{P=1}^{\infty} Z_P a^P \quad (47)$$

where  $a$  is a parameter independent of  $P$  whose value is to be determined later. Then by eq. (46),

$$\Xi = \sum_{P=1}^{\infty} m_P a^P + (1-u)a_- a \sum_{P=1}^{\infty} m_{P-1} a^{-1} \quad (48)$$

But, by eq. (45)

$$\sum_{P=1}^{\infty} m_P a^P = \sum_{P=1}^{\infty} \sum_{t=0}^{[P/3]} \sum_{s=0}^{[(P-3t)/2]} \frac{(P-s-2t)!}{(P-2s-3t)!s!t!} (am)^{P-2s-3t} (a^2n)^s (a^3q)^t$$

$$\begin{aligned}
 &= \sum_{P=1}^{\infty} (am + a^2n + a^3q)^P \\
 &= (1 - am - a^2n - a^3q)^{-1} - 1
 \end{aligned} \tag{49}$$

Hence

$$\Xi = \frac{1 + (1 - u)a_-a}{1 - am - a^2n - a^3q} - 1 \tag{50}$$

The binding parameters are determined from the equations

$$\theta_- = (\partial \Xi / \partial \ln a_-) / (\partial \Xi / \partial \ln a) \tag{51}$$

$$\theta_A = (\partial \Xi / \partial \ln a_A) / (\partial \Xi / \partial \ln a) \tag{52}$$

$$\theta_C = (\partial \Xi / \partial \ln a_C) / (\partial \Xi / \partial \ln a) \tag{53}$$

in the limit of arbitrarily large  $\Xi$ . This limit is obtained by choosing  $a$  so that  $\Xi$  just fails to converge, i.e., if  $a$  is chosen as the smallest positive solution of the equation

$$1 - am - a^2n - a^3q = 0 \tag{54}$$

By dividing this equation by  $a^3$  and comparing it with the secular eq. (26), we find

$$a = \lambda_{\max}^{-1} \tag{55}$$

which shows the equivalence of the quasi-grand partition function and matrix methods.

After carrying out the operation indicated by eqs. (51)–(53), simplifying the resulting expressions and subsequently applying eq. (54), we obtain

$$\theta_- = a_-[u + a_A(1 - u)a + a_C(1 - u)a^{-2}]F \tag{56}$$

$$\theta_A = a_A[1 + a_-(1 - u)a]F \tag{57}$$

$$\theta_C = a_C a[1 + a_-(1 - u)a]F \tag{58}$$

where

$$F = (m + 2na + 3qa^2)^{-1} \tag{59}$$

It remains to eliminate  $a$  from eqs. (56)–(58) by means of eq. (54). This objective can be accomplished without solving the latter equation as follows:

From eq. (54), and remembering the definitions (27)–(29), it can be shown that

$$[u + a_A(1 - u)a + a_C(1 - u)a^2][1 + a_-(1 - u)a] = 1 \tag{60}$$

Then multiplication of eqs. (56) and (57) leads to

$$F = (\theta_- \theta_A / a_- a_A)^{1/2} \tag{61}$$

The positive root is chosen because all the quantities contributing to  $F$  in eq. (59) are positive. Applying this to eq. (57) and solving for  $a$  we obtain

$$a = (w^{-1} - 1)/[a_-(1 - u)] \quad (62)$$

where  $w$  is defined as

$$w = (a_A\theta_-/a_-\theta_A)^{1/2} \quad (63)$$

Dividing eq. (58) by eq. (57) gives

$$a_C a = a_A \theta_C / \theta_A \quad (64)$$

which together with eqs. (62) and (63) leads to

$$a_C / \theta_C = (a_A / \theta_A) a_-(1 - u) / (w^{-1} - 1) \quad (65)$$

$$a_C / a_-^2 = (\theta_C / \theta_-) (1 - u) w^3 / (1 - w) \quad (66)$$

Equation (66) together with eq. (63) is one of the desired relations.

Another relation, giving  $w$  as a function of the  $\theta$ 's, will be obtained next.

Combining eqs. (56)–(58), we find

$$\theta_A + \theta_C - \theta_- = (a_A + a_C a - a_- u) F \quad (67)$$

After applying eqs. (61) and (64) to eliminate  $F$  and  $a_C a$ , respectively, eq. (63) to eliminate  $(a_A / a_-)$ , and rearranging terms, we find

$$(\theta_A + \theta_C) w^2 + (\theta_- - \theta_C - \theta_A) w - u \theta_- = 0 \quad (68)$$

The physically meaningful solution of this quadratic equation is

$$w = (1/2) (1 - R) + (1/2) [(1 - R)^2 + 4uR]^{1/2} \quad (69)$$

where  $R$ , the ratio of the number of ionized sites to the total number of bound counterions, is given by

$$R = \theta_- / (\theta_A + \theta_C) \quad (70)$$

With the use of eqs. (3) and (4), eqs. (63) and (66) can now be written

$$(\theta_A / \theta_- a_M) w^2 = K_M \quad (71)$$

$$(\theta_C / \theta_- a_D) (1 - u) w^3 / (1 - w) = K_D \quad (72)$$

where  $w$  is given by eqs. (69) and (70). These equations demonstrate how the mass action law is modified when the binding anions are no longer independent kinetic units but are tied into a chain.

When  $u = 1$ , which corresponds to no interactions between adjacent ionized sites, then  $w = 1$  by eq. (69), and eq. (72) cannot be used in its present form. Here the following power series expansion of eq. (69), valid for  $(1 - u) \ll 1$ , is useful:

$$w = 1 - [R/(1 + R)] (1 - u) - [R^2/(1 + R)^3] (1 - u)^2 + \dots \quad (73)$$

Equation (72) now simplifies to

$$\theta_C(1 - \theta_{-C})/\theta_{-}^2 a_D = K_D \quad (74)$$

where use has been made of eq. (70) and the relation

$$\theta_{-} + \theta_A + 2\theta_C = 1 \quad (75)$$

For the limiting case,  $u = 0$ , corresponding to infinitely strong interactions, it is necessary that  $R < 1$ . Then, by equation (69),  $w = 1 - R$ .

Two other limiting cases are of interest. When  $R \ll 1$  (large binding) eqs. (73) and (74) are both valid for all values of  $u$ , and it is seen that the results are independent of  $u$ . When  $R \gg 1$  (small binding), the expansion (73) is also valid for all values of  $u$ . For this important case eq. (72) simplifies to

$$(\theta_C/a_D)u^3 = K_D \quad R \gg 1 \quad (76)$$

It should be noted that eq. (72) and its simplified versions, eqs. (74) and (76), are also correct when there is no bound univalent ion. Similarly, eq. (71) applies in the absence of divalent ion and has already been derived for this case previously.<sup>12</sup>

If both bound univalent and bound divalent ions are present, it is frequently useful to combine eqs. (71) and (72) into the expression

$$\frac{(\theta_C/a_D')}{(\theta_A/a_M')^2} \frac{\theta_{-}(1-u)}{w(1-w)} = \frac{K_D}{K_M^2} \quad (77)$$

where  $a_M'$  and  $a_D'$  are given by eqs. (5) and (6). In this form, the equation can be applied without a knowledge of the potential  $\psi$ .

Some further insight can be obtained into the meaning of  $K_D$  by relating it to the binding constant for the dimer,  $K_2$ . The latter is given by the expression

$$[\mathcal{O}_2D]/[\mathcal{O}_2^{--}]a_D' = K_2 \quad (78)$$

where  $[\mathcal{O}_2D]$  and  $[\mathcal{O}_2^{--}]$  are the molar concentrations of the species  $\mathcal{O}_2D$  and  $\mathcal{O}_2^{--}$  whose activity coefficients have been neglected. In our notation, this equation can be written

$$2\theta_C/\theta_{-}a_D' = K_2 \quad (79)$$

provided there are no bound univalent ions. With the same proviso, eq. (46) gives the partition function

$$Z_2 = ua_{-}^2 + a_C \quad (80)$$

which, on applying eqs. (8), (10), and (4), becomes

$$2\theta_C/\theta_{-}a_D = K_D/u \quad (81)$$

In this case, the quantity  $u$  should account completely for electrostatic effects, and, therefore,  $\psi$  must be taken as zero.\* Then  $a_D = a_D'$ , and by

\* To be completely consistent, the values of  $\psi$  for the higher polymers should also be based on this zero point.

comparing eqs. (79) and (81) we obtain

$$K_D = uK_2 \quad (82)$$

which gives us the desired interpretation of  $K_D$ .

### References

1. Gregor, M. P., L. B. Luttinger, and E. M. Loebl, *J. Phys. Chem.*, **59**, 34, 366 (1955).
2. Morawetz, H., *J. Polymer Sci.*, **17**, 442 (1955); *ibid.*, **23**, 247 (1957).
3. Kotliar, A. M., and H. Morawetz, *J. Am. Chem. Soc.*, **77**, 3692 (1955).
4. Wall, F. T., and S. J. Gill, *J. Phys. Chem.*, **58**, 1128 (1954).
5. Irani, R. R., and C. F. Callis, *J. Phys. Chem.*, **64**, 1398 (1960).
6. Strauss, U. P., and A. Siegel, *J. Phys. Chem.*, **67**, 2683 (1963).
7. Zubay, G., and P. Doty, *Biochim. Biophys. Acta*, **29**, 47 (1958).
8. Felsenfeld, G., and S. Huang, *Biochim. Biophys. Acta*, **24**, 234 (1959); *ibid.*, **37**, 425 (1960); *ibid.*, **51**, 19 (1961).
9. Hill, T. L., *J. Polymer Sci.*, **23**, 549 (1957).
10. Kramers, H. A., and G. H. Wannier, *Phys. Rev.*, **60**, 252 (1951).
11. Onsager, L., *Phys. Rev.*, **65**, 117 (1944).
12. Lifson, S., *J. Chem. Phys.*, **26**, 727 (1957).
13. Lifson, S., and A. Roig, *J. Chem. Phys.*, **34**, 1963 (1961).
14. Lifson, S., and B. H. Zimm, *Biopolymers*, **1**, 15 (1963).
15. Lifson, S., *J. Chem. Phys.*, **29**, 89 (1958).

### Résumé

Le problème de la liaison d'un contre-ion bivalent par deux sites de liaison adjacents dans un polyélectrolyte linéaire uniforme a été étudié pour des longueurs de chaîne finie et infinie. On a tenu compte des interactions entre les groupements ionisés adjacents et de la présence d'un contre-ion monovalent qui peut également être lié. Dans le cas des longueurs de chaîne finies, la fonction de partage est obtenue à partir d'une matrice  $3 \times 3$  contenant les probabilités conditionnelles des états possibles d'un groupement polyélectrolytique. Par une nouvelle méthode, l'expression de la fonction de partage est alors simplifiée pour obtenir un polynôme fini contenant seulement les coefficients de l'équation séculaire, mais pas ses valeurs propres. A partir de cette expression de la fonction de partage, on calcule la quasi-grande fonction de partage des longues chaînes à l'infini. On a montré que dans le cas de longueur de chaîne finie et infinie, les expressions explicites reliant les degrés d'ionisation et la liaison ionique aux activités ioniques et au paramètre d'interaction peuvent être obtenues à partir de celle où les valeurs propres de la matrice ont été éliminées. On discute brièvement de l'application de cette nouvelle méthode de calcul à d'autres problèmes impliquant des réseaux linéaires finis d'Ising.

### Zusammenfassung

Das Problem der Bindung eines zweiwertigen Gegenions durch zwei benachbarte Bindungsstellen eines einheitlichen linearen Polyelektrolyten wurde sowohl für endliche als auch unendlich Kettenlänge untersucht. Die Wechselwirkung zwischen benachbarten ionisierten Gruppen und die Anwesenheit eines einwertigen Gegenions, das ebenso gebunden sein kann, wurde berücksichtigt. Für den Fall endlicher Kettenlänge wird die Verteilungsfunktion als  $3 \times 3$ -Matrix erhalten, die die Wahrscheinlichkeiten der möglichen Zustände einer Polyelektrolytgruppe enthält. Durch eine neue Methode wird der Ausdruck für die Verteilungsfunktion zu einem endlichen Polynom vereinfacht, das nur die Koeffizienten der Säkulargleichung, aber nicht ihre Eigenwerte enthält.

Aus diesem Ausdruck für die Verteilungsfunktion wird die quasi-Grand Verteilungsfunktion für die unendlich lange Kette berechnet. Es wird gezeigt, dass sowohl für den Fall der endlichen als auch der unendlichen Kettenlänge geschlossene explizite Ausdrücke, aus denen die Eigenwerte der Matrix eliminiert werden, für den Zusammenhang zwischen Ionenbindung sowie Ionenaktivität und Wechselwirkungsparameter erhalten werden können. Die Anwendbarkeit der neuen Berechnungsmethode auf andere Probleme, darunter endliche lineare Ising-Gitter, wird kurz diskutiert.

Received January 8, 1964



## Effect of Gamma Radiation on the Specific Volume of Polytetrafluoroethylene from $-80^{\circ}\text{C.}$ to $+40^{\circ}\text{C.}$

W. R. LICHT and D. E. KLINE, *Nuclear Engineering Department, The Pennsylvania State University, University Park, Pennsylvania*

### Synopsis

Specific volume vs. temperature relationships for  $\gamma$ -irradiated polytetrafluoroethylene (PTFE) samples ( $1/2$  in. diameter rods) have been studied over the  $-80$  to  $+40^{\circ}\text{C.}$  temperature range for radiation doses up to 890 Mrads. At low doses, the overall specific volume decreases with increasing dose. Between 100 and 300 Mrads the effect reverses, and the specific volume increases with dose up to 890 Mrads. As reported in the literature, an inflection point associated with the first-order crystalline transition appears in the specific volume curve near  $19^{\circ}\text{C.}$  for unirradiated PTFE. This inflection point loses definition and shifts to lower temperatures with increasing radiation dose. At 890 Mrads the inflection point has decreased about  $50^{\circ}\text{C.}$  to near  $-33^{\circ}\text{C.}$  Effects noted in irradiated PTFE are attributed to chain scission, changes in per cent crystallinity, and eventual disordering of the crystallites with increasing radiation dose. No significant difference in results are detected between samples irradiated in air and samples irradiated in vacuum-sealed containers.

### I. Introduction

It has been shown<sup>1,2</sup> that the irradiation of polytetrafluoroethylene (PTFE) can result in rather large changes in the density at relatively low doses (25 Mrads). At very low doses ( $\sim 10^3$  rads), one investigation<sup>1</sup> showed a slight decrease in density followed by a relatively sharp increase as the radiation dose increased. For doses in the range of 1-100 Mrads, both studies indicated significant increases in density.

Other effects have been noted to accompany the increase in density of PTFE with irradiation.<sup>2</sup> Per cent crystallinity by infrared techniques and density-based calculations both indicated an increase in crystallinity from approximately 60 to 80% for a 100-Mrad dose. X-ray analysis<sup>1</sup> has also confirmed the increase in crystallinity with dose. Dynamic mechanical property studies<sup>2</sup> have indicated that significant changes take place upon nuclear irradiation, to some extent consistent with increasing crystallinity. For instance, a reduction in the size of the damping peak at  $200^{\circ}\text{K.}$  (a peak which is presumed to be related to molecular motion in the amorphous regions) was considered to be indicative of an increase in crystallinity. The observed increase in dynamic modulus with dose between

175 and 500°C. was also consistent with increased crystallinity, as has been shown by McCrum.<sup>3</sup>

Usually the percentage of crystallinity in polymers decreases because the crystallites become disordered under irradiation. Since the density and crystallinity at room temperature were noted to increase in PTFE at doses up to 100 Mrads, one purpose of this study was to investigate the possibility of a decrease in density at higher doses due to gas evolution and break-up of the crystallites. Another purpose of the study was the investigation of the behavior of the crystalline transitions (19 and 30°C.) under irradiation. This work is a report of detailed volume-temperature studies of irradiated PTFE over the temperature range -80 to +40°C. and for  $\gamma$ -radiation doses ranging from 0 to 890 Mrads.

## II. Procedures and Sample Preparation

The specific volume of PTFE, as a function of temperature, was determined by first weighing samples in air and subsequently weighing them when submerged in a liquid of known density. The specific volume is then given by  $v_s = (W_a - W_1)/(W_a \rho_{liq})$  where  $W_a$  is the weight in air,  $W_1$  is the weight when immersed, and  $\rho_{liq}$  is the density of the liquid at the given temperature.

Polytetrafluoroethylene is well known for its resistance to solvents, therefore, selection of a liquid in which to weigh the samples depended primarily upon the temperature range over which the measurements were to be made. Ethyl alcohol (f.p. -117°C., b.p. 78°C.) was selected, and measurements showed that PTFE absorbed less than 0.01% its own weight in alcohol over the temperature range of interest. Density of the alcohol used was measured as a function of temperature employing a material of low expansion coefficient (Pyroceram). Measurements were made to establish the coefficient of expansion for Pyroceram over the -200°C. to +100°C. temperature range. This was found to be about  $1.9 \times 10^{-6}/^\circ\text{C}$ .

The room temperature volume of a piece of Pyroceram rod 2 in. long was determined from its weight loss when weighed in distilled water. The volume of a wire basket used to hold the specimen was determined in the same way. The value  $1.8 \times 10^{-5}/^\circ\text{C}$ . was taken as the coefficient of linear thermal expansion of the stainless steel basket. Since this volume is small, the coefficient is not critical. The volume expansion coefficient of both the Pyroceram standard and the basket was assumed to be three times the linear coefficient. When taking measurements, the sample was first cooled to about -100°C., then a rate of temperature rise of  $0.27 \pm 0.02^\circ\text{C}/\text{min}$ . was established and maintained by electrical heaters. Measurements were made every two degrees from -80°C. to +40°C.

Samples were received in the form of  $1/2$ -in. diameter rods formed from TFE #7 resin (a commercial product, E. I. du Pont de Nemours and Company, Inc.). The number-average molecular weight is thought to be more than  $5 \times 10^6$ . All irradiation of PTFE samples was carried out

in the 50 kc. Co<sup>60</sup>  $\gamma$ -ray source at the National Bureau of Standards in Washington, D. C. The exposure rate in air was approximately 10 Mr/hr. The conversion factor from roentgens in air to rads in PTFE is:

$$\frac{\text{Rads in PTFE}}{\text{Roentgens in air}} = \frac{(Z/A) \text{ for PTFE}}{(Z/A) \text{ for air}} \times \frac{0.877 \text{ rads in air}}{\text{Roentgens in air}} = 0.843$$

This is in agreement with the dose conversion of Florin, Wall, and Brown.<sup>4</sup> The estimated average dose received by each sample in this investigation is indicated in Table I.

TABLE I  
Characteristics of Samples Tested

Sample	Irradiation environment	Dose received, Mrads
A	Unirradiated	0
B	Air	9.6
C	Air	29
D	Air	96
E	Air	290
F	Air	890
G	Unirradiated	0
H	Vacuum-sealed	8.9
I	Vacuum-sealed	89
J	Vacuum-sealed	890

Variations in the dose rate which occur over the dimensions of the sample, combined with the limits of accuracy on the calibration of the source, make it necessary to place an accuracy limit of  $\pm 10\%$  on dose values of Table I. Samples H, I, and J were first heated and maintained at 100°C. in a partial vacuum maintained by a mechanical pump for approximately 24 hr., then sealed under vacuum in glass tubing for irradiation.

### III. Experimental Results

The specific volume of each sample was measured every two degrees from  $-80^{\circ}\text{C.}$  through  $+40^{\circ}\text{C.}$  Figure 1 is a plot of specific volume versus temperature for unirradiated sample A and the five samples irradiated in air (B through F). Figure 2 is a similar plot for unirradiated sample G and the three samples sealed in vacuum prior to irradiation (H through J). Comparison of the curves in Figure 2 with the corresponding curves in Figure 1 reveals that there is very little difference in the shape of the curves between the samples irradiated in air and those irradiated in vacuum sealed glass tubes. It is presumed that little of the oxygen already trapped in the PTFE samples was removed during the vacuum-sealing treatment.

Inspection of Figures 1 and 2 shows that radiation produced three significant changes in the specific volume versus temperature relationships of PTFE. First, it initially caused a decrease in specific volume at any tem-

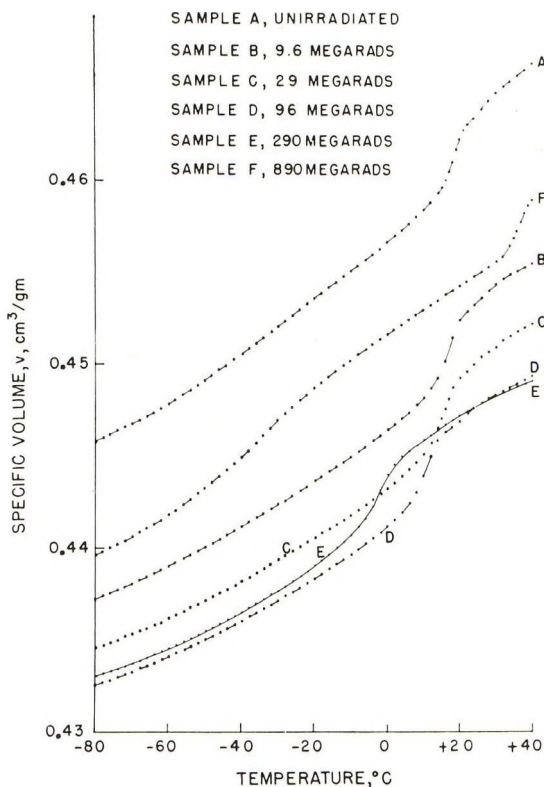


Fig. 1. Specific volume vs. temperature for PTFE samples irradiated in air.

perature. This appears to reach a minimum with doses in the range 100–300 Mrads. Additional radiation then resulted in an increase in specific volume. With doses up to 890 Mrads, the specific volume did not get as high as its initial value. Secondly, an increase in radiation dose lowered the temperature at which the first-order transition occurred. Finally, as dose was increased, the transition became broader, and identification of the temperature of the transition became more difficult.

The transition temperature was determined by plotting the derivative of the specific volume versus temperature curves. Figure 3 is a plot of the derivative versus temperature for the samples irradiated in vacuum-sealed containers. The transition was assumed to be at the temperature at which the derivative curve reached a peak. In the case of sample J (890 Mrads), the derivative did not have a sharp peak and the transition temperature was approximated to be  $-33^{\circ}\text{C}$ . It should be noted that the derivative curves also show some evidence of the second transition in PTFE at a slightly higher temperature ( $30^{\circ}\text{C}$ .) than the primary one, but the data are not conclusive here because of the scatter.

An unexpected sudden increase in specific volume with temperature occurred, beginning at about  $+30^{\circ}\text{C}$ ., for the sample which had received

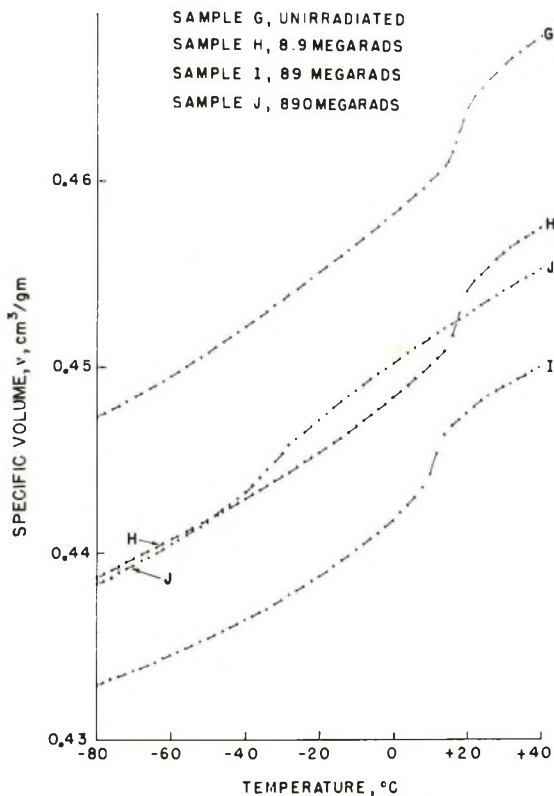


Fig. 2. Specific volume vs. temperature for PTFE samples irradiated in vacuum-sealed glass tubes.

890 Mrads in air (sample F). A similar phenomenon has been observed at higher temperatures and lower doses by Havlik, Udlock, and Kline<sup>5</sup> during preliminary linear expansion studies of irradiated PTFE.

It can be observed in Figure 3 that at first the radiation (8.9 Mrads) resulted in reducing the transition temperature approximately 1°C. A tenfold increase in dose lowered the transition temperature approximately another 6°C. Another tenfold increase in dose lowered the transition temperature to about -33°C. Figure 4 is a semilog plot of transition temperature versus dose for the samples irradiated in air. The line drawn represents the equation:

$$T = 292 \exp\{-2.5 \times 10^{-4}D\} \quad (6)$$

where  $T$  is the transition temperature (absolute) and  $D$  is the dose in megarads.

#### IV. Discussion of Results

The shape of the curves of specific volume versus temperature for the two unirradiated PTFE samples (sample A of Fig. 1 and sample G of Fig. 2) are

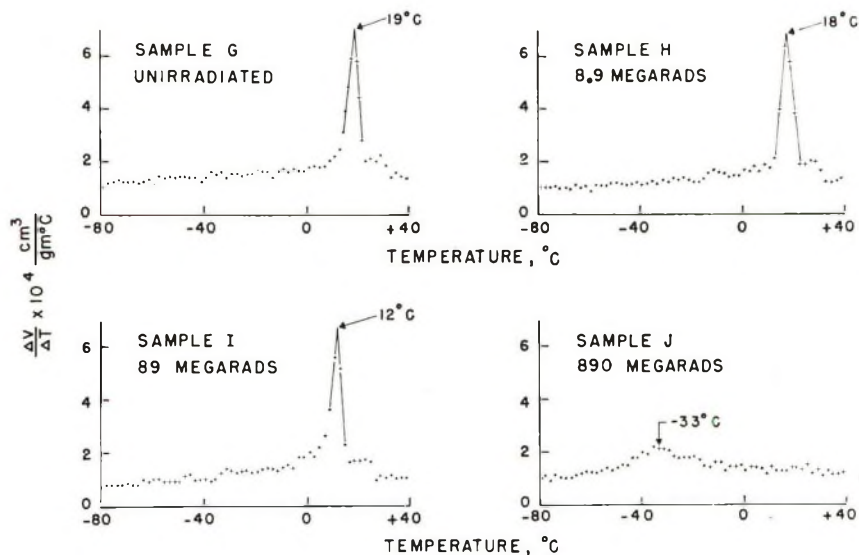


Fig. 3. Temperature derivative of specific volume as a function of temperature for PTFE samples irradiated in vacuum-sealed glass tubes.

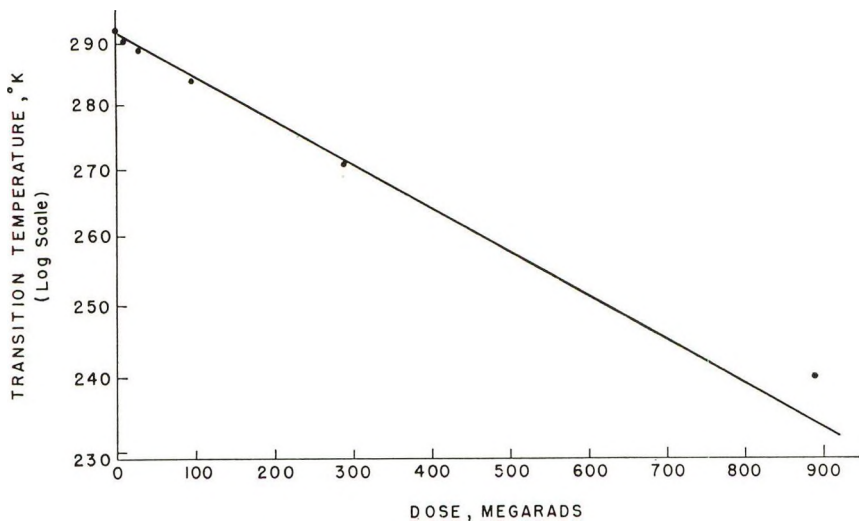


Fig. 4. Transition temperature vs. dose for PTFE samples irradiated in air.

essentially the same as those reported by previous investigators.<sup>6-8</sup> The specific volume of a PTFE sample at any temperature appears to be primarily dependent upon three variables: average molecular weight,<sup>9</sup> per cent crystallinity,<sup>10</sup> and void content.<sup>11</sup> Variations in these parameters result from difference in the polymerization and fabrication techniques.<sup>12</sup> Therefore, the absolute value of the specific volume of PTFE at any given temperature can be expected to vary from one specimen to another. This has been clearly demonstrated by Rigby and Bunn.<sup>6</sup>

In agreement with recent work done by Pierce et al., the first order crystalline transition was found to be in the vicinity of 19°C.<sup>13</sup> However, an error analysis based on our experimental procedure indicated that the exact temperature of the transition reported here may be subject to a variation of a few degrees, because of the possible accumulation of experimental errors. Since the same procedure was followed for all samples, the relative error from sample to sample is much less. Quinn et al.<sup>7</sup> showed that the temperature at which the transition appeared to take place was dependent upon the rate of temperature rise of the sample. The faster the temperature was increased, the higher the apparent transition temperature.

The initial decrease in specific volume with radiation observed in this investigation is in agreement with the results reported by Kline and Sauer<sup>2</sup> and by Nishioka, Tajima, and Owaka.<sup>1</sup> Kline and Sauer used infrared measurements to show that the increase in density with radiation dose (up to 100 Mrads of reactor radiation) was associated with an increase in per cent crystallinity. Similarly, Nishioka et al. used x-ray diffraction patterns to show that the increase in density at 21°C., with exposures in the range at  $10^4$ – $10^7$  rads of  $\gamma$ -radiation, was the result of an increase in crystallinity. This increase in density with dose can probably be considered to be the result of chain scission in PTFE irradiated in the presence of oxygen. Scission in the amorphous regions would tend to relieve strains or entanglements and permit further crystallization of the network. In partial support of this hypothesis, it has been shown by Doban, Knight, Peterson, and Sperati<sup>9</sup> that for unirradiated PTFE, with a given thermal history, the lower the average molecular weight of the PTFE specimen, the higher the density, and correspondingly the higher the crystallinity. Their work covered the range of number-average molecular weights of 500,000–8,000,000.

It is reasonable to assume that some disordering is produced in the existing crystallites during irradiation, and it has also been shown that gases, such as  $CF_4$ <sup>14</sup> and some higher fluorocarbons, are produced and evolved. Both of these effects would be associated with an increase in specific volume at any temperature, but, at low doses, the increase in overall per cent of crystallization causes a decrease in specific volume which masks these effects.

An estimation can be made of the expected increase in specific volume from sample E (290 Mrads) to sample F (890 Mrads), due to gas evolution only (i.e., assuming no corresponding decrease in dimensions). Assuming that the product evolved is fluorine and that the  $G$  value (atoms liberated per 100 e.v. absorbed) for this is about 0.6,\* the increase in specific volume would be about 0.7% compared to the observed increase of about 1.6%. It would thus appear that all the change in specific volume at this dose level is not entirely a result of gas evolution.

The first-order transition of PTFE, which occurs far below its melting point of 327°C., is considered rather unique among polymers, but it is not

\* The  $G$  value was estimated from the data of Florin and Wall<sup>14</sup> by taking the total fluorine contained in all the volatile products liberated as a result of irradiation.

unique among fluorocarbons. Bunn and Howells<sup>15</sup> used x-ray diffraction to study crystals of perfluorocetane,  $C_{16}F_{34}$ , which has a molecular weight of 838. They found that at room temperature its crystalline structure is very similar to that of PTFE well above 30°C., in that the molecules have a helical configuration and are packed in a hexagonal array which is highly ordered in two dimensions but not in the third. They reported that the diffraction patterns indicated a transition to a full-ordered crystal at about -170°C., which may be similar to the room temperature transition in PTFE. Thus, the lowering of the transition temperature in PTFE with radiation could be associated with decreasing the average molecular weight.

For an estimated overall  $G$  (scission) value of 0.3<sup>16</sup> for PTFE irradiated with oxygen present, the decrease in molecular weight can be calculated. As earlier stated, samples used in this investigation were fabricated from a resin which has a high number-average molecular weight, apparently more than  $5 \times 10^6$ . If it is assumed that main chain fracture occurs at random and is proportional to dose, a dose of 890 Mrads should reduce the number-average molecular weight to about  $4 \times 10^3$ . For an initial molecular weight in the range of  $5 \times 10^6$ , the exact value is not important to the calculation.

In addition to the shift in the temperature of the transition, which occurs with radiation dose, the transition becomes broader. This can be observed from the derivatives of the specific volume curves (Fig. 3). These infer that the very narrow temperature region, normally associated with a first-order transition is occurring over a range on the order of 20–30°C. for the samples which received 890 Mrads. This could be the result of disorder produced in the crystallites by the radiation, which has left them in states of varying degrees of perfection.

The presence of oxygen in PTFE during irradiation or after irradiation while radiation-induced free radicals are still present is known to greatly affect the post-irradiation properties,<sup>14,17,18</sup> and scission has been shown to predominate under these conditions. In the studies reported here, it is observed from Figures 1 and 2 that the results for air-irradiated samples are essentially the same as the results for samples maintained at 100°C. in vacuum for 24 hr. and subsequently vacuum-sealed for irradiation. This might imply that oxygen was initially present within the samples in both cases and that comparatively little diffusion of oxygen took place during heat treatment before vacuum-sealing or during irradiation. High temperatures were avoided to prevent any changes in crystallinity and specific volume which could be induced by annealing processes.

This research was supported in part by the National Science Foundation.



## References

1. Nishioka, A., M. Tajima, and M. Owaka, *J. Polymer Sci.*, **28**, 617 (1958).
2. Kline, D. E., and J. A. Sauer, *J. Polymer Sci.*, **A1**, 1621 (1963).
3. McCrum, N. G., *J. Polymer Sci.*, **34**, 355 (1959).
4. Florin, R. E., L. A. Wall, and D. W. Brown, *J. Res. Natl. Bur. Stds.*, **64A**, 269 (1960).
5. Havlik, A. J., D. E. Udlock, and D. E. Kline, unpublished preliminary results.
6. Rigby, H. A., and C. W. Bunn, *Nature*, **164**, 583 (1949).
7. Quinn, F. A., Jr., D. E. Roberts, and R. N. Work, *J. Appl. Phys.*, **22**, 1085 (1951).
8. Yasuda, T., and Y. Araki, *J. Appl. Polymer Sci.*, **5**, 331 (1961).
9. Doban, R. C., A. C. Knight, J. H. Peterson, and C. A. Sperati, paper presented at 130th National Meeting of the American Chemical Society, Atlantic City, New Jersey, September 18, 1956.
10. Sperati, C. A., and J. L. McPherson, paper presented at the 130th National Meeting of the American Chemical Society, Atlantic City, New Jersey, September 18, 1956.
11. N. G. McCrum, *ASTM Bull.*, **242**, 80 (1959).
12. Thomas, P. E., J. F. Lontz, C. A. Sperati, and J. L. McPherson, *SPE J.*, **12**, 89 (1956).
13. Pierce, R. H. H., Jr., E. S. Clark, J. F. Whitney, and W. M. D. Bryant, paper presented at the 130th National Meeting of the American Chemical Society, Atlantic City, New Jersey, September 18, 1956.
14. Florin, R. E., and L. A. Wall, *J. Res. Natl. Bur. Std.*, **65A**, 375 (1961).
15. Bunn, C. W., and E. R. Howells, *Nature*, **174**, 549 (1954).
16. Florin, R. E., and L. A. Wall, private communication.
17. Resroad, H. N., and W. Gordy, *J. Chem. Phys.*, **30**, 399 (1959).
18. Wall, L. A., *ASTM Spec. Tech. Publ. No. 276*, 208 (1959).

## Résumé

On a étudié le volume spécifique en fonction de la température pour des échantillons de polytétrafluoroéthylène (PTFE) (barres de  $1/2''$  de diamètre) irradiés par les rayons gamma dans un domaine de température s'étendant de  $-80^{\circ}\text{C}$  à  $+40^{\circ}\text{C}$  et pour des doses de radiations allant jusqu'à 890 mégarads. Pour des faibles doses le volume spécifique global diminue avec une augmentation de la dose. Entre 100 et 300 mégarads, les effets sont inversés et le volume spécifique augmente pour des doses allant jusqu'à 890 mégarads. En accord avec la littérature, un point d'inflexion associé à la transition cristalline de premier ordre apparaît dans la courbe du volume spécifique près de  $19^{\circ}\text{C}$  pour le PTFE non irradié. Ce point d'inflexion perd sa définition et se déplace vers les températures plus basses pour une augmentation de la dose de radiation. A 890 mégarads, le point d'inflexion a diminué d'environ  $50^{\circ}\text{C}$  aux environs de  $-33^{\circ}\text{C}$ . Les effets observés dans le PTFE irradié est attribué à une scission de chaîne, au changement dans le pourcentage de cristallinité et à un éventuel désordre dans les cristallites avec une augmentation de la dose. On n'a observé aucune différence importante dans les résultats pour des échantillons irradiés dans l'air et pour des échantillons irradiés dans des tubes scelés sous vide.

## Zusammenfassung

Die Temperaturabhängigkeit des spezifischen Volumens von gammabestrahlten Polytetrafluoräthylenproben (PTFE) (Stäbe mit Durchmesser von  $1/2''$ ) wurde über den Temperaturbereich von  $-80^{\circ}\text{C}$  bis  $+40^{\circ}\text{C}$  für Bestrahlungsdosen bis zu 890 Megarad untersucht. Bei niedrigen Dosen nimmt das spezifische Bruttovolumen mit steigender Dosis ab. Zwischen 100 und 300 Megarad kehrt sich der Effekt um, und das spezifische Volumen steigt mit der Dosis bis zu 890 Megarad an. Wie schon in der Literatur berichtet, erscheint bei nichtbestrahltem PTFE ein mit der kristallinen Umwandlung erster

Ordnung zusammenhängender Wendepunkt in der spezifischen-Volums-Kurve nahe bei  $19^{\circ}\text{C}$ . Dieser Wendepunkt verliert mit zunehmender Bestrahlungsdosis an Schärfe und verschiebt sich zu niedrigeren Temperaturen. Bei 890 Megarad hat der Wendepunkt um etwa  $50^{\circ}\text{C}$  auf  $-33^{\circ}\text{C}$  abgenommen. Die an bestrahltem PTFE beobachteten Effekte werden auf Kettenspaltung, Änderung der prozentuellen Kristallinität und Störung der Ordnung der Kristallite mit zunehmender Bestrahlungsdosis zurückgeführt. Zwischen den Ergebnissen an unter Luft bestrahlten Proben und im Vakuum eingeschmolzenen Proben treten keine signifikanten Unterschiede auf.

Received April 23, 1964

## Association Phenomena in Carboxyl-Containing Polymers\*

JOSEPH S. YUDELSON and RANDALL E. MACK,  
*Research Laboratories, Eastman Kodak Company, Rochester, New York*

### Synopsis

Gelation effects were studied as a function of pH for the following polymeric materials: alginic acid, poly(methyl acrylate *co* acrylic acid), poly(ethyl acrylate *co* acrylic acid), and phthalated ethylcellulose. The effects of various addenda were also studied. The results suggest a gelation mechanism for all the polymers which consists of a balance of repulsive force interactions due to ionization of carboxyl groups, and of attractive force interactions due to hydrogen bonding. The groups involved in hydrogen-bonding interactions are deduced. The melting points of phthalated ethylcellulose and poly(ethyl acrylate *co* acrylic acid) gels were obtained as a function of concentration and plots of  $\log c$  versus reciprocal absolute temperature of melting gave linear curves. The heat of reaction for the formation of crosslinks was  $-8 \pm 0.4$  kcal./mole crosslinks. This is much lower than values obtained for gelatin gels and suggests that a single crosslink contains 1-2 hydrogen bonds.

### INTRODUCTION

The change in viscosity that occurs when a solution of a carboxyl-containing polymer is made alkaline is well known. The molecular coil expands owing to the electrostatic repulsion of the carboxylate ions in the polymer chain, thus increasing the hydrodynamic dimensions. Therefore, as the pH of the solution is raised, the viscosity increases. As the degree of ionization approaches 100%, the viscosity value reaches a maximum.<sup>1,2</sup>

However, certain carboxyl-containing polymers show extraordinary viscosity maxima in a narrow pH region at degrees of ionization that are much less than 100%. Since this behavior occurs at concentrations greater than a critical value, it appears that intermolecular interactions are causing the viscosity increase. The viscosity value at the maximum is so great as to indicate gelation, yet the molecular volume (as determined by intrinsic viscosity measurements) in this narrow pH region (which we will call the "gelation pH") is usually one-third to one-half that measured at full ionization. In this paper we shall deduce the mechanism of this type of gelation phenomenon. In the work, we have followed the viscosity changes which occur upon the introduction of various addenda to aqueous solutions of algin, poly(ethyl acrylate *co* acrylic acid), poly(methyl acrylate *co*

\* Presented in part at the Symposium on Molecular Association Complexes of Polymers, 138th Meeting of the American Chemical Society, New York City, Sept. 13, 1960.

acrylic acid), and phthalated ethylcellulose. We have been particularly interested in addenda which would eliminate the gelation region for these polymers. Many of these addenda are well-known hydrogen-bond-breaking agents. By observation of their effects, we shall describe the important interactions leading to intermolecular association and gelation. The results should have a bearing on other polymer systems.

## EXPERIMENTAL

### Preparation of Polymers

Algin (sodium salt) was obtained from the Kelco Corporation. Potentiometric titration with 0.1*N* HCl gave a neutralization equivalent of 202.6 (theoret. 198.2) and the material was used without purification. Phthalated ethylcellulose (from the Cellulose Technology Division, Eastman Kodak Co., Rochester, N. Y.) was prepared by reaction of phthalic anhydride with ethylcellulose (Dow G-100) in glacial acetic acid at 80°C. for 6 hr., using sodium acetate as catalyst. The material was precipitated and washed with water. It contained 21.5% (by wt.) of phthaloyl group and 45.0% of ethoxyl. This corresponds to 2.3 and 0.4 ethoxyl and phthaloyl groups, respectively, per glucose ring. Poly(alkyl acrylate *co* acrylic acid) was prepared (by Dr. Donald A. Smith of these Laboratories) by refluxing alkyl acrylate and acrylic acid in acetone with azobisisobutyronitrile as catalyst. Refluxing overnight causes the polymerizations to go to completion. The polymers were precipitated and washed with water. Intrinsic viscosities in acetone ranged from 0.2 to 0.4. The acrylic acid content of these copolymers was obtained by potentiometric titration of the sodium salt with 0.1*N* HCl in isopropanol-water (1:1).

### Viscosity Measurements

Measurements of viscosity as a function of pH were made with a Brookfield LVT Viscometer, using the No. 2 spindle. The majority of the measurements were made at 6 rpm. Determinations of dilute solution of intrinsic viscosities were made with an Ostwald Funke-Cannon viscometer, S-100, which had a flow time of 67 sec. at 25°C. for water. All viscosity determinations were made at this temperature unless otherwise specified.

### pH Changes

The pH changes were produced by adding HCl or acetic anhydride to an aqueous solution of sodium or ammonium salt of the carboxyl-containing polymers. Dilute HCl (0.01 to 0.2*N*) was used for algin. For the other polymers, particularly those containing acrylic acid, the lowering of pH must be done with great care to avoid local precipitation. This was accomplished by adding acetic anhydride (Eastman Grade) by means of a microburet to a rapidly stirred polymer solution. The anhydride was added in small increments (ca. 0.02 ml.) and 10–15 min. elapsed from the time of addition before viscosity and pH measurements were taken.

## Melting Points

The melting points of the gels were measured by gelling a solution of the polymer in a 100-ml. beaker which contained a 1-in. magnetic stirring bar. The gels were aged for 24 hr. at 25°C. and the beaker was put into a small water bath which was on a magnetic stirrer-heater (Gyratherm-Will Corp.) The rotor was turned to full speed and the temperature of the bath raised at the rate of 0.5°C./min. The temperature at which the bar began to rotate was taken as the melting point. The melting points were reproducible to within  $\pm 0.3^\circ\text{C}$ . if the gel annealed at 25°C. for 24 hr. before the melting point determination. If the solution obtained by melting the gel was chilled rapidly and the melting point redetermined without the annealing period, the values varied erratically by  $\pm 2^\circ\text{C}$ .

## RESULTS

### Viscosity—pH Behavior of the Polymers

#### *Gelling Types*

Table I summarizes the data on the polymers which gelled. The polymer concentration is that needed to produce a maximum viscosity above 10,000 cpoise. The degree of ionization  $\alpha$  at the viscosity maximum obtained by titrations of 0.1–0.25% solutions, is an approximation because the degree of ionization is dependent on concentration. All of the polymers listed have viscosities below 500 cpoise when fully ionized at the concentrations listed. The viscosity maximum represents at least 50- to 100-fold increase over this value. Figure 1 shows the viscosity behavior of algin at several concentrations. For a 1% concentration, the viscosity rises to over 30,000 cpoise at pH 3.5 (the gelation pH). The maximum exists at 0.5% and is eliminated by further dilution to 0.25%. This demonstrates that intermolecular interactions are causing the maximum. The dotted curve illustrates the increase in molecular volume with pH as measured by the

TABLE I  
Carboxyl-Containing Polymers Which Showed Gelation Behavior

Polymer	COOH, mole-%	Concn., %	Gel point (pH)	$\alpha$
Algin (AA)		1	3.5	0.56
Phthalated ethylcellulose (PEC)	21.5*	2	5.0	0.13
Poly(ethyl acrylate <i>co</i> acrylic acid) (EAAA)	25	3	6.3	0.52
Poly(methyl acrylate <i>co</i> acrylic acid)(MAAA)	10	3	6.9	0.65
	15	3	6.3	0.72
	20	3	5.5	0.40
	25	3	5.4	0.44

\* Wt.-% Phthaloyl (45 wt.-% ethoxyl).

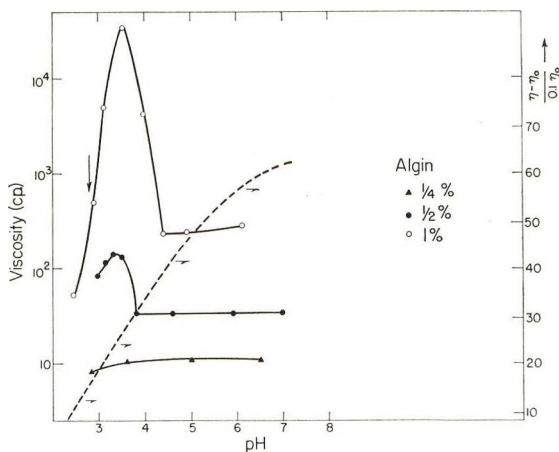


Fig. 1. Viscosity-pH data for algin (inherent viscosity on right side in dl./g.).

inherent viscosity of 0.1% solutions. The hydrodynamic volume of the algin molecule at the gelation point is estimated to be one-third of that which would be found at full ionization. It must be emphasized that the algin molecules are not precipitating out of solution at the gelation point. The solutions do not show any visible turbidity until the pH reaches 2.8, as shown by the arrow on the 1% curve. All the cases discussed showed no turbidity until the pH was lowered 0.5–1 pH unit below the value at the viscosity maximum.

The other gelling polymers, phthalated ethylcellulose and the alkyl acrylate-acrylic acid copolymers, behave as does algin. The acrylic acid-containing polymers showed no viscosity maxima (at the gelation pH) at concentrations of 1% or less, and the phthalated ethylcellulose showed no maximum at 0.75% or less. Ethyl acrylate copolymers made with 35 mole-% of acrylic acid showed very weak gelation behavior and methyl acrylate copolymers containing 30 mole-% acrylic acid did not show any gelation or viscosity increases at pH's that correspond to less than 100% ionization.

#### *Nongelling Carboxyl-Containing Polymers*

Polymers which did not show viscosity maxima but instead gave monotonically decreasing viscosity values with lowering of pH were: poly(alkyl methacrylate *co* acrylic acid) (30–60 mole-% of acid), poly(butyl acrylate *co* acrylic acid) (15–40 mole-%), poly(styrene *co* acrylic acid) (30–50%), poly(butadiene *co* acrylic acid) (15–35 mole-%), poly(butadiene *co* methacrylic acid) (15–35 mole-%), poly(vinyl acetate *co* crotonic acid) (5–12 mole-%), poly(vinyl methyl ether *co* maleic acid), poly(vinyl methyl ether *co* maleamic acid), poly(styrene *co* maleic acid) poly(acrylic acid), poly(methacrylic acid), pectin (citrus), gum arabic, and carboxymethyl cellulose (Hercules CMC-7HP and CMC-12HP). In this group of nongelling

polymers, concentrations as high as 10% were tested to bring out any intermolecular effects which might lead to viscosity maxima. Poly(galacturonic acid) showed gelation effects at the 5% level at pH 2.8. However, it precipitates out of solution at this pH and therefore was not included in this study.

### Addenda

The results obtained with the addenda will be divided into two parts: (1) the effects of addenda on the viscosity maximum using the concentrations listed in Table I for the various polymers, and (2) the effects of addenda on inherent viscosity values of dilute solutions of the polymers.

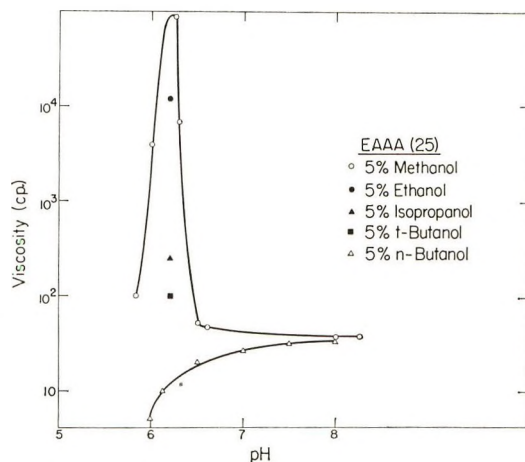


Fig. 2. Viscosity behavior of 3% EAAA (25) solutions. Maximum values only are shown for ethanol, isopropanol, and *tert*-butanol.

**Alcohols.** Alcohols had a pronounced effect on reducing the viscosity maxima. Figure 2 illustrates the effect for poly(ethyl acrylate *co* acrylic acid) [EAAA (25)] when a solvent mixture of 95/5 water-alcohol (v./v.) was used. Essentially the same results were observed with the methyl acrylate-acrylic acid (MAAA) copolymers and with phthalated ethylcellulose (PEC).<sup>\*</sup> Algin could not be studied because of precipitation caused by the addition of the alcohol. In Figure 2 only the maximum viscosity values are shown for ethanol, isopropanol, and *tert*-butanol; *n*-propanol (not shown) behaves in approximately the same way as does isopropanol.

The amounts of alcohol necessary to prevent gelation in 3% EAAA(25) solutions are listed in Table II. Also, in order to demonstrate the effect of varying the carboxyl content, Table III lists the amounts of isopropanol required to prevent gelation in 3% solutions of methyl acrylate-acrylic acid copolymers. We see that the amount of alcohol required increases as

\* Because of the similarity of results observed in the MAAA and EAAA series, the effects of addenda on EAAA(25) are shown in Figure 2 and in subsequent figures.

TABLE II  
Gelation Prevention by Alcohols in 3% EAAA (25) Solutions

Alcohol	Amt. alcohol required to prevent gelation, vol.-%
CH <sub>3</sub> OH	25
CH <sub>3</sub> CH <sub>2</sub> OH	15
(CH <sub>3</sub> ) <sub>2</sub> CHOH	10
CH <sub>3</sub> CH <sub>2</sub> CH <sub>2</sub> OH	10
(CH <sub>3</sub> ) <sub>3</sub> COH	7.5
CH <sub>3</sub> CH <sub>2</sub> CH <sub>2</sub> CH <sub>2</sub> OH	5

TABLE III  
Gelation Prevention by Isopropanol in 3% MAAA Solutions

Polymer	Amt. isopropanol required to prevent gelation, vol.-%
MAAA (10)	17.5
MAAA (15)	15
MAAA (20)	10
MAAA (25)	10

the acrylate component is increased. Similar results were found in the ethyl acrylate-acrylic acid (EAAA) series over the same range of monomer ratios.

**Urea.** Urea eliminated gelation in algin (Fig. 3) and PEC but had no effect on the acrylic acid-containing polymers. Guanidine hydrochloride was even more effective than urea, since only 1M solutions were needed to eliminate any appreciable viscosity rise.

**Sodium Chloride.** Sodium chloride at the 0.5M level eliminates gelation in algin, PEC and the acrylates (Fig. 4).

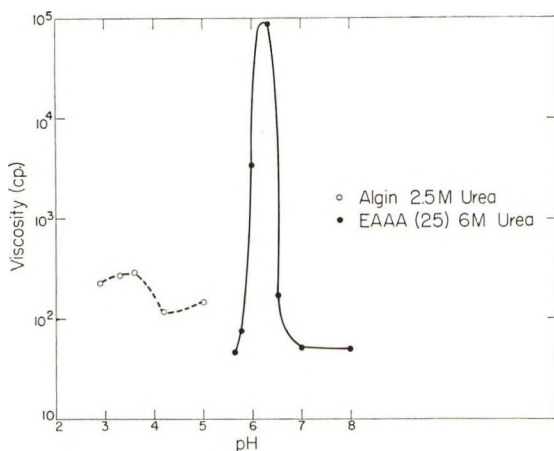


Fig. 3. Viscosity behavior of 1% algin and 3% EAAA (25) solutions.



**Surfactants.** Nonionic types (Fig. 5), such as Triton X-100 (*tert*-octylphenoxy polyethoxy ethanol), did not suppress gelation of alginate. Relatively small concentrations eliminated the gelation of the acrylate copolymers. Even at 0.25% the viscosity rise of EAAA(25) was limited

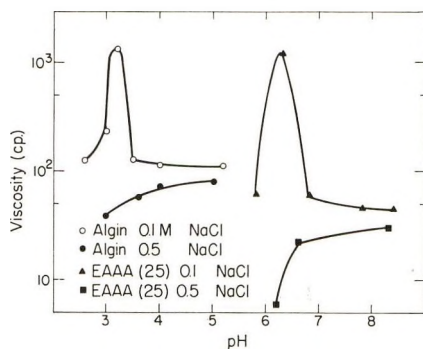


Fig. 4. Viscosity behavior of 1% alginate and 3% EAAA (25) solution.

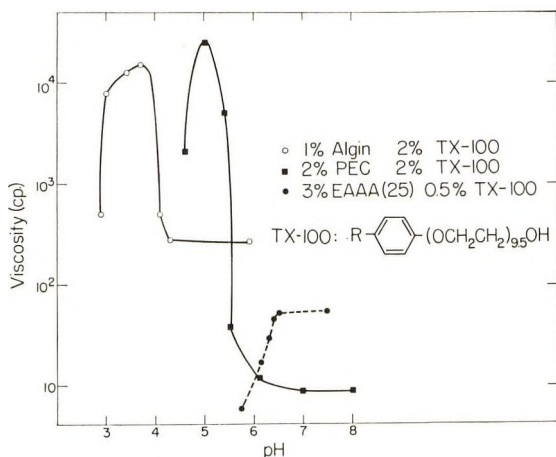


Fig. 5. Effect of Triton X-100 on gelation ( $R = \textit{tert}$ -octyl).

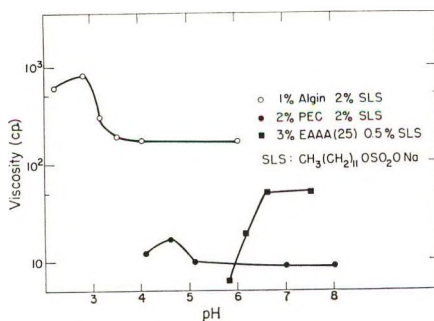


Fig. 6. Effect of sodium lauryl sulfate (SLS) on gelation.

to less than 500 cpoise. Anionic surfactants (Fig. 6), such as sodium lauryl sulfate (Duponol C), eliminated or severely reduced the viscosity rise at the gelation pH.

**Other Addenda.** Glycols up to hexylene had no effect on suppression of gelation. Butoxyethanol resembled *n*-butanol in its effect on PEC. (It was incompatible, however, with the other polymers.) Methoxyethanol resembled methanol in its effect on the acrylate polymers and on PEC. Glycol ethers, such as diethoxyethylene glycol, had no effect. Ketones resembled the alcohols, 2-butanone being much more effective than acetone. However, 2-butanone at the 20% level still allowed a 3- to 4-fold viscosity rise at the gelation pH.

### Melting Points

Melting points were obtained for gelled PEC and EAAA(25). Algin crosslinked irreversibly during the melting point determinations, giving rise to erratic results. The melting point data were treated (Fig. 7) by the

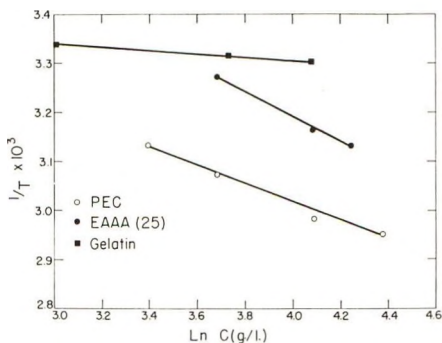


Fig. 7. Melting-point data for gels. Gelatin data from Eldridge and Ferry.<sup>2</sup>

method of Eldridge and Ferry,<sup>3</sup> who derived eq. (1) (on the basis of the three-dimensional network theory of gelation) for the dependence of the melting point of gelation gels on concentration.

$$\ln c = \Delta H^\circ / RT + \text{constant} \quad (1)$$

where  $c$  is concentration of the polymer (g./liter);  $T$  is the melting point of gel (absolute); and  $\Delta H^\circ$  is the heat of reaction for:



### Effects of Addenda on Inherent Viscosity

The inherent viscosity determinations were made at the gelation pH's of the polymers in solutions sufficiently dilute to minimize intermolecular effects. Data are shown for EAAA(25) at 0.5% concentration and for algin at 0.1%. Figure 8 shows the effects of methanol and isopropanol, Figure 9 shows the effects of urea, and Figure 10 shows the effects of the surfactants on algin.

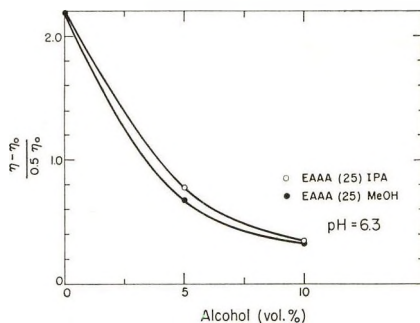


Fig. 8. Effect of alcohols on inherent viscosity (dl./g.) on EAAA (25) at the gelation pH.

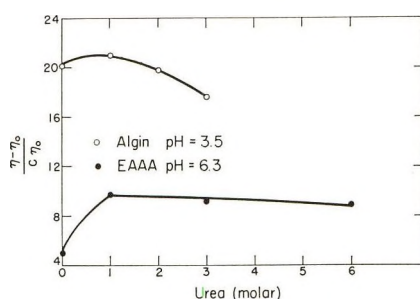


Fig. 9. Effect of urea on inherent viscosity (dl./g.) of alginate (0.1%) and EAAA (25) (0.5%) at the gelation pH.

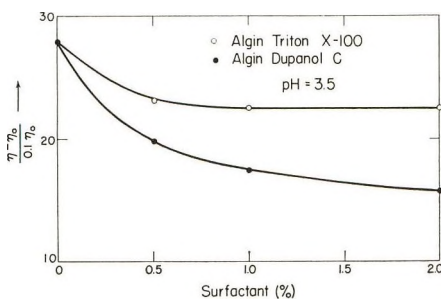


Fig. 10. Effect of surfactants on inherent viscosity (dl./g.) of alginate at the gelation pH.

## DISCUSSION

Many of the effects of adding addenda presented are reminiscent of a protein-protein interaction such as is found in the gelation of gelatin. These include the behavior of alginate and PEC with urea, the greater effectiveness of guanidine HCl compared with urea, and the action of anionic surfactants on both types of polymers. The effect of urea and nonionic surfactants on the acrylate copolymers is quite different from the gelatin case. Also, unlike the case of gelatin gels, the electrostatic effect demonstrated by NaCl

is an important factor. This last point makes it quite clear that the gelation mechanism cannot be based on hydrogen bonding alone.

The evidence presented indicates that both hydrogen bonding and electrostatic-repulsive effects are operating in the gelation mechanism. Gelation in a narrow pH region for these relatively dilute systems must be caused by a balance of intermolecular forces. Since the polymers at their gelation points are ionized to a considerable extent (with the exception of PEC) (Table I), the gelation phenomena cannot be considered to be due simply to the precipitating tendency of the solute.<sup>4-6</sup>

If this were the case, then the viscosity of the polymer solutions could not be lowered from the maximum viscosity values without precipitation of the polymer. Also, the tendency to gelation would have been observed with many of the other carboxyl-containing polymers which are listed in the results. Finally, many of the addenda which did not prevent gelation, such as diethoxyethylene glycol, are solvents for the free acid form of polymers such as the acrylate-acrylic acid series.

The data suggest the following gelation mechanism. At the gelation pH, attractive force interactions and repulsive force effects are equal. The attractive force interactions are due to hydrogen bonding and the repulsive forces are due to the coulombic repulsion of charged carboxylate ions. Addenda which can solvate the hydrogen-bond sites eliminate the attractive force interactions and allow the repulsive forces to prevent the molecules from forming a three-dimensional network. Electrolytes such as NaCl create a more extensive counterion atmosphere around the charged groups and reduce the repulsive forces so that as the pH is lowered, the possibility of an extended three-dimensional network is eliminated. Association takes place, together with low degrees of swelling.

In the acrylates, bonding can occur between uncharged carboxyl groups and between carboxyl and ester groups. The carboxyl-ester interaction must contribute the greater part to the attractive force effects. Otherwise poly(acrylic acid) would be expected to show a viscosity maximum at pH's far below the value at 100% ionization and the butadiene-acrylic acid copolymers would certainly be expected to show gelation effects. Also, the acrylate-acrylic acid copolymers required more alcohol to prevent gelation as the acrylate content increased (Table III), indicating the importance of the acrylate group in the attractive force interactions. Urea and guanidine hydrochloride do not break the hydrogen bonds in these copolymers because the environment around the groups constituting such a bond must be quite hydrophobic. The importance of the size of the alkyl group in the alcohol used as the addendum bears this out. Eliasaff and Silberberg<sup>7</sup> have shown that a hydrogen-bond breaker for one polymer need not necessarily have any effect on another polymer. In addition, it has recently been demonstrated<sup>8</sup> that urea does not have very much effect on intramolecular carboxyl-carboxyl or carboxyl-carboxylate bonds. One would expect their results to apply also to intermolecular bonds between such groups. Therefore, all evidence points to the carboxyl-ester interaction as the important attractive force interaction in the acrylate copolymers.

The effectiveness with which relatively small amounts of surface-active agents eliminate gelation with the acrylate-acrylic acid copolymers is particularly striking. The nonionic surfactant acts as the limiting case of the alcohol series; as the alkyl group increases in size, less addendum is needed to prevent gelation.

In the case of algin and PEC, the attractive forces could be due to hydroxyl-hydroxyl, hydroxyl-carboxyl, carboxyl-carboxyl, and carboxyl-carboxylate hydrogen bonding. In view of the findings with the acrylates, we assume that carboxyl-carboxyl and carboxyl-carboxylate contributions are of lesser importance. The degree of ionization of PEC at the gelation pH (13%) shows that the amount of coulombic repulsion needed to balance the attractive forces is much lower for PEC than that for algin, which is more than 50% ionized at the gelation point. PEC has very few hydroxyl groups available because of its high degree of substitution. Here again it is demonstrated that carboxyl-carboxyl or carboxyl-carboxylate attractive interactions are very weak compared with those produced by hydroxyl groups. Otherwise, PEC would have a larger degree of ionization at the gelation point. One would expect the large phthaloyl group to block the carboxylate group so that it could not be involved in the degree of carboxyl-carboxylate interaction that was found with the acrylate copolymers. Urea was very effective in eliminating gelation in algin and PEC, indicating that its effect is similar to that observed with aggregation and hydrogen bonding in poly(vinyl alcohol) solutions.<sup>9</sup> The failure of nonionic surfactants to eliminate associative effects in the celluloses is similar to results of interaction studies reported with such materials and with proteins.<sup>10</sup>

The absence of gelation effects in the case of carboxymethylcellulose is puzzling. One would expect it to show associative effects through hydroxyl-carboxyl and hydroxyl-hydroxyl interactions. The ether linkage introduced during the carboxymethylation of cellulose is quite hydrophilic and possibly reduces the associative tendencies of the remaining hydroxyl groups. It is possible to prepare aqueous solutions of the free acid form of this polymer.

It is interesting to note that acrylic acid copolymers with butyl acrylate show no gelation tendencies. The butyl group probably obstructs the formation of associative bonds.

Plots of the concentration versus the melting point of PEC and EAAA-(25) gave reasonably straight lines, indicating the applicability of eq. (1) to these gels. The heats of reaction for both gels were  $-8 \pm 0.4$  kcal./mole crosslinks. Melting point data obtained by Eldridge and Ferry<sup>3</sup> for one of their gelatin samples (Fig. 1 in their work) which was gelled without annealing are also shown in Figure 7, and the  $\Delta H^\circ$  value found by them is more than  $-50$  kcal./mole crosslinks. If one considers the crosslinks due to hydrogen bonds, then the crosslinks for the gelling polymers contain 1-2 hydrogen bonds per crosslink. This is in contrast to the highly associated crosslinks that seem to be indicated for gelatin gels. One would not expect amorphous polymers such as the acrylate copolymers when gelled to contain highly associated crosslinks.

The effects of the addenda on the inherent viscosity (Figs. 8–10) show essentially that intramolecular effects could not account for the viscosity changes that have been found with these polymers at their gelation points. An addendum causing a large increase in the inherent viscosity would have meant that there was a large increase in the molecular hydrodynamic volume caused by a decrease in the intramolecular bonding. Methanol or isopropanol (Fig. 8) did not differ in their effect on the hydrodynamic volume of EAAA(25), yet they behaved differently with regard to the prevention of gelation at the higher polymer concentrations used. Urea (Fig. 9) appears to expand the polymer coil for EAAA somewhat and has little effect on the size of algin molecules. The anionic surfactant (Fig. 10) has a greater effect than does the nonionic on the viscosity of 0.1% algin solutions, but at the 1% polymer concentration the anionic surfactant eliminated intermolecular bonding. Intermolecular association then still persists for algin at the 0.1% level at the gelation pH. Measurements made at still lower concentrations (0.01–0.03%) gave erratic results.

The concept of attractive force interactions affecting the shape of viscosity versus degree of ionization curves has been reported for poly(acrylic acid),<sup>11</sup> acacia catechuic acid,<sup>12</sup> and for poly(aspartic acid).<sup>13</sup> In the first two cases, it was found that 10% of the carboxyl groups must be ionized in order to overcome weak hydrogen-bonding interactions. No viscosity maxima were found at degrees of ionization much less than 100%. We have studied poly(acrylic acid) at concentrations as high as 10% without observing any gelation tendencies. This is to be expected in view of the weakness of the hydrogen-bonding. Poly(aspartic acid), on the other hand, shows extremely strong hydrogen-bonding tendencies, and 40% of the acid groups must be ionized in order to overcome the hydrogen-bonding interactions due to the peptide groups. In this case one would expect viscosity maxima at degrees of ionization much less than 100%. This was not observed by Berger and Katchalski,<sup>13</sup> possibly because they worked with low concentrations (ca. 0.1%).

The gelation of alginic acid at pH 3.5 has been reported by Saric and Schofield.<sup>14</sup> They attribute the gelation to hydrogen bonding between the carboxyl groups. It is apparent from our work that the hydroxyl groups must be much more strongly involved than the carboxyl. However, we were not able to ascertain the importance of heterologous bonding between the hydroxyl and the carboxyl groups.

In conclusion, the model of a balance of forces of association due to hydrogen bonding and repulsion resulting from coulombic forces accounts for the gelation behavior which has been observed. The detailed study of the effect of addenda on the gelation of these polymers gives valuable information on the nature of the groups involved in the interactions.

We wish to thank Dr. Donald A. Smith for the preparation of the acrylate-acrylic acid copolymers.

## References

1. Hermans, J. J., and J. Th. G. Overbeek, *Bull. Soc. Chim. Belg.*, **57**, 154 (1948).
2. Kuhn, W., O. Kuntze, and A. Katchalsky, *Helv. Chim. Acta*, **31**, 1944 (1948).
3. Eldridge, J. E., and J. D. Ferry, *J. Phys. Chem.*, **58**, 992 (1954).
4. Evans, E. F., and H. M. Spurlin, *J. Am. Chem. Soc.*, **72**, 4750 (1950).
5. Flory, P. J., *Principles of Polymer Chemistry*, Cornell Univ. Press, Ithaca, N. Y., 1953, p. 595.
6. Silberberg, A., J. Eliassaf, and A. Katchalsky, *J. Polymer Sci.*, **23**, 259 (1957).
7. Eliassaf, J., and A. Silberberg, *J. Polymer Sci.*, **41**, 33 (1959).
8. Levy, M., and J. P. Magoulas, *J. Am. Chem. Soc.*, **84**, 1345 (1962).
9. Stacey, K. A., and P. Alexander, *Symposio Intern. Chim. Macromol. Milan-Turin (1954)*, Arti Grafiche Panetto, Rome, Italy, 1955, p. 889.
10. Putnam, F. W., in *The Proteins, Chemistry, Biological Activity, and Methods*, Vol. I, Part B, H. Neurath and K. Bailey, Eds., Academic Press, New York, 1953, Chap. 9, pp. 807-891.
11. Katchalsky, A., *J. Polymer Sci.*, **7**, 393 (1951).
12. Mukherjee, S. N., and V. K. Kulshrestha, *J. Polymer Sci.*, **39**, 552 (1959).
13. Berger, A., and E. Katchalski, *J. Am. Chem. Soc.*, **73**, 4084 (1951).
14. Saric, S. P., and R. K. Schofield, *Proc. Roy. Soc. (London)*, **A185**, 431 (1946).

## Résumé

Des effets de formation de gels ont été étudiés en fonction du pH pour les matières polymériques suivantes: l'acide alginique, le poly(acrylate de méthyle-co-acide acrylique), le poly(acrylate d'éthyle-co-acide acrylique), et l'éthyl-cellulose phtalée. Les effets de différents additifs ont été également étudiés. Les résultats suggèrent un mécanisme de formation de gels pour tous les polymères qui consiste en une balance d'interactions de force répulsives, dues à l'ionisation des groupements carboxyliques et d'interactions de forces attractives, dues à la formation de ponts hydrogène. Les groupements participant aux interactions, dues à la formation de ponts hydrogène ont été déduits. Les points de fusion des gels de l'éthylcellulose phtalée, et du poly(acrylate d'éthyle co acide acrylique) ont été obtenus en fonction de la concentration et les  $\log c$  donnaient en fonction de l'inverse des températures absolues de fusion des droites linéaires. La chaleur de la réaction de pontage était de  $-8 \pm 0.4$  kcal/mole. Ceci est beaucoup moins élevé que les valeurs obtenues pour des gels de gélatine et suggère qu'un pont simple contient une à deux liaisons hydrogène.

## Zusammenfassung

Gelbildungseffekte wurden als Funktion des pH-Wertes an folgenden polymeren Stoffen untersucht: Alginsäure, Poly-(Methylacrylat-co-Acrylsäure), Poly-(Äthylacrylat-co-Acrylsäure) und Äthylcellulosephthalat. Auch der Einfluss verschiedener Zusätze wurde untersucht. Die Ergebnisse lassen bei allen Polymeren einen Gelbildungsmechanismus als wahrscheinlich erscheinen, der die abstossenden Kräfte der ionisierten Karboxylgruppen und die anziehenden Kräfte der Wasserstoffbindungen berücksichtigt. Die bei der Wasserstoffbindung wirksamen Gruppen werden bestimmt. Die Schmelzpunkte von Äthylcellulosephthalat- und Poly-(Äthylacrylat-co-Acrylsäure)-gelen wurden als Funktion der Konzentration ermittelt und lieferten beim Auftragen von  $\log c$  gegen die reziproke absolute Schmelztemperatur eine lineare Abhängigkeit. Die Reaktionswärme der Vernetzungsbildung betrug  $-8 \pm 0,4$  kcal/Mol Vernetzung. Dieser Wert ist bedeutend niedriger als die an Gelatinegelen erhaltenen Werte und spricht dafür, dass eine einzelne Vernetzung 1 bis 2 Wasserstoffbindungen enthält.

Received December 30, 1963

## Adsorption of Poly(vinyl Acetate-C<sup>14</sup>) on Smooth, Geometrically Simple Surfaces

R. C. WEATHERWAX and HAROLD TARKOW,  
*Forest Products Laboratory, Forest Service, U.S. Department of Agriculture,  
Madison, Wisconsin\**

### Synopsis

Poly(vinyl acetate-C<sup>14</sup>)(PVA) was adsorbed from a variety of benzene and carbon tetrachloride solutions on swollen and shrunken cellophane film, on glass, and on cellulose acetate film. The surfaces were geometrically simple, permitting mechanical measurements of the areas. Glass, shrunken cellophane, and cellulose triacetate adsorbed equal amounts of PVA. Swollen cellophane, however, adsorbed 40 times as much PVA as shrunken cellophane. Desorption experiments indicated that the high PVA adsorption on swollen cellophane showed the high reactivity of the surface rather than the diffusion of PVA into the cellophane.

### INTRODUCTION

The adsorption of polymers from solution plays an important role in the gluing and finishing of wood. A better understanding of these operations may result from knowledge of the early interactions between polymer and wood. The Forest Products Laboratory has completed a study of the adsorption of polyvinyl acetate on cellophane as part of a broader program. Cellophane, as an adsorption substrate, is related to wood substance, but has the advantage of a well-defined surface, which allows adsorptions to be related to unit area, rather than unit mass of substrate.

### EXPERIMENTAL

Poly(vinyl acetate-C<sup>14</sup>), specific activity 1.15  $\mu\text{c.}/\text{mg.}$ , (Tracerlab) was used without purification or dilution. The viscosity-determined molecular weight<sup>1</sup> was 45,000. The solvents were reagent-grade carbon tetrachloride and benzene, dried and freed of polar impurities by percolation through anhydrous silica gel. Commercial absolute alcohol and reagent acetone were dried by percolation through a Linde molecular sieve, type 3A, and then redistilled. Spectroscopic grade chloroform was used without purification. Glassware was cleaned with chromic-sulfuric acid.

The principal substrate, DuPont, type 215 PD, uncoated cellophane, 0.0009 in. thick, was leached free of plasticizer in distilled water. The 24 hr.

\* Maintained at Madison, Wis., in cooperation with the University of Wisconsin.



of extraction exceeded the 18 hr. period considered adequate by Stamm.<sup>2</sup> Swollen anhydrous films were produced by solvent exchange from the water-swollen condition through alcohol to benzene or carbon tetrachloride. To produce smooth shrunken films, the water-swollen films were clamped across glass rings and slowly equilibrated at 90% and then 30% R.H. The air-dry films were then vacuum-dried at 40°C. The films were clear without apparent crazing after removal from the rings. Glass microscope cover slides were degreased by 24 hr. of Soxhlet extraction with acetone and then oven-dried. Eastman cellulose acetate film (39.4% acetyl) was formed by evaporation of 2% acetone solution in quiet air. The clear film was freed from residual acetone by three cycles of humidification and air drying, followed by vacuum drying at 40°C.

The area of the glass substrate was measured by a micrometer to  $\pm 0.75\%$ . The area of the other substrates, twice the area of the die used to cut out the adsorption disks, was known to  $\pm 0.1\%$ .

The quantity of PVA adsorbed on a film or in the dry residue of a solution was determined by burning the material to C<sup>14</sup>-tagged carbon dioxide by Van Slyke<sup>3</sup> combustion, and assaying the gas with an ionization chamber and a vibrating reed electrometer (Nuclear Chicago Company).<sup>4</sup> The mean error for oxidation and assay of identical PVA aliquots was 0.95% at the 95% confidence level.

## RESULTS

### Time Required for Equilibrium Adsorption and for Rinsing

Minimum rinse time and equilibration time had to be determined before meaningful adsorption data could be obtained.

The several substrates with adsorbed PVA were rinsed for periods from 2 to 35 min., passing through five vessels of pure solvent before being blotted, dried, and assayed. These attempts to measure the rate of desorption of PVA from swollen and shrunken cellophane, glass, and cellulose acetate showed no statistically significant desorption after 5 min. of preliminary rinsing (Table I), which probably removed physically entrained PVA. Previous experience with PVA-C<sup>12</sup> adsorption on wood also indicated the polymer had very little tendency to desorb in pure solvent at room temperature. All subsequent films were rinsed a minimum of 5 min. in five successive vessels of pure solvent.

Shrunken cellophane disks, separated by 1 mm. glass spacers, were placed in unstirred benzene and carbon tetrachloride solutions of PVA. Pairs of films were removed periodically, rinsed, and assayed for polymer. The data, given in Table II, show that 24 hr. were adequate for equilibration in benzene, but that 48 hr. were required for adsorption from carbon tetrachloride. A minimum of 3 days was allowed for adsorption from either solution on shrunken film. A similar experiment (Table II) with swollen cellophane showed 12 days were required for equilibrium adsorption under these unstirred conditions. Two weeks were allowed. These data have no

TABLE I  
Effect of Rinse Time in Pure Solvent on Retention of PVA-C<sup>14</sup> by Various Substrates

Substrate	Rinse time, min.	Specific adsorption of PVA, $\mu\text{g./cm.}^2$
Cellulose acetate	4.5	0.42
	9	0.42
Shrunken cellophane	14	0.41
	5	0.46
	15	0.48
	25	0.46
	35	0.43
Swollen cellophane	5	19.70
	15	17.30
	25	20.30
	35	20.20
Glass	15	0.52
	15	0.46
	25	0.49
	35	0.43

TABLE II  
Time Required for Equilibrium Adsorption of PVA on Cellophane

Type of film	Solvent	Adsorption days	Mean specific adsorption of PVA, $\mu\text{g./cm.}^2$
Shrunken	CCl <sub>4</sub>	0.33	0.16
		0.66	0.19
		1.33	0.24
		2.00	0.47
		3.00	0.45
Shrunken	Benzene	0.33	0.18
		0.66	0.19
		1.33	0.19
		2.00	0.21
		3.00	0.20
Swollen	Benzene	4.00	5.2
		7.00	6.7
		12.00	9.0
		14.00	10.6

kinetic significance. They merely establish the minimum time for equilibration.

#### Adsorption of PVA on Dry, Shrunken Cellophane, Glass, and Cellulose Acetate

The substrates were allowed to adsorb PVA from benzene and carbon tetrachloride solutions of widely varying concentrations. The results are shown in Figure 1. At concentrations greater than about 100  $\mu\text{g./ml.}$ , the equilibrium specific adsorption is independent of concentration. Table III



shows that the mean specific adsorptions of PVA from solutions above 100  $\mu\text{g./ml.}$  on shrunken cellophane, glass, and cellulose acetate are in good agreement with each other. The table also includes, for comparison, the PVA adsorption data of Koral, Ullman, and Eirich,<sup>5</sup> which are recalculated to show specific adsorption (in  $\mu\text{g./cm.}^2$  of surface). Koral's specific adsorptions are about twice the specific adsorptions observed on shrunken cellophane, glass, and cellulose acetate. However, Koral based his measurement of the surface area of his powders primarily on the adsorption of palmitic acid from carbon tetrachloride solution. He assumed a close-packed film of palmitic acid, an assumption that may be questioned. Assuming his areas were actually somewhat greater than those reported, the agreement of adsorption values on all five substrates is good.

TABLE III  
Mean Maximum Specific Adsorption of PVA on Various Substrates of Known Area

Solvent	Mean specific adsorption of PVA, $\mu\text{g./cm.}^2$					
	Tin <sup>a</sup>	Iron <sup>a</sup>	Glass	Cellulose acetate	Shrunken dry cellophane	Swollen anhydrous cellophane
Benzene	0.58	0.32			0.21	9.0
CCl <sub>4</sub>	0.97	0.98	0.54	0.43	0.47	18.7

<sup>a</sup> Data of Koral, Ullman, and Eirich.<sup>5</sup>

The nature of the substrate in the present work is such that the roughness factor must be very close to unity. The close agreement in specific adsorption among the various substrates must mean that the forces responsible are similar. The hydrogen-bonding capability of cellulose hydroxyl groups is not available in dry, shrunken cellophane, so the only forces common to all five substrates are the nonspecific van der Waals' forces.

#### Adsorption of PVA on Anhydrous, Swollen Cellophane

Table III and Figure 1 also show the adsorption of PVA from benzene and from carbon tetrachloride solutions on swollen, anhydrous cellophane. Each datum point in the figure is the mean of four samples. At saturation, the swollen cellophane adsorbed about 40 times as much PVA as did the shrunken cellophane. The onset of saturation occurred at a higher external solution concentration.

The extremely high adsorption on swollen cellophane may be explained as (1) penetration into the swollen film as suggested by Luce and Robertson<sup>6</sup> for pulps or (2) interaction only at the immediate surface.

The possibility of penetration depends on the relative size of the polymer coil and the interchain distance in the amorphous region of the cellophane. There is reason to believe that such penetration was not possible for the polymer used in this work. Craig and King<sup>7</sup> studied the dialysis of a

variety of proteins through water-swollen cellophane. They found rather rapid penetration up to molecular weights of about 4,000, but no detectable penetration above 6,000. Furthermore, a literal comparison of the probable unperturbed root-mean-square, end-to-end distance for PVA of molecular weight 45,000,<sup>8,9</sup> shows it is over seven times the intermicellar distance in water-swollen cellophane.<sup>8</sup> That the ratio is even greater when the water is solvent-exchanged with benzene is shown by the 30% reduction in film area following solvent exchange. Further evidence for ruling out penetration was obtained from desorption studies.

### Desorption Experiments

The intermicellar spaces are the only channels through which a polymer molecule can diffuse into or out of swollen cellophane. Evaporation of the solvent from the swollen cellophane would partially collapse these channels, and would therefore tend to immobilize any polymer in the interior of the cellophane. The hypothesis that PVA does not penetrate the swollen cellophane was tested by allowing PVA to adsorb on a set of swollen cellophane disks. The rates of PVA desorption from the still swollen disks were then compared with the rate from disks shrunken by evaporation of the solvent. The hypothesis would be confirmed if the rates of PVA desorption from the shrunken disks were equal to or greater than the desorption rate from swollen disks. An hypothesis that PVA penetration into the film can occur requires the rate of PVA diffusion from the shrunken film to be less than that from the swollen film.

Swollen cellophane films (exchanged to benzene) were equilibrated with PVA. Entrained PVA was removed by a 20-min. rinse in pure benzene, and

TABLE IV  
Desorption of PVA from Swollen Cellophane and Cellophane Shrunken after Adsorption

Solvent	Desorption time, days <sup>a</sup>	Temperature, °C.	Residual PVA in film, $\mu\text{g./cm.}^{2b}$		
			After desorption from swollen condition		After desorption from shrunken condition, group 3
			Group 1	Group 2	
—	0	25	5.63 $\pm$ 0.43	5.38 $\pm$ 0.47	5.19 $\pm$ 0.29
CHCl <sub>3</sub>	3	25		4.84 $\pm$ 0.23	1.86 $\pm$ 0.24
CHCl <sub>3</sub>	7	25		4.81 $\pm$ 0.23	1.80 $\pm$ 0.24
CHCl <sub>3</sub>	10	25		4.82 $\pm$ 0.23	1.56 $\pm$ 0.24
CHCl <sub>3</sub>	14	25		4.86 $\pm$ 0.23	1.35 $\pm$ 0.24
CHCl <sub>3</sub>	3	61		4.67 $\pm$ 0.13	1.28 $\pm$ 0.16
Acetone	1	56		1.00 $\pm$ 0.13	0.74 $\pm$ 0.16
Acetone	3	56		0.53 $\pm$ 0.02	0.60 $\pm$ 0.09

<sup>a</sup> Errors at 75% confidence level.

<sup>b</sup> The films were given a preliminary 20-min. rinse in pure benzene to remove entrained PVA.

the films were divided into three sets. The first group was dried and assayed for adsorbed polymer. The second group, still swollen, was transferred to pure chloroform. The third set was air-dried, vacuum-dried at 40°C., and transferred to chloroform. Chloroform was chosen because it is a good solvent for PVA but does not swell cellophane. The films remained in chloroform for 14 days and, during this time, aliquots of the chloroform were analyzed for desorbed PVA. The films were then transferred to fresh chloroform, which was boiled under total reflux for 3 days, and the PVA desorption determined as before. The films were then transferred to acetone, under reflux for 3 days, and PVA desorption again measured.

The films were then assayed for residual adsorbed polymer. From results of these various analyses, Table IV was prepared.

The desorption from the swollen film (group 2) by chloroform was only about 10%, whereas the shrunken film (group 3) lost about 75% of its originally adsorbed polymer to the chloroform. Moreover, the loss occurred in the first 3 days without any statistically significant further loss in the next 11 days. This is contrary to the postulated behavior if penetration into the film had occurred. Very little additional loss occurred after 3 days in boiling chloroform.

The very appreciable loss to chloroform from the shrunken film is probably due to the breaking of hydrogen bonds between cellophane and PVA as the films were dried. These hydrogen bonds remained intact in the swollen film and prevented any appreciable desorption. Irreversible adsorption has been reported by others.<sup>5</sup> It should be emphasized, however, that the original adsorption on swollen film is a surface phenomenon.

Acetone is also a good solvent for PVA, but unlike chloroform, it can form strong hydrogen bonds with surface hydroxyl groups on cellophane. As a consequence, the remaining adsorbed polymer is removed from both substrates in time. Koral<sup>5</sup> found similar results for acetonitrile on his PVA-substrate systems.

## DISCUSSION

This work emphasizes the marked difference in equilibrium adsorption of PVA onto a substrate like swollen cellophane where opportunities for hydrogen bonding are excellent and substrates like glass, cellulose acetate, shrunken cellophane, and powdered metals where such opportunities are poor. The generally accepted mechanism for the adsorption of flexible chains is that of occasional linkages between polymer and substrate,<sup>10</sup> with portions extending into solution. If one takes Ries' value<sup>11</sup> for the area required for the adsorption of a monomer unit of PVA, the amount of polymer adsorbed on shrunken cellophane is 4 to 10 times greater (depending on solvent) than the substrate could hold if the polymer lies flat on the surface. Where appreciable hydrogen bonding can occur, as between the carbonyl group in PVA and hydroxyl groups in swollen cellophane, the amount adsorbed is several hundred times greater. This must require a high degree of

lateral compression or an interpenetration of polymer coils or both. The approach to an equilibrium configuration is very likely responsible for the long equilibration times necessary with swollen cellophane. This high adsorption on swollen cellophane does emphasize the enormously high reactivity of surfaces of swollen cellulosic materials, and therefore should be pertinent to the bonding of resins to pulps and of adhesives and finishes to wood. Comparable results, as yet unpublished, are found for swollen wood substance.

### References

1. Varadaiah, V. V., *J. Polymer Sci.*, **19**, 477 (1956).
2. Stamm, A. J., *J. Phys. Chem.*, **60**, 76 (1956).
3. Van Slyke, D. D., F. Plazin, and J. R. Weiseger, *J. Biol. Chem.*, **191**, 299 (1951).
4. Tolbert, B. M., U.S. Atomic Energy Commission, University of California Radiation Laboratory Report No. 3499, 315 (1956).
5. Koral, J., R. Ullman, and F. R. Eirich, *J. Phys. Chem.*, **62**, 541 (1958).
6. Luce, J. E., and A. A. Robertson, *J. Polymer Sci.*, **51**, 317 (1961).
7. Craig, L. C., and T. P. King, *J. Am. Chem. Soc.*, **77**, 6620 (1955).
8. Sato, M., Y. Koshiishi, and M. Asahina, *J. Polymer Sci.*, **B1**, 233 (1963).
9. Stamm, A. J., *Tappi*, **40**, 761 (1957).
10. Jenckel, E., and B. Rumbach, *Z. Electrochem.*, **55**, 612 (1951).
11. Ries, H. E., and D. C. Walker, *J. Colloid Sci.*, **16**, 361 (1961).

### Résumé

L'acétate de polyvinyle C<sup>14</sup> (PVA) a été adsorbé à partir de solutions dans le benzène et le tétrachlorure de carbone sur un film de cellophane gonflé et rétréci, sur le verre et sur un film d'acétate de cellulose. Les surfaces étaient géométriquement simples, permettant des mesures mécaniques de surfaces. Le verre, le cellophane rétréci et le triacétate de cellulose adsorbent la même quantité de PVA. La cellophane gonflée cependant adsorbe 40 fois plus de PVA que le cellophane rétrécie. Des expériences de désorption ont fait apparaître que l'adsorption élevée du PVA sur cellophane gonflée montrait la réactivité élevée de la surface plutôt que la diffusion du PVA dans la cellophane.

### Zusammenfassung

Polyvinylacetat-C<sup>14</sup> (PVA) wurde aus einer Reihe von Benzol- und Tetrachlorkohlenstofflösungen an gequollenem und geschrumpftem Zellophanfilm, auf Glas und Zelloseacetatfilm adsorbiert. Die Oberfläche war geometrisch einfach und erlaubte mechanische Flächenmessung. Glas, geschrumpftes Zellophan und Zellosetriacetat adsorbieren gleiche Mengen an PVA. Gequollenes Zellophan jedoch adsorbierte 40 mal soviel PVA wie geschrumpftes. Desorptionsversuche zeigen, dass die hohe PVA-Adsorption an gequollenem Zellophan durch die hohe Reaktivität der Oberfläche und nicht durch die Diffusion von PVA in das Zellophan bedingt ist.

Received October 31, 1963

Revised January 29, 1964

## BOOK REVIEW

N. G. GAYLORD, Editor

**Grundriss der Makromolekularen Chemie**, B. VOLLMERT. Springer-Verlag, Berlin-Göttingen-Heidelberg, 1962, 507 + xii, DM 48.00.

This book, at first glance, seems rather small. Yet it contains an amazing amount of information. Dr. Vollmert who straddles both the industrial and academic fields at Badische Anilin- & Soda-Fabrik and at the Technische Hochschule at Karlsruhe has produced a work that will be most useful in both spheres for reference and as a text.

The book begins with a discussion of basic principles. A lengthy section on the synthesis and reactions of macromolecular compounds follows that includes radical polymerization, ionic polymerization, polymerization with complex initiators, polycondensation, polyaddition, ring-opening polymerization, enzymatic polymerization, graft and block copolymers, and chemical reactions of polymers, including degradation. The properties of "free" macromolecules are then discussed, such as molecular weight and its determination, molecular structure, and configuration. Finally, macromolecular aggregates are covered, including solution properties, gels, and the rubbery, glassy, and crystalline states. There is thus a good balance of the organic and physical aspects of polymer chemistry.

Many practical aspects, such as reinforced and impact-resistant polymers, and foams, are also presented, as is a somewhat too brief list of tradenames. There is an extensive bibliography of key articles and books by subject, but there are only very few references cited directly in the text. The book is abundantly illustrated with structures, tables, graphs, and photographs.

This reviewer feels that Dr. Vollmert's book is among the best of the single-volume treatises covering the entire field of polymers and heartily recommends it to all able to understand German.

*Norbert M. Bikales*

Gaylord Associates, Inc.  
Newark, New Jersey, 07104



## ERRATUM

### Linear Condensation Polymers from Phenolphthalein and Related Compounds

(article in *J. Polmer Sci.*, A2, 437-459, 1964)

P. W. MORGAN

*Pioneering Research Division, Textile Fibers Department, E. I. du Pont de Nemours & Company, Inc., Wilmington, Delaware*

On p. 442, para. 4, line 6 should read: <sup>26</sup> rather than <sup>25</sup>; the reaction which follows should begin with compound I.

On p. 449, the caption for Figure 1 should read diacetate rather than dibenzoate; the caption for Figure 2 should read dibenzoate rather than diacetate; and the caption for Figure 4 should read sebacate rather than isophthalate.

On p. 450, the caption for Figure 5 should read isophthalate rather than sebacate.

On p. 458, transpose the bibliographic data of references 24 and 25.